An application of Doppler echocardiography and Tissue Doppler Imaging in the evaluation of cardiac function of normal cats and cats with hypertrophic cardiomyopathy

Haralambos Koffas

PhD
The University of Edinburgh
May 2003

Abstract

Hypertrophic cardiomyopathy (HCM) of cats is the most common cardiac disease of this species. Feline HCM shares many of the morphological characteristics recorded with human HCM. Diastolic impairment is believed to be the main abnormality of the disease and evidence for this has been provided by both invasive and Doppler echocardiographic studies. Tissue Doppler Imaging (TDI) has emerged in the last decade as an alternative tool for the non-invasive quantification of regional and global myocardial function. TDI studies in affected humans and experimental animals have shown that systolic impairment is also evident in HCM, despite the presence of normal or supernormal contractile state of the LV in this cardiac entity.

The aims of this study were (1) to produce Doppler echocardiographic criteria of normality in cats; (2) to identify differences in ventricular function using Doppler echocardiography between normal cats and cats with HCM; (3) to investigate diastolic and systolic function in normal cats and cats with HCM, by means of TDI.

There was no significant difference in LV FS% between normal and HCM cats although affected cats tended to have higher FS%. Apart from the E deceleration time of mitral inflow, which was prolonged in HCM cats, neither the E/A of mitral inflow nor the IVRT were different between the two groups. The LV flow propagation velocity was significantly lower in the affected group compared to that in normal. Asymptomatic affected cats had a higher S wave and S/D ratio and a lower D wave of pulmonary venous flow (PVF) than normal cats. The time from the Q wave of the ECG to peak systolic velocities of PVF was significantly prolonged in the HCM than in the normal group. HCM cats showed significantly higher aortic and pulmonic velocities than normal cats.

The TDI technique revealed evidence of both diastolic and systolic dysfunction in HCM cats. On pulsed TDI data, diastolic dysfunction was expressed with decreased early diastolic velocities, lower early diastolic acceleration and deceleration, prolonged IVRt and decreased E'/A', mainly along the longitudinal axis of the heart. The physiologic time and space non-uniformity recorded in the LV motion of normal cats was lost in affected cats. Systolic dysfunction in the HCM group was less prominent than the diastolic, and was expressed with decreased late systolic velocities and systolic acceleration mainly along the longitudinal axis. This decrease was independent from left ventricular out-flow tract obstruction and was present in asymptomatic affected cats. Cats with CHF showed a tendency for decreased systolic myocardial indices. On colour M-mode TDI, certain colour velocity stripes were appeared on the LVPW of cats and were corresponded to certain peaks occurring in tracings of both the Myocardial Velocity Gradients (MVG) and Mean Myocardial Velocity (MMV). Biphasic shifts were recorded in the LVPW during early diastole and the two isovolumic periods. MVG followed wall thickness changes during the different phases of the cardiac cycle. Peak MVG during early diastole and systole was significantly reduced in HCM cats compared to that in normals. Peak MMV during the second phase of the isovolumic contraction period was significantly reduced in HCM cats.

This study, for the first time, offers evidence for systolic dysfunction in feline HCM. The data presented here provide reference data for future studies in the investigation and better classification of feline cardiac diseases. The successful application of TDI in cats, despite the very small size of their heart and the inherent high heart rates often encountered in this species, provides evidence for possible successful application of the technique in human neonatal hearts and experimental small animal models of human diseases.

Declaration

Tom Anderson made the tissue mimicking material phantom and helped in setting up the relevant experiment. Bill Adams performed the analysis of covariance. Joanna Dukes McEwan acquired all the TDI images in the repeatability study and Paul Smith participated in the repeatability study for colour M-mode TDI images. The rest of this thesis has been entirely composed by the author, Haralambos Koffas, and has not been presented to any university other than the University of Edinburgh.

Haralambos Koffas

May 2003

To my parents, Ismini and Christo

To my sisters, Lena and Domna

and to little Ismini.

Acknowledgements

This project was funded by the Greek State Scholarship Foundation, and I am extremely grateful for their continuous financial support.

I am also indebted to my supervisor Dr. Joanna Dukes-McEwan, who conceived the idea of this project, for her tireless support, valuable advice, and encouragement. Thank you Jo. Without you, this work would have been impossible. I am especially grateful to my supervisor, Dr. Brendan Corcoran, for his invaluable help and trust. Thank you Brendan, for being always there, when I needed it. Particular thanks are due to Vassilis Sboros, my mentor and friend from the Medical Physics department, who has been an inexhaustible source of inspiration and support. Thank you Vassili. I was very lucky to meet you. I am also grateful to my supervisors from the Medical Physics department, Dr. Carmel Moran and Professor Norman McDicken, for their assistance and valuable guidance. I must acknowledge the support of Tom Anderson from the Medical Physics department, who set the phantom study. Thank you all guys from the Medical Physics department. It was wonderful to feel part of your group.

I am especially indebted to Mo Clarke from the Dundas Veterinary Group who provided cases for this project, to Bill Adams from the Medical statistics department for carrying out the analysis of covariance, to Dr Graham Mackenzie for his assistance with the analysis software and to the owners who allowed us to carry out these studies on their cats. Special thanks are due to Anne French and Kerry Simpson for their general assistance and also to Paul Smith for providing clinical cases for this project and participating in the repeatability study. I would like also to acknowledge my supervisor from Greece, Professor Alexander Koutinas for his valuable advice and encouragement at the initial stages of this project.

Finally, I must acknowledge Irini for her love, support and patience, throughout this study. Thank you Irini.

Contents

SECTION A

INTRODUCTION HYPERTROPHIC CARDIOMYOPATHY: GENERAL REVIEW

SECTION B

ECHOCARDIOGRAPHIC / DOPPLER EVALUATION OF HYPERTROPHIC CARDIOMYOPATHY

SECTION C

TISSUE DOPPLER IMAGING ECHOCARDIOGRAPHY: A REVIEW OF THE LITERATURE

SECTION D

PULSED DOPPLER TISSUE IMAGING IN NORMAL CATS AND CATS WITH HYPERTROPHIC CARDIOMYOPATHY: ASSESSMENT OF MYOCARDIAL MOTION ALONG THE RADIAL AND LONGITUDINAL AXIS

SECTION E

PEAK MEAN MYOCARDIAL VELOCITIES AND VELOCITY GRADIENTS MEASURED BY COLOUR M-MODE TISSUE DOPPLER IMAGING IN THE LEFT VENTRICULAR FREE WALL OF HEALTHY CATS

SECTION F

PEAK MEAN MYOCARDIAL VELOCITIES AND VELOCITY GRADIENTS MEASURED BY COLOUR M-MODE TISSUE DOPPLER IMAGING IN THE LEFT VENTRICULAR FREE WALL OF HEALTHY CATS AND CATS WITH HYPERTROPHIC CARDIOMYOPATHY

SECTION G

REPEATABILITY STUDY

SECTION H

SECTION I

List of tables

List of figures

List of appendices

List of abbreviations used in text and tables

A	Mitral (or tricuspid) inflow late diastolic velocity or late diastolic peak of MVG or MMV
A'	Late diastolic myocardial velocity
AC	Atrial contraction
Acc. t	Acceleration time of aortic velocity
ACE	Angiotensin converting enzyme
A' dur	Duration of A' wave
A dur	Duration of late ventricular filling
ANCOVA	Analysis of covariance
Ar dur	Duration of Ar wave of the PVF
Adur/Ardur	Ratio of duration of A wave of mitral inflow to duration of Ar of PVF
Ao diam d	Aortic diameter during diastole (2D rpsa)
Aort.v Aod	Aortic diameter during diastole (M-mode)
Aort.v:LAs	Left atrial diameter during systole (M-mode)
Ao.vmax	Aortic peak velocity
Ao VTI	Velocity time integral of aortic velocity
Ar	Pulmonary venous flow atrial reversal wave
Ar VTI	Velocity time integral of the Ar wave of the PVF
A' VTI	Velocity time integral of A' wave
A VTI	Velocity time integral of A wave of mitral inflow
bpm	Beats per minute
bS'-Sl'	Time from onset of S' wave to Sl'
CFDE	Colour flow Doppler echocardiography
CHF	Congestive heart failure
cm	Centimetres
cm/sec	Centimetres per second
CP	Constrictive pericarditis
cTnT	Cardiac troponin T
CV%	Coefficient of variation
D	Pulmonary venous flow peak diastolic velocity
DCM	Dilated cardiomyopathy
D dur	Duration of D wave of PVF
D dec	Deceleration time of D wave of the PVF
dP/dt	Rate of pressure development during isovolumic contraction
D VTI	Velocity time integral of the D wave of the PVF
Diast t	Duration of diastole
E	Mitral (or tricuspid) inflow early diastolic velocity
E'	Early diastolic myocardial velocity
E/A	Ratio of early to late diastolic velocity of mitral (or tricuspid) inflow or of MMV
E'/A'	Ratio of early to late diastolic myocardial velocity
EA	Combined E and A peak of mitral inflow or of MVG or MMV
EA'	Combined E' and A' myocardial velocity
E acc t	Acceleration time of early filling
EA' VTI	Velocity time integral of EA'
ECG	Electrocardiogram
E dec t	Deceleration time of early filling
E' dec	Deceleration of E' wave
E dur	Duration of early filling
E' dur	Duration of E' wave
EF%	Ejection fraction
E max	Maximal early diastolic peak of MVG or MMV
EPSS	Mitral E point to septal separation
ET	Ejection time

EVE	Early ventricular ejection
EVF	Early ventricular filling
E VTI	Velocity time integral of E wave of mitral inflow
E' VTI	Velocity time integral of E' wave
E1 acc	Mean acceleration of E1 of MMV
E12 acc	Mean acceleration of E12 of MMV
E1 dec	Mean deceleration of E1 of MMV
E12 dec	Mean deceleration of E12 of MMV
E2 dec	Mean deceleration of E2 of MMV
E1	First early diastolic peak of MVG or MMV
E12	Combined E1 and E2 peak of MVG or MMV
E2	Second early diastolic peak of MVG or MMV
FPV	Flow propagation velocity
FS%	Fractional shortening
HCM	Hypertrophic cardiomyopathy
HOCM	Hypertrophic obstructive cardiomyopathy
II-E'	Time from end of S' wave to peak E'
IGF-1	Insulin-like growth factor-1
I-Se'	Time from end of A' wave to Se'
IVA	Myocardial acceleration of the free wall of the RV
IVC	Isovolumic contraction phase
IVCa	Myocardial shift during the first phase of the isovolumic contraction period
IVCb	Myocardial shift during the second phase of the isovolumic contraction period
IVCt	Isovolumic contraction time
IVR	Isovolumic relaxation phase
IVRa	Myocardial shift during the first phase of the isovolumic relaxation period
IVRb	Myocardial shift during the second phase of the isovolumic relaxation period
IVRt	Isovolumic relaxation time (myocardial)
IVRT	Isovolumic relaxation time (LV flow)
IVSs	Interventricular septal wall thickness (systole)
IVS	Interventricular septum
LA	Left atrium
LA area d	Left atrial area during diastole
LA area s	Left atrial area during systole
LAd/Aod	Left atrial to aortic diastolic diameter (2D rpsa)
LA dist d	Left atrial distance during diastole (2D rpla)
LA dist s	Left atrial distance during systole (2D rpla)
LA FS%	Left atrial fractional shortening
LA length d	Left atrial length during diastole (2D rpsa)
LAs/Aod	Left atrium (systole) to aorta ratio (diastole) (M-mode)
lat MA	Lateral mitral annulus
LV	Left ventricle
LVA	Left ventricular pressure during atrial contraction
LV diam.s	Left ventricular end-systolic diameter
LV diam.d	Left ventricular end-diastolic diameter
LVE	Late ventricular ejection
LVEDP	Left ventricular end diastolic pressure
LV FS%	Left ventricular fractional shortening
LVOT	Left ventricular outflow tract
LVOTO	Left ventricular outflow tract obstruction
LVPW	Left ventricular posterior wall
LVPWs	Left ventricular posterial wall thickness (systole)
m	Metres
MAM lat	Mitral annulus excursion (lateral)

MAM sep	Mitral annulus excursion (septal)
MI	Mitral inflow
MMV	Mean myocardial velocity
m/sec	Metres per second
msec	Millisecond
MV	Mitral valve
MVG	Myocardial velocity gradient
n	Number
nRCWT	Normalized rate of change of wall thickness
ns	Not significant
PA. vmax	Pulmonary artery peak velocity
PCWP	Pulmonary capillary wedge pressure
PEP	Pre-ejection period
PEP/ET	Pre-ejection period to ejection time ratio
pre-A LV pressure	Left ventricular pressure before atrial contraction
PVF	Pulmonary venous flow
Q-A'	Time from Q wave of the ECG to peak A' wave
Q-Ar	Time from Q wave of the ECG to Ar of PVF
Q-bE'	Time from Q wave of the ECG to the onset of E' wave
Q-bS	Time from Q wave of the ECG to onset of S wave of PVF
Q-bS'	Time from Q wave of the ECG to the onset of S' wave
Q-D	Time from Q wave of the ECG to D of PVF
Q-E'	Time from Q wave of the ECG to peak E'
Q-Sl'	Time from Q wave of ECG to Sl'
Q-Smax	Time from Q wave of the ECG to Smax of PVF
Q-S1	Time from Q wave of the ECG to S1 of PVF
Q-S12	Time from Q wave of the ECG to S12 of PVF
Q-S2	Time from Q wave of the ECG to S2 of PVF
PST	Post-systolic thickening
RCM	Restrictive cardiomyopathy
R(D)SVS	Royal (Dick) School of Veterinary Studies
rpla	Right parasternal long axis
rpsa	Right parasternal short axis
R-R	Mean interval between R waves on ECG
RVOTO	Right ventricular outflow tract obstruction
S'	Myocardial systolic wave
SAM	Systolic anterior motion
S/D	Ratio of maximal systolic to diastolic PVF velocity
sd or SD	Standard deviation
S dur	Duration of S wave of PVF
S' dur	Duration of S' wave
SE	Standard error
SEE	Standard error of estimate
Se	Early systolic peak of MVG or MMV
Se'	Early systolic myocardial velocity
Se acc	Mean early systolic acceleration of MMV
Se' acc	Acceleration of systolic myocardial velocity
Sl	Late systolic peak of MVG or MMV
Sl'	Late systolic myocardial velocity
S max	Pulmonary venous flow maximal systolic velocity
S VTI	Velocity time integral of S wave of PVF
S' VTI	Velocity time integral of S' wave
S1	Pulmonary venous flow peak S1 wave velocity
S2	Pulmonary venous flow peak S2 wave velocity
S12	Pulmonary venous flow peak S12 wave velocity
syst t	Duration of systole
τ or tau	Time constant of left ventricular pressure decay during the isovolumic relaxation period

TDI	Tissue Doppler Imaging
tE'acc	Acceleration time of E' wave
tE'dec	Deceleration time of E' wave
TGF-β1	Transforming growth factor-β1
TI	Tricuspid inflow
TMM	Tissue-mimicking material
TNF-a	Tumor necrosis factor
tSe'acc	Acceleration time of systolic wave
WHO	World Health Organization
vs	Versus
4 ch	4 chamber apical view
β-MHC	β-myosin heavy chain

SECTION A
INTRODUCTION
HYPERTROPHIC CARDIOMYOPATHY: GENERAL REVIEW

A.1. Definition

The original report of the World Health Organization (WHO/ISFC Task force, 1980), defined cardiomyopathies as "heart muscle diseases of unknown cause" distinct from specific heart muscle diseases of known aetiology. The original classification of the WHO included three major morphological types of cardiomyopathy; dilated, hypertrophic and restrictive. According to the new WHO report, cardiomyopathies are classified by the dominant pathophysiology or, when possible, by aetiological/pathogenetic factors (Richardson *et al*, 1996). Cardiomyopathies are defined as diseases of the myocardium associated with cardiac dysfunction (Richardson *et al*, 1996). The revised WHO classification now recognizes the following types of cardiomyopathy: dilated, hypertrophic, restrictive, and arrhythmogenic right ventricular. Unclassified cardiomyopathies are those, which are difficult to classify, and may share common characteristics with other types of cardiomyopathy. Hypertrophic cardiomyopathy in humans is currently defined as a familial cardiac disease, which is transmitted with an autosomal dominant trait and results from mutations in the genes responsible for encoding sarcomeric proteins (Richardson *et al*, 1996). Hypertrophic cardiomyopathy is characterized by left and/or right ventricular hypertrophy, which is usually asymmetric and predominantly involves the interventricular septum. The left ventricular volume may be normal or

reduced and systolic gradients may be present. Typical pathological changes encountered in hypertrophic cardiomyopathy are: myocyte hypertrophy, disarray and increased fibrosis of the loose connective tissue.

A.2.1. Aetiology and pathogenesis of HCM in humans

HCM of humans is an inherited disease, which is transmitted as an autosomal dominant trait (Marian and Roberts, 1995a). Although current data indicate that the significant proportion (> 90%) of HCM cases is familial, sporadic cases due to *de novo* mutations also occur (Watkins *et al*, 1993). Currently 10 genes responsible for encoding sarcomere proteins, with nearly 100 different mutations, have been found to contribute to the pathogenesis of HCM (Roberts and Sigwart, 2001). Mutations in the β-myosin heavy chain (β-MHC) and the Troponin T genes constitute the great majority of the mutations related to the disease (Roberts and Sigwart, 2001).

The genetic diversity of HCM is a significant determinant of the phenotypic and clinical diversity of the disease (Marian and Roberts, 1995a). Genetic-phenotypic studies have shown that carriers of certain mutations exhibit severe hypertrophy and also severe clinical manifestation, whereas carriers of others show mild hypertrophy and have a more benign clinical course (Epstein *et al*, 1992; Fananapazir and Epstein, 1994; Marian and Roberts, 1995a). Some mutations (Troponin T) are associated with mild hypertrophy and very poor prognosis with high incidence of sudden cardiac death (Marian and Roberts, 1995a). Interestingly, the individual magnitude and extent of hypertrophy varies dramatically, even among carriers of the same mutation (Fananapazir and Epstein, 1994).

The phenotypic diversity of the disease and the fact that mutant genes encode sarcomeric proteins, which implicitly must influence the contractile properties of the myocytes, led many investigators to suspect the additional effect of modifier genes or factors in the genesis of hypertrophy. According to this hypothesis, impaired contractility is the primary deficit, which triggers the release of growth factors that result in compensatory myocardial growth and fibroblast proliferation (Rust *et al*, 1999; Marian, 2000; Roberts and Sigwart, 2001). Several different studies have shown that certain mutations related to HCM significantly impair the contractile properties of the cardiac myocytes. Marian and colleagues (1997) showed that expression of the mutant $Arg^{92}Gln$ human cardiac troponin T (cTnT) in isolated adult feline myocardial cells decreased cell fractional shortening and peak velocity of shortening in the absence of significant disruption in the sarcomere structure. Expression of the mutant $Arg^{403}Gln$ human β-MHC, again in isolated adult feline myocardial cells, caused disruption of sarcomeric assembly and myofibrillar disarray suggesting that this abnormality maybe a possible cause of impaired myocardial contractility in HCM (Marian *et al*, 1995b). Moreover, it has been shown that the 179N and R92Q mutant cardiac cTnT caused reduced calcium sensitivity and contraction force in isolated adult human myocardial cells without altering the gross sarcomeric structure (Rust *et al*, 1999).

Other studies have investigated the role of modifying factors in the pathogenesis of HCM. Ortlepp and colleagues (2002) showed that certain genetic polymorphisms of the renin-angiotensin-aldosterone-system increased penetrance and degree of

hypertrophy in gene carriers from a single family with a myosin binding protein C mutation. Li and colleagues (1997) showed that the levels of transforming growth factor-β1 (TGF-β1) and insulin-like growth factor-1 (IGF-1) from hypertrophied intraventricular segments of patients with HCM were significantly elevated when compared with those from corresponding myocardial segments of patients with aortic stenosis, stable angina and ischemic cardiomyopathy. In an effort to investigate the role of modifying factors in the magnitude of regional hypertrophy, the same group of investigators compared the levels of IGF-1 and TGF-β1 between the hypertrophied septum and non-hypertrophied myocardium of patients who underwent septal myectomy for severe hypertrophic obstructive cardiomyopathy (HOCM) (Li *et al*, 2002). IGF-1 messenger RNA and protein levels in the hypertrophied myocardium were 2.6 and 2.9 times greater, respectively, than in the non-hypertrophic myocardium of the same patient. Similarly, TGF-β1 messenger RNA and protein levels in the hypertrophied myocardium were 2.5 and 2.8 times greater, respectively, than the levels in the non-hypertrophied segments. Tumor necrosis factor (TNF-a) was also suspected to be associated with cardiac hypertrophy (Patel *et al*, 2000).

The results from the aforementioned studies provide evidence that cardiac stress due to impaired contractile performance enhances the expression of stress-responsive mitotic and trophic factors, which in turn induce compensatory hypertrophy and myocardial fibrosis. Although the above theory accepts that diastolic impairment is also evident in HCM, this is believed to be the consequence of hypertrophy and fibrosis rather the primary defect (Marian, 2000). Preserved or increased contractility

as assessed by FS% in HCM results from the concentric hypertrophy of the disease, which leads to increased wall thickness and decreased LV end diastolic volume, both resulting in decreased afterload. However, reduced contractility of the individual myocardial fibres remains the fundamental functional deficit of the disease (Marian, 2000).

On the other hand, *in vitro* studies have shown that isolated human and mouse mutant β-MHC R403Q myocytes exhibit enhanced actin-activated ATPase activity, increased generated force and accelerated filament sliding, suggesting increased contractile performance at cellular level induced by this particular mutation (Palmiter *et al*, 2000; Tyska *et al*, 2000). These findings may provide an alternative explanation of the supra normal cardiac performance, which may be evident in humans with hypertrophic cardiomyopathy. It has been suggested that the consequences of enhanced myosin function would be detrimental rather beneficial. Heterogeneity of motor performance of mutant and wild-type myosin proteins within the sarcomere is believed to result in loss of mechanical co-ordination between the myosin heads. In addition, enhanced ATPase activity would result in higher energy consumption by the hypertrophied heart. This, in the presence of reduced energy supply could be detrimental and lead to premature death of individual cardiac cells. Fibroblast proliferation and replacement fibrosis may occur under these circumstances as a consequence of the myocyte death and contribute to the overall pathological consequences of the disease (Seidman and Seidman, 2001).

A.2.2. Aetiology of HCM in cats

Evidence for genetic transmission of feline HCM has been provided by several studies over the last few years. An inherited pattern of transmission of HCM has been described in a highly interrelated colony of Maine coon cats, compatible with autosomal dominant transmission and 100 percent penetrance (Kittleson *et al*, 1999). An autosomal dominant trait of HCM has been also documented in a family of American shorthair cats with systolic anterior motion (SAM) of the anterior mitral valve leaflet and LV hypertrophy and in an inbred colony of Persian cats (Martin *et al*, 1994; Meurs *et al*, 1997). HCM has also been reported in two families of mixed-breed cats (Kraus *et al*, 1999; Nakagawa *et al*, 2002). HCM is seen with increased prevalence in certain breads of cats, such as Ragdoll, British shorthair, Norwegian Forest and Rex cats. Exotic breeds, such as Siamese and Burmese, are rarely affected by HCM (Harpster, 1986). Recently, in a limited study, Meurs and colleagues (2001) showed that myomesin was decreased or absent in the myocardium of affected with Maine coon cats when compared to that in normal animals. The same study showed that within the myocardium of affected animals, anomalously migrating beta myosin heavy chain (β-MHC) was detected along with concomitant decrease in β-MHC. This study provided additional evidence that HCM of cats is a disease of the sarcomere and set new targets for further studies in the feline genome. However, no causal mutation of feline HCM has been reported to date.

A.3. Naturally occurring HCM in domestic animals

Apart from humans and cats with naturally occurring HCM, HCM has also been described in dogs and pigs (Liu and Tilley, 1980; Thomas *et al*, 1984; Liu *et al*, 1993; Dai *et al*, 1996; Huang *et al*, 1996).

A.4. Animal models of HCM

A number of transgenic animal models of HCM have been created in order to investigate the pathophysiological mechanisms of the disease (Oberst *et al*, 1998; Tardiff *et al*, 1998; Yang *et al*, 1998; Marian *et al*, 1999). These models exhibited many characteristics of the human disease, including cardiac hypertrophy and histopathological features of myocyte disarray, with increased interstitial fibrosis and altered cardiac physiology. The natural history of the mutant α-myosin heavy chain-arginine^{403} mouse was investigated by one group and offered valuable information about the impact of genotype and physical activity on phenotype (Geisterfer-Lowrance *et al*, 1996). The wild-type β-myosin heavy chain-arginine^{403} and the mutant β-myosin heavy chain-glutamic acid^{403} transgenic rabbits of human HCM have been used in assessing the sensitivity of Tissue Doppler Imaging (TDI) echocardiography in detecting mutant rabbits in the absence of LV hypertrophy (Nagueh *et al*, 2000).

Recently, the genetic cause of naturally occurring HCM in the Syrian hamster has been described (Sakamoto *et al*, 1997). Interestingly, it has been shown that in this animal model the defect responsible for HCM (mutation in the gene encoding for delta-sarcoglycan) causes also DCM in some animals. Other genetic factors are

suspected for determining the phenotypic expression of the disease (HCM or DCM) in the mutation carriers.

A.5. Prevalence of HCM in humans and cats

The Coronary Artery Risk Development in Adults (CARDIA) study showed a prevalence of HCM in humans of 0.17% (7/4111) (Maron *et al*, 1995). In this study HCM was estimated to be 2.9 times more common in men than women and 2.4 times more common in blacks than whites. However, the sample used in the above study was relatively small and therefore the reported figures may not represent the exact prevalence of HCM in humans (Fananapazir and Epstein, 1995).

After the significant reduction in the presence of Dilated Cardiomyopathy due to supplementation of commercial food with taurine, HCM has become the most commonly diagnosed cardiac disease of the cat (Atkins *et al*, 1992a; Kittleson, 1999). One study carried out at the Animal Medical Centre in New York showed that in a period of two years, 46 cats out of 143 were diagnosed to have HCM. (Fox *et al*, 1995). Similar prevalence of HCM in cats during a period of 10 years is reported by Kittleson (1999). In the latter report the number of HCM cases was more than twice the number of congenital cardiac defects diagnosed in cats over the some period. A male predisposition in HCM of cats has been reported in many studies (Atkins *et al*, 1992a; Fox *et al*, 1995), but this is not a consistent finding of all reports (Martin *et al*, 1994; Meurs *et al*, 1997).

A.6. Clinical presentation and physical findings in cats with HCM

Cats with HCM may be asymptomatic or may present with signs of CHF or clinical manifestations of thromboembolism (Bright *et al*, 1992; Peterson *et al*, 1993; Fox *et al*, 1995; Fox, 1998). Detection of HCM in asymptomatic animals is usually incidental during routine examination and based on the presence of a murmur, gallop rhythm or arrhythmia. Cats with moderate to severe heart failure present with tachypnoea, dyspnoea or orthopnoea due to pulmonary oedema or pleural effusion or both. Coughing is uncommon in cats with congestive heart failure (Bonagura, 1994). Cats with right-sided heart failure may have ascites, hepatomegaly and distended jugular veins with abnormal pulse. Inappetence and vomiting may sometimes precede the respiratory signs of CHF. Arterial thromboembolism, mainly at the aortic trifurcation, results in peracute onset of posterior paresis or paralysis and pain. Thromboembolism of the brachial artery occurs less often and results in paresis or paralysis mainly of the front right leg. Syncope in cats with HCM is a rare presentation and may result from tachyarrhythmia or dynamic left ventricular outflow tract obstruction (Kittleson, 1999). Sudden death is another possible clinical manifestation, although the precise mechanism remains uncertain. Ventricular tachyarrhythmia that degenerates into ventricular fibrillation has been proposed as one possible explanation for sudden death in cats with HCM (Kittleson, 1999).

Palpation may detect marked precordial impulse and abnormally weak femoral pulses, attributed to arrhythmia or decreased cardiac output. Auscultation in cats with HCM may reveal a murmur, gallop rhythm, tachycardia or arrhythmia. The murmur is systolic, better audible over the left apex and cranial sternum and is either due to

left ventricular outflow tract obstruction or mitral regurgitation, or both (Kittleson, 1999). Recently, dynamic obstruction of the right ventricular outflow tract was described and suggested as a possible cause of systolic right sternal border murmur in cats with HCM (Rishniw and Thomas, 2002). The gallop rhythm is usually due to fourth heart sound (S4) associated with atrial contraction (Luis Fuentes, 1992). Moreover, auscultation may detect increased respiratory noise and crackles resulting from pulmonary oedema. Muffled cardiac and lung sounds may be present if there is pericardial or pleural effusion, both referable to heart failure (Kittleson, 1999). Typically the latter is the usual finding. Interestingly, cats with HCM may be bradycardic and it is suggested this may be due to hypoxia.

A.7. Radiography in feline HCM

Radiographic findings in cats with HCM may be variable. Cats may present with moderate to mild cardiomegaly related, mainly, to left sided enlargement (Harpster, 1986). Left atrial enlargement occurs more frequently (Harpster, 1986). Biatrial enlargement with concomitant right ventricular enlargement and shifting of the apex towards to the midline may cause the so-called "valentine-shape" in the dorsoventral projection (Tilley, 1976). However, this finding is not consistent in cats with HCM (Fox, 1998). In asymptomatic cats, a normal cardiac shape or mild left atrial enlargement is more likely (Harpster, 1986). Cats with left-sided heart failure may present with pulmonary vascular congestion with interstitial or alveolar oedema (Harpster, 1986; Fox, 1998). Pulmonary oedema in cats with HCM may be patchy or focal rather than localized in the perihilar region as seen in dogs, and tends to be more prominent in the dorso-caudal lung fields (Medinger and Bruyette, 1992; Fox,

1998). With severe heart failure, some cats often present with pleural effusion and may develop pericardial effusion, giving a globoid heart silhouette (Kittleson, 1999). Although many authors attribute pleural effusion to right heart failure (Lord *et al*, 1974; Bright *et al*, 1992), there is strong anatomical evidence to suggest it can be caused by left-side congestive heart failure (Kittleson, 1999). Based on early studies, which showed that cats' visceral pleura is supplied by pulmonary arteries instead of bronchial arteries (McLaughlin *et al*, 1961), Kittleson (1998) speculated that pulmonary veins are likely to be involved in the drainage of visceral pleura of this species. An increase in the LA pressure could therefore lead to increased pulmonary hypertension and eventually to pleural effusion.

A.8. Electrocardiography in feline HCM

Electrocardiography in cats with HCM may reveal variable findings. Electrocardiographic changes suggestive of left atrial and left ventricular enlargement, such as tall P and R waves, are frequently encountered (Tilley, 1992). Ventricular and supraventricular arrhythmias, such as sinus tachycardia, atrial and ventricular premature complexes, atrial fibrillation and ventricular tachycardia may also be present. Profound sinus bradycardia and paroxysmal bigeminy are also included in the ECG disturbances related with HCM of cats (Goodwin *et al*, 1992; Medinger and Bruyette, 1992). The presence of left anterior fascicular block, which results in left axis deviation, is a common electrocardiographic finding in cats with HCM, and is infrequently recorded in other feline myocardial diseases (Moise *et al*, 1986; Bright *et al*, 1992; Fox, 1998). Other conduction abnormalities may occur in

the ECG of cats with HCM, such as pre-excitation conduction pattern and left or right bundle branch block.

A.9. Natural history and prognosis of HCM in cats

HCM can occur in cats of any age, although an increased incidence among young and middle-aged cats has been reported by many investigators (Harpster, 1986). Severe obstructive HCM has been reported in two 2-month-old kittens (Fujii *et al*, 2001). In a highly interrelated colony of Maine coon cats, echocardiographic findings suggestive of HCM occurred in offspring of affected animals between 4 and 6 months of age (Kittleson, 1999). In this study, cats, which were offspring of affected animals, showed a more severe form of HCM and developed heart failure earlier than affected animals, which resulted from the mating of one affected and one normal cat. Furthermore, affected males progressed to severe HCM and death more commonly than affected females.

The clinical presentation or survival time of cats with HCM does not relate absolutely to the severity of left ventricular thickening (Rush *et al*, 2002). Cats with moderate to severe left ventricular thickening may be asymptomatic or have subtle signs of heart failure (Bright *et al*, 1992; Peterson *et al*, 1993; Fox *et al*, 1995; Kittleson, 1999). However, these cats have the potential to develop heart failure. In a study with 46 cats with HCM, non-survivals (n=21) due to cardiac reasons (died or euthanized) showed a greater extent and magnitude of LV hypertrophy, larger LA size and had a lower incidence of outflow tract obstruction than cats, which survived (n=18) (Fox *et al*, 1995). Unfavourable prognosis was associated with greater size of

the LA and depressed fractional shortening in another study (Peterson *et al*, 1993). Left atrial size was a significant negative predictor for survival time in a retrospective study of 260 cats with HCM (Rush *et al*, 2002). Cats with asymmetric hypertrophy with predominant free wall thickening were more prone to develop thromboembolism than those with diffuse hypertrophy or with predominant thickening of the interventricular septum (Peterson *et al*, 1993). Additionally, a heart rate > 200 bpm was a negative predictor for survival in a group of cats with HCM (Atkins *et al*, 1992a). However, this finding has not been confirmed by other studies (Rush *et al*, 2002). In Atkin's study (1992a), median survival time after the development of CHF or thromboembolism was 92 and 61 days respectively. All cats with thromboembolism were dead by six months, whereas nearly 40% of animals in heart failure survived more than 6 months. Less than 20% of cats in failure survived up to 3 years. Higher survival times have been documented in cats with HCM and CHF (median survival time 563 days, range 2 to 4418 days) or aortic thromboembolism (median survival time 184 days, range 2 to 2278 days) in another study (Rush *et al*, 2002). The occurrence of CHF in HCM of cats is not associated with a steady worsening of clinical signs. Instead, a variable duration between the first and consecutive episodes of CHF has been reported (Rush *et al*, 2002).

A.10. Pathology of HCM

Since the first systematic description of HCM by Teare (1958), who described a disease characterized by an asymmetrically hypertrophied ventricular septum containing bizarrely arranged cells, numerous pathological studies have investigated the pathological characteristics of this cardiac entity in humans, and also in animals,

with spontaneous form of the disease (Liu and Tilley, 1980; Liu *et al*, 1993; Huang *et al*, 1996). Pathological studies have shown that humans and animals with HCM share common gross and histopathological characteristics. Gross pathology of HCM of humans often discloses a non-dilated LV with disproportionate hypertrophy of the IVS, although hypertrophy may involve other parts of the left and sometimes of the right ventricular wall (Roberts and Ferrans, 1975). Absolute heart weight in patients with HCM is often higher than that in normal subjects. The size of the left and right ventricular cavities is small or normal and the left or sometimes both atria are dilated. Endocardial mural plaque on the basal ventricular septum in apposition with the anterior mitral valve leaflet is commonly present. The mitral valve leaflets and especially the anterior leaflet may be thickened and elongated. Endocardial scars and foci of fibrosis may be observed in different parts of the LV. Similar gross pathological findings are encountered in HCM of cats, although hypertrophy appears to be more symmetric, involving substantial portions of all ventricular walls (Liu *et al*, 1981; Liu *et al*, 1993). Myocardial infarcts in the LV free wall and apex have been reported in cats with HCM without significant extramural coronary artery disease (Liu and Fox, 1995). Similar findings have been reported also in humans with HCM (Maron *et al*, 1979a).

Histopathology reveals myocardial hypertrophy, cardiomyocyte disarray, increased interstitial fibrosis and abnormal intramural coronary arteries. Myocardial fibres may be thick with large hyperchromatic nuclei (Tilley *et al*, 1977; Van Vleet *et al*, 1980). The extent, but not the presence, of myofibre disarray is considered as a specific marker of HCM in humans. Histopathological studies have shown that, in hearts

from patients with HCM, the amount of myofibre disarray (areas with myofibre disarray occupying more than 5% of the tissue section) is significantly higher than in normal hearts or in hearts from patients with other cardiac diseases (Maron and Roberts, 1979b; St John Sutton *et al*, 1980). It has been shown that the amount of myofibre disorganization in HCM is not related to the extent of hypertrophy, the presence of outflow tract obstruction, general symptoms or the incidence of sudden death (Maron and Roberts, 1979b). These findings underline that cellular disorganization is more likely to be a morphologic manifestation of the underlying genetic defect, rather than a consequence of abnormal mechanical strains developed in the LV wall of patients with HCM (Maron and Epstein, 1980). However, a higher percentage of myofibre disorganization has been reported in young individuals (< 18 years of age) who died suddenly, compared to that in older patients (Maron *et al*, 1979a; Maron and Epstein, 1980). Maron and Roberts (1981b) speculated that the dispersed myocardial fibres might disrupt the physiologic transmission of electrical impulses and induce fatal ventricular arrhythmias. Marked myocardial disarray has been documented in members of families with HCM, in the absence of macroscopic cardiac hypertrophy, suggesting that cellular disorganization is one pathological manifestation of the disease with potential detrimental effects, which cannot be detected by standard echocardiographic criteria (Maron *et al*, 1990; McKenna *et al*, 1990). In some studies the extent of cellular disorganization in the IVS of humans with HCM was higher compared to that in the LVPW (Liu *et al*, 1993), although equal involvement of disarray in both ventricular walls has been reported in others (St John Sutton *et al*, 1980). Cats with HCM appear to have less frequent and

extensive cardiac cell disorganization than humans and it is likely to be confined to the IVS (Liu *et al*, 1993).

Intramural coronary artery disease is another common pathological characteristic of HCM, with small coronary arteries presenting with increased size and thickened walls. In humans thickening of the arterial wall results from thickening of both the media and the intima due to increase of smooth muscle cells, fibrous tissue and elastic or mucoid deposits (Liu *et al*, 1993). In cats, arterial thickening results more frequently from increased connective tissue elements (Liu *et al*, 1993). Abnormal intramural coronary arteries are present more frequently and to a higher extent in the myocardium of humans with HCM compared to that of normal individuals or that from patients with other cardiac diseases (Maron *et al*, 1986b; Tanaka *et al*, 1987). This particular pathological lesion of HCM is not associated with the extent of hypertrophy, the presence of outflow tract obstruction or the clinical course of the disease, and has been also documented in infants (Maron *et al*, 1986b; Tanaka *et al*, 1987). It has been suggested that the presence of abnormal intramural arteries constitutes either an independent marker of HCM or results secondarily to substantial or transmural fibrous tissue formation as a form of neovascularization (Maron *et al*, 1986b). Increased numbers of abnormal myocardial coronary vessels have been identified in close vicinity with excessive myocardial fibrosis both in humans and cats indicating a causal relation between these two pathological characteristics of HCM (Maron *et al*, 1986b; Tanaka *et al*, 1987; Liu *et al*, 1993). It is possible that the decreased coronary flow, due to the narrowing of the small intramural arteries, results in myocardial ischaemia, which if severe and prolonged may produce in turn

necrosis and fibrous tissue formation (Maron *et al*, 1986b). Abnormal small intramural vessels have been identified in both the IVS and the LVPW wall of humans and cats with HCM (Liu *et al*, 1993). In one study by Tanaka and colleagues (1987), patients with DCM-like HCM showed a more severe narrowing of the intramural small arteries than patients with typical HCM did.

A.11. Treatment of HCM in cats

Treatment in HCM is aimed at improving diastolic function and alleviating the signs of congestive heart failure when necessary. Calcium channel and β-blockers have been traditionally used to improve lusitropy through direct action (Ca-channel blockers) or indirectly (β-blockers) through the decrease of heart rate. Experimental studies have shown that diltiazem appears to have beneficial effects in HCM of cats, by controlling successfully the signs of congestive heart failure, prolonging survival and reducing significantly LV thickness (Bright *et al*, 1991). The only reported clinical study related to the efficacy of β-blockers in cats with HCM refers to esmolol (short acting β1-blocker) (Bonagura *et al*, 1991). Esmolol infusions in cats with obstructive form of HCM decreased the left ventricular out-flow tract velocities and systolic gradient and also increased the R-R interval. The efficacy of β-blockers in cats with HCM remains to be proven.

The use of angiotensin-converting-enzymes inhibitors has recently gained ground in the treatment of HCM of cats. Their efficacy in reducing preload along with their arteriodilating effects renders them as a useful tool in reducing congestion in animals with heart failure. Administration of enalapril, along with other medication, resulted

in a significant increase in the survival of a group of HCM cats with CHF (Rush *et al*, 1998). Mean survival time for cats (n=11) that had CHF at the time of initiation of enalapril was 1,147 days, with nine animals being still alive during the following up period (the two animals, which died, lived for 875 and 699 days, respectively). In another study, administration of benazepril, sometimes in combination with other medication, showed beneficial effects on clinical signs and marginal reduction in the thickness of the LV free wall in a group of HCM cats (Amberger *et al*, 1999). The use of ACE inhibitors in HCM is further supported by experimental findings, which showed that hypertrophy is mediated by the action of Angiotensin II and other mitotic and trophic factors (Li *et al*, 1997; Li *et al*, 2002; Ortlepp *et al*, 2002). Contraindications to the use of ACE inhibitors arise from their arteriodilating effects, which theoretically can increase left ventricular outflow pressure gradients and augment mitral regurgitation (Kittleson, 1999). However, no clinical deterioration or worsening of the outflow tract obstruction was caused by the administration of ACE inhibitors in a group of HCM cats (Rush *et al*, 1998).

SECTION B

ECHOCARDIOGRAPHIC / DOPPLER EVALUATION OF HYPERTROPHIC CARDIOMYOPATHY

B.1. 2D and M-mode echocardiography in HCM of humans

HCM of humans is defined echocardiographically as a hypertrophied (thickness ≥ 15 mm) non-dilated LV in the absence of other cardiac or systemic disease known to cause increased LV mass (Maron *et al*, 1981a). The phenotypic variability of HCM of humans has been described extensively by 2-dimensional and M-mode echocardiography. Although a variety of patterns of left ventricular hypertrophy have been documented, the vast majority of patients show asymmetric and predominant thickening of the ventricular septum, whereas the posterior free wall is usually the least thickened part of the ventricle (Maron *et al*, 1981a; Shapiro and McKenna, 1983; Klues *et al*, 1995). In a study carried out in 600 patients with HCM, the anterior ventricular septum was the most frequently hypertrophied segment of the left ventricle (96%) and also the predominant region of hypertrophy (83%) (Klues *et al*, 1995). Less commonly involved was the posterior septum (66%), the lateral free wall (42%) and the posterior wall (18%). In 28% of patients in the above study, hypertrophy was confined to only one myocardial segment, in 38%, hypertrophy involved two segments of the LV wall and in 34% of patients wall thickening involved 3 myocardial segments. Symmetrical hypertrophy (increased myocardial thickening to similar extent in all myocardial segments) was present in only 1% of

the study population. Klues and colleagues (1995) described, in many patients with HCM, a heterogeneous pattern of hypertrophy "with transitions between thickened and non-thickened regions being commonly sharp and abrupt, not infrequently creating right-angled contour of the ventricular wall". Marked, asymmetric thickening of the posterior LV free wall (Lewis and Maron, 1991) and predominant apical hypertrophy have been reported in other studies (Yamaguchi *et al*, 1979; Maron *et al*, 1982). Furthermore, patients with characteristic histological cardiac abnormalities compatible with HCM in the absence of gross increase in LV hypertrophy have been also documented (Maron *et al*, 1990; McKenna *et al*, 1990).

A series of case reports have described the evolution of "typical" HCM (hypertrophied, hyperdynamic and non-dilated LV) into a morphological and functional phase, which resembled dilated cardiomyopathy (Beder *et al*, 1982; Fujiwara *et al*, 1984; Kanemoto *et al*, 1995). Progressive increase in LV dimensions (average increase up to 10 mm), with maintenance of normal cavity size, along with substantial wall thinning (average decrease in thickness up to 8 mm) and systolic impairment (EF < 50%) was also evident in a subgroup of HCM patients (Spirito *et al*, 1986; Spirito *et al,* 1987).

An inverse correlation was found between age and severity of hypertrophy in a number of clinical trials, with younger patients (<35 years) more frequently showing a diffuse hypertrophy and markedly increased wall thickness (Louie and Maron, 1986; Spirito and Maron, 1989; Lewis and Maron, 1991; Klues *et al*, 1995). The observed gradual LV thinning seen in some patients with HCM was speculated to be

one possible explanation for the above inverse correlation identified between age and severity of thickness (Spirito and Maron, 1989; Klues *et al*, 1995).

Although several studies have tried to correlate the magnitude and extent of thickness with the clinical manifestation or prognosis, controversy still exists regarding this issue. Neither in Klues's study (1995) nor in Louie's one (1986) (34 patients with maximal thickness of ≥35 mm), was there a substantial relationship between the extent of hypertrophy and maximum thickness with the severity of symptoms or the clinical course of the disease. However, in Maron's study (1981a), patients with widespread hypertrophy had a significantly higher prevalence of moderate to severe functional limitation. Similarly, the majority of patients with marked asymmetrical hypertrophy of the posterior LV free wall had severe symptoms that quite often prove refractory to medical therapy (Lewis and Maron, 1991).

B.2. 2D and M-mode echocardiography in feline HCM

Echocardiography is the most sensitive modality for diagnosing HCM in cats. Thickness of >6 mm at any part of the LV wall measured by 2D or M-mode echocardiography has been accepted from many investigators as the cut-off value for defining LV hypertrophy in HCM of this species (Peterson *et al*, 1993; Fox *et al*, 1995). In contrast to the predominant asymmetrical thickening of the IVS in humans with HCM, LV hypertrophy in feline HCM is present in a more diverse pattern. In a group of 79 cats with HCM, 41% exhibited symmetrical hypertrophy, which involved equally all the parts of the LV, 42% showed predominant thickening of the

IVS and 17% showed greater thickening of the LV free wall (Peterson *et al*, 1993). Diffuse symmetrical hypertrophy has been documented in 67% of a group of HCM cats (n=46), with the rest presenting with asymmetrical hypertrophy, mainly involving the IVS (Fox *et al*, 1995). In the above study, nearly 2/3 of the affected animals showed substantially greater wall thickening in the basal portion of the LV than in the apical region, when viewed in the right parasternal long axis view. In a colony of Maine coon cats, hypertrophy more frequently involved the papillary muscles and the LV free wall than the IVS (Kittleson *et al*, 1999). Prominent thickening of the basal portion of the IVS, which protrudes into the left ventricular outflow tract, has also been documented in a number of affected animals (Peterson *et al*, 1993; Fox *et al*, 1995). The left atrial size may be normal irrespective of the magnitude of hypertrophy. However, left atrial enlargement is most likely to develop earlier in cats with severe hypertrophy than those with mild to moderate hypertrophy (Kittleson, 1999).

Echocardiography may also reveal reduced ventricular dimensions, mainly end systolic volume and normal or increased fractional shortening, although decreased fractional shortening is sometimes reported (Peterson *et al*, 1993; Fox *et al*, 1995). The evolution of "typical" HCM in humans (hypertrophied, hyperdynamic and non-dilated LV) into a morphologically and functionally phase which resembles dilated cardiomyopathy, is not often documented in cats with HCM. However, reports of affected animals with mild LV hypertrophy and concomitant severe heart failure and also the reported inverse association between decreased fractional shortening and survival, may indicate that some cats with HCM evolve to a dilating phase at a later

stage in the disease course (Bright *et al*, 1992; Peterson *et al*, 1993). Recently, Baty and colleagues (2001) reported a family of cats with an end stage HCM, which was characterised by hypodynamic LV systolic function and relative LV chamber dilatation.

Regional wall motion abnormalities (hyperkinesis, hypokinesis, akinesis, dyskinesis) with wall thinning (especially of the apex) and aneurysms may be caused by myocardial infarction in cats with HCM (Liu and Fox, 1995). Usually, the LV free wall and the apex and occasionally the free wall of the RV are involved (Fox, 1998). More infrequently, echocardiographic evaluation may detect decreased interventricular septal and left ventricular free wall thickening and aortic root excursion (Moise *et al*, 1986). Right atrial enlargement or hypertrophy of the right ventricle may be rarely observed (Fox, 1998). Echocardiography may also reveal increased thickening of the mitral valve leaflets and the presence of thrombus in the left atrium.

B.3. Left ventricular outflow tract obstruction in HCM

Increased pressure gradients in the LVOT is one of the main characteristics of HCM in humans and for many investigators one of the main determinants of clinical course of the disease (Maron and Epstein, 1986a; Wigle *et al*, 1995). According to the most widely accepted theory, increased pressure gradients are due to true mechanical obstruction caused by the Systolic Anterior Motion (SAM) of the mitral valve when its anterior leaflet is moving towards the intraventricular septum obstructing the blood flow in the LVOT during systole (Wigle *et al*, 1995; Sherrid *et al*, 2000).

Several different causal determinants of SAM have been proposed so far. These include narrowing of the LVOT due to septal basal hypertrophy (Panza *et al*, 1992; Nakatani *et al*, 1996), anterior displacement of the mitral apparatus with concomitant elongation of the anterior mitral leaflet and increased angle between the ejection flow and the mitral valve (Klues *et al*, 1993; Levine *et al*, 1995). However, the nature of the haemodynamic force causing the SAM and consequently the significance of different determinants in the genesis of this phenomenon remains a subject of unresolved debate. Many investigators have implicated the Venturi effect as the main force causing the anterior motion (Wigle *et al*, 1995). According to this theory, the high velocity ejection flow caused by outflow narrowing due to septal hypertrophy results in a local under-pressure in the LVOT, which pulls the protruding mitral leaflet towards the septum. However, in many patients with HCM, SAM occurs at a time that flow velocities in the LVOT are relatively low and therefore unable to generate significant Venturi forces (lift forces). It has therefore been proposed that drag forces (pushing force of the flow) are the main cause of SAM (Sherrid *et al*, 2000). The latter theory suggests that flow forces are exerted on the anteriorly positioned mitral leaflets (due to displacement of mitral apparatus associated with chordal slack and general distortion of papillary muscles) from a positive angle (mid-septal thickening favours the redirection of flow so as to come from a relatively lateral direction) and therefore push them towards the septum rather than lift them towards it. Contrary to the Venturi theory, which accepts narrowing of the outflow tract as a major determinant of SAM, the drag theory is substantially supported by the fact that SAM was developed after displacement of papillary muscles in the absence of LV hypertrophy in an experimental study with dogs (Klues *et al*, 1993).

Moreover, other studies have shown that many patients with severe septal thickening had no evidence of LVOT obstruction (Louie and Maron, 1986) and that SAM was evident more frequently in patients with widespread hypertrophy rather than in those with one hypertrophied segment (Klues *et al*, 1995). However, findings in other studies directly connect the narrowing of LVOT due to increased basal septal thickness with a higher incidence of SAM (Panza *et al*, 1992; Nakatani *et al*, 1996).

The SAM of the anterior leaflet of the mitral valve also results in a failure of systolic coaptation of the mitral leaflets and therefore leads to mitral regurgitation (Wigle *et al*, 1995). The degree of mitral regurgitation is determined by the time of onset and duration of mitral leaflet-septal contact in systole (Wigle *et al*, 1995) and also by the length and ability of the posterior leaflet to move anteriorly and participate in SAM coapting effectively with the anterior leaflet (Schwammenthal *et al*, 1998). This latter observation explains interindividual differences in regurgitation for comparable degrees of SAM.

According to the "cavity obliteration" theory, increased intracavitary systolic pressure gradients in HCM are not due to mechanical obstruction caused by SAM, but the result of the hyperdynamic contraction of the LV. The latter creates a significant pressure difference between the rapidly eliminated and isometrically contracting, even after its emptying, submitral area and the non-contractile outflow tract with the lower pressure due to its communication with the aorta (Criley and Siegel, 1985). The above theory invokes the fact that ventricles with dynamic gradients have better systolic function than those that do not and also that

enhancement of the gradient is associated with an increase in the rate and degree of LV emptying (Siegel and Criley, 1985). This is in contrast with the concept of physical mechanical obstruction, which if true, would hinder the rate of LV emptying. According to the "obliteration" theory, SAM is the result (the pressure gradient bends the elongated leaflet tips towards the low pressure zone of the LVOT) of the intracavitary pressure gradient rather than its cause and is not of significant clinical importance.

It has been shown by many studies that intraventricular pressure gradients are variable (Kizilbash *et al*, 1998) and subject to many factors such as myocardial contractility, preload and afterload (Maron *et al*, 1987).

Systolic anterior motion of the mitral valve is believed to be the cause of LVOT obstruction (Hypertrophic Obstructive Cardiomyopathy, (HOCM)) in cats with HCM. SAM can be seen in 2D and M-mode echocardiography. On colour flow Doppler echocardiography, it can result in two turbulent jets, one projecting into the aorta and one regurgitating through the mitral valve towards the posterior aspect of the LA (Fox, 1998; Kittleson *et al*, 1999). Left ventricular out-flow tract obstruction in cats is highly variable and quite often depends on the level of stress or excitement (Kittleson *et al*, 1999). SAM in cats with HCM does not correlate absolutely with the severity of the disease (Kittleson, 1999). In one survey, SAM occurred at the same frequency regardless of the distribution of wall thickening (segmental or diffuse) and its absence was an unfavourable indicator in the prognosis (Fox *et al*, 1995). Dynamic right ventricular outflow obstruction, caused by the apposition of the right

ventricular free wall with the interventricular septum may be detected by colour Doppler echocardiography as a turbulent systolic jet in the right ventricular outflow tract in cats with HCM (Rishniw and Thomas, 2002).

B.4. Assessment of mitral inflow characteristics by Doppler echocardiography

Assessment of LV haemodynamics in the past was feasible only by invasive, instantaneous, pressure and volume measurements, which are difficult to use on a routine clinical basis. Over the last two decades, Doppler echocardiography has been established as an non-invasive alternative to cardiac catheterization for the evaluation of cardiac haemodynamics. Mitral inflow measurements with Doppler echocardiography have become a valuable and necessary tool in the assessment of LV diastolic properties in the clinical setting. Several investigations in humans and experimental animals have provided insight into interpretation of the flow velocity pattern of mitral inflow recorded by Doppler echocardiography.

The LV pressure decay during the isovolumic relaxation period results in the mitral valve opening and the consequent influx of blood from the LA into the LV (early diastolic mitral inflow E wave) (Appleton *et al*, 1988). The blood flow during early diastole is driven by the atrioventricular pressure gradient, which is determined by a complex interaction of multiple factors. These include the left atrial pressure at the time of mitral valve opening, the rate of relaxation of the left ventricle, the compliance of the left atrium and ventricle, the size of the mitral annulus, as well as variable conditions, such as load, age and heart rate (Ishida *et al*, 1986; Appleton *et al*, 1988; DeMaria *et al*, 1991). The initial acceleration of blood into the left

ventricle, immediately after the opening of the mitral valve, continues until the risen LV pressure becomes equal to LA pressure (Nishimura *et al*, 1996). Once the latter exceeds the LV pressure then the deceleration of the flow within the LV begins. The deceleration rate of blood flow is measured as the mitral deceleration time and is dependent mainly on the effective operating compliance of the LV. During diastasis, there is equilibration of LV and LA pressures, with a low velocity of forward flow as a result of inertial forces. During late diastole, the atrial contraction results in the reacceleration of transmitral flow as left atrial pressure rises above left ventricular pressure (late diastolic mitral inflow A wave). The late diastolic mitral inflow velocity reflects the contractile state of the left atrium and is affected from the atrioventricular pressure gradient and LV compliance (Lewis, 1996).

Because of the complexity of interacting factors affecting LV filling, mitral inflow patterns recorded by Doppler echocardiography should be always interpreted as the reflection of LV haemodynamics and function rather than as indicators of specific type of cardiac diseases (Appleton *et al*, 1988). A primary abnormality of relaxation is associated with specific changes in the mitral inflow curve, such as a decreased peak early mitral inflow velocity, a normal or increased mitral inflow velocity at atrial contraction, a reduced E/A ratio, a prolonged early deceleration and isovolumic relaxation times (Appleton *et al*, 1988; DeMaria *et al*, 1991; Nishimura *et al*, 1996). This pattern has been encountered in several different cardiac diseases and is accompanied by a prolongation of the time constant of isovolumic relaxation (tau) in the presence of normal or slightly elevated left atrial pressures. A slower rate of isovolumic pressure fall results in late mitral valve opening, longer isovolumic

relaxation time and a lower initial atrioventricular driving force, which produces a low early diastolic mitral inflow E wave. Prolongation of relaxation into mid or late diastole prolongs the deceleration time of early diastolic mitral inflow. Under these circumstances, the contribution of LA contraction in the LV filling is augmented in a compensatory fashion. This leads to an increased late diastolic mitral inflow A wave and E/A reversal (E/A velocity < 1).

However, with further deterioration of the disease process and worsening of abnormal relaxation, the consequent LA pressure rise, leads to the "normalization" of the transmitral pressure gradient (Appleton *et al*, 1988; DeMaria *et al*, 1991; Nishimura *et al*, 1996). As a result, the transmitral inflow curve shifts to the so-called "pseudonormal" pattern, in which the early diastolic mitral inflow wave exceeds the late diastolic wave. This change is usually followed by a decrease in the deceleration time.

In the late stages of the disease, the ventricular compliance decreases further and LA pressure becomes even higher, leading to a large early diastolic atrioventricular gradient, which forces the blood to accelerate fast into the left ventricle. A high E wave occurs normally under these circumstances. Because the LV pressure rises abruptly after the mitral valve opening, the deceleration of early diastolic mitral inflow is rapid (short E wave deceleration time). The isovolumic relaxation time decreases further. The forward flow caused by left atrial contraction at this stage is low because the LA is operating at the lower part of its Frank-Starling curve (atrial dysfunction induced by a long-standing increase in atrial afterload due to increased

atrial and ventricular pressures). A restrictive filling pattern occurs under these conditions and it is characterized by a high E velocity, a short E deceleration time, a low A velocity and a high E/A ratio, > 2:1 (Appleton *et al*, 1988; DeMaria *et al*, 1991; Nishimura *et al*, 1996).

Transmitral flow velocity characteristics may be affected by a number of additional factors, which must be taken into consideration when mitral inflow patterns are interpreted. Decreased preload caused by nitroglycerin (Choong *et al*, 1987) or ACE inhibitor administration (Keren *et al*, 1992) has been shown to decrease the amplitude of the early diastolic wave resulting in an "abnormal relaxation" mitral inflow pattern. On the other hand, increased preload due to mitral regurgitation it is believed to mask abnormal diastolic function (Takenaka *et al*, 1986), although this effect depends on the presence of elevated LV filling pressures (Lavine and Arends, 1989). An increased afterload prolongs the rate of ventricular relaxation and slows the decrease of diastolic pressure decay, leading to decreased early diastolic velocities (Nishimura *et al*, 1996). An abnormal relaxation pattern has been described by numerous Doppler echocardiographic studies in older humans, reflecting probably impaired diastolic properties induced by aging (Gardin *et al*, 1987; Kuo *et al*, 1987; Appleton *et al*, 1988). Heart rate is another factor, which can affect the mitral inflow pattern. Sinus tachycardia (short R-R interval) may decrease the time available for early diastolic filling, increasing the proportion of filling occurring during atrial contraction (Appleton, 1991; Yamamoto *et al*, 1993).

Pulsed Doppler echocardiographic studies of mitral inflow in humans with HCM have revealed that the most common encountered inflow pattern in this cardiac entity is the abnormal relaxation pattern, which is characterized by decreased early and increased late diastolic velocities and prolonged deceleration and isovolumic contraction times (Takenaka *et al*, 1986; Bryg *et al*, 1987; Maron *et al*, 1987; Spirito and Maron, 1990). However, due to the load dependency of transmitral inflow and its tendency to shift to a "pseudonormal" pattern with increased LA pressures, Doppler mitral inflow indices cannot consistently reflect abnormal relaxation properties and increased intracavitary pressures in HCM (Nishimura *et al*, 1996; Rodriguez *et al*, 1996; Naqvi *et al*, 2001). It has been shown that diastolic filling abnormalities in HCM of humans are independent of the magnitude and extent of hypertrophy, suggesting that the myopathic process responsible for diastolic impairment involves the nonhypertrophied areas of the ventricular wall (Spirito and Maron, 1990).

The influence of left ventricular outflow tract obstruction in mitral inflow in HCM of humans has been investigated in a number of studies. Patients with the non-obstructive form of the disease tended to show more severe alterations in Doppler indices of diastolic function in comparison to patients with obstruction. In particular, patients with non-obstructive hypertrophic cardiomyopathy had a more prolonged isovolumic relaxation time, slower deceleration and lower peak flow velocity during early diastole compared with patients with outflow obstruction (Takenaka *et al*, 1986; Maron *et al*, 1987). The presence of mitral regurgitation in patients with outflow obstruction was proposed as a possible factor, which may increase preload

and therefore can mask abnormal diastolic function in patients with this form of HCM (Takenaka *et al*, 1986; Bryg *et al*, 1987; Maron *et al*, 1987).

B.5. Assessment of pulmonary venous flow by Doppler echocardiography in humans

Pulmonary venous flow (PVF) velocities recorded by transthoracic and transesophageal Doppler echocardiography have been used in addition to mitral inflow velocities to assess systolic and diastolic function of the LA and ventricle. It has been shown by numerous Doppler studies that PVF has three distinct phases (Keren *et al*, 1986; Rossvoll and Hatle, 1993). A systolic forward flow (S wave) caused by LA expansion during ventricular systole, a diastolic forward flow (D wave) occurring after the opening of the mitral valve during the early ventricular filling and a reversal flow (Ar wave) corresponding to atrial contraction. Occasionally, systolic biphasic peaks (S1 and S2) have been recorded in PVF with the S1 representing forward inflow driven by atrial relaxation at the onset of systole and S2 forward flow driven by the apical displacement of the atrioventricular ring (Nishimura *et al*, 1990; Castello *et al*, 1991). Various factors may influence the systolic wave of pulmonary venous flow including left atrial effects (LA relaxation, compliance, pressure, contraction and rhythm) as well as ventricular factors (ventricular systolic function and left ventricular pressures, which partially reflect compliance and relaxation) (Keren *et al*, 1986; Kuecherer *et al*, 1990; Nishimura *et al*, 1990; Klein and Tajik, 1991; Hofmann *et al*, 1995). During systole, the pulmonary systolic flow corresponds to the x-descent of left atrial pressure curve, which is caused by the contribution of atrial relaxation and mitral annulus

displacement (Kuecherer *et al*, 1990; Castello *et al*, 1991). The diastolic wave of pulmonary venous flow appears approximately 50 msec after the mitral peak E wave, when LA pressure decreases and allows the pulmonary veins to fill the LA. The diastolic wave of PVF corresponds to the y-descent of left atrial pressure (Kuecherer *et al*, 1990). During this phase, the atrium is opened to the ventricle, thus, it represents an open conduit between the pulmonary veins and the LV. Therefore, pulmonary veins essentially "see" ventricular pressure and flow is determined by the ventricular-venous gradient (Kuecherer *et al*, 1990). Several studies have demonstrated the close correlation between the mitral E wave and the diastolic pulmonary wave (Kuecherer *et al*, 1990; Nishimura *et al*, 1990; Appleton *et al*, 1993). The Ar wave of PVF occurs during atrial contraction and atrial contractility seems to be the main determinant of it (Kuecherer *et al*, 1990).

It is important to emphasise that LV properties (e.g. compliance, relaxation) significantly influence LA properties; thus, the determinants of PVF must be investigated not as single and independent factors, but as a part of a very complicated and continuously altering mechanism, which partially involves both left ventricular and atrial properties (Kuecherer *et al*, 1990; Appleton *et al*, 1993). Additional factors, such as mitral regurgitation, loading conditions, heart rhythm and age and also body posture and the particular vein, which is sampled, must always be taken into consideration when interpreting PVF patterns (Nishimura *et al*, 1990; Gentile *et al*, 1997; Seiler *et al*, 1998; Izumi *et al*, 1999).

The influence of ageing on PVF indices has been investigated by Doppler echocardiographic studies. It has been shown that peak systolic velocity of PVF in normal humans increases progressively with age, whereas peak diastolic velocity shows an inverse correlation with ageing (Gentile *et al*, 1997). A positive association has been documented between the S/D peak velocity ratio and age in normal individuals ($r = 0.70$, $p < 0.001$) (Gentile *et al*, 1997). Furthermore, the difference between the pulmonary atrial reversal duration and the mitral A wave duration has been shown to be independent of age and therefore a potentially useful index for assessing LV diastolic properties and pressures even in elderly humans (Klein *et al*, 1998). It is speculated that age related changes in the LV compliance do not significantly influence LVEDP sufficiently to influence the duration of either the Ar or of the A wave of mitral inflow (Klein *et al*, 1998).

Several studies have tried to assess the haemodynamic determinants of PVF and their relation with LV and LA functional properties in various cardiac diseases. Combined haemodynamic and Doppler echocardiographic studies have consistently documented a strong negative association between systolic indices of PVF and LA or pre-A LV pressure (pressure before atrial contraction). A decreased systolic fraction (the ratio of systolic to the sum of systolic and diastolic velocity integral) or systolic VTI, and an S/D ratio < 1 have all been shown to associate negatively with LA or pre-A LV pressure and to predict elevated LA pressures in the disease state with high accuracy (Kuecherer *et al*, 1990; Appleton *et al*, 1993; Rossvoll and Hatle, 1993; Hofmann *et al*, 1995). The time between the Q deflection of the ECG to the occurrence of the maximal peak velocity during either the systolic or the diastolic

phase of PVF has been shown to be the strongest predictor for elevated LA pressures (Hofmann *et al*, 1995). In the diseased state, the reduction of systolic forward flow in pulmonary veins reflects mainly the decreased LA compliance induced by the elevated LA pressure (Kuecherer *et al*, 1990). This, of course, is the consequence of elevated LV filling pressures and it is supported by the strong inverse association between the pre-A LV pressure and systolic PVF indices (Rossvoll and Hatle, 1993). Other factors that may influence the degree of systolic flow in pulmonary veins are atrial relaxation, left ventricular systolic function (suction by the downward motion of the mitral ring during ventricular contraction) and mitral regurgitation.

The pulmonary Ar wave tends to be influenced mainly from changes in the LV pressure due to atrial contraction (LVA). Several studies have shown that the duration of Ar correlates significantly with the LVA pressure (Appleton *et al*, 1993; Rossvoll and Hatle, 1993). The atrial pressure waveform during atrial systole is probably the main determinant of the velocity and duration of reverse flow (Appleton *et al*, 1993). Atrial pressure generation during atrial systole is dependent on atrial preload, contractility and left ventricular properties.

The difference in the duration between the Ar and the mitral inflow wave has been used widely as an noninvasive index for the assessment of LV filling pressures. A longer Ar duration than that of the mitral A wave has been shown accurately to predict LVEDP and it has been suggested as an indicator of decreased LV compliance (Appleton *et al*, 1993; Rossvoll and Hatle, 1993). Matsuda and colleagues investigated the influence of the increase in LVEDP (induced by

angiotensin infusion in patients and experimental animals), in the relation between LV and LA pressures during atrial contraction (Matsuda *et al*, 1990). They showed that when LV pressure increases the atrial pressure curve becomes biphasic. The first peak preceded the pressure increase in the ventricle. The second and largest peak occurred at the time of maximal ventricular A wave pressure. This second peak was believed to be a passive reflection of an increased pressure build up within a stiff ventricle, superimposed on the decay of atrial contraction. It was suggested that the mitral A wave is due to the first atrial pressure peak that generates a positive atrioventricular pressure gradient. When LV chamber compliance is reduced, LV pressure at atrial contraction increases at a steeper and faster rate than that of LA pressure. This results in a shorter duration of positive transmitral pressure gradient at left atrial contraction and an abrupt termination of transmitral flow (shorter A wave duration). In this situation maximal atrial pressure appears delayed at the second peak, which means that reverse pulmonary venous flow continues for longer (longer Ar duration). Similar findings have been reported from combined hemodynamic and Doppler echocardiographic studies in humans with various diseases. In the presence of moderate decreases in ventricular compliance, the Ar duration increases, whereas the duration of mitral A wave remains unchanged. With severe deterioration of ventricular compliance and markedly elevated filling pressures at advanced stages of the disease process, the Ar duration does not increase further, whereas the A duration reduces (Yamamoto *et al*, 1997; Abdalla *et al*, 1998).

Ito and colleagues (1996) compared the velocity of Ar and that of A mitral wave between patients with HCM and DCM. They showed that the level of atrial

contractility plays a significant role in determining the amplitude of both waves. In this study, both the DCM and HCM groups were divided into two subgroups with a normal PCWP (<15 mm Hg) or an elevated PCWP (>15 mm Hg). There was no significant difference in Ar velocity between the DCM subgroups, but in the HCM group, Ar was higher in patients with elevated PCWP than in those with a normal PCWP. The velocity of A mitral wave was significant lower in the DCM subgroup with elevated PCWP when compared to that of the corresponding HCM subgroup. Furthermore, in the DCM group, left atrial systolic function was depressed with an elevated PCWP, as shown by the reduction in the LA appendage emptying flow velocity and in LA appendage ejection fraction. In contrast, LA systolic function was preserved in the HCM group and was not influenced by the severity of heart failure.

The above studies reveal that both the amplitude and duration of PVF Ar wave are influenced by LV filling pressure, provided LA contractility is preserved at a level, which allows LA to oppose a proportional and opposite force to the elevated LA pressure. When LA contractility is preserved, then an elevation in LV filling pressures not only delays the time that maximum LA pressure occurs, leading to prolonged atrial contraction, but also increases the contractile force of the LA. The result is an increase in the duration and in the amplitude of Ar wave. Moreover, when the LA loses its ability to contract properly, then its response to increased LV filling pressures is minimized. In this situation even a very high LV pre-A pressure does not result in further increases of PVF Ar duration. Similarly, under these circumstances, the contribution of LA contraction in the generation of the A mitral wave is very low, therefore the duration and the amplitude of this wave decreases. In the above

situation a restrictive transmitral flow pattern is predominantly present. When LA contractility is not impaired, the transmitral flow tends to show an E and A reversal pattern. Whether the impairment of LA contractility is due to an intrinsic myopathic process or to prolonged elevation in left atrial preload (an overstretched left atrium operating on the descending part of its Frank-Starling curve) or both, is debatable.

Many studies have shown that patients with high pre-A pressure or PCWP tend to have increased mitral E wave peak velocity, reduced A wave velocity, increased E/A ratio and a shorter deceleration time of early mitral flow in comparison to patients with normal pre-A pressure (Appleton *et al*, 1993; Rossvoll and Hatle, 1993; Giannuzzi *et al*, 1994). Pre-A pressure seems to be the main determinant of the E/A ratio, whereas LVA and LVEDP show a very weak correlation with it (Rossvoll and Hatle, 1993). In one study a deceleration time of E wave < 120 ms was the best cut off point in predicting PCWP > 12 mm Hg with high sensitivity and specificity. In addition, the value of 153 ms deceleration time was the best cut off point in predicting PCWP < 12 mm Hg with high accuracy. Consequently, the level of pre-A pressure does not only influence the duration of the A mitral wave (Rossvoll and Hatle, 1993), but also the amplitude of E/A ratio and A mitral wave as well. High level of LV pre-A pressure seem to be the most significant determinant of the "so-called" pseudonormal mitral filling pattern, in which, although abnormal relaxation of the LV may be present, the mitral inflow velocity pattern is shifted to a normal pattern, in which the amplitude of the E-wave increases and the amplitude of the A wave decreases.

In patients with HCM, normal or slightly elevated LV filling pressures lead to elevated systolic and decreased diastolic PVF velocities (Ito *et al*, 1996; Oki *et al*, 1996). When LV filling pressures increase further, the systolic and diastolic waves become relatively equal, with the S wave tending to decrease and the D wave to increase. The above change in the amplitude of the S and D wave is accompanied by a similar change in the amplitude of the E and A mitral waves, which tends to result in the so-called pseudonormal pattern. It has been shown that a very strong positive association exists between the A/E ratio of mitral inflow and the S/D of PVF in various cardiac diseases including HCM (Rossvoll and Hatle, 1993; Ito *et al*, 1996; Oki *et al*, 1996). This further emphasizes the potential of PVF in unmasking pseudonormal mitral inflow patterns in the diseased state. High mitral A wave and PVF systolic velocities reflect slight elevation in LV filling pressures and especially of pre-A LV pressure, which seems to be the main determinant of these waves. During the early stages of impairment of LV relaxation, a slightly elevated pre-A LV pressure forces the LA to contact stronger (increased mitral A and Ar wave) without significantly affecting its compliance. An increase in the PVF S wave at this stage indicates that the LA expands more in order to contract more vigorously (Frank-Starling law). As the pre-A pressure increases further, left atrial compliance decreases and the mitral inflow velocities swift to a pseudonormal pattern, whereas the PVF shows a gradual reduction in the S/D ratio.

Doppler echocardiographic studies of PVF in normal dogs have revealed similar findings with those reported in healthy humans (Schober *et al*, 1998; Schober and Luis Fuentes, 2001). Interestingly, in a big group of normal dogs of various breeds, it

has been shown that the A dur/Ar dur was independent of age, suggesting that it could be used as an alternative tool in the noninvasive assessment of LV filling pressures in the diseased state (Schober and Luis Fuentes, 2001).

B.6. Doppler echocardiography in cats

Despite the wide application of Doppler echocardiography in the assessment of LV diastolic properties in humans, Doppler echocardiographic studies in normal cats and cats with HCM are limited. In one of the few of them, Santilli and Bussadori (1998) investigated the mitral inflow and pulmonary venous flow characteristics in 20 unsedated, normal cats. They showed that age was a significant independent predictor for many Doppler filling indices, with the late diastolic mitral inflow wave and the peak systolic velocity (S) of the pulmonary venous flow showing a positive association with age, reflecting changes in diastolic function associated with aging. Investigation of diastolic LV function by Doppler echocardiography in cats with HCM has shown that asymptomatic animals exhibit the typical abnormal relaxation mitral inflow pattern (E/A > 1) (Santilli 1996, Bright 1999). In these animals, pulmonary venous flow presents an increase of the systolic velocity, a decrease of the diastolic velocity (D) with an elevation of S/D ratio and of systolic fraction (S VTI/[S VTI+D VTI]). Prolonged isovolumic relaxation time has been documented in cats with HCM indicating impaired diastolic properties (Santilli 1996, Bright 1999). A confounding effect in the recording of mitral inflow velocities by Doppler echocardiography in cats, arises from the high heart rates of this species which can result in summated E and A waves and therefore can make it difficult to interpret the recordings (Santilli and Bussadori, 1998). This problem is exacerbated in affected animals, which normally have high heart rates due to increased sympathetic drive.

Pulmonary venous flow in cats is not affected by summation effects due to high heart rates and therefore its assessment with Doppler echocardiography can unmask abnormal relaxation properties in cats with HCM.

In the presence of LVOT obstruction induced by SAM of the anterior MV leaflet, continuous Doppler echocardiography may reveal increased flow velocities in the left ventricular out-flow tract. The shape of Doppler wave is characteristic of dynamic subaortic stenosis, showing slow increase in early systole and abrupt rise in mid systole (Fox, 1998; Kittleson, 1999). A similar aortic velocity pattern can be recorded in the right ventricular outflow tract when dynamic right ventricular obstruction is present (Rishniw and Thomas, 2002).

B.7. Colour M-mode Doppler echocardiography

Colour M-mode Doppler echocardiography has been used widely in the evaluation of LV diastolic properties. In contrast to pulsed Doppler echocardiography, which provides the estimation of blood flow velocities at a single location, colour M-mode echocardiography allows evaluation of the temporal and also spatial aspects of LV filling (Moller *et al*, 2000). Colour M-mode recordings are obtained using the 4 chamber apical view, which allows the parallel placement of the ultrasonic beam to the LV diastolic flow and its investigation from mitral valve plane to LV apex. A typical colour M-mode recording displays a first propagating wave of blood flow, which corresponds to early ventricular filling and a second propagating wave, which corresponds to atrial contraction. Several clinical trials have been carried out using manual or semiautomatic indices derived by colour M-mode echocardiography.

Jacobs and colleagues (1990) firstly investigated the time delay of propagating flow (time required for blood to travel from mitral valve to LV apex). Later on, Brun and colleagues (1992) measured the velocity of flow propagation (FPV) as the slope of the flow wave front (transition from no colour to colour) during early ventricular filling. Using a different approach, Stugaard and colleagues (1993) calculated the time delay between occurrence of peak velocity in the apical region and the mitral valve plane. Others calculated FPV as the slope of the first aliasing isovelocity of the early propagating wave. Using this method, the velocity scale is usually adjusted to the 75% of maximum E transmitral velocity until an aliased core is achieved in the early propagating wave (Garcia *et al*, 1999; Moller *et al*, 2000).

In the 1980's, Brutsaert (1987) proposed that nonuniformity of relaxation, a time and space dependent process, modulates LV relaxation, along with loading conditions and rate of relaxation, under normal circumstances. Later studies showed that, in the normal LV, the presence of intraventricular pressure gradients is the main driving force for the early diastolic ventricular filling (Courtois *et al*, 1988). It is now accepted that any alteration in the physiologic nonuniformity of LV relaxation or its rate disrupts the normal intraventricular pressure gradient between apex and base, consequently leading to a lower flow propagation velocity during early diastole (Brun *et al*, 1992; Duval-Moulin *et al*, 1997). Several different studies have shown that FPV is reduced in the diseased myocardium irrespective of the underlying cause (Brun *et al*, 1992; Takatsuji *et al*, 1996; Duval-Moulin *et al*, 1997; Steine *et al*, 1998). In a study with patients with various cardiac diseases (dilated cardiomyopathy, ischaemic myocardial disease, hypertrophic cardiomyopathy,

systemic hypertension or aortic valve disease), FPV was found to be reduced in affected individuals when compared with that from normal subjects (Brun *et al*, 1992). FVP has been shown to correlate inversely with age in normal individuals, reflecting the reduced diastolic function associated with aging (Brun *et al*, 1992; Mego *et al*, 1998).

Invasive haemodynamic studies have shown that FPV and time delay of maximum peak velocity between mitral valve plane and apex correlate strongly in an inverse manner with the time constant of the isovolumetric relaxation (τ), providing evidence that they may be used as alternative tools for noninvasively assessing LV diastolic properties (Brun *et al*, 1992; Stugaard *et al*, 1994; Takatsuji *et al*, 1996; Garcia *et al*, 2000). Moreover, it has been proven that a low FPV is always accompanied by an increase in left ventricular -dP/dt and in minimum LV pressure following impaired diastolic function (Stugaard *et al*, 1994; Takatsuji *et al*, 1996; Duval-Moulin *et al*, 1997). Other studies have shown that FVP is independent from changes in preload, in contrast to mitral inflow pattern, which is subject to loading alterations and therefore can mask impaired LV properties (Garcia *et al*, 1999; Garcia *et al*, 2000; Moller *et al*, 2000). Moller and colleagues (2000) showed that changes in preload induced by the Valsalva maneuver, passive leg lifting and after administration of nitroglycerine in healthy volunteers and patients with previous myocardial infarction, caused no significant changes in FVP, whereas peak E wave of mitral inflow, E/A ratio and E deceleration time were significantly altered. Similar findings were found in Garcias' studies (1999 and 2000). The finding that FPV is independent from changes in loading is reflected in the fact that, although it correlates positively with peak early

diastolic flow and the E/A ratio in normal subjects, this correlation is absent in affected individuals (Brun *et al*, 1992; Takatsuji *et al*, 1996; Mego *et al*, 1998). This finding is mainly attributed to the pseudonormalized transmitral inflow pattern of patients with advanced stage of disease, due to significantly elevated LA pressures. According to Garcia and colleagues (1998) the discrepancy between high peak E mitral inflow and low FPV in diseased left ventricles is probably explained by vortex formation, where the velocity (E) in the centre the vortex ring exceeds the velocity at which the whole ring (FPV) travels. Using an experimental filling model of left ventricle, Steen and colleagues (1994) suggested that vorticity is generated due to shear stresses between the inflowing blood and the blood in the ventricle, because of the difference in axial velocity. The close correlation between E and FPV in normal subjects and the lack of their correlation in patients with LV dysfunction probably reflects the fact that FPV is less affected by compliance and LA pressure than peak early mitral inflow velocity (Moller *et al*, 2000). The preload independence of FPV renders it a more sensitive and accurate means of assessing LV diastolic properties when compared to pulsed Doppler echocardiography.

A number of studies have investigated the potential of FPV to predict LA and pulmonary capillary wedge pressure respectively (Garcia *et al*, 1997; Gonzalez-Vilchez *et al*, 1999). In a study of patients with variable cardiac diseases (45 patients; 22 acute ischemic event, 5 DCM, 3 aortic valve disease, the rest had variable conditions which required cardiac catheterization) a combination of FPV and peak early mitral inflow velocity was shown to be highly predictive of LA pressure according to the equation:

$LAP = 5.27*(E/FPV) + 4.6$ mm Hg ($r = 0.8$, $p < 0.001$, $SE = 3.1$ mm Hg)

The combination of FPV and isovolumic relaxation time correlated strongly with pulmonary capillary wedge pressure in another study:

$PCWP = 4.5*(10^3/[2IVRT + FPV]) - 9$ ($r = 0.89$, $p < 0{,}001$, $SE = 3.3$ mm Hg)

and predicted capillary wedge pressure > 15 mm Hg with a sensitivity of 90% and specificity of 100%. In a group of 35 patients with HCM, Nagueh and colleagues (1999) showed that E/FPV ratio correlated positively with pre-A pressure (LV pressure prior to atrial contraction) ($r = 0.67$, SEE = 4 mm Hg) and that in patients with serial measurements pre-A pressure changes correlated quite well with changes in E/FPV ($r = 0.68$, $p < 0.01$). The ability of E/FPV to predict pre-A pressure was strong ($r = 0.76$). In an effort to establish predictors of death or readmission due to worsening of heart failure in patients with previous myocardial infarction, Moller and colleagues (2001) showed that one-year event free survival was 97% and 33% in patients with a ratio of E/FPV < 1.5 and ≥1.5 respectively. In the same study the positive predictive value of E/FPV ≥1.5 to identify patients with Killip class > II during hospitalization was 90% and the negative predictive value was 92%.

The FPV was found to correlate significantly with tau in normal cats showing promise for the non-invasive quantification of LV diastolic function in feline cardiomyopathies (Schober *et al*, 2003).

AN ECHOCARDIOGRAPHIC / DOPPLER EVALUATION OF HYPERTROPHIC CARDIOMYOPATHY IN CATS

B.8. Aims

To define echocardiographic / Doppler criteria of normality in healthy cats, particularly pertaining to left ventricular diastolic function and to investigate the echocardiographic / Doppler abnormalities associated with feline Hypertrophic cardiomyopathy.

B.9. Criteria for selection

Amenable cats owned by the staff and students of the Royal (Dick) School of Veterinary Studies R(D)SVS, with no clinical abnormalities indicating cardiac disease were selected for further investigation in order to comprise the normal group of this study. Cases for the affected group were selected from cats presented to the cardiopulmonary service at the R(D)SVS with signs of cardiac disease or where incidental murmurs, gallops or arrhythmias were identified either from the referring veterinary surgeon or the clinical staff of the R(D)SVS.

B.10. Examination of individual cats

A detailed history was obtained for every animal. A thorough clinical examination was performed and details were kept in the animal's records. Animals were weighed and their weight was recorded for analysis purposes. All normal cats above seven years of age and all affected animals underwent haematology and biochemical testing. Cats with azotaemia and elevated total thyroxine hormone (T4) were

excluded from the study. When necessary a urine sample was taken by cystocentisis for urine examination to assist assessment of renal function. Systolic blood pressure was recorded using the Doppler technique (Parks medical electronics, Aloha, Oregon, USA). Blood pressure measurements were obtained from the coccygeal artery using a purpose designed probe and an inflatable cuff, which was placed on the base of the tail. The systolic blood pressure was calculated after averaging several consecutive pressure measurements. A systolic blood pressure of < 180 mm Hg was considered normal. Hypertensive cats were excluded from further evaluation. All affected animals underwent an ECG examination using a six-lead electrocardiogram (Schiller; Switzerland).

B.11. Study group

The study population comprised 24 normal cats, which were pets of staff and students of the R(D)SVS and 23 cats with HCM, which were referred to the cardiopulmonary service of the R(D)SVS for cardiac screening. Diagnosis of HCM was done on the basis of LV thickness ≥6 mm, at any part of the LV wall, on 2D or M-mode echocardiography in the absence of volume overload (no obvious valvular abnormalities) and systemic diseases known to cause LV hypertrophy. All affected animals were in sinus rhythm except for one, which had atrial fibrillation. Nineteen animals with HCM were asymptomatic and one of them was receiving β-blockers. Four affected animals were in congestive heart failure at the time of evaluation and were treated with a combination of diuretics, ACE inhibitors with or with out β-blockers. No drug withdrawal was done prior to assessment. All animals were unsedated.

B.12. Conventional Echocardiographic/Doppler examination

B.12.1. Patient preparation

The hair coat was clipped over the site of precordial impulse on the left and right hemithoraces.

Animals were scanned unsedated and manually restrained in lateral recumbency on a purpose-designed table, which allowed placement of the transducer on the dependent part of the thorax from below through a hole. A simultaneous ECG was recorded (lead II) using adhesive electrodes, which were attached to the main pads of the feet and secured with a tape.

B.12.2. Ultrasound machine and set up

Conventional echocardiographic and Doppler examination was carried out in the cardiopulmonary service of the Royal (Dick) School of Veterinary Studies. Echocardiographic examination was performed using an Esaote SIM 7000 Challenge ultrasound system (Esaote Biomedica, Firenze, Italy) with a 7.5 MHz phased array transducer. Images were recorded onto S-VHS videotapes by a videocassette recorder (SV0-9500MDP; Sony Corporation, Japan).

The sector width and depth setting were adjusted to include the entire heart in the screen and to maximize the cardiac image. Overall gain and time gain compensation controls were set to optimize the image quality. Colour flow Doppler echocardiography (CFDE) provided information about the direction of motion of the blood flow. Blood flow moving towards and away the transducer was colour coded, red and blue, respectively, and turbulent flow was encoded green (velocity-variance

map). During CFDE, the colour sector was kept as small as a possible to increase the frame rate and consequently the quality of the colour signal. The focus of the ultrasonic beam was adjusted to the level of the region of interest. Colour gain was adjusted to achieve optimal CFDE and avoid over-gaining. M-mode measurements were always guided by 2D images. The maximum M-mode sweep speed was used every time. During pulsed Doppler echocardiography, a sample volume (2 or 4 mm) was placed in the region of interest and the ultrasonic beam was kept as parallel as possible to the blood flow. Gain and filter settings were adjusted to achieve optimal spectral signal with clarity of envelope contour. Velocity scale and baseline position were set to achieve maximum envelope size. All Doppler echocardiographic measurements were recorded using the maximum available sweep speed (100 mm/sec). Continuous wave Doppler echocardiography was used when recording of high blood flow velocities was required.

B.12.3. Recorded images

Using the right parasternal long axis view the LV and LA areas were maximized and several cardiac cycles were recorded. The smallest sector width, which allowed visualization of the entire LV and LA, was used. Qualitative assessment of LV myocardial motion was performed. LV wall was qualitatively assessed to identify areas with segmental hypertrophy. The interventricular and interatrial septae were scrutinized. The appearance and motion of mitral and tricuspid valve leaflets were assessed carefully. CFDE was used to record blood flow through the mitral valve. On the long axis LV outflow view assessment of the appearance and motion of the aortic leaflets was performed. Using this view, CFDE was used to record simultaneously blood flow through the mitral valve and the left ventricular outflow tract. The

ultrasound beam was placed perpendicular to the left ventricular axis to achieve a horizontal image.

A right parasternal short axis view was then obtained by rotating the transducer 90^{o} anticlockwise. The sector width was reduced to improve the image resolution. A base to apex sweep was performed by angling the transducer to record LV thickness at different levels. Once the LV cavity was symmetrical and rounded the M-mode cursor was carefully positioned through the centre of the LV at chordae tendineae level. An M-mode measurement was recorded. Angling the transducer cranio-dorsally, a short axis view at mitral valve level was obtained ensuring that both the anterior and posterior leaflets of the mitral valve could be visualized. An M-mode recording at this level was recorded to document SAM if present and to measure the mitral E point to septal separation (EPSS). Further cranio-dorsal angling of the transducer allowed recording of the short axis view at aortic valve level. Care was taken to ensure that aortic valve leaflets were always included in the image and also that the left atrium and auricle could be clearly seen (permitting 2D measurement of aorta and LA during diastole). The M-mode cursor was then positioned through the aortic root and the left atrium and an M-mode was recorded. Slight anticlockwise rotation of the transducer disclosed the right ventricular outflow tract and the pulmonary artery. CFDE of blood flow was assessed in these areas. Once the ultrasonic beam was parallel to the blood flow in the pulmonary trunk, the pulsed wave Doppler sample volume was placed just beyond the pulmonic valve. Spectral Doppler flow recording of the blood flow in the pulmonary artery was then performed.

With the animal in left lateral recumbency, a 4-chamber apical view was obtained. CFDE of blood flow through the mitral valve was recorded. The sample volume was placed on the tips of the mitral valve leaflets to record mitral inflow. By positioning the ultrasonic beam parallel to mitral inflow and retaining the CFDE on, the M-mode was activated to record the colour flow propagation of mitral inflow. Pulmonary venous flow was recorded by placing the sample volume (2 to 4 mm) of spectral Doppler in the lateral pulmonary vein. Care was taken to avoid sampling the pulmonary vein wall or placing the sample volume in the left atrium. To achieve optimal velocity signal, gain was maximized and filter was set at the lowest possible level. While in the 4-chamber apical view, the ultrasonic cursor was placed parallel to the lateral and septal corners of the mitral annulus and an M-mode measurement was recorded. From the left parasternal apical four chamber view, spectral and CFDE recordings of the tricuspid inflow were obtained.

Rotating the transducer slightly anticlockwise the left ventricular outflow tract was revealed, providing a 5-chamber apical view. CFDE was then used to record simultaneously blood velocity in the left ventricular outflow tract (blue colour map) and mitral inflow (red colour map). The ultrasonic beam was placed on the interface of the two flows as they were defined by the 2 different colour maps. Continuous Doppler echocardiography was then used to record aortic and mitral inflow simultaneously and care was taken to ensure the optimal delineation of the end of outflow envelope and the beginning of the inflow trace, which defined the isovolumic relaxation time.

In the 5-chamber apical view placement of the sample volume just beyond the aortic leaflets allowed the measurement of aortic velocity. When left ventricular outflow tract obstruction was present, continuous Doppler echocardiography was used to record the aortic velocity. In these cases, care was taken to avoid measuring the mitral regurgitation jet.

B.13. Analysis of echocardiographic measurements

B.13.1. General methods

Analysis of echocardiographic measurements was done off-line, from the videocassette recordings. Diastolic events were analyzed at end diastole, which was defined as the start of the QRS complex of the ECG. Systolic events were analyzed at end systole, at the end part of the T wave of the ECG. Values from six consecutive cardiac cycles were measured for each variable and their mean was calculated and used for further analysis. In cases of atrial fibrillation, values from 12 cardiac cycles were averaged. Events related to supraventricular or ventricular premature complexes were ignored.

Colour flow Doppler echocardiography was performed from the right and left parasternal views interrogating all valves and observation was made of valvular morphology, any incompetence and LVOT turbulence. Valvular regurgitation was subjectively graded as 1+ to 4+.

B.13.2. Right parasternal view measurements

B.13.2.1. Left atrial parameters

Left atrial area was calculated on the right-parasternal-four-chamber view by tracing the internal perimeter of the left atrium as described previously by O' Grady and colleagues (1986). The LA internal diameter was calculated on the same view in the middle of the left atrium and parallel to the mitral valve. LA area and diameter were measured in both diastole and systole. The fractional shortening of the LA was defined as the ratio of the difference between the LA systolic and diastolic diameter to the LA systolic diameter.

B.13.2.2. Left ventricular M-mode

LV M-mode measurements were carried out using the leading edge-leading edge method (Sahn *et al*, 1978). Diastolic measurements were performed on the Q wave of the ECG and systolic when minimum LV dimensions were achieved. The right ventricular diastolic diameter was measured, but because of the suboptimal quality of the near field, this measurement was unreliable and therefore it was excluded from further analysis. The systolic and diastolic thickness of the IVS and the LVPW and also the LV dimensions were measured. The fractional shortening (the ratio of the difference between end diastolic and systolic LV diameter to the LV diastolic diameter) was computed automatically by the software.

B.13.2.3. Assessment of hypertrophy

Hypertrophy was considered asymmetrical when the difference in M-mode diastolic thickness between the IVS and the LVPW was > 1.3 and symmetric when it was <

1.3 (Maron *et al*, 1981a). When both the IVS and the LVPW were hypertrophied (end diastolic thickness > 6 mm) then the hypertrophy was considered diffuse. When the hypertrophy involved only one myocardial segment then it was considered as segmental.

When segmental hypertrophy was suspected, measurement of diastolic thickness of the interrogated myocardial segment was performed on 2D images (rpla and rpsa views). Mean regional thickness was the average of at least 6 cardiac cycles. Measurement of regional thickness was performed only for diagnostic purposes (differentiating normal from affected cats) and not for assessing the magnitude of thickness of the different myocardial segments of the LV.

B.13.2.4. Mitral M-mode

The E point to septal separation was measured from the M-mode at mitral valve level. The observation of SAM was made on this view.

B.13.2.5. Left atrial and aortic diameter on 2D mode

The left atrial and aortic internal diameters were measured on the short axis view at aortic valve level as described previously by Häggström and colleagues (1994). The left atrial to aortic diameter ratio was than calculated.

B.13.2.6. Aortic M-mode

An M-mode of the aorta and the LA was obtained on the short axis view at aortic valve level. The leading edge-leading edge method was used to measure the LA and

aortic dimensions (Sahn *et al*, 1978). The aortic root was measured at the end of diastole (Q wave of the ECG) and the LA diameter when maximum dimension was achieved during end systole. The M-mode LA to aortic diameter was then calculated.

B.13.2.7. Pulmonary artery

The peak pulmonic velocity was measured. The right ventricular pre-ejection period was calculated from the Q wave of the ECG to the onset of the pulmonic velocity. The right ventricular ejection time was measured from the beginning of the pulmonic velocity to its end. The ratio of the pre-ejection period to the ejection time then was calculated.

B.13.3. Left parasternal view measurements

B.13.3.1. Mitral inflow

Peak mitral early and late diastolic (E and A wave) velocities were recorded. The ratio of early to late diastolic mitral inflow velocity was determined. The velocity time integral of early and late diastolic waves was calculated by tracing the modal velocity along the envelopes, but only when full separation was present (Quinones *et al*, 2002). The acceleration and deceleration time of early diastolic mitral inflow wave were assessed by recording the time from the onset of E to peak E and from the peak E to the intersection of E with the baseline respectively. E deceleration time was measured only when the two diastolic waves were fully separated. Early and late diastolic duration were determined by the duration of E and A waves, respectively, when there was no summation effect.

B.13.3.2. Colour M-mode of the mitral inflow

Flow propagation velocity was determined as the ratio of the distance covered by the wave-front of the early propagating wave, from the mitral valve plane to as much possible within the LV in certain time, to the time needed to cover this distance (Figure B1). Where a summating propagating flow wave was identified, the flow propagation velocity was determined using the wave front of the summating wave. To identify the wave front of the propagating wave, the transition from colour to no colour method, described by Brun (1992), was used.

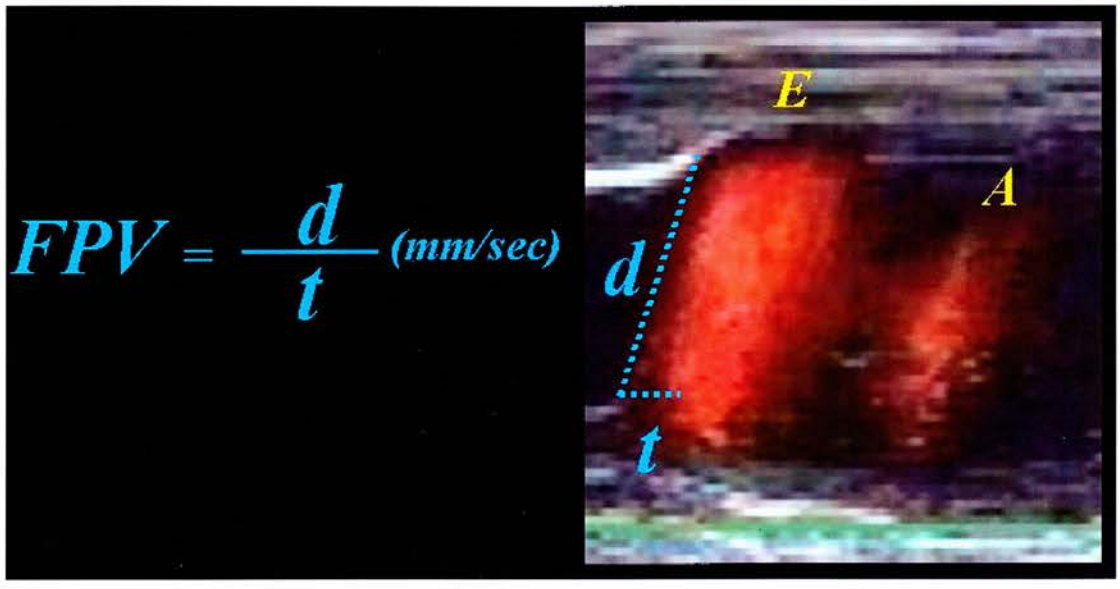

Figure B 1. *Flow propagation velocity was determined as the ratio of the distance (d) covered by the wave-front of the early propagating wave, from the mitral valve plane to as long as possible within the LV in a time (t), to the time (t) needed to cover this distance.*

B.13.3.3. Isovolumic relaxation time

When good quality spectral signals of aortic flow and of mitral inflow were obtained then the time from the end of the aortic envelope to the beginning of the inflow envelope was defined as the isovolumic relaxation time.

B.13.3.4. Aortic flow

The peak aortic velocity was recorded. The velocity time integral of the aortic flow was calculated by tracing the modal velocity along the outflow envelope (Quinones *et al*, 2002). The pre-ejection period of the LV was defined as the time interval from the Q wave of the ECG to the beginning of the aortic flow. LV ejection time was determined by the duration of the outflow envelope. The ratio of the LV pre-ejection period to ejection time then was calculated. Acceleration time of the aortic velocity was defined as the time from the onset of aortic flow to its maximum velocity.

B.13.3.5. Pulmonary venous flow

The peak first (S1), second (S2) and combined (S12) systolic velocities and also the diastolic (D) and atrial reversal (Ar) velocities were recorded in the PVF pulsed wave Doppler spectral signal. The ratio of maximal peak systolic (Smax) to diastolic velocity (S/D) was calculated. To assess the velocity time integral of the systolic, diastolic and atrial reversal waves of the PVF tracing, along their modal velocity was performed. Where the systolic and the diastolic waves were merged, a perpendicular line was drawn to baseline to define their borders. The intersection point on the baseline was used to define the duration of the systolic and the diastolic waves. The duration of atrial reversal wave was determined by the duration of the corresponding

envelope. The time from the Q wave of the ECG to the peak systolic (Q-S), the diastolic (Q-D) and the atrial reversal velocities (Q-Ar), were recorded. The time from the Q wave of the ECG to the beginning of the systolic wave (Q-bS) was also recorded. The ratio of the duration of the late diastolic wave of mitral inflow to the duration of the atrial reversal of the pulmonary venous flow (Adur/Ardur) was calculated.

B.13.3.6. Mitral annulus motion

The septal (MAM sep) and lateral (MAM lat) mitral annulus motion was calculated as the maximum excursion between end diastole and systole.

B.14. Statistical analysis

Statistical analysis was carried out using Genstat^{TM} 5 (release 3, Rothmsted experimental station, U.K) and SigmaStat (V2.03; SPSS Inc 1997). Values are expressed as the mean ± standard deviation or median. Analysis of covariance was used to control conventional echocardiographic indices for RR interval, age, weight and sex. A t-test was used to compare values between the two groups. A t-test was used to compare age, weight and heart rate between the two groups and a Chi-square or a Fisher's Exact test to compare the number of male and female cats within the groups. Stepwise regression was carried out to assess the influence of RR interval, age, weight and sex on echocardiographic indices. Linear and multiple linear regression analysis were used to define the association between echocardiographic indices and independent predictors. For the purposes of regression analysis, male cats were defined as number 1 and female cats as number 2. A t test or a Mann-Whitney

Rank Sum test was used to compare echocardiographic variables between male and female cats within the same group when sex was found to be a significant predictor in linear or multiple linear regression analysis. A Kolmogorov-Smirnov test was used to determine whether data were normally distributed. To achieve normality of the non-normally distributed variables logarithmic transformation was used. A p value of < 0.05 was considered statistically significant.

B.15. Results

B.15.1. Population details

Normal cats (n=24) of the following breeds were included in the study: 20 Domestic Short-haired, 1 Domestic Semilong-haired, 1 Maine-coon, 1 Abyssinian, 1 Siamese (12 female and 12 male neutered cats). Mean (± sd) for body weight was: 4.52 (± 0.8) Kg. All normal cats were in good body condition (none were obese or excessively thin). Their mean (± sd) age was 6.2 (± 3.5) years, with ages ranging from 10 months to 14 years. The mean (± sd) heart rate measured by the RR interval recorded during the acquisition of images from at least 6 cardiac cycles was 150 (± 26) bpm. Affected cats (n=23) consisted of the following breeds (21 Domestic Short-haired and 2 Persian; 3 female and 20 male neutered cats) had a mean (± sd) of body weight of 5.2 (± 1) Kg, mean (± sd) of age 7.1 (± 2.8) years (range: 1 to 12 years) and their heart rate was 158 ± 35 bpm. HCM cats had greater weight than normal animals ($p<0.05$). There was no statistical difference in age and heart rate between the two groups. Male and female cats were equally represented in the normal group, but male cats were over-represented in the HCM group ($p<0.001$).

B.15.2. 2D/Doppler echocardiographic variables

Results for 2D/Doppler echocardiographic parameters from normal and HCM cats are shown in Tables App.B1 and App.B2, Appendix B1.

B.15.2.1. 2D parameters

The 2D echocardiographic parameters for the LA and the LV are shown in Table B1. LA area (mm^2) during diastole and systole was significantly greater in the HCM group compared to that in the normal group (223.6 ± 190 vs 105.8 ± 28, $p<0.05$ and 299 ± 183 vr 164 ± 47.5, $p<0.05$, respectively). Similarly, LA distance (mm), as measured in the right parasternal long axis view, during diastole and systole was greater in the HCM than in the normal group (13.8 ± 6.1 vs 9.3 ± 1.5, $p<0.05$ and 16.2 ± 5.5 vs 12.5 ± 2.3, $p<0.05$, respectively). There was no significant difference in the LA fractional shortening between the two groups. The LA diastolic length (mm) in the short axis view at aortic valve level was significantly greater in affected than in normal animals (15.3 ± 4.6 vs 11.2 ± 1.4, $p<0.01$). No differences were recorded in the diameter of aorta between the two groups at this level. The ratio of left atrial to aortic diameter was higher in HCM cats compared to that in normals (1.9 ± 0.7 vs 1.4 ± 0.2, $p<0.05$). With the exception of LA distance during systole, differences in the 2D echocardiographic parameters persisted between affected and normal cats even when animals with CHF were excluded from the analysis.

Table B 1. 2D echocardiographic parameters

?D measurements	Normal (n)	HCM (n)	p
LA area d (mm^2)	105.8 ± 28 (20)	223.6 ± 190 (21)	<0.05
LA dist d (mm)	9.5 ± 1.5 (20)	13.8 ± 6.1 (21)	<0.05
LA area s (mm^2)	164.8 ± 47.5 (20)	299 ± 183 (21)	<0.05
LA dist s (mm)	12.5 ± 2.3 (20)	16.2 ± 5.5 (21)	<0.05
LA FS%	22.4 ± 13.4 (20)	17.1 ± 9.8 (21)	ns
LA length d (mm)	11.2 ± 1.4 (21)	15.3 ± 4.6 (21)	<0.01
Ao diam d (mm)	8 ± 0.8 (21)	8.3 ± 0.9 (21)	ns
LAd/Aod	1.4 ± 0.2 (21)	1.9 ± 0.7 (21)	<0.05

B.15.2.2. M-mode parameters

M-mode echocardiographic parameters are given in Table B2. Diastolic thickness (mm) of the IVS and the LVPW at chordae tendineae level was significantly greater in the HCM group than in the normal group (6.6 ± 1.5 vs 3.8 ± 0.8, $p<0.001$ and 5.9 ± 1.6 vs 3.8 ±0.9, $p<0.001$, respectively). The thickness (mm) of the IVS and the LVPW at chordae tendineae level remained significantly greater during systole in the HCM group when compared with that from the normal group (9.1 ± 1.6 vs 6.4 ± 1.2, $p<0.001$ and 9.2 ± 1.6 vs 6.8 ± 1.1, $p<0.001$, respectively). There was no significant difference in the LV diameter during systole and diastole between the two groups. However, LV diameter during systole was significantly higher in the normal than in the HCM group, when affected cats with CHF were excluded from the analysis (8.3 ± 2.2 vs 6.1 ± 2, $p<0.01$). The fractional shortening (%) appeared to be higher in the HCM group than in the normal group and, although this difference did not reach statistical significance, it became significant when only asymptomatic affected animals were considered in the analysis (normal: 44 ± 11 vs asymptomatic: 60 ± 12, $p<0.001$). The mitral valve E point to septal separation was not different between the two groups. LA systolic diameter (mm) was significantly greater in HCM cats than in normal ones (16 ± 4.2 vs 12.4 ± 2, $p<0.001$). There was no significant difference in aortic diameter during diastole between the two groups. The ratio of left atrial to

aortic diameter at aortic valve level was significantly higher in the affected group compared to that in the normal group (1.8 ± 0.6 vs 1.3 ± 0.2, $p<0.05$). Differences in M-mode echocardiographic variables between the two groups remained unchanged even after the exclusion of cats with CHF from the analysis with the exemption of variables mentioned above. No significant difference was found in septal or lateral mitral annulus excursion between normal and HCM cats. Exclusion of HCM cats with CHF from the analysis did not alter significantly the relation in septal or lateral mitral annulus between the two groups.

Table B 2. M-mode echocardiographic parameters

M-mode measurements	Normal (n)	HCM (n)	p
IVSd (mm)	3.8 ± 0.8 (23)	6.6 ± 1.5 (23)	<0.001
LV diam.d (mm)	14.9 ± 2.2 (23)	15.1 ± 2.1 (23)	ns
LVPW d (mm)	3.8 ± 0.9 (23)	5.9 ± 1.6 (23)	<0.001
IVSs (mm)	6.4 ± 1.2 (23)	9.1 ± 1.6 (23)	<0.001
LV diam.s (mm)	8.3 ± 2.2 (23)	6.8 ± 2.6 (23)	ns
LVPWs (mm)	6.8 ± 1.1 (23)	9.2 ± 1.6 (23)	<0.001
LV FS%	44 ± 10.8 (23)	55.4 ± 14.9 (23)	ns
MV EPSS (mm)	1.2 ± 0.7 (19)	1 ± 0.6 (20)	ns
Aort.v Aod (mm)	9.4 ± 1.5 (24)	9.1 ± 1.1 (23)	ns
Aort.v:Las (mm)	12.4 ± 2 (24)	16 ± 4.2 (23)	<0.01
LAs/Aod	1.3 ± 0.2 (24)	1.8 ± 0.6 (23)	<0.05
MAM sep (mm)	4.2 ± 1 (18)	3.5 ± 1 (17)	ns
MAM lat (mm)	5.4 ± 1.7 (18)	5 ± 1.7 (15)	ns

B.15.3. Doppler parameters of pulmonic flow

Doppler echocardiographic variables of pulmonic flow are presented in Table B3. Pulmonic velocity (m/sec) was significantly higher in HCM cats than in normal animals (1.03 ± 0.4 vs 0.75 ± 0.11, $p<0.05$). Although there was no significant difference in ejection and pre-ejection period times between the two groups, the PEP/ET ratio was significantly higher in the affected group compared to that in the normal group (0.3 ± 0.08 vs 0.23 ± 0.05, $p<0.05$). Differences in Doppler parameters

of pulmonic flow between the two groups persisted even when cats with CHF were excluded from the analysis.

Table B 3. Doppler echocardiographic parameters

Pulmonic flow: Right	**Normals (n)**	**HCM (n)**	**p**
PA. vmax (m/sec)	0.75 ± 0.11 (22)	1.03 ± 0.4 (21)	<0.05
ET (sec)	0.161 ± 0.023 (18)	0.147 ± 0.017 (20)	ns
PEP (sec)	0.037 ± 0.008 (18)	0.044 ± 0.012 (21)	ns
PEP/ET	0.231 ± 0.046 (18)	0.305 ± 0.084 (20)	<0.05
Aortic flow: Left apical			
Ao.vmax (m/sec)	0.8 ± 0.11 (22)	1.94 ± 1.54 (18)	<0.01
Ao VTI (m)	0.08 ± 0.02 (22)	0.18 ± 0.13 (18)	<0.01
PEP (sec)	0.042 ± 0.009 (22)	0.044 ± 0.011 (16)	ns
ET (sec)	0.156 ± 0.021 (22)	0.152 ± 0.019 (18)	ns
PEP/ET	0.272 ± 0.06 (22)	0.29 ± 0.091 (16)	ns
Acc. t (sec)	0.039 ± 0.009 (22)	0.061 ± 0.029 (18)	<0.05
Mitral inflow			
E (m/sec)	0.64 ± 0.12 (20)	0.64 ± 0.2 (12)	ns
A (m/sec)	0.59 ± 0.12 (20)	0.61 ± 0.19 (11)	ns
E/A	1.12 ± 0.28 (20)	1.05 ± 0.4 (11)	ns
E VTI (m)	0.04 ± 0.01 (13)	0.05 ± 0.02 (8)	ns
A VTI (m)	0.03 ± 0.03 (13)	0.03 ± 0.01 (5)	ns
E dec t (sec)	0.055 ± 0.01 (13)	0.072 ± 0.017 (9)	<0.01
E acc t (sec)	0.043 ± 0.012 (16)	0.045 ± 0.008 (9)	ns
E dur (sec)	0.102 ± 0.01 (13)	0.118 ± 0.019 (9)	<0.05
A dur (sec)	0.071 ± 0.009 (13)	0.085 ± 0.02 (5)	<0.05
Colour M-mode of mitral inflow			
FPV (mm/sec)	590 ± 243 (17)	394 ± 127 (15)	<0.05
IVRT (LV)			
IVRT (sec)	0.048 ± 0.009 (19)	0.054 ± 0.015 (14)	ns
Tricuspid inflow			
E vmax (m/sec)	0.45 ± 0.12 (18)	0.51 ± 0.09 (11)	ns
A vmax (m/sec)	0.43 ± 0.11 (18)	0.43 ± 0.07 (11)	ns
E/A	1.12 ± 0.44 (18)	1.25 ± 0.42 (11)	ns

B.15.4. Doppler parameters of aortic flow

Doppler indices of aortic flow are shown in Table B3. The aortic velocity (m/sec) and the velocity time integral (m) of aortic velocity were significantly higher and greater, respectively in the HCM group compared to that in the normal group (1.94 ± 1.54 vs 0.8 ± 0.11 and 0.18 ± 0.13 vs 0.08 ± 0.02, $p<0.01$, respectively). There was no significant difference in the PEP, the ET or the PEP/ET between the two groups.

The mean acceleration time of aortic velocity (sec) was significantly prolonged in the affected group in comparison to that in the normal group (0.061 ± 0.029 vs 0.039 ± 0.009, $p<0.05$). No differences were recorded in the maximum and mean acceleration of aortic velocity between the two groups. Differences in Doppler parameters of aortic flow between the two groups remained unchanged even when cats with CHF were removed from the analysis.

B.15.5. Doppler parameters of mitral flow

Doppler mitral inflow indices are displayed in Table B3. No statistically significant differences were identified between the two groups for peak early and late diastolic velocities of mitral inflow and also for their velocity time integrals. Similarly, the E/A of mitral inflow was not different between the two groups. E deceleration, E and A duration (sec) were found to be significantly prolonged in HCM cats compared to that in normals (0.072 ± 0.017 vs 0.055 ± 0.01, $p<0.01$; 0.118 ± 0.019 vs 0.102 ± 0.01 and 0.085 ± 0.02 vs 0.071 ± 0.009, $p<0.05$, respectively). Differences in Doppler parameters of mitral inflow between the two groups persisted even when only affected asymptomatic cats were included in the analysis.

B.15.6. Isovolumic relaxation time

No statistical significant differences were found in the IVRT between the two groups (Table B3). Cats with CHF did not influence the difference between the two groups.

B.15.7. Colour M-mode of mitral inflow

HCM cats exhibited significantly lower flow propagation velocity (mm/sec) than normal animals (394 ± 127 vs 590 ± 243, $p<0.05$) (Table B3). This difference persisted between asymptomatic and normal animals when cats with CHF were excluded from the analysis. A typical example of FPV from a normal and a HCM cat is shown in Figure B2.

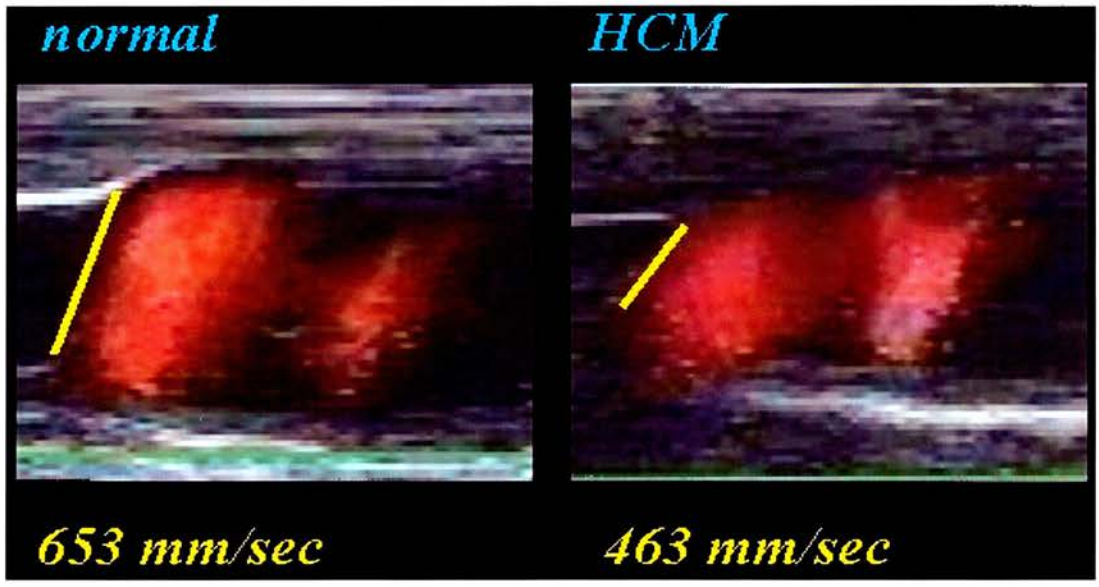

Figure B 2. *Note that the FPV in the normal cat is higher than that in the affected cat.*

B.15.8. Doppler parameters of tricuspid inflow

None of the tricuspid inflow indices was statistically different between the two groups irrespective of whether animals with CHF were included in the analysis or not (Table B3).

B.15.9. Doppler parameters of pulmonary venous flow

There were no significant differences between the two groups regarding the peak systolic and diastolic velocities (Tables B4 and B5). However, when only asymptomatic animals (n=14) were included in the analysis, HCM cats showed significantly higher maximal systolic (Smax, m/sec) and S12 velocity and also lower diastolic (D, m/sec) velocity in comparison with the normal group (0.48 ± 0.01 vs 0.39 ± 0.01, $p<0.01$; 0.52 ± 0.11 vs 0.37 ± 0.12, $p<0.001$; 0.3 ± 0.06 vs 0.41 ± 0.08, $p<0.001$, respectively). The S/D ratio was found to be lower in the normal group compared to that in the affected group irrespective of whether animals with CHF were included in the analysis or not (1.01 ± 0.34 vs 1.38 ± 0.53, $p<0.05$; without animals in CHF: 1.01 ± 0.34 vs 1.63 ± 0.23, $p<0.001$). None of the asymptomatic animals in the affected group exhibited an S/D < 1, whereas in the normal group seven animals had an S/D < 1. In the all three affected animals with CHF the S/D was less than 1. The peak atrial reversal velocity (m/sec) was significantly higher in the affected than in the normal group (0.33 ± 0.13 vs 0.23 ± 0.08, $p<0.05$). This difference remained significant even when only asymptomatic animals were considered (0.3 ± 0.06 vs 0.23 ± 0.08, $p<0.05$). No statistically significant differences were identified between the two groups for the VTI of the PVF waves. However, asymptomatic HCM cats had lower diastolic D VTI compared with that from normal animals (0.027 ± 0.01 vs 0.037 ± 0.012, $p<0.001$). The time from the Q wave of the ECG to the beginning of the systolic wave (Q-bS, sec) and also to the maximum systolic peak (Q-Smax, sec) and to peak S12 and peak S1 was significantly prolonged in the affected group than in the normal group (0.034 ± 0.014 vr 0.028 ± 0.015, $p<0.01$; 0.064 ± 0.022 vs 0.089 ± 0.025, $p<0.01$; 0.061 ± 0.029 vs 0.093 ±

0.025, p<0.01; 0.066 ± 0.013 vs 0.088 ± 0.024, p<0.05). The difference in the above time intervals between the two groups persisted even when the asymptomatic HCM cats were not included in the comparison. However, there was no significant difference between the normal and the asymptomatic HCM cats regarding the Q-bS.

Table B 4. Doppler echocardiographic indices of pulmonary venous flow from normal and HCM cats (asymptomatic + CHF)

Pulmonary venous flow	Normals (n)	HCM (n)	p
Smax (m/sec)	0.39 ± 0.1 (20)	0.43 ± 0.14 (17)	ns
S12	0.37 ± 0.12 (10)	0.44 ± 0.16 (12)	ns
S1 (m/sec)	0.41 ± 0.07 (10)	0.42 ± 0.04 (5)	ns
S2 (m/sec)	0.26 ± 0.06 (10)	0.25 ± 0.06 (5)	ns
D (m/sec)	0.4 ± 0.08 (20)	0.34 ± 0.12 (18)	ns
Ar (m/sec)	0.23 ± 0.08 (20)	0.33 ± 0.13 (17)	<0.05
S/D	1.01 ± 0.34 (20)	1.38 ± 0.53 (18)	<0.05
S VTI (m)	0.05 ± 0.01 (20)	0.05 ± 0.02 (18)	ns
D VTI (m)	0.04 ± 0.01 (20)	0.03 ± 0.02 (18)	ns
Ar VTI (m)	0.01 ± 0.003 (19)	0.01 ± 0.004 (17)	ns
S dur (sec)	0.204 ± 0.037 (20)	0.191 ± 0.042 (18)	ns
D dur (sec)	0.147 ± 0.04 (20)	0.143 ± 0.037 (18)	ns
D dec (sec)	0.072 ± 0.034 (20)	0.076 ± 0.029 (17)	ns
Ar dur (sec)	0.078 ± 0.013 (18)	0.088 ± 0.021 (17)	ns
Adur/Ardur	0.93 ± 0.134 (11)	0.97 ± 0.35 (4)	ns
Q-bS (sec)	0.028 ± 0.015 (18)	0.034 ± 0.014 (16)	<0.05
Q-Smax (sec)	0.064 ± 0.022 (20)	0.089 ± 0.025 (17)	<0.01
Q-S12 (sec)	0.061 ± 0.029 (10)	0.093 ± 0.025 (12)	<0.01
Q-S1 (sec)	0.066 ± 0.013 (10)	0.088 ± 0.024 (5)	<0.05
Q-S2 (sec)	0.19 ± 0.018 (10)	0.206 ± 0.021 (5)	ns
Q-D (sec)	0.298 ± 0.033 (20)	0.297 ± 0.04 (16)	ns
Q-Ar (sec)	0.376 ± 0.104 (20)	0.366 ± 0.063 (15)	ns

Table B 5. Doppler echocardiographic indices of pulmonary venous flow from normal and asymptomatic HCM cats

Pulmonary venous flow	Normals (n)	asymptomatic HCM (n)	p
Smax (m/sec)	0.39 ± 0.1 (20)	0.48 ± 0.10 (14)	<0.01
S12	0.37 ± 0.12 (10)	0.52 ± 0.11 (9)	<0.001
S1 (m/sec)	0.41 ± 0.07 (10)	0.42 ± 0.04 (5)	ns
S2 (m/sec)	0.26 ± 0.06 (10)	0.25 ± 0.06 (5)	ns
D (m/sec)	0.4 ± 0.08 (20)	0.30 ± 0.06 (14)	<0.001
Ar (m/sec)	0.23 ± 0.08 (20)	0.33 ± 0.14 (14)	<0.05
S/D	1.01 ± 0.34 (20)	1.63 ± 0.23 (14)	<0.01
S VTI (m)	0.05 ± 0.01 (20)	0.057 ± 0.01 (14)	ns
D VTI (m)	0.04 ± 0.01 (20)	0.027 ± 0.01 (14)	<0.001
Ar VTI (m)	0.01 ± 0.003 (19)	0.013 ± 0.004 (14)	ns
S dur (sec)	0.204 ± 0.037 (20)	0.206 ± 0.036 (14)	ns
D dur (sec)	0.147 ± 0.04 (20)	0.139 ± 0.026 (14)	ns
D dec (sec)	0.072 ± 0.034 (20)	0.074 ± 0.023 (14)	ns
Ar dur (sec)	0.078 ± 0.013 (18)	0.087 ± 0.021 (14)	ns
Adur/Ardur	0.93 ± 0.134 (11)	0.97 ± 0.35 (4)	ns
Q-bS (sec)	0.028 ± 0.015 (18)	0.029 ± 0.01 (12)	ns
Q-Smax (sec)	0.064 ± 0.022 (20)	0.086 ± 0.026 (12)	<0.01
Q-S12 (sec)	0.061 ± 0.029 (10)	0.090 ± 0.027 (7)	<0.01
Q-S1 (sec)	0.066 ± 0.013 (10)	0.08 ± 0.025 (5)	<0.05
Q-S2 (sec)	0.19 ± 0.018 (10)	0.206 ± 0.021 (5)	ns
Q-D (sec)	0.298 ± 0.033 (20)	0.301 ± 0.034 (14)	ns
Q-Ar (sec)	0.376 ± 0.104 (20)	0.378 ± 0.059 (14)	ns

B.15.10. Influence of age, sex, weight, and R-R interval on conventional 2D/Doppler echocardiographic variables

Results of stepwise regression analysis, linear and multiple linear regression analysis between 2D/Doppler echocardiographic variables and independent predictors are presented in Tables App.B3, 4 and 5, Appendix B2.

B.15.10.1. Normal group

In the normal group, age associated inversely with the E velocity and the E/A ratio of the tricuspid inflow and the E/A ratio of the mitral inflow. Age inversely influenced the flow propagation velocity and the isovolumic relaxation time in normal cats. A positive association was found between age and the duration of the E wave of mitral inflow, the S max and S/D of the pulmonary venous flow and also the duration of the S wave.

The PEP and PEP/ET of the left ventricle was positively related to weight. A positive relationship was found also between the IVRT, the D wave of PVF and its velocity time integral and weight. Weight inversely influenced the ejection time of the right ventricle, the S/D ratio and the VTI of the Ar of the PVF and also the lateral mitral annulus excursion.

A positive association was found between sex and the PEP/ET of the left ventricle, the deceleration time of the E wave of mitral inflow and its velocity time integral and also the velocity time integral of the D wave of the PVF. Sex was associated inversely with the LA systolic area, the 2D aortic to LA diameter, the M-mode LA diameter during systole, the ejection time in both ventricles and the acceleration time of the aortic flow. Male cats had a higher LA systolic area (mm^2) and M-mode LA systolic diameter (mm) than female cats (182 vs 142, $p<0.01$; 13.4 vr 11.5, $p<0.05$, respectively). Normal female cats showed a greater E VTI (m) and a higher D wave (m/sec) of PVF than normal male cats (0.045 vs 0.038, $p<0.05$; 0.45 vs 0.36, $p<0.01$). There were no significant differences between male and female normal cats regarding the rest of the echocardiographic variables.

The diameter of the LA and the LV during diastole and systole, respectively, tended to increase with longer R-R interval. A positive association was found between the diastolic thickness of the LVPW and the R-R interval. The ejection time of both ventricles and the pre-ejection period of the LV showed a positive relation with the R-R interval. A positive association was found between the R-R interval and the

velocity time integrals of aortic flow and the D wave of the PVF. The E/A ratio and the duration of E wave of the mitral inflow tended to increase and prolong, respectively, with longer R-R intervals. The R-R interval associated positively with the following indices of PVF: duration of S and D waves, deceleration of D wave, time from the Q wave of the ECG to Smax, Sl, S12, S2, D and Ar waves. An inverse association was found between the A wave velocity of the mitral inflow and the R-R interval.

B.15.10.2. HCM group

Age was positively associated with the E and A wave velocities of the mitral inflow in the HCM group. Similarly, a positive association was found between age and the FPV and the S max of the PVF in affected cats. Although age was found to be a significant predictor for the early diastolic wave of tricuspid inflow and the pre-ejection period of the right ventricle in forward stepwise regression analysis, no significant association was found between age and the aforementioned indices.

The aortic diameter during diastole correlated with increasing weight in the affected group.

In forward stepwise regression analysis, the factor sex was found to be a significant predictor for S max, S12 and S/D of PVF. However, no significant association was found between these indices and sex.

A positive association was found between the R-R interval and the ejection time of both ventricles. Similarly, the R-R interval was associated positively with the velocity time integral, the duration and the deceleration time of the D wave of the PVF and the Q-D and Q-Ar intervals. The R-R interval inversely influenced the FPV and the pulmonic velocity in the HCM group.

B.15.11. Patterns of hypertrophy

Six cats exhibited diffuse symmetric hypertrophy (26%). Ten cats had segmental asymmetric type of hypertrophy with 7 (30%) presenting predominant thickening of the IVS and 3 (13%) of the LVPW. In 5 cats, the hypertrophy involved only parts of the IVS without being asymmetrical. In 5 affected cats the basilar portion of the IVS was thickened and protruded in the LVOT (septal budge).

B.15.12. Mitral regurgitation and SAM

CFDE identified mitral regurgitation in 19 HCM cats. Regurgitant jets were most often directed towards the posterior aspect of the LA wall. Twelve affected cats had documented SAM of the anterior leaflet of the mitral valve on mitral M-mode.

B.16. Discussion

B.16.1. Introduction

In our study, we defined HCM by the presence of a 6 mm LV end diastolic thickness measured on either 2D or M-mode recordings at any part of the LV wall on the absence of volume or pressure overload or other systematic disease known to cause LV hypertrophy (Peterson *et al*, 1993; Fox *et al*, 1995). That the mean end diastolic thickness of the LVPW wall in the affected group was 5.9 mm, which was less than

the cut-off value of 6 mm used to discriminate between normal and affected cats, resulted from the fact that some HCM cats had asymmetric septal hypertrophy. Some of these cats had a LVPW diastolic thickness of < 6 mm. Assessment of asymmetrical hypertrophy was done using the 1.3 value for the ratio of IVS to LVPW thickness, as described previously by others (Maron *et al*, 1981a). The most common pattern of hypertrophy encountered in our group of HCM cats was asymmetric septal hypertrophy. In nearly 50% of affected animals the hypertrophy involved parts of the IVS. This finding is in partial agreement with the results reported by Peterson and colleagues (1993), who showed that in a group of 86 HCM cats, up to 40% exhibited asymmetric hypertrophy with predominant involvement of the IVS. In our study, cats with diffuse hypertrophy represented a smaller percentage in the HCM group than that reported by Fox and colleagues (1995). Cats with predominant hypertrophy of the LVPW were less frequently seen and this is in agreement with previous reports (Peterson *et al*, 1993; Fox *et al*, 1995). In some cats, hypertrophy was prominent in the basilar portion of the IVS (septal bulge), a finding that has been previously described in both humans and cats with HCM (Fox *et al*, 1995; Klues *et al*, 1995).

A high percentage of affected cats had mitral regurgitation recorded by CFDE. However, mitral regurgitation was not always accompanied by SAM of the anterior leaflet of the mitral valve. This finding is in agreement with the findings of other studies in cats with HCM (Fox *et al*, 1995). Nearly half of the affected cats had SAM of the anterior leaflet of the mitral valve, similar to that documented in other reports (Fox *et al*, 1995).

B.16.2. 2D and M-mode echocardiographic variables in normal and HCM cats

The positive association reported in the current study between LA diameter during diastole and LV diameter during systole is in agreement with the increased chamber dimensions occurring with decreasing heart rate reported in healthy cats by Jacobs and Knight (1985).

The results reported in the current study show that cats with hypertrophic cardiomyopathy, irrespective of their clinical status (asymptomatic or not), had larger LA in comparison to normal animals. This was reflected in both 2D and M-mode measurements by the greater LA area and diameter recorded in the affected group during diastole and systole. LA enlargement in the diseased state is the consequence of elevated LA pressures, which result from elevated filling pressures due to abnormal relaxation and impaired compliance. Affected cats with CHF exhibited significantly larger LA and lower LA FS% compared with asymptomatic animals, indicating the presence of high LA pressures and loss of LA contractility at the end stage of the disease. The loss of LA contractility was indicated by the very low values of LA FS% recorded in this subgroup of affected cats.

M-mode measurements showed that HCM cats had significantly increased IVS and LVPW diastolic thickness and also LV FS% compared to that in normal cats. These findings are in agreement with previously published data (Fox *et al*, 1995) and reconfirm the hypercontractile state of the LV, at least in asymptomatic animals.

B.16.3. Doppler indices of aortic and pulmonic flow

The increased aortic velocity recorded in affected cats is compatible with the presence of LV outflow tract obstruction, a frequent complication encountered in HCM. The prolonged acceleration time of aortic velocity recorded in HCM cats results probably from the mid-systolic obstruction of the blood flow due to the systolic anterior motion of the mitral valve.

Increased peak pulmonic velocities were recorded in the affected group and it is believed to result by right ventricular outflow tract obstruction (RVOTO), which possibly occurred in some animals. Unfortunately, systematic evaluation of the right ventricular outflow tract with CFDE was not carried out in this study, so it is impossible to quote the exact number of animals with RVOTO. Interestingly, HCM cats exhibited higher right ventricular PEP/ET than normal animals did. It has been shown that the ratio PEP/ET is a sensitive indicator of contractility, which prolongs in the presence of abnormal global systolic function. Increased PEP/ET results from increased pre-ejection period (reduced rate of ventricular pressure rise) and reduced ventricular ejection time (reduced fibre shortening) (Atkins and Snyder, 1992b; Allworth *et al*, 1995). Although the exact mechanism, which led to the increased RV PEP/ET recorded in the HCM group is unknown, possible impairment of the contractile performance of the RV can not be ruled out. It is peculiar that, despite the fact that LV is apparently predominantly affected in HCM, no significant difference in the PEP/ET ratio between the two groups was found for the LV assessed for aortic outflow.

B.16.4 Mitral inflow

B.16.4.1. Mitral inflow in normal cats

Age-related changes in mitral and tricuspid inflow Doppler indices similar to those reported in normal humans have been recorded in our group of normal cats (Appleton *et al*, 1988; Nishimura *et al*, 1997). Age showed an inverse association with the E/A ratio of both the mitral and tricuspid inflow and also with the E wave of tricuspid inflow. The E/A ratio of mitral inflow was also found to be associated inversely with age by Santili and Bussadori (1998). With advanced age, the duration of early left ventricular filling tended to prolong. These findings indicate altered diastolic properties associated with age-induced changes in both ventricles of normal cats.

In the normal group, late diastolic wave (A) and E/A ratio of mitral inflow showed an inverse and positive association, respectively, with the R-R interval, reflecting the prominent role of left atrial contraction in the LV filling with elevated heart rates. The inverse association between the A wave of the mitral inflow and R-R is in agreement with the findings presented by Santilli and Bussadori (1998).

B.16.4.2. Doppler echocardiographic findings of mitral inflow in HCM cats

There was no significant difference in E, A, E/A ratio of mitral inflow and the IVRT between the two groups. Although, Doppler echocardiographic studies have shown that humans with HCM quite often exhibit decreased early and increased late diastolic velocities, elevated LA pressures tend to pseudonormalize the mitral inflow pattern and consequently to mask abnormal relaxation properties. This may be one

contributing factor for the absence of difference in early and late diastolic mitral inflow velocities between our two study groups. In the presence of elevated LV filling pressures, the IVRT decreases and therefore is not a very reliable index for disclosing abnormal relaxation properties (Takenaka *et al*, 1986; Bryg *et al*, 1987; Maron *et al*, 1987; Spirito and Maron, 1990; Bright *et al*, 1999). This may possibly explain that IVRT was not different between the two groups. IVRT is also technically difficult to accurately measure and, thus difficult to document differences between groups. An abnormal relaxation mitral inflow pattern was often recorded in older animals, suggesting reduced relaxation properties induced by aging. This finding has probably affected the comparison of mitral inflow indices between the two groups. In the presence of high heart rates, affected animals showed summated E and A waves, making impossible to interpret mitral inflow patterns and also reducing the number of quantifiable tracings, which otherwise may have probably helped to show differences between the two groups. The prolonged deceleration time and duration of early diastolic mitral inflow velocity in affected animals are in agreement with previous reports in humans and cats with HCM and reflect abnormal relaxation properties. However, due to summation effects induced by high heart rates measurement of these two indices was possible only in less than half of affected animals. The prolongation of late diastolic velocity in cats with HCM results from a possible increase in LA pressure, which in turn forces the LA to contract longer during late diastole. Because measurement of the duration of A wave was feasible in only few affected animals the value of this finding is questionable.

B.16.5 Colour flow propagation in normal and HCM cats

An inverse association was found between age and FPV in the normal group. A similar association has been documented in normal humans and it is believed to result from age-related changes, which increase myocardial stiffness and impair relaxation properties (Mego *et al*, 1998).

The decreased flow propagation velocity in the affected group results from the delayed LV relaxation and elevated filling pressures and is in agreement with previous reports of humans with HCM (Brun *et al*, 1992; Nagueh *et al*, 1999).

B.16.6. Pulmonary venous flow

B.16.6.1. Pulmonary venous flow characteristics in normal cats

Age appeared to influence positively the S wave and the S/D ratio of pulmonary venous flow. These findings show that the LA is performing in a higher level of its Frank-Starling curve possibly due to elevated filling pressures caused by alterations in relaxation and compliance properties induced by aging. The positive association between the S wave of the PVF and age in normal cats has been also documented by Santilli and Bussadori (1998).

B.16.6.2. Pulmonary venous flow characteristics in HCM cats

It has been shown that in patients with HCM, slightly elevated LV filling pressures lead to elevated systolic and decreased diastolic PVF velocities (Ito *et al*, 1996; Oki *et al*, 1996). This finding is compatible with the higher systolic velocities and S/D ratio and the decreased diastolic PVF velocities recorded in the asymptomatic group

of HCM cats in the current study. During the early stages of impairment of LV relaxation, a slight elevation in LV filling pressure forces the LA to contact more strongly without significantly affecting its compliance. An increase in the PVF S wave at this stage indicates that the LA expands more in order to contract more vigorously during late diastole (Frank-Starling law). This also results in higher Ar PVF velocities, which is confirmed by the results of our study. As LV filling pressures increase further, left atrial compliance decreases resulting in decreased PVF systolic velocities. Diastolic velocities show a compensatory increase, since during early diastole the atrio-pulmonary venous pressure gradient is higher than the one developed during systole and consequently the S/D becomes < 1. At the end stage of the disease, when LA contractility is minimal and LV filling pressures are maximal, the systolic wave becomes very low and most of the forward PVF takes place during early diastole (high D wave) (restrictive pattern). This was clearly depicted in the HCM cats with CHF. Because of its pulsatile nature, PVF is not affected by the summation effects induced by high heart rates, therefore can be a valuable tool in the non-invasive assessment of LV diastolic properties in feline cardiac diseases, overcoming the limitations of mitral inflow. Although, quantification of PVF has technical difficulties, particularly in cats because of the small size of their heart, in the diseased state, it becomes easier due to the widening of the pulmonary veins. This study shows that in normal animals the S/D ratio of PVF shows a gradual increase with increasing age and although it tends to become > 1, especially in old animals, it rarely exceeds 1.5. Although the data presented in the current study is not compared with invasive hemodynamic indices, it is highly possible that an S/D > 1.5 indicates elevated LV pressures induced by a disease

process rather than aging. Using this cut-off value only 2 asymptomatic HCM (the S/D ratio for these two cases was 1.35 and 1.27, respectively) cats could not be identified and only 1 normal cat (9 year-old) could be falsely diagnosed as affected (S/D ratio, 1.85). When the S/D ratio is close to 1 or < 1 and the Ar is > 40 cm/sec and has a duration of > 100 msec then significantly elevated LV filling pressures should be suspected. This speculation, although arbitrary, is based on the fact that only 1 normal cat had an Ar > 40 cm/sec (41 cm/sec) and another had Ar dur > 100 msec (105 msec). Although these cut-off values for Ar indices are quite sensitive for concluding that an animal in not normal, they fail to identify nearly 2/3 of the affected animals (lack of specificity). However, one needs to keep in mind that quantification of the Ar wave in cats was probably the most difficult among the PVF waves and therefore its true values may be underestimated. The widely used difference between the A wave of mitral inflow duration and the Ar duration in the prediction of LV filling pressures in humans, is confounded in cats by the high heart rates, which result in summation and make impossible to record the duration of the mitral A wave. In affected cats, the time from the electrocardiographic Q wave to the peak systolic velocities was prolonged compared to that in normal animals. This finding shows that PVF during systole peaks later in the presence of elevated LA pressures.

SECTION C

Tissue Doppler Imaging echocardiography: a review of the literature

C.1. Introduction

Tissue Doppler Imaging (TDI) has emerged in the last decade as new alternative tool in the non-invasive quantification of myocardial motion. Based on the Doppler principle, which is applied to the myocardium instead of to the blood pool, the technique selects only the high amplitude, low frequency ultrasonic shifts returning from the interrogated myocardium and therefore allows the estimation of myocardial velocities (Fleming *et al*, 1994b; Miyatake *et al*, 1995). This is feasible by appropriate modifications in signal processing of the returned Doppler signals. The high-pass wall filters, which are used to eliminate the low-velocity and high-amplitude signals of myocardial walls for detection of blood flow velocities in conventional Doppler/colour flow modalities, are bypassed for TDI. In addition, gain amplification is used to enhance low-velocity myocardial signals and to eliminate the blood flow signals within the cardiac chambers (Sutherland *et al*, 1999).

Quantification of myocardial motion can be performed using different applications of the TDI technique, such as pulsed, colour M-mode and 2D TDI modalities (Trambaiolo *et al*, 2001; Waggoner and Bierig, 2001). Pulsed TDI allows measurement of the instantaneous velocities of different myocardial segments. This is feasible by placing the sample volume on the dependent myocardial site and

obtaining the instantaneous myocardial velocities passing through the sample volume during the cardiac cycle. Although pulsed TDI has no spatial resolution within the sample volume, it offers excellent temporal resolution and requires minimal off-line analysis. Limitations of this particular application of TDI arise from the fact that only regional quantification of myocardial velocities at selected sites is possible and that sampling can not be localized to the endocardial or epicardial layers. Additionally, myocardial velocities measured by pulsed TDI are affected by the overall heart motion and motion of adjacent myocardial segments and therefore do not represent an accurate estimate of true myocardial velocities (Shimizu *et al*, 1998).

When the colour M-mode and 2D TDI modalities are used, myocardial motion is colour coded with red and blue colours, which indicate myocardial movement towards and away from the transducer, respectively. The intensity of colour represents the magnitude of motion, with dark hues representing low velocities and bright hues representing higher velocities. Colour M-mode TDI provides very high temporal resolution and also quantification of myocardial motion of different myocardial layers (Trambaiolo *et al*, 2001; Waggoner and Bierig, 2001). However, an inherent disadvantage of this modality is that it allows interrogation of myocardial velocities only along the M-mode scan-line and therefore it can only be used in quantifying myocardial motion along the radial axis of the heart, and in limited number of segments, using the parasternal views. Using the velocity estimates along every single M-mode scan-line the myocardial velocity gradient (MVG), from endocardium to epicardium, can be calculated (Fleming *et al*, 1994b). MVG is not influenced by either cardiac rotation or displacement and thus, it offers the potential

for a more accurate quantification of regional myocardial function. The clinical value of MVG will be discussed later in this thesis.

The colour 2D TDI mode allows the simultaneous quantification of myocardial motion in multiple segments in a 2D image. This reduces the influence of beat-to-beat variability when velocities from different myocardial segments are compared. The ability to collect full sector image data in real time also reduces patient scanning time compared to the more time consuming segment-by-segment sampling inherent in acquiring pulsed TDI data. A disadvantage of the colour 2D TDI is that, with the currently available systems, it offers lower temporal resolution in comparison to pulsed and colour M-mode TDI techniques (Trambaiolo *et al*, 2001; Waggoner and Bierig, 2001). Moreover, it has a lower signal to noise ratio compared to colour M-mode TDI, which may lead to underestimation of true myocardial velocities (Garot *et al*, 1998). Using 2D TDI images it is possible to calculate the MVG and strain and strain rate in different myocardial segments (Uematsu *et al*, 1995; Heimdal *et al*, 1998). The latter two variables are recently introduced TDI indices, which allow the quantification of deformation characteristics along different parts of the myocardial wall, irrespective of translational effects and overall heart motion. Further description of strain and strain rate is beyond the scope of this thesis.

The myocardial velocity tracings recorded by different applications of the TDI technique exhibit a characteristic pattern of positive and negative waves, with each one of them corresponding to myocardial motion during certain cardiac phases. Systole is represented by a positive deflection (S' wave), which commences after

aortic valve opening and peaks during early ventricular ejection following a fast acceleration period. During late systole, the systolic wave shows a characteristic plateau shape and immediately after that decelerates until the end of systole. The systolic wave reflects the contractile state of the myocardium and results from inward myocardial movement during systole. Early diastole is represented by a negative deflection (E' wave) occurring after mitral valve opening and late diastole by a negative wave (A') appearing after the P wave of the ECG (Rodriguez *et al*, 1996; Ohte *et al*, 1998; Pai and Gill, 1998; Nagueh *et al*, 2001b). The E' wave results from the early diastolic myocardial expansion and reflects the energy dependant myocardial relaxation and also the elastic properties of the myocardium (elastic recoil of myocardial fibres). Late diastolic myocardial motion is passive and related to filling due to atrial contraction. During the 2 isovolumic periods, short duration biphasic shifts have been recorded in all myocardial segments, and although it has been shown that they correlate with the opening and closure of atrioventricular and semilunar valves, their main determinants remain elusive (Garcia *et al*, 1996a).

TDI, apart from offering an alternative means in the non-invasive assessment of regional myocardial function, also allows the simultaneous quantification of myocardial motion during all phases of the cardiac cycle along the two major axes of the heart. The myocardium is constructed of longitudinally arranged oblique fibres in the subepicardial and subendocardial regions and circumferential fibres in the mid-wall (Greenbaum *et al*, 1981). Systolic shortening and diastolic lengthening along the longitudinal and radial axis of the heart is attributed to the contraction and relaxation of the longitudinal and circumferential/radial fibres, respectively (Galiuto *et al*,

1998). Optimal mechanical performance during diastole and systole requires a highly organized coordination between these two different types of myocardial fibres (Jones *et al*, 1990). Although conventional echocardiography enables the indirect assessment of myocardial function based on morphological and blood flow characteristics, it does not always offer an accurate means for assessing global myocardial properties and its contribution in quantifying regional myocardial function is limited. By contrast, the use of TDI allows for the first time the direct quantification of myocardial motion, and more specifically, assessment of motion of the differently oriented types of fibres. It has been proposed that regional abnormalities in myocardial motion may precede and lead to changes in global systolic and diastolic dysfunction (Bonow *et al*, 1987). Thus, quantification of regional myocardial function is of particular importance in the early detection and prevention of cardiac diseases. TDI has shown great promise in this respect.

Because of the angle dependence of the TDI technique, quantification of myocardial motion along the two major axes of the heart is feasible using certain echocardiographic views, which allow the parallel placement of the ultrasonic beam to the myocardial movement investigated every time (Trambaiolo *et al*, 2001; Waggoner and Bierig, 2001). Assessment of radial motion is made using the parasternal long or short axis views. When the pulsed TDI technique is applied, placement of the sample volume on the mid-portions of the IVS or the LVPW is recommended for optimising the interrogation of circumferentially arranged fibres. Quantification of longitudinal motion is feasible when the apical views are used.

When the pulsed TDI is applied, the sample volume is either placed on different sites of the atrioventricular rings or in the endocardial areas of ventricular walls.

C.2. Pulsed Tissue Doppler Imaging

C.2.1. Pulsed Tissue Doppler Imaging studies in healthy humans. Identification of physiologic non-uniformity

A physiologic non-uniformity in the myocardial motion of normal humans and of experimental animals has been described during diastole and systole and it is believed to be, along with load and activation-inactivation mechanisms, one of the main determinants of optimal myocardial performance under normal circumstances (Lew and Lewinter, 1983; Hammermeister *et al*, 1986; Brutsaert, 1987). This heterogeneous and asynchronous motion is the result of myocardial fibre orientation, asynchronous activation and of different electrophysiological and mechanical features of myocardial fibres in different parts of the myocardium (Brutsaert, 1987). Quantification of the normal human myocardium with the TDI technique has confirmed the presence of this physiologic time and space non-uniformity among the different walls of the LV. Knowledge of the physiologic heterogeneity of myocardial motion is essential in recognising changes induced by disease. This phenomenon has been identified for a wide range of TDI variables. TDI studies in humans have shown that the posterior and lateral sides of the LV along both axes exhibit higher myocardial velocities than the septal side of the heart during all cardiac phases (Garcia *et al*, 1996a; Oki *et al*, 1997; Galiuto *et al*, 1998; Pai and Gill, 1998; Alam *et al*, 1999; Yamada *et al*, 1999a; Tabata *et al*, 2000; Cardim *et al*, 2002a). Peak early diastolic velocities in the septal side of the heart occur later than those in the LVPW

along both axes in normal individuals (Oki *et al*, 1997; Yamada *et al*, 1999a; Cardim *et al*, 2002a). It also has been shown that early diastolic myocardial motion in the IVS of normal individuals lasts significantly longer compared to that in the LVPW wall along the longitudinal axis (Pai and Gill, 1998). Moreover, the time from the first component of the first heart sound to Se' (I-Se') was shorter in the septal mitral annulus than in the other annular sites (Cardim *et al*, 2002a). Additionally, a gradual reduction in all velocities has been reported from LV base to apex in normal subjects (Galiuto *et al*, 1998; Pai and Gill, 1998).

Investigation of the tricuspid annular motion with pulsed TDI has shown that this myocardial segment exhibits higher systolic velocities than those recorded in the mitral annulus of normal individuals (Alam *et al*, 1999). This denotes the higher contractile state of the right ventricle. Differences in the myosin isoenzyme composition between the myocardial cells of the two ventricles have been shown to attribute to their different mechanical states (Samuel *et al*, 1983; Pagani and Julian, 1984; Litten *et al*, 1985). In normal subjects, the tricuspid annulus also exhibits higher late diastolic velocities compared to that in mitral annular sites (Alam *et al*, 1999). However, early diastolic tricuspid annular velocities were higher only when compared with those from the septal mitral annulus, with the rest of the mitral annular sites showing the same velocities with the tricuspid annulus during this particular cardiac phase (Alam *et al*, 1999).

Yamada and colleagues (1999a) compared TDI indices derived from the middle IVS and the LVPW along both axes of the heart in normal subjects. Their study showed

that E' of the posterior wall was significantly greater along the radial axis than along the longitudinal axis, whereas A' of the LVPW was significantly greater along the longitudinal axis than along the radial axis. Conversely, E' and A' at the IVS were significantly higher along the longitudinal axis than along the radial axis. Based on the above findings, it was suggested that relaxation of the circumferential fibres is greater than that of longitudinal fibres during early diastole and that elongation of longitudinally arranged fibres resulting from atrial contraction is greater than that of circumferential ones (Yamada *et al*, 1999a). Additionally, greater peak Se' has been documented along the longitudinal axis compared to that along the radial axis in the LVPW of normal subjects.

The physiologic, asynchronous, myocardial motion of the different parts of the LV has been shown by many TDI studies in normal humans. The time from the aortic component of the second heart sound to E' (II-E') in the middle IVS was longer than that of the LVPW along both axes in normal individuals (Yamada *et al*, 1999a). In the LVPW, II-E' was significantly longer along the longitudinal axis than along the radial axis. Similar to the above results, II-E' in all regions (basal, middle, apical) of the IVS along the radial axis was significantly prolonged in comparison to that of the corresponding ones in the LVPW along the same axis (Oki *et al*, 1997). II-E' of the lateral and inferior sites of the mitral annulus was shorter in duration than that of the septal and anterior regions (Cardim *et al*, 2002a). On the other hand, E' duration of the septal, lateral, anterior and inferior walls along the longitudinal axis was reduced between their mid and distal segments (Pai and Gill, 1998). E' duration was the shortest in the lateral walls and the longest in the septum (Pai and Gill, 1998).

Regarding systolic time intervals, Pai and Gill (1998) showed that, although S' duration and the time from the Q wave of the ECG to the beginning of S' wave (Q-bS') were similar among segments of the same level in the four LV myocardial walls along the longitudinal axis, S' duration was reduced between their mid and distal regions. The time from the first component of the first heart sound to Se' (I-Se') was shorter in the septal annulus of normal subjects than in the other annular sites (Cardim *et al*, 2002a). Equal Q-Se' in the IVS and the LVPW along the radial axis have been reported in normal subjects (Oki *et al*, 1998b).

C.2.2. Age related changes in the normal human myocardium reflected by pulsed TDI

TDI studies have reflected age-related changes in the diastolic and systolic performance of the normal human myocardium. A decrease in early diastolic velocity with a concomitant increase in the amplitude of the late diastolic myocardial component have been shown with increasing age in many studies (Garcia *et al*, 1996a; Rodriguez *et al*, 1996; Sohn *et al*, 1997; Alam *et al*, 1999; Yamada *et al*, 1999a; Naqvi *et al*, 2001). An inverse association between systolic mitral annular velocities and age has been documented in others (Alam *et al*, 1999). Similarly, decreased early systolic velocities with increasing age have been recorded in the LVPW along the longitudinal axis in normal individuals (Onose *et al*, 1999a). Changes in the active state of myocardial fibres and in visco-elasticity are induced due to aging and it has been shown to affect the diastolic properties of the myocardium (Weisfeldt, 1971; Lakatta, 1975). Increased myocardial stiffness due to increased quantity of interstitial connective tissue, along with increase of the

connective tissue of the fibrous skeleton of the heart, may play an additional role in the age-related decrease in LV diastolic function. Interestingly, with increasing age, a decline in the ability of beta-adrenergic receptor stimulation to increase contractility has been reported in isolated myocytes of rats and this finding might explain the age-related TDI changes (Xiao *et al*, 1994).

C.2.3. Haemodynamic determinants of Tissue Doppler Imaging indices

Several studies have tried to assess the haemodynamic determinants of TDI indices. Knowledge of this would allow better interpretation and understanding of the TDI data, when quantification of myocardial motion is attempted, using the TDI technique. In an experimental study in dogs, Nagueh and colleagues (2001b) showed the load independence (caval compression) of annular E' (septal and lateral mitral annulus) in the presence of impaired LV relaxation (increased τ) induced by esmolol infusion. In normal and enhanced relaxation states (after dobutamine infusion), annular E' decreased with caval compression at baseline and after dobutamine infusion and increased with volume loading at baseline. The load independence of myocardial early diastolic velocity, when impaired relaxation is present, is of significant clinical value, since myocardial E' wave can prove useful in unmasking pseudonormal mitral inflow patterns in the presence of elevated LV filling pressures, and therefore can be used as a more accurate tool in quantifying impaired diastolic properties. The load independence of E' in the diseased state has been proven in many clinical settings and it will be discussed more extensively later on. In Nagueh's study (2001), dobutamine infusion with its inotropic effects enhanced early diastolic recoil (decreased τ) and decreased LVEDP, which resulted in an increase in the

amplitude of annular E'. By contrast, esmolol had the opposite effect. Annular E' showed a strong inverse correlation with tau and –dP/dt. The correlation between annular E' and LV stroke volume was positive. On the other hand dobutamine infusion led to an increase in annular A' through the lower LVEDP (decreased LA afterload) and the enhancement of LA contractility and relaxation. Conversely, esmolol resulted in impairment of LV relaxation, elevated LVEPD and therefore atrial afterload. This occurred alongside depression of LA function and concomitant reduction in A' velocity. Similar to the above findings were the experimental observations by Firstenberg and colleagues (2001) who confirmed the load independence of annular E' during impaired LV relaxation and its strong inverse correlation with τ. In an experimental animal setting, Vogel and colleagues (2002) studied the influence of loading and heart rate changes and also of pharmacologically induced alterations in myocardial acceleration of the free wall of the RV during isovolumic contraction (IVA). IVA was unaffected from increased preload and decreased afterload. During esmolol infusion IVA and dP/dt decreased and both were increased after dobutamine infusion. IVA was considered as an alternative index for the assessment of RV contractile performance in different clinical settings. Increased afterload, induced by angiotensin infusion in normal subjects, has been shown to decrease Se' and E', but not A', and to prolong the time from the aortic component of the second heart sound to peak early diastolic velocity (II-E') (Oki *et al*, 1999).

The above findings are in agreement with the results of combined invasive haemodynamic and TDI studies in human subjects with various cardiac diseases. TDI indices have been found to correlate very well with invasive haemodynamic

variables, thus they can be used as alternative tools in the non-invasive quantification of global systolic and diastolic function. Mitral annular E' or E' of the LVPW and the IVS along the radial axis of the heart have been shown to correlate negatively with tau in patients with various cardiac diseases and a wide range of diastolic and systolic performance (Oki *et al*, 1997; Sohn *et al*, 1997; Ohte *et al*, 1998). A positive association between annular E' and –dP/dt has been also documented in patients with coronary artery disease (Ohte *et al*, 1998). The correlation between annular E' and tau persisted even in patients with atrial fibrillation and an E' value of < 8 cm/sec could predict prolonged tau (> 50 msec) with high sensitivity and specificity (Sohn *et al*, 1999). Similarly, Se' and Q-Se' of the middle LVPW along the radial axis correlated positively and inversely, respectively, with –dP/dt in a group of patients with diverse cardiac disease (Yamada *et al*, 1998). Similar correlations, but less strong, were found between the above systolic TDI indices and –dP/dt in the IVS along the same axis (Yamada *et al*, 1998).

Other studies have confirmed the load independence of myocardial E' in the diseased state. In patients with an abnormal relaxation pattern of mitral inflow, saline loading changed the mitral inflow pattern towards the pseudonormalized pattern, whereas the septal annular E' and E'/A' remained unchanged (Sohn *et al*, 1997). Nitroglycerin infusion caused an increase in E deceleration time and a decrease in E/A of mitral inflow. However, E' and E'/A' did not change significantly. Furthermore, in patients with chronic ischaemic syndrome and pseudonormal LV filling pattern, standard Doppler filling indices were significantly affected by alterations in preload (Trendelenberg maneuvre, reverse Trendelenberg maneuvre, amylnitrate

administration), whereas early diastolic annular velocities recorded by pulsed TDI remained unaltered (Yalcin *et al*, 2002). Additionally, mitral annular E' had the strongest discriminating value in differentiating patients with normal from those with abnormal diastolic function and showed a significant and steady decline with progressive diastolic dysfunction, suggesting lack of a reversing effect caused by preload compensation (Farias *et al*, 1999). Similarly, the lateral annular E' and Se' were significantly reduced in patients with pseudonormal mitral inflow pattern compared to that in patients with an impaired relaxation pattern and normal subjects (Nagueh *et al*, 1997). In this study lateral annular E', E'/A', E' acceleration and E' deceleration were significantly reduced in the pseudonormalized and abnormal relaxation groups in comparison to those in the normal group.

The ability of non-invasive Doppler echocardiographic measurements to predict intracardiac pressures in the diseased state has been of major interest. Evidence would suggest that TDI is a very powerful tool in this respect. TDI indices have been found to predict with a relatively high accuracy, the level of LVEPD, in patients with diverse cardiac disease (Dagdelen *et al*, 2001). A lateral annular E'/A' > 1, an A' duration of 90 to 110 msec and an E' deceleration time of > 120msec have been shown to be the best discriminators for a LVEPD < 10 mm Hg, 10 to 15 mm Hg and > 15 mm Hg, respectively, with high accuracy. Additionally, the early diastolic mitral inflow to mitral annular velocity ratio (E/E') can correct for the influence of elevated LA pressures in transmitral E, and has been shown to correlate very strongly with LV filing pressures (Nagueh *et al*, 1997). The ability of E/E' to predict elevated LV filling pressures persisted even in atrial fibrillation and sinus tachycardia. E/E'

correlated strongly with LVEDP in patients with atrial fibrillation and an E/E' > 8cm/sec could predict elevated LVEDP > 15 mmHg with high sensitivity and specificity (Sohn *et al*, 1999). Moreover, E/E' could estimate PCWP with reasonable accuracy in sinus tachycardia even with complete merging of E' and A' velocity waves (Nagueh *et al*, 1998). The relation between E/E' and PCWP remains strong irrespective of the mitral inflow pattern and the LVEF (Nagueh *et al*, 1998). Septal annular E/E' also correlated strongly with pre-A LV pressure and it was the single predictor for mean LVDP in patients with wide range of EF (Kim *et al*, 2000; Ommen *et al*, 2000). E/E' of the tricuspid annulus could estimate with reasonable accuracy right atrial pressure (Nageh *et al*, 1999).

In addition to TDI predicting intracardiac pressures, there is also interest in it being able to discriminate between reversible and irreversible disease. Sohn and colleagues (2000) investigated the predictive value of A' in discriminating a reversible from an irreversible restrictive LV filling pattern. They showed that a septal annular A' > of 5 cm/sec could differentiate a reversible from an irreversible filling pattern in a highly sensitive and a specific manner, highlighting that the amplitude of A' is an indicator of LA contractility. Patients with reversible restrictive LV filling had a higher E', A' and A and also a lower E/A than patients with an irreversible pattern at baseline (before onset of treatment). Similarly, another study showed that, although E' of the lateral mitral annulus and of the LVPW along the long axis were similar in patients with an abnormal relaxation and those with a pseudonormal or a restrictive LV filling pattern, A' in the restrictive group was the lower among the three groups (Abe *et al*, 1999). Moreover, A' of the LVPW could discriminate the three affected and also the

normal group relatively well. The marked decrease in A' documented in the restrictive group was accompanied by a significant decrease in LA contractility and functional reserve of pulmonary venous system (decreased Ar) and also by a marked increase in PCWP.

C.2.4. Pulsed TDI in hypertrophic cardiomyopathy.

Numerous TDI studies have investigated LV dysfunction in HCM of humans. Changes in TDI indices indicative of abnormal relaxation properties, such as decreased E' and E'/A', prolonged E' deceleration and isovolumic relaxation are often encountered in all myocardial segments along both axes in patients with HCM (Oki *et al*, 1998b; Severino *et al*, 1998; Cardim *et al*, 2002a; Matsumura *et al*, 2002). The E'/A' reversal myocardial pattern seen in human HCM resembles the abnormal relaxation pattern of mitral inflow often recorded in patients with this disease. However, a poor association between myocardial and mitral inflow E/A ratio has been reported in patients with HCM, reflecting the different influence of loading on these two echocardiographic variables (Naqvi *et al*, 2001). Additionally, it has been shown that the degree of asynchrony is more marked in patients with HCM than in normal subjects (Oki *et al*, 2000; Cardim *et al*, 2002a). The time from the aortic component of the second heart sound to peak E' it has been found to be markedly prolonged in patients with HCM, not only in the hypertrophied IVS, but also in the non-hypertrophied LVPW (Oki *et al*, 2000). Based on these findings it was speculated that abnormalities in LV relaxation in HCM are determined by the severity of regional LV asynchrony and that the typical pathologic alterations seen in this cardiac entity also are present in the nonhypertrophied myocardial segments (Oki

et al, 2000). A decreased mitral annular A' wave has been reported in patients with HCM and it was believed to reflect intrinsic atrial disease (Cardim *et al*, 2002a). However, an increased late diastolic myocardial velocity has been reported in other studies, probably reflecting increased atrial response to the elevated LA pressures (Cardim *et al*, 2002c).

Comparing the annular motion between patients with obstructive HCM and those with the non-obstructive form of the disease, Cardim and colleagues (2002d) showed that there was no differences in annular Se', E' and E'/A' between the two groups, although the presence of obstruction was associated with a significant increase in the number of annular sites with an E'/A' < 1, especially in the septal and anterior annular regions. Increased incidence of E'/A' < 1 in these annular sites in patients with the obstructive form of the disease was attributed to the increased load dependence of the septal annular side. Thus, quantification of the lateral mitral annulus was suggested when detection of pseudonormalization of the mitral inflow is sought (Cardim *et al*, 2002d).

A number of findings derived by TDI measurements have highlighted the presence of systolic dysfunction in HCM of humans. These findings, along with experimental data, led many investigators to implicate systolic dysfunction as the primary deficit of HCM, responsible for inducing compensatory hypertrophy and fibrosis through the release of growth and mitotic factors (Marian *et al*, 1995b; Marian *et al*, 1997; Marian and Roberts, 2001; Marian, 2000; Li *et al*, 1997; Rust *et al*, 1999; Roberts and Sigwart, 2001; Li *et al*, 2002; Ortlepp *et al*, 2002). Decreased peak systolic myocardial velocities and prolonged Q-Se' in the middle IVS and the LVPW along

both axes have been documented in HCM patients, with a more prominent decrease in Se' along the longitudinal axis (Oki *et al*, 1998b; Tabata *et al*, 2000). Another study has shown that Se' and Sl' of the LVPW and Se' of the IVS were decreased in HCM patients when compared with those from normal subjects only along the longitudinal axis, and not along the radial axis (Mishiro *et al*, 2000). Interestingly, systolic impairment has been documented not only in the hypertrophied IVS, but also in the non-hypertrophied LVPW (Tabata *et al*, 2000). Impaired contractility, as assessed by TDI in HCM patients, was impaired even in the presence of a normal or supernormal FS% or EF% (Oki *et al*, 1998b; Cardim *et al*, 2002a). Impairment of systolic and also diastolic function was evident in mitral annular regions adjacent to walls with and without myocardial hypertrophy, excluding hypertrophy as the sole causal factor for these findings (Cardim *et al*, 2002a). These observations further were supported by the findings of Mishiro and colleagues (2000), who showed that increased afterload induced by angiotensin II infusions resulted in a more prominent decrease in Se' and Sl' in the non-hypertrophied LVPW along both axes in comparison to the decrease seen in normal subjects.

Although decreased systolic velocities have been reported in humans with HCM, this finding is not reported consistently in all studies. Severino and colleagues (1998) failed to show differences in Se' of the middle IVS and the LVPW along the long axis between normal and HCM subjects. Ho and colleagues (2002) found that decreased systolic annular velocities were present only in carriers of β-myosin heavy chain mutations with LV hypertrophy and not in those without LV hypertrophy. The fact that systolic impairment is not always evident in HCM of humans may reflect differences in the effect that certain mutations have in the contractile state of

sarcomere proteins. Although, it has been reported that some mutations are associated with impaired sarcomere contractility (Marian *et al*, 1995b; Marian *et al*, 1997; Marian and Roberts, 2001; Marian, 2000), other experimental studies, particularly those evaluating β-MHC mutations, have shown that a hypercontractile state is induced by certain sarcomere mutations (Palmiter *et al*, 2000; Tyska *et al*, 2000; Witt *et al*, 2001). This latter finding may explain the hypercontractile LV state seen often in HCM and the lack of significant reduction in systolic TDI indices reported by some studies in humans with this particular disease.

Recent studies have tried to investigate the ability of TDI in predicting affected genotype in HCM. This is of particular importance because, although HCM is conventionally diagnosed by the presence of unexplained LV hypertrophy, this is neither a sensitive nor an early marker for the disease (Nagueh *et al*, 2000; Nagueh *et al*, 2001a). Because of the variable penetrance (Fananapazir and Epstein, 1995), and the confounding effects of modifier genes (Brugada *et al*, 1997), sex (Abchee and Marian, 1997), and environmental factors, LV hypertrophy is absent in a significant number of mutation carriers. Moreover, LV hypertrophy is minimal in individuals with HCM due to certain mutations, such as those in cardiac troponin T, despite such patients having a high incidence of sudden death (Marian and Roberts, 2001). An alternative non-invasive diagnostic tool capable of detecting mutation carriers, irrespective of hypertrophy, could help in the early prevention and modification of the clinical history of the disease. TDI has shown great promise regarding this aspect. In a study by Nagueh and colleagues (2001a), it was shown that patients with familial HCM and LV hypertrophy and also mutation carriers without LV

hypertrophy, had reduced Se' and E' velocities at both septal and lateral corners of mitral annulus, in comparison with normal subjects. However, TDI velocities were lowest in the HCM group with LV hypertrophy. Lateral and septal annular E' and Se' both had a sensitivity and specificity between 90% and 100% in distinguishing between abnormal nonhypertrophied and normal genotype. Similar findings have been reported in the mutant β-MHC-Q^{403} transgenic rabbit model of human HCM (Nagueh *et al*, 2000). Low systolic and early diastolic LV myocardial velocities along the longitudinal axis have been reported in a family with a missense mutation in the myosin binding protein C gene (Arg 502 Gln), in the absence of LV hypertrophy (Cardim *et al*, 2002c). However, in a study by Ho and colleagues (2002), there was a substantial overlap in mitral E' between mutation carriers with no LV hypertrophy and control subjects.

TDI has also been used to investigate right ventricular involvement in humans with HCM (Galderisi *et al*, 2001). Patients with asymptomatic HCM (class I and II) have decreased E' and E'/A', increased A' and prolonged E' deceleration and IVR times in tricuspid annulus when compared with normal subjects. The commonly absent IVRt in tricuspid annular motion in normal subjects (IVRt is seen in only 53%) was present in all HCM patients. It has been speculated that RV relaxation abnormalities in HCM might be due to the extension of myopathic process to walls other than that of the IVS (Galderisi *et al*, 2001; D'Andrea *et al*, 2003). In 34 patients with asymmetric septal hypertrophy and no evidence of hypertrophy in the free wall of the RV, quantification of the middle free wall of the RV along the longitudinal axis

revealed that the only altered TDI index in the HCM group was the prolonged IVRt (Severino *et al*, 2000).

A further major interest, however in TDI is its application in evaluating cardiac function in athleticism. Pulsed TDI has managed to discriminate between pathologic hypertrophy and physiologic hypertrophy induced by athleticism. Both systolic and diastolic annular TDI indices were impaired in patients with HCM even in sites adjacent to walls without hypertrophy (Cardim *et al*, 2002b). In athletes the E'/A' was never < 1. In HCM patients E'/A' was < 1 in 27% of annular sites (Cardim *et al*, 2002b). Patients with pathologic hypertrophy due to HCM and hypertension had lower systolic and early diastolic mitral annular velocities than athletes (Vinereanu *et al*, 2001). However, velocities along the radial axis did not differ between the two groups. A mean annular (mean from 4 annular sites) systolic velocity of > 9cm/sec could discriminate between pathologic from physiologic hypertrophy with a sensitivity of 87% and specificity of 97% (Vinereanu *et al*, 2001).

TDI has also been used to a limited extend, to assess drug response. The influence of cibenzoline (class Ia antiarrhythmic drug) and bisopropol in LV diastolic function in patients with obstructive and non-obstructive HCM was investigated by Kondo and colleagues (2001). After cibenzoline administration, the E/FPV and E/E' were significantly reduced and the lateral annular E' increased in both HOCM and non-obstructive HCM groups. However, TDI indices did not change with bisopropol in the HCM group, but they did change in the HOCM one. The above findings led the investigators to suggest that the direct lusitropic effects of cibenzoline rather the

reduction in afterload might have contributed to the improvement of diastolic function in HOCM cases.

C.2.5. Pulsed TDI in Restrictive cardiomyopathy and Constrictive pericarditis

Differentiating constrictive pericarditis (CP) from restrictive cardiomyopathy (RCM) is crucial for choosing the appropriate therapy (Schoenfeld *et al*, 1987). Various hemodynamic, M-mode, 2D and Doppler echocardiographic criteria have been used to differentiate these cardiac entities (Khuller and Lewis, 1976; Tyberg *et al*, 1981; Hirota *et al*, 1983; Vaitkus and Kussmaul, 1991). However, differentiation of constrictive from restrictive heart disease, remains challenging, since a significant overlap exists among the commonly used diagnostic techniques and in human patients surgical exploration in often utilized (Vaitkus and Kussmaul, 1991). TDI has shown promise as an alternative non-invasive tool in distinguishing between these two cardiac diseases with high accuracy. Patients with constrictive pericarditis (CP) have a significantly higher early diastolic and systolic lateral annular velocity than normal subjects and patients with RCM (Garcia *et al*, 1996b; Rajagopalan *et al*, 2001). A peak E' lateral annular velocity > 8 cm/sec could discriminate between patients with CPC and RCM with a sensitivity of 89% and specificity of 100% (Rajagopalan *et al*, 2001). The acceleration and deceleration rates of E' are also significantly higher in patients with constrictive pericarditis compared to those in normal subjects and patients with RCM. Exaggerated longitudinal motion reflected as increased E' annular velocity in patients with constrictive pericarditis was attributed to limited lateral expansion of the entire heart by the constricting pericardium (Ha *et al*, 2001). However, higher E' and shorter Q-E' have been

recorded in the middle regions of the IVS and the LVPW along both axes in patients with CP compared to that in normal subjects, confounding further the explanation of high early diastolic velocities in patients with CP (Oki *et al*, 1998a). In contrast to the positive correlation found between E/E' and LV filling pressures in patients with primary myocardial disease, it has been shown that in patients with CP the E/E' ratio is inversely associated with PCWP and LVEDP (Ha *et al*, 2001). Hence, the term "annulus paradoxous" was proposed to describe the paradoxical behaviour of the mitral annulus in CP (Ha *et al*, 2001).

TDI studies in humans with restrictive cardiomyopathy have shown reduced early diastolic velocities along both axes of the heart compared to that in normal subjects (Garcia *et al*, 1996b; Koyama *et al*, 2002). Koyama and colleagues showed that cardiac amyloidosis is initially characterized by impaired early relaxation, but the presence of CHF was associated mainly with impairment of LV contraction along the longitudinal axis (decreased annular systolic velocities), even when FS was normal (Koyama *et al*, 2002). Consequently, it was suggested that CHF in cardiac amyloidosis is also the result of systolic longitudinal dysfunction and is not attributed exclusively to diastolic impairment.

C.2.6. Pulsed TDI in human dilated cardiomyopathy

TDI has been used in the investigation of human DCM. TDI indices such as Se' and Sl' have been found to correlate strongly with dP/dt and LVEF, suggesting that they could be used as alternatives in the non-invasive assessment of myocardial function in DCM. Se' along the longitudinal axis and Sl' along the radial axis showed the

strongest correlation with dP/dt (Mishiro *et al*, 1999). Impaired contractility in patients with DCM has been expressed with lower early and late diastolic myocardial velocities in the LVPW and also the IVS along both axes of the heart (Yamada *et al*, 1998; Mishiro *et al*, 1999). Se' of the middle IVS along the radial axis has been found to be lower in DCM patients than in patients with HCM, hypertension, patients with ischemic heart disease and normal subjects. However, the discriminatory ability of Se' of the LVPW along the radial axis was minimal for the above diseased groups (Yamada *et al*, 1998). In one study, it was shown that, although in control subjects Se' in the LVPW along the longitudinal axis was significantly greater than Se' and Sl' along the radial axis, and Sl' along the radial axis was significantly greater than Sl' along the longitudinal axis, in DCM patients these relationships between Se' and Sl' were lost (no significant differences were seen between Se' and Sl' along both axis). The delayed peak of early and late systolic myocardial velocities is another indicator of abnormal contractile state in humans with DCM (Yamada *et al*, 1998; Mishiro *et al*, 1999).

Interestingly, it has been documented that signs of CHF in a group of patients with DCM were exclusively related to diastolic failure and not to a transient deterioration of systolic function (Richartz *et al*, 2002). It has been shown that at baseline, mitral annular E' was lower in DCM patients with CHF than in asymptomatic DCM patients and healthy individuals. Se' was higher in normal subjects than in both the DCM subgroups. There was not significant difference in Se' between the latter two groups. Clinical improvement after medication in the symptomatic DCM group was accompanied by a gradual increase of E', but not of LVEF or Se'. With improving

symptoms the E'/Se' in the CHF group became > 1 within 3 days, whereas E'/Se', E', Se', remained unchanged during the following up period in the group with stable clinical condition. The above results show that loss of ventricular compliance is the main determinant of signs of CHF in DCM rather than terminal deterioration of systolic function.

C.2.7. Pulsed TDI in patients with heart failure and preserved global systolic function

Two studies have shown that systolic dysfunction, as assessed by TDI echocardiography, is evident in patients with CHF even in the presence of normal LV EF%. Decreased mitral annular systolic velocities were recorded in a group of patients with variable cardiac disease and normal LV EF% (> 45%) and also significant LV hypertrophy (Yip *et al*, 2002). However, in these patients early diastolic annular velocity was reduced to a greater extent than Se'. Similarly, decreased Se', E' and A' mitral annular velocities were documented in patients with heart failure and preserved global systolic function (LV EF% > 45%) (Nikitin *et al*, 2002). These findings show that TDI indices are a more accurate means in assessing the contractile state of the LV in comparison to traditional echocardiographic methods.

C.2.8. Temporal relation between myocardial motion and flow

The use of TDI has helped our understanding of the temporal relationship between mitral inflow and LV myocardial motion in the normal and diseased myocardium. Doppler and TDI echocardiographic studies in normal individuals have shown that

the onset of early diastolic annular motion either precedes or coincides with the onset of early diastolic mitral inflow wave and that peak annular early diastolic velocity precedes the corresponding peak of mitral inflow (Rodriguez *et al*, 1996; Pai and Gill, 1998; Onose *et al*, 1999b; Naqvi *et al*, 2001). Similarly, it has been shown that the onset of both the late diastolic and systolic annular velocities precedes the onset of late diastolic mitral inflow and that of LV ejection respectively (Pai and Gill, 1998). These findings prove that under physiological circumstances, it is the early myocardial activation, which governs the timing of blood flow events. In contrast, in the diseased state these temporal relationships are altered. In patients with various cardiac diseases, it has been shown that the onset and peak of the early diastolic wave of mitral inflow precede those of early diastolic mitral annulus motion (Rodriguez *et al*, 1996; Onose *et al*, 1999b; Naqvi *et al*, 2001). In the presence of impaired diastolic recoil, which causes a delayed onset of myocardial relaxation, high LA pressures lead to an earlier opening of the mitral valve (Rodriguez *et al*, 1996; Onose *et al*, 1999b).

C.2.9. Pulsed TDI in the assessment of cardiac function in systematic diseases.

TDI has also been used in the evaluation of myocardial properties in patients with systematic diseases, such as acromegaly and hyperthyroidism. In patients with active acromegaly, the E' and E'/A' of the septal mitral annulus have been shown to be significantly reduced in comparison to that in control subjects and patients with stable acromegaly (Bruch *et al*, 2002). E' and E'/A' ratio could identify patients with active acromegaly with a relatively high sensitivity and specificity. In another study reduced E'/A' and prolonged IVRt were recorded in the basal segments of the lateral,

posterior and septal walls of patients with active acromegaly along the long axis (Mercuro *et al*, 2000). Se' of the basal lateral wall in acromegalic patients was decreased when compared with that from normal subjects. Moreover, in patients with subclinical hyperthyroidism, mitral annular TDI indices, such as Q-bS', IVRt and Q-bS' were reduced significantly in comparison to that of normal individuals (Vitale *et al*, 2002). However, the overlap in TDI indices between the two groups was large. Of comparative interest is that impaired myocardial properties are believed to be caused by a number of systematic diseases in cats. However, evidence for this is limited. TDI may be proved a useful tool in the assessment of myocardial dysfunction in systemic diseases of this species.

C.3. Colour M-mode TDI

Colour M-mode TDI is one of the applications of the TDI technique, which has been used widely in various clinical and experimental settings for quantification of myocardial motion (Palka *et al*, 1995; Palka *et al*, 1997a; Palka *et al*, 1997b; Palka *et al*, 1999; Palka *et al*, 2002; Zamorano *et al*, 1997; Dutka *et al*, 2000). The high temporal resolution and signal to noise ratio of this particular mode offers advantages over other applications of the TDI technique. Although 2D TDI mode enables the simultaneous quantification of myocardial motion in different areas of the LV wall, it often provides poor temporal resolution and has a low signal to noise ratio (Garot *et al*, 1998). This can result in underestimation of myocardial velocities and failure to quantify accurately myocardial motion during short duration events, especially with high heart rates (often encountered in cats). Pulsed TDI offers high temporal resolution, but allows only the estimation of instantaneous myocardial velocities,

which can be affected by overall heart motion and motion of adjacent myocardial areas (Shimizu *et al*, 1998). The use of colour M-mode TDI allows the calculation of MVG, which describes the spatial distribution of transmyocardial velocities throughout the myocardium from endocardium to epicardium and reflects wall thickness changes during diastole and systole (Fleming *et al*, 1994b). Under normal circumstances the contribution of the endocardial area in the wall thickening and thinning during systole and diastole respectively, is greater compared to that of the epicardial area (Myers *et al*, 1986). This results in a physiologic velocity gradient between endocardium and epicardium. Traditionally, quantification of regional myocardial function was based on either the visual qualitative assessment of myocardial motion using 2D images or the calculation of the rate of change of wall thickening and thinning by M-mode echocardiography. However, the former approach is based on the assessment of morphological features without taking into consideration the true structural and functional properties of the myocardium and it is subject to the temporal limitations of human vision, which makes it difficult to assess myocardial motion during short duration events (Kvitting *et al*, 1999). Although a series of studies have proved the usefulness of assessment of wall thickness changes in investigating LV properties in different human cardiac diseases, the calculation of the rate of thinning and thickening from digitized M-mode images has some inherent disadvantages (Sutton *et al*, 1978; Traill *et al*, 1978; Lee *et al*, 1991; Carvalho *et al*, 1996). Firstly, it is based only on the displacement of endocardial and epicardial borders and therefore does not accurately reflect changes within the myocardium. Furthermore, it is highly dependent on the clear identification of the cardiac boundaries, which sometimes are blurred or ambiguous. Additionally, it is affected

by the overall heart motion (Fleming *et al*, 1994b). On the other hand, the calculation of MVG from colour M-mode TDI images is based on the estimation of myocardial estimates along the entire thickness of the myocardium. Therefore, MVG more accurately depicts the inherent properties of the myocardium, presuming that myocardial velocity estimates reflect the structural and functional characteristics of different points along it. Moreover, the estimation of MVG is independent of the accurate identification of endocardial and epicardial borders, since it is the slope of the linear regression of velocity estimates and it is also not affected by translational effects (Fleming *et al*, 1994b; Uematsu *et al*, 1997). In contrast to mitral inflow pattern, which is subject to loading changes and therefore can be masked by increased LV filling pressures, so switching to a pseudonormal pattern, early diastolic MVG has been shown to be independent from preload increases in the diseased state (Shimizu *et al*, 1998; Shimizu *et al*, 2003). Additionally, MVG correlates strongly with invasive hemodynamic indices, such as the peak positive and negative pressure development (dP/dt) and the time constant of pressure decay in isovolumetric relaxation (tau), suggesting that apart from being a very sensitive tool in assessing regional myocardial function, it can also reflect global systolic and diastolic properties (Oki *et al*, 2000; Ueno *et al*, 2002). The sensitivity of MVG in quantifying myocardial properties has been shown in variable cardiac settings. MVG has managed to discriminate between hypertrophy of different aetiologies (HCM from left ventricular hypertrophy induced by hypertension and athleticism) and between restrictive cardiomyopathy and constrictive pericarditis (Palka *et al*, 1997a; Palka *et al*, 2000). Its application was particularly useful in detecting wall motion abnormalities in ischaemic myocardial segments, especially when visual assessment

failed to do so, and also in differentiating the extent of experimentally induced infarction (transmural from endocardial) (Gorcsan *et al*, 1998; Derumeaux *et al*, 2001; Marcos-Alberca *et al*, 2002). Recently, MVG was used in the assessment of regional functional effects of transplanted skeletal myoblasts in an experimentally induced infarcted area in the LV of a sheep model (Ghostine *et al*, 2002). The use of MVG also allowed the quantification of myocardial function in various cardiac diseases, such as dilated cardiomyopathy, cardiac amyloidosis, hypertensive cardiomyopathy, Friedreich's ataxia and coronary artery disease (Palka *et al*, 1997a; 2002; Dutka *et al*, 2000; Tsutsui *et al*, 2000; Iwakami and Numano, 2001). In one of the few applications of colour M-mode TDI in animals, Chetboul and colleagues (2001) showed that peak systolic MVG could identify early and accurately the dystrophin mutant Golden Retriever Muscular Dystrophy dogs, despite normal echocardiographic findings (LV dimensions and FS%).

SECTION D

Pulsed Doppler Tissue Imaging in normal cats and cats with hypertrophic cardiomyopathy: assessment of myocardial motion along the radial and longitudinal axis

D.1. Introduction

Hypertrophic cardiomyopathy of cats is the most common cardiac disease of this species, and by convention is characterised by a concentrically hypertrophied, non-dilated left ventricle, in the absence of other systematic diseases know to cause left ventricular hypertrophy (Atkins *et al*, 1992a; Bright *et al*, 1992; Fox *et al*, 1995). HCM of cats appears to be a hereditary cardiac disorder, which is transmitted as an autosomal dominant trait, and shares many morphological characteristics in common with human HCM (Fox *et al*, 1995; Kittleson *et al*, 1999). Diastolic impairment is believed to be the main abnormality of the disease (Atkins *et al*, 1992a; Bright *et al*, 1992; Fox *et al*, 1995; Kittleson *et al*, 1999) and evidence for this has been provided by both invasive and Doppler echocardiographic studies (Golden and Bright, 1990; Bright *et al*, 1999). Tissue Doppler Imaging has emerged in the last decade as an alternative tool for the non-invasive quantification of regional and global myocardial function (McDicken *et al*, 1992; Ohte *et al*, 1998; Yamada *et al*, 1998; Mishiro *et al*, 1999; Sohn *et al*, 1999). Its use offered a unique opportunity for the direct quantification of myocardial motion, as opposed to the indirect assessment of myocardial function using morphological, 2D characteristics and Doppler derived indices (McDicken *et al*, 1992; Miyatake *et al*, 1995). It has been shown that TDI

indices correlate very well with global systolic and diastolic invasive haemodynamic variables and that they are independent from changes in preload in the diseased state (Nagueh *et al*, 1997; Sohn *et al*, 1997; Ohte *et al*, 1998; Yamada *et al*, 1998; Farias *et al*, 1999; Sohn *et al*, 1999; Yalcin *et al*, 2002). TDI indices have been shown to correlate well with invasive hemodynamic parameters in normal anaesthetised cats, showing promise in the non-invasive quantification of myocardial function in feline cardiac diseases (Schober *et al*, 2003). Recently, in the first application of TDI in cats, Gavaghan and colleagues (1999) showed that cats with HCM had decreased myocardial diastolic velocities, acceleration and deceleration and also prolonged isovolumic relaxation time (IVRt). These findings offered further evidence for diastolic impairment in HCM of this species. The recent wide application of TDI in humans with HCM also has revealed interesting aspects in the pathophysiology of the disease (Cardim *et al*, 2002a; Cardim *et al*, 2002b; Cardim *et al*, 2002d; Severino *et al*, 1998; Mishiro *et al*, 2000; Oki *et al*, 2000; Tabata *et al*, 2000; Nagueh *et al*, 2001a; Ho *et al*, 2002; Matsumura *et al*, 2002). Apart from the classical diastolic changes, such as decreased early diastolic velocities and prolonged IVRt, the presence of marked asynchrony in myocardial motion in different parts of the LV wall has also been detected and it is believed to be another significant determinant of diastolic impairment in HCM (Oki *et al*, 2000). Furthermore, in contrast to traditional techniques, which consider diastolic dysfunction as the main abnormality of the disease, TDI studies have shown that systolic impairment is also evident in human HCM, despite the normal or supernormal contractile state of the LV in this cardiac entity (Oki *et al*, 1998b; Mishiro *et al*, 2000; Tabata *et al*, 2000; Nagueh *et al*, 2001a; Cardim *et al*, 2002a; Ho *et al*, 2002). Based on these findings and findings

from experimental studies, some investigators suggested that systolic dysfunction may be the primary abnormality of the disease, which leads to the classical pathological changes seen in HCM (Marian *et al*, 1995b; Marian *et al*, 1997; Marian and Roberts 2001; Marian, 2000; Li *et al*, 1997; Rust *et al*, 1999; Nagueh *et al*, 2000; Roberts and Sigwart, 2001; Li *et al*, 2002; Ortlepp *et al*, 2002). These results emphasise the need for investigating HCM of cats in a more detailed way. Using a purpose designed 7.4 MHz transducer equipped to record pulsed TDI, the aim of this study was to quantify feline myocardial motion in multiple myocardial segments in a larger number of cats with HCM than previously attempted. It was hoped this would offer new insights in to the pathophysiologic mechanisms of the disease, thereby helping to better define therapeutic regimes for future use.

D.2. Materials and methods

D.2.1 Study group

The study population comprised 25 normal cats, which were pets of staff and students of the Royal (Dick) School of Veterinary Studies the University of Edinburgh and 23 cats with HCM, which were referred to the Cardiopulmonary Service of the R(D)SVS for cardiac investigation. None of the normal cats had evidence of cardiovascular or other significant abnormalities on clinical examination. All normal cats underwent a complete standard 2D, M-mode and colour flow and spectral Doppler echocardiographic examination and were found to have echocardiographic results within normal published limits (Sisson *et al*, 1991; Fox *et al*, 1995). All normal animals above seven years of age and all affected animals underwent haematology and biochemical testing, and had values within reference

ranges. Cats with azotaemia and elevated total thyroxine hormone (T4) were excluded. All cats from both groups had systolic blood pressure measured by the Doppler technique and were found to be normal (< 180 mm Hg). The method followed to measure the blood pressure has been described in Section B.

Affected cats also had a complete standard echocardiographic examination. Diagnosis of HCM was made on the basis of LV thickness ≥6 mm on 2D or M-mode echocardiography, in the absence of volume overload (no obvious valvular abnormalities) and systemic diseases known to cause LV hypertrophy (Fox *et al*, 1995). All affected cats were in sinus rhythm except one, which had atrial fibrillation. Nineteen animals with HCM were asymptomatic and one was receiving β-blockers. Four affected animals were in congestive heart failure at the time of evaluation and were being treated with a combination of diuretics, ACE inhibitors with or with out β-blockers. No drug withdrawal was done prior to assessment. All animals were unsedated.

D.2.2. Conventional echocardiography

Conventional echocardiographic and Doppler examination was carried out in the cardiopulmonary service of the Royal (Dick) School of Veterinary Studies. Echocardiographic examination was performed using an Esaote SIM 7000 Challenge ultrasound system (Esaote Biomedica, Firenze, Italy) with a 7.5 MHz phased array transducer. Images were recorded onto S-VHS videotapes by a videocassette recorder (SV0-9500MDP; Sony Corporation, Japan). The method followed to

acquire conventional and Doppler echocardiographic measurements has been described in Section B.

D.2.3. Tissue Doppler Imaging echocardiography

TDI measurements were obtained from all animals in the Medical Physics and Engineering Department of the University of Edinburgh the evening of the same day that conventional echocardiography was carried out in the Cardiopulmonary Service of the R(D)SVS. All pulsed TDI recordings were made with an ATL HDI 5000 ultrasound system (ATL Bothell, Washington, USA) using a 7.4 MHz phased array transducer, which used prototype TDI software. Off-line analysis of the images was done using a special analysis software (HDIlab) developed by ATL Bothell, Washington, USA.

Animals were scanned unsedated and manually restrained in lateral recumbency on a purpose-designed table, which allowed placement of the transducer on the dependant part of the thorax from below through a hole. A simultaneous ECG was recorded (lead II) using adhesive electrodes, which were attached to the main pads of the feet and secured with tape.

The sector width and depth setting were adjusted to include the entire heart in the screen and to maximize the cardiac image. Overall gain and time gain compensation controls were set to optimize the image quality. A 2-dimensional guided 1 mm sample volume was placed on the subendocardial portions of the intraventricular septum and the LV free wall at chordae tendineae level in the 4 chamber apical view

(Figure D1). The septal and lateral corner of the mitral annulus and also the tricuspid annulus were sampled using the same echocardiographic view (Figure D1). In the right parasternal long axis view, the sample volume was placed on the mid-wall portions of the IVS and the LV free wall at chordae tendineae level (Figure D1). The Nyquist limit was adjusted to achieve maximum velocity signal while avoiding aliasing. Gain was optimized to reduce noise and the maximum sweep rate was used (values obtained every 3 msec).

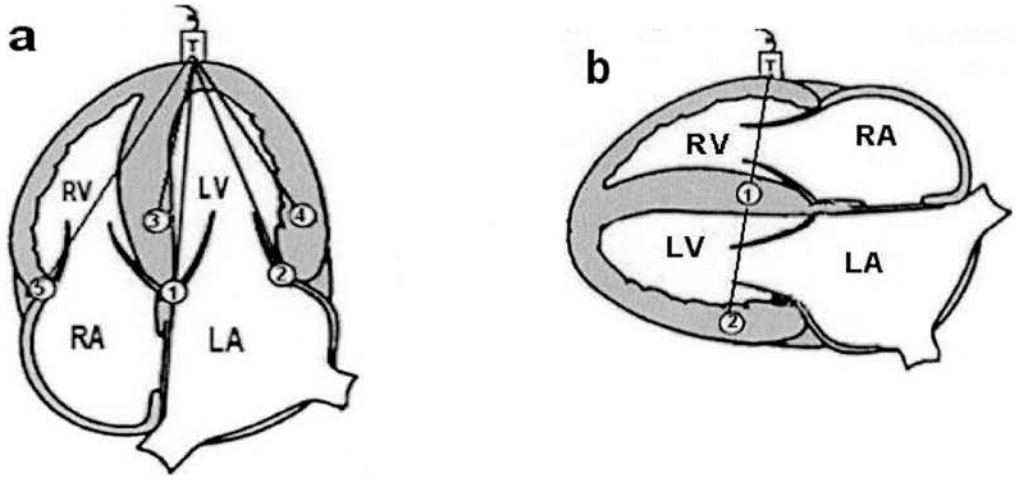

Figure D 1. *Sample volume recording of motion velocity patterns along the longitudinal (4-chamber apical view) (a) and the radial (right parasternal long axis view) (b) axis. Sample volumes (white circles) were set on the septal (1) and lateral (2) mitral annulus, on the tricuspid annulus (5) and on the subendocardial portions of the interventricular septum (3) and the left ventricular free wall (4) at chordae tendineae level using the 4-chamber apical view. Sample volumes were also set on the midwall of the interventricular septum (1) and the left ventricular free wall (2) at chordae tendineae level on the right parasternal long axis view.*

On the basis of myocardial velocity patterns recorded from all myocardial segments, assessment of certain pulsed TDI indices was carried out as follows (Figure D2). The velocity wave recorded during LV ejection (at the end of the QRS complex and ending at the end of the T wave of the ECG) was the systolic (S') component of myocardial motion. Se' and Sl' were the peak early and late systolic velocities, respectively. Se' acc and tSe' acc. were the mean early acceleration (measured from the beginning of S' wave to Se') and time of mean acceleration of S' respectively. bS'-Sl' was the time from the beginning of S' to Sl'. E' and A' were the early and late diastolic velocities corresponding to early diastolic relaxation and atrial contraction, respectively. Mean acceleration (E' acc) and deceleration (E' dec) of the E' wave were recorded from the beginning and the end of this wave to its peak, respectively. Acceleration (tE' acc) and deceleration (tE' dec) times were the corresponding times of E' acc and E' dec, respectively. When E' and A' waves were partially summated, then only their peaks were measured. In cases of full summation the peak velocity of the summated wave (EA') was measured. However, EA' values were excluded from further analysis. When possible, the ratio of E' to A' wave (E'/A') was calculated from each pulsed TDI tracing. The biphasic oppositely directed and brief duration shifts during the 2 isovolumic periods were the IVCa and IVCb for the isovolumic contraction and IVRa and IVRb for the isovolumic relaxation phases, respectively. Only IVCb values were included in the analysis. Isovolumic contraction time (IVCt) was measured from the end of A' wave to the beginning of S' wave and isovolumic relaxation time from the end of S' wave to the beginning of E' wave. The time from the Q wave of the ECG to the beginning of S', E' (Q-bS', Q-bE') and also to their peaks (Q-Se', Q-Sl', Q-E') was recorded. Similarly, the time from the Q wave of the

ECG to A' (Q-A') was measured. The time from the end of S' wave to peak early diastolic velocity (II-E') and the time from the end of late diastolic wave to early systolic peak (I-Se') were also measured. Velocity time integrals (VTI) and duration of S', E' and A' were also measured. In the latter two, this was only done when a full separation between the two waves was achieved. All TDI indices were calculated from the mean of at least six cardiac cycles. In the single cat with atrial fibrillation, the mean of twelve cardiac cycles was used.

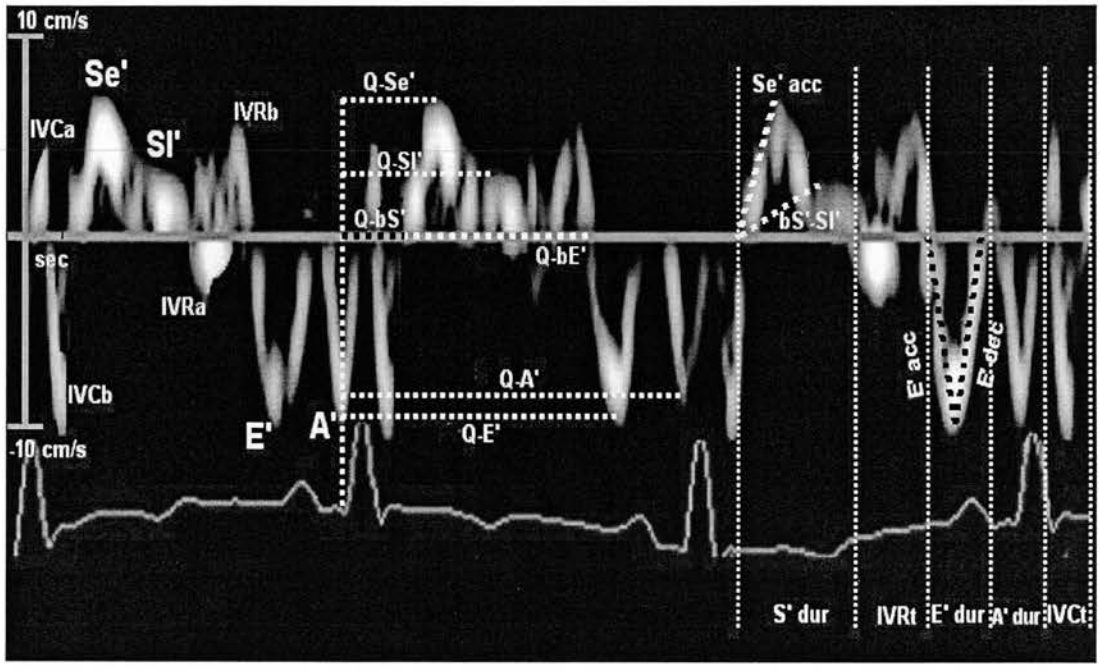

Figure D 2. *Pulsed TDI tracing obtained from the LVPW along the longitudinal axis of a 7-year-old cat. Se': peak early systolic velocity, Sl': peak late systolic velocity. E': peak early diastolic velocity. A': peak late diastolic velocity. IVCa and IVCb: myocardial shifts during the isovolumic contraction period. IVRa and IVRb: myocardial shifts during the isovolumic relaxation period. Q-Se': time from the Q wave of the ECG to Se'. Q-Sl': time from the Q wave to Sl'. Q-bS': time from the Q wave to the onset of the systolic wave. Q-bE': time from the Q wave to the onset of E' wave. Q-A': time from the Q wave to A'. Q-E': time from the Q wave to E'. S' dur: duration of systolic velocity. IVRt: isovolumic relaxation period. E' dur: duration of early diastolic velocity. A' dur: duration of late diastolic velocity. IVCt: isovolumic contraction period. Se' acc: mean early systolic acceleration. bS'-Sl': time from beginning of S' wave to peak late systolic velocity. E' acc: early diastolic acceleration. E' dec: early diastolic deceleration.*

D.2.4. Statistical analysis

Statistical analysis was carried out by using Genstat^{TM} 5 (release 3, Rothmsted experimental station, U.K) and SigmaStat (V2.03; SPSS Inc 1997). Values are expressed as the mean ± standard deviation. Analysis of covariance was used to control TDI indices for R-R, age, weight and sex. A t-test was used to compare values between the two groups. Comparisons between the two groups were repeated by excluding from the analysis affected cats with CHF. To assess the influence of left ventricular outflow tract obstruction on systolic TDI indices, only affected cats with outflow tract pressure gradient < 4 mm Hg and without evidence of SAM of the mitral valve were considered. Stepwise regression analysis was used to assess the influence of R-R, age, weight, sex and thickness on TDI indices. Multiple linear or linear regression analysis was used to assess the association of independent predictors on TDI indices in both groups. For the purposes of regression analysis, male cats were defined as number 1 and female cats as number 2. A t test or a Mann-Whitney Rank Sum test was used to compare TDI variables between male and female cats within the same group when sex was found to be a significant predictor in linear or multiple linear regression analysis. Time intervals were controlled for heart rate (divided by the square root of the RR interval) before were compared between male and female cats. A Kolmogorov-Smirnov test was used to assess the distribution of variables. To achieve normality of non-normally distributed variables logarithmic transformation was used. A p value of < 0.05 was considered statistically significant.

D.3. Results

D.3.1. Study population

Normal cats (n=25) of the following breeds were included in the study: 21 Domestic Short-haired, 1 Domestic Semilong-haired, 1 Maine-coon, 1 Abyssinian, 1 Siamese (12 female and 13 male neutered cats). Mean (± sd) for body weight was: 4.56 ± 0.8 Kg. All normal cats were in good body condition (none were obese or excessively thin). Their mean (± sd) age was 6 ± 3.5 years, with ages ranging from 10 months to 14 years. The mean (± sd) heart rate measured by the RR interval recorded during the acquisition of images from at least 6 cardiac cycles was 150 ± 26 bpm. Affected cats (n=23) consisted of the following breeds (22 Domestic Short-haired and 1 Persian; 4 female and 19 male neutered cats) had a mean (± sd) of body weight of 5.2 ± 1 Kg, mean (± sd) of age 6.9 ± 3 years (range: 1 to 12 years) and their HR was 158 ± 35 bpm.

D.3.2. Conventional echocardiography

The results of the LV M-mode measurements are displayed in Table D1. Thickness of the IVS and the LVPW at chordae tendineae level were significantly higher in the HCM group than in the normal group ($p<0.001$). Although affected animals appeared to have higher FS% than normal animals this difference did not reach statistical significance. In 10 cats the outflow tract pressure gradient was < 4 mm Hg (mean Ao.v ± sd: 0.85 ± 0.14), in 8 animals was > 4 mm Hg (mean Ao.v ± sd: 3.18 ± 1.47) and in 5 it was technically impossible to acquire good quality aortic velocity envelopes. In this latter group, 4 animals had systolic anterior motion of the mitral valve. CFDE identified mitral regurgitation in 19 HCM cats.

Table D 1. M-mode measurements (mean ± SD) of normal (n=25) and HCM cats (n=23)

	normal	HCM	p
IVSd (mm)	3.8 ± 0.8	6.6 ± 1.5	<0.001
LVd (mm)	14.9 ± 2.2	15.1 ± 2.1	ns
LVPWd (mm)	3.8 ± 0.9	5.9 ± 1.6	<0.001
IVSs (mm)	6.4 ± 1.2	9.1 ± 1.6	<0.001
LVs (mm)	8.3 ± 2.2	6.8 ± 2.6	ns
LVPWs (mm)	6.8 ± 1.1	9.2 ± 1.6	<0.001
FS (%)	44 ± 11	55 ± 15	ns
LA:Aod	1.4 ± 0.2	1.8 ± 0.6	<0.01

IVSd = Interventricular septal wall thickness (diastole), LVd = Left ventricular end-diastolic diameter, LVPWd = Left ventricular posterial wall thickness (diastole), IVSs = Interventricular septal wall thickness (systole), LVs = Left ventricular end-systolic diameter, LVPWs = Left ventricular posterial wall thickness (systole), FS = Fractional shortening, LA:Aod = Left atrium (systole) to aorta ratio (diastole).

D.3.3.1 TDI myocardial velocities in different myocardial segments in both normal and HCM cats

Good quality pulsed TDI tracings adequate for measurement and interpretation were obtained from the different myocardial segments (number and [percentage]) in the normal and HCM group, respectively, as follows: septal mitral annulus: 25 (100%) and 23 (100%). Lateral mitral annulus: 24 (96%) and 18 (78%). IVS along the longitudinal axis: 25 (100%) and 23 (100%). LVPW along the longitudinal axis: 24 (96%) and 18 (78%). IVS along the radial axis: 17 (68%) and 17 (74%). LVPW along the radial axis: 24 (96%) and 23 (100%). Tricuspid annulus: 8 (100%) and 12 (100%).

The number of traces with fully merged E' and A' diastolic waves as a percentage of the measurable tracings obtained from each myocardial segment was for the HCM group as follows: septal mitral annulus: 2 (9%), lateral mitral annulus: 3 (16%), IVS along the longitudinal axis 4 (17%), LVPW along the longitudinal axis 3 (17%), IVS along the radial axis 3 (18%), LVPW along the radial axis 1 (4%), tricuspid annulus 3 (25%). In some tracings obtained from the HCM group fully merged E' and A' waves along with partially summated waves occur (1 in each of the following segments: septal mitral annulus, IVS along both axes and LVPW along the radial axis). One tracing from the lateral mitral annulus of normal animals exhibited only fully merged E' and A' waves and those obtained from the tricuspid annulus none. The number of tracings obtained from the normal group with fully merged E' and A' waves along with partially summated waves was: 1 from the lateral mitral annulus, 2 from the septal mitral annuls and the IVS and the LVPW along the radial axis and 3 from the IVS and the LVPW along the longitudinal axis. Pulsed TDI results obtained from both groups are presented in Table D2 (estimates, standard error) and Table D3 (mean, standard deviation). Mean values of pulsed TDI indices from all myocardial segments of the cats included in the study are presented in Appendix D1, Tables App.D1 to D14 (App.D1-D8 normal group; App.D9-D14 HCM group).

Table-D2. Estimates (standard error) of Tissue Doppler myocardial indices produced by ANCOVA from normal cats and cats with hypertrophic cardiomyopathy

	sep MA		lat MA		4ch IVS		4ch LVPW		rpla IVS		rpla LVPW		Tr	
	normal	HCM	normal	HCM	normal	HCM	normal	HCM	normal	HCM	normal	HCM	normal	HCM
E' (cm/sec)	6.62 (0.36)	4.02 (0.43)	8.3 (0.37)	5.04 (0.51)	6.9 (0.36)	4.52 (0.44)	9.08 (0.37)	5.76 (0.46)	5.11 (0.49)	4.91 (0.51)	5.75 (0.36)	4.75 (0.42)	10.43 (0.89)	7.36 (0.68)
E' VTI (cm)	0.34 (0.03)	0.26 (0.03)	0.42 (0.03)	0.35 (0.04)	0.33 (0.03)	0.25 (0.03)	0.44 (0.03)	0.37 (0.04)	0.3 (0.04)	0.27 (0.06)	0.29 (0.03)	0.3 (0.04)	0.68 (0.05)	0.67 (0.07)
E' dur (msec)	88 (4)	103 (4)	84 (4)	108 (6)	78 (4)	88 (5)	81 (4)	104 (6)	87 (5)	92 (10)	79 (4)	99 (5)	112 (8)	124 (10)
E' acc (cm/s²)	181 (14)	93 (17)	231 (14)	124 (23)	206 (14)	143 (19)	308 (14)	169 (21)	143 (19)	135 (35)	189 (14)	121 (20)	220 (30)	181 (34)
tE'acc (msec)	37 (2)	46 (3)	37 (2)	46 (4)	37 (2)	35 (3)	30 (2)	42 (3)	45 (2)	40 (6)	34 (2)	41 (3)	49 (5)	47 (5)
E' dec (cm/s²)	131 (12)	90 (14)	189 (12)	95 (19)	170 (12)	89 (16)	188 (12)	120 (18)	144 (16)	95 (30)	136 (12)	90 (17)	168 (26)	117 (29)
tE'dec (msec)	51 (3)	56 (4)	49 (3)	63 (5)	45 (3)	55 (4)	54 (3)	60 (5)	43 (4)	58 (5)	47 (3)	58 (4)	59 (7)	73 (8)
A' (cm/sec)	6.68 (0.47)	6 81 (0.56)	6.04 (0.49)	5.88 (0.7)	6.22 (0.46)	7.04 (0.59)	5.32 (0.48)	6.05 (0.63)	5.27 (0.63)	6.59 (0.63)	5.63 (0.47)	6.97 (0.56)	9.71 (1.16)	17.11 (0.95)
A' VTI (cm)	0.27 (0.03)	0.3 (0.03)	0.22 (0.03)	0.23 (0.03)	0.25 (0.02)	0.29 (0.03)	0.22 (0.02)	0.19 (0.04)	0.25 (0.02)	0.27 (0.03)	0.25 (0.02)	0.27 (0.03)	0.4 (0.04)	0.8 (0.05)
A' dur (msec)	68 (2)	70 (3)	60 (2)	62 (4)	61 (2)	67 (3)	61 (2)	60 (4)	60 (3)	66 (5)	64 (2)	67 (3)	75 (5)	79 (6)
E'/A'	1.04 (0.08)	0 64 (0.09)	1.48 (0.08)	0.89 (0.12)	1.15 (0.08)	0.69 (0.1)	1.85 (0.08)	1.05 (0.1)	1.14 (0.1)	0.78 (0.11)	1.08 (0.08)	0.74 (0.09)	1.16 (0.2)	0.46 (0.16)
Se' (cm/sec)	6.96 (0.43)	6.43 (0.47)	7.05 (0.43)	5.36 (0.52)	6.16 (0.42)	6.28 (0.49)	6.23 (0.43)	5.44 (0.51)	5.76 (0.57)	5.93 (0.52)	6.22 (0.43)	5.99 (0.48)	12.93 (1.05)	10.33 (0.69)
S' VTI (cm)	0.59 (0.04)	0.48 (0.04)	0.58 (0.04)	0.48 (0.04)	0.56 (0.04)	0.47 (0.05)	0.60 (0.04)	0.46 (0.04)	0.43 (0.05)	0.51 (0.05)	0.56 (0.04)	0.53 (0.04)	0.85 (0.08)	0.9 (0.06)
S' dur (msec)	155 (5)	145 (5)	159 (5)	151 (6)	156 (5)	139 (6)	157 (5)	143 (6)	142 (7)	161 (6)	148 (5)	152 (5)	159 (12)	151 (8)
Se'acc (cm/s²)	288 (18)	222 (20)	309 (18)	182 (23)	224 (18)	196 (22)	252 (19)	188 (22)	208 (25)	205 (22)	218 (18)	199 (21)	287 (45)	338 (30)
tSe'acc (msec)	27 (2)	30 (2)	24 (2)	33 (2)	29 (2)	34 (2)	27 (2)	32 (2)	30 (2)	34 (2)	31 (2)	35 (2)	33 (4)	32 (2)
Sl' (cm/sec)	4.7 (0.25)	3.24 (0.29)	4.18 (0.25)	3.27 (0.35)	4.85 (0.25)	3.38 (0.37)	3.7 (0.27)	3.6 (0.39)	3.34 (0.37)	3.48 (0.36)	4.12 (0.27)	3.4 (0.32)	4.89 (1.24)	6.58 (0.44)
bS'-Sl' (msec)	77 (4)	87 (5)	81 (4)	104 (6)	86 (4)	92 (6)	102 (4)	93 (6)	83 (6)	100 (6)	89 (4)	97 (5)	100 (20)	86 (7)
IVCb (cm/sec)	5.78 (0.42)	5.06 (0.52)	5.72 0.43)	5.43 (0.55)	4.17 (0.68)	4.42 (0.8)	5.28 (0.45)	5.04 (0.49)	4.78 (0.53)	4.03 (0.76)	6.87 (0.38)	5.52 (0.45)	4.75 (1.8)	5.36 (1.27)
Q-Se' (msec)	87 (3)	86 (4)	88 (3)	93 (4)	87 (3)	85 (4)	91 (3)	89 (4)	87 (6)	83 (4)	98 (3)	102 (4)	82 (9)	82 (6)
Q-Sl' (msec)	137 (4)	144 (5)	146 (4)	166 (6)	144 (4)	144 (6)	162 (5)	147 (7)	146 (8)	133 (6)	156 (5)	168 (5)	160 (22)	141 (9)
Q-E' (msec)	311 (5)	311 (6)	317 (5)	315 (7)	312 (5)	307 (6)	311 (5)	321 (6)	310 (8)	312 (7)	303 (5)	317 (6)	292 (12)	299 (12)
Q-A' (msec)	471 (4)	406 (5)	418 (4)	398 (6)	415 (4)	407 (5)	412 (4)	407 (5)	423 (7)	423 (6)	405 (4)	411 (5)	431 (10)	387 (10)
Q-bS' (msec)	63 (5)	58 (5)	69 (4)	66 (5)	62 (4)	57 (5)	67 (4)	63 (5)	60 (7)	50 (5)	71 (4)	72 (5)	57 (10)	57 (7)
Q-bE (msec)	284 (6)	268 (6)	275 (6)	269 (7)	284 (7)	279 (7)	282 (7)	275 (6)	262 (8)	280 (7)	269 (6)	280 (6)	246 12)	264 (12)
IVRt (msec)	60 (4)	76 (4)	50 (4)	71 (5)	60 (4)	84 (5)	58 (4)	76 (5)	64 (6)	74 (5)	58 (4)	64 (4)	54 (10)	60 (7)
IVCt (msec)	36 (3)	31 (3)	48 (3)	52 (4)	35 (3)	33 (3)	47 (3)	48 (4)	34 (4)	40 (4)	49 (3)	50 (3)	30 (7)	41 (5)
II-E' (msec)	100 (4)	123 (5)	92 (4)	107 (6)	98 (4)	125 (6)	90 (4)	120 (6)	120 (6)	113 (10)	91 (4)	105 (6)	105 (9)	116 (10)
I-Se' (msec)	64 (4)	62 (4)	73 (4)	84 (5)	65 (4)	67 (4)	74 (4)	80 (5)	72 (5)	74 (5)	80 (4)	84 (4)	64 (9)	74 (6)

Table-D3. Mean values (standard deviation) of Tissue Doppler myocardial indices from normal cats and cats with hypertrophic cardiomyopathy

	sep MA		lat MA		4ch IVS		4ch LVPW		rpla IVS		rpla LVPW		Tr	
	normal	**HCM**	**normal**	**HCM**	**normal**	**HCM**	**normal**	**HCM**	**normal**	**HCM**	**normal**	**HCM**	**normal**	**HCM**
E' (cm/sec)	6.42 (1.83)	4.12 (0.85)	8.39 (2.58)	5.24 (1.22)	6.8 (1.9)	5.12 (1.96)	9.28 (2.14)	5.87 (1.39)	5.2 (1.69)	4.93 (1.55)	5.6 (1.58)	5.04 (1.99)	9.78 (2.27)	7.08 (1.24)
E' VTI (cm)	0.33 (0.12)	0.27 (0.09)	0.42 (0.15)	0.37 (0.17)	0.31 (0.09)	0.28 (0.1)	0.44 (0.11)	0.36 (0.07)	0.3 (0.1)	0.3 (0.08)	0.28 (0.11)	0.3 (0.12)	0.71 (0.18)	0.55 (0.15)
E' dur (msec)	88 (11)	104 (29)	84 (16)	114 (26)	78 (14)	92 (22)	81 (13)	105 (28)	87 (28)	96 (15)	80 (20)	108 (38)	122 (20)	120 (20)
E' acc (cm/s²)	179 (58)	94 (33)	240 (75)	120 (73)	206 (78)	150 (80)	317 (82)	165 (73)	147 (59)	128 (30)	186 (63)	122 (49)	203 (63)	157 (37)
tE'acc (msec)	38 (8)	47 (12)	36 (6)	47 (10)	36 (8)	37 (10)	31 (6)	43 (14)	44 (18)	43 (10)	34 (9)	41 (11)	50 (9)	47 (7)
E' dec (cm/s²)	128 (41)	96 (52)	190 (88)	88 (35)	169 (68)	98 (36)	192 (66)	118 (58)	147 (63)	99 (26)	135 (47)	84 (36)	140 (44)	110 (32)
tE'dec (msec)	51 (7)	55 (23)	48 (12)	68 (19)	44 (11)	55 (15)	54 (19)	60 (18)	43 (11)	54 (8)	47 (16)	64 (27)	72 (18)	68 (17)
A' (cm/sec)	6.57 (2.4)	6.55 (2.09)	6.2 (2.43)	6.05 (1.89)	6.16 (1.61)	7.26 (3.12)	5.37 (1.92)	5.98 (2.42)	5.34 (2.22)	7.08 (2.74)	5.58 (1.78)	7.27 (2.28)	10.26 (3.59)	16.29 (4.7)
A' VTI (cm)	0.26 (0.09)	0.28 (0.09)	0.22 (0.07)	0.21 (0.08)	0.24 (0.06)	0.27 (0.09)	0.21 (0.09)	0.19 (0.05)	0.20 (0.09)	0.24 (0.08)	0.23 (0.08)	0.27 (0.07)	0.48 (0.17)	0.75 (0.17)
A' dur (msec)	68 (11)	69 (9)	60 (10)	62 (16)	60 (9)	67 (9)	60 (10)	62 (12)	58 (14)	64 (10)	65 (11)	68 (17)	84 (13)	80 (7)
E'/A'	1.02 (0.25)	0.74 (0.47)	1.47 (0.59)	0.92 (0.2)	1.15 (0.38)	0.79 (0.44)	1.87 (0.59)	1.12 (0.48)	1.15 (0.64)	0.77 (0.27)	1.07 (0.37)	0.74 (0.29)	1.04 (0.37)	0.46 (0.09)
Se' (cm/sec)	7 (1.8)	6.26 (1.72)	7.1 (2.34)	5.77 (2.22)	6.17 (1.5)	6.46 (2.18)	6.34 (1.85)	5.37 (1.72)	5.65 (1.26)	6.1 (1.11)	6.16 (1.26)	6.05 (1.48)	12.18 (6.08)	10.46 (3.31)
S' VTI (cm)	0.58 (0.14)	0.47 (0.1)	0.58 (0.14)	0.47 (0.16)	0.55 (0.13)	0.49 (0.17)	0.6 (0.16)	0.45 (0.12)	0.44 0.09	0.5 (0.07)	0.54 (0.12)	0.54 (0.16)	1 (0.31)	0.88 (0.25)
S' dur (msec)	155 (19)	147 (16)	158 (20)	149 (37)	156 (20)	139 (28)	158 (35)	141 (33)	146 (23)	154 (28)	150 (20)	152 (19)	174 (31)	149 (14)
Se'acc (cm/s²)	290 (110)	219 (58)	310 (128)	191 (80)	225 (78)	207 (74)	256 (68)	181 (60)	207 (75)	221 (100)	216 (67)	195 (81)	303 (102)	335 (103)
tSe'acc (msec)	27 (5)	30 (4)	24 (4)	33 (9)	29 (5)	33 (7)	27 (9)	33 (8)	30 (8)	33 (11)	31 (8)	36 (12)	35 (5)	33 (4)
Sl' (cm/sec)	4.65 (1.26)	3.31 (0.63)	4.2 (1)	3.18 (0.78)	4.79 (1.41)	3.78 (1.02)	3.8 (1.02)	3.56 (0.94)	3.17 (0.72)	3.42 (0.68)	3.98 (1.35)	3.52 (1.52)	6.64 (2.17)	6.57 (1.7)
bS'-Sl' (msec)	77 (13)	88 (9)	81 (19)	102 (30)	87 (12)	92 (14)	99 (30)	94 (22)	89 (17)	99 (16)	92 (25)	96 (22)	95 (10)	94 (33)
IVCb (cm/sec)	5.96 (2.38)	4.68 (1.61)	5.62 (2.12)	5.4 (1.21)	4.46 (1.24)	4.55 (1.11)	5.21 (1.93)	4.96 (1.68)	5.03 (1.43)	4.03 (1.15)	6.89 (2.14)	5.48 (1.23)		5.44 (1.73)
Q-Se' (msec)	87 (13)	86 (10)	88 (13)	94 (15)	87 (14)	84 (14)	91 (14)	90 (16)	81 (23)	84 (42)	98 (16)	103 (24)	89 (15)	82 (16)
Q-Sl' (msec)	137 (24)	146 (14)	145 (25)	164 (38)	144 (19)	145 (18)	160 (28)	149 (26)	146 13	135 (29)	161 (32)	165 (35)	153 (22)	137 (16)
Q-E' (msec)	309 (35)	312 (40)	312 (36)	322 (22)	308 (33)	308 (40)	305 (30)	322 (33)	306 (47)	309 (40)	305 (41)	314 (42)	315 (53)	297 (19)
Q-A' (msec)	414 (87)	407 (82)	415 (86)	406 (51)	413 (82)	395 (89)	406 (66)	410 (72)	424 (95)	421 (65)	413 (85)	402 (67)	459 (98)	391 (54)
Q-bS' (msec)	63 (13)	58 (12)	79 (54)	67 (13)	61 (12)	57 (14)	67 (16)	64 (10)	56 (20)	48 (15)	72 (12)	71 (16)	60 (14)	56 (15)
Q-bE' (msec)	281 (36)	270 (37)	271 (32)	273 (19)	277 (34)	278 (35)	275 (30)	277 (25)	265 (42)	274 (36)	272 (40)	275 (36)	265 (48)	261 (32)
IVRt (msec)	61 (13)	75 (22)	54 (11)	72 (32)	61 (15)	81 (33)	57 (10)	75 (25)	67 (25)	71 (22)	61 (16)	62 (21)	53 (19)	66 (21)
IVCt (msec)	36 (14)	34 (10)	49 (17)	53 (16)	36 (13)	34 (11)	46 (19)	49 (14)	39 (24)	36 (19)	50 (15)	47 (16)	28 (6)	39 (11)
II-E' (msec)	97 (20)	125 (27)	90 (13)	112 (26)	98 (16)	119 (26)	88 (11)	119 (26)	119 (30)	119 (19)	93 (20)	105 (19)	103 (26)	109 (15)
I-Se' (msec)	63 (15)	63 (10)	73 (19)	85 (21)	65 (15)	66 (13)	73 (20)	79 (18)	69 (27)	69 (25)	81 (16)	82 (17)	63 (9)	71 (13)

D.3.3.2. Differences between the longitudinal and radial axis

Velocities: Peak early diastolic velocity of the LVPW was significantly higher in normal animals along the longitudinal axis than it was along the radial axis ($p<0.001$). There was no significant difference in E' of the LVPW or of the IVS in affected animals between the two axes. A significantly higher E'/A' was recorded in the LVPW along the longitudinal axis when compared with that from the radial axis in both groups ($p<0.001$). SI' was significantly higher in the IVS of normal animals along the longitudinal axis than it was along the radial axis ($p<0.001$). The IVCb was significantly higher in the LVPW of normal animals along the radial axis than it was along the longitudinal axis ($p<0.01$).

Velocity integrals: In normal animals, E' VTI of the LVPW along the longitudinal axis was significantly greater than it was along the radial axis ($p<0.001$) and S' VTI of the IVS was significantly greater along the longitudinal axis than along the radial axis ($p<0.05$).

Acceleration-deceleration: In normal animals, acceleration of the E' wave was significantly higher in the IVS and the LVPW along the long axis than along the radial axis ($p<0.01$ for the IVS and $p<0.001$ for the LVPW). Acceleration time of E' in the IVS along the radial axis in normal animals was significantly longer when compared with that along the longitudinal axis ($p<0.05$). E' deceleration in the LVPW of normal animals was higher along the longitudinal axis than along the radial axis ($p<0.01$). Mean early systolic acceleration time in the LVPW of normal animals along the radial axis was significantly longer than it was along the

longitudinal axis ($p<0.05$). The bS'-Sl' in the LVPW of normal animals along the longitudinal axis was significantly prolonged compared to that along the radial axis ($p<0.05$).

Time intervals: In the HCM group, Q-Se' and Q-Sl' of the LVPW along the long axis was significantly longer in comparison to those along the radial axis ($p<0.05$). In normal animals II-E' in the IVS along the longitudinal axis was shorter than that along the radial axis ($p<0.01$).

D.3.3.3. Differences along the longitudinal axis

Velocities: In normal animals, the IVCb of the septal mitral annulus was significantly higher than that of the IVS ($p<0.05$).

Acceleration-deceleration: Acceleration and time of acceleration of the E' wave in the LVPW of normal animals were significantly higher and shorter respectively compared to that in the lateral mitral annulus ($p<0.001$). In affected animals acceleration of the E' wave was significantly higher in the IVS than it was in the septal mitral annulus ($p<0.001$) and acceleration time of the E' wave in the septal mitral annulus was significantly longer than it was in the IVS ($p<0.01$). Deceleration of the E' wave in the IVS of normal animals was significantly higher compared to that from the septal mitral annulus ($p<0.05$). Early systolic acceleration in the septal and lateral mitral annulus of normal animals was higher than it was in the IVS and the LVPW respectively ($p<0.05$). bS'-Sl' wave in the lateral mitral annulus of normal animals was shorter than that in the LVPW ($p<0.001$).

Time intervals: The Q-SI' in the LVPW of normal animals was longer in comparison to that in the lateral mitral annulus ($p<0.05$).

D.3.3.4. Differences between septal and posterior side

Velocities: Significantly higher E' and E'/A' were recorded in the posterior than in the septal side along the longitudinal axis in normal animals ($p<0.01$ for E' and $p<0.001$ for E'/A'). In affected animals, a higher E'/A' was recorded in the LVPW than in the IVS along the longitudinal axis ($p<0.001$). The SI' of the IVS was significantly higher compared with the LVPW of normal animals along the longitudinal axis ($p<0.01$).

Velocity integrals: In affected animals, the A' VTI of the IVS along the longitudinal axis was significantly greater than that of the LVPW ($p<0.05$). The S' VTI of the LVPW along the radial axis was significantly higher compared to that of the IVS in the normal group ($p<0.05$).

Acceleration-deceleration: In normal animals, the E' acceleration in the septal mitral annulus and in the IVS along both axes was significantly lower than they were in the lateral mitral annulus and in the LVPW along both axes respectively ($p<0.001$ and $p<0.05$ respectively). Acceleration time of the E' wave was significantly longer in the IVS of normal animals compared to that of LVPW along both axes ($p<0.05$ for the longitudinal axis and $p<0.001$ for the radial axis). E' deceleration in the lateral mitral annulus of normal animals was significantly higher compared to that from the

septal mitral annulus ($p<0.001$). In normal cats, the bS'-Sl' interval in the IVS along the longitudinal axis was shorter than that in the LVPW ($p<0.01$).

Time intervals: A' duration in the septal mitral annulus of normal animals was significantly longer compared to that in the lateral mitral annulus ($p<0.05$). The Q-Se' in the LVPW of affected animals along the radial axis was longer compared to that from the IVS ($p<0.01$). The Q-Sl' in the LVPW of normal animals along the longitudinal axis was significantly prolonged compared to that in the IVS ($p<0.05$). The Q-bS' of the LVPW of HCM cats along the radial axis was significantly longer compared to that in the IVS ($p<0.001$). The IVCt in the posterial side along the longitudinal axis was significantly longer compared to that from the septal side in both groups ($p<0.001$). The II-E' in the IVS of normal animals along the radial axis was significantly longer compared to that in the LVPW ($p<0.001$). In affected animals, the I-Se' in the posterial side of the heart along the longitudinal axis was significantly longer than that in the septal side ($p<0.001$ for the annular sites and $p<0.05$ for the myocardial segments at chordae tendineae level).

D.3.3.5. Differences between mitral and tricuspid annular sites

Velocities: Diastolic and early systolic velocities in the tricuspid annulus were significantly higher than that recorded in both mitral annular sites in both groups ($p<0.01$).

Velocity integrals: Diastolic and systolic VTI were significantly greater in the tricuspid annulus compared to that in the mitral annular sites of both groups ($p<0.001$).

Acceleration-deceleration: Acceleration time of E' in the tricuspid annulus of normal animals was significantly longer compared to that in the both annular sites ($p<0.001$). In affected animals, acceleration of E' was significantly lower in the septal mitral annulus compared to that in the tricuspid annulus ($p<0.05$). Early and late mean systolic acceleration in both annular sites of the affected group were significantly lower compared with that from the tricuspid annulus ($p<0.01$). The time of early systolic acceleration in the lateral mitral annulus of normal animals was significantly shorter than that recorded in the tricuspid annulus ($p<0.01$). In affected cats, the bS'-Sl' interval in the lateral mitral annulus was significantly longer compared to that recorded in the tricuspid annulus ($p<0.05$).

Time intervals: The duration of early diastolic wave was significantly longer in the tricuspid annulus of normal animals compared to that in both mitral annular sites ($p<0.01$ for the lateral mitral annulus and $p<0.05$ for the septal mitral annulus). The A' wave duration in the tricuspid annulus of normal animals was longer than that recorded in their lateral mitral annulus ($p<0.05$). The Q-Sl' in the lateral mitral annulus of affected animals was significantly longer than that recorded in the tricuspid annulus ($p<0.05$). The IVCt in the tricuspid annulus of normal animals was significantly shorter than that in the lateral mitral annulus ($p<0.05$).

D.3.3.6. Differences in TDI indices between normal and HCM cats

Velocities: HCM cats exhibited significantly lower peak early diastolic velocities in all myocardial segments along the longitudinal axis in comparison to normal cats ($p<0.001$). A cut-off value of E' in the LVPW along the longitudinal axis > 7 cm/sec could discriminate normal from affected cats with a sensitivity of 92 % and a specificity of 87% (Figure D3).

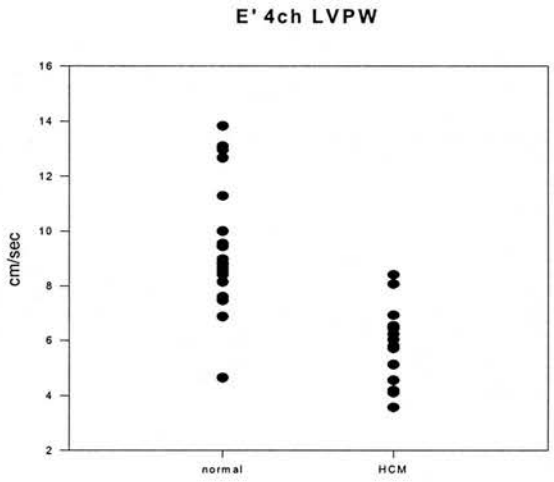

Figure D 3. *Point plot of early diastolic velocity of the LVPW along the longitudinal axis between normal and HCM cats.*

There was no significant difference in E' of the IVS and the LVPW along the radial axis between the two groups. Tricuspid annular peak early diastolic velocity was significantly lower in the affected group when compared with that in the normal group ($p<0.01$). Although A' in all myocardial segments was higher in the affected group than in the normal one, this trend never reached statistical significance. However, peak late diastolic velocity of the tricuspid annulus was significantly higher in the HCM group that in the normal group ($p<0.001$). The E'/A' was

significantly higher in all myocardial segments in the normal group than in the affected one ($p<0.05$ for the IVS along the radial axis, $p<0.01$ for the septal and tricuspid annulus and $p<0.001$ for the remaining myocardial segments). Peak early systolic velocity was significantly lower only in the lateral mitral annulus of affected animals ($p<0.05$). Peak late systolic velocity was significantly lower in the septal ($p<0.001$) and lateral ($p<0.05$) mitral annulus and also in the IVS along the longitudinal axis ($p<0.001$) in affected animals than in normal ones. The second myocardial shift (IVCb) during the isovolumic contraction period was lower in the LVPW of affected animals along the radial axis when compared with that from normal animals ($p<0.05$). There was no significant difference in IVCb in other myocardial segments between the two groups.

Velocity integrals: A' VTI in the tricuspid annulus of affected animals was significantly greater than that in normal ones ($p<0.001$). S' VTI of the septal mitral annulus in affected animals was significantly lower than that in the normal group ($p<0.05$).

Acceleration-deceleration: Acceleration of the E' wave was higher in all myocardial segments along the longitudinal axis and also in the LVPW along the radial axis in the normal group compared with that from the corresponding segments in the affected group ($p<0.01$ for the IVS and the LVPW along the longitudinal and radial axis respectively and $p<0.001$ for the remaining of the myocardial segments). Acceleration time of the E' wave was prolonged in the septal and lateral mitral annulus and in the LVPW of affected animals along both axes compared to that from

normal ones ($p<0.01$ for the LVPW along the longitudinal axis and $p<0.05$ for the other of the myocardial segments). E' deceleration was higher in all myocardial segments along the longitudinal axis and also in the LVPW along the radial axis in the normal group compared with that from the corresponding segments in the affected group ($p<0.05$ for the septal mitral annulus and the LVPW along the radial axis, $p<0.01$ for the LVPW along the longitudinal axis and $p<0.001$ for the lateral mitral annulus and the IVS along the longitudinal axis). Deceleration time of E' was significantly prolonged in the lateral mitral annulus and the LVPW along the radial axis in affected animals in comparison to that from normal ones ($p<0.05$). The mean early acceleration of S' wave in both mitral annular sites and also in the LVPW along the longitudinal axis, was significantly higher in the normal group compared to that in the affected group ($p<0.001$ for the lateral mitral annulus and $p<0.05$ for the septal mitral annulus and the LVPW along the longitudinal axis). Early systolic acceleration time was significantly prolonged in the lateral mitral annulus and in the IVS and the LVPW along the longitudinal axis in affected animals compared to that in normal animals ($p<0.05$). The bS'-Sl' in the lateral mitral annulus and in the IVS along the radial axis was significantly prolonged in normal animals compared to that in affected ones ($p<0.01$ and $p<0.05$, respectively).

Time intervals: Duration of E' was significantly prolonged in the septal and lateral mitral annulus and in the LVPW along both axes in the HCM group when compared with that from the corresponding myocardial segments of normal animals ($p<0.05$ for the septal mitral annulus and $p<0.01$ for the rest myocardial segments). The duration of S' was significantly longer in the IVS of normal animals along the longitudinal

axis than it was in affected animals and it was significantly prolonged in the IVS of affected animals along the radial axis compared with that of normal animals ($p<0.05$). Q-A' was significantly longer in the lateral mitral and tricuspid annulus of normal animals than in affected ones ($p<0.05$). Q-SI' was significantly longer in the lateral mitral annulus of affected animals than in the normal ones ($p<0.05$). Significantly longer IVRt were recorded in all myocardial segments along the longitudinal axis in affected animals than in normal ones ($p<0.01$). The II-E' interval was significantly longer in all myocardial segments along the longitudinal axis and also in the LVPW along the radial axis in affected cats compared to that in nomral ones ($p<0.05$ for the lateral mitral annulus and the LVPW along the radial axis, $p<0.001$ for the rest myocardial segments). The IVCt was not significantly different in any of the myocardial segments between the two groups.

D.4. Influence of CHF on TDI indices

Changes in the level of significance of TDI indices between the two groups when HCM cats with CHF were excluded from the analysis are discussed in this section.

D.4.1. Systole

Se' of the lateral mitral annulus was not statistically different between the two groups when only asymptomatic HCM and normal cats were compared. In the asymptomatic HCM group, S' VTI of the LVPW along the longitudinal axis was significantly lower than that in the radial axis ($p<0.05$). There was no statistical difference in the duration of the S' wave of the IVS along both axes between the two groups when only asymptomatic animals were considered in the analysis. Similarly, no difference was found in the duration of the S' wave in the IVS between the two axes in the

asymptomatic affected group. The duration of the S' wave in the posterior side of the heart along the longitudinal axis in the normal group was longer compared to that recorded in asymptomatic HCM animals ($p<0.01$). No statistically significant difference was found in bS'-Sl' between the septal mitral annulus and the IVS along the longitudinal axis in asymptomatic HCM cats.

D.4.2. Early diastole

Early diastolic peak and VTI of the septal mitral annulus in the asymptomatic group were significantly lower than that of the IVS along the longitudinal axis ($p<0.05$). E' VTI of the LVPW along the longitudinal axis was significantly higher in the normal compared to the affected group, when CHF animals were excluded from the analysis ($p<0.05$). The duration of E' wave in the IVS along the longitudinal axis of normal animals became statistically shorter than that of affected cats, when animals in CHF were excluded from the analysis ($p<0.05$). There was no statistical difference in the duration of the E' wave of the septal mitral annulus when only asymptomatic animals were included in the analysis. No statistical difference was found in the deceleration of the E' wave of the septal mitral annulus between the two groups, when cats with CHF were excluded from the analysis. Acceleration of the E' wave of the tricuspid annulus was significantly higher in normal cats than that in the asymptomatic group ($p<0.01$). There was no difference in the acceleration time of the E' wave of the LVPW along the radial axis of the heart between normal and asymptomatic animals.

D.4.3. Late diastole

A' of the IVS along both axes of the heart was significantly higher in asymptomatic than in normal animals ($p<0.05$). In the asymptomatic group, A' duration of the septal and lateral mitral annulus was significantly shorter compared to that of the tricuspid annulus ($p<0.05$). The duration of A' wave in the septal mitral annulus of asymptomatic animals was significantly longer than that of the lateral mitral annulus ($p<0.05$).

D.4.4. Time intervals

There was no statistical difference in the Q-A' of the tricuspid annulus between the two groups when only asymptomatic animals were considered in the analysis. The difference in Q-SI' of the lateral mitral annulus between the two groups was lost when only asymptomatic HCM animals were included in the analysis. There was no statistical difference in Q-SI' between the two annular segments in the asymptomatic group. Q-SI' become statistically longer in the normal group when only asymptomatic animals were considered in the analysis

D.5. Influence of independent predictors on TDI indices

The influence of independent variables, age, gender, R-R interval, thickness and weight on pulsed TDI indices is presented in Appendix D2, in Tables App.D15 to D28. Results of forward stepwise regression analysis, of linear regression or multiple linear regression analysis and R, R^2 and adjusted R^2 values along with the level of significance are also shown.

D.5.1. Influence of aging on pulsed TDI indices in normal cats

An inverse association was found between the early diastolic myocardial velocity in both mitral annular sites and age in the normal group. Similarly, early diastolic myocardial velocities in the LVPW along both axes of the heart were negatively associated with age. The E'/A' ratio in all myocardial segments along the longitudinal axis was negatively influenced by age. The acceleration of early diastolic myocardial velocity in the septal mitral annulus and the LVPW along both axes showed an inverse relationship with age. An inverse association between age and the deceleration of early diastolic myocardial velocity was found in all myocardial segments except for lateral mitral annulus. Age was a positive predictor for the deceleration time of E' in the tricuspid annulus of normal animals. The late systolic velocity in the LVPW along the longitudinal axis was associated inversely with age. Q-Se', Q-bS' and Q-bE' of the lateral mitral annulus and also the Q-Sl' in the IVS along the radial axis were prolonged with advancing age in normal animals.

D.5.2. Influence of aging on pulsed TDI indices in HCM cats

In forward stepwise regression analysis age was found to be a significant predictor for the E'/A' ratio in the septal side of the heart along the longitudinal axis. However, in multiple linear regression analysis age was eliminated from the model. Age was negatively associated with the E' VTI of the posterior side along the longitudinal axis in HCM cats. Age was a positive predictor for the acceleration of early diastolic myocardial velocity in the IVS along the radial axis. Although multiple regression analysis showed that age was a significant predictor for the acceleration of E' in the tricuspid annulus, the association between these two

variables was not statistically significant. The deceleration time of E' in the IVS along the longitudinal axis was associated inversely with age. Age was a positive predictor for A' VTI in the LVPW along the longitudinal axis in the affected group. The Q-Sl' and the Q-bE' in the LVPW of HCM cats along the radial axis of the heart were associated positively with age. Similarly a positive association was found between the acceleration time of early systole and age in the affected group.

D.5.3. Influence of thickness on pulsed TDI indices in normal cats

Thickness was negatively related the E'/A' ratio in the lateral mitral annulus and the LVPW along the radial axis in normal cats. A positive association was found between thickness and the VTI of A' wave in the LVPW along the radial axis in the normal group. The acceleration and time of acceleration of the systolic wave in the LVPW along the radial axis showed an inverse association with thickness. Thickness was a negative predictor for Q-Sl' in the LVPW along the radial axis in normal cats. A positive relationship was found between the acceleration time of late systole and age in the lateral mitral annulus of normal animals.

D.5.4. Influence of thickness on pulsed TDI indices in HCM cats

A negative association was found between thickness and the early diastolic velocity in the lateral mitral annulus of HCM cats. Thickness was a negative predictor for the acceleration and deceleration of E' in the IVS along the radial axis in the affected group. With the exception of the LVPW, thickness was a negative predictor for E' VTI in the other myocardial segments along the longitudinal axis. However, there was no statistically significant association between E' VTI in the lateral mitral

annulus and thickness in the HCM group. Thickness was inversely associated with the late diastolic velocity and its integral in both annular sites and in the IVS along both axes in affected cats. IVCb in the IVS along the radial axis showed an inverse association with thickness.

Thickness was a negative predictor for S' VTI in the IVS along the longitudinal axis in HCM cats. Q-bS' was related positively with thickness in the lateral mitral annulus and the LVPW along the longitudinal axis. Although thickness was a significant predictor for Q-bS' in the IVS and the LVPW along the longitudinal axis in affected cats, their association did not reach statistical significance. Thickness was a positive predictor for Q-Sl' in the LVPW along the radial axis. The early systolic acceleration time showed an inverse association with thickness in the lateral mitral annulus and the IVS along the longitudinal axis in the HCM group. Thickness appeared to inversely and positively influence the duration of the systolic wave in septal mitral annulus and in the IVS along the radial axis, respectively. An inverse association was found between thickness and IVCt in the LVPW along the radial axis in affected cats.

D.5.5. Influence of weight on pulsed TDI indices in normal cats

Weight was a significant positive predictor for E' in the septal mitral annulus and for E'/A' ratio of the lateral mitral annulus in normal cats. Acceleration of E' was positively associated with weight in the septal mitral annulus and the LVPW along the radial axis in the normal group. Weight was a significant predictor for IVCb in the septal side of the heart along the longitudinal axis. However, there was no

statistically significant association between the IVCb and weight in these myocardial segments. IVRt in the septal mitral annulus of normal cats was related inversely to weight. A positive relation was found between the Q-bS' and weight in the septal mitral annulus of normal animals. Weight was a significant positive predictor for Q-Se' and Q-Sl' in the LVPW along the radial axis.

D.5.6. Influence of weight on pulsed TDI indices in HCM cats

Weight was a significant positive predictor for E' in the IVS and the LVPW along the longitudinal axis and also for the A' and S' waves in the lateral mitral annulus in affected cats. The duration of E' in the LVPW along the radial axis and the duration of S' in the IVS along the longitudinal axis were positively associated with weight. An inverse association was found between weight and acceleration of E' in the IVS along the radial axis and the IVCt of the tricuspid annulus in the HCM group. Weight was a significant predictor for E'/A', E' duration and deceleration and time of early diastolic acceleration in the LVPW along the longitudinal axis in affected cats. However, none of the above TDI indices showed a significant association with weight. The E'VTI and the duration of S' in the septal mitral annulus showed a positive relation with weight in the affected group.

D.5.7. Influence of sex on pulsed TDI indices in normal cats

Sex was a significant negative predictor for the duration of S' wave in the IVS along the longitudinal axis and the lateral mitral annulus of normal cats. A positive association was found between sex and Q-Sl' in the LVPW along the radial axis and the septal mitral annulus in the normal group. Sex was found to associate positively

with the time of early systolic acceleration in the LVPW along the radial axis. The time of early diastolic acceleration in both annular sites showed an inverse association with sex. Q-bE' in the lateral mitral annulus and in the Q-E' in the IVS along the longitudinal axis were related inversely with sex. A positive association was found between the Q-bS' in the septal mitral annulus and sex in the normal group. Sex was a significant negative predictor for the deceleration of E' in the septal mitral annulus of normal animals and was positively related with the deceleration time of the E' wave of the same myocardial segment. When all of the above TDI indices were corrected for heart rate (divided by the square root of the R-R interval), no statistical significant difference was found between male and female cats.

D.5.8. Influence of sex on pulsed TDI indices in HCM cats

A positive association was found between sex and the A' and its VTI in the septal mitral annulus of affected animals. Sex was a significant positive predictor for the acceleration of early diastolic velocity and for the duration of the systolic wave in the IVS along the radial axis in the HCM group. However, no statistical significant difference was found between male and female cats regarding the above TDI indices.

D.5.9. Influence of heart rate on pulsed TDI indices in normal cats

A' of the IVS along the longitudinal axis and of the lateral mitral annulus showed an inverse association with R-R. Se' of both annular sites was related negatively with R-R. R-R was a significant positive predictor for the E'/A' ratio of the lateral mitral annulus. Duration of the E' wave in the septal mitral annulus, in the LVPW along the radial axis and in the tricuspid annulus was related positively with the R-R interval.

Similar associations were found between the R-R and the duration of A' wave in the septal side of the heart along the longitudinal axis. With the exception of the LVPW along the longitudinal axis and of the IVS along the radial axis, the duration of systolic wave was influenced positively by the R-R interval in the other myocardial segments. The time of deceleration of E' in the septal mitral annulus and in the LVPW along the radial axis showed a positive relation with the R-R. The early systolic acceleration in the IVS along the longitudinal axis and in the LVPW along the radial axis were associated inversely with the R-R interval. A positive relationship was found between the R-R interval and the acceleration time of early systole in the IVS along the longitudinal axis in the normal group. The IVCb in the LVPW along the radial axis was associated inversely with R-R interval. The time from the beginning of the S' wave to Sl' in the IVS along the longitudinal axis and in the lateral mitral annulus showed a positive association with the R-R interval. With the exception of the tricuspid annulus and the IVS along the radial axis, the Q-Se' interval was positively influenced with R-R in the other myocardial segments in the normal group. Similar associations were found between Q-Sl' and Q-bS' and R-R in the above myocardial segments. The Q-E', the Q-A' and the Q-bE', all showed a positive association with the R-R interval. The IVCt in the LVPW along both axes of the heart was influenced positively with R-R. The R-R interval was a significant predictor for IVRt in the septal mitral annulus and the IVS along the radial axis of normal cats. However, only in the latter, IVRt showed a significant positive association with R-R.

D.5.10. Influence of heart rate on pulsed TDI indices in HCM cats

R-R was a negative predictor for E' in the LVPW along the longitudinal axis in the affected group. Se' showed an inverse association with R-R interval in the IVS along the radial axis. There was a similar relationship between Sl' in the LVPW along the longitudinal axis and R-R in the affected group. In the LVPW along the radial axis, the deceleration and time of deceleration of E' showed an inverse and positive association with R-R, respectively. The duration of E' in the septal mitral annulus and in the LVPW along the radial axis of affected cats was positively related with the R-R interval. R-R was a significant predictor for S' VTI in the LVPW along the longitudinal axis and in the lateral mitral annulus in the affected group. However, a positive association between S' VTI and R-R was found only for the LVPW along the radial axis. With the exception of the IVS along the longitudinal axis, the duration of S' wave showed a positive association with R-R in all the other myocardial segments. The time of early systolic acceleration and the time from the beginning of S' wave to Sl' in the lateral mitral annulus were positively related with the R-R interval. With the exception of the tricuspid annulus, the Q-E' and the Q-A' were positively associated with R-R in all the other myocardial segments in the affected group. A positive association was found between the Q-Se' and the R-R interval in the IVS along the longitudinal axis and in the lateral mitral annulus. The Q-Sl' in the LVPW along the radial axis and in the lateral mitral annulus showed a positive relation with the R-R interval. A positive association was found between the Q-bS' and the R-R interval in the IVS of affected cats along the radial axis. The IVRt in the septal mitral annulus was positively associated with R-R.

D.6. Discussion

D.6.1. Introduction

This study documents that diastolic dysfunction in feline HCM is expressed as decreased early diastolic velocities, reduced E' wave acceleration and deceleration, and also as loss of the physiological non-uniformity of myocardial motion during early diastole. Systolic dysfunction was evident in a number of TDI indices, irrespective of degree of hypertrophy, suggesting that systolic impairment is an inherent component of HCM of this species. The study also shows the influence of aging, weight, R-R, thickness and sex on myocardial velocity indices recorded by the pulsed TDI technique in normal and HCM cats.

TDI has evolved as a very useful and sensitive tool in the non-invasive assessment of regional and global myocardial function. The use of TDI allowed the simultaneous quantification of myocardial motion during all phases of the cardiac cycle along the two major axes of the heart. The myocardium is constructed of longitudinally arranged oblique fibres in the subepicardial and subendocardial regions and circumferential fibres in the mid-wall (Greenbaum *et al*, 1981). Systolic shortening and diastolic lengthening along the longitudinal and radial axis of the heart is attributed to the contraction and relaxation of the longitudinally and circumferentially fibres respectively (Galiuto *et al*, 1998). Optimal mechanical performance, during diastole and systole, requires therefore, a highly organised co-ordination between these two different types of myocardial fibres (Jones *et al*, 1990). Although, conventional echocardiography allows the indirect assessment of myocardial function based on morphological and blood flow characteristics, it does

not always offer an accurate means for assessing global myocardial properties and its contribution in quantifying regional myocardial function is limited. By contrast, the use of TDI has allowed, for the first time, the direct quantification of myocardial motion, and more specifically, assessment of motion of the differently oriented fibres types. This is feasible by using different echocardiographic projections such as, right parasternal short and long axis views for quantifying motion of the radially oriented fibres and apical views for assessing the longitudinally arranged fibres. Moreover, TDI indices, such as peak early diastolic and systolic myocardial velocities, correlate strongly with invasive haemodynamic variables, such as the time constant of pressure decay in isovolumetric relaxation (τ) and the peak positive and negative rate of pressure development (dP/dt), suggesting that they could be used as alternative tools in the non-invasive assessment of global diastolic and systolic function (Oki *et al*, 1997; Sohn *et al*, 1997; 1999; Ohte *et al*, 1998; Yamada *et al*, 1998). Peak early diastolic myocardial velocity has been proved to be preload independent and therefore capable in unmasking pseudonormal mitral inflow patterns in patients with elevated LA pressures (Sohn *et al*, 1997; Farias *et al*, 1999; Yalcin *et al*, 2002). Additionally, the ratio of early mitral inflow to early mitral annular diastolic velocity (E/E') has predicted with relatively high accuracy LV filling pressures in various cardiac settings (Nagueh *et al*, 1998; Sohn *et al*, 1999; Kim and Sohn, 2000).

In a recent study, Schober and colleagues (2003) showed that most peak annular systolic and diastolic TDI indices were increased with increased preload induced by saline infusion in anaesthetized normal cats. Moreover, the E/E' ratio in both annular sites did not show any association with LV filling pressures (Schober *et al*, 2003).

The above results re-confirm the observations of studies in normal humans and experimental animals and show that the preload independence of TDI indices and their sensitivity in predicting LV pressures are enhanced in the disease state (Firstenberg *et al*, 2000; Nagueh *et al*, 2001b).

Early diastolic myocardial velocity represents the energy dependent myocardial relaxation and also the elastic properties of the myocardium (Rodriguez *et al*, 1996; Ohte *et al*, 1998; Nagueh *et al*, 2001b). Late diastolic velocities in the normal myocardium represent passive myocardial expansion due to LA contraction rather than late diastolic mitral inflow (Pai and Gill, 1998). Early and late systolic velocities represent myocardial contraction during early and late ventricular ejection respectively. The biphasic short duration shifts during the 2 isovolumic phases involve the entire myocardium and although it has been shown that they correlate with the opening and closure of atrioventricular and semilunar valves they probably represent adjustment myocardial movements governed by the Frank-Starling law (Hawthorne, 1961; Garcia *et al*, 1996a).

D.6.2. Age related changes in pulsed TDI indices

TDI studies have detected age-related changes in the diastolic and systolic performance of the normal human myocardium. A decrease in early diastolic velocity with a concomitant increase in the amplitude of the late diastolic myocardial component have been shown with increasing age in many studies (Garcia *et al*, 1996a; Rodriguez *et al*, 1996; Sohn *et al*, 1997; Alam *et al*, 1999; Yamada *et al*, 1999a; Naqvi *et al*, 2001). An inverse association between systolic velocities along

the longitudinal axis and age has been documented in others (Alam *et al*, 1999; Onose *et al*, 1999a). In our group of normal cats, changes associated with aging were found mainly in diastolic TDI indices and were reflected as a significant decrease in early diastolic velocities along both axes with increasing age. That the E'/A' was inversely associated with age in all myocardial segments is attributed primarily to the decreased early diastolic velocities, and to lesser extent to a compensatory increased contribution of LA contraction in the LV filling. The decreased early diastolic performance due to aging documented in normal cats is in agreement with findings of TDI studies in normal humans. Evidence for systolic changes induced by aging was found in some systolic time intervals, which were prolonged with advancing age in normal cats. Similar changes associated with aging were found in both diastolic and systolic TDI indices in the affected group. However, these changes were not reflected to the same extent as in the normal group.

Changes in the active state of myocardial fibres and in visco-elasticity are induced due to aging and it has been shown to affect the diastolic properties of the myocardium (Weisfeldt, 1971; Lakatta, 1975). Increased myocardial stiffness due to increased quantity of interstitial connective tissue, along with increase of the connective tissue of the fibrous skeleton of the heart may play an additional role in the age-related decrease in LV diastolic function. Furthermore, with increasing age a decline in the ability of beta-adrenergic receptor stimulation to increase contractility has been reported in isolated myocytes of rats (Xiao *et al*, 1994).

D.6.3. Influence of sex on pulsed TDI indices

Male cats were over-represented in the current study in the HCM group. This is in agreement with the high incidence of male affected cats reported in other studies and may reflect possible contribution of modifying factors related to sex in the phenotypic expression of the disease (Atkins *et al,* 1992a; Fox *et al,* 1995; Geisterfer-Lowrance *et al,* 1996; Rush *et al,* 2002). Stepwise regression analysis showed that the factor sex contributed mainly in the variance of TDI time intervals, especially in the normal group and scarcely in those of the affected group. However, when TDI time intervals were corrected for heart rate there was no significant difference found between male and female cats. Although the high incidence of male cats in the affected group indicates the possible influence of sex in the development of the disease, pulsed TDI indices were proved insensitive in reflecting these changes in the affected population of this study.

D.6.4. Physiological non-uniformity in feline myocardial motion

Several studies have documented the presence of a physiological non-uniformity in the myocardial motion of normal humans and of experimental animals. This has been described during both phases of the cardiac cycle and it is believed to be along with load and activation-inactivation mechanisms one of the main determinants of optimal myocardial performance under normal circumstances (Lew and Lewinter, 1983; Hammermeister *et al*, 1986; Brutsaert, 1987). This heterogeneous and asynchronous motion is the result of myocardial fibre orientation, asynchronous activation and of special electrophysiological and mechanical features of myocardial fibres in different parts of the myocardium (Brutsaert, 1987). Quantification of the normal human

myocardium with the TDI technique has confirmed the presence of this physiological time and space non-uniformity involving the different walls of the LV. TDI studies have shown that the posterior and lateral sides of the LV along both axes exhibit higher myocardial velocities than the septal side of the heart during all cardiac phases (Garcia *et al*, 1996a; Oki *et al*, 1997; Galiuto *et al*, 1998; Pai and Gill, 1998; Alam *et al*, 1999; Yamada *et al*, 1999a; Cardim *et al*, 2002a). Peak early diastolic velocities in the septal side of the heart occur later than those in the LVPW along both axes in normal individuals (Oki *et al*, 1997; Yamada *et al*, 1999a; Cardim *et al*, 2002a). It has also been shown that early diastolic myocardial motion in the IVS of normal individuals lasts significantly longer compared to that in the LVPW wall along the longitudinal axis (Pai and Gill, 1998). Moreover, the time from the first component of the first heart sound to Se' is shorter in the septal mitral annulus than in the other annular sites (Cardim *et al*, 2002a). Our study demonstrates that differences in myocardial motion between the posterior and septal side of the normal feline myocardium are mainly along the longitudinal axis, in which the posterior side exhibited higher early diastolic velocities and acceleration and also E'/A' compared to that in the septal side. Peak early diastolic velocity of the LVPW along the longitudinal axis occurred earlier than in the IVS along the same axis. The deceleration of E' wave at the lateral mitral annulus was higher than that in the septal mitral annulus. Differences between the LVPW and the IVS along the radial axis were confined in the acceleration and time of acceleration of the E' wave, which were significantly higher and shorter, respectively, in the former than in the latter. These findings support evidence for the higher compliance of the LVPW in the normal feline myocardium, and are in agreement with previous observations in normal

humans (Pai and Gill, 1998). Clinical and experimental invasive studies have shown that electrical activation and onset of contraction among the different myocardial layers and walls of the LV is asynchronous, with the endocardial area of the IVS being activated first and the septal side contracting earlier than other parts of the LV (Clayton *et al*, 1979; Hammermeister *et al*, 1986). Although, IVCt was shorter in the septal side of the heart along the longitudinal axis compared to that in the corresponding segments of the posterior side, one needs to take in to account that IVCt does not reflect true time of electrical activation since its onset was defined as the end of late diastolic myocardial motion and this occurs quite often during the pre-ejectional period. The shorter IVCt probably reflects more the tendency of longitudinal fibres in the IVS to expand for longer after LA contraction than those in the LVPW, rather than shorter pre-ejectional period. However, this was not reflected as a statistically longer A' duration in the septal side of the heart.

Although a gradual reduction in all myocardial velocities has been reported from LV base to apex, and also in the duration of E' and S' waves between mid and distal LV segments along the longitudinal axis in normal humans, similar findings are not reported to this extent in our group of normal cats (Galiuto *et al*, 1998; Pai and Gill, 1998). The LVPW showed significantly higher acceleration and shorter time of acceleration during early diastole than the lateral mitral annulus. Similarly, the IVS exhibited higher early diastolic myocardial deceleration than the septal mitral annulus. Conversely, early systolic acceleration (Se'acc) was significantly higher in both mitral annular sites compared to that in myocardial segments along the corresponding side.

Investigation of myocardial motion with TDI along both axes has shown that, with the exception of E' wave of the LVPW along the radial axis, myocardial motion along the longitudinal axis in normal humans is more prominent than it is along the radial axis during all phases of the cardiac cycle (Yamada *et al*, 1999a; Tabata *et al*, 2000). II-E' in the LVPW along the longitudinal axis was significantly longer compared to that from the radial axis (Yamada *et al*, 1999a). In our group of normal animals, myocardial motion along the longitudinal axis during early diastole was more prominent than along the radial axis. This was reflected in the higher velocities and accelerations recorded during early diastole in almost all myocardial segments along the longitudinal axis. Additionally, higher early myocardial deceleration was documented in the LVPW along the longitudinal axis in comparison to that recorded along the radial axis. Peak early diastolic myocardial velocity occurred earlier in the IVS along the longitudinal than along the radial axis. These findings reflect the predominant role of early diastolic myocardial expansion along the longitudinal axis in the normal feline myocardium. During systole, myocardial motion was more uniform among the different myocardial segments along both axes. However, the S' VTI of the IVS along the longitudinal axis was greater than that along the radial axis. IVCb in the LVPW along the radial axis was the most prominent myocardial shift during this period among all myocardial segments.

Quantification of tricuspid annular motion in normal cats showed that this part of the myocardium developed higher velocities compared to that in mitral annular sites during all cardiac phases. This denotes the higher contractile state and compliance of the right ventricle. Differences in the myosin isoenzyme composition between the

myocardial cells of the two ventricles have been shown to contribute to their different mechanical states (Samuel *et al*, 1983; Pagani and Julian, 1984; Litten *et al*, 1985). TDI studies in normal humans have shown that the tricuspid annulus exhibits higher systolic and late diastolic velocities compared to that in mitral annular sites (Alam *et al*, 1999). However, early diastolic tricuspid annular velocities in humans were higher only when compared with those from the septal mitral annulus, with the rest of mitral annular sites showing the same velocities with the tricuspid annulus during this particular cardiac phase (Alam *et al*, 1999).

D.6.5. Diastolic dysfunction in cats with HCM

Diastolic impairment was evident in a number of TDI indices obtained in the affected group. Decreased early diastolic velocities were recorded in all myocardial segments along the longitudinal axis in cats with HCM (Figure D4). Early diastolic acceleration and deceleration were lower in all myocardial segments along the longitudinal axis and also in the LVPW along the radial axis in affected animals. Diastole lasted longer at both annular sites and in the LVPW along both axes in HCM cats compared to that in normal animals. Peak early diastolic velocity in all myocardial segments, apart from the IVS along the radial axis, occurred later in the HCM group compared to that in normal ones. This was reflected mainly in the prolonged II-E' interval recorded in these segments. The early diastolic acceleration time was also prolonged and the early diastolic duration lasted longer in all myocardial segments in the HCM group apart from the IVS along both axes. Decreased early diastolic deceleration was recorded in the lateral mitral annulus and in the LVPW along the radial axis in HCM cats. The prolonged IVRt recorded in

many myocardial segments in the affected group was additional evidence of diastolic impairment in HCM of this species. CHF appeared to negatively affect some diastolic TDI indices in the HCM group, mainly by contributing to a further decrease in the acceleration (tricuspid annulus and LVPW along the radial axis) and deceleration (septal mitral annulus) of early diastolic velocities and by prolonging, on some occasions (septal mitral annulus), the duration of early diastolic myocardial expansion.

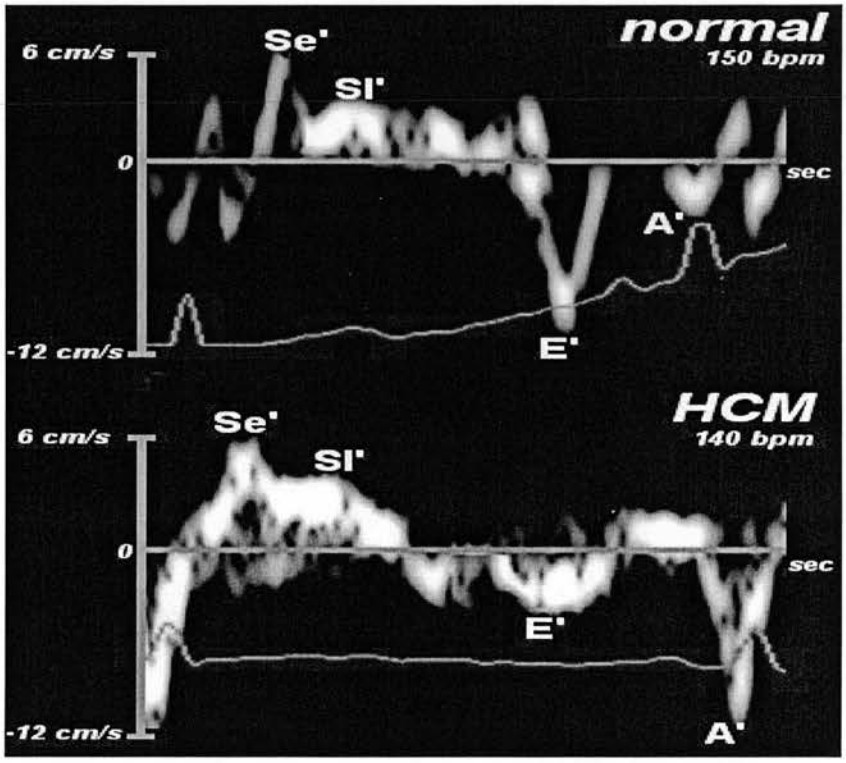

Figure D 4. *Myocardial velocities recorded from the IVS along the longitudinal axis of a normal (upper panel) and an affected (bottom panel) cat. The normal cat exhibits a normal velocity diastolic pattern with the early diastolic velocity (E') exceeding the late diastolic velocity (A'). The affected animal presents an abnormal relaxation pattern with very low early diastolic velocity and increased late diastolic component. Se' and Sl' peak early and late systolic velocities.*

Numerous TDI studies have shown that humans with HCM exhibit decreased early diastolic myocardial velocities and prolonged isovolumic relaxation time (Tabata *et al,* 2000; Naqvi *et al,* 2001; Vinereanu *et al,* 2001; Cardim *et al,* 2002a; Ho *et al,* 2002). These changes reflect impaired intrinsic diastolic properties caused by the classical pathological changes seen in HCM and/or abnormal cytosolic kinetics (Oki *et al*, 2000; Cardim *et al*, 2002a). In the first ever application of pulsed TDI in cats, Gavaghan and colleagues (1999) reported decreased diastolic velocities, acceleration and deceleration and also prolonged IVRt in both the lateral mitral annulus and the LVPW along the radial axis at papillary muscle level in cats with HCM.

These findings are in general agreement with the results reported in the current study. However, in our analysis we did not include summated E' and A' waves. Although it has been shown that the ratio of mitral inflow EA to myocardial EA' can be used to predict with relatively high accuracy pulmonary capillary wedge pressure (PCWP), we believe, based on the currently available data, that diastolic velocities, (early, late or summated early and late diastolic velocities) can not be used interchangeably in assessing feline diastolic myocardial properties and that a combined interpretation of their characteristics is required in order to do so. This is supported by the fact that early and late diastolic velocities have different physiologic and haemodynamic determinants, and hence, to a certain extent, they reflect different physiological processes. Affected asymptomatic animals can exhibit very low early diastolic velocities, suggesting impaired active relaxation properties and decreased elastic recoil, and on the other hand, prominent late diastolic velocities, reflecting preserved LA contractility. Under these circumstances in the presence of relatively high heart

rates (> 180 bpm) asymptomatic animals can present high amplitude EA' waves, due to the increased contribution of LA contraction (A' wave) in the genesis of the summated velocity wave despite impaired ventricular early diastolic properties. There is further support for this idea in that heart rate was found to be a positive predictor of A' wave in some myocardial segments in both groups (LVPW along the longitudinal axis in affected animals and both annular sites in the normal group). Decreased summated EA' waves is most likely to occur in animals with CHF, in which both early and late diastolic myocardial velocity components are decreased. Interestingly, affected animals tended to provide summated EA' waves at lower heart rates than normal animals did, suggesting that summation may be an indicator of diastolic impairment. The comparison of a relatively large number of EA' waves obtained from the same myocardial segment, between normal and HCM would help to clarify the utility of summated EA' waves in the assessment of feline diastolic myocardial properties. Pacing studies in affected and normal animals would probably overcome the difficulty in obtaining summated EA' waves in normal animals and further elucidate this issue.

Marked temporal and spatial nonuniformity is another common finding in the HCM of humans and is believed to be a significant determinant of diastolic impairment in this cardiac entity (Bonow *et al*, 1987; Oki *et al*, 2000). The physiological heterogeneity and asynchrony seen in the myocardial motion of normal cats was lost in HCM cats. This was evident in the loss of differences in peak early diastolic velocities between the posterior and septal side of the heart mainly along the longitudinal axis and also between the two axes in the posterior side. Differences in

the early diastolic acceleration and deceleration between the two groups followed a similar pattern. Although early diastolic velocities peaked significantly later in affected animals, they occurred in a more uniform pattern than those in the normal group. The role of physiological non-uniformity in the mechanical efficiency of the myocardium during contraction and especially during relaxation has been highlighted from earlier studies (Brutsaert, 1987). A number of factors such as architectural changes, electrical disturbances, alterations in the activation-inactivation coupling could alone or in combination disturb the physiologic non-uniformity under different pathological conditions. The result is an unbalanced or inappropriately increased non-uniformity, which in turn exacerbates further the mechanical insufficiency of the myocardium (Bonow *et al*, 1987). Our results show that in cats with HCM the physiologic asynchrony and heterogeneity of myocardial motion during diastole is lost rather than increased. We suggest this is an extra contributing factor in the deterioration of diastolic function of the myocardium, with potential negative haemodynamic effects.

The reduction in peak early diastolic velocities in the posterior side of the heart along the longitudinal axis was higher than that recorded at the septal side along the same axis. This probably reflects the greater susceptibility of the longitudinally arranged myocardial fibres in the LVPW of cats to myocardial damaged caused by HCM. Whether or not their magnitude of damage is greater than that seen in the septum needs pathologic confirmation. Changes in early diastolic motion along the radial axis in the affected group were identified exclusively in the LVPW. That there was no significant difference in peak early diastolic velocities in the LVPW along the

radial axis between the two groups does not imply that circumferential fibres at this part of the feline myocardium are less affected in HCM. One needs to take into account that motion of the LVPW along the radial axis is affected favourably by overall heart motion (Tabata *et al*, 2000). This makes it more difficult for TDI myocardial velocities to unmask impaired functional properties in this myocardial segment along the radial axis.

Myocardial wall thickness appeared to associate inversely, mainly with the VTI of early diastolic velocities, and with limited number of early diastolic TDI indices in the affected group. This highlights the fact that diastolic impairment in HCM of cats is not likely to be the cause of increased hypertrophy. Furthermore, it suggests that the typical pathologic alterations occurring in HCM is also likely to involve the non-hypertrophied parts of the LV (Cardim *et al*, 2002a).

The late diastolic myocardial component results from atrial contraction and it is believed to be an index of atrial contractility. A' wave was significantly higher along both axes of the heart in the IVS and the tricuspid annulus in asymptomatic animals compared to that in normal cats. This finding reflects increased atrial response to the elevated LA pressures and it is indicative of preserved atrial contractility in the early stages of the disease (Nagueh *et al*, 2001b; Naqvi *et al*, 2001). That the A' wave was not higher in the rest of the myocardial segments in the asymptomatic group when compared to that from the normal group, probably represents a lower response to atrial contraction or greater reduction of compliance rather than decreased atrial contractility. The absence of difference in the A' wave between the two groups, when

CHF animals were included in the analysis results from the loss of LA contractility in the failing myocardium. Thickness in the affected group, most of the time, appeared to be the only significant negative predictor for late diastolic velocities and their VTI, mainly along the longitudinal axis. This finding shows that hypertrophy is one of the main determinants of reduced compliance in HCM.

The E'/A' was significantly reduced in all myocardial segments of affected animals compared to that of normal ones. This was the only TDI index, which was significantly different in all myocardial segments between the two groups. The reduction in the E'/A' in affected animals was attributed mainly to the decreased early diastolic velocities. The number of tracings with an E'/A' > 1 was lower in affected animals compared to that in the normal group (number and percentage of tracings with an E'/A' > 1 in affected animals was: 3 (15%) and 4 (28%) in the septal and lateral mitral annulus respectively, 2 (10%) and 3 (25%) in the IVS along the longitudinal and radial axis respectively, 2 (9%) in the LVPW along the radial axis and none in the tricuspid annulus. Seven affected animals (50%) had an E'/A' > 1 in the LVPW along the longitudinal axis. This, along with the fact that none of the normal animals showed an E'/A' < 1, reflects the decreased response of longitudinal fibres in the LVPW during passive motion induced by atrial contraction.

The decreased early diastolic velocities recorded in the tricuspid annulus of affected animals, indicates right ventricular involvement in the myopathic process (Galderisi *et al*, 2001).

IVCb in the LVPW along the radial axis was a distinct diastolic shift, which was recorded in almost all animals and was not affected from summation effects. This is in agreement with the decreased myocardial velocities reported during the two isovolumic phases in humans with HCM (Naqvi *et al*, 2001).

D.6.6. Systolic dysfunction in feline HCM

A number of findings in this study provided evidence for systolic dysfunction in feline HCM. This was reflected in the decreased late systolic velocities recorded along the longitudinal axis and the reduced peak systolic acceleration of both annular sites and also of the LVPW along the longitudinal axis in the affected group compared to that in normal cats. Peak late systolic velocity occurred (bS'-Sl') later in both the lateral mitral annulus and the IVS along the radial axis in affected animals than in normals. The systolic VTI in the septal mitral annulus of affected animals was also decreased compared to that from normal ones. Moreover, the relatively uniform myocardial motion seen during systole in normal animals was absent in the HCM group. This was particularly reflected in the delayed occurrence of Se' and Sl' (Q-Se' and Q-Sl', respectively) in the LVPW along the radial axis compared to that along the longitudinal axis. Additionally, contraction in the LVPW commenced later (Q-bS') in comparison to that in the IVS along the radial axis. None of the differences in the above systolic TDI indices between the two groups was attributed to CHF or to LV outflow tract obstruction. Although peak early systolic velocity of the lateral mitral annulus appeared to be lower in HCM than in normal cats, this difference was lost when only asymptomatic animals were considered in the analysis. All cats in CHF had very low systolic mitral annular velocities (3 of them < 3 cm/sec

and 1 < 5 cm/sec). Low early systolic velocities were recorded in almost all myocardial segments in animals with CHF. These findings suggest that deterioration of systolic dysfunction in cats with HCM may play an important role in the development of CHF. However, higher number of animals with end-stage disease would be required in order to confirm this hypothesis.

Systolic impairment in HCM of humans is however, now accepted as a key component in the pathophysiology of the disease and was evident in numerous TDI studies in patients with this cardiac entity. It has been shown that impaired contractility as assessed by TDI indices is depressed in humans with HCM even in the presence of normal or supernormal global systolic function (FS% of EF%) and that it is not always associated with LV hypertrophy (Cardim *et al*, 2002a; Cardim *et al*, 2002c; Oki *et al*, 1998b; Tabata *et al*, 2000;). Increased afterload, induced by angiotensin infusions, resulted in a more prominent decrease of systolic velocities, even in the non-hypertrophied LVPW of HCM patients, compared to the decrease seen in normal individuals (Mishiro *et al*, 2000). Annular systolic velocities could differentiate with high degrees of sensitivity human mutation carriers without LV hypertrophy from normal subjects (Nagueh *et al*, 2001a). Moreover, systolic lateral annular velocity could identify the mutant β- MHC-Q^{403} transgenic rabbit with high sensitivity even in the absence of LV hypertrophy (Nagueh *et al*, 2000). These findings, along with experimental data, led many investigators to implicate the impaired contractile performance of individual cardiac cells as the primary deficit in HCM, which triggers the release of stress-responsive mitotic and trophic factors, which in turn induce compensatory hypertrophy and myocardial fibrosis (Marian *et*

al, 1995b; Marian *et al*, 1997; Marian and Roberts, 2001; Marian, 2000; Li *et al*, 1997; Li *et al*, 2002; Rust *et al*, 1999; Roberts and Sigwart, 2001; Ortlepp *et al*, 2002). According to this theory although diastolic impairment is also evident in HCM, it is believed to be the consequence of hypertrophy and fibrosis rather than the primary defect (Marian, 2000). That indices of global systolic function such as FS% or EF% are normal or supernormal in HCM is attributed to the concentric nature of the disease, which leads to decreased LV end diastolic volume and consequently decreased afterload (Marian, 2000).

Although decreased systolic velocities have been reported in humans with HCM, this finding is not reported constantly in all studies. Severino and colleagues (1998) failed to show differences in Se' of the middle IVS and the LVPW along the long axis between normal and HCM subjects. Ho and colleagues (2002) found that decreased systolic annular velocities were present only in carriers of β-myosin heavy chain mutations with LV hypertrophy and not in those without LV hypertrophy. The fact that systolic impairment is not always evident in HCM of humans may reflect differences in the effect that certain mutations have in the contractile state of sarcomere proteins. Although, it has been reported that some mutations are associated with impaired sarcomere contractility (Marian *et al*, 1995b; Marian *et al*, 1997; Marian and Roberts, 2001; Marian, 2000), other experimental studies, particularly those evaluating β-MHC mutations, have shown that a hypercontractile state is induced by certain sarcomere mutations (Palmiter *et al*, 2000; Tyska *et al*, 2000; Witt *et al*, 2001). This latter finding may explain the hypercontractile LV state often seen in HCM and the lack of significant reduction in systolic TDI indices reported by some studies in humans with this particular disease.

In the present study, decreased contractility was detected in a number of systolic TDI indices in cats with HCM, despite having similar FS% to that recorded in normal cats. These observations are in partial agreement with previous findings in humans and experimental animals with HCM and shows that traditional methods of assessment of global systolic function are less sensitive in accurately reflecting LV systolic properties. However, the reduction in systolic TDI indices documented in the current group of HCM cats was not of the magnitude reported in some TDI studies in humans with HCM. Peak early systolic velocities appeared to be lower only in the lateral mitral annulus and this finding was attributed mainly to CHF. The genetic diversity of HCM in humans along with the role that modifier genes (Brugada *et al*, 1997), sex (Abchee and Marian, 1997), environmental factors and variable penetrance (Fananapazir and Epstein, 1995) exert on the pathogenesis of the disease, contribute to a variable extent to the phenotypic and clinical diversity of the this cardiac entity (Marian and Roberts, 1995a). Differences between the data reported in the current study and that from TDI studies in humans with HCM may reflect differences in the contributing factors resulting in the genesis of the disease in the two species. Despite peak early systolic velocity of the lateral mitral annulus, the decrease reported in the rest of the systolic TDI indices in the affected group was not positively correlated with wall thickness. Interestingly, thickness negatively affected indices, such as the tSe' acc of the lateral mitral annulus and of the IVS along the longitudinal axis, despite being significantly prolonged in the affected group. These findings show that depressed contractility in feline HCM is an inherent component in the disease, which is likely to be independent from hypertrophy.

In human HCM, systolic impairment has been expressed as prolonged Q-Se' in all myocardial segments, along both axes with the prolongation being greater in the LVPW along the radial axis (Oki *et al*, 2000). Although, our results did not confirm the above findings, we believe that the asynchrony seen in some of the systolic events in affected animals reflects altered systolic properties.

D.6.7. General comments about the acquisition of images

Quantification of myocardial motion was easier in the septal side of the heart along the longitudinal axis and in the posterior side of the heart along the radial axis. This was reflected in the higher number of quantifiable tracings acquired from these regions. That the septal side along the longitudinal axis was always feasible to quantify may represent the increased number of longitudinal fibres in that part of the feline myocardium. Similarly, one could argue that the increased number of circumferential fibres in the LVPW was a contributing factor, but the fact that motion of this myocardial wall, along the radial axis, is affected favourably by translational effects needs also to be considered. Quantification of motion of the IVS at chordae tendineae level along the radial axis often provided quite erratic velocity signals. Studies with 2-dimensional colour TDI have revealed that even in the normal human myocardium the IVS during systole exhibits a paradoxical movement with its upper-basal part moving anteriorly while the lower-apical part moves posteriorly (Iwasaki *et al*, 1999). Although qualitative assessment of motion of the IVS with 2-dimensional TDI was not performed in our study, we believe that the presence of a similar pattern of motion in the IVS of cats is a possible cause of the erratic velocity signals obtained from these region along the radial axis. The motion of the IVS is

influenced by ventricular interdependence and right ventricular filling (Gorcsan *et al*, 1996; Gorcsan *et al*, 1998). It is also influenced more from overall heart motion than other parts of the myocardium, especially along the radial axis of the heart (Garcia *et al*, 1996a; Tabata *et al*, 2000). These factors make it more difficult to quantify its motion with routine echocardiographic methods. Quantification of the LVPW along the longitudinal axis was quite often unsuccessful and provided unidentifiable sequence of velocity signals, especially in affected cats. In six affected animals, the LVPW along the longitudinal axis exhibited very prominent positive velocities during the second phase of the IVR period, which were substantially higher than the preceding systolic velocities (Figure D5). A similar velocity pattern, that is called post-systolic thickening, has been documented in variable clinical conditions, such as myocardial ischaemia and stunning, left bundle branch block and syndrome X in human patients and various explanations have been given so far for its genesis (Takayama *et al*, 1988; Henein *et al*, 1994; Hosokawa *et al*, 2000; Galderisi *et al*, 2002). Some investigators suggest that post-systolic thickening represents delayed active contraction and it is associated with viable myocardium, whereas others support that it is a passive motion caused by the interaction of affected myocardial segments with normal surrounding contracting muscle (Takayama *et al*, 1988; Ehring and Heusch, 1990; Henein *et al*, 1994; Jamal *et al*, 1999; Edvardsen *et al*, 2000; Hosokawa *et al*, 2000; Derumeaux *et al*, 2001; Pislaru *et al*, 2001; Galderisi *et al*, 2002). However, the fact that post-systolic thickening was present in patients with left bundle branch block suggests that this myocardial pattern of motion could be the result of interaction between normally and delayed activated myocardial segments and therefore can not be solely attributed to myocardial infarction (Grines *et al*,

1989; Galderisi *et al*, 2002). It has been shown that the typical narrowed lumens of small intramural coronary arteries seen in patients with HCM can increase microvascular resistance and decrease coronary reserve resulting in myocardial ischaemia (Cannon *et al*, 1985; Camici *et al*, 1991). This, along with myocardial disarray, interstitial fibrosis and thickening, may cause loss of the mechanical efficiency of myocardial fibres and prolong the depolarization at areas with significant myocardial damage. This could reduce the contractile performance of myocardial fibres and result either in delayed contraction or passive contraction induced by the shortening of less affected adjacent myocardial areas. Whether myocardial infarction, as seen in humans with coronary artery disease is related to the reduced systolic velocities and the augmented post-systolic thickening recorded in the LVPW along the longitudinal axis in some cats with HCM is something that, to our knowledge, can not be supported on the basis of current pathological data. Combining TDI and pathological data would help to elucidate the mechanisms of this phenomenon in affected cats. However, irrespective of the underline causative mechanism, the presence of post-systolic thickening is indicative of impaired systolic function. The fact that erratic, unidentifiable velocity signals and post-systolic thickening were recorded in the LVPW of cats only along the longitudinal axis and not along the radial one suggests the more profound impairment of longitudinally arranged fibres in this myocardial wall of cats with HCM.

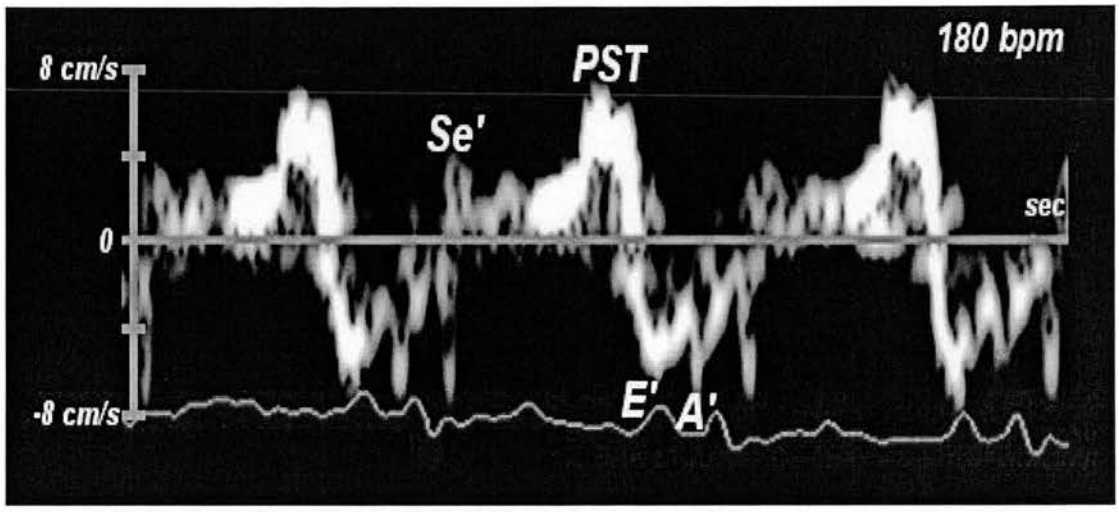

Figure D 5. *Post-systolic thickening (PST) recorded in the LVPW along the longitudinal axis of a HCM cat. Note that the systolic velocity (Se') is substantially lower from that recorded just before the onset of early diastole. E' and A', peak early and late diastolic velocities.*

D.6.8. Limitations

This study was carried out using pet owned animals. Consequently, we were unable to generate invasively determined haemodynamic data to provide gold standards with which to compare our results. Some of the affected animals were treated for CHF. To what extent their status and treatment may have influenced TDI indices remains unclear, mainly because of their small number. Future studies with larger numbers of cats in CHF due to HCM will elucidate further this issue and help in monitoring the influence of drug therapy in asymptomatic and animals with end-stage disease. Classification of different groups, and especially of the affected group, was based on morphological rather than pathological criteria. This may have resulted in falsely including affected animals in the normal group and affected animals with other cardiac diseases, apart from HCM, to the affected group. Myocardial velocities

recorded by the TDI technique are affected by overall heart motion and therefore do not truly represent absolute myocardial motion. This may mask impaired myocardial properties, especially in areas, which are favourably affected by translational effects. TDI indices such as Myocardial Velocity Gradients and strain, which are independent from overall heart motion, can offer a more accurate means of myocardial function and will overcome the confounding effects of translational motion. Due to the angle dependence of the TDI technique, only the velocity component parallel to the ultrasonic beam was recorded. This may have underestimated true myocardial velocities. However, sampling of myocardial segments was consistently done by using the same echocardiographic view every time. Nineteen of the affected cats had mitral regurgitation. Mitral regurgitation is known to increase preload (Takenaka *et al*, 1986; Bryg *et al*, 1987; Maron *et al*, 1987). It is a limitation that TDI indices were not controlled for mitral regurgitation. However, taking into consideration that TDI indices are supposed to be independent from preload in the diseased state and that the magnitude of mitral regurgitation in HCM is not usually big, it is safe to assume that TDI indices were not affected significantly from the presence of mitral regurgitation.

D.6.9. Conclusion

In this study, the pulsed TDI technique was applied in a higher number of normal and affected animals from that in previous studies. Quantification of myocardial motion of multiple myocardial segments along both axes of the heart was performed. In normal animals, aging was found to affect inversely mainly early diastolic myocardial properties and to a lesser extent the systolic performance of the

myocardium. A physiological time and space non-uniformity was recorded in myocardial motion of different myocardial segments during early diastole in the normal group. In normal animals myocardial relaxation along the longitudinal axis was more prominent than along the radial axis during early diastole, suggesting the greater compliance of longitudinally arranged fibres in the normal feline myocardium. Evidence of diastolic and systolic impairment, irrespective of myocardial thickness, was documented in HCM cats. The physiologic nonuniformity of myocardial motion recorded in the normal feline myocardium during early diastole was lost in the affected group. Decreased early systolic acceleration and late systolic velocities were recorded in HCM cats mainly along the longitudinal axis and along with the presence of post-systolic thickening in the LVPW in a number of affected animals were the main systolic abnormalities found in this group. A very prominent decrease in early diastolic velocity was recorded in the LVPW of affected animals along the longitudinal axis, which along with the presence of post-systolic thickening and an increased number of erratic, unquantifiable velocity signals suggest that damage of the longitudinally arranged fibres in this myocardial segment may be more prominent than in other parts of the LV, and may play a significant role in the progress of the disease.

SECTION E

Peak mean myocardial velocities and velocity gradients measured by colour M-mode Tissue Doppler Imaging in the left ventricular free wall of healthy cats

E.1. Introduction

Myocardial disease is a major cause of morbidity and mortality in cats, particularly hypertrophic cardiomyopathy (HCM) (Atkins *et al*, 1992a; Bright *et al*, 1992; Fox *et al*, 1995). HCM of this species is characterized by a concentrically hypertrophied, non-dilated left ventricle with diastolic dysfunction being the main abnormality of the disease (Fox *et al*, 1995). However, it is believed that diastolic dysfunction also is involved in some other cardiac diseases of cats, which have been labelled as restrictive cardiomyopathy (RCM) (Fox, 1998), unclassified cardiomyopathy (UCM) (Gavaghan *et al*, 1999) and intermediate cardiomyopathy (Harpster, 1986). These entities are poorly classified and their assessment often is subjective and based on morphologic features. Consequently, much effort has been spent in the investigation of feline cardiomyopathies with the intention of improving the classification of these diseases in recent years. Moreover, studies of feline myocardial disease have shown the potential of using cats as an animal model for human cardiac disease (Fox *et al*, 1995; Kittleson *et al*, 1999; Fox *et al*, 2000). This possibility further emphasizes the importance of investigating feline myocardial function in a more detailed way.

Tissue Doppler Imaging recently has emerged as a new ultrasonic technique, which is able to quantify myocardial motion (McDicken *et al*, 1992; Miyatake *et al*, 1995). Based on the Doppler principle, which is applied to the myocardium instead of to the blood pool, the technique selects only the high amplitude, low frequency ultrasonic shifts returning from the interrogated myocardium and therefore allows the estimation of myocardial velocities (Fleming *et al*, 1994b; Miyatake *et al*, 1995). A series of studies have proved the usefulness of TDI in investigating different cardiac diseases in both humans and animals (Palka *et al*, 1997b; Oki *et al*, 1998c; Gavaghan *et al*, 1999; Edvardsen *et al*, 2000). More specifically, colour M-mode TDI allows the estimation of myocardial velocity gradient (MVG) and mean myocardial velocity (MMV). MVG describes the spatial distribution of transmyocardial velocities throughout the myocardium from endocardium to epicardium and reflects wall thickness changes during diastole and systole (Fleming *et al*, 1994b). It is one of the few ultrasonic variables that is independent of preload and also of the overall heart motion and correlates strongly with invasive haemodynamic variables such as the peak positive rate of pressure development (dP/dt) and the time constant of pressure decay in isovolumetric relaxation (τ). Therefore, it is a very sensitive tool for non-invasively assessing regional and global myocardial systolic and diastolic function (Fleming *et al*, 1994b; Shimizu *et al*, 1998; Oki *et al*, 2000; Ueno *et al*, 2002). MVG can differentiate myocardial hypertrophy of different aetiologies and also is a useful tool in the investigation of different myocardial diseases in humans (Palka *et al*, 1997a; Palka *et al*, 1997b; 2000; Shimizu *et al*, 1998; Dutka *et al*, 1999; Marcos-Alberca *et al*, 2002). The technique has also allowed investigation of age-related changes in the normal human myocardium (Palka *et al*, 1996; Palka *et al*, 1999).

MMV describes the mean value of myocardial velocity estimates from endocardium to epicardium and has been widely used in the investigation of human myocardial physiology and myocardial diseases (Palka *et al*, 1996; Palka *et al*, 1999; Zamorano *et al*, 1997). In addition, the use of colour M-mode has offered a unique opportunity to assess the different phases of the cardiac cycle accurately and non-invasively (Zamorano *et al*, 1997).

We sought to assess the feasibility of measuring MVG and MMV in the free wall of normal cats using a purpose-designed 7.4 MHz transducer equipped to record colour M-mode TDI. The velocity estimation accuracy and the spatial resolution of the system used to record colour M-mode TDI images were assessed using rotating phantoms made from tissue-mimicking material (TMM). The cyclic variation of MVG and its consistency with wall thickness changes, as determined by the normalized rate of change of wall thickness (nRCWT), were assessed. We also aimed to provide reference data for MVG and MMV from healthy cats for ongoing studies in the investigation of feline myocardial diseases. Such data may offer additional information in the classification of myocardial diseases of this species.

E.2. Materials and methods

E.2.1. Study group

The study population comprised 18 unsedated normal cats, which were pets owned by students and staff at the University of Edinburgh. None of the animals had clinical evidence of cardiovascular disease or other significant clinically relevant abnormalities. Each cat underwent a complete 2D, M-mode and colour flow and

spectral Doppler echocardiographic examination and had results within normal limits (Sisson *et al*, 1991; Fox *et al*, 1995). All cats > 7 years of age also underwent haematology and biochemical testing primarily for the assessment of azotaemia and thyroid status and had values within reference ranges. All cats had normal systolic blood pressure (<180 mm Hg) as measured by the Doppler technique. The method followed to measure the blood pressure has been described in Section B.

E.2.2. Conventional echocardiography

Conventional echocardiographic and Doppler examination was carried out in the cardiopulmonary service of the Royal (Dick) School of Veterinary Studies. Echocardiographic examination was performed using an Esaote SIM 7000 Challenge ultrasound system (Esaote Biomedica, Firenze, Italy) with a 7.5 MHz phased array transducer. Images were recorded onto S-VHS videotapes by a videocassette recorder (SV0-9500MDP; Sony Corporation, Japan). The method followed to acquire conventional and Doppler echocardiographic measurements has been described in Section B.

E.2.3. Tissue Doppler Imaging echocardiography

Colour M-mode TDI measurements were obtained from all animals in the Medical Physics and Engineering department of the University of Edinburgh the evening of the same day that conventional echocardiography was carried out in the Cardiopulmonary Service of the R(D)SVS. All colour M-mode TDI recordings were made with an ATL HDI 5000 ultrasound system (ATL Bothell, Washington, USA) using a 7.4 MHz phased array transducer, which used prototype TDI software. Off-

line analysis of the images was done using a special analysis software (HDIlab) developed by ATL Bothell, Washington, USA.

Animals were scanned unsedated and manually restrained in lateral recumbency on a purpose-designed table, which allowed placement of the transducer on the dependant part of the thorax from below through a hole. A simultaneous ECG was recorded (lead II) using adhesive electrodes, which were attached to the main pads of the feet and secured with a tape.

Colour M-mode TDI provides the potential for assessing the spatial distribution of transmyocardial velocities throughout the myocardium by detecting the consecutive Doppler shifts returning from the interrogated myocardium (McDicken *et al*, 1992; Miyatake *et al*, 1995). Based on this information, the myocardial velocity gradient (MVG) and the mean myocardial velocity (MMV) can be calculated (Fleming *et al*, 1994b; Miyatake *et al*, 1995). In this study, MVG was defined as the slope of the linear regression of the velocity estimates across each M-mode scan-line throughout the myocardium, from endocardium to epicardium (Figure E1). Peak MVG was defined as the maximal value of MVG during a particular cardiac phase. MMV was defined as the mean value of the myocardial velocity estimates along each M-mode scan-line from endocardium to epicardium (Figure E1). Peak MMV was the maximal MMV value over the duration of each cardiac phase.

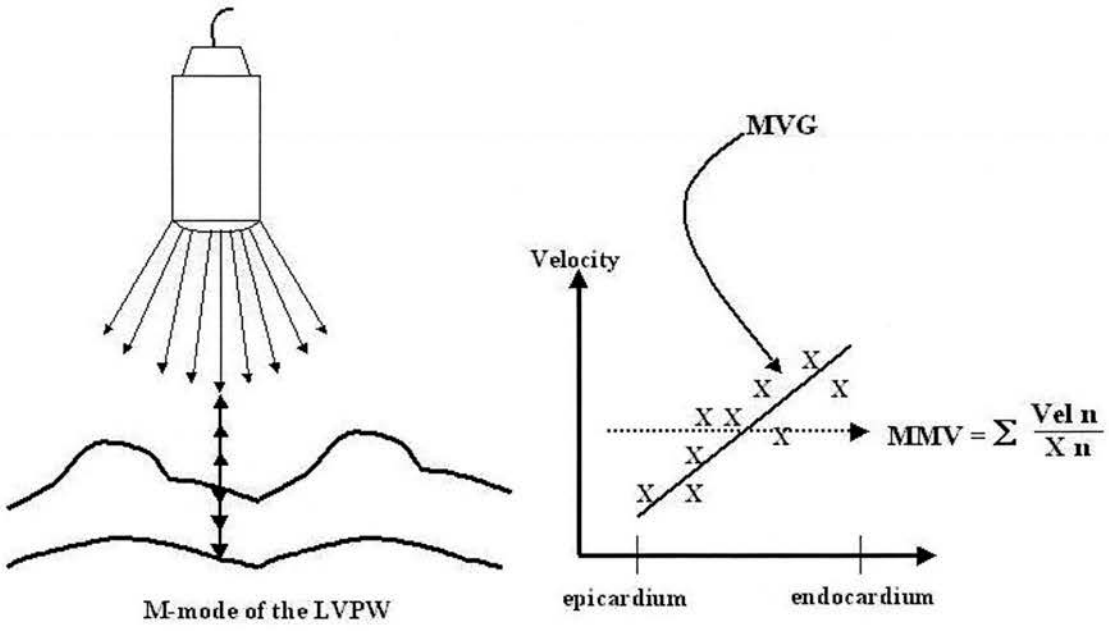

Figure E 1. *Graphical representation of the calculation of myocardial velocity gradient and mean myocardial velocity. Myocardial velocity gradient is defined as the slope of the linear regression of the velocity estimates across every single M-mode scan line throughout the myocardium from endocardium and epicardium. Mean myocardial velocity was defined as the mean value of the velocity estimates along each M-mode scan line from endocardium to epicardium.*

Colour M-mode TDI images of the left ventricular posterior wall were obtained from the right parasternal long-axis view at mitral valve level. Mitral valve level was chosen to permit timing of cardiac events and to optimize alignment. Throughout the study, care was taken to ensure that the ultrasonic beam was always parallel to the movement of the free wall. The Doppler velocity range was set at the minimal point at which no aliasing occurred. Doppler velocity gain was adjusted to achieve proper colour filling of the free wall. Grey-scale gain was optimized so that the endocardial and epicardial borders could be clearly seen. The maximal available M-mode sweep rate was used (values obtained every 3 msec). The focus of the ultrasonic beam was set at the free wall level in order to optimize the quality of grey and colour scales.

Both the grey and colour scales were captured simultaneously with the colour scale being superimposed on the grey scale. Assessment of the quality of the grey scale was possible by turning the colour scale off before downloading the images. To assess the region of interest, the endocardial and epicardial borders were traced manually on the grey scale (Figure E2). This method was chosen because the wall boundaries were seen more clearly on the digitized grey-scale image. These traces were automatically superimposed onto the corresponding colour image (Figure E2). In previous studies of humans in which colour M-mode TDI was used, myocardial velocities were calculated by converting colour-coded velocities into velocity estimates using the colour bar data as a reference table (Palka *et al*, 1996; Palka *et al*, 1997a; Palka *et al*, 1997b; Palka *et al*, 1999). In contrast to these studies, an advantage of the system used in the current study was that determination of the velocity estimates was possible from the direct quantification of the image data so a conversion from the colour bar velocities was not required (the number of data points collected for each column of M-Mode data was 512). However, the use of colour played an important role in selecting the optimal velocity range for every frame.

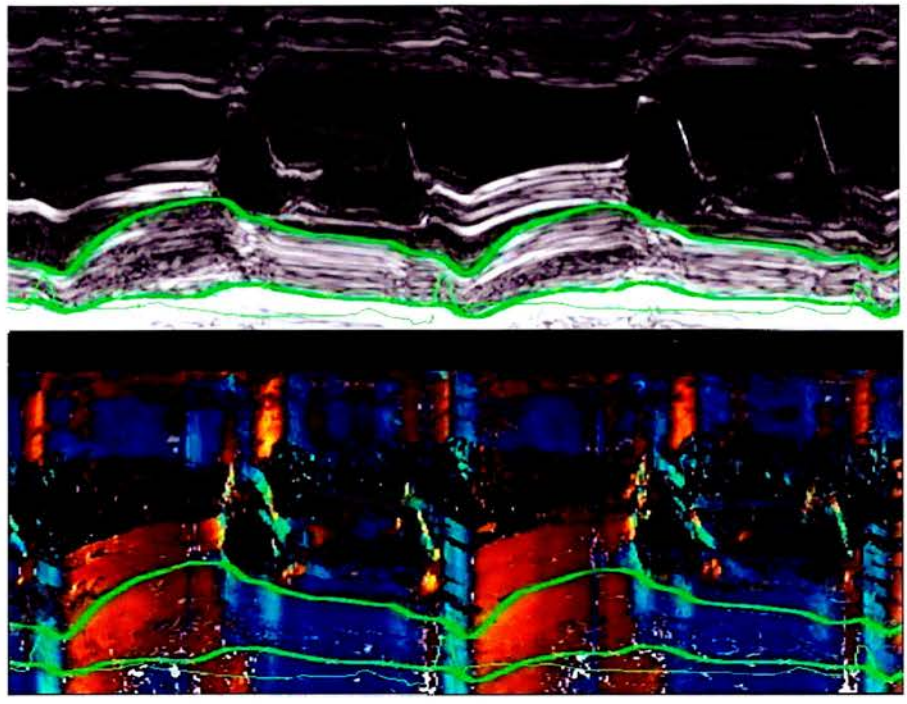

Figure E 2. *M-mode at the level of the mitral valve (right parasternal long axis view). Tracing of the cardiac boundaries took place on the grey-scale image. Colour M-mode images were automatically superimposed onto the corresponding grey-scale image.*

E.2.4. Phantom Study

To test the velocity estimation accuracy of the system used to record TDI images, a rotating circular-shaped phantom made out of tissue-mimicking material (TMM) was used (Figure E3). The TMM phantom was manufactured in the following manner: a disc of reticulated foam was glued to a nylon disc (a) (Figure E4 and E5) and inserted into a close fitting tube of 4.2 cm internal diameter. Tissue-mimicking material was prepared (see Appendix E) and poured into the tube and left to set overnight (Teirlinck *et al*, 1998; Moran *et al*, 2000). The following morning, the tube was removed leaving a circular disc of TMM material of 4.2 cm diameter (b) (Figure E4 and E5) (this size was chosen to mimic a cat heart) attached to the nylon

disc. The nylon disc was attached to a motor (c) (McLennon Ltd, Grand Falls-Windsor, Canada) (Figure E4 and E5) which rotated the disc at a constant velocity, the magnitude of which was set by means of a variable voltage supply (d) (Farnell Instruments, Texas, U.S) (Figure E5) applied to the motor drive unit. The speed of rotation was assessed using a photo-electric detector (e) (RS components Ltd, Corby, UK) (Figure E4 and E5) attached to the motor rear shaft extension. The detector produced 360 pulses per revolution of the disc and the pulses were observed and measured on a Tektronix 2236 (Bracknell, UK) 100MHz oscilloscope (f) (Figure E6). The rotating phantom was set in motion while submerged in an off- centre circular-shaped hole filled with water in a base made out of tissue mimicking material (g) (Figure E4 and E5). Measurements were acquired by placing the probe on the outer surface of the TMM base. The off-centre circular shaped hole allowed the adjustment of depth in order to be similar with that used during the acquisition of images from cats.

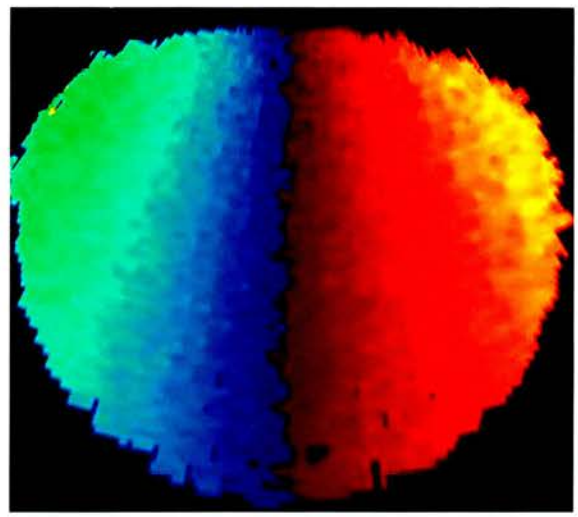

Figure E 3. *An actual image of the rotating phantom*

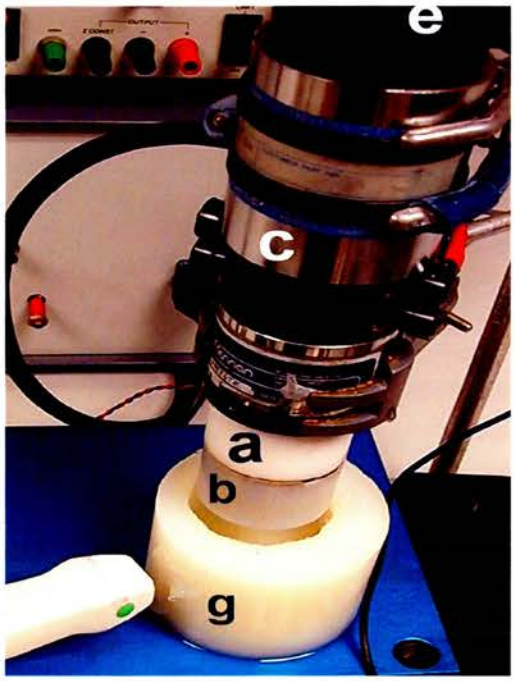

Figure E 4. *a) nylon disc, (b) circular TMM phantom, (c) motor (McLennon Ltd, Grand Falls-Windsor, Canada), (e) photo-electric detector (RS components Ltd, Corby, UK), (g) TMM base.*

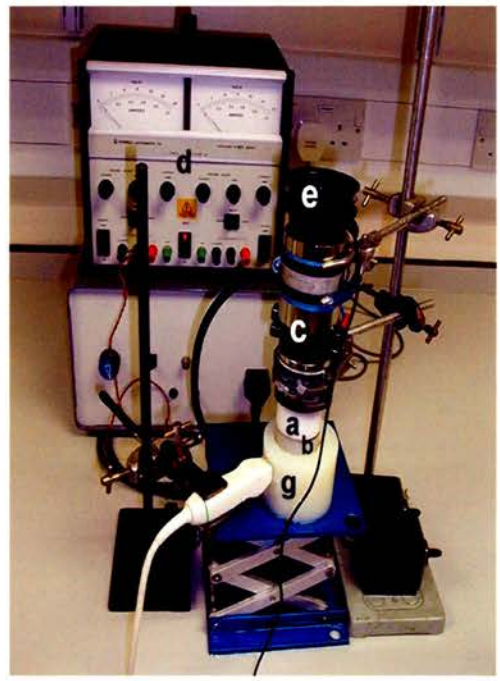

Figure E 5. *a) nylon disc, (b) circular disc TMM phantom, (c) motor (McLennon Ltd, Grand Falls-Windsor, Canada), (d) voltage supply unit (Farnell Instruments, Texas, U.S), (e) photo-electric detector (RS components Ltd, Corby, UK), (g) TMM base.*

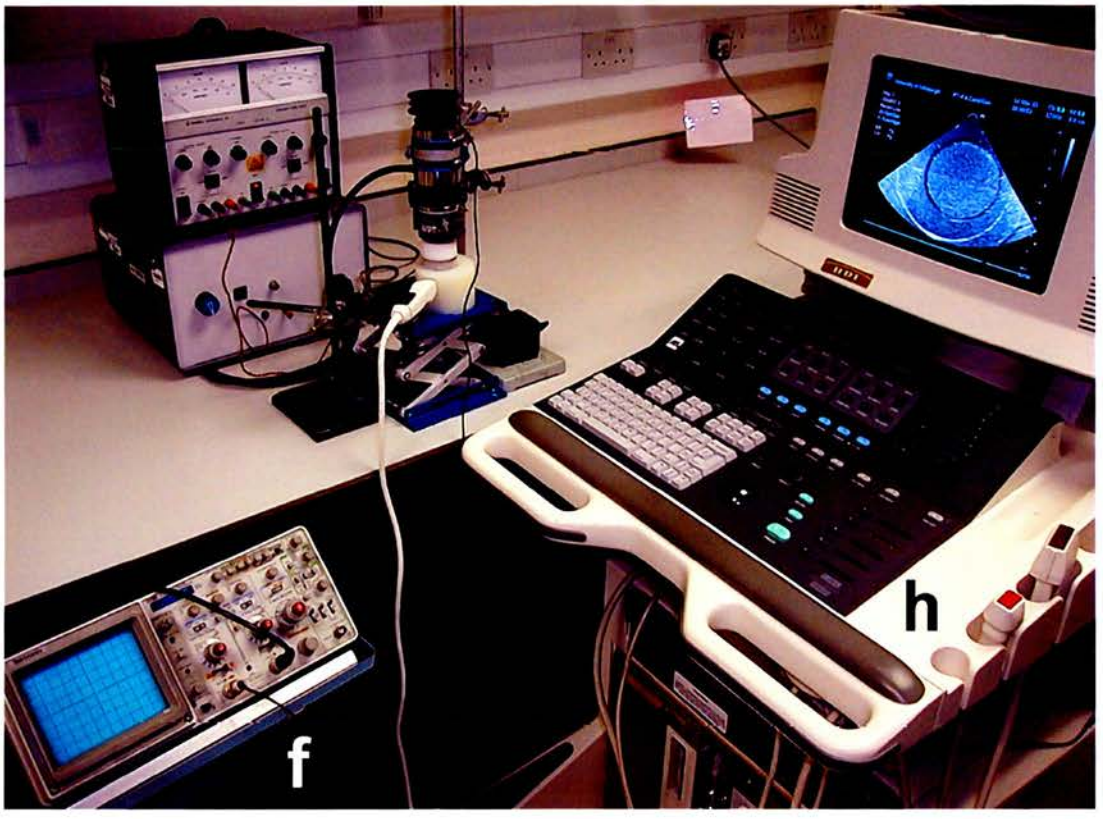

Figure E 6. *(h) ATL 5000 ultrasound system used for the phantom study (ATL Bothell, Washington, USA), (f) Tektronix 2236 100MHz oscilloscope (Bracknell, UK)*

Mean Doppler velocities measured by the system along different scan lines were compared with the actual velocities of the rotating phantom at the same points. Calculation of the actual velocities was based on the concept that a straight line through a rotating phantom has a constant velocity component in the direction of the line at all points along it (Fleming *et al*, 1994a). This velocity can be calculated by the following equation:

$$\upsilon = 2 \pi r f \cos\theta \quad (1)$$

where υ is the velocity, r is the distance between the scan line and the centre of rotation; f is the rotational frequency (revolutions per second); and θ is the angle of incidence of the scan line. Rotational speed of the phantom was set at 17, 26 and 47

revs/min. Actual velocities were measured at 7 different points from either side of the centre of the phantom. Mean Doppler velocities were calculated from colour M-mode TDI images acquired from the same points using the special analysis software (HDIlab). All actual velocities then were compared with Doppler velocities.

To assess the spatial resolution of the current system, a rotating circular-shaped TMM phantom (diameter, 4.2 cm) with a wedge was used (Figure E7 A and B). Spatial resolution was assessed as the minimal distance in which the 2 edges of the wedge could be resolved, while using the 2D TDI mode, and it was calculated as the mean value of several measurements obtained at 8 different levels and at 2 different rotating velocities (26 and 40 rev/min). All phantom measurements were obtained using similar echocardiographic settings as those used during the acquisition of images from cats.

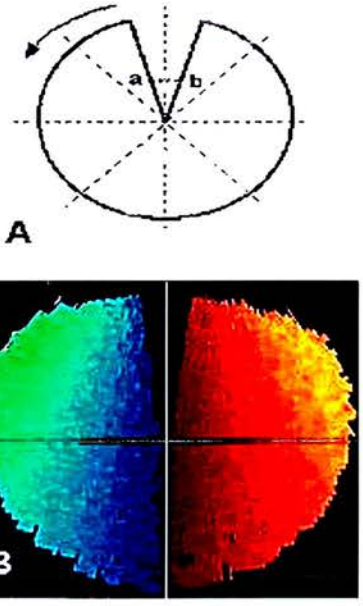

Figure E 7. *A. Diagram of rotating wedged phantom. Spatial resolution was assessed as the minimal distance (thick vertical dashed line) in which the two edges of the wedge (a and b) could be clearly resolved. Thin dashed lines indicate levels at which spatial resolution was assessed. B. Actual image of rotating wedged phantom.*

E.2.5. MVG and wall thickness changes

Fleming et al (Fleming *et al*, 1994b) proposed that velocity gradients are linear in the myocardium and can be estimated from Doppler velocity estimates throughout the muscle. According to their initial study, if the ultrasound beam is parallel to movement of the interrogated muscle then the following relationship between MVG and the wall thickness holds:

$$\text{Myocardial Velocity Gradient} = -\,dPW/PW \times dt \quad (\text{cm/cm} \times \text{sec}) \quad (2)$$

where dPW is the change in wall thickness that occurs during time dt and PW is the average wall thickness during dt. The second part of the above equation represents the normalized rate of change of wall thickness (nRCWT).

To assess if MVG follows wall thickness changes measured by the nRCWT in the free wall of cats, 2 methods were used. First, the correlation coefficient between the overall amplitude of MVG and nRCWT was calculated for each M-mode sequence. Secondly, the correspondence between peaks of MVG and nRCWT during systole and diastole was assessed. These determinations were made by noting the presence or absence of a MVG peak when a nRCWT peak was used as a reference and *vice versa*. Only peaks of MVG and nRCWT that reached 1 sec^{-1} were considered. Peaks less than 1 sec^{-1} were ignored. Calculation of the nRCWT was achieved by using the data acquired by tracing the cardiac boundaries on the digitized grey scale (Figure E2). Figure E8b shows a characteristic tracing of the nRCWT. Peak nRCWT was the maximal nRCWT value during a particular cardiac phase.

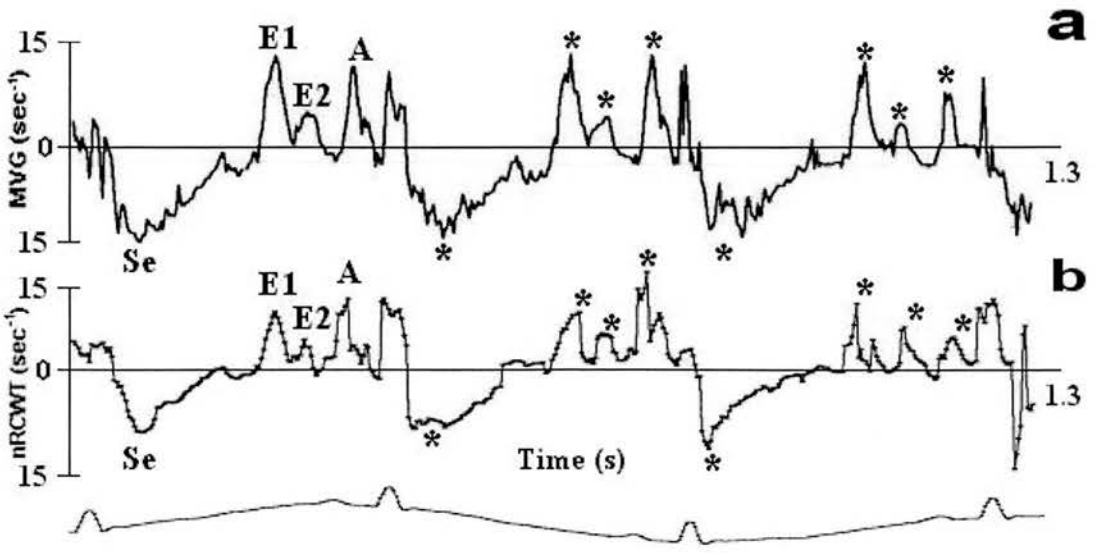

Figure E 8. *Examples of tracings of MVG (a) and nRCWT (b) from the free wall (mitral valve level, long axis view) of a 7-year-old domestic short-haired cat. Note that there is a very good correspondence in terms of timing in all three cardiac cycles, between peaks in both curves. However, peak values of nRCWT are lower than the corresponding peak values of MVG. Asterisks indicate peak values during the different phases of the cardiac cycle.*

Assessment of every cardiac phase was done using the combined information obtained from the M-mode colour and grey scale at mitral valve level and the simultaneously recorded ECG (Figure E9). Each cardiac cycle was divided into 6 standarized phases: early ventricular filling (EVF) (opening of mitral valve to P wave of the ECG), atrial contraction (AC) (P wave of the ECG to mitral valve closure), early ventricular ejection (EVE) (systolic inward movement indicated by a red colour velocity pattern occurring in the LVPW after the S wave of the ECG to end of T wave of the ECG), late ventricular ejection (LVE) (end of T wave of the ECG to end of inward systolic movement indicated by the end of red colour velocity pattern), isovolumic contraction (IVC) and isovolumic relaxation phase (IVR), (intervals occurring between diastole and systole). All peak values of MVG, MMV and nRCWT are expressed as the mean value of at least 6 cardiac cycles.

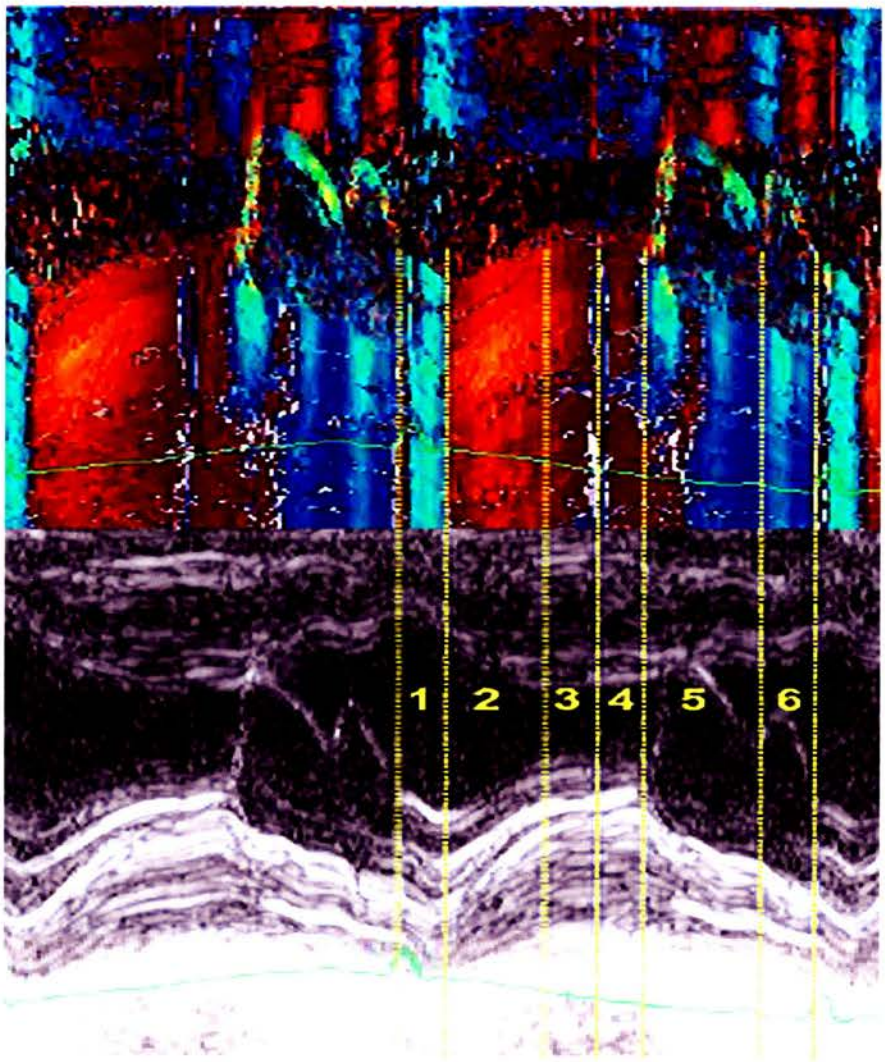

Figure E 9. *Colour M-mode TDI image and the corresponding grey-scale. 1= isovolumic contraction phase. The beginning of IVC was marked by a narrow red strip, which coincided with the closure of the mitral valve (after left atrial contraction) and the QR wave of the ECG. A bright blue strip (RS wave of the ECG) followed immediately after (second part of the IVC). 2 = early systole. This phase was represented by a yellow-red colour transition coming after the S wave of the ECG. 3 = late systole; corresponds to a dark red strip, which coincided with the last part of the T wave of the ECG. 4 = isovolumic relaxation time. The beginning of IVR marked with a blue strip, which corresponded to a descending movement of the myocardium more easily seen in the endocardial area on grey-scale. The second part of the IVR represented by a red strip before the opening of the mitral valve. 5 = early diastole. This phase started immediately after the opening of the mitral valve (first bright-blue transition) and lasted until the opening of the mitral valve during left atrial contraction (P wave of the ECG). 6 = late diastole. Note that early diastole exhibits two bright-blue columns separated by a red column.*

E.2.6. Statistical analysis

Statistical analysis was carried out using SigmaStat (V2.03; SPSS Inc 1997). Values are expressed as the mean ± standard deviation. The Kolmogorov-Smirnov test was used to assess the distribution of the variables. To achieve normality of non-normally distributed variables, logarithmic transformation was used. Pearson's correlation coefficients were calculated to assess the linear relationship between 2 variables (e.g MVG and nRCWT). Linear regression analysis was used to assess the association between the following variables of interest: peak TDI myocardial indices with age and heart rate and Doppler-derived and actual velocities in the phantom study. Stepwise regression was used to assess the influence of age and heart rate as independent predictors of peak MVG and MMV values. A p value of <0.05 was considered statistically significant.

E.3. Results

E.3.1. Study population

Cats of the following breeds were included in the study: 14 domestic short-haired, 1 domestic semilong-haired, 1 Maine coon, 1 Abyssinian, 1 Siamese. There were 11 female and 7 male neutered cats. Mean ± SD body weight was 4.3 ± 0.5 kg. All cats were in good body condition (none were obese or excessively thin). The mean ± SD age was 6.2 ± 3.7 years, with ages ranging from 10 months to 14 years. The results of 2D, M-mode and conventional Doppler echocardiographic analysis were all within previously published reference ranges (Sisson *et al*, 1991; Fox *et al*, 1995). The M-mode results are presented in Table E1. The mean ± SD heart rate measured by the

RR interval recorded during the acquisition of images from at least 6 cardiac cycles was 151 ± 28 bpm.

Table E 1. M-mode measurements (mean ± SD) of clinically normal cats (n=18)

IVSd (mm)	3.8 ± 0.9
LVd (mm)	14.4 ± 2.1
LVPWd (mm)	3.8 ± 0.9
IVSs (mm)	6.3 ± 1.2
LVs (mm)	8.1 ± 1.9
LVPWs (mm)	6.7 ± 1.1
FS (%)	42.5 ± 8.4
LA:Aod	1.4 ± 0.35

IVSd = Interventricular septal wall thickness (diastole), LVd = Left ventricular end-diastolic diameter, LVPWd = Left ventricular posterial wall thickness (diastole), IVSs = Interventricular septal wall thickness (systole), LVs = Left ventricular end-systolic diameter, LVPWs = Left ventricular posterial wall thickness (systole), FS = Fractional shortening, LA:Aod = Left atrium (systole) to aorta ratio (diastole).

E.3.2. Description of Colour M-mode TDI

Using combined information obtained from the simultaneously recorded ECG and the digitized grey scale, several distinct color phases were detected in the colour TDI images (Figure E10). Systole was represented by a red colored strip, which began immediately after the S wave of the ECG and was comprised in most cases of 2 distinct phases: an early phase that corresponded to a bright red band (early systole, Se) followed by a dark red band (late systole, Sl), which commenced at the end of the T wave of the ECG. The beginning of the isovolumic relaxation phase (IVR) was

marked by the occurrence of a very brief duration blue strip (IVRa) at the end of systole and coincided with a slight descending motion of the endocardium, which was clearly seen in the digitized grey scale. A red and relatively wider strip followed immediately after and represented the inward movement of the free wall during the IVR (IVRb). Diastole was represented by a blue band, which commenced at mitral valve opening and ended with the appearance of a red, brief duration strip during the QR wave of the ECG and mitral valve closure (inward movement of the free wall during the IVC, IVCa). Early diastole exhibited 2 brighter blue columns, which reflected the biphasic motion of the free wall of cats during this particular phase of the cardiac cycle. In some animals, a short duration red strip was noticed between the 2 bright columns of early diastole probably reflecting a rebounding movement of the free wall during the middle part of this phase (Figure E9). Late diastole was represented by another bright blue column appearing after the P wave of the ECG (Figure E10). In only a few animals (n=4), a second bright blue column was noticed during this phase, reflecting the biphasic motion of the free wall of cats that occasionally may occur during late diastole. A bright blue band occurred throughout the myocardium between the R and the end of the S wave of the ECG (outward movement of the free wall during the isovolumic contraction phase, IVCb). This band actually consisted of successive narrow strips with interchangeable pattern (Figure E11): 2 narrow bright blue strips separated by a deep blue strip appearing at the beginning and the end of the sequence. The movement of the free wall of cats during the IVCb was very prominent and involved the endocardial and epicardial regions equally.

E.3.3. MVG and MMV traces

Both tracings of MVG and MMV exhibited consistent characteristic peaks during the different phases of the cardiac cycle (Figure E10), which corresponded to the colour velocity patterns described above. The early (Se) and late ventricular (Sl) systolic peaks of MMV were positive indicating the inward movement of the free wall during the corresponding phases of the cardiac cycle. The early systolic peak of MMV was biphasic, and consisted of 2 smaller sub-peaks. Early diastole in the MMV tracing was represented by 2 distinct negative shifts, E1 and E2, which in some cases were separated by a positive shift corresponding to the inward movement of the myocardium during mid-early diastole. A third negative peak occurred during late diastole. IVC and IVR in the MMV tracing exhibited 2 oppositely directed biphasic peaks. The outward movement of the free wall during IVCb provided in many cases the most prominent negative peak in the MMV tracing and showed the same biphasic pattern, comprised of 2 smaller sub-peaks, as the one seen during early systole. The same pattern of peaks occurred in the MVG tracing, although the peaks in it showed the opposite direction from those in the corresponding MMV tracing (Figure E10).

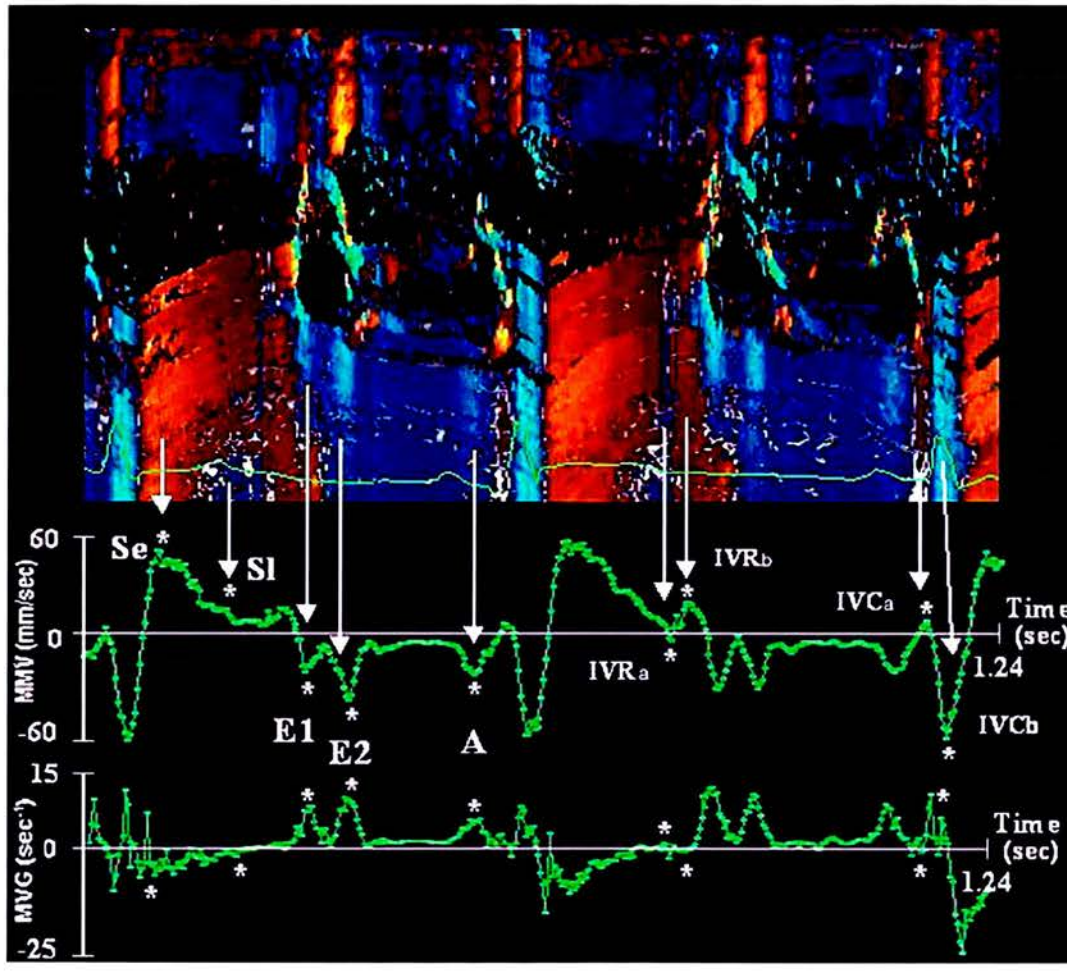

Figure E 10. *Colour M-mode TDI from a 10-month-old domestic short-haired cat (right parasternal long axis view, mitral valve level). Early systole is represented by a prominent peak (Se) in both tracings of MMV and MVG occurring after the S wave of the QRS complex of the ECG (yellow-red phase in the TDI image). During late systole (T wave) a less prominent peak (Sl) appears (red dark strip). Early diastole exhibits a biphasic shift (E1 and E2 peaks) each one of them corresponding to one of the 2 bright blue strips occurring in the colour TDI image during this phase. Late diastole is represented by peak A, which corresponds to the third bright blue strip of diastole coming after the P wave of the ECG. During the IVR and IVC oppositely directed shifts were recorded in both tracings. Note that at the beginning of IVR the free wall undergoes an outward movement (narrow blue strip in the colour TDI image; IVRa peak) which is followed by an inward movement (red strip before the opening of the mitral valve; IVRb peak). In contrast, during the IVC the movement of the free wall follows the opposite pattern. An inward movement of the free wall (narrow red strip during the QR wave of the ECG; IVCa peak) is followed by a very prominent outward movement (blue strip during the RS wave of the ECG; IVCb).* The asterix (*) indicates where peak values were measured during the different phases of the cardiac cycle.

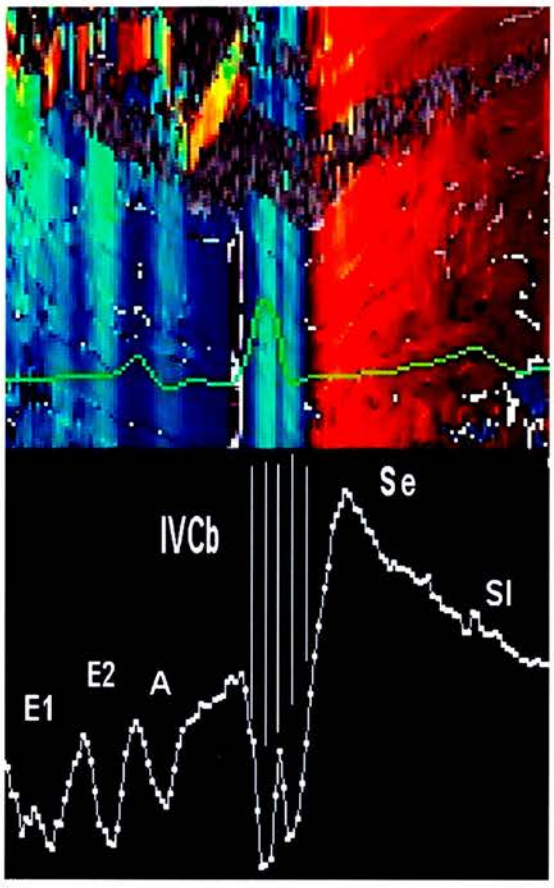

Figure E 11. *Colour M-mode image (free wall, mitral valve level). Note that during IVCb the free wall exhibits a sequence of very short duration blue strips with interchangeable pattern representing the oscillating movements of the myocardium during this phase. The tracing of MMV depicts the corresponding pattern of motion.*

E.3.4. Peak MVG and MMV values and influence of heart rate and age

Peak mean values of MVG and MMV during the defined cardiac phases and the influence of age and heart rate are given in Table E2. A significant and relatively strong inverse association was found between the second peak of early diastole (E2) of MMV and age ($r=-0.71$, $r^2=0.50$, $p<0.01$) (Figure E12). The relationship between E1 of MMV and age was similarly inverse, but did not achieve statistical significance. The peak MMV during late diastole showed a positive association with

age ($r=0.54$, $r^2=0.29$, $p<0.05$) (Figure E12). With advancing age, both early and late systolic peaks of MMV decreased significantly ($r=-0.55$, $r^2=0.30$, $p<0.05$ and $r=-0.62$, $r^2=0.39$, $p<0.01$, respectively) (Figure E12).

A relatively strong inverse association was found between E2 and age for MVG ($r=-0.79$, $r^2=0.63$, $p<0.001$) (Figure E12), but not between E1 of MVG and age. The late diastolic peak MVG was associated positively with age ($r=0.50$, $r^2=0.25$, $p<0.05$). We did not find any age association for the peak MVG during early or late systole. Neither peak values of IVR or IVC showed a significant association with age. A comparison between a 2-year-old and a 10-year-old cat for MMV and MVG is illustrated in Figure E13.

Peak values of MVG and MMV were influenced by heart rate, but to a variable extent during the different phases of the cardiac cycle (Table E2). In our group of normal cats, only E2 of MVG showed a statistically significant inverse association with heart rate ($r=-0.64$, $r^2=0.41$, $p<0.01$). E2 was absent in 3 cats with heart rates > 170 bpm. In these 3 cats, the myocardial motion during early diastole became monophasic. However, E2 also was absent in 2 animals (both of them 8 years of age) with relatively low heart rates (146 and 140 bpm, respectively). No other peak values of MVG and MMV showed a significant association with heart rate. Stepwise regression analysis in which age and heart rate were used as independent predictors of peak MVG and MMV showed that age was the only significant independent predictor of these indices.

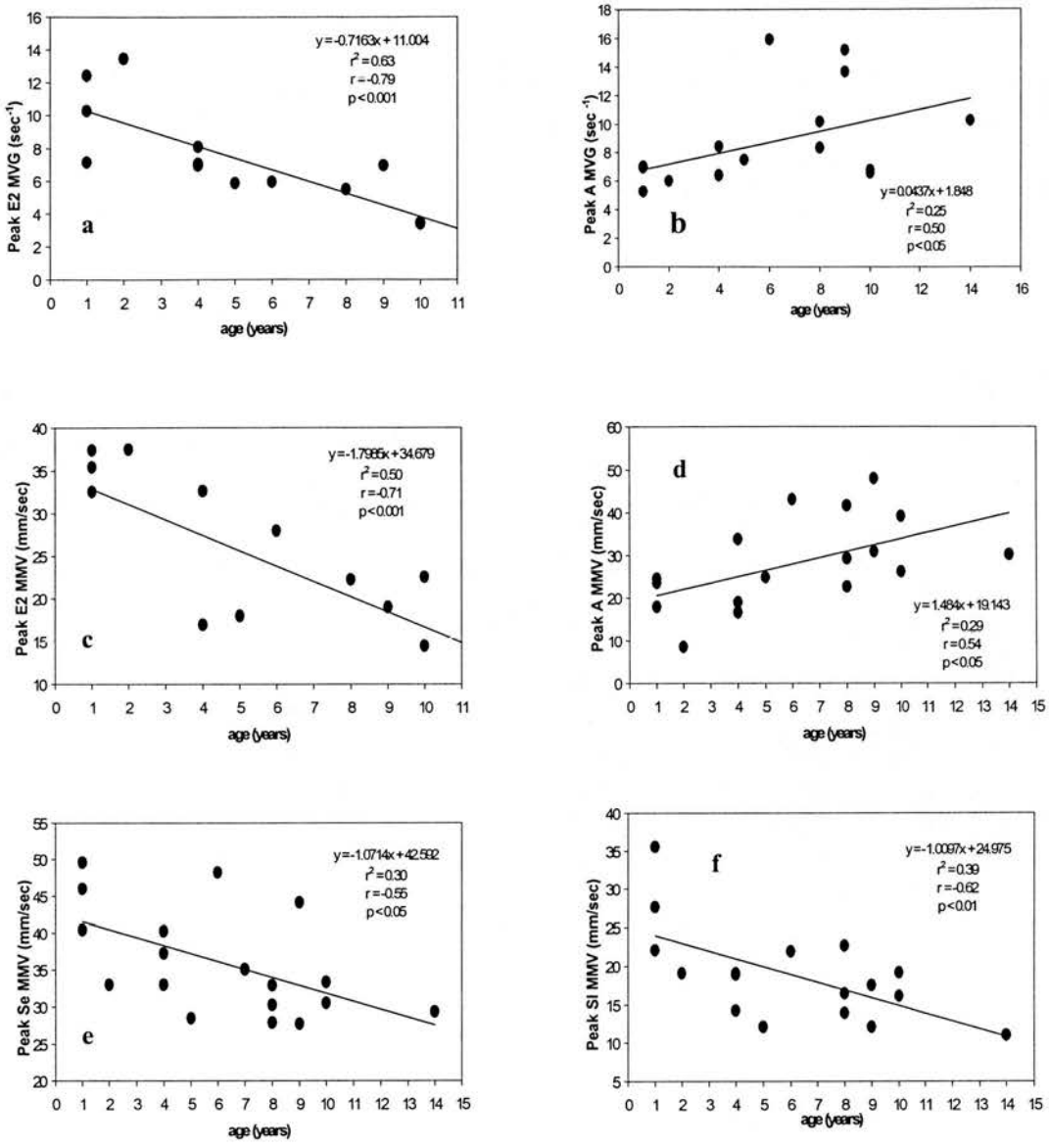

Figure E 12 . *Linear regression plots showing:*
a) the association between age and peak MVG during the second phase of early diastole
b) the association between age and peak MVG during late diastole
c) the association between age and peak MMV during the second phase of early diastole
d) the association between age and peak MMV during late diastole
e) the association between age and peak MMV during early systole and
f) late systole.

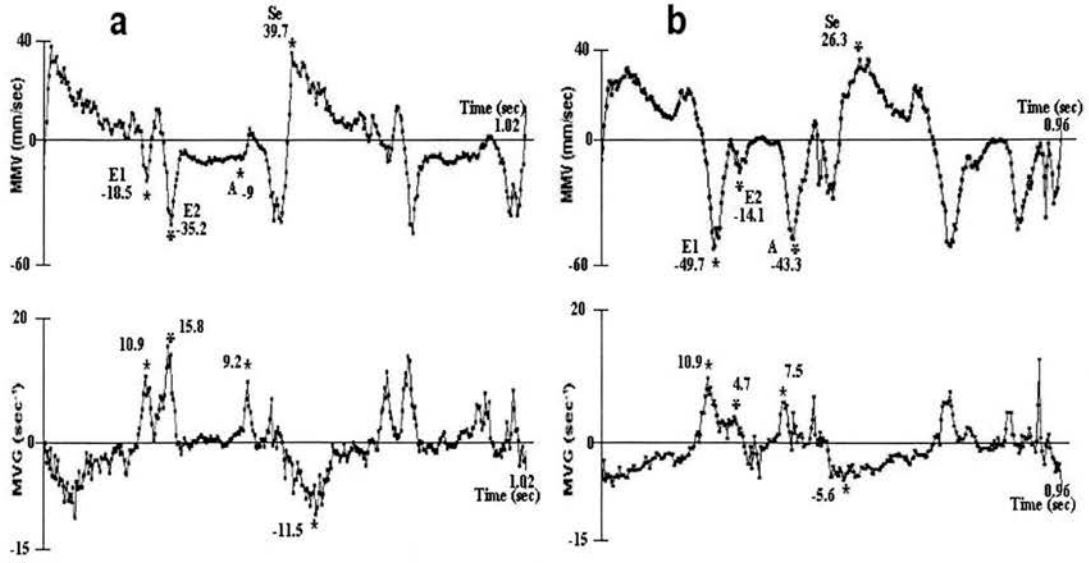

Figure E 13. *Tracings of MVG and MMV from a) a 2-year-old Maine coon cat and b) a 10-year-old domestic short-haired cat. Note that during E1, the MMV of the old animal was higher than it was in the young animal. However, there was no difference in the peak MVG during this phase between the two animals. During E2 the peak MMV and MVG were substantially higher in the young animal. Similarly, peak MMV and MVG were higher during early systole (Se) in the young animal than they were in the older one. A: late diastolic peak. Asterix indicates peak values during the different cardiac phases.*

Table E 2. Colour M-mode Tissue Doppler Imaging measurements (mean ± SD) from the free wall of normal cats and their association with age and heart rate.

	MVG	age		HR		MMV	age		HR	
		r	r^2	r	r^2		r	r^2	r	r^2
E1	11.4 ± 3.7	*ns*	*ns*	*ns*	*ns*	-31.8 ± 11.5	*ns*	*ns*	*ns*	*ns*
E2	7.4 ± 3	-0.79	0.63, p<0.001	-0.64	0.41 p<0.01	-22.3 ± 15.9	-0.71	0.50, p<0.01	*ns*	*ns*
A	8.8 ± 3.2	0.50	0.25, p<0.05	*ns*	*ns*	-28.2 ± 10.5	0.54	0.29, p<0.05	*ns*	*ns*
Se	-8.9 ± 2.9	*ns*	*ns*	*ns*	*ns*	36 ± 7.2	-0.55	0.30, p<0.05	*ns*	*ns*
Sl	-4.4 ± 2.1	*ns*	*ns*	*ns*	*ns*	18.8 ± 6.3	-0.62	0.39, p<0.01	*ns*	*ns*
IVRa	2.3 ± 2.4	*ns*	*ns*	*ns*	*ns*	1.9 ± 10.2	*ns*	*ns*	*ns*	*ns*
IVRb	-1.7 ± 1.9	*ns*	*ns*	*ns*	*ns*	12.7 ± 4.1	*ns*	*ns*	*ns*	*ns*
IVCa	-1.1 ± 3.6	*ns*	*ns*	*ns*	*ns*	2 ± 3.9	*ns*	*ns*	*ns*	*ns*
IVCb	5.6 ± 3.3	*ns*	*ns*	*ns*	*ns*	-39.1 ± 10.4	*ns*	*ns*	*ns*	*ns*

r values were calculated using absolute values of myocardial indices. ns = not significant, HR = heart rate. MVG = Myocardial velocity gradient (sec^{-1}), MMV = Mean myocardial velocity (mm/sec), E1= first early diastolic peak, E2 = second early diastolic peak, A = late diastolic peak, Se = early systolic peak, Sl = late systolic peak, IVRa and IVRb = first and second phase of isovolumic relaxation, IVCa and IVCb = first and second phase of isovolumic contraction

E.3.5. Phantom study

A very strong association (r^2=0.99, p<0.001) was found between measured and calculated velocities in all speeds used (17, 26 and 47 rev/min) (Figure E14). Spatial resolution assessed by the method used was 1.3 ± 0.4 mm.

E.3.6. Comparison between MVG and wall thickness changes (nRCWT)

The overall amplitude correlation (r) between the MVG and the nRCWT ranged between 0.34 and 0.8 (mean ± SD, 0.6 ± 0.13). The correspondence between peak values of the 2 variables during diastole and systole is shown in Table E3. An example is shown in Figure 4. All peaks of MVG during early diastole and systole had a corresponding peak of nRCWT. Peak values of MVG occurred more consistently than peak values of the nRCWT mainly during the second phase of early diastole.

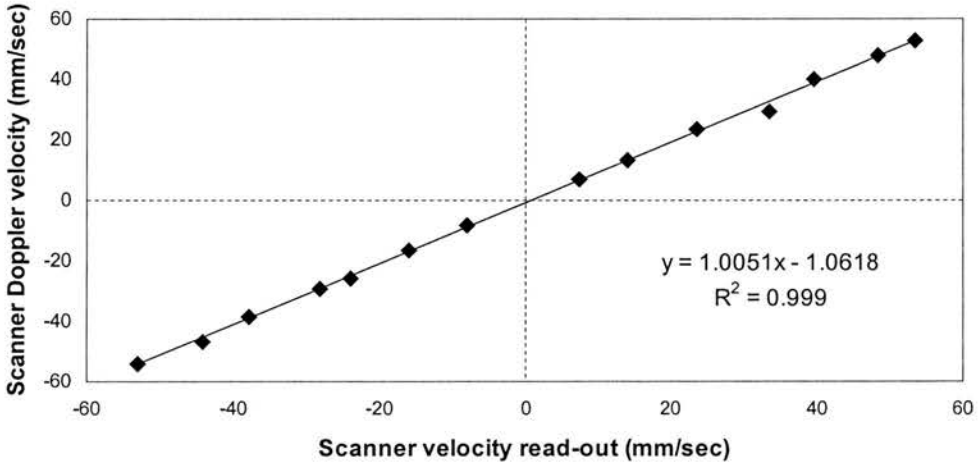

Figure E 14. *Phantom study. Comparison of calculated actual velocities from a rotating tissue mimicking phantom with the Doppler velocities measured by the ultrasound machine (26 rev/min).*

Table E 3. Percentage of cardiac cycles with MVG peak having a concurrent peak of nRCWT and vice versa. Also, percentage of cardiac cycles with peak MVG and nRCWT during four different cardiac phases. Only peaks of MVG and nRCWT that reached 1 sec^{-1} were considered.

	E1	E2	A	Se
MVG peaks with a concurrent nRCWT peak	100%	82%	98%	100%
NRCWT peaks with a concurrent MVG peak	100%	93%	100%	100%
Cycles with MVG peak	100%	94%	100%	100%
Cycles with nRCWT peak	100%	70%	97%	100%

E.4. Discussion

This study documents for the first time the successful application of colour M-mode TDI in the feline myocardium. Due to the very high temporal and spatial resolution of the system used, recording of MVG and MMV was feasible in cats despite the very small size of their hearts and the very fast heart rates that may develop.

The cat population used in this study was similar to diseased cats referred to the cardiopulmonary service of the Small Animal Hospital of the University of Edinburgh with respect to breed and age. In order to produce reliable reference data, we excluded cats with obesity, hypertension, chronic renal failure, hyperthyroidism and acromegaly because of the influence these conditions may have on myocardial properties (Bond *et al*, 1988; Peterson *et al*, 1990; Taugner *et al*, 1996; Snyder *et al*, 2001). However, this exclusion made it more difficult to recruit older healthy cats, particularly above 10 years of age.

Several different studies in humans have shown the ability of colour M-mode TDI to describe changes in wall motion during individual phases of the cardiac cycle by certain colour velocity patterns (Palka *et al*, 1995; Palka *et al*, 1996; Zamorano *et al*,

1997). Colour M-mode TDI measurements in the free wall of humans have disclosed that this part of the myocardium is displayed alternatively in red and blue as it moves towards and away from the transducer, respectively. Our study shows that similar velocity patterns occur in the LV free wall of cats (Palka *et al*, 1996; Zamorano *et al*, 1997).

Zamorano and colleagues (1997) have proven that colour M-mode TDI has the potential to accurately assess the different phases of the cardiac cycle non-invasively. Their study showed that colour velocity patterns recorded by colour M-mode TDI echocardiography in the IVS of humans correlated very well with the different phases of the cardiac cycle as assessed by invasive hemodynamic measurements. In our non-invasive study, assessment of the cardiac phases in the free wall of cats was done by using the combined information obtained from the colour and grey scale including mitral valve motion and the simultaneously recorded ECG. However, the consistency of colour velocity patterns and their good correlation with the events seen on the grey scale and with ECG timing ensures that assessment of the cardiac phases can be carried out accurately.

Differences in the color intensity between early and late ventricular ejection reflected differences in the type of motion (fast acceleration during early systole and deceleration during late systole). Studies of humans in which colour M-mode TDI has been used have shown that anteroseptal endocardial motion exhibits biphasic shifts during early diastole (Gorcsan *et al*, 1996; Gorcsan *et al*, 1998). Ventricular interdependence and right ventricular filling were proposed as 2 possible factors

contributing to this phenomenon. Our study documented the biphasic character of early diastolic movement in the free wall of cats. This movement actually involved the entire myocardium and it was not confined to the endocardial area. This observation was confirmed by quantification of myocardial motion for different layers of the left ventricular wall. The first shift (E1) coincided with the opening of the anterior mitral valve leaflet, as shown in the grey scale of the M-mode, whereas the second shift (E2) was associated with the descending movement of the mitral valve during the later stage of early diastole. Although the energy dependence of myocardial relaxation during early diastole is well known, it is still unclear whether the second early diastolic shift (E2) is part of this energy dependent process or if it merely reflects a passive movement of the myocardium caused by the influx of blood into the left ventricle. Additional studies are needed to investigate the physiological significance of this biphasic movement during early diastole in the feline myocardium. According to the pattern of colour strips seen in the IVS during early diastole (2 red strips separated by a narrower blue strip) (data not shown), it is believed that this part of the myocardium undergoes a similar biphasic motion during early diastole as shown in the free wall of this species and reported in the anteroseptal endocardium of humans (Gorcsan *et al*, 1996; Gorcsan *et al*, 1998). The passive dependence of myocardial motion due to the influx of blood into the LV cavity after atrial contraction has been described by others (Yamada *et al*, 1999a).

Quantification of the motion of the human myocardium with TDI has identified the oppositely directed shifts that occur during IVR and IVC (Palka *et al*, 1995; Garcia *et al*, 1996a; Galiuto *et al*, 1998; Naqvi *et al*, 2001). Our study recorded a similar

pattern of motion in the free wall of cats during these phases. During both parts of IVR and IVC, a uniform motion was recorded along the entire myocardium and resulted in relatively low MVG especially during their initial phases. However, myocardial motion was more prominent during IVRb and IVCb. This finding was reflected in the higher MMV recorded during these phases and especially during IVCb. Pellerin and colleagues (1997), using the colour M-mode TDI technique, described a "bayadere" colour pattern of successive vertical strips with reverse velocity signals in the IVS and the free wall of humans during the pre-ejection period (beginning of the Q wave of the ECG to onset of the ejection). However, in the free wall of cats, reverse velocity signs existed only between IVCa and IVCb with the latter presenting a pattern of very narrow successive strips, which were depicted more clearly in the MMV tracing (Figure E11). The presence of these successive strips reflects the very brief duration of oscillating movements occurring in the feline myocardium during IVCb.

Several different studies in humans and in experimental animals have tried to investigate myocardial motion and LV volume and shape changes during the 2 isovolumic periods. Some of them proposed that the IVC phase is characterized by asynchronous contraction during which the early activation and contraction of papillary muscles and trabeculae carnae result in sudden downward movement of the atrioventricular valves and passive outward stretch of the circumferentially-oriented fibres, particularly those in the basilar two-thirds of the ventricle (Rushmer, 1956; Hawthorne, 1966). This sequence of events results in a more spherical configuration of the LV during IVC (Rushmer, 1956; Hawthorne, 1966; Jones *et al*, 1990). During

the IVR period, an outward movement of the anterior wall and of the apex, accompanied by an inward movement of the inferior and posterior wall of the basal area of the LV, has been described by others (Altieri *et al*, 1973; Hammermeister *et al*, 1986). The outward movement during the second part of the IVC phase and also the inward movement during the second part of the IVR period seen in the free wall of cats by us may be explained by the aforementioned findings of invasive, physiological studies. However, none of these studies provides a substantial clue for the first part of the 2 isovolumic periods. Rankin and colleagues (1976) documented occasional biphasic changes in the thickness of the anterior wall consisting of alternative thickening and thinning during IVC. We believe that the oppositely directed shifts recorded during the 2 isovolumic periods represent adjustment movements of the myocardial fibres determined by the Frank-Starling law (Hawthorne, 1961). The outward movement of the myocardium during IVCb precedes the initiation of the main inward movement during systole and follows (IVRa) the cessation of it. The same relationship holds between the observed inward movements (IVRb and IVCa) during the 2 isovolumic periods and the diastolic movement. An investigation of the timing of occurrence of these biphasic shifts in different myocardial segments when sampled from different projections would offer significant clues for the role and interrelation between longitudinal and circumferential fibres during these periods. Moreover, myocardial motion during the 2 isovolumic phases has been shown to affect overall myocardial performance, and its quantification may be of value in assessing LV properties (Gibson *et al*, 1976b; Gibson *et al*, 1978; Palka *et al*, 1995).

Peak MVG in our group of normal cats was higher than that reported in sedentary humans during all cardiac phases (Palka *et al*, 1996; Palka *et al*, 1997b; Palka *et al*, 1999). However, values of peak MVG during E1 (11.4 ± 3.7 sec^{-1}) in cats were close to those reported during early diastole from the free wall of athletes (10.2 ± 1.5 sec^{-1}) (Palka *et al*, 1999). On the other hand, peak MMV during E1 was substantially lower in the feline free wall (31.8 ± 11.5 mm/sec) compared with that from the free wall of humans (66 ± 22 mm/sec) (Palka *et al* 1996; Palka *et al*, 1997b; Palka *et al*, 1999). Only peak MMV during IVCb (39.1 ± 10.4 mm/sec) exceeded the corresponding value recorded from the human myocardium (13 ± 12 mm/sec) (Palka *et al*, 1996; Palka *et al*, 1997b; Palka *et al*, 1999). The above differences in peak MVG and MMV values probably reflect physiological differences in myocardial function between the 2 species. We speculate that the high velocity gradient between endocardium and epicardium in the free wall of cats is likely to be a compensatory mechanism, which allows the normal feline myocardium to perform efficiently despite the very short R-R intervals that occur normally in this species.

Many studies in humans and in experimental animals have shown the influence of aging on LV properties. Prolongation of both contraction and relaxation times is believed to be attributed to an altered active state and to changes in visco-elastisity (Weisfeldt, 1971; Lakatta, 1975). Increased myocardial stiffness due to increased quantity of interstitial connective tissue, along with increase of the connective tissue of the fibrous skeleton of the heart, may play a significant role in the age-related decrease in LV diastolic function. Furthermore, with increasing age, a decline in the ability of β-adrenergic receptor stimulation to increase contractility has been reported

in isolated myocytes of rats (Xiao *et al*, 1994). Age-related changes in the myocardium of humans have been reflected in colour M-mode TDI measurements. Peak velocity gradient and peak mean velocity during late diastole were positively associated with age, whereas peak MVG during rapid ventricular filling decreased with increasing age in the free wall of normal humans (Palka *et al*, 1996). No association between age and systolic indices have been reported in humans (Palka *et al*, 1996). However, our study demonstrated that the systolic performance of the myocardium of cats also is reduced in association with aging. This association was shown mainly in the decrease of peak systolic MMV values during both the early and late ventricular ejection periods. Another study has shown that the negative correlation between peak early diastolic MVG and age was more prominent in the free wall of sedentary humans than in the free wall of athletes (Palka *et al*, 1999). In our group of normal cats, the influence of aging on diastolic performance proved to be more prominent in the second phase (E2) of early diastole with significant decrease in the amplitude of peak MVG and MMV (Figure E13). Interestingly, all animals without a defined separate E2 wave, regardless of their heart rate, were > 7 years of age. This finding suggests that absence of this wave may reflect, at least in part, failure of the older myocardium to relax adequately during early diastole. On the other hand, our results show that the E1 wave remains uninfluenced by age-related changes in the myocardium of non-diseased animals. Peak MVG during late diastole showed a relatively weak positive association with age in contrast to the strong relationship reported with age in the free wall of normal humans. However, the above findings complement the results presented by Santilli and Bussadori (1998), where a positive correlation was shown between the A wave of mitral inflow

and age in healthy cats. A negative association was also found between age and the velocity time integral of the E mitral inflow wave, but not with the peak E mitral inflow wave velocity. The fact that the E1 remains unaltered by advancing age may explain partially why the peak E wave of mitral inflow did not correlate with age in the study presented by Santilli and Bussadori (1998). The augmentation of passive myocardial motion in cats during late diastole (peak A wave of MVG and MMV) is attributed to the increasingly dominant role of left atrial contraction in left ventricular filling (increased A wave of mitral inflow) with increasing age (Yamada *et al*, 1999a).

Although heart rate appeared to significantly influence only E2 of MVG, stepwise regression analysis showed that this factor was not a significant independent predictor of myocardial indices for any stage of the cardiac cycle. This heart rate independence offers advantages over other methods of assessing systolic or diastolic function. However, we believe that only an invasive study where heart rate is controlled by pacing will reliably investigate the influence of this factor on MMV or MVG indices (Vogel *et al*, 2002).

Fleming and colleagues (1994a) previously showed that measurement of MVG is feasible only within a distance double the spatial resolution available. Therefore, we thought that an in vitro assessment of the spatial resolution of our system would be essential considering the normal, thin LV wall of cats (3-4 mm). The TMM phantoms used in this study were designed to have similar size to a cat heart. Rotational velocities and echocardiographic settings resembled those used during the

acquisition of images from cats. Our results show that with the current system, successful determination of MVG is only possible over a distance exceeding twice the spatial resolution assessed in this study (2 x 1.3 ± 0.4 mm). This finding provides further evidence for the potential accurate measurement of MVG in cats under most circumstances. The lower spatial resolution documented by us compared to that reported by Fleming et al (3 mm), is attributed to the higher frequency probe used in the current study. The excellent correlation found between actual and estimated velocities shows the ability of the system used to accurately assess myocardial velocities and further validates this technique in cats.

Several studies have proved the usefulness of assessment of wall thickness changes in investigating LV properties in different cardiac diseases of humans (Sutton *et al*, 1978; Traill *et al*, 1978; Papademetriou *et al*, 1985; Lee *et al*, 1991; Carvalho *et al*, 1996). However, the calculation of the rate of thinning and thickening from the digitized M-mode images has some inherent disadvantages (Fleming *et al*, 1994b). Firstly, it is based only on the displacement of endocardial and epicardial borders and therefore does not accurately reflect changes within the myocardium. Furthermore, it is highly dependent on the clear identification of the cardiac boundaries, which sometimes are blurred or ambiguous. It also is affected by the overall heart motion. In contrast, the calculation of MVG and MMV from colour M-mode TDI images is based on the estimation of myocardial estimates through the entire thickness of the myocardium. Therefore, it more accurately depicts the inherent properties of the myocardium, assuming that myocardial velocity estimates reflect the structural and functional characteristics of different points along the myocardium (Fleming *et al*,

1994b). Moreover, the estimation of MVG is independent of the accurate identification of endocardial and epicardial borders and it also is not affected by translational effects.

The results of our study are in agreement with those reported from studies of humans, in which it has been shown that MVG follows wall thickness changes (Fleming *et al*, 1994b) (Figure E8). Differences in the overall amplitude between the 2 variables reflect the difficulty in obtaining optimal images rather than failure to prove that equation (2) is valid. Blurred cardiac boundaries, especially in animals with increased subcutaneous or intrathoracic fat, resulted in less accurate calculation of the nRCWT from the digitized grey scale and consequently in poor correlation between the 2 variables. Another factor that explains the discrepancy observed in the amplitude of MVG and the nRCWT is the fact that even subtle errors in accurately tracing the cardiac boundaries resulted in significant changes in the amplitude of nRCWT. Overall heart motion also may have contributed to the difference seen in the overall amplitude between the 2 variables because it affects the nRCWT and not the MVG.

The fact that peak values of MVG occurred more consistently during E2 shows that the colour M-mode TDI was more sensitive than the nRCWT in accurately depicting changes in wall movement during this particular phase of the cardiac cycle. The correspondence between peak values of MVG and nRCWT was very strong during all phases of cardiac cycle. This finding supports further that MVG is consistent with

wall thickness changes and therefore can be used as a more accurate and sensitive means of quantifying myocardial motion of cats.

E.5. Limitations

This was a non-invasive study carried out on pet animals. Consequently, we were unable to generate any invasively determined haemodynamic data to provide "gold standards" with which to compare our results. Due to the angle dependence of Doppler measurements, the estimation of MVG and MMV was confined only to the free wall by using the right parasternal long-axis view in which the ultrasonic beam was visually determined to be parallel to myocardial movement. Although this study showed a significant influence of age on MMV, this parameter is influenced by translational movement of the heart within the thorax. Analysis of very short duration events, such as those occurring during the 2 isovolumic periods and especially their first part, requires very high temporal resolution. Higher rates of data acquisition than those used in the current study (values acquired every 3 msec) will allow a more accurate quantification of myocardial motion during these periods. Lack of simultaneous recording of phonocardiogram may have caused less accurate estimation of the duration of the different cardiac phases than that reported in other studies. However, we believe that the colour and grey scale events and the simultaneously recorded ECG offered consistent definition of the phases of the cardiac cycle used to define our analyses. Although previous studies have reported the influence of respiration on the amplitude of MMV and MVG (Palka *et al*, 1995), we were unable to simultaneously record phases of respiration during acquisition of

images, and it was impossible for us to investigate the relationship between the timing of each phase of respiration and the occurrence of peak MVG or MMV.

E.6. Conclusion

Myocardial disease is a major cause of morbidity and mortality in cats, with patients presenting with dyspnoea or thromboembolism (Atkins *et al*, 1992a; Fox, 1998; Kittleson, 1999). Dilated cardiomyopathy, related or unrelated to taurine deficiency, now is rare (Fox, 1998). At present, hypertrophic cardiomyopathy is the most common feline cardiac disease and it is well described and diagnosed by standard echocardiography (Atkins *et al*, 1992a; Bright *et al*, 1992; Fox *et al*, 1995). Restrictive cardiomyopathy is another known cardiac disease of cats, but its diagnosis by echocardiography is difficult or controversial. Pathologic confirmation is usually required (Kittleson, 1999). On the other hand, some poorly defined myocardial disease presentations have been identified in a subset of feline patients, and are believed to be associated with clinically relevant diastolic dysfunction. They present with marked left atrial enlargement, with a high risk of thromboembolism, without meeting the criteria for the diagnosis of hypertrophic or restrictive cardiomyopathy. These atypical cases are poorly characterized on the basis of ultrasonography and their aetiopathogenesis is not understood. Various terms such as restrictive, intermediate, intergrade or unclassified cardiomyopathy have been used to describe them and so far their classification is based mainly on morphologic features and subjective assessment (Harpster, 1986; Kittleson, 1999). Major limitations occur in assessing myocardial diastolic function even with traditional echocardiographic approaches including mitral inflow and pulmonary venous flow

studies. Mitral inflow is subject to loading conditions and pulmonary venous flow is technically difficult to measure (Shimizu *et al*, 1998; Ommen *et al*, 2000).

Recently, in the first application of pulsed TDI in cats, Gavaghan and colleagues (1999) reported that some cats with unclassified cardiomyopathy showed a "restrictive" myocardial pattern of motion whereas others had an entirely "unclassified" one. Studies of humans have shown that MVG is preload independent and correlates well with invasive hemodynamic indices, which reflect global systolic and diastolic myocardial properties, such as dP/dt and τ (Oki *et al*, 2000; Ommen *et al*, 2000; Ueno *et al*, 2002). Furthermore, in contrast to myocardial velocities measured by pulsed TDI, MVG is not affected by overall heart motion (Shimizu *et al*, 1998). Palka and colleagues (1997a) have shown that MVG recorded in the LV free wall of humans can be used to differentiate between myocardial hypertrophy of different aetiologies, reflecting the great sensitivity of this novel echocardiographic variable in assessing and differentiating LV properties of various cardiac entities with similar morphological characteristics. These advantages of MVG render it a more sensitive tool in assessing LV properties, and offer potential in better classifying feline cardiac diseases and elucidating the mechanisms of their pathophysiology. These findings may help further establish better therapeutic regimens for cardiac diseases in cats.

To the authors' knowledge, this is the first study to record myocardial velocities and velocity gradients of cats using colour M-mode TDI. Based on the very high temporal resolution of this particular application of TDI, we identified interesting

physiological aspects of myocardial movement in cats. Our results describe these features, including the influence of aging and biphasic motion during early diastole and the isovolumic periods. MVG showed cyclic variation consistent with wall thickness changes suggesting that it has the potential to be a very useful tool in the assessment of myocardial function in feline cardiac diseases. Furthermore, the study proved that measurement of MVG and MMV was feasible in the myocardium of this species despite the small size of the feline heart and the very fast heart rates that may develop. This study also provides evidence for the potential utility of color TDI in human neonatal hearts or experimental models in small animals.

SECTION F

Peak mean myocardial velocities and velocity gradients measured by colour M-mode Tissue Doppler Imaging in the left ventricular free wall of healthy cats and cats with hypertrophic cardiomyopathy

F.1. Introduction

Hypertrophic cardiomyopathy (HCM) of cats is the most common cardiac disease of this species and is characterised by a concentrically hypertrophied, non-dilated left ventricle in the absence of other systematic diseases known to cause left ventricular hypertrophy (Atkins *et al*, 1992a; Bright *et al*, 1992; Peterson *et al*, 1993; Fox *et al*, 1995). HCM of cats is a hereditary cardiac disorder, which is probably transmitted as an autosomal dominant trait and shares many common morphological characteristics with human HCM (Fox *et al*, 1995; Kittleson *et al*, 1999). Diastolic impairment is traditionally believed to be the main abnormality of the disease (Atkins *et al*, 1992a; Bright *et al*, 1992; Peterson *et al*, 1993; Fox *et al*, 1995). Evidence for this has been provided by both invasive and Doppler echocardiographic studies (Golden *et al*, 1990; Bright *et al*, 1992). More recently, Tissue Doppler Imaging (TDI) has emerged as an alternative tool for the non-invasive quantification of myocardial motion, which can overcome the confounding effects of loading in the assessment of mitral inflow (Farias *et al*, 1999; Sohn *et al*, 1999; Yalcin *et al*, 2002). Recently in the first ever application of TDI in cats, Gavaghan and colleagues (1999) showed that cats with HCM had decreased myocardial diastolic velocities, acceleration and

deceleration and also prolonged isovolumic relaxation time (IVRt). These findings offered further evidence for diastolic impairment in HCM of this species. TDI studies have shown that systolic impairment is also evident in human HCM, despite the presence of normal or supernormal contractile state of the LV in this cardiac entity (Tabata *et al*, 2000; Cardim *et al*, 2002a). Based on these findings and findings from experimental studies, some investigators suggested systolic dysfunction as the primary abnormality of the disease, which leads to the classical pathological changes seen in HCM (Marian *et al*, 1995b; Marian *et al*, 1997; Marian, 2000; Li *et al*, 1997; Rust *et al*, 1999; Tabata *et al*, 2000; Roberts and Sigwart, 2001; Cardim *et al*, 2002a; Li *et al*, 2002; Ortlepp *et al*, 2002). To date, there is lack of systematic investigation of the systolic myocardial properties in cats with HCM. Myocardial Velocity Gradients (MVG) derived from colour M-mode TDI is one of the few TDI indices, which is independent of the overall heart motion and it has been shown to be a very sensitive tool in the investigation of regional myocardial function (Palka *et al*, 1995; Palka *et al*, 1997a; Palka *et al*, 1997b; Palka *et al*, 1999; Palka *et al*, 2000; Palka *et al*, 2002; Dutka *et al*, 2000). Using a purpose designed 7.4 MHz transducer equipped to record colour M-mode TDI, we sought to quantify myocardial function in the LVPW of cats with HCM by measuring the MVG during all phases of the cardiac cycle. This we hoped would offer new insights into the pathophysiologic mechanisms of the disease and assess better the diastolic and contractile state of the diseased myocardium. A better understanding of the pathophysiology of this entity will undoubtedly help to define better therapeutic regimes in the future.

F.2. Materials and methods

F.2.1. Study group

The study population comprised 20 normal cats, which were pets of staff and students of the Royal (Dick) School of Veterinary Studies and 23 cats with HCM, which were referred to the Cardiopulmonary Service of the R(D)SVS for cardiac screening. None of the normal animals had evidence of cardiovascular or other significant abnormalities on clinical examination. All normal animals underwent a complete 2D, M-mode and colour flow and spectral Doppler echocardiographic examination and had echocardiographic results within reference normal limits (Sisson *et al*, 1991; Fox *et al*, 1995). Normal cats above seven years of age and all affected cats underwent haematology and biochemical testing and had values within reference range. Cats with azotaemia and elevated total thyroxine hormone (T4) were excluded. All cats had normal systolic blood pressure defined as <180 mm Hg using the Doppler technique. The method followed to measure the blood pressure has been described in Section B.

Affected cats had a complete echocardiographic examination. Diagnosis of HCM was done on the basis of LV wall thickness ≥6 mm at any region on 2D or M-mode echocardiography, in the absence of volume or pressure overload (no obvious valvular abnormalities) and systemic diseases known to cause LV hypertrophy. All affected animals were in sinus rhythm except one, which had atrial fibrillation. Eighteen of the cats with HCM were asymptomatic and one was receiving β-blockers. Five affected cats were in congestive heart failure (CHF) at the time of evaluation and were being treated with a combination of diuretics, ACE inhibitors

with or with out β-blockers. No drug withdrawal was done prior to assessment. All animals were unsedated during echocardiographic evaluation.

F2.2. Conventional echocardiography

Conventional echocardiographic and Doppler examination was carried out in the cardiopulmonary service of the Royal (Dick) School of Veterinary Studies. Echocardiographic examination was performed using an Esaote SIM 7000 Challenge ultrasound system (Esaote Biomedica, Firenze, Italy) with a 7.5 MHz phased array transducer. Images were recorded onto S-VHS videotapes by a videocassette recorder (SV0-9500MDP; Sony Corporation, Japan). The method followed to acquire conventional and Doppler echocardiographic measurements has been described in Section B.

F.2.3. Tissue Doppler Imaging echocardiography

Colour M-mode TDI measurements were obtained from all animals in the Medical Physics and Engineering department of the University of Edinburgh the evening of the same day that conventional echocardiography was carried out in the Cardiopulmonary Service of the R(D)SVS. All colour M-mode TDI recordings were made with an ATL HDI 5000 ultrasound system (ATL Bothell, Washington, USA) using a 7.4 MHz phased array transducer, which used prototype TDI software. Off-line analysis of the images was done using a special analysis software (HDIlab) developed by ATL Bothell, Washington, USA.

Animals were scanned unsedated and manually restrained in lateral recumbency on a purpose-designed table, which allowed placement of the transducer on the dependant part of the thorax from below, through a hole. A simultaneous ECG was recorded (lead II) using adhesive electrodes, which were attached to the main pads of the feet and secured with a tape.

Colour M-mode TDI provides the potential for assessing the spatial distribution of transmyocardial velocities throughout the myocardium by detecting the consecutive Doppler shifts returning from the interrogated myocardium (McDicken *et al*, 1992; Miyatake *et al*, 1995). Based on this information, the Myocardial Velocity Gradient (MVG) and the Mean Myocardial Velocity (MMV) can be calculated (Fleming *et al*, 1994b). In this study, MVG was defined as the slope of the linear regression of the velocity estimates across each M-mode scan-line throughout the myocardium, from endocardium to epicardium. Peak MVG was defined as the maximum value of MVG during a particular cardiac phase. MMV was defined as the mean value of the myocardial velocity estimates along each M-mode scan-line from endocardium to epicardium. Peak MMV was the maximum MMV value over the duration of each cardiac phase.

Colour M-mode TDI images of the left ventricular posterior wall were obtained from the right parasternal long-axis view at mitral valve level. Mitral valve level was chosen to permit timing of cardiac events and to optimize alignment. Throughout the study, care was taken to ensure the ultrasonic beam was always parallel to the movement of the free wall. The Doppler velocity range was set at the minimum point

at which no aliasing occurred. Doppler velocity gain was adjusted to achieve proper colour filling of the free wall. Grey-scale gain was optimized so that the endocardial and epicardial borders could be clearly seen. The maximum available M-mode sweep rate was used (values obtained every 3 msec). The focus of the ultrasonic beam was set at the free wall level in order to optimize the quality of grey and colour scale.

Both the grey and colour scale was captured simultaneously, with the colour scale being superimposed on the grey scale. Assessment of the quality of the grey scale was possible by turning the colour scale off before downloading the images. To assess the region of interest, the endocardial and epicardial borders were traced manually on the grey-scale. This method was chosen since the wall boundaries were more clearly seen on the digitized grey-scale image. These traces were automatically superimposed onto the corresponding colour image. Determination of the velocity estimates was possible from the direct quantification of the image data (the number of data points collected for each column of M-Mode data was 512).

Assessment of every cardiac phase was done using the combined information obtained from the M-mode colour and grey scale at mitral valve level and the simultaneously recorded ECG. Each cardiac cycle was divided into 6 standarized phases: early ventricular filling (EVF) (opening of mitral valve to P wave of the ECG), atrial contraction (AC) (P wave of the ECG to mitral valve closure), early ventricular ejection (EVE) (systolic inward movement indicated by a red colour velocity pattern occurring in the LVPW after the S wave of the ECG to end of T wave of the ECG), late ventricular ejection (LVE) (end of T wave of the ECG to end

of inward systolic movement indicated by the end of red colour velocity pattern), isovolumic contraction (IVC) and isovolumic relaxation phase (IVR), (intervals occurring between diastole and systole).

Based on the sequence of peaks occurring in MVG and MMV tracings during the different phases of the cardiac cycle the following peak values were identified (Figure F1): E1 and E2 were the first and second early diastolic peaks respectively, E12 was the peak resulting from the combined E1 and E2 peaks, EA was the combined early and late diastolic peak, Emax was defined as the maximum early diastolic peak and A was the late diastolic peak. Se was the early systolic peak and Sl was the late systolic peak. IVRa and IVRb were the peaks during the first and second phase of isovolumic relaxation period, respectively, and IVCa and IVCb the peaks during the first and second phase of isovolumic contraction period, respectively. In the MMV tracing, the ratio of maximum early diastolic velocity to peak late diastolic velocity (E/A) was also measured. Mean early systolic acceleration (Se acc) was measured from the beginning of systole to peak early systolic velocity. Acceleration of the first (E1 acc) early diastolic wave was measured from the onset of diastole to peak E1. Deceleration of the first (E1 dec) and the second (E2 dec) early diastolic shifts was measured from E1 and E2 to the their ends, respectively. Acceleration (E12 acc) and deceleration (E12 dec) of E12 were measured from the beginning and end of early diastole to peak E12, respectively. All peak values of MVG, MMV are expressed as the mean value of at least six cardiac cycles.

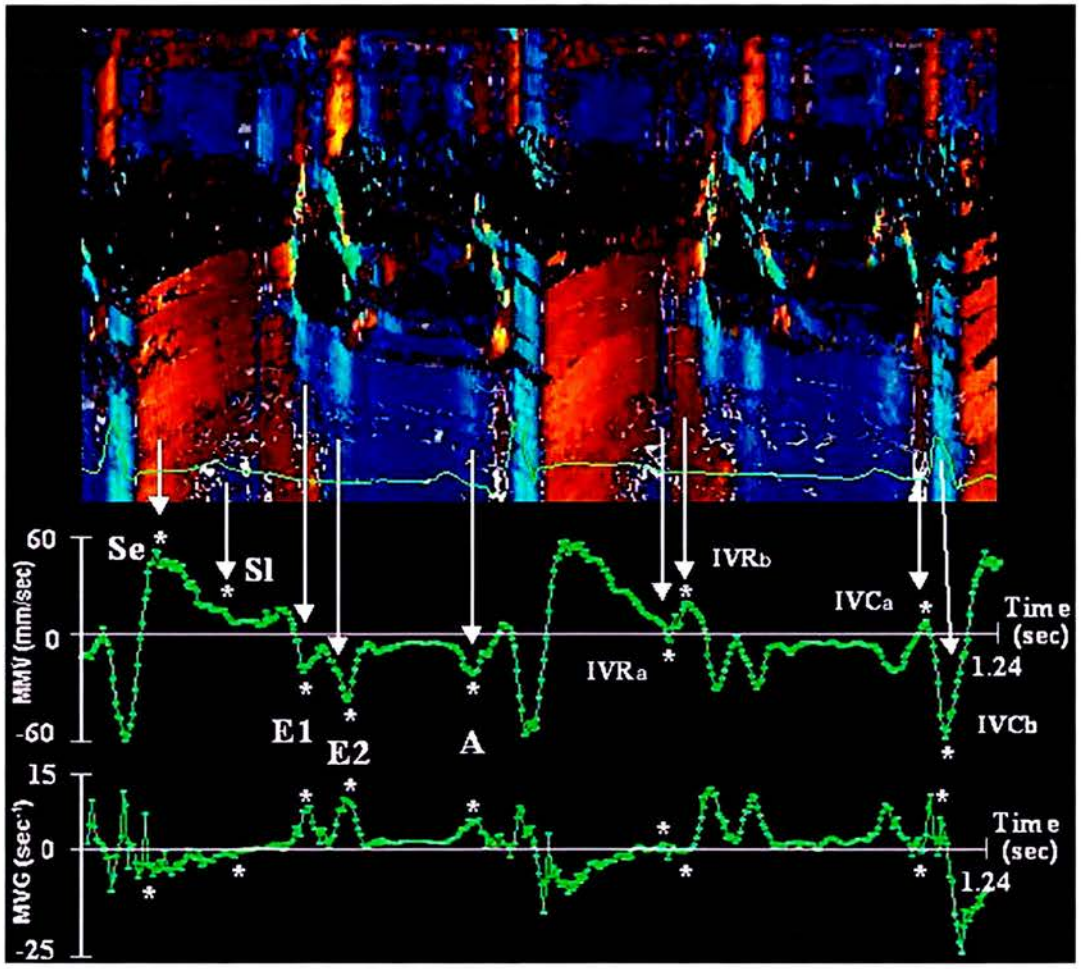

Figure F 1. *Colour M-mode DTI from a 10-month-old Domestic short-haired cat (right parasternal long axis view, mitral valve level) and corresponding tracings of Myocardial Velocity Gradient (MVG) and Mean Myocardial Velocity (MMV). Se and Sl: peak values during early and late systole respectively. E1, E2 and A: peak values during the first and second phase of early diastole and during late diastole respectively. IVRa and IVRb: first and second myocardial shift during the isovolumic relaxation period. IVCa and IVCb: first and second myocardial shift during the isovolumic contraction period. The asterix (*) indicates where peak values were measured.*

F.2.4. Statistical analysis

Statistical analysis was carried out by using Genstat^{TM} 5 (release 3, Rothmsted experimental station, U.K) and SigmaStat (V2.03; SPSS Inc 1997). Values are expressed as the mean ± standard deviation. Analysis of covariance was used to control TDI and M-mode indices for RR interval, age, weight and sex. A t-test was used to compare values between the two groups. To eliminate the influence of congestive heart failure on the results, comparisons between the two groups were repeated by excluding affected cats with CHF from the analysis. To assess the influence of left ventricular outflow tract obstruction on systolic TDI indices, only affected cats with outflow tract pressure gradient < 4 mm Hg and without evidence of SAM of the mitral valve, were considered. Stepwise regression was carried out to assess the influence of RR interval, age, weight, sex and thickness on peak MVG and MMV values and also on IVRt and IVCt. Linear and multiple linear regression analysis were used to define the association between TDI indices and independent predictors. For the purposes of regression analysis, male cats were defined as number 1 and female cats as number 2. A t test or a Mann-Whitney Rank Sum test was used to compare TDI variables between male and female cats within the same group when sex was found to be a significant predictor in linear or multiple linear regression analysis. A Kolmogorov-Smirnov test was used to assess the normal distribution of the variables. To achieve normality of the non-normally distributed variables logarithmic transformation was used. A p value of < 0.05 was considered statistically significant.

F.3. Results

F.3.1. Study population

Normal cats of the following breeds were included in the study: 18 Domestic Short-haired, 1 Maine-coon, 1 Abyssinian (8 female and 12 male neutered cats). Mean ± sd body weight was: 4.5 ± 0.9 Kg. All normal cats were in good body condition (none were obese or excessively thin). Their mean ± sd age was 6.5 ± 3.6 years, with ages ranging from 10 months to 14 years. The mean ± sd heart rate calculated from the RR interval recorded during the acquisition of images from at least 6 cardiac cycles was 147 ± 24 bpm. Affected animals (22 Domestic Short-haired and one Persian; 3 female and 20 male neutered cats) had a mean ± sd of body weight of 5.2 ± 1 Kg, mean ± sd of age 6.7 ± 2.9 years (range: 1 to 12 years) and their HR was 155 ± 30 bpm.

F.3.2. Conventional echocardiography

The results of the LV M-mode measurements are displayed in Table F1. Thickness of the IVS and the LVPW at chordae tendineae level were significantly higher in the HCM group than in the normal group ($p<0.001$). HCM cats had significantly thicker LVPW at mitral level than normal cats (6 ± 1.4 vs 4.2 ± 0.66, $p<0.001$). Affected animals had a higher left atrium to aorta ratio than normal animals ($p<0.01$). Although affected animals appeared to have significantly higher FS% than normal animals this difference did not reach statistical significance. In 10 affected cats the outflow tract pressure gradient was < 4 mm Hg (mean Ao.v ± sd: 0.85 ± 0.14), while in 8 cats it was > 4 mm Hg (mean Ao.v ± sd: 3.18 ± 1.47) and in 5 it was technically impossible to acquire good quality aortic velocity envelopes. In this latter group, 4

cats had systolic anterior motion of the mitral valve. CFDE identified mitral regurgitation in 19 HCM cats.

Table F 1. M-mode measurements (mean ± SD) of normal (n=20) and HCM cats (n=23)

	normal	HCM	p
IVSd (mm)	3.74 ± 0.8	6.5 ± 1.5	<0.001
LVd (mm)	15 ± 2.2	15.2 ± 2.1	ns
LVPWd (mm)	3.85 ± 0.9	5.9 ± 1.6	<0.001
IVSs (mm)	6.17 ± 1.2	9.07 ± 1.6	<0.001
LVs (mm)	8.66 ± 2.1	6.92 ± 2.5	ns
LVPWs (mm)	6.82 ± 1.2	9.17 ± 1.6	<0.001
FS (%)	42.4 ± 9.1	54.7 ± 14.8	ns
LA:Aod	1.32 ± 0.2	1.79 ± 0.6	<0.01

IVSd = Interventricular septal wall thickness (diastole), LVd = Left ventricular end-diastolic diameter, LVPWd = Left ventricular posterior wall thickness (diastole), IVSs = Interventricular septal wall thickness (systole), LVs = Left ventricular end-systolic diameter, LVPWs = Left ventricular posterior wall thickness (systole), FS = Fractional shortening, LA:Aod = Left atrium (systole) to aorta ratio (diastole).

F.3.3. Peak MVG and MMV between the two groups

Peak mean MVG values during the different phases of the cardiac cycle in the two groups are given in Table F2. MVG indices from all cats included in the study are shown in Appendix F1, Tables App.F1 and App.F2. Mean peak first (E1) and second (E2) early diastolic MVG were significantly higher in the normal group compared with that in the affected group ($p<0.01$ and $p<0.001$ respectively) (Table F2). Mean peak E12 MVG was significantly higher in the normal than in the affected group

($p<0.05$). Maximum early diastolic MVG (Emax) was significantly higher in normal than in affected cats ($p<0.001$). A cut-off value of Emax MVG > 8 sec^{-1} could discriminate normal from affected animals with a sensitivity of 85% and a specificity of 90% (Figure F2).

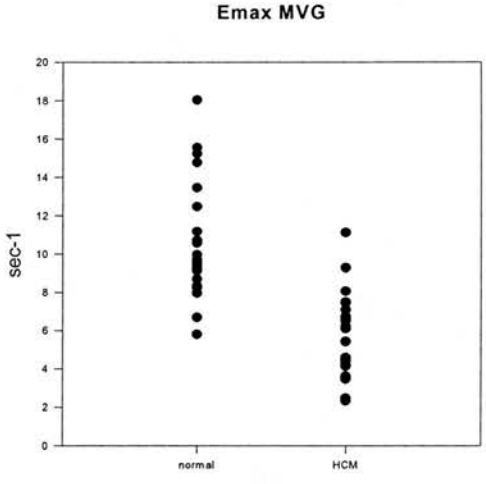

Figure F 2. *Point Plot of maximum early diastolic (Emax) Myocardial Velocity Gradient (MVG) between normal and HCM cats.*

Fully merged early and late diastolic waves and consequently MVG were recorded in only 2 affected animals and none of the normal cats. Mean peak late diastolic (A) MVG did not differ between the two groups. Mean peak early systolic (Se) MVG was significantly greater in the normal than in the affected group ($p<0.05$). There was no significant difference in mean peak late systolic (Sl) MVG between the two groups. Peak MVG values during the two phases of the IVR period were significantly higher in the normal group compared with that in the HCM group. No significant difference in MVG during the two phases of the IVC period was found between the two groups.

Table F 2. Peak MVG values (mean and sd) in normal (n=20) and HCM (n=23) cats

MVG sec^{-1}	normal mean ± sd (n)	HCM mean (sd) (n)	p
E1	11.38 ± 3.1 (15)	5.65 ± 2.5 (9)	< 0.01
E2	7.02 ± 3.1 (15)	3.47 ± 1.6 (9)	< 0.001
E12	7.99 ± 1.7 (5)	5.61 ± 2.5 (12)	<0.05
EA	-	8.85 ± 5.2 (2)	-
Emax	10.75 ± 3.2 (20)	5.8 ± 2.2 (23)	< 0.001
A	8.68 ± 3.1 (20)	6.85 ± 2.7 (20)	ns
Se	-8.67 ± 2.83 (20)	-5.8 ± 2.6 (23)	< 0.05
Sl	-4.36 ± 2 (20)	-3 ± 1.2 (19)	ns
IVRa	1.94 ± 2.4 (20)	0.64 ± 0.6 (21)	< 0.05
IVRb	-2.41 ± 1.1 (20)	-0.89 ± 1 (22)	< 0.05
IVCa	-1.58 ± 4 (19)	-0.99 ± 2.1 (21)	ns
IVCb	5.61 ± 3.1 (19)	2.83 ± 3.3 (22)	ns

n = number, MVG = Myocardial Velocity Gradient (sec^{-1}), E1= first early diastolic peak, E2 = second early diastolic peak, E12 = combined E1 and E2 peak, EA = combined E and A peak, Emax = maximum early diastolic peak, A = late diastolic peak, Se = early systolic peak, Sl = late systolic peak, IVRa and IVRb = peaks during the first and second phase of isovolumic relaxation respectively, IVCa and IVCb = peaks during the first and second phase of isovolumic contraction respectively.

Peak mean values of MMV are given in Table F3. MMV indices from all cats included in the study are presented in Appendix F1, Tables App.F3 and App.F4. There was no significant difference in any diastolic peak MMV or the early systolic MMV between the two groups. Mean peak late systolic (Sl) MMV in the normal group was significantly higher in the normal than in the affected group ($p<0.05$). The ratio of peak early systolic MMV to peak IVCb MMV was significantly greater in normal than in affected cats ($p<0.05$). Among the mean peak values of MMV during the 2 isovolumic periods, only IVRb and IVCb were significantly higher in the normal group compared with that from the HCM group ($p<0.001$). A cut-off value of

IVCb of MMV > 34 mm/s could discriminate normal from affected animals with a sensitivity of 80% and a specificity of 87% (Figure F3).

Isovolumic relaxation time (IVRt) was significantly prolonged in the affected group when compared with that from the normal group ($p<0.001$). No difference was found in the rest of the MMV indices between the two groups.

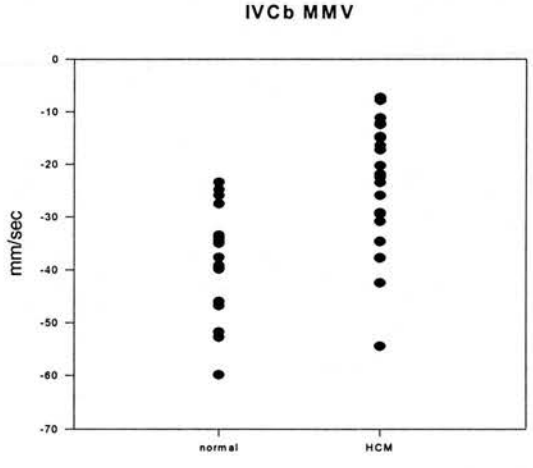

Figure F 3. *Point Plot of mean peak values of the second myocardial shift during the isovolumic contraction period (IVCb) of Mean Myocardial Velocity (MMV) between normal and HCM cats.*

Table F 3. MMV indices (mean and sd) in normal (n=20) and HCM (n=23) cats

MMV	normal mean ± sd (n)	HCM mean ± sd (n)	p
E1 (mm/s)	-31.7 ± 10.4 (15)	-29.6 ± 14.2 (9)	ns
E2 (mm/s)	-24.5 ± 8.6 (15)	-24.1 ± 14.8 (9)	ns
E12 (mm/s)	-26.1 ± 10.5 (5)	-22.5 ± 9.5 (12)	ns
EA (mm/s)	-	-39.7 ± 2.9 (2)	ns
Emax (mm/s)	-32.2 ± 9.1 (20)	-28.5 ± 12.3 (23)	ns
E/A	1.4± 0.9 (20)	1.1 ± 0.9 (21)	ns
A (mm/s)	-27.1 ± 10.6 (20)	-32.3 ± 12.2 (21)	ns
Se (mm/s)	34.7 ± 7.1 (20)	33.9 ± 10.4 (23)	ns
Sl (mm/s)	18 ± 6 (20)	13.6 ± 5.4 (22)	< 0.05
IVRa (mm/s)	0.3 ± 7.4 (20)	-3.9 ± 7.7 (21)	ns
IVRb (mm/s)	12.7 ± 5.5 (20)	4.4 ± 7 (22)	< 0.001
IVCa (mm/s)	1.8 ± 3.9 (20)	4.6 ± 6.6 (23)	ns
IVCb (mm/s)	-38.7 ± 10.1(20)	-22.5 ± 11.8 (23)	< 0.001
Se acc (mm/sec^2)	2093 ± 622 (20)	1688 ± 738 (23)	ns
E1 acc (mm/sec^2)	726 ± 142 (8)	679 ± 199 (7)	ns
E1 dec (mm/sec^2)	925 ± 250 (15)	686 ± 374 (9)	ns
E2 dec (mm/sec^2)	822 ± 351(15)	940 ± 987 (8)	ns
E12 acc (mm/sec^2)	707 ± 61 (3)	631 ± 338 (11)	ns
E12dec (mm/sec^2)	653 ± 349 (5)	556 ± 330 (12)	ns
IVRt (sec)	0.044 ± 0.01 (20)	0.062 ± 0.02 (21)	<0.001
IVCt (sec)	0.051 ± 0.01 (20)	0.052 ± 0.01 (23)	ns
Diast t (sec)	0.182 ± 0.06 (20)	0.167 ± 0.07 (22)	ns
Syst t (sec)	0.153 ± 0.03 (20)	0.135 ±0.03 (22)	ns

n = number, MMV = Mean Myocardial Velocity (mm/sec), E1= first early diastolic peak, E2 = second early diastolic peak, E12 = combined E1 and E2 peak, EA = combined E and A peak, Emax = maximum early diastolic peak, E/A = ratio of maximum early to maximum late diastolic peak, A = late diastolic peak, Se = early systolic peak, Sl = late systolic peak, IVRa and IVRb = peaks during the first and second phase of isovolumic relaxation respectively, IVCa and IVCb = peaks during the first and second phase of isovolumic contraction respectively, Se acc = mean early systolic acceleration, E1 = mean acceleration of E1, E1 and E2 dec = mean deceleration of E1 and E2 respectively, IVRt = duration of isovolumic relaxation phase, IVCt = duration of isovolumic contraction phase, diast t = duration of diastole, syst t = duration of systole.

F.3.4. Influence of CHF on colour M-mode TDI indices

Differences in MVG indices between the two groups remained unchanged even after excluding from the analysis affected cats with CHF.

The peak A wave and the E/A ratio of MMV were found to be significantly higher ($p<0.05$) and lower ($p<0.01$), respectively in asymptomatic affected cats compared to that in normal animals. Systole lasted for longer in normal cats compared to asymptomatic HCM animals ($p<0.05$).

F.3.5. Influence of independent predictors on colour M-mode TDI indices

The influence of independent variables, age, gender, R-R interval, thickness and weight on colour M-mode TDI indices is presented in Tables App.F5 and App.F6, Appendix F2.

F.3.5.1. Influence of independent predictors on MVG indices

Results of forward stepwise regression, linear and multiple linear regression analysis between MVG indices and independent predictors (age, RR, weight, sex, thickness) in both groups are presented in Table App.F5, Appendix F2. In the normal group E2 and IVRa of MVG were associated inversely and positively, respectively, with age. E2 of MVG was also influenced positively by sex, weight and R-R interval. However, there was no significant difference in E2 between male and female normal cats. IVRa was also influenced inversely by thickness. Although thickness, age and R-R interval were significant predictors of the IVRb in forward stepwise regression analysis, none of these independent factors significantly contributed to the variance of IVRb in multiple linear regression analysis.

Thickness was inversely associated with E2, E max and A of MVG in the affected group. The R-R interval showed an inverse relation with E2 of MVG in HCM cats. An inverse association was found between thickness and Se and Sl of MVG in HCM cats. IVCb and E1-2 of MVG were influenced inversely by sex in the affected group. Male affected cats showed lower E1-2 MVG values than female cats. There was no significant difference in IVCb of MVG between male and female cats in the affected group.

F.3.5.2. Influence of independent predictors on MMV indices

Results of forward stepwise regression, linear and multiple linear regression analysis between MMV indices and independent predictors (age, RR, weight, sex, thickness) in both groups are presented in Table App.F6, Appendix F2. An inverse association was found between age and E2, E max, E/A, Se and Sl of MMV in the normal group. Thickness positively influenced the IVRa of MMV in normal cats. Weight was associated positively with the early systolic acceleration of MMV in the normal group and, although it was found to be a significant predictor for E1 and the acceleration of E1, it did not contribute in the variance of these two latter indices in multiple linear regression analysis. The duration of diastole and systole showed as positive association with the R-R interval in the normal group.

Age was related positively with Sl of MMV in the affected group. The isovolumic relaxation time showed a positive association with thickness in HCM cats. Weight was inversely associated with IVRb and positively with E2 in the HCM group. E2

and SI of MMV were influenced positively by the R-R interval in HCM cats. E1-2 deceleration of MMV showed an inverse association with the R-R interval in the affected group.

F.4. Discussion

This study shows that differences in the LVPW between normal and HCM cats are mainly due to decreased MVG rather than MMV. Decreased early diastolic and systolic MVG were recorded in the LVPW of affected animals providing evidence for both diastolic and systolic impairment in HCM of this species.

Colour M-mode TDI is one of the applications of the TDI technique, which has been used widely in various clinical and experimental settings for quantification of myocardial motion (Palka *et al*, 1995; Palka *et al*, 1997a; Palka *et al*, 1997b; Palka *et al*, 1999; Palka *et al*, 2002; Zamorano *et al*, 1997; Dutka *et al*, 2000). The high temporal resolution and signal to noise ratio of this particular mode offers advantages over other applications of the TDI technique. Although 2D TDI mode enables the simultaneous quantification of myocardial motion in different areas of the LV wall, it often provides poor temporal resolution and has a low signal to noise ratio (Garot *et al*, 1998). This can result in underestimation of myocardial velocities and failure to quantify accurately myocardial motion during short duration events, especially with high heart rates (often encountered in cats). Pulsed TDI offers high temporal resolution, but allows only the estimation of instantaneous myocardial velocities, which can be affected by overall heart motion and motion of adjacent myocardial areas (Shimizu *et al*, 1998). The use of colour M-mode TDI allows the calculation of

Myocardial Velocity Gradient, which describes the spatial distribution of transmyocardial velocities throughout the myocardium from endocardium to epicardium and reflects wall thickness changes during diastole and systole (Fleming *et al*, 1994b). Under normal circumstances, the contribution of the endocardial area in the wall thickening and thinning during systole and diastole, respectively, is greater compared to that of the epicardial area (Myers *et al*, 1986) (Figure F4). This results in a physiologic velocity gradient between endocardium and epicardium. Traditional quantification of regional myocardial function was based on either the visual qualitative assessment of myocardial motion using 2D images, or the calculation of the rate of change of wall thickening and thinning by M-mode echocardiography. However, the former is based on the assessment of morphological features without taking into consideration the true structural and functional properties of the myocardium and it is subject to the temporal limitations of human vision, which makes it difficult to assess myocardial motion during short duration events (Kvitting *et al*, 1999). Although a series of studies have proved the usefulness of assessment of wall thickness changes in investigating LV properties in different human cardiac diseases, the calculation of the rate of thinning and thickening from digitized M-mode images has some inherent disadvantages (Sutton *et al*, 1978; Traill *et al*, 1978; Lee *et al*, 1991; Carvalho *et al*, 1996). Firstly, it is based only on the displacement of endocardial and epicardial borders and therefore does not accurately reflect changes within the myocardium. Furthermore, it is highly dependent on the clear identification of the cardiac boundaries, which sometimes are blurred or ambiguous. Additionally, it is affected by the overall heart motion (Fleming *et al*, 1994b). On the other hand, the calculation of MVG from colour M-mode TDI images

is based on the estimation of myocardial estimates along the entire thickness of the myocardium. Therefore, MVG more accurately depicts the inherent properties of the myocardium, presuming that myocardial velocity estimates reflect the structural and functional characteristics of different points along it. Moreover, the estimation of MVG is independent of the accurate identification of endocardial and epicardial borders, since it is the slope of the linear regression of velocity estimates and it is also not affected by translational effects (Fleming *et al*, 1994b; Uematsu *et al*, 1997). In contrast to mitral inflow pattern, which is subject to loading changes and therefore can be masked by increased LV filling pressures, so switching to a pseudonormal pattern, MVG has been shown to be independent from preload increases in the diseased state (Shimizu *et al*, 1998). Additionally, MVG correlates strongly with invasive hemodynamic indices, such as the peak positive and negative pressure development (dP/dt) and the time constant of pressure decay in isovolumetric relaxation (τ), suggesting that, apart from being a very sensitive tool in assessing regional myocardial function, it can also reflect global systolic and diastolic properties (Oki *et al*, 2000; Ueno *et al*, 2002). The sensitivity of MVG in quantifying myocardial properties has been shown in various cardiac settings in humans. MVG has managed to discriminate between hypertrophy of different aetiologies (HCM from left ventricular hypertrophy induced by hypertension and athleticism) and between restrictive cardiomyopathy and constrictive pericarditis (Palka *et al*, 1997a; Palka *et al*, 2000). Its application was particularly useful in detecting wall motion abnormalities in ischemic myocardial segments, especially when visual assessment failed to do so and also in differentiating the extent of experimentally induced infarction (transmural from endocardial) (Gorcsan *et al*, 1998; Derumeaux *et al*,

2001; Marcos-Alberca *et al*, 2002). Recently, MVG was used in the assessment of regional functional effects of transplanted skeletal myoblasts in an experimentally induced infarcted area (Ghostine *et al*, 2002). The use of MVG allowed also the quantification of myocardial function in variable cardiac diseases (Palka *et al*, 1997a; Palka *et al*, 2002; Dutka *et al*, 2000; Tsutsui *et al*, 2000; Iwakami and Numano, 2001).

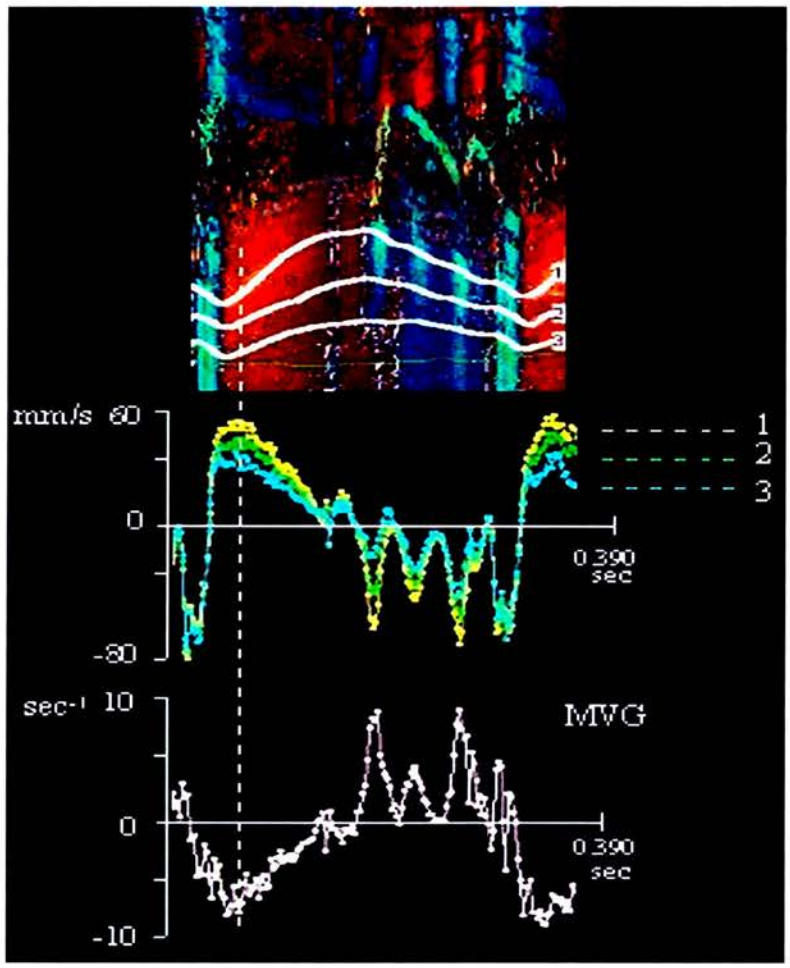

Figure F 4. *Myocardial Velocity Gradient (MVG) across the myocardium results from the physiological difference in velocity motion of different myocardial layers. Normally the endocardial area exhibits higher velocities than the epicardial area, especially during diastole and systole. Note that the endocardial velocity (1) is higher than the mid-wall (2) and the epicardial velocity (3). The mid-wall velocity is also higher than the epicardial one. The MVG is decreased in the diseased myocardium.*

In our previous report (Koffas *et al,* 2003; Section E), we have shown that recording of MVG was feasible in the LVPW of normal cats and that it correlated well with wall thickness changes. We also showed that peak MVG during the different phases of the cardiac cycle corresponded to certain colour velocity patterns occurring in the LVPW of cats. Feline myocardial motion exhibited biphasic shifts during early diastole (E1 and E2) and also during the isovolumic relaxation (IVR) and contraction (IVC) phases. These shifts were represented with certain waves in the MVG tracing.

The current study shows that MVG was reduced during early diastole and systole in the LVPW of our population of HCM cats compared with that from normal animals. These findings support evidence for diastolic and systolic impairment in HCM of this species. Diastolic impairment has traditionally been believed to be the main abnormality in HCM of cats (Bright *et al*, 1992; Fox *et al*, 1995). Evidence for this has been provided by both invasive and Doppler echocardiographic studies (Golden *et al*, 1990; Bright *et al*, 1999). Recently the application of TDI has confirmed the presence of diastolic impairment in HCM of cats (Gavaghan *et al*, 1999). Decreased myocardial diastolic velocities, acceleration and deceleration and prolonged isovolumic relaxation time were recorded in affected animals. Similar findings have been reported from TDI studies in humans with HCM (Oki *et al*, 1998b; Oki *et al*, 2000; Tabata *et al*, 2000; Nagueh *et al*, 2001a; Naqvi *et al*, 2001; Cardim *et al*, 2002a). Impaired intrinsic diastolic properties result from the classical pathological changes seen in HCM (disarray, fibrosis, hypertrophy) and/or abnormal cytosolic kinetics (Oki *et al*, 1998b). Our study shows that cats with HCM had lower early diastolic (E1, E2 and E12) MVG than normal animals. E2 and Emax MVG

associated inversely with thickness in the affected group. Emax was the best discriminator between normal and affected cats and shows great promise for the assessment of cardiac function in other feline cardiac diseases, especially those with equivocal characteristics. Although peak MVG during late diastole was lower in affected animals compared to that in the normal group, this difference was not statistically significant. Thickness showed an inverse association with the late diastolic peak MVG, suggesting decreased passive myocardial response to atrial contraction, probably due to decreased LV compliance. The above results are in general agreement with those reported by colour M-mode TDI studies in humans with HCM. Decreased peak early diastolic MVG was documented in the LVPW of patients with HCM even in the absence of significant hypertrophy (Palka *et al*, 1997a; Oki *et al*, 1998b). Peak MVG during late diastole was also significantly lower in the LVPW of patients with HCM compared to that in normal individuals (Palka *et al*, 1997a).

We have previously described that myocardial motion in the LVPW of many normal cats is biphasic during early diastole (Koffas *et al,* 2003; Section E). Cats with HCM more frequently showed monophasic early diastolic shifts compared with normal animals, mainly because they had higher heart rates. The origin of the second early diastolic shift remains unknown. A similar pattern of biphasic motion during early diastole has been described in the IVS of humans and ventricular interdependence and right ventricular filling were suggested as possible causes of this phenomenon (Gorcsan *et al*, 1996; Gorcsan *et al*, 1998). However, this suggestion does not explain the occurrence of this pattern of motion in the LVPW of cats. LV pressure

tracings in cats show that the diastolic pressure curve sometimes exhibits three distinct peaks, with the two of them occurring before atrial contraction (Lord *et al*, 1974). These pressure deflections may result from the biphasic myocardial shifts recorded in the LV of cats. Further studies are needed in order to elucidate the physiological significance of this biphasic early diastolic shift in the myocardium of cats.

TDI studies have shown that systolic impairment is evident in humans and experimental animals with HCM in the absence of significant intraventricular pressure gradient and normal indices of global systolic function (Palka *et al*, 1997a; Nagueh *et al*, 2001a; Cardim *et al*, 2002a). This reduction in contractility is not always accompanied by LV hypertrophy (Palka *et al*, 1997a; Nagueh *et al*, 2000; Nagueh *et al*, 2001a; Cardim *et al*, 2002c). Reduced systolic MVG have been documented in the IVS and LVPW of humans with HCM (Palka *et al*, 1997a; Yamada *et al*, 1999b). These findings, along with experimental data, led many investigators to implicate systolic dysfunction of the individual cardiac cells as the primary deficit in HCM, which leads to compensatory hypertrophy and fibrosis through the release of stress-responsive mitotic and trophic factors (Marian *et al*, 1995b; Marian *et al*, 1997; Marian and Roberts, 2001; Marian, 2000; Li *et al*, 1997; Rust *et al*, 1999; Roberts and Sigwart, 2001; Li *et al*, 2002; Ortlepp *et al*, 2002). That indices of global systolic function such as FS% or EF% are normal or supernormal in HCM is attributed to the concentric nature of the disease, which leads to decreased LV end diastolic volume and consequently in decreased wall stress and afterload (Marian, 2000). The reduction in peak early systolic MVG in the LVPW of HCM

cats was not associated with high intraventricular pressure gradients (even in cats with intraventricular pressure gradient < 4 mm Hg, the peak Se MVG was significantly lower than that in normal cats), and it was accompanied by normal FS%. These findings show that systolic impairment is evident in HCM of cats and that traditional methods of assessment of global systolic function are less sensitive in accurately reflecting LV systolic properties. However, thickness was a significant negative independent predictor for peak early and late systolic MVG in the affected group, suggesting that systolic impairment in the LVPW of HCM cats is attributed to a certain extent to hypertrophy. This finding underlines the hypothesis that hypertrophy is not only resulting in reduced myocardial compliance, but also in reduced contractility. That thickness was a significant negative independent predictor for peak early systolic MVG in the HCM group does not rule out the possibility that reduced contractile performance is attributable to the systolic deficit of individual cardiac cells. It rather represents regional characteristics between thickness and systolic MVG in the LVPW of cats. This is supported by our previous observations in HCM cats, which showed that decreased systolic TDI indices in other parts of the LV were not associated with LV hypertrophy (Section D). A series of case reports have described the evolution of "typical" HCM in humans (hypertrophied, hyperdynamic and non-dilated LV) into a morphologically and functionally phase which resembled dilated cardiomyopathy (Beder *et al*, 1982; Fujiwara *et al*, 1984; Kanemoto *et al*, 1995). Progressive increase in LV dimensions with maintenance of normal cavity size, along with substantial wall thinning and systolic impairment, was also evident in a subgroup of HCM patients (Spirito *et al*, 1986; Spirito *et al*, 1987; Tabata *et al*, 2000). Recently, Baty and colleagues (2001) reported a family of cats

with an end stage HCM, which was characterized by hypodynamic LV systolic function and relative LV chamber dilatation. Whether the decreased systolic MVG in HCM of cats reflects primary contractile deficit or is related to the dilating changes seen in a subset of patients remains unclear. It would be of clinical importance to assess the association between changes in MVG during all phases of the cardiac cycle and heart failure in cats with HCM. This, apart from offering possible early markers for CHF, would be useful in monitoring the efficacy of different therapeutic regimes and help in optimising drug selection. Larger number of cats with CHF than those used in the current study and long term monitoring of the disease progress will elucidate further these issues.

Our study shows that differences in the LVPW between normal and HCM cats are due to decreased early diastolic and systolic MVG (Figure F5). Corresponding peak MMV velocities were similar between the two groups. We attribute the discrepancy between MVG and MMV to the influence of the overall heart motion on these TDI indices. It has been proven by theoretical calculations and clinical data that MVG, in contrast to MMV, is not affected by the overall heart motion, and so it can be a more accurate index of intrinsic myocardial function (Fleming *et al*, 1994b; Uematsu *et al*, 1995; Uematsu *et al*, 1997). Myocardial velocities measured by the TDI technique are affected by the overall heart motion and motion of adjacent myocardial segments and therefore do not always represent true myocardial velocities. This is particularly exacerbated in myocardial walls, which are affected favourably by the overall heart motion, such as the LVPW, especially along the radial axis of the heart (Tabata *et al*, 2000). We have shown that with the exception of IVCb, pulsed TDI velocities failed

to reveal impaired myocardial properties in the LVPW of HCM cats along the radial axis (Section D). Similar to this, MMV measured by colour M-mode TDI was not different between normal and HCM cats. These findings highlight the superiority of MVG in accurately quantifying myocardial properties and also the limitations of TDI derived velocities.

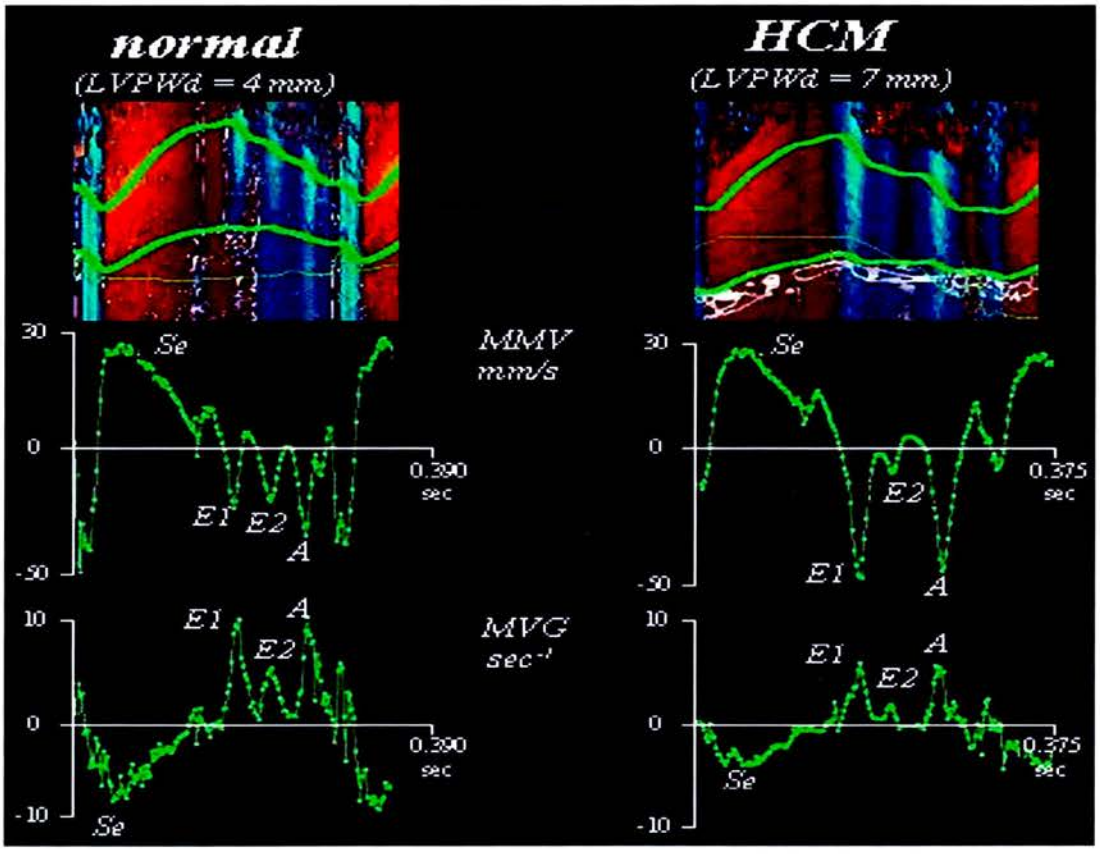

Figure F 5. *Myocardial Velocity Gradient (MVG) and Mean Myocardial Velocity (MMV) from a normal and a HCM cat. Note that the affected animal presents higher peak first early (E1) and late diastolic (A) MMV than the normal animal. Peak early systolic (Se) MMV is slightly higher in the affected animal than in the normal one. However, peak MVG during these phases were significantly higher in the normal animal compared with that in the HCM cat. E2: second early diastolic peak. LVPWd: thickness of left ventricular free wall during diastole.*

Myocardial function appeared to be impaired during the 2 isovolumic periods in cats with HCM. This was reflected by the prolonged IVRt, the reduced MVG during the two phases of the isovolumic relaxation period and the reduced MMV during the second phase of both isovolumic periods. Reduced myocardial velocities have also been reported during the 2 isovolumic periods in humans with HCM (Naqvi *et al*, 2001). Myocardial motion during these short duration periods occurs in a similar fashion across the myocardium (biphasic oppositely directed shifts), irrespective of heart rate, and apart from regulating the transition of myocardial fibres from a contractile to a relaxation state and *vice versa,* it results in abrupt changes in intracavitary pressures, which are essential for the physiologic sequence of cardiac events during the cardiac cycle (opening and closure of cardiac valves). Earlier studies have shown that changes in myocardial motion during the 2 isovolumic periods can cause loss of the mechanical efficiency of the myocardium during both systole and diastole (Gibson and Brown, 1976a). Changes in the myocardial motion characteristics during these short duration periods can also result in altered LV haemodynamics. Invasive hemodynamic studies have shown that humans with HCM have prolonged time constant of pressure decay in isovolumetric relaxation (τ) and decreased peak positive rate of pressure development (dP/dt) during the isovolumic contraction period (Yamada *et al*, 1998; Oki *et al*, 2000). Similar findings have been reported in cats with HCM (Golden *et al*, 1990). These changes reflect impaired global diastolic and systolic function and result from impaired myocardial motion during the two isovolumic periods. IVCb of MMV appeared to be a very sensitive index in discriminating between the two groups. Peak IVCb of MMV was independent of heart rate, age, weight, sex and thickness in both groups and it was

consistently identified in the MMV tracing without being affected by summation effects due to high heart rates. The above characteristics of IVCb of the MMV suggest that it is a very sensitive marker for differentiating normal cats and cats with HCM and that it could be used for investigating myocardial properties in other feline cardiomyopathies. Myocardial motion during the isovolumic contraction time coincides with the electrical activation of the myocardium and its characteristics have been an issue of debate among investigators (Clayton *et al*, 1979). Some have proposed that the IVC phase is characterized by asynchronous contraction during which the early activation and contraction of papillary muscles and trabeculae carnae result in a sudden downward movement of the atrioventricular valves and passive outward stretch of the circumferentially oriented fibres, particularly those in the basilar two-thirds of the ventricle (Hawthorne, 1966; Jones *et al*, 1990). Based on this theory one could argue that the prominent outward movement in the LVPW of cats during the second phase of the ICVt probably represents a passive reaction of the myocardial fibres rather than an active phenomenon and the reduction seen in the IVCb of MMV in the HCM group reflects decreased response of the circumferentially oriented fibres in a less vigorous contraction of the longitudinally arranged fibres of the endocardial area. However, we believe that other factors, such as the need for adjustment against rapid load changes (transition from a contractile to a relaxation state and *vice versa*) should be taken into account when interpretation of myocardial motion during the 2 isovolumic periods is sought (Hawthorne, 1961). Further studies are needed to elucidate the behaviour of myocardial fibres in the different parts of the myocardium during this short duration periods in the normal and the diseased state.

Male cats were over represented in the current study. This is in agreement with the high prevalence of male affected cats reported in other studies and may reflects possible contribution of modifying factors related to sex in the phenotypic expression of the disease (Atkins *et al*, 1992a; Fox *et al*, 1995). However, stepwise regression analysis showed that the factor sex did not contribute often to the variance of TDI indices derived from the LVPW of cats.

F.5. Limitations

This was a non-invasive study carried out on pet animals. Consequently, we were unable to generate any invasively determined haemodynamic data to provide gold standards with which to compare our results. Due to the angle dependence of Doppler measurements, the estimation of MVG and MMV was confined to the free wall by using the right parasternal long-axis view in which the ultrasonic beam was visually checked to be parallel to the myocardial movement. Analysis of very short duration events, such as those occurring during the 2 isovolumic periods and especially their first part, requires very high temporal resolution. Higher sampling rates than those used in the current study will allow a more accurate quantification of myocardial motion during these periods. Lack of simultaneous recording of phonocardiogram may have caused a less accurate estimation of the duration of the different cardiac phases than that reported in other studies. However, we believe that the grey and colour scale events and the simultaneously recorded ECG offered consistent definition of the phases of the cardiac cycle used to define our analyses. Although previous studies have reported the influence of respiration in the amplitude of MMV and MVG, we were unable to simultaneously record phases of respiration

during acquisition of images, so it was impossible for us to investigate the relationship between the timing of each phase of respiration and the occurrence of peak MVG or MMV. We averaged peak values from several cardiac cycles, which would have probably helped to minimise the significance of this problem. Some of the animals in this study were treated for CHF during assessment. To what extent this may have influenced TDI indices, is unknown. However, most of the affected animals were asymptomatic and not treated during the time of evaluation. Nineteen of the affected cats had mitral regurgitation. Mitral regurgitation is known to increase preload (Takenaka *et al*, 1986; Bryg *et al*, 1987; Maron *et al*, 1987). It is a limitation that TDI indices were not controlled for mitral regurgitation. However, taking into consideration that TDI indices are supposed to be independent from preload in the diseased state and that the magnitude of mitral regurgitation in HCM is not usually big, it is safe to assume that TDI indices were not affected significantly from the presence of mitral regurgitation.

F.6. Conclusions

This study for the first time describes the successful application of colour M-mode TDI and measurement of MVG in cats with HCM. The decreased MVG recorded in the LVPW of affected animals during diastole and systole suggests that both diastolic and systolic impairment are involved in HCM of this species. The high temporal resolution of colour M-mode TDI allowed the quantification of myocardial motion during the 2 isovolumic periods. Cats with HCM had decreased TDI indices during both the IVC and IVR phases. MMV failed to show differences between the two groups and proved to be a less sensitive means in quantifying myocardial function

and that it should be always interpreted cautiously. MVG is a very sensitive tool in quantifying feline myocardial motion and it could be used in the classification of feline cardiac diseases and in monitoring the efficacy of different therapeutic strategies in the cardiomyopathies of this species.

SECTION G

Repeatability study

G.1. Materials and methods

To assess intra-operator and intra-observer variability, five cats (2FN and 3MN; 4 normal [cat 1, 2, 3, and 4] and 1 HCM [cat 5]) were scanned twice with a 1-week interval apart. The same person acquired and analyzed the images for the 2D/Doppler echocardiographic study. All TDI images were acquired by the same operator and analysed by the same observer. The coefficient of variation (standard deviation of measurements / mean of measurements x 100) (CV%) was calculated for all 2D/Doppler echocardiographic and TDI variables. Repeatability was assessed by calculating the mean difference and limits of agreement (mean difference ± 2 x standard deviation of difference) between two measurements, according to the Bland-Altman method (Bland and Altman, 1986). The coefficient of repeatability (2 x standard deviation of differences) was also calculated. All the above parameters of repeatability were additionally calculated for the 4 normal cats of the repeatability study (excluding the affected cat). "Real" lower and upper values for each variable were also calculated by subtracting and adding from the mean value of each parameter the lower and upper limits of agreement, respectively, determined only from the normal animals of the repeatability study. This permitted evaluation of the clinical significance of the repeatability study.

Additionally, inter- and intra-observer variability for every peak MVG and MMV index were assessed in 5 randomly selected colour M-mode TDI images by calculating the mean difference and limits of agreement (mean difference ± 2 x standard deviation [SD] of difference) of the image readings between 2 observers (one experienced and one inexperienced to assess inter-observer variability) and between the 2 separate readings of the experienced observer to assess intra-observer variability (Bland and Altman, 1986).

G.2. Results

G.2.1. Repeatability results for 2D/Doppler echocardiographic variables

The results of repeatability (CV%, limits of agreement, coefficient of reproducibility and "real" values) in acquiring 2D/Doppler echocardiographic data are presented in Table App.G1, Appendix G. Only results of the CV%, for certain 2D/Doppler echocardiographic indices, are presented in the following text.

The CV% for 2D echocardiographic variables was usually < 10% in all animals. A CV% between 10 and 20% was found for the LA area during systole in cats 1 and 4, for the LA FS% in cats 2, and 5, for LA area during diastole in cats 2 and 4, for LA length (aortic valve level) during diastole in cat 4 and for LA systolic distance in cat 5. The CV% for the LA FS% in cat 1 was 65%.

Most M-mode echocardiographic variables had a CV% < 10% in all cats included in the reproducibility study. In cats 4 and 5 the CV% for the EPSS was between 10-20%. In cats 1, 4, and 5 the CV% for the ratio of LA to aorta diameter and the

diastolic diameter of aorta ranged between 10-20% and in cat 3 between 20-30%. The CV% for the LV systolic diameter in cat 1 was 13% and for the LV FS% in cat 4, 16%.

Doppler echocardiographic variables measured from the pulmonary artery had generally a CV% < 10%. In cats 3 and 4, the CV% for the PEP and the PEP/ET of the right ventricle ranged between 10 and 20%. In cat 1, the CV% for the pulmonary artery velocity was 13%.

Doppler echocardiographic variables measured from the aorta had usually a CV% < 10%. Cat 1 had a CV% between 10 and 20% for peak aortic velocity, PEP and PEP/ET. In cat 5 the CV% for the VTI of aortic velocity was 31%.

With the exception of the following variables; E deceleration time in cat 3, E and A in cat 1, E/A, A VTI, E deceleration and acceleration in cat 4, and E, E/A and E VTI in cat 5, which had a CV% between 10-20%, the CV% for the rest of the mitral inflow echocardiographic variables was < 10%.

FVP showed a CV% of < 15% in all cats. In two of them it was <10%.

All cats, apart from cat 2, had a CV% of <10% for IVRT. In cat 2 the CV% for the IVRT was 13%.

In cats 3 and 4, the CV% for Doppler echocardiographic indices of tricuspid annulus was < 10%. In all cats the CV% for the A wave of tricuspid inflow was < 10%. The

CV% for the E wave of the tricuspid inflow was in the range between 10-20% in cats 1 and 2, and between 20-30% in cat 5. In cats 2 and 5 the CV% for the E/A ratio of the tricuspid inflow was in the range between 20-30% and in cat 1 it was 11%.

In cats 1, 2 and 3, the CV% for Smax, D, Ar and the S/D ratio of PVF was < 15%. In cat 4, the CV% for Smax, Ar and the S/D of PVF was in the range between 20-30% and D had a CV% of 2. In cat 5 the CV% for the Smax and D wave of the PVF was between 20-30% and < 10% for the Ar and the S/D ratio. The CV% for the rest of the Doppler echocardiographic variables of PVF are shown in Table App.G1.

G.2.2. Repeatability results for pulsed TDI variables

Results of repeatability (CV%, limits of agreement, coefficient of reproducibility and "real" values) in acquiring pulsed TDI data are presented in Tables App.G2 to App.G8, Appendix G. Bland-Altman plots for peak early diastolic velocities are shown in Figure G1. Only results of the CV%, for certain pulsed TDI indices are presented in the following text.

The coefficient of variation for E' was < 20% in the great majority of myocardial segments and more frequently varied between 10 and 20%. The CV% for E' was < 20% in the IVS of cats 2, 3, 4 and 5, in the LVPW along the longitudinal axis of cats 1, 2, 3 and 4 and also in the lateral mitral annulus of cats 1, 2, 3, and 4. All cats included in the reproducibility study showed a CV% < 20% for E' of the LVPW along the radial axis. The CV% for E' was < 20% in the septal mitral annulus of cats 1, 3 and 4 and also in the IVS along the radial axis and the tricuspid annulus of cats 2, 3 and 5. The CV% for E' was between 20 and 30% in the IVS along the radial axis

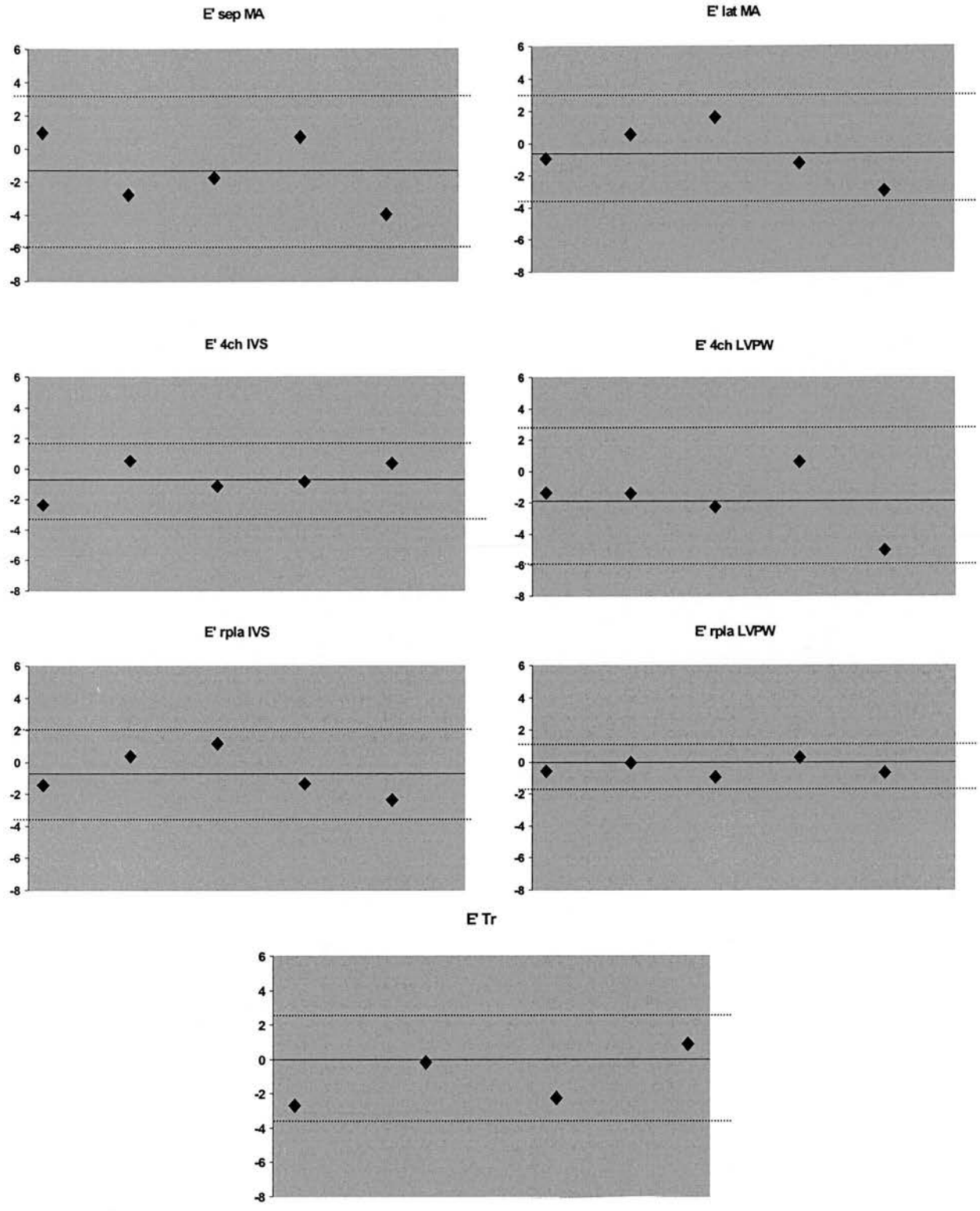

Figure G1. *Bland-Altman plots for early diastolic myocardial velocities (cm/sec). Continuous parallel line indicates the mean of all differences between the two sets of measurements. Dashed lines indicate the upper and lower limits of agreement (mean of differences ± 2 standard deviation of differences) and the diamonds the differences between the two measurements from each individual cat.*

and the tricuspid annulus of cat 1 and also in the lateral mitral annulus of cat 5 and the IVS along the radial axis of cat 4. Cat 4 showed a CV% for E' > 30% in the septal mitral annulus and the LVPW along the longitudinal axis. Cats 1 and 2 had a CV% > 30% for E' in the IVS along the longitudinal axis and the septal mitral annulus, respectively.

The coefficient of variation for A' was < 20% in the great majority of myocardial segments and was < 10% and between 10 and 20% in equal numbers of cats. The CV% was < 20% for A' in the septal side, the LVPW along the longitudinal axis and the tricuspid annulus in almost all cats included in the reproducibility study. Cat 5 showed a CV% > 30% for A' of the LVPW along the longitudinal axis. The CV% for A' in the lateral mitral annulus was between 20 and 30% in cats 1 and 3 and > 30% in cats 2 and 4. In cats 1, 2 and 4 the CV% for A' was < 10% in the IVS along the radial axis and between 20-30% in the same myocardial segment in cats 3 and 5. A CV% of < 10% was found for A' in the LVPW along the radial axis in cats 2 and 4 and between 10-20% and 20-30% in the same myocardial segment in cats 5 and 1, respectively.

The CV% for Se' was < 10% in the septal mitral annulus and the LVPW along the radial axis in all animals. A CV% of < 10% was found for Se' in the IVS along the longitudinal axis in cat 4, in the LVPW along the longitudinal axis in cat 1, in the lateral mitral annulus of cats 3 and 4 and also in the IVS along the radial axis in cats 4 and 5. The CV% for Se' was between 10 and 20% in the IVS along the longitudinal axis in cats 3 and 5, in the LVPW along the longitudinal axis in cats 3

and 4, in the lateral mitral annulus in cat 2 and also in the tricuspid annulus in cats 1, 2 and 3. The CV% for Se' was between 20 and 30% in the IVS along the longitudinal axis in cats 1 and 2, in the LVPW along the longitudinal axis in cats 2 and 5, in the lateral mitral annulus in cats 1 and 4 and also in the IVS along the radial axis in cats 1, 2 and 3. Only in the tricuspid annulus of cat 4 the CV% of Se' was > 30%.

In general, the CV% for the acceleration of E' was < 10% more frequently than the deceleration of E' in the interrogated myocardial segments. The CV% for the deceleration of E' was > 30% more often than it was for the acceleration of E'. In cats 2, 3 and 4 the CV% of the acceleration of E' was < 10% in the LVPW along the longitudinal axis, the IVS along the radial axis and in the tricuspid annulus.

The CV% for the acceleration of Se' was < 20% in most instances.

G.2.3. Repeatability results for colour M-mode TDI variables

Results of repeatability (CV%, limits of agreement, coefficient of reproducibility and "actual values") in acquiring colour M-mode TDI data are presented in Tables App.G9 and App.G10, Appendix G. Results of inter-observer and intra-observer variability (standard deviation of differences and limits of agreement) between the two readings of the same colour M-mode TDI images are shown in Table App.G11, Appendix G. Only results of the CV%, for certain MVG indices are presented in the following text.

With the exception of E2 in cat 3, all cats showed a CV% < 20% for peak diastolic MVG indices. The CV% for Se of the MVG was > 30% in cats 1 and 3 (35 and 32%, respectively), 21 and 19% in cats 4 and 5, respectively and 8% for cat 2. The CV% for Sl of the MVG was 18, 29, 14 and 7% for cats 1, 2, 3, and 4, respectively. The CV% for MVG indices during the isovolumic phases is shown in Table G9. The CV% and limits for agreement for MMV indices are presented in Table G10. Table G11 shows the mean differences and limits of agreement of the two readings of the 5 colour M-mode TDI images (two readings of the same observer and of two different observers).

G.3. Discussion

Assessing reproducibility in acquiring and analysing echocardiographic data and also knowing the level of natural/random variability occurring in these measurements, is crucial for assessing whether changes in sequentially acquired data are genuine due to disease progress or in response to treatment. Different studies in humans and animals have investigated variability in 2D/Doppler and TDI echocardiographic variables (Kuecherer *et al*, 1991; Vinereanu *et al*, 1999; Dukes-McEwan *et al*, 2002). Dukes-McEwan and colleagues (2002) in a serial echocardiographic examination in boxer dogs, showed that most echocardiographic variables had a CV% of < 20%, with the most reproducible being the M-mode and LV volumetric measurements and the worst those of tricuspid and pulmonary venous flow. Vinereanu and colleagues (1999) investigated the reproducibility in acquiring and measuring pulsed TDI data in humans, and showed that TDI indices were more reproducible along the longitudinal axis (intraobserver variability between 10 and 16%) than in the short

axis (intraobserver variability between 14 and 24%) of the heart, and that recordings from the lateral mitral annulus had the lower variability among the investigated myocardial segments (intraobserver variability < 16% for all peak myocardial velocities).

The CV% for most of the 2D and M-mode conventional echocardiographic variables was usually < 20% and quite often < 10%. The corresponding limits of agreement were, in general terms, relatively narrow and therefore the variability of the above variables was small. Very low CV%, usually < 10% and less frequently between 10-20%, and very small limits of agreement were found in most occasions for Doppler echocardiographic variables measured over the pulmonary and aortic valves. Similar findings, regarding the CV% and the limits of agreement, were found for the mitral inflow variables. The tricuspid inflow variables, showed a similar trend of variability, although the CV% was sometimes > 20% and quite often between 10-20%. The CV% for the FPV and the IRVT was always <15%. Although peak PVF indices, such as Smax, D, Ar and also the S/D ratio showed in some instances a CV% >20%, this never exceeded 30%. The peak PVF indices had a CV% < 10% and between 10-20% with the same frequency. The CV% for the PVF VTI was generally greater than that of the corresponding velocities. Considering that measurement of PVF in cats is probably one of the most difficult to acquire, the variability of PVF indices as assessed in the current study by means of CV% and limits of agreement, is judged satisfactory. This can be stated for all 2D/Doppler echocardiographic variables. Although, a CV% between 10-20% and occasionally >20%, but almost always < 30%, was found for some 2D/Doppler echocardiographic parameters, the

inherent technical difficulties in scanning cats and also the natural variability due to the highly variable heart rate of this species and their dynamic cardiac function, make a variability of this level inevitable. The level of the CV% for conventional echocardiographic variables in our group of cats was similar to that reported by Dukes-McEwan and colleagues (2002) in boxer dogs. The "real" values for 2D/Doppler echocardiographic variables calculated from the normal cats used in the repeatability study, showed, in most occasions, no overlap with the corresponding mean values from the affected group. This means that the variability documented for the above parameters in normal cats is unlikely to result in values outside reference ranges.

The variability for early and late diastolic indices of MVG was satisfactory. Emax of the MVG was the variable with the lowest variability, suggesting that it would be unlikely differences found in the magnitude of this variable to result from natural variability. This finding renders Emax of the MVG a reliable index for investigation of the early diastolic properties of the feline myocardium in serial studies. With the exception of E2 of the MVG in cat 3, all of the other diastolic MVG indices showed an acceptable CV%, which was always <20% and quite often < 10%. In contrast to diastolic MVG indices, the variability in systolic MVG indices was higher, particularly in peak Se MVG. This find may reflect the dynamic character of the contractile performance of thc feline myocardium and its increased response in neurohormonal and heart rate alterations. The variability for all MVG indices during the two isovolumic periods was large. This is partially explained by their low magnitude, which increases the possibility for measurement error. MMV indices

showed larger variability than the corresponding MVG indices, probably because they are influenced from overall heart motion, which may act as an extra contributing factor in the natural variability of myocardial velocities. Although the CV% for the IVCb of the MMV was particularly large in cats 2 (normal) and 5 (HCM), the two sets of values of this variable in each one those cats, did not show overlap with the mean values of the other group. We believe that the IVCb of the MMV could be a useful index for the evaluation of feline myocardial properties without significantly affected by natural variability. With the exception of peak early diastolic MVG indices and IVCb of the MMV, all the rest of the MVG and MMV variables had "real" values, which overlapped with the corresponding mean values from the affected group. This means that, given that acquisition and analysis of the two sets of data were carried out by the same operator and observer, respectively, natural variability and variability due to the inherent difficulty of sampling exactly the same myocardial site each time, may considerably decrease the sensitivity, particularly of those variables with "real" values considerably overlapping the corresponding mean values from HCM cats.

Intra-observer and inter-observer limits of agreement for the colour M-mode TDI image readings between 2 observations (two readings of the same image by the same observer and two readings of the same image by different observers) were satisfactory for most indices of both variables (MMV and MVG). Very wide inter-observer limits of agreement for some indices (IVCa and IVRa of MMV) may reflect differences in analyzing experience between observers rather than true difficulties in reproducing peak values successfully during these phases. In general, intra-observer

variability was lower than inter-observer variability. This observation emphasizes that analysis of colour M-mode TDI images requires a minimal level of analysing experience. Narrower limits of agreement of MMV indices when compared with those of MVG are due to the fact that the MMV tracing showed a more consistent and recognisable sequence of peaks than the MVG tracings. Peak indices with very low mean values (especially MVG during the IVC and IVR phases) were difficult to identify consistently and thus more prone to measurement error. The very low intra-observer variability found in the two readings of the same colour M-mode images, indicates that the variability documented in acquiring the two sets of data from the same cat at two different occasions, is more likely to result from natural variability and variability caused by the difficulty to sample the exact myocardial site each time.

The early diastolic myocardial velocities measured by pulsed TDI showed a CV%, which usually was < 20% and quite often <10%. Less frequently the CV% for E' was between 20-30% or > 30% and most of the times this happened in animals 1 and 4 (the former was not very co-operative, so it was difficult to consistently sample the same myocardial segment and the latter showed a heart rate variability between the two measurements, which may have contributed to the large variability seen in E' in some myocardial segments). The LVPW along the radial axis and the IVS along the longitudinal axis had the narrower limits of agreement for E', presumably because it was easy to quantify them and they provided consistently good quality tracings (Figure G1). The CV% for A' was generally < 20% and more frequently < 10% than it was for the early diastolic velocity. The variability for A' was the larger in the lateral mitral annulus, a finding which probably reflects the general difficulty in

acquiring late diastolic myocardial signals from this particular myocardial segment. We believe that quantification of the systolic properties of the LA in cats by means of A' it should be done on the septal side of the heart along the longitudinal axis. The variability of the E'/A' ratio followed the trends described for the early and late diastolic myocardial velocities. The lower variability and narrower limits of agreement for the E'/A' ratio were found in the LVPW along both axes and the tricuspid annulus. Early systolic myocardial velocities were the most reproducible among the pulsed TDI indices. The CV% for the Se' was < 10% in the septal mitral annulus and the LVPW along the radial axis in all animals. The SI' velocities were less reproducible than Se', in the corresponding myocardial segments. Acceleration and deceleration of E' and acceleration of Se' were in general less reproducible than peak myocardial velocities. Although on many occasions, they showed a CV% of < 10%, quite often they had a CV% > 30%. The acceleration of E' and Se' waves showed a lower CV% than the deceleration of E' in most instances. In general, pulsed TDI indices from all myocardial segments from the normal animals used in the repeatability study had "real" values, which overlapped with the corresponding values from the affected group. This indicates that interpretation of pulsed TDI indices from individual animals should be done cautiously. The level of variability of pulsed TDI indices in our group of cats was higher than that reported in humans (Vinereanu *et al*, 1999). This finding is reasonable considering the relatively small heart rate variability of humans and the fact that cats are less cooperative compared with humans.

G.4. Conclusion

The repeatability study described in the current section was limited by the relatively low number of animals and because not all were normal. Higher number of cats would have provided a more accurate estimate of the variability of the echocardiographic variables assessed. When reproducibility in acquiring echocardiographic measurements in a serial way in cats is examined, one always needs to consider the existence of natural variability, due to respiratory and especially due to heart rate variability. The dynamic nature of the feline myocardial function, which is compatible with rapid adjustments in increasingly variable high heart rates is another factor, which may contribute to natural variability. The variability in 2D/Doppler echocardiographic variables was less than that found for TDI indices. This finding is reasonable to certain extent, since conventional echocardiographic variables are related to global characteristics of the heart and its function and therefore must be less dependent on factors contributing to natural variability than the characteristics of segmental myocardial motion, assessed by means of TDI indices. A relatively higher variability in TDI indices results also from the fact that it is very difficult, almost impossible, to always sample exactly the same part of the interrogated myocardial segment. This confounding factor may be exacerbated in the small heart of cats, since, sampling of slightly different myocardial regions may result in quantification of areas with significantly different structural and functional characteristics from those sampled at first instance. Considering the finite size of the sample volume used in the current study (1 mm), quantification of exactly the same myocardial segment in two occasions would be highly unlikely (Vinereanu *et al*, 1999). Despite the above confounding factors, the

variability of peak myocardial pulsed TDI indices remained usually < 20% and quite often < 10%. This level of variability is generally acceptable. However, it means that changes < 30 % in the magnitude of TDI indices between serial scans, should be considered as normal, presuming the way of acquisition and analysis of the data remained unchanged. We believe that changes > 30% should be accepted as significant changes indicating progress of disease or improvement due to certain medications or due to other factors, when serial evaluation of cardiac function is performed by means of pulsed TDI. Peak diastolic MVG parameters showed the lower variability among the TDI indices, suggesting that they may be very sensitive indices in assessing diastolic properties in feline cardiac diseases, in a serial way.

Another limitation of the current study was that intra-observer and inter-observer variability in analysing pulsed TDI tracings and 2D/Doppler echocardiographic data was not carried out. However, the results of intra-observer and inter-observer variability from the analysis of the same colour M-mode images indicate that when data analysis is carried out by experienced observers, the observer variability is low. As a conclusion, we could say that the measurement process is more repeatable than acquisition of images, particularly for TDI echocardiography. Although repeatability problems of TDI echocardiography may limit the value of serially scanning one individual cat, the utility of the technique in population screening, or comparing groups of cats with various diseases, provided there are enough cats in each group, remains valuable.

Section H

Correlations between echocardiographic variables

H.1. Materials and methods

Selective correlations were investigated between 2D/Doppler echocardiographic variables and also between TDI indices and 2D/Doppler echocardiographic parameters within the same group. Only pulsed TDI indices from both annular sites and those from the radial axis of the heart were included in the analysis.

Linear regression analysis was carried out using SigmaStat (V2.03; SPSS Inc 1997). A Kolmogorov-Smirnov test was used to assess the normal distribution of the variables. To achieve normality of the non-normally distributed variables logarithmic transformation was used. A p value of < 0.05 was considered statistically significant.

H.2. Results

Results of correlations are presented in Tables H1-H4.

H.2.1. Comparisons between 2D/Doppler echocardiographic variables

Results are shown in Table H1. A positive association was found between the E/A ratio of mitral inflow and the FPV in the normal group. The E/A ratio of mitral inflow showed an inverse association with the S/D ratio of the PVF. In normal cats, the A wave of mitral inflow was associated positively with the Smax and the S/D of PVF.

Table H 1. Correlations between 2D/Doppler echocardiographic variables within the same group

	normals	r p	HCM	r p
E vs FPV	ns	ns	ns	ns
E/A vs FPV	E/A = 0.448 + (0.001 * FPV)	0.49 =0.056	ns	ns
LA area d vs Smax	ns	ns	LA area d = 494.5 - (676.1 * Smax)	0.65 <0.01
LA area s vs Smax	ns	ns	LA area s = 563.1 - (646.7 * Smax)	0.62 <0.01
LA FS% vs Smax	ns	ns	LA FS% = -6.55 + (55.69 * Smax)	0.80 <0.001
LA area d vs D	ns	ns	ns	ns
LA area s vs D	ns	ns	ns	ns
LA FS% vs D	ns	ns	LA FS% = 34.339 - (51.989 * D)	0.59 <0.01
LA area d vs Ar	ns	ns	ns	ns
LA area s vs Ar	ns	ns	ns	ns
LA FS% vs Ar	ns	ns	ns	ns
LA area d vs S/D	ns	ns	LA area d = 618.82 - (278.26 * S/D)	0.71 <0.001
LA area s vs S/D	ns	ns	LA area s = 651.23 - (245.29 * S/D)	0.66 <0.01
LA FS% vs S/D	ns	ns	LA FS% = -6.509 + (16.902 * S/D)	0.87 <0.001
LV FS% vs FPV	ns	ns	ns	ns
E vs Smax	ns	ns	ns	ns
E vs D	ns	ns	E = 0.248 + (1.152 * D)	0.73 <0.05
E vs S/D	ns	ns		
A vs Smax	A = 0.259 + (0.864 * Smax)	0.69 <0.01	A = 0.159 + (0.959 * Smax)	0.76 <0.05
A vs D	ns	ns	ns	ns
A vs S/D	A = 0.345 + (0.245 * S/D)	0.68 <0.01	A = 0.253 + (0.225 * S/D)	0.62 =0.055
E/A vs S/D	E/A = 1.624 - (0.487 * S/D)	0.59 <0.05	E/A = 2.053 - (0.651 * S/D)	0.80 <0.01

In the affected group, an inverse association was found between the Smax and S/D of PVF with the LA area during diastole and systole. The Smax and S/D were positively correlated with LA FS% in HCM cats. In contrast, the D wave of PVF showed and inverse association with LA FS%. The E wave of mitral inflow was related positively with the D wave of PVF in the affected group. The A wave of mitral inflow showed a positive relationship with the Smax and S/D of PVF. An inverse association was found between the E/A of mitral inflow and the S/D of PVF in HCM cats.

H.2.2. Comparisons between pulsed TDI indices and 2D/Doppler echocardiographic variables

Results are shown in Tables H2 and H3. A positive, but weak association was found between the E' wave of the septal mitral annulus of normal animals and the LV FS%.

Table H2. Correlations between 2D/Doppler echocardiographic variables and pulsed TDI annular indices from normal and HCM cats

	normal				HCM			
	sep MA	r p	lat MA	r p	sep MA	r p	lat MA	r p
E' vs LV FS%	E' = 26.555 + (2.83 * LV FS%)	0.42 <0.05	ns	ns	ns	ns	ns	ns
E' vs E	ns	ns	ns	ns	ns	ns	ns	ns
E' vs FPV	ns	ns	E' = 1.813 + (0.0115 * FPV)	0.55 <0.05	ns	ns	ns	ns
E' vs Smax	ns	ns	ns	ns	ns	ns	ns	ns
E' vs D	ns	ns	ns	ns	ns	ns	ns	ns
E' vs S/D	ns	ns	ns	ns	ns	ns	ns	ns
A' vs LA FS%	ns	ns	ns	ns	A' = 3.342 + (0.155 * LA FS%)	0.66 <0.01	A' = 2.95 + (0.13 * LA FS%)	0.63 <0.05
A' vs LA area d	ns	ns	ns	ns	A' = 8.487 - (0.0127 * LA area d)	0.76 <0.01	A' = 16.08 - (2.14 * LA area d)	0.69 <0.05
A' vs LA area s	ns	ns	ns	ns	A' = 9.287 - (0.0118 * LA area s)	0.75 <0.01	A' = 7.86 - (0.009 * LA area s)	0.69 <0.05
A' vs A	A' = 0.433 + (9.611 * A)	0.64 <0.01	A' = -1.947 + (13.296 * A)	0.67 <0.05	ns	ns	ns	ns
A' vs Smax	A' = 2.247 + (9.723 * Smax)	0.52 <0.05	ns	ns	A' = 1.599 + (10.237 * Smax)	0.67 <0.01	A' = 0.593 + (11.340 * Smax)	0.72 <0.05
A' vs D	ns	ns	ns	ns	ns	ns	ns	ns
A' vs Ar	ns	ns	ns	ns	ns	ns	ns	ns
A' vs S/D	ns	ns	ns	ns	A' = 1.601 + (3.016 * S/D)	0.59 <0.05	A' = -0.169 + (3.755 * S/D)	0.62 <0.05
Se' vs LA area s	ns	ns	ns	ns	Se' = 7.462 - (0.0049 * LA area s)	0.53 <0.05	Se' = 7.52 - (0.007 * LA area s)	0.55 <0.05
Se' vs LA area d	ns	ns	ns	ns	ns	ns	Se' = 16.48 - (2.16 * LA area d)	0.64 <0.05
Se' vs LA FS%	ns	ns	ns	ns	ns	ns	Se' = 3.20 + (0.13 * LA FS%)	0.58 <0.05
Se' vs LV FS%	ns	ns	ns	ns	Se' = 1.802 + (0.0780 * LV FS%)	0.67 <0.01	Se' = 0.15 + (0.10 * LV FS%)	0.64 <0.01
Se' vs Ao. vmax	ns	ns	ns	ns	ns	ns	ns	ns
Se' vs E	ns	ns	ns	ns	ns	ns	ns	ns
Se' vs FPV	ns	ns	ns	ns	ns	ns	ns	ns
Se' vs IVRT	ns	ns	Se' = 0.82 + (136.03 * IVRT)	0.52 <0.05	ns	ns	ns	ns
Se' vs Smax	ns	ns	ns	ns	Se' = 2.702 + (7.252 * Smax)	0.72 <0.01	Se' = 1.002 + (11.619 * Smax)	0.64 <0.05
Se' vs D	ns	ns	ns	ns	ns	ns	ns	ns
Se' vs Ar	ns	ns	ns	ns	ns	ns	ns	ns
Se' vs S/D	ns	ns	ns	ns	Se' = 3.220 + (1.775 * S/D)	0.57 <0.05	ns	ns
E'/A' vs S/D	E'/A' = 1.617 - (0.556 * S/D)	0.74 <0.001	E'/A' = 2.785 - (1.233 * S/D)	0.72 <0.01	ns	ns	E'/A' = 1.797 - (0.540 * S/D)	0.72 <0.05
E'/A' vs E/A (MI)	E'/A' = 0.168 + (0.886 * E/A)	0.81 <0.001	E'/A' = -0.44 + (1.79 * E/A)	0.86 <0.01	E'/A' = -0.461 + (1.222 * E/A)	0.79 <0.01	ns	ns
E'/A' vs E/A (TI)	E'/A' = 0.741 + (0.275 * E/A)	0.50 <0.05	ns	ns	ns	ns	ns	ns
IVRt vs IVRT	ns	ns	ns	ns	ns	ns	ns	ns

Table H3. Correlations between 2D/Doppler echocardiographic variables and pulsed TDI indices from the LVPW and the IVS along the radial axis from normal and HCM cats

	normal				HCM			
	rpla LVPW	r p	rpla IVS	r p	rpla LVPW	r p	rpla IVS	r p
E' vs LV FS%	ns	ns	ns	ns	ns	ns	ns	ns
E' vs E	ns	ns	ns	ns	ns	ns	ns	ns
E' vs FPV	E' = 3.934 + (0.00233 * FPV)	0.51 <0.05	ns	ns	ns	ns	ns	ns
E' vs Smax	ns	ns	ns	ns	ns	ns	ns	ns
E' vs D	E' = 2.537 + (6.990 * D)	0.47 <0.05	ns	ns	ns	ns	ns	ns
E' vs S/D	ns	ns	ns	ns	ns	ns	ns	ns
A' vs LA FS%	ns	ns	ns	ns	ns	ns	ns	ns
A' vs LA area d	ns	ns	ns	ns	ns	ns	ns	ns
A' vs LA area s	ns	ns	ns	ns	ns	ns	ns	ns
A' vs A	ns	ns	A' = -3.605 + (15.016 * A)	0.83 <0.001	ns	ns	ns	ns
A' vs Smax	ns	ns	ns	ns	A' = 0.683 + (13.397 * Smax)	0.72 <0.01	ns	ns
A' vs D	ns	ns	ns	ns	ns	ns	ns	ns
A' vs Ar	ns	ns	ns	ns	A' = 3.631 + (10.190 * Ar)	0.65 <0.01	ns	ns
A' vs S/D	ns	ns	A' = 1.574 + (3.998 * S/D)	0.67 <0.01	ns	ns	ns	ns
Se' vs LA area s	ns	ns	ns	ns	Se' = 7.367 - (0.0046 * LA area s)	0.55 <0.05	ns	ns
Se' vs LA area d	ns	ns	ns	ns	Se' = 12.180 - (1.203 * LA aread)	0.53 <0.05	Se' = 0.64 + (1.08 * LA area d)	0.53 <0.05
Se' vs LA FS%	ns	ns	ns	ns	Se' = 4.289 + (0.0975 * LA FS%)	0.59 <0.01	ns	ns
Se' vs LV FS%	ns	ns	ns	ns	Se' = 2.147 + (0.0698 * LV FS%)	0.68 <0.01	ns	ns
Se' vs Ao. vmax	ns	ns	ns	ns	ns	ns	ns	ns
Se' vs E	ns	ns	ns	ns	Se' = 8.889 - (4.668 * E)	0.61 <0.05	ns	ns
Se' vs FPV	ns	ns	ns	ns	ns	ns	ns	ns
Se' vs IVRT	ns	ns	ns	ns	ns	ns	ns	ns
Se' vs Smax	ns	ns	ns	ns	Se' = 4.195 + (4.159 * Smax)	0.56 <0.05	ns	ns
Se' vs D	ns	ns	ns	ns	Se' = 9.186 - (10.461 * D)	0.74 <0.001	ns	ns
Se' vs Ar	ns	ns	ns	ns	ns	ns	ns	ns
Se' vs S/D	ns	ns	ns	ns	Se' = 2.289 + (2.460 * S/D)	0.86 <0.001	ns	ns
E'/A' vs S/D	ns	ns	E'/A' = 1.904 - (0.841 * S/D)	0.60 <0.05	E'/A' = 1.788 - (0.644 * S/D)	0.51 <0.05	ns	ns
E'/A' vs E/A (MI)	E'/A' = 0.375 + (0.632 * E/A)	0.44 <0.05	E'/A' = -0.029 + (1.131 * E/A)	0.54 <0.05	ns	ns	ns	ns
E'/A' vs E/A (TI)	ns	ns	ns	ns	ns	ns	ns	ns
IVRt vs IVRT	ns	ns	ns	ns	IVRt = -0.0066 + (1.22 * IVRT)	0.68 <0.05	ns	ns

In normal cats, the septal and lateral mitral annular A' wave showed a positive association with the A wave of mitral inflow. A similar positive association was found between the A' wave of the septal mitral annulus and the Smax of PVF. The septal and lateral mitral annular E'/A' were found to correlate inversely and positively with the S/D ratio of PVF and the E/A of mitral inflow, respectively, in a very strong manner. The E'/A' of the septal mitral annulus of normal cats showed a positive, but weak association with the E/A ratio of the tricuspid inflow. Relatively weak, but positive associations were found between the lateral annular E' and the FPV and also between the lateral annular Se' and the IVRT.

In the affected group, the A' wave from both annular sites showed an inverse relationship with the LA area during diastole and systole and a positive association with the LA FS% and also with the Smax and the S/D ratio of the PVF. In HCM cats, a positive association was found between the Se' of both annular sites and the Smax of PVF and also with the LV FS%. The Se' in both annular sites of affected cats showed an inverse, but relatively weak association with the LA area during systole. The Se' in the lateral mitral annulus of HCM cats was correlated positively and inversely, with the LA FS% and the LA area during diastole, respectively. The Se' in the septal mitral annulus of HCM cats was found to correlate positively with the S/D ratio of PVF. The E'/A' ratio in the septal and lateral mitral annulus of affected animals showed a positive and an inverse association with the E/A of mitral inflow and the S/D of PVF, respectively.

In the normal group, the E' wave of the LVPW along the radial axis showed a positive association with the FPV and the D wave of the PVF. In the both the LVPW and the IVS (radial axis) of normal cats, a positive, but weak association was found between the E'/A' and the E/A ratio of mitral inflow. In normal cats, the A' wave of the IVS along the radial axis was correlated positively with the A wave of mitral inflow and the S/D ratio of PVF.

In the LVPW of HCM cats along the radial axis, a positive association was found between the Se' wave and the following 2D/Doppler echocardiographic indices: LA and LV FS%, Smax and S/D of PVF. The Se' in the LVPW along the radial axis in affected cats was associated inversely with the LA area during diastole and systole, the E wave of mitral inflow and the D wave of PVF. A positive relationship was found between the A' wave of the LVPW along the radial axis and the Ar wave and the Smax of PVF. In the LVPW (radial axis) of affected cats a positive association was found between the myocardial IVRt and the LV IVRT. In the same myocardial segment of HCM cats a negative, but weak, correlation was found between the E'/A' ratio and the S/D of PVF.

The only significant association found in the IVS of affected cats along the radial axis was between the Se' and the LA area during diastole.

H.2.3. Comparisons between colour M-mode TDI indices and 2D/Doppler echocardiographic variables

Results are shown in Table H4. E12 of the MMV and MMV values, in both groups, did not correlate significantly with any of the conventional echocardiographic variables used in the above analysis. Peak E1 MVG was found to associate positively and negatively with FPV in the normal group and the affected group, respectively. A positive association was found between peak E1 of the MVG and peak aortic velocity in the HCM group. Peak E2 of the MVG in normal cats showed an inverse association with the LV FS%, and the S wave and S/D ratio of PVF. A very strong positive relationship was found between the E2 of the MVG and the E/A ratio and the FPV in the normal group. Emax of the MVG in the normal group showed a positive association with the FPV. Similarly, a positive association was found between the Emax of MVG and the LV FS% in HCM cats. Peak A of the MVG showed a positive and inverse association with the A wave and the E/A ratio of mitral inflow, respectively, in both groups. Peak A of the MVG was correlated positively with the Smax and S/D of PVF and also with the LA FS% in HCM cats. An inverse association was found between the peak A of MVG and the LA area during diastole and systole in affected cats.

The E2 of the MMV showed a positive association with the FPV and the E wave of mitral inflow in the normal group. An inverse association was found between the Se of the MMV and the Smax of PVF in normal cats. The Se of the MMV was associated inversely with the E wave of mitral inflow and the D wave of PVF in HCM cats.

Table H 4. Correlations between colour M-mode TDI indices and 2D/Doppler echocardiographic variables in the normal and HCM group

MVG	normal	r p	HCM	r p
E1 vs E	ns	ns	ns	ns
E1 vs LV FS%	ns	ns	ns	ns
E1 vs Ao. vmax	ns	ns	E1 = 2.484 + (1.272 * Ao.vmax)	0.83 <0.05
E1 vs E/A	ns	ns	ns	ns
E1 vs FPV	E1 = 2.138 + (0.0173 * FPV)	0.64 <0.05	E1 = 12.930 - (0.0236 * FPV)	0.88 <0.05
E1 vs IVRT	ns	ns	ns	ns
E1 vs Smax	ns	ns	ns	ns
E1 vs D	ns	ns	ns	ns
E1 vs S/D	ns	ns	ns	ns
E2 vs E	ns	ns	ns	ns
E2 vs LV FS%	E2 = 16.28 - (0.22 * LVFS%)	0.55 <0.05	ns	ns
E2 vs Ao. vmax	ns	ns	ns	ns
E2 vs E/A	E2 = -4.637 + (9.846 * E/A)	0.81 <0.001	ns	ns
E2 vs FPV	E2 = -2.539 + (0.0172 * FPV)	0.80 <0.01	ns	ns
E2 vs IVRT	ns	ns	ns	ns
E2 vs Smax	E2 = 13.925 - (18.156 * Smax)	0.60 <0.05	ns	ns
E2 vs D	ns	ns	ns	ns
E2 vs S/D	E2 = 14.349 - (7.491 * S/D)	0.78 <0.01	ns	ns
Emax vs E	ns	ns	ns	ns
Emax vs LV FS%	ns	ns	Emax = 0.707 + (0.091 * LV FS%)	0.54 <0.05
Emax vs Ao. vmax	ns	ns	ns	ns
Emax vs E/A	ns	ns	ns	ns
Emax vs FPV	Emax = 0.516 + (0.019 * FPV)	0.67 <0.05	ns	ns
Emax vs IVRT	ns	ns	ns	ns
Emax vs Smax	ns	ns	ns	ns
Emax vs D	ns	ns	ns	ns
Emax vs S/D	ns	ns	ns	ns
A vs LA area s	ns	ns	A = 10.811 - (0.0162 * LA area s)	0.84 <0.001
A vs LA area d	ns	ns	A = 23.334 - (3.337 * LA area d)	0.78 <0.001
A vs LA FS%	ns	ns	A = 2.966 + (0.194 * LA FS%)	0.66 <0.01
A vs A (MI)	A = 0.160 + (13.828 * A)	0.55 <0.05	A = -1.852 + (13.351 * A)	0.83 <0.01
A vs E/A	A = 14.473 - (5.563 * E/A)	0.55 <0.05	A = 12.029 - (5.450 * E/A)	0.73 <0.05
A vs FPV	ns	ns	ns	ns
A vs Smax	ns	ns	A = 0.200 + (13.507 * Smax)	0.67 <0.05
A vs D	ns	ns	ns	ns
A vs Ar	ns	ns	ns	ns
A vs S/D	ns	ns	A = -0.695 + (4.724 * S/D)	0.69 <0.05
Se vs LV FS%	ns	ns	ns	ns
Se vs Ao. vmax	ns	ns	ns	ns
Se vs E	ns	ns	ns	ns
Se vs FPV	ns	ns	ns	ns
Se vs Smax	ns	ns	ns	ns
Se vs D	ns	ns	ns	ns
Se vs S/D	ns	ns	ns	ns
MMV	**normal**	**r p**	**HCM**	**r p**
E1 vs E	ns	ns	ns	ns
E2 vs E	E2 = 3.691 + (43.092 * E)	0.61 <0.05	ns	ns
Emax vs E	ns	ns	ns	ns
E1 vs FPV	ns	ns	ns	ns
E2 vs FPV	E2 = 2.134 + (0.0454 * FPV)	0.68 <0.05	ns	ns
Emax vs FPV	ns	ns	ns	ns
A vs LA area s	ns	ns	A = -45.011 - (0.0481 * LA area s)	0.58 <0.05
A vs LA area d	ns	ns	A = -80.265 - (9.611 * LA area d)	0.49 <0.05
A vs A	ns	ns	A = -0.819 + (46.105 * A)	0.64 <0.05
A vs Smax	ns	ns	ns	ns
A vs D	ns	ns	ns	ns
Se vs LV FS%	ns	ns	ns	ns
Se vs Ao. vmax	ns	ns	ns	ns
Se vs E	ns	ns	Se = 64.920 - (47.226 * E)	0.85 <0.001
Se vs FPV	ns	ns	ns	ns
Se vs Smax	Se = 48.989 - (38.338 * Smax)	0.51 <0.05	ns	ns
Se vs D	ns	ns	Se = 50.514 - (54.731 * D)	0.62 <0.01
Se vs S/D	ns	ns	ns	ns

H.3. Discussion

H.3.1. Comparisons between 2D/Doppler echocardiographic variables

The strong association found between peak mitral inflow and PVF velocities in both groups of cats is in agreement with Doppler echocardiographic findings in normal and affected humans. Several studies in humans have demonstrated the close correlation between the mitral E and the diastolic pulmonary wave and also between the A wave of mitral inflow and the S wave of PVF (Kuecherer *et al*, 1990; Nishimura *et al*, 1990; Appleton *et al*, 1993). These strong associations determine the strong negative association found between the E/A of mitral inflow and the S/D ratio of PVF (Rossvoll and Hatle, 1993; Ito *et al*, 1996; Oki *et al*, 1996). The association between the E/A ratio of mitral inflow and the S/D of PVF was particularly strong in the affected group of HCM cats. This finding further emphasises that PVF indices can be used as alternatives in the quantification of LV diastolic properties in cats, capable in unmasking pseudonormal mitral inflow patterns in the diseased state and overcoming the limitations caused by the high heart rates, often encountered in this species (summation effects), in the assessment of mitral inflow.

The relative strong positive association found between the LA FS% and the S wave and particularly with the S/D ratio of PVF in HCM cats, supports the concept that a slight elevation in LV filling pressures at the early stages of the diseased state lead to increased atrial contractility (increased mitral A and Ar wave), and therefore enhanced relaxation during systole (S wave of PVF). As LV filling pressures increase further, left atrial contractility and compliance decrease, and the S/D ratio of PVF shows a gradual reduction. The inverse association between LA area during

systole and diastole and the S wave, as well with the S/D ratio of PFV in affected cats, mainly reflects the fact that LA distension (loss of contractility and reduced compliance) at the end stages of the disease, leads to decreased systolic PVF velocities. The compensatory elevated diastolic PVF velocities at this stage contribute further to the decreased S/D ratio.

H.3.2. Comparisons between pulsed TDI indices and 2D/Doppler echocardiographic variables

The E'/A' in all four myocardial segments showed a significant positive correlation with the E/A ratio of mitral inflow in the normal group. This is in agreement with findings from studies in normal humans. In the affected group, the E'/A' was associated strongly with the E/A of mitral inflow only in the septal mitral annulus. This finding may provide evidence for the load independence of the E'/A' in the diseased state, and may also indicate that the septal mitral annulus is load sensitive in affected cats. However, safe conclusions about the significance and actual meaning of the association between the E'/A' and the E/A of mitral inflow in HCM cats, can not be extrapolated, since not all affected animals provided separate E and A mitral inflow or myocardial waves.

The positive association found between A' and the A wave of mitral inflow in normal animals, shows that myocardial A' wave results from atrial contraction. However, no correlation was found for A' and A of mitral inflow in the affected group. An interesting finding was that the A' wave in both annular sites in the affected group, not only correlated positively with the Smax of the PVF, but showed

a similar association with LA FS% and also with LA area during diastole and systole, as the Smax. This observation is supportive of the close association between the contractile properties (A' annular wave) and compliance (Smax of PVF) of the LA, and suggest that these two indices could be used interchangeably in the assessment of LA function.

The early systolic myocardial wave (Se') in the lateral mitral annulus, in the LVPW along the radial axis and partially in the septal mitral annulus of affected cats, exhibited the same associations with LA FS% and also the LA area during diastole and systole, as had the Smax of the PVF and the A' annular wave. This finding is probably suggestive of a gradual decline in the systolic performance of the LV in HCM cats during the course of the disease.

The E'/A' ratio appeared to be inversely related to the S/D ratio of PVF in some myocardial segments of both normal and affected cats, suggesting that impaired LV diastolic properties result in increased S/D of PVF, at least at the early stages of the disease process.

H.3.3. Comparisons between colour M-mode TDI indices and 2D/Doppler echocardiographic variables

The positive association found between E1 and E2 of the MVG with the FPV in normal animals may reflect the significance of MVG in the genesis of the intraventricular pressure gradient, which under normal circumstances results in the blood flow propagation within the LV during early diastole. The strong, inverse

association found between the E1 of the MVG and the FPV in affected cats is difficult to interpret. Similarly, the inverse association between the E1 of the MVG and the peak aortic velocity in HCM cats was unexpected. However, the statistical power for the two latter correlations was weak and the above relationships need be interpreted cautiously. The inverse association between E2 of the MVG and Smax and also the S/D of PVF in normal cats was expected, since these variables were influenced inversely and positively, respectively, by ageing. A similar explanation can be given for the inverse association found between the Se of the MMV and Smax of PVF in normal cats. The associations found between the peak A of the MVG and the 2-dimensional LA indices reconfirm the concept that late diastolic myocardial motion is determined by LA contraction. Loss of LA contractility expressed with decreased LA FS% and increased LA area, results in decreased myocardial response during late diastole (reduced A wave of mitral inflow or of MVG and MMV).

H.4. Limitations

The above comparisons are limited by the fact that the 2D/Doppler echocardiographic and TDI data were not acquired sequentially or with the same echocardiographic machine. This means that acquisition of the two sets of data was not done under the same conditions or in the same environment, particularly, given the inherent highly variable heart rate of cats. Comparisons between time intervals from the two sets of data were not performed, not only, because of the influence of heart rate variability on these indices, but also, because of the different rates of acquisition of data by the two systems used. This latter factor may result in significant differences in the duration of time intervals, especially those small magnitude intervals encountered normally in cats. However, the variables correlated

in this section were derived from the same animals and obtained the same day, making it more likely that the above results are genuine.

Several Doppler echocardiographic measurements were obtained in this study from both normal and HCM cats. There was no significant difference in LV FS% between normal and HCM cats, although affected cats tended to have higher FS%. Apart from the E deceleration time of mitral inflow, which was prolonged in the affected group, neither the E/A of mitral inflow nor the IVRT were different between the two groups. Despite the technical difficulties in acquiring Doppler measurements of PVF, its quantification was possible in a high proportion of animals used in this study. Asymptomatic affected cats had a higher S wave and S/D ratio and a lower D wave of PVF than normal cats. Pulmonary venous flow measurements can be used as alternative to mitral inflow measurements for the quantification of LV diastolic function in cats, without being affected from summation effects induced by high heart rates, and may be useful in unmasking pseudonormal mitral inflow patterns.

Our study describes the physiologic asynchrony and heterogeneous motion of the different myocardial segments in the LV of normal cats. Myocardial expansion during early diastole was more prominent along the longitudinal axis than along the radial axis. The posterior side of the heart along the longitudinal axis showed signs of earlier activation during early diastole and also higher compliance in comparison to the septal side along the same axis. During systole, motion of the different myocardial segments of the LV was more uniform. The tricuspid annulus exhibited higher velocities during all cardiac phases of the cardiac cycle, indicating the higher

contractile state and compliance of the right ventricle compared to the LV. Age was found to affect inversely, mainly, the diastolic LV properties of healthy cats and it should be always considered as an influencing factor of myocardial velocities. The results of the current study are in agreement with findings from previous TDI studies in humans and cats with HCM, which showed that diastolic dysfunction is represented with decreased early diastolic myocardial velocities and deceleration, prolonged IVRt and increased E'/A' ratio (Gavaghan *et al*, 1999; Oki *et al*, 2000; Cardim *et al*, 2002a). The physiologic time and space nonuniformity of myocardial motion in the LV of normal cats was lost in affected animals. Interestingly, some changes noted in a number of TDI indices are indicative of systolic impairment in feline HCM. These changes were accompanied by normal FS%, suggesting that TDI is a more accurate means of quantifying true myocardial properties compared with conventional echocardiographic approaches. The systolic impairment, as expressed by the decrease found in some systolic pulsed TDI indices, was not of the magnitude seen in some humans or experimental animals with HCM. However, this finding does not rule out the possibility that primary systolic dysfunction of the individual myocardial cells may play an important role in the pathogenesis and the morphological manifestation of HCM in cats. Although diastolic changes in TDI indices were more prominent than those documented during systole, there is strong evidence to support the idea that cats with an end-stage disease demonstrate a significant reduction in myocardial contractile performance. Application of the TDI technique in a higher number of affected cats with CHF is needed to support this hypothesis.

This study describes, for the first time, the successful application of colour M-mode TDI and measurement of MVG in cats. Based on the very high temporal resolution of this particular application of TDI, we identified interesting physiological aspects of myocardial movement in cats. Our results describe these features, including the biphasic motion during early diastole and the isovolumic periods. MVG showed cyclic variation in the LVPW of cats, consistent with wall thickness changes as described by the nRCWT. The fact that MVG is the slope of the linear representation of myocardial velocity estimates throughout the myocardium, from endocardium to epicardium, renders this novel echocardiographic technique as a more accurate means in quantifying regional myocardial functional and structural properties. In contrast to MMV, the MVG was significantly decreased in the LVPW of affected cats, indicating that its independence from the overall heart motion makes it a superior tool for quantifying myocardial motion compared to TDI velocities. Although the latter may be of value for myocardial quantification, caution is needed in their interpretation. MVG was found to be decreased during diastole and systole in affected cats, providing additional evidence for both diastolic and systolic impairment in feline HCM. MVG may prove to be a very useful tool in the investigation and better classification of feline cardiac diseases, especially those with equivocal characteristics. Given the very small size of the feline heart and the inherent high heart rates of this species, the measurement of MVG in the LVPW of cats provides evidence for the successful application of this variable in the myocardium of human neonatal hearts and in experimental animal models.

References

Abchee, A. and Marian, A. J. Prognostic significance of beta-myosin heavy chain mutations is reflective of their hypertrophic expressivity in patients with hypertrophic cardiomyopathy (1997) *J Investig Med,* **45,** 191-196.

Abdalla, I., Murray, R., Lee, J., Stewart, W., Tajik, A. and Klein, A. Duration of Pulmonary Venous Atrial Reversal Flow Velocity and Mitral Inflow A Wave: New Measure of Severity of Cardiac Amyloidosis (1998) *Journal of the American Society of Echocardiography,* **11,** 1125-1133.

Abe, M., Oki, T., Tabata, T., Yamada, H., Onose, Y., Matsuoka, M., Mishiro, Y., Wakatsuki, T. and Ito, S. Evaluation of the hemodynamic relationship between the left atrium and left ventricle during atrial systole by pulsed tissue Doppler imaging in patients with left heart failure (1999) *Jpn Circ J,* **63,** 763-769.

Alam, M., Wardell, J., Andersson, E., Samad, B. A. and Nordlander, R. Characteristics of mitral and tricuspid annular velocities determined by pulsed wave Doppler tissue imaging in healthy subjects (1999) *J Am Soc Echocardiogr,* **12,** 618-628.

Allworth, M. S., Church, D. B., Maddison, J. E., Einstein, R., Brennan, P., Abdul Hussein, N. and Matthews, R. Effect of enalapril in dogs with pacing-induced heart failure (1995) *Am J Vet Res,* **56,** 85-94.

Altieri, P. I., Wilt, S. M. and Leighton, R. F. Left ventricular wall motion during the isovolumic relaxation period (1973) *Circulation,* **48,** 499-505.

Amberger, C. N., Glardon, O., Glaus, T., Hörauf, A., King, J. N., Schmidli, H., Schröter, L. and Lombard, C. W. Effects of benazepril in the treatment of feline hypertrophic cardiomyopathy. Results of a prospective, open-label, multicenter clinical trial (1999) *Journal of Veterinary Cardiology,* **1,** 19-26.

Appleton, C. P. Influence of incremental changes in heart rate on mitral flow velocity: assessment in lightly sedated, conscious dogs (1991) *J Am Coll Cardiol,* **17,** 227-236.

Appleton, C. P., Galloway, J. M., Gonzalez, M. S., Gaballa, M. and Basnight, M. A. Estimation of left ventricular filling pressures using two-dimensional and Doppler echocardiography in adult patients with cardiac disease. Additional value of analyzing left atrial size, left atrial ejection fraction and the difference in duration of pulmonary venous and mitral flow velocity at atrial contraction (1993) *J Am Coll Cardiol,* **22,** 1972-1982.

Appleton, C. P., Hatle, L. K. and Popp, R. L. Relation of transmitral flow velocity patterns to left ventricular diastolic function: new insights from a combined hemodynamic and Doppler echocardiographic study (1988) *J Am Coll Cardiol,* **12,** 426-440.

Atkins, C. E., Gallo, A. M., Kurzman, I. D. and Cowen, P. Risk factors, clinical signs, and survival in cats with a clinical diagnosis of idiopathic hypertrophic cardiomyopathy: 74 cases (1985-1989) (1992a) *J Am Vet Med Assoc,* **201,** 613-618.

Atkins, C. E. and Snyder, P. S. Systolic time intervals and their derivatives for evaluation of cardiac function (1992b) *J Vet Intern Med,* **6,** 55-63.

Baty, C. J., Malarkey, D. E., Atkins, C. E., DeFrancesco, T. C., Sidley, J. and Keene, B. W. Natural history of hypertrophic cardiomyopathy and aortic thromboembolism in a family of domestic shorthair cats (2001) *J Vet Intern Med,* **15,** 595-599.

Beder, S. D., Gutgesell, H. P., Mullins, C. E. and McNamara, D. G. Progression from hypertrophic obstructive cardiomyopathy to congestive cardiomyopathy in a child (1982) *Am Heart J,* **104,** 156-156.

Bland, J. M. and Altman, D. G. Statistical methods for assessing agreement between two methods of clinical measurement (1986) *Lancet,* **1,** 307-310.

Bonagura, J. D. (1994) In *The cat diseases and clinical management* (Ed, Sherding, R.) Churchill Livingstone, New York, pp. 819-946.

Bonagura, J. D., Stepien, R. L. and Lehmkuhl, L. B. Acute effects of esmolol on left ventricular outflow obstruction in cats with hypertrophic cardiomyopathy: a Doppler echocardiographic study (1991) *J Vet Intern Med,* **5,** 123.

Bond, B. R., Fox, P. R., Peterson, M. E. and Skavaril, R. V. Echocardiographic findings in 103 cats with hyperthyroidism (1988) *J Am Vet Med Assoc,* **192,** 1546-1549.

Bonow, R. O., Vitale, D. F., Marron, B. J., Bacharach, S. L., Frederick, T. M. and Green, M. V. Regional left ventricular asynchrony and impaired global left ventricular filling in hypertrophic cardiomyopathy: effect of verapamil (1987) *J Am Coll Cardiol,* **9,** 1108-1116.

Bright, J. M., Golden, A. L. and Daniel, G. B. Feline hypertrophic cardiomyopathy: Variations on a theme (1992) *J Small An Pr,* **33,** 266-274.

Bright, J. M., Golden, A. L., Gompf, R. E., Walker, M. A. and Toal, R. L. Evaluation of the calcium channel-blocking agents diltiazem and verapamil for treatment of feline hypertrophic cardiomyopathy (1991) *J Vet Intern Med,* **5,** 272-282.

Bright, J. M., Herrtage, M. E. and Schneider, J. F. Pulsed Doppler assessment of left ventricular diastolic function in normal and cardiomyopathic cats (1999) *J Am Anim Hosp Assoc,* **35,** 285-291.

Bruch, C., Herrmann, B., Schmermund, A., Bartel, T., Mann, K. and Erbel, R. Impact of disease activity on left ventricular performance in patients with acromegaly (2002) *Am Heart J,* **144,** 538-543.

Brugada, R., Kelsey, W., Lechin, M., Zhao, G., Yu, Q. T., Zoghbi, W., Quinones, M. A., Elstein, E., Omran, A., Rakowski, H., Wigle, D., Liew, C. C., Sole, M., Roberts, R. and Marian, A. J. Role of candidate modifier genes on the phenotypic expression of hypertrophy in patients with hypertrophic cardiomyopathy (1997) *J Investig Med,* **45,** 542-551.

Brun, P., Tribouilloy, C., Duval, A. M., Iserin, L., Meguira, A., Pelle, G. and Dubois-Rande, J. L. Left ventricular flow propagation during early filling is related to wall relaxation: a color M-mode Doppler analysis (1992) *J Am Coll Cardiol,* **20,** 420-432.

Brutsaert, D. L. Nonuniformity: a physiologic modulator of contraction and relaxation of the normal heart (1987) *J Am Coll Cardiol,* **9,** 341-348.

Bryg, R. J., Pearson, A. C., Williams, G. A. and Labovitz, A. J. Left ventricular systolic and diastolic flow abnormalities determined by Doppler echocardiography in obstructive hypertrophic cardiomyopathy (1987) *Am J Cardiol,* **59,** 925-931.

Camici, P., Chiriatti, G., Lorenzoni, R., Bellina, R. C., Gistri, R., Italiani, G., Parodi, O., Salvadori, P. A., Nista, N. and Papi, L. Coronary vasodilation is impaired in both hypertrophied and nonhypertrophied myocardium of patients with hypertrophic cardiomyopathy: a study with nitrogen-13 ammonia and positron emission tomography (1991) *J Am Coll Cardiol,* **17,** 879-886.

Cannon, R. O. I. I. I., Rosing, D. R., Maron, B. J., Leon, M. B., Bonow, R. O., Watson, R. M. and Epstein, S. E. Myocardial ischemia in patients with hypertrophic cardiomyopathy: contribution of inadequate vasodilator reserve and elevated left ventricular filling pressures (1985) *Circulation,* **71,** 234-243.

Cardim, N., Castela, S., Cordeiro, R., Longo, S., Ferreira, T., Pereira, A., Gouveia, A., Reis, R. P. and Correia, J. M. [Tissue Doppler imaging assessment of long axis left ventricular function in hypertrophic cardiomyopathy.] (2002a) *Rev Port Cardiol,* **21,** 953-985.

Cardim, N., Cordeiro, R., Correia, M. J., Gomes, E., Longo, S., Ferreira, T., Pereira, A., Gouveia, A., Reis, R. P. and Correia, J. M. Tissue Doppler imaging and long axis left ventricular function: hypertrophic cardiomyopathy versus athlete's heart (2002b) *Rev Port Cardiol,* **21,** 679-707.

Cardim, N., Perrot, A., Ferreira, T., Pereira, A., Osterziel, K. J., Palma Reis, R. and Martins Correia, J. F. Usefulness of Doppler myocardial imaging for identification of mutation carriers of familial hypertrophic cardiomyopathy (2002c) *The American Journal of Cardiology,* **90,** 128-132.

Cardim, N., Torres, D., Morais, H., Candido, A., Duarte, R., Longo, S., Ferreira, T., Pereira, A., Gouveia, A., Reis, R. P. and Correia, J. M. [Tissue Doppler imaging in hypertrophic cardiomyopathy: impact of intraventricular obstruction on longitudinal left ventricular function.] (2002d) *Rev Port Cardiol,* **21,** 271-297.

Carvalho, J. S., Silva, C. M., Shinebourne, E. A. and Redington, A. N. Prognostic value of posterior wall thickness in childhood dilated cardiomyopathy and myocarditis (1996) *Eur Heart J,* **17,** 1233-1238.

Castello, R., Pearson, A. C., Lenzen, P. and Labovitz, A. J. Evaluation of pulmonary venous flow by transesophageal echocardiography in subjects with a normal heart: comparison with transthoracic echocardiography (1991) *J Am Coll Cardiol,* **18,** 65-71.

Chetboul, V., Escriou, C., Blot, S., Tessier, D., Pouchelon, J. L., Litzler, P. Y. and Derumeaux, G. Early detection of myocardial dysfunction in a dog model of dilated cardiomyopathy by Tissue Doppler Imaging (2001) *Circulation,* **104,** II-351.

Choong, C. Y., Herrmann, H. C., Weyman, A. E. and Fifer, M. A. Preload dependence of Doppler-derived indexes of left ventricular diastolic function in humans (1987) *J Am Coll Cardiol,* **10,** 800-808.

Clayton, P. D., Bulawa, W. F., Klausner, S. C., Urie, P. M., Marshall, H. W. and Warner, H. R. The characteristic sequence for the onset of contraction in the normal human left ventricle (1979) *Circulation,* **59,** 671-679.

Courtois, M., Kovacs, S. J. and Ludbrook, P. A. Transmitral pressure-flow velocity relation. Importance of regional pressure gradients in the left ventricle during diastole (1988) *Circulation,* **78,** 661-671.

Criley, J. M. and Siegel, R. J. Has 'obstruction' hindered our understanding of hypertrophic cardiomyopathy? (1985) *Circulation,* **72,** 1148-1154.

Dagdelen, S., Eren, N., Karabulut, H., Akdemir, I., Ergelen, M., Saglam, M., Yuce, M., Alhan, C. and Caglar, N. Estimation of left ventricular end-diastolic pressure by color M-mode Doppler echocardiography and tissue Doppler imaging (2001) *Journal of the American Society of Echocardiography,* **14,** 951-958.

Dai, K. S., Chen, S. P., Yang, P. C., Liu, C. Y. and Mao, S. J. Ultrastructural alterations in pigs with naturally occurring hypertrophic cardiomyopathy (1996) *Br Vet J,* **152,** 333-338.

D'Andrea, A., Caso, P., Severino, S., Sarubbi, B., Forni, A., Cice, G., Esposito, N., Scherillo, M., Cotrufo, M. and Calabro, R. Different involvement of right ventricular myocardial function in either physiologic or pathologic left ventricular hypertrophy: A Doppler tissue study (2003) *J Am Soc Echocardiogr,* **16,** 154-161.

DeMaria, A. N., Wisenbaugh, T. W., Smith, M. D., Harrison, M. R. and Berk, M. R. Doppler echocardiographic evaluation of diastolic dysfunction (1991) *Circulation,* **84,** I288-I295.

Derumeaux, G., Loufoua, J., Pontier, G., Cribier, A. and Ovize, M. Tissue Doppler Imaging Differentiates Transmural From Nontransmural Acute Myocardial Infarction After Reperfusion Therapy (2001) *Circulation,* **103,** 589-596.

Dukes-McEwan, J., French, A. T. and Corcoran, B. M. Doppler echocardiography in the dog: measurement variability and reproducibility (2002) *Vet Radiol Ultrasound,* **43,** 144-152.

Dutka, D. P., Donnelly, J. E., Nihoyannopoulos, P., Oakley, C. M. and Nunez, D. J. Marked variation in the cardiomyopathy associated with Friedreich's ataxia (1999) *Heart,* **81,** 141-147.

Dutka, D. P., Donnelly, J. E., Palka, P., Lange, A., Nunez, D. J. and Nihoyannopoulos, P. Echocardiographic characterization of cardiomyopathy in Friedreich's ataxia with tissue Doppler echocardiographically derived myocardial velocity gradients (2000) *Circulation,* **102,** 1276-1282.

Duval-Moulin, A. M., Dupouy, P., Brun, P., Zhuang, F., Pelle, G., Perez, Y., Teiger, E., Castaigne, A., Gueret, P. and Dubois-Rande, J. L. Alteration of left ventricular diastolic function during coronary angioplasty-induced ischemia: a color M-mode Doppler study (1997) *J Am Coll Cardiol,* **29,** 1246-1255.

Edvardsen, T., Aakhus, S., Endresen, K., Bjomerheim, R., Smiseth, O. and Ihlen, H. Acute regional myocardial ischemia identified by 2-dimensional multiregion Doppler imaging tissue technique (2000) *Journal of the American Society of Echocardiography,* **13,** 986-994.

Ehring, T. and Heusch, G. Left ventricular asynchrony: an indicator of regional myocardial dysfunction (1990) *Am Heart J,* **120,** 1047-1057.

Epstein N. D., Cohn, G. M., Cyran, F., Fananapazir, L. Differences in clinical expression of hypertrophic cardiomyopathy associated with two distinct mutations in the beta-myosin heavy chain gene. A 908Leu----Val mutation and a 403Arg----Gln mutation (1992) *Circulation,* **86,** 345-352.

Fananapazir, L. and Epstein, N. D. Genotype-phenotype correlations in hypertrophic cardiomyopathy. Insights provided by comparisons of kindreds with distinct and identical beta-myosin heavy chain gene mutations (1994) *Circulation,* **89,** 22-32.

Fananapazir, L. and Epstein, N. D. Prevalence of Hypertrophic Cardiomyopathy and Limitations of Screening Methods (1995) *Circulation,* **92,** 700-704.

Farias, C. A., Rodriguez, L., Garcia, M. J., Sun, J. P., Klein, A. L. and Thomas, J. D. Assessment of diastolic function by tissue Doppler echocardiography: comparison with standard transmitral and pulmonary venous flow (1999) *J Am Soc Echocardiogr,* **12,** 609-617.

Firstenberg, M. S., Greenberg, N. L., Main, M. L., Drinko, J. K., Odabashian, J. A., Thomas, J. D. and Garcia, M. J. Determinants of diastolic myocardial tissue Doppler velocities: influences of relaxation and preload (2001) *J Appl Physiol,* **90,** 299-307.

Firstenberg, M. S., Levine, B. D., Garcia, M. J., Greenberg, N. L., Cardon, L., Morehead, A. J., Zuckerman, J. and Thomas, J. D. Relationship of echocardiographic indices to pulmonary capillary wedge pressures in healthy volunteers (2000) *Journal of the American College of Cardiology,* **36,** 1664-1669.

Fleming, A. D., McDicken, W. N., Sutherland, G. R. and Hoskins, P. R. Assessment of colour Doppler tissue imaging using test-phantom (1994a) *Ultrasound Med Biol,* **20,** 937-951.

Fleming, A. D., Xia, X., McDicken, W. N., Sutherland, G. R. and Fenn, L. Myocardial velocity gradients detected by Doppler imaging (1994b) *Br J Radiol,* **67,** 679-688.

Fox, P. R. (1998) In *Textbook of Canine and Feline Cardiology. Principles and clinical practice, 2n ed* (Eds, Fox, P. R., Sisson, D. and Moise, N. S.) WB Saunders, Philadelphia, pp. 621-678.

Fox, P. R., Liu, S. K. and Maron, B. J. Echocardiographic assessment of spontaneously occurring feline hypertrophic cardiomyopathy. An animal model of human disease (1995) *Circulation,* **92,** 2645-2651.

Fox, P. R., Maron, B. J., Basso, C., Liu, S. K. and Thiene, G. Spontaneously occurring arrhythmogenic right ventricular cardiomyopathy in the domestic cat: A new animal model similar to the human disease (2000) *Circulation,* **102,** 1863-1870.

Fujii, Y., Masuda, Y., Takashima, K., Ogasawara, J., Machida, N., Yamane, Y., Chimura, S., Awazu, T., Yamane, T. and Wakao, Y. Hypertrophic cardiomyopathy in two kittens. (2001) *J Vet Med Sci,* **63,** 583-585.

Fujiwara, H., Onodera, T., Tanaka, M., Shirane, H., Kato, H., Yoshikawa, J., Osakada, G., Sasayama, S. and Kawai, C. Progression from hypertrophic obstructive cardiomyopathy to typical dilated cardiomyopathy-like features in the end stage (1984) *Jpn Circ J,* **48,** 1210-1214.

Galderisi, M., Cicala, S., Sangiorgi, G., Caso, P. and de Divitiis, O. Tissue Doppler-derived postsystolic motion in a patient with left bundle branch block: a sign of myocardial wall asynchrony (2002) *Echocardiography,* **19,** 79-81.

Galderisi, M., Severino, S., Caso, P., Cicala, S., Petrocelli, A., De Simone, L., Mininni, N. and de Divitiis, O. Right ventricular myocardial diastolic dysfunction in different kinds of cardiac hypertrophy: analysis by pulsed Doppler tissue imaging (2001) *Ital Heart J,* **2,** 912-920.

Galiuto, L., Ignone, G. and DeMaria, A. N. Contraction and relaxation velocities of the normal left ventricle using pulsed-wave tissue Doppler echocardiography (1998) *Am J Cardiol,* **81,** 609-614.

Garcia, M. J., Ares, M. A., Asher, C., Rodriguez, L., Vandervoort, P. and Thomas, J. D. An index of early left ventricular filling that combined with pulsed Doppler peak E velocity may estimate capillary wedge pressure (1997) *J Am Coll Cardiol,* **29,** 448-454.

Garcia, M. J., Palac, R. T., Malenka, D. J., Terrell, P. and Plehn, J. F. Color M-mode Doppler flow propagation velocity is a relatively preload-independent index of left ventricular filling (1999) *J Am Soc Echocardiogr,* **12,** 129-137.

Garcia, M. J., Rodriguez, L., Ares, M., Griffin, B. P., Klein, A. L., Stewart, W. J. and Thomas, J. D. Myocardial wall velocity assessment by pulsed Doppler tissue imaging: characteristic findings in normal subjects (1996a) *Am Heart J,* **132,** 648-656.

Garcia, M. J., Rodriguez, L., Ares, M., Griffin, B. P., Thomas, J. D. and Klein, A. L. Differentiation of constrictive pericarditis from restrictive cardiomyopathy: assessment of left ventricular diastolic velocities in longitudinal axis by Doppler tissue imaging (1996b) *J Am Coll Cardiol,* **27,** 108-114.

Garcia, M. J., Smedira, N. G., Greenberg, N. L., Main, M., Firstenberg, M. S., Odabashian, J. and Thomas, J. D. Color M-mode Doppler flow propagation velocity is a preload insensitive index of left ventricular relaxation: animal and human validation (2000) *J Am Coll Cardiol,* **35,** 201-208.

Garcia, M. J., Thomas, J. D. and Klein, A. L. New Doppler echocardiographic applications for the study of diastolic function (1998) *J Am Coll Cardiol,* **32,** 865-875.

Gardin, J. M., Rohan, M. K. and Davidson, D. M. Doppler transmitral flow velocity parameters: relationship between age, body surface area, blood pressure and gender in normal subjects (1987) *Am J Noninvasive Cardiol,* **1,** 3-10.

Garot, J., Diebold, B., Derumeaux, G. A., Monin, J. L., Bosio, P., Duval-Moulin, A. M., Castaigne, A., Dubois-Rande, J. L. and Gueret, P. Comparison of regional myocardial velocities assessed by quantitative 2- dimensional and M-mode color Doppler tissue imaging: influence of the signal-to-noise ratio of color Doppler myocardial images on velocity estimators of the Doppler tissue imaging system (1998) *J Am Soc Echocardiogr,* **11,** 1093-1105.

Gavaghan, B. J., Kittleson, M. D., Fisher, K. J., Kass, P. H. and Gavaghan, M. A. Quantification of left ventricular diastolic wall motion by Doppler tissue imaging in healthy cats and cats with cardiomyopathy (1999) *Am J Vet Res,* **60,** 1478-1486.

Geisterfer-Lowrance, A. A., Christe, M., Conner, D. A., Ingwall, J. S., Schoen, F. J., Seidman, C. E. and Seidman, J. G. A mouse model of familial hypertrophic cardiomyopathy (1996) *Science,* **272,** 731-734.

Gentile, F., Mantero, A., Lippolis, A., Ornaghi, M., Azzollini, M., Barbier, P., Beretta, L., Casazza, F., Corno, R., Faletra, F., Giagnoni, E., Gualtierotti, C., Lombroso, S., Mattioli, R., Morabito, A., Pepi, M., Todd, S. and Pezzano, A. Pulmonary venous flow velocity patterns in 143 normal subjects aged 20 to 80 years old. An echo 2D colour Doppler cooperative study (1997) *Eur Heart J,* **18,** 148-164.

Ghostine, S., Carrion, C., Souza, L. C., Richard, P., Bruneval, P., Vilquin, J. T., Pouzet, B., Schwartz, K., Menasche, P. and Hagege, A. A. Long-term efficacy of myoblast transplantation on regional structure and function after myocardial infarction (2002) *Circulation,* **106,** I131-136.

Giannuzzi, P., Imparato, A., Temporelli, P. L., de-Vito, F., Silva, P. L., Scapellato, F. and A., G. Doppler-derived mitral deceleration time of early filling as a strong predictor of pulmonary capillary wedge pressure in postinfarction patients with left ventricular systolic dysfunction (1994) *J Am Coll Cardiol,* **23,** 1630-1637.

Gibson, D. G. and Brown, D. J. Assessment of left ventricular systolic function in man from simultaneous echocardiographic and pressure measurements (1976a) *Br Heart J,* **38,** 8-17.

Gibson, D. G., Doran, J. H., Traill, T. A. and Brown, D. J. Abnormal left ventricular wall movement during early systole in patients with angina pectoris (1978) *Br Heart J,* **40,** 758-766.

Gibson, D. G., Prewitt, T. A. and Brown, D. J. Analysis of left ventricular wall movement during isovolumic relaxation and its relation to coronary artery disease (1976b) *Br Heart J,* **38,** 1010-1019.

Golden, A. L. and Bright, J. M. Use of relaxation half-time as an index of ventricular relaxation in clinically normal cats and cats with hypertrophic cardiomyopathy (1990) *Am J Vet Res,* **51,** 1352-1356.

Gonzalez-Vilchez, F., Ares, M., Ayuela, J. and Alonso, L. Combined use of pulsed and color M-mode Doppler echocardiography for the estimation of pulmonary capillary wedge pressure: an empirical approach based on an analytical relation (1999) *J Am Coll Cardiol,* **34,** 515-523.

Goodwin, J. K., Lombard, C. W. and Ginex, D. D. Results of continuous ambulatory electrocardiography in a cat with hypertrophic cardiomyopathy (1992) *J Am Vet Med Assoc,* **200,** 1352-1354.

Gorcsan, J., Deswal, A., Mankad, S., Mandarino, W. A., Mahler, C. M., Yamazaki, N. and Katz, W. E. Quantification of the myocardial response to low-dose dobutamine using tissue Doppler echocardiographic measures of velocity and velocity gradient (1998) *Am J Cardiol,* **81,** 615-623.

Gorcsan, J., Gulati, V. K., Mandarino, W. A. and Katz, W. E. Color-coded measures of myocardial velocity throughout the cardiac cycle by tissue Doppler imaging to quantify regional left ventricular function (1996) *Am Heart J,* **131,** 1203-1213.

Greenbaum, R. A., Ho, S. Y., Gibson, D. G., Becker, A. E. and Anderson, R. H. Left ventricle fibre architecture in man (1981) *Br Heart J,* **45,** 248-258.

Grines, C. L., Bashore, T. M., Boudoulas, H., Olson, S., Shafer, P. and Wooley, C. F. Functional abnormalities in isolated left bundle branch block. The effect of interventricular asynchrony (1989) *Circulation,* **79,** 845-853.

Ha, J.-W., Oh, J. K., Ling, L. H., Nishimura, R. A., Seward, J. B. and Tajik, A. J. Annulus Paradoxus: Transmitral Flow Velocity to Mitral Annular Velocity Ratio Is Inversely Proportional to Pulmonary Capillary Wedge Pressure in Patients With Constrictive Pericarditis (2001) *Circulation,* **104,** 976-978.

Haggstrom, J., Hansson, K., Karlberg, B. E., Kvart, C. and Olsson, K. Plasma concentration of atrial natriuretic peptide in relation to severity of mitral regurgitation in Cavalier King Charles Spaniels (1994) *Am J Vet Res,* **55,** 698-703.

Hammermeister, K. E., Gibson, D.G, Hughes, D Regional variation in the timing and extent of left ventricular wall motion in normal subjects (1986) *British Heart Journal,* **56,** 226-235.

Harpster, N. K. (1986) In *Current Veterinary Therapy* (Ed, Kirk, R. W.) Saunders, Philadelphia, pp. 380-398.

Hawthorne, E. W. Instantaneous dimensional changes of the left ventricle in dogs (1961) *Circ Res,* **9,** 110-119.

Hawthorne, E. W. Symposium on measurements of left ventricular volume. Part III. Dynamic geometry of the left ventricle. (1966) *Am J Cardiol,* **18,** 566-573.

Heimdal, A., Stoylen, A., Torp, H. and Skjaerpe, T. Real-time strain rate imaging of the left ventricle by ultrasound (1998) *J Am Soc Echocardiogr,* **11,** 1013-1019.

Henein, M. Y., Rosano, G. M., Underwood, R., Poole-Wilson, P. A. and Gibson, D. G. Relations between resting ventricular long axis function, the electrocardiogram, and myocardial perfusion imaging in syndrome X (1994) *Br Heart J,* **71,** 541-547.

Hirota, Y., Kohriyama, T., Hayashi, T., Kaku, K., Nishimura, H., Saito, T., Nakayama, Y., Suwa, M., Kino, M. and Kawamura, K. Idiopathic restrictive cardiomyopathy: differences of left ventricular relaxation and diastolic wave forms from constrictive pericarditis (1983) *Am J Cardiol,* **52,** 421-423.

Ho, C. Y., Sweitzer, N. K., McDonough, B., Maron, B. J., Casey, S. A., Seidman, J. G., Seidman, C. E. and Solomon, S. D. Assessment of Diastolic Function With Doppler Tissue Imaging to Predict Genotype in Preclinical Hypertrophic Cardiomyopathy (2002) *Circulation,* **105,** 2992-2997.

Hofmann, T., Meinertz, T., Keck, A., van Ingen, G., Simic, O. and Ostermeyer, J. Simultaneous Measurement of Pulmonary Venous Flow by Intravascular Catheter Doppler Velocimetry and Transesophageal Doppler Echocardiography: Relation to Left Atrial Pressure and Left Atrial and Left Ventricular Function (1995) *Journal of the American College of Cardiology,* **26,** 239-249.

Hosokawa, H., Sheehan, F. H. and Suzuki, T. Measurement of postsystolic shortening to assess viability and predict recovery of left ventricular function after acute myocardial infarction (2000) *Journal of the American College of Cardiology,* **35,** 1842-1849.

Huang, S. Y., Tsou, H. L., Chiu, Y. T., Shyu, J. J., Wu, J. J., Lin, J. H. and Liu, S. K. Heritability estimate of hypertrophic cardiomyopathy in pigs (Sus scrofa domestica) (1996) *Lab Anim Sci,* **46,** 310-314.

Ishida, Y., Meisner, J. S., Tsujioka, K., Gallo, J. I., Yoran, C., Frater, R. W. and Yellin, E. L. Left ventricular filling dynamics: influence of left ventricular relaxation and left atrial pressure (1986) *Circulation,* **74,** 187-196.

Ito, T., Suwa, M., Hirota, Y., Otake, Y., Moriguchi, A. and Kawamura, K. Influence of left atrial function on Doppler transmitral and pulmonary venous flow patterns in dilated and hypertrophic cardiomyopathy: evaluation of left atrial appendage function by transesophageal echocardiography (1996) *Am Heart J,* **131,** 122-130.

Iwakami, M. and Numano, F. Regional wall motion abnormalities during early diastole in patients with hypertensive left ventricular hypertrophy: a Doppler tissue echocardiographic study (2001) *J Med Dent Sci,* **48,** 45-49.

Iwasaki, Y., Satomi, G. and Yasukochi, S. Analysis of ventricular septal motion by doppler tissue imaging in atrial septal defect and normal heart (1999) *Am J Cardiol,* **83,** 206-210.

Izumi, C., Iga, K., Himura, Y., Gen, H. and Konish, i. T. Influence of gravity on pulmonary venous flow velocity patterns: analysis of left and right pulmonary venous flow velocities in left and right decubitus positions (1999) *Am Heart J,* **137,** 419-426.

Jacobs, G. and Knight, D. H. M-mode echocardiographic measurements in nonanesthetized healthy cats: effects of body weight, heart rate, and other variables (1985) *Am J Vet Res,* **46,** 1705-1711.

Jacobs, L. E., Kotler, M. N. and Parry, W. R. Flow patterns in dilated cardiomyopathy: a pulsed-wave and color flow Doppler study (1990) *J Am Soc Echocardiogr,* **3,** 294-302.

Jamal, F., Kukulski, T., D'hooge, J., De Scheerder, I. and Sutherland, G. Abnormal Postsystolic Thickening in Acutely Ischemic Myocardium During Coronary Angioplasty: A Velocity, Strain, and Strain Rate Doppler Myocardial Imaging Study (1999) *Journal of the American Society of Echocardiography,* **12,** 994-996.

Jones, C. J. H., Raposo, L. and Gibson, D. G. Functional importance of the long axis dynamics of the human left ventricle (1990) *Br Heart J,* **63,** 215-220.

Kanemoto, N., Takigawa, O., Morimoto, K., Oguma, T., Nakayama, K., Yoshioka, K. and Handa, S. [Identical male twins showing progression from hypertrophic cardiomyopathy to dilated cardiomyopathy-like features] (1995) *J Cardiol,* **26,** 249-257.

Keren, G., Bier, A., Sherez, J., Miura, D., Keefe, D. and LeJemtel, T. Atrial contraction is an important determinant of pulmonary venous flow (1986) *J Am Coll Cardiol,* **7,** 693-695.

Keren, G., Pardes, A., Eschar, Y., Hansch, E., Scherez, J. and Laniado, S. Left ventricular filling dynamics by Doppler echocardiography in dilated cardiomyopathy: one-year follow-up in patients treated with captopril compared to placebo (1992) *Cardiology,* **81,** 196-206.

Khuller, S. and Lewis, R. Usefulness of systolic time intervals in the differential diagnosis of constrictive pericarditis and restrictive cardiomyopathy (1976) *Br Heart J,* **38**.

Kim, Y.-J. and Sohn, D.-W. Mitral annulus velocity in the estimation of left ventricular filling pressure: Prospective study in 200 patients (2000) *Journal of the American Society of Echocardiography,* **13,** 980-985.

Kittleson, M. D. (1999) *Small Animal Cardiovascular Medicine,* Mosby, St.Louis.

Kittleson, M. D., Meurs, K. M., Munro, M. J., Kittleson, J. A., Liu, S. K., Pion, P. D. and Towbin, J. A. Familial hypertrophic cardiomyopathy in maine coon cats: an animal model of human disease (1999) *Circulation,* **99,** 3172-3180.

Kizilbash, A. M., Heinle, S. K. and Grayburn, P. A. Spontaneous Variability of Left Ventricular Outflow Tract Gradient in Hypertrophic Obstructive Cardiomyopathy (1998) *Circulation,* **97,** 461-466.

Klein, A., Abdalla, I., Murray, R., Lee, J., Vandervoort, P., Thomas, J., Appleton, C. and Tajik, A. Age Independence of the Difference in Duration of Pulmonary Venous Atrial Reversal Flow and Transmitral A-Wave Flow in Normal Subjects (1998) *Journal of the American Society of Echocardiography,* **11,** 458-465.

Klein, A. L. and Tajik, A. J. Doppler assessment of pulmonary venous flow in healthy subjects and in patients with heart disease (1991) *J Am Soc Echocardiogr,* **4,** 379-392.

Klues, H., Roberts, W. C. and Maron, B. J. Morphological determinants of echocardiographic patterns of mitral valve systolic anterior motion in obstructive hypertrophic cardiomyopathy (1993) *Circulation,* **87,** 1570-1579.

Klues, H. G., Schiffers, A. and Maron, B. J. Phenotypic spectrum and patterns of left ventricular hypertrophy in hypertrophic cardiomyopathy: morphologic observations and significance as assessed by two-dimensional echocardiography in 600 patients (1995) *J Am Coll Cardiol,* **26,** 1699-1708.

Koffas, H., Dukes-McEwan, J., Corcoran, B. M., Moran, C. M., French, A., Sboros, V., Anderson, T., Smith, P., Simpson, K. and McDicken, W. N. Peak mean myocardial velocities and velocity gradients measured by color M-mode Tissue Doppler Imaging in the left ventricular free wall of healthy cats (2003) *J Vet Intern Med,* **17,** 125-139. (in press).

Kondo, I., Mizushige, K., Nozaki, S., Iwado, Y., Masugata, H., Kohno, M. and Matsuo, H. Effect of cibenzoline, a class ia antiarrhythmic agent, on left ventricular diastolic function in hypertrophic cardiomyopathy (2001) *Cardiovasc Drugs Ther,* **15,** 459-465.

Koyama, J., Ray-Sequin, P. A., Davidoff, R. and Falk, R. H. Usefulness of pulsed tissue Doppler imaging for evaluating systolic and diastolic left ventricular function in patients with AL (primary) amyloidosis (2002) *Am J Cardiol,* **89,** 1067-1071.

Kraus, M. S., Calvert, C. A. and Jacobs, G. J. Hypertrophic cardiomyopathy in a litter of five mixed-breed cats (1999) *J Am Anim Hosp Assoc,* **35,** 293-296.

Kuecherer, H. F., Kee, L. L., Modin, G., Cheitlin, M. D. and Schiller, N. B. Echocardiography in serial evaluation of left ventricular systolic and diastolic function: importance of image acquisition, quantitation, and physiologic variability in clinical and investigational applications (1991) *J Am Soc Echocardiogr,* **4,** 203-214.

Kuecherer, H. F., Muhiudeen, I. A., Kusumoto, F. M., Lee, E., Moulinier, L. E., Cahalan, M. K. and Schiller, N. B. Estimation of mean left atrial pressure from transesophageal pulsed Doppler echocardiography of pulmonary venous flow (1990) *Circulation,* **82,** 1127-1139.

Kuo, L. C., Quinones, M. A., Rokey, R., Sartori, M., Abinader, E. G. and Zoghbi, W. A. Quantification of atrial contribution to left ventricular filling by pulsed Doppler echocardiography and the effect of age in normal and diseased hearts (1987) *Am J Cardiol,* **59,** 1174-1178.

Kvitting, J.-P., Wigstrom, L., Strotmann, J. and Sutherland, G. How Accurate Is Visual Assessment of Synchronicity in Myocardial Motion? An In Vitro Study with Computer-Simulated Regional Delay in Myocardial Motion: Clinical Implications for Rest and Stress Echocardiography Studies (1999) *Journal of the American Society of Echocardiography,* **12,** 698-705.

Lakatta, E. G., Gerstenblith, G., Angell, C.S, Shock, N.W., Weisfeldt, M.L., Prolonged contraction duration in aged myocardium (1975) *The Journal of Clinical Investigation,* **55,** 61-68.

Lavine, S. J. and Arends, D. Importance of the left ventricular filling pressure on diastolic filling in idiopathic dilated cardiomyopathy (1989) *Am J Cardiol,* **64,** 61-65.

Lee, C. H., Hogan, J. C. and Gibson, D. G. Diastolic disease in left ventricular hypertrophy: comparison of M mode and Doppler echocardiography for the assessment of rapid ventricular filling (1991) *Br Heart J,* **65,** 194-200.

Levine, R. A., Vlahakes, G. J., Lefebvre, X., Guerrero, J. L., Cape, E. G., Yoganathan, A. P. and Weyman, A. E. Papillary Muscle Displacement Causes Systolic Anterior Motion of the Mitral Valve : Experimental Validation and Insights Into the Mechanism of Subaortic Obstruction (1995) *Circulation,* **91,** 1189-1195.

Lew, W. Y. W. and Lewinter, M. M. Regional circumferential lengthening patterns in canine left ventricle (1983) *Am J Physiol,* **245,** H741-H748.

Lewis, B. S. Doppler diastolic transmitral ventricular filling patterns--towards a better understanding (1996) *Eur Heart J,* **17,** 493-495.

Lewis, J. F. and Maron, B. J. Hypertrophic cardiomyopathy characterized by marked hypertrophy of the posterior left ventricular free wall: significance and clinical implications (1991) *J Am Coll Cardiol,* **18,** 421-428.

Li, G., Borger, M., Williams, W., Weisel, R., Mickle, D., Wigle, E. and Li, R.-K. Regional overexpression of insulin-like growth factor-I and transforming growth factor-[beta]1 in the myocardium of patients with hypertrophic obstructive cardiomyopathy (2002) *Journal of Thoracic and Cardiovascular Surgery,* **123,** 89-95.

Li, R.-K., Li, G., Mickle, D. A. G., Weisel, R. D., Merante, F., Luss, H., Rao, V., Christakis, G. T. and Williams, W. G. Overexpression of Transforming Growth Factor-ß1 and Insulin-Like Growth Factor-I in Patients With Idiopathic Hypertrophic Cardiomyopathy (1997) *Circulation,* **96,** 874-881.

Litten, R. Z., Martin, B. J., Buchthal, R. H., Nagai, R., Low, R. B. and Alpert, N. R. Heterogeneity of myosin isozyme content of rabbit heart (1985) *Circ Res,* **57,** 406-414.

Liu, S. K. and Fox, P. R. (1995) In *Kirk's Current veterinary therapy*, Vol. XI (Eds, Kirk, R. W. and Bonagura, J. D.) Saunders, W.B, Philadelphia ; London, pp. 791-794.

Liu, S. K., Maron, B. J. and Tilley, L. P. Feline hypertrophic cardiomyopathy: gross anatomic and quantitative histologic features (1981) *Am J Pathol,* **102,** 388-395.

Liu, S. K., Roberts, W. C. and Maron, B. J. Comparison of morphologic findings in spontaneously occurring hypertrophic cardiomyopathy in humans, cats and dogs (1993) *Am J Cardiol,* **72,** 944-951.

Liu, S. K. and Tilley, L. P. Animal models of primary myocardial diseases (1980) *Yale J Biol Med,* **53,** 191-211.

Lord, P. F., Wood, A., Tilley, L. P. and Liu, S. K. Radiographic and hemodynamic evaluation of cardiomyopathy and thromboembolism in the cat (1974) *J Am Vet Med Assoc,* **164,** 154-165.

Louie, E. K. and Maron, B. J. Hypertrophic cardiomyopathy with extreme increase in left ventricular wall thickness: functional and morphologic features and clinical significance (1986) *J Am Coll Cardiol,* **8,** 57-65.

Luis Fuentes, V. Feline heart disease: an update (1992) *J Small Anim Pract,* **33,** 130-137.

Marcos-Alberca, P., Garcia-Fernandez, M. A., Ledesma, M. J., Malpica, N., Santos, A., Moreno, M., Bermejo, J., Antoranz, J. C. and Desco, M. Intramyocardial analysis of regional systolic and diastolic function in ischemic heart disease with Doppler tissue imaging: role of the different myocardial layers (2002) *J Am Soc Echocardiogr,* **15,** 99-108.

Marian, A. J. Pathogenesis of diverse clinical and pathological phenotypes in hypertrophic cardiomyopathy (2000) *The Lancet,* **355,** 58-61.

Marian, A. J. and Roberts, R. Recent Advances in the Molecular Genetics of Hypertrophic Cardiomyopathy (1995a) *Circulation,* **92,** 1336-1347.

Marian, A. J. and Roberts, R. The Molecular Genetic Basis for Hypertrophic Cardiomyopathy (2001) *Journal of Molecular and Cellular Cardiology,* **33,** 655-670.

Marian, A. J., Wu, Y., Lim, D.-S., McCluggage, M., Youker, K., Yu, Q.-t., Brugada, R., DeMayo, F., Quinones, M. and Roberts, R. A transgenic rabbit model for human hypertrophic cardiomyopathy (1999) *J. Clin. Invest.,* **104,** 1683-1692.

Marian, A. J., Yu, Q.-T., Mann, D. L., Graham, F. L. and Roberts, R. Expression of a Mutation Causing Hypertrophic Cardiomyopathy Disrupts Sarcomere Assembly in Adult Feline Cardiac Myocytes (1995b) *Circ Res,* **77,** 98-106.

Marian, A. J., Zhao, G., Seta, Y., Roberts, R. and Yu, Q.-t. Expression of a Mutant (Arg92Gln) Human Cardiac Troponin T, Known to Cause Hypertrophic Cardiomyopathy, Impairs Adult Cardiac Myocyte Contractility (1997) *Circ Res,* **81,** 76-85.

Maron, B. J., Bonow, R. O., Cannon, R. O., 3rd, Leon, M. B. and Epstein, S. E. Hypertrophic cardiomyopathy. Interrelations of clinical manifestations, pathophysiology, and therapy (1) (1987) *N Engl J Med,* **316,** 780-789.

Maron, B. J., Bonow, R. O., Seshagiri, T. N., Roberts, W. C. and Epstein, S. E. Hypertrophic cardiomyopathy with ventricular septal hypertrophy localized to the apical region of the left ventricle (apical hypertrophic cardiomyopathy) (1982) *Am J Cardiol,* **49,** 1838-1848.

Maron, B. J. and Epstein, S. E. Hypertrophic cardiomyopathy. Recent observations regarding the specificity of three hallmarks of the disease: asymmetric septal hypertrophy, septal disorganization and systolic anterior motion of the anterior mitral leaflet (1980) *Am J Cardiol,* **45,** 141-154.

Maron, B. J. and Epstein, S. E. Clinical significance and therapeutic implications of the left ventricular outflow tract pressure gradient in hypertrophic cardiomyopathy (1986a) *Am J Cardiol,* **58,** 1093-1096.

Maron, B. J., Epstein, S. E. and Roberts, W. C. Hypertrophic cardiomyopathy and transmural myocardial infarction without significant atherosclerosis of the extramural coronary arteries (1979a) *Am J Cardiol,* **43,** 1086-1102.

Maron, B. J., Gardin, J. M., Flack, J. M., Gidding, S. S., Kurosaki, T. T. and Bild, D. E. Prevalence of Hypertrophic Cardiomyopathy in a General Population of Young Adults : Echocardiographic Analysis of 4111 Subjects in the CARDIA Study (1995) *Circulation,* **92,** 785-789.

Maron, B. J., Gottdiener, J. S. and Epstein, S. E. Patterns and significance of distribution of left ventricular hypertrophy in hypertrophic cardiomyopathy. A wide angle, two dimensional echocardiographic study of 125 patients (1981a) *Am J Cardiol,* **48,** 418-428.

Maron, B. J., Kragel, A. H. and Roberts, W. C. Sudden death in hypertrophic cardiomyopathy with normal left ventricular mass (1990) *Br Heart J,* **63,** 308-310.

Maron, B. J. and Roberts, W. C. Quantitative analysis of cardiac muscle cell disorganization in the ventricular septum of patients with hypertrophic cardiomyopathy (1979b) *Circulation,* **59,** 689-706.

Maron, B. J. and Roberts, W. C. Hypertrophic cardiomyopathy and cardiac muscle cell disorganization revisited: relation between the two and significance (1981b) *Am Heart J,* **102,** 95-110.

Maron, B. J., Wolfson, J. K., Epstein, S. E. and Roberts, W. C. Intramural ("small vessel") coronary artery disease in hypertrophic cardiomyopathy (1986b) *J Am Coll Cardiol,* **8,** 545-557.

Martin, L., VandeWoude, S., Boon, J. and Brown, D. Left ventricular hypertrophy in a closed colony of Persian cats (1994) *J Vet Intern Med,* **8,** 143.

Matsuda, Y., Toma, Y., Matsuzaki, M., Moritani, K., Satoh, A., Shiomi, K., Ohtani, N., Kohno, M., Fujii, T. and Katayama, K. Change of left atrial systolic pressure waveform in relation to left ventricular end-diastolic pressure (1990) *Circulation,* **82,** 1659-1667.

Matsumura, Y., Elliott, P. M., Virdee, M. S., Sorajja, P., Doi, Y. and McKenna, W. J. Left ventricular diastolic function assessed using Doppler tissue imaging in patients with hypertrophic cardiomyopathy: relation to symptoms and exercise capacity (2002) *Heart,* **87,** 247-251.

McDicken, W. N., Sutherland, G. R., Moran, C. M. and Gordon, L. N. Colour Doppler velocity imaging of the myocardium (1992) *Ultrasound Med Biol,* **18,** 651-654.

McKenna, W. J., Stewart, J. T., Nihoyannopoulos, P., McGinty, F. and Davies, M. J. Hypertrophic cardiomyopathy without hypertrophy: two families with myocardial disarray in the absence of increased myocardial mass (1990) *Br Heart J,* **63,** 287-290.

McLaughlin, R. F., Tyler, W. S. and Canada, R. O. A study of the subgross pulmonary anatomy in various mammals (1961) *Am J Anat,* **108,** 149.

Medinger, T. L. and Bruyette, D. S. Feline hypertrophic cardiomyopathy (1992) *The Compendium North American Edition-Small Animal,* **14,** 479-492.

Mego, D. M., DeGeare, V. S., Nottestad, S. Y., Lamanna, V. P., Oneschuk, L. C., Rubal, B. J. and Zabalgoitia, M. Variation of flow propagation velocity with age. (1998) *J Am Soc Echocardiogr,* **11,** 20-25.

Mercuro, G., Zoncu, S., Colonna, P., Cherchi, P., Mariotti, S., Pigliaru, F., Petrini, L. and Iliceto, S. Cardiac dysfunction in acromegaly: evidence by pulsed wave tissue Doppler imaging (2000) *Eur J Endocrinol,* **143,** 363-369.

Meurs, K., Kittleson, M. D. and Towbin, J. Familial systolic anterior motion of the mitral valve and/or hypertrophic cardiomyopathy is apparently inherited as an autosomal dominant trait in a family of American shorthair cats (1997) *J Vet Intern Med,* **11,** 138.

Meurs, K. M., Kittleson, M. D., Reiser, P. J., Magnon, A. L. and Towbin, J. A. (2001) In *Proceedings of the 11th congress of the ESVIM,*Dublin, Ireland, pp 137

Mishiro, Y., Oki, T., Yamada, H., Onose, Y., Matsuoka, M., Tabata, T., Wakatsuki, T. and Ito, S. Use of Angiotensin II Stress Pulsed Tissue Doppler Imaging to Evaluate Regional Left Ventricular Contractility in Patients with Hypertrophic Cardiomyopathy (2000) *Journal of the American Society of Echocardiography,* **13,** 1065-1073.

Mishiro, Y., Oki, T., Yamada, H., Wakatsuki, T. and Ito, S. Evaluation of left ventricular contraction abnormalities in patients with dilated cardiomyopathy with the use of pulsed tissue Doppler imaging (1999) *J Am Soc Echocardiogr,* **12,** 913-920.

Miyatake, K., Yamagishi, M., Tanaka, N., Uematsu, M., Yamazaki, N., Mine, Y., Sano, A. and Hirama, M. New method for evaluating left ventricular wall motion by color-coded tissue Doppler imaging: in vitro and in vivo studies (1995) *J Am Coll Cardiol,* **25,** 717-724.

Moise, N. S., Dietze, A. E., Mezza, L. E., Strickland, D., Erb, H. N. and Edwards, N. J. Echocardiography, electrocardiography, and radiography of cats with dilatation cardiomyopathy, hypertrophic cardiomyopathy, and hyperthyroidism (1986) *Am J Vet Res,* **47,** 1476-1486.

Moller, J., Poulsen, S., Sondergaard, E. and Egstrup, K. Preload dependence of color M-Mode Doppler flow propagation velocity in controls and in patients with left ventricular dysfunction (2000) *Journal of the American Society of Echocardiography,* **13,** 902-909.

Moller, J. F., Sondergaard, E., Poulsen, S. H., Seward, J. B., Appleton, C. P. and Egstrup, K. Color M-mode and pulsed wave tissue Doppler echocardiography: powerful predictors of cardiac events after first myocardial infarction (2001) *J Am Soc Echocardiogr,* **14,** 757-763.

Moran, C. M., Anderson, T., Pye, S. D., Sboros, V. and McDicken, W. N. Quantification of microbubble destruction of three fluorocarbon-filled ultrasonic contrast agents (2000) *Ultrasound in Medicine & Biology,* **26,** 629-639.

Myers, J. H., Stirling, M. C., Choy, M., Buda, A. J. and Gallagher, K. P. Direct measurement of inner and outer wall thickening dynamics with epicardial echocardiography (1986) *Circulation,* **74,** 164172.

Nageh, M. F., Kopelen, H. A., Zoghbi, W. A., Quinones, M. A. and Nagueh, S. F. Estimation of mean right atrial pressure using tissue Doppler imaging (1999) *The American Journal of Cardiology,* **84,** 1448-1451.

Nagueh, S. F., Bachinski, L. L., Meyer, D., Hill, R., Zoghbi, W. A., Tam, J. W., Quinones, M. A., Roberts, R. and Marian, A. J. Tissue Doppler Imaging Consistently Detects Myocardial Abnormalities in Patients With Hypertrophic Cardiomyopathy and Provides a Novel Means for an Early Diagnosis Before and Independently of Hypertrophy (2001a) *Circulation,* **104,** 128-130.

Nagueh, S. F., Kopelen, H. A., Lim, D. S., Zoghbi, W. A., Quinones, M. A., Roberts, R. and Marian, A. J. Tissue Doppler imaging consistently detects myocardial contraction and relaxation abnormalities, irrespective of cardiac hypertrophy, in a transgenic rabbit model of human hypertrophic cardiomyopathy (2000) *Circulation,* **102,** 1346-1350.

Nagueh, S. F., Lakkis, N. M., Middleton, K. J., Spencer, W. H., Zoghbi, W. A. and Quinones, M. A. Doppler estimation of left ventricular filling pressures in patients with hypertrophic cardiomyopathy (1999) *Circulation,* **99,** 254-261.

Nagueh, S. F., Middleton, K. J., Kopelen, H. A., Zoghbi, W. A. and Quinones, M. A. Doppler tissue imaging: a noninvasive technique for evaluation of left ventricular relaxation and estimation of filling pressures (1997) *J Am Coll Cardiol,* **30,** 1527-1533.

Nagueh, S. F., Mikati, I., Kopelen, H. A., Middleton, K. J., Quinones, M. A. and Zoghbi, W. A. Doppler estimation of left ventricular filling pressure in sinus tachycardia. A new application of tissue doppler imaging (1998) *Circulation,* **98,** 1644-1650.

Nagueh, S. F., Sun, H., Kopelen, H. A., Middleton, K. J. and Khoury, D. S. Hemodynamic determinants of the mitral annulus diastolic velocities by tissue Doppler (2001b) *J Am Coll Cardiol,* **37,** 278-285.

Nakagawa, K., Takemura, N., Machida, N., Kawamura, M., Amasaki, H. and Hirose, H. Hypertrophic cardiomyopathy in a mixed breed cat family (2002) *J Vet Med Sci,* **64,** 619-621.

Nakatani, S., Marwick, T. H., Lever, H. M. and Thomas, J. D. Resting Echocardiographic Features of Latent Left Ventricular Outflow Obstruction in Hypertrophic Cardiomyopathy (1996) *The American Journal of Cardiology,* **78,** 662-667.

Naqvi, T. Z., Neyman, G., Broyde, A., Mustafa, J. and Siegel, R. J. Comparison of myocardial tissue Doppler with transmitral flow Doppler in left ventricular hypertrophy (2001) *J Am Soc Echocardiogr,* **14,** 1153-1160.

Nikitin, N. P., Witte, K. K., Clark, A. L. and Cleland, J. G. Color tissue Doppler-derived long-axis left ventricular function in heart failure with preserved global systolic function (2002) *Am J Cardiol,* **90,** 1174-1177.

Nishimura, M., FACC, Rick A. and Tajik, M., FACC, A. Jamil Evaluation of Diastolic Filling of Left Ventricle in Health and Disease: Doppler Echocardiography Is the Clinician's Rosetta Stone (1997) *Journal of the American College of Cardiology,* **30,** 8-18.

Nishimura, R. A., Abel, M. D., Hatle, L. K. and Tajik, A. J. Relation of pulmonary vein to mitral flow velocities by transesophageal Doppler echocardiography. Effect of different loading conditions. (1990) *Circulation,* **81,** 1488-1497.

Nishimura, R. A., Appleton, C. P., Redfield, M. M., Ilstrup, D. M., Holmes Jr., D. R. and Tajik, A. J. Noninvasive Doppler Echocardiographic Evaluation of Left Ventricular Filling Pressures in Patients With Cardiomyopathies: A Simultaneous Doppler Echocardiographic and Cardiac Catheterization Study (1996) *Journal of the American College of Cardiology,* **28,** 1226-1233.

Oberst, L., Zhao, G., Park, J. T., Brugada, R., Michael, L. H., Entman, M. L., Roberts, R. and Marian, A. J. Dominant-negative Effect of a Mutant Cardiac Troponin T on Cardiac Structure and Function in Transgenic Mice (1998) *J. Clin. Invest.,* **102,** 1498-1505.

O'Grady, M. R., Bonagura, J. D., Powers, J. D. and Herring, D. S. Quantitative cross-sectional echocardiography in the normal dog (1986) *Veterinary Radiology,* **27,** 34-49.

Ohte, N., Narita, H., Hashimoto, T., Akita, S., Kurokawa, K. and Fujinami, T. Evaluation of left ventricular early diastolic performance by color tissue Doppler imaging of the mitral annulus (1998) *The American Journal of Cardiology,* **82,** 1414-1417.

Oki, T., Fukuda, K., Tabata, T., Mishiro, Y., Yamada, H., Abe, M., Onose, Y., Wakatsuki, T., Iuchi, A. and Ito, S. Effect of an Acute Increase in Afterload on Left Ventricular Regional Wall Motion Velocity in Healthy Subjects (1999) *Journal of the American Society of Echocardiography,* **12,** 476-483.

Oki, T., Fukuda, N., Iuchi, A., Tabata, T., Kiyoshige, K., Fujimoto, T., Manabe, K., Yamada, H. and Ito, S. Changes in Left Ventricular Inflow and Pulmonary Venous Flow Velocities During Preload Alteration in Hypertrophic Cardiomyopathy (1996) *The American Journal of Cardiology,* **77,** 430-435.

Oki, T., Mishiro, Y., Yamada, H., Onose, Y., Matsuoka, M., Wakatsuki, T., Tabata, T. and Ito, S. Detection of left ventricular regional relaxation abnormalities and asynchrony in patients with hypertrophic cardiomyopathy with the use of tissue Doppler imaging (2000) *Am Heart J,* **139,** 497-502.

Oki, T., Tabata, T., Yamada, H., Abe, M., Onose, Y., Wakatsuki, T., Fujinaga, H., Sakabe, K., Ikata, J., Nishikado, A., Iuchi, A. and Ito, S. Right and left ventricular wall motion velocities as diagnostic indicators of constrictive pericarditis (1998a) *Am J Cardiol,* **81,** 465-470.

Oki, T., Tabata, T., Yamada, H., Manabe, K., Fukuda, K., Abe, M., Onose, Y., Iuchi, A., Fukuda, N. and Ito, S. Difference in systolic motion velocity of the left ventricular posterior wall in patients with asymmetric septal hypertrophy and prior anteroseptal myocardial infarction. Evaluation by pulsed tissue Doppler imaging (1998b) *Jpn Heart J,* **39,** 163-172.

Oki, T., Tabata, T., Yamada, H., Wakatsuki, T., Mishiro, Y., Abe, M., Onose, Y., Iuchi, A. and Ito, S. Left ventricular diastolic properties of hypertensive patients measured by pulsed tissue Doppler imaging (1998c) *J Am Soc Echocardiogr,* **11,** 1106-1112.

Oki, T., Tabata, T., Yamada, H., Wakatsuki, T. and Shinohara, H. Clinical Application of Pulsed Doppler Tissue Imaging for Assessing Abnormal Left Ventricular Relaxation (1997) *The American Journal of Cardiology,* **79,** 921-928.

Ommen, S. R., Nishimura, R. A., Appleton, C. P., Miller, F. A., Oh, J. K., Redfield, M. M. and Tajik, A. J. Clinical utility of Doppler echocardiography and tissue Doppler imaging in the estimation of left ventricular filling pressures: A comparative simultaneous Doppler-catheterization study (2000) *Circulation,* **102,** 1788-1794.

Onose, Y., Oki, T., Mishiro, Y., Yamada, H., Abe, M., Manabe, K., Kageji, Y., Tabata, T., Wakatsuki, T. and Ito, S. Influence of aging on systolic left ventricular wall motion velocities along the long and short axes in clinically normal patients determined by pulsed tissue doppler imaging (1999a) *J Am Soc Echocardiogr,* **12,** 921-926.

Onose, Y., Oki, T., Tabata, T., Yamada, H. and Ito, S. Assessment of the temporal relationship between left ventricular relaxation and filling during early diastole using pulsed Doppler echocardiography and tissue Doppler imaging (1999b) *Jpn Circ J,* **63,** 209-215.

Ortlepp, J. R., Vosberg, H. P., Reith, S., Ohme, F., Mahon, N. G., Schroder, D., Klues, H. G., Hanrath, P. and McKenna, W. J. Genetic polymorphisms in the renin-angiotensin-aldosterone system associated with expression of left ventricular hypertrophy in hypertrophic cardiomyopathy: a study of five polymorphic genes in a family with a disease causing mutation in the myosin binding protein C gene (2002) *Heart,* **87,** 270-275.

Pagani, E. D. and Julian, F. J. Rabbit papillary muscle myosin isozymes and the velocity of muscle shortening (1984) *Circ Res,* **54,** 586-594.

Pai, R. and Gill, K. Amplitudes, Durations, and Timings of Apically Directed Left Ventricular Myocardial Velocities: I. Their Normal Pattern and Coupling to Ventricular Filling and Ejection (1998) *Journal of the American Society of Echocardiography,* **11,** 105-109.

Palka, P., Lange, A., Donnelly, J. E. and Nihoyannopoulos, P. Differentiation Between Restrictive Cardiomyopathy and Constrictive Pericarditis by Early Diastolic Doppler Myocardial Velocity Gradient at the Posterior Wall (2000) *Circulation,* **102,** 655-662.

Palka, P., Lange, A., Fleming, A. D., Donnelly, J. E., Dutka, D. P., Starkey, I. R., Shaw, T. R. D., Sutherland, G. R. and Fox, K. A. A. Differences in Myocardial Velocity Gradient Measured Throughout the Cardiac Cycle in Patients With Hypertrophic Cardiomyopathy, Athletes and Patients With Left Ventricular Hypertrophy Due to Hypertension (1997a) *Journal of the American College of Cardiology,* **30,** 760-768.

Palka, P., Lange, A., Fleming, A. D., Fenn, L. N., Bouki, K. P., Shaw, T. R., Fox, K. A., McDicken, W. N. and Sutherland, G. R. Age-related transmural peak mean velocities and peak velocity gradients by Doppler myocardial imaging in normal subjects. (1996) *Eur Heart J,* **17,** 940-950.

Palka, P., Lange, A., Fleming, A. D., Sutherland, G. R., Fenn, L. N. and McDicken, W. N. Doppler tissue imaging: myocardial wall motion velocities in normal subjects (1995) *J Am Soc Echocardiogr,* **8,** 659-668.

Palka, P., Lange, A. and Nihoyannopoulos, P. The effect of long-term training on age-related left ventricular changes by Doppler myocardial velocity gradient (1999) *The American Journal of Cardiology,* **84,** 1061-1067.

Palka, P., Lange, A., Wright, R. A., Starkey, I. R., Fleming, A. D., Bouki, K. P., Sutherland, G. R., Shaw, T. R. D. and Fox, K. A. A. Myocardial velocity gradient measured throughout the cardiac cycle in dilated cardiomyopathy hearts-a potential new parameter of systolic and diastolic myocardial function by Doppler myocardial imaging (1997b) *Eur J Ultrasound,* **5,** 141-154.

Palka, P., Lange, A., Donnelly, J., Scalia, G., Burstow, D. and Nihoyannopoulos, P. Doppler tissue echocardiographic features of cardiac amyloidosis (2002) *Journal of the American Society of Echocardiography,* **15,** 1353-1360.

Palmiter, K. A., Tyska, M. J., Haeberle, J. R., Alpert, N. R., Fananapazir, L. and Warshaw, D. M. R403Q and L908V mutant beta-cardiac myosin from patients with familial hypertrophic cardiomyopathy exhibit enhanced mechanical performance at the single molecule level (2000) *J Muscle Res Cell Motil,* **21,** 609-620.

Panza, J. A., Maris, T. J. and Maron, B. J. Development and determinants of dynamic obstruction to left ventricular outflow in young patients with hypertrophic cardiomyopathy (1992) *Circulation,* **85,** 1398-1405.

Papademetriou, V., Gottdiener, J. S., Fletcher, R. D. and Freis, E. D. Echocardiographic assessment by computer-assisted analysis of diastolic left ventricular function and hypertrophy in borderline or mild systemic hypertension (1985) *Am J Cardiol,* **56,** 546-550.

Patel, R., Lim, D.-S., Reddy, D., Nagueh, S. F., Lutucuta, S., Sole, M. J., Zoghbi, W. A., Quinones, M. A., Roberts, R. and Marian, A. J. Variants of Trophic Factors and Expression of Cardiac Hypertrophy in Patients with Hypertrophic Cardiomyopathy (2000) *Journal of Molecular and Cellular Cardiology,* **32,** 2369-2377.

Pellerin, D., Cohen, L., Larrazet, F., Pajany, F. and Witchitz, S. Preejectional Left Ventricular Wall Motion in Normal Subjects Using Doppler Tissue Imaging and Correlation With Ejection Fraction (1997) *Am J Cardiol,* **80,** 601-607.

Peterson, E. N., Moise, N. S., Brown, C. A., Erb, H. N. and Slater, M. R. Heterogeneity of hypertrophy in feline hypertrophic heart disease (1993) *J Vet Intern Med,* **7,** 183-189.

Peterson, M. E., Taylor, R. S., Greco, D. S., Nelson, R. W., Randolph, J. F., Foodman, M. S., Moroff, S. D., Morrison, S. A. and Lothrop, C. D. Acromegaly in 14 cats (1990) *J Vet Intern Med,* **4,** 192-201.

Pislaru, C., Belohlavek, M., Bae, R. Y., Abraham, T. P., Greenleaf, J. F. and Seward, J. B. Regional asynchrony during acute myocardial ischemia quantified by ultrasound strain rate imaging (2001) *Journal of the American College of Cardiology,* **37,** 1141-1148.

Quinones, M., Otto, C., Stoddard, M., Waggoner, A. and Zoghbi, W. Recommendations for quantification of Doppler echocardiography: A report from the Doppler quantification task force of the nomenclature and standards committee of the American Society of Echocardiography (2002) *Journal of the American Society of Echocardiography,* **15,** 167-184.

Rajagopalan, N., Garcia, M. J., Rodriguez, L., Murray, R. D., Apperson-Hansen, C., Stugaard, M., Thomas, J. D. and Klein, A. L. Comparison of new Doppler echocardiographic methods to differentiate constrictive pericardial heart disease and restrictive cardiomyopathy (2001) *Am J Cardiol,* **87,** 86-94.

Rankin, J. S., McHale, P. A., Arentzen, C. E., Ling, D., Greenfield, J. C. J. and Anderson, R. W. The three-dimensional dynamic geometry of the left ventricle in the conscious dog (1976) *Circ Res,* **39,** 304-313.

Richardson, P., McKenna, W., Bristow, M., Maisch, B., Mautner, B., O'Connell, J., Olsen, E., Thiene, G., Goodwin, J., Gyarfas, I., Martin, I. and Nordet, P. Report of the 1995 World Health Organization/International Society and Federation of Cardiology Task Force on the Definition and Classification of Cardiomyopathies (1996) *Circulation,* **93,** 841-842.

Richartz, B. M., Werner, G. S., Ferrari, M. and Figulla, H. R. Comparison of left ventricular systolic and diastolic function in patients with idiopathic dilated cardiomyopathy and mild heart failure versus those with severe heart failure (2002) *Am J Cardiol,* **90,** 390-394.

Rishniw, M. and Thomas, W. P. Dynamic right ventricular outflow obstruction: a new cause of systolic murmurs in cats (2002) *J Vet Intern Med,* **16,** 547-552.

Roberts, R. and Sigwart, U. New concepts in hypertrophic cardiomyopathy, part I (2001) *Circulation,* **104,** 2113-2116.

Roberts, W. C. and Ferrans, V. J. Pathologic anatomy of the cardiomyopathies. Idiopathic dilated and hypertrophic types, infiltrative types, and endomyocardial disease with and without eosinophilia (1975) *Hum Pathol,* **6,** 287-342.

Rodriguez, L., Garcia, M., Ares, M., Griffin, B. P., Nakatani, S. and Thomas, J. D. Assessment of mitral annular dynamics during diastole by Doppler tissue imaging: comparison with mitral Doppler inflow in subjects without heart disease and in patients with left ventricular hypertrophy (1996) *Am Heart J,* **131,** 982-987.

Rossvoll, O. and Hatle, L. K. Pulmonary venous flow velocities recorded by transthoracic Doppler ultrasound: relation to left ventricular diastolic pressures (1993) *J Am Coll Cardiol,* **21,** 1687-1696.

Rush, J. E., Freeman, L. M., Brown, D. J. and Smith, F. W., Jr. The use of enalapril in the treatment of feline hypertrophic cardiomyopathy (1998) *J Am Anim Hosp Assoc,* **34,** 38-41.

Rush, J. E., Freeman, L. M., Fenollosa, N. K. and Brown, D. J. Population and survival characteristics of cats with hypertrophic cardiomyopathy: 260 cases (1990-1999) (2002) *J Am Vet Med Assoc,* **220,** 202-207.

Rushmer, R. F. Initial phase of ventricular systole: asynchronous contraction (1956) *Am J Physiol,* **184,** 188-194.

Rust, E. M., Albayya, F. P. and Metzger, J. M. Identification of a contractile deficit in adult cardiac myocytes expressing hypertrophic cardiomyopathy–associated mutant troponin T proteins (1999) *J. Clin. Invest.,* **103,** 1459-1467.

Sahn, D. J., DeMaria, A. N., Kisslo, J. and Weyman, A. Recommendations regarding quantitation in M-mode echocardiography: results of a survey of echocardiographic measurements (1978) *Circulation,* **58,** 1072-1083.

Sakamoto, A., Ono, K., Abe, M., Jasmin, G., Eki, T., Murakami, Y., Masaki, T., Toyo-oka, T. and Hanaoka, F. Both hypertrophic and dilated cardiomyopathies are caused by mutation of the same gene, delta -sarcoglycan, in hamster: An animal model of disrupted dystrophin-associated glycoprotein complex (1997) *PNAS,* **94,** 13873-13878.

Samuel, J. L., Rappaport, L. and Mercadier, J. J. Distribution of myosin isozymes within cardiac cells (1983) *Circ Res,* **52,** 200-209.

Santilli, R. A. and Bussadori, C. Doppler echocardiographic study of left ventricular diastole in non-anaesthetized healthy cats (1998) *Vet J,* **156,** 203-215.

Schober, K. E. and Luis Fuentes, V. Effects of age, body weight, and heart rate on transmitral and pulmonary venous flow in clinically normal dogs (2001) *Am J Vet Res,* **62,** 1447-1454.

Schober, K. E., Luis Fuentes, V. and Bonagura, J. D. Comparison between invasive hemodynamic measurements and noninvasive assessment of left ventricular diastolic function by use of Doppler echocardiography in healthy anesthetized cats (2003) *Am J Vet Res,* **64,** 93-103.

Schober, K. E., Luis Fuentes, V., McEwan, J. D. and French, A. T. Pulmonary venous flow characteristics as assessed by transthoracic pulsed Doppler echocardiography in normal dogs (1998) *Vet Radiol Ultrasound,* **39,** 33-41.

Schoenfeld, M. H., Supple, E. W., Dec, G. W. J., Fallon, J. T. and Palacios, I. F. Restrictive cardiomyopathy versus constrictive pericarditis: role of endomyocardial biopsy in avoiding unnecessary thoracotomy (1987) *Circulation,* **75,** 1012-1017.

Schwammenthal, E., Nakatani, S., He, S., Hopmeyer, J., Sagie, A., Weyman, A. E., Lever, H. M., Yoganathan, A. P., Thomas, J. D. and Levine, R. A. Mechanism of Mitral Regurgitation in Hypertrophic Cardiomyopathy : Mismatch of Posterior to Anterior Leaflet Length and Mobility (1998) *Circulation,* **98,** 856-865.

Seidman, J. G. and Seidman, C. The genetic basis for cardiomyopathy: from mutation identification to mechanistic paradigms (2001) *Cell,* **104,** 557-567.

Seiler MD, F., Christian, Aeschbacher MD, B. C. and Meier MD, F., FACC, Bernhard Quantitation of Mitral Regurgitation Using the Systolic/Diastolic Pulmonary Venous Flow Velocity Ratio (1998) *Journal of the American College of Cardiology,* **31,** 1383-1390.

Severino, S., Caso, P., Cicala, S., Galderisi, M., de Simone, L., D'Andrea, A., D'Errico, A. and Mininni, N. Involvement of right ventricle in left ventricular hypertrophic cardiomyopathy: analysis by pulsed Doppler tissue imaging (2000) *Eur J Echocardiogr,* **1,** 281-288.

Severino, S., Caso, P., Galderisi, M., De Simone, L., Petrocelli, A., de Divitiis, O. and Mininni, N. Use of pulsed Doppler tissue imaging to assess regional left ventricular diastolic dysfunction in hypertrophic cardiomyopathy (1998) *Am J Cardiol,* **82,** 1394-1398.

Shapiro, L. M. and McKenna, W. J. Distribution of left ventricular hypertrophy in hypertrophic cardiomyopathy: a two-dimensional echocardiographic study (1983) *J Am Coll Cardiol,* **2,** 437-444.

Sherrid, M. V., Gunsburg, D. Z., Moldenhauer, S. and Pearle, G. Systolic anterior motion begins at low left ventricular outflow tract velocity in obstructive hypertrophic cardiomyopathy (2000) *Journal of the American College of Cardiology,* **36,** 1344-1354.

Shimizu, Y., Uematsu, M., Nagaya, N., Yamagishi, M., Yamamoto, H., Miyatake, K., Imazu, M. and Kohno, N. Myocardial velocity gradient reflects the severity of myocardial damage regardless of the presence or absence of mitral regurgitation (2003) *Journal of the American Society of Echocardiography,* **16,** 246-253.

Shimizu, Y., Uematsu, M., Shimizu, H., Nakamura, K., Yamagishi, M. and Miyatake, K. Peak negative myocardial velocity gradient in early diastole as a noninvasive indicator of left ventricular diastolic function: comparison with transmitral flow velocity indices (1998) *J Am Coll Cardiol,* **32,** 1418-1425.

Siegel, R. J. and Criley, J. M. Comparison of ventricular emptying with and without a pressure gradient in patients with hypertrophic cardiomyopathy (1985) *Br Heart J,* **53,** 283-291.

Sisson, D. D., Knight, D. H., Helinski, C., Fox, P. R., Bond, B. R., Harpster, N. K., Moise, N. S., Kaplan, P. M., Bonagura, J. D., Czarnecki, G. and et al. Plasma taurine concentrations and M-mode echocardiographic measures in healthy cats and in cats with dilated cardiomyopathy (1991) *J Vet Intern Med,* **5,** 232-238.

Snyder, P. S., Sadek, D. and Jones, G. L. Effect of amlodipine on echocardiographic variables in cats with systemic hypertension (2001) *J Vet Intern Med,* **15,** 52-56.

Sohn, D. W., Chai, I. H., Lee, D. J., Kim, H. C., Kim, H. S., Oh, B. H., Lee, M. M., Park, Y. B., Choi, Y. S., Seo, J. D. and Lee, Y. W. Assessment of mitral annulus velocity by Doppler tissue imaging in the evaluation of left ventricular diastolic function (1997) *J Am Coll Cardiol,* **30,** 474-480.

Sohn, D.-W., Kim, Y.-J., Lee, M.-M., Park, Y.-B., Choi, Y.-S. and Lee, Y.-W. Differentiation between reversible and irreversible restrictive left ventricular filling patterns with the use of mitral annulus velocity (2000) *Journal of the American Society of Echocardiography,* **13,** 891-895.

Sohn, D.-W., Song, J.-M., Zo, J.-H., Chai, I.-H., Kim, H.-S., Chun, H.-G. and Kim, H.-C. Mitral Annulus Velocity in the Evaluation of Left Ventricular Diastolic Function in Atrial Fibrillation (1999) *Journal of the American Society of Echocardiography,* **12,** 927-931.

Spirito, P. and Maron, B. J. Relation between extent of left ventricular hypertrophy and age in hypertrophic cardiomyopathy (1989) *J Am Coll Cardiol,* **13,** 820-823.

Spirito, P. and Maron, B. J. Relation between extent of left ventricular hypertrophy and diastolic filling abnormalities in hypertrophic cardiomyopathy (1990) *J Am Coll Cardiol,* **15,** 808-813.

Spirito, P., Maron, B. J., Bonow, R. O. and Epstein, S. E. Severe functional limitation in patients with hypertrophic cardiomyopathy and only mild localized left ventricular hypertrophy (1986) *J Am Coll Cardiol,* **8,** 537-544.

Spirito, P., Maron, B. J., Bonow, R. O. and Epstein, S. E. Occurrence and significance of progressive left ventricular wall thinning and relative cavity dilatation in hypertrophic cardiomyopathy (1987) *Am J Cardiol,* **60,** 123-129.

St John Sutton, M. G., Lie, J. T., Anderson, K. R., O'Brien, P. C. and Frye, R. L. Histopathological specificity of hypertrophic obstructive cardiomyopathy. Myocardial fibre disarray and myocardial fibrosis (1980) *Br Heart J,* **44,** 433-443.

Steen, T. and Steen, S. Filling of a model left ventricle studied by colour M mode Doppler (1994) *Cardiovasc Res,* **28,** 1821-1827.

Steine, K., Flogstad, T., Stugaard, M. and Smiseth, O. A. Early diastolic intraventricular filling pattern in acute myocardial infarction by color M-mode Doppler echocardiography (1998) *J Am Soc Echocardiogr,* **11,** 119-125.

Stugaard, M., Risoe, C., Ihlen, H. and Smiseth, O. A. Intracavitary filling pattern in the failing left ventricle assessed by color M-mode Doppler echocardiography (1994) *J Am Coll Cardiol,* **24,** 663-670.

Stugaard, M., Smiseth, O. A., Risoe, C. and Ihlen, H. Intraventricular early diastolic filling during acute myocardial ischemia, assessment by multigated color m-mode Doppler echocardiography (1993) *Circulation,* **88,** 2705-2713.

Sutherland, G. R., Bijnens, B. and McDicken, W. N. Tissue Doppler Echocardiography: Historical Perspective and Technological Considerations (1999) *Echocardiography,* **16,** 445-453.

Sutton, M. G., Tajik, A. J., Gibson, D. G., Brown, D. J., Seward, J. B. and Guiliani, E. R. Echocardiographic assessment of left ventricular filling and septal and posterior wall dynamics in idiopathic hypertrophic subaortic stenosis (1978) *Circulation,* **57,** 512-520.

Tabata, T., Oki, T., Yamada, H., Abe, M., Onose, Y. and Thomas, J. Subendocardial Motion in Hypertrophic Cardiomyopathy: Assessment from Long- and Short-Axis Views by Pulsed Tissue Doppler Imaging (2000) *Journal of the American Society of Echocardiography,* **13,** 108-115.

Takatsuji, H., Mikami, T., Urasawa, K., Teranishi, J., Onozuka, H., Takagi, C., Makita, Y., Matsuo, H., Kusuoka, H. and Kitabatake, A. A new approach for evaluation of left ventricular diastolic function: spatial and temporal analysis of left ventricular filling flow propagation by color M-mode Doppler echocardiography (1996) *J Am Coll Cardiol,* **27,** 365-371.

Takayama, M., Norris, R. M., Brown, M. A., Armiger, L. C., Rivers, J. T. and White, H. D. Postsystolic shortening of acutely ischemic canine myocardium predicts early and late recovery of function after coronary artery reperfusion (1988) *Circulation,* **78,** 994-1007.

Takenaka, K., Dabestani, A., Gardin, J. M., Russell, D., Clark, S., Allfie, A. and Henry, W. L. Left ventricular filling in hypertrophic cardiomyopathy: a pulsed Doppler echocardiographic study (1986) *J Am Coll Cardiol,* **7,** 1263-1271.

Tanaka, M., Fujiwara, H., Onodera, T., Wu, D. J., Matsuda, M., Hamashima, Y. and Kawai, C. Quantitative analysis of narrowings of intramyocardial small arteries in normal hearts, hypertensive hearts, and hearts with hypertrophic cardiomyopathy (1987) *Circulation,* **75,** 1130-1139.

Tardiff, J. C., Factor, S. M., Tompkins, B. D., Hewett, T. E., Palmer, B. M., Moore, R. L., Schwartz, S., Robbins, J. and Leinwand, L. A. A Truncated Cardiac Troponin T Molecule in Transgenic Mice Suggests Multiple Cellular Mechanisms for Familial Hypertrophic Cardiomyopathy (1998) *J. Clin. Invest.,* **101,** 2800-2811.

Taugner, F., Baatz, G. and Nobiling, R. The renin-angiotensin system in cats with chronic renal failure. (1996) *J Comp Pathol,* **115,** 239-252.

Teare, D. Asymmetrical hypertrophy of the heart in young patients (1958) *Br Heart J,* **20,** 1.

Teirlinck, C. J., Bezemer, R. A., Kollmann, C., Lubbers, J., Hoskins, P. R., Ramnarine, K. V., Fish, P. J., Fredeldt, K. E. and Schaarschmidt, U. G. Development of an example flow test object and comparison of five of these test objects, constructed in various laboratories (1998) *Ultrasonics,* **36,** 653-660.

Thomas, W. P., Mathewson, J., Suter, P. F., Reed, J. R. and Meierhenry, E. F. Hypertrophic obstructive cardiomyopathy in a dog: clinical, hemodynamic angiographic, and pathologic studies (1984) *J Am Anim Hosp Assoc,* **20,** 253-260.

Tilley, L. P. Feline cardiology (1976) *Veterinary Clinics of North America,* **6,** 415-432.

Tilley, L. P. (1992) *Essentials of canine and feline electrocardiography: interpretation and treatment,* Lea & Febiger, Philadelphia ; London.

Tilley, L. P., Liu, S. K., Gilbertson, S. R., Wagner, B. M. and Lord, P. F. Primary myocardial disease in the cat. A model for human cardiomyopathy (1977) *Am J Pathol,* **86,** 493-522.

Traill, T. A., Gibson, D. G. and Brown, D. J. Study of left ventricular wall thickness and dimension changes using echocardiography (1978) *Br Heart J,* **40,** 162-169.

Trambaiolo, P., Tonti, G., Salustri, A., Fedele, F. and Sutherland, G. New insights into regional systolic and diastolic left ventricular function with tissue doppler echocardiography: from qualitative analysis to a quantitative approach (2001) *Journal of the American Society of Echocardiography,* **14,** 85-96.

Tsutsui, H., Uematsu, M., Yamagishi, M., Haruta, S., Shimakura, T. and Miyatake, K. Usefulness of the subendocardial myocardial velocity gradient in low-dose dobutamine stress echocardiography (2000) *Heart Vessels,* **15,** 11-17.

Tyberg, T. I., Goodyer, A. V., Hurst, V. W., Alexander, J. and Langou, R. A. Left ventricular filling in differentiating restrictive amyloid cardiomyopathy and constrictive pericarditis (1981) *Am J Cardiol,* **47,** 791-796.

Tyska, M. J., Hayes, E., Giewat, M., Seidman, C. E., Seidman, J. G. and Warshaw, D. M. Single-Molecule Mechanics of R403Q Cardiac Myosin Isolated From the Mouse Model of Familial Hypertrophic Cardiomyopathy (2000) *Circ Res,* **86,** 737-744.

Uematsu, M., Miyatake, K., Tanaka, N., Matsuda, H., Sano, A., Yamazaki, N., Hirama, M. and Yamagishi, M. Myocardial velocity gradient as a new indicator of regional left ventricular contraction: detection by a two-dimensional tissue Doppler imaging technique (1995) *J Am Coll Cardiol,* **26,** 217-223.

Uematsu, M., Nakatani, S., Yamagishi, M., Matsuda, H. and Miyatake, K. Usefulness of myocardial velocity gradient derived from two-dimensional tissue Doppler imaging as an indicator of regional myocardial contraction independent of translational motion assessed in atrial septal defect (1997) *Am J Cardiol,* **79,** 237-241.

Ueno, Y., Nakamura, Y., Ohbayashi, Y. and Kinoshita, M. Evaluation of left ventricular systolic and diastolic global function: peak positive and negative myocardial velocity gradients in M-mode Doppler tissue imaging (2002) *Echocardiography,* **19,** 15-25.

Vaitkus, P. T. and Kussmaul, W. G. Constrictive pericarditis versus restrictive cardiomyopathy: a reappraisal and update of diagnostic criteria. (1991) *Am Heart J,* **122,** 1431-1441.

Van Vleet, J. F., Ferrans, V. J. and Weirich, W. E. Pathologic alterations in hypertrophic and congestive cardiomyopathy of cats (1980) *Am J Vet Res,* **41,** 2037-2048.

Vinereanu, D., Florescu, N., Sculthorpe, N., Tweddel, A. C., Stephens, M. R. and Fraser, A. G. Differentiation between pathologic and physiologic left ventricular hypertrophy by tissue doppler assessment of long-axis function in patients with hypertrophic cardiomyopathy or systemic hypertension and in athletes (2001) *The American Journal of Cardiology,* **88,** 53-58.

Vinereanu, D., Khokhar, A. and Fraser, A. G. Reproducibility of pulsed wave tissue Doppler echocardiography (1999) *J Am Soc Echocardiogr,* **12,** 492-499.

Vitale, G., Galderisi, M., Lupoli, G. A., Celentano, A., Pietropaolo, I., Parenti, N., De Divitiis, O. and Lupoli, G. Left ventricular myocardial impairment in subclinical hypothyroidism assessed by a new ultrasound tool: pulsed tissue Doppler (2002) *J Clin Endocrinol Metab,* **87,** 4350-4355.

Vogel, M., Schmidt, M. R., Kristiansen, S. B., Cheung, M., White, P. A., Sorensen, K. and Redington, A. N. Validation of myocardial acceleration during isovolumic contraction as a novel noninvasive index of right ventricular contractility: comparison with ventricular pressure-volume relations in an animal model (2002) *Circulation,* **105,** 1693-1699.

Waggoner, A. and Bierig, S. Tissue Doppler imaging: A useful echocardiographic method for the cardiac sonographer to assess systolic and diastolic ventricular function (2001) *Journal of the American Society of Echocardiography,* **14,** 1143-1152.

Watkins, H., Thierfelder, L., Anan, R., Jarcho, J., Matsumori, A., McKenna, W., Seidman, J. G. and Seidman, C. E. Independent origin of identical beta cardiac myosin heavy-chain mutations in hypertrophic cardiomyopathy (1993) *Am J Hum Genet,* **53,** 1180-1185.

Weisfeldt, M. L., Loeven, W.A., Shock, N.W., Resting and active mechanical properties of trabeculae carnae from aged male rats (1971) *American Journal of Physiology,* **220,** 1921-1927.

Wigle, E. D., Rakowski, H., Kimball, B. P. and Williams, W. G. Hypertrophic Cardiomyopathy : Clinical Spectrum and Treatment (1995) *Circulation,* **92,** 1680-1692.

Witt, C. C., Gerull, B., Davies, M. J., Centner, T., Linke, W. A. and Thierfelder, L. Hypercontractile Properties of Cardiac Muscle Fibers in a Knock-in Mouse Model of Cardiac Myosin-binding Protein-C (2001) *J. Biol. Chem.,* **276,** 5353-5359.

Xiao, R. P., Spurgeon, H. A., O'Connor, F. and Lakatta, E. G. Age-associated changes in beta-adrenergic modulation on rat cardiac excitation-contraction coupling (1994) *J Clin Invest,* **94,** 2051-2059.

Yalcin, F., Kaftan, A., Muderrisoglu, H., Korkmaz, M. E., Flachskampf, F., Garcia, M. and Thomas, J. D. Is Doppler tissue velocity during early left ventricular filling preload independent? (2002) *Heart,* **87,** 336-339.

Yamada, H., Oki, T., Mishiro, Y., Tabata, T., Abe, M., Onose, Y., Wakatsuki, T. and Ito, S. Effect of aging on diastolic left ventricular myocardial velocities measured by pulsed tissue Doppler imaging in healthy subjects (1999a) *J Am Soc Echocardiogr,* **12,** 574-581.

Yamada, H., Oki, T., Tabata, T., Iuchi, A. and Ito, S. Assessment of left ventricular systolic wall motion velocity with pulsed tissue Doppler imaging: comparison with peak dP/dt of the left ventricular pressure curve (1998) *J Am Soc Echocardiogr,* **11,** 442-449.

Yamada, H., Oki, T., Tabata, T., Mishiro, Y., Abe, M., Onose, Y., Wakatsuki, T., Iuchi, A. and Ito, S. Assessment of the Systolic Left Ventricular Myocardial Velocity Profile and Gradient Using Tissue Doppler Imaging in Patients with Hypertrophic Cardiomyopathy (1999b) *Echocardiography,* **16,** 775-783.

Yamaguchi, H., Ishimura, T., Nishiyama, S., Nagasaki, F., Nakanishi, S., Takatsu, F., Nishijo, T., Umeda, T. and Machii, K. Hypertrophic nonobstructive cardiomyopathy with giant negative T waves (apical hypertrophy): ventriculographic and echocardiographic features in 30 patients (1979) *Am J Cardiol,* **44,** 401-412.

Yamamoto, K., Masuyama, T., Tanouchi, J., Doi, Y., Kondo, H., Hori, M., Kitabatake, A. and Kamada, T. Effects of heart rate on left ventricular filling dynamics: assessment from simultaneous recordings of pulsed Doppler transmitral flow velocity pattern and haemodynamic variables, (1993) *Cardiovasc Res* **27,** 935-941.

Yamamoto, K., Nishimura, R., Burnett, J. and Redfield, M. Assessment of left ventricular end-diastolic pressure by Doppler echocardiography: Contribution of duration of pulmonary venous versus mitral flow velocity curves at atrial contraction (1997) *Journal of the American Society of Echocardiography,* **10,** 52-59.

Yang, Q., Sanbe, A., Osinska, H., Hewett, T. E., Klevitsky, R. and Robbins, J. A Mouse Model of Myosin Binding Protein C Human Familial Hypertrophic Cardiomyopathy (1998) *J. Clin. Invest.,* **102,** 1292-1300.

Yip, G., Wang, M., Zhang, Y., Fung, J. W., Ho, P. Y. and Sanderson, J. E. Left ventricular long axis function in diastolic heart failure is reduced in both diastole and systole: time for a redefinition? (2002) *Heart,* **87,** 121-125.

Zamorano, J., Wallbridge, D. R., Ge, J., Drozd, J., Nesser, J. and Erbel, R. Non-invasive assessment of cardiac physiology by tissue Doppler echocardiography. A comparison with invasive haemodynamics (1997) *Eur Heart J,* **18,** 330-339.

Published papers

H.Koffas, J.Dukes-McEwan, B.M.Corcoran, C.M.Moran, A.French, V.Sboros, T.Anderson, P.Smith, K.Simpson, W.N.McDicken. (2003). Peak mean myocardial velocities and velocity gradients measured by color M-mode Tissue Doppler Imaging in the left ventricular free wall of healthy cats. *Journal of Veterinary Internal Medicine vol 17(4), p.125-139, 2003.*

Abstracts

published from scientific meetings where this research has been presented

H.Koffas, J.Dukes-McEwan, C.Moran, V.Sboros, A.French, B.M.Corcoran, W.N.McDicken. (2001). Myocardial Velocity Gradients in cats and correlation with dynamic wall thickness changes. *Proceedings of the 44th annual congress of the British Small Animal Veterinary Association, 5-8th April 2001, Birmingham, UK.* p. 501.

H.Koffas, J. Dukes-McEwan, C.Moran, A.French, V.Sboros, K.Thorp, B. M.Corcoran, W.N.McDicken. (2001). Left ventricular wall motion velocities measured by pulsed Doppler Tissue Imaging in healthy cats. Normal values and the influence of ageing. *Proceedings of the 11th congress of the European Society of Veterinary Internal Medicine, 5-8th September 2001, Dublin, Ireland.* p. 101.

H.Koffas, J.Dukes-McEwan, C.Moran, A.French, V.Sboros, K.Simpson, B.M.Corcoran, W.N.McDicken. (2001). Age dependent peak transmural mean velocities and myocardial velocity gradients in normal cats measured by Doppler Tissue Imaging. *Proceedings of the 33rd British Medical Ultrasound Society and the 13th Euroson congress, 11-14th December 2001, Edinburgh, UK.* p.47. *European Journal of Ultrasound vol 15(S1); S4: 2002.*

H. Koffas, J.Dukes-McEwan, C.Moran, A. French, V. Sboros, K. Simpson, B.M. Corcoran. (2002) Colour M-mode Doppler flow propagation velocity in normal cats and cats with left ventricular dysfunction. *Proceedings of the 45th annual congress of the British Small Animal Veterinary Association, 4-7th April 2002, Birmingham, UK.* p.647. *Journal of Small Animal Practice vol 43(9), 2002.*

H.Koffas, J.Dukes-McEwan, B.M.Corcoran, C.Moran, A.French, V.Sboros, K.Simpson, W.N.McDicken. (2002). Myocardial Velocity Gradient and Mean Myocardial Velocity measured by colour M-mode Doppler Tissue Imaging in normal cats and cats with hypertrophic cardiomyopathy. *Proceedings of the 20th annual forum of the American College of Veterinary Internal Medicine, May 29th-June 1st 2002, Dallas-Texas, US.* p.777. *Journal of Veterinary Internal Medicine vol 16(3), p.343, 2002.*

H.Koffas, J.Dukes-McEwan, C.Moran, A.French, V.Sboros, K.Simpson, B. M.Corcoran, W.N.McDicken. (2002). Myocardial velocities measured by pulsed Doppler tissue imaging (DTI) in normal cats and cats with hypertrophic cardiomyopathy (HCM). *Proceedings of the 12th European Congress of Veterinary Internal Medicine, 19-21 September 2002, Munich, Germany.* p.157. *Journal of Veterinary Internal Medicine vol 16(5), p. 627, 2002.*

H.Koffas, A.Stevens, J.Dukes-McEwan, C.Moran, A.French, V.Sboros, K.Simpson, B. M.Corcoran, W.N.McDicken. (2002). Unclassified cardiomyopathy (UCM) in a cat. *Proceedings of the 12th European Congress of Veterinary Internal Medicine, 19-21 September 2002, Munich, Germany.* p.178.

Appendix B1

Table App.B1- 2D/Doppler echocardiographic variables from normal cats

cat	sex	age	weight	*Two-Dimensional measurements*								*M-mode measurements*													*Mitral annulus m.*	
		(years)	(Kg)	LA area d (mm^2)	LA diat d (mm)	LA area s (mm^2)	LA diat s (mm)	LA FS%	LA length d (mm)	Ao diam d (mm)	LAd/Aod	IVSd (mm)	LV diam.d (mm)	LVPW d (mm)	IVSs (mm)	LV diam.s (mm)	LVPWs (mm)	LV FS%	R-R (sec)	MV EPSS (mm)	Aort.v Aod (mm)	Aort.v-LAo (mm)	LAo/Aod	MAM ant (mm)	MAM lat (mm)
F010	MN	10	6.30	108	9.6	190	13.0	26.28	13.6	7.3	1.86	4.5	12.9	3.7	7.9	5.3	7.5	59	0.335	0.78	8.14	11.62	1.43	3.6	3.1
F011	FN	2	4.00	53	5.7	87	19.3	70.39	8.9	8.4	1.05	3.9	10.8	4.1	7.4	3.4	7.8	70	0.292	0.97	8.53	10.33	1.21	2.9	2.8
F012	FN	2	5.60						11.0	8.3	1.32	3.6	18.6	3.8	7.3	10.6	6.6	43	0.422	2.24	11.36	12.82	1.13	5.6	4.5
F014	MN	6	4.80						10.1	8.3	1.21	3.2	17.4	3.6	6.8	9.0	6.7	49	0.428	1.38	7.60	13.48	1.77	4.6	4.9
F015	MN	6	4.40						11.2	8.4	1.33									0.73	8.38	13.43	1.60		
F025	FN	9	4.70	102	9.5	124	10.9	12.64				3.3	14.2	3.5	4.9	7.9	5.3	44	0.375	0.83	8.02	9.84	1.23		
F028	FN	7	4.90	93	8.8	152	11.0	19.96	11.8	7.6	1.56	4.8	14.3	3.6	7.9	6.3	7.2	57	0.295		9.66	12.16	1.26	4.6	4.4
F031	FN	4	3.50						10.2	6.2	1.64	3.3	14.2	2.7	5.1	8.8	5.6	38	0.312		8.64	9.22	1.07	4.1	7.1
F033	FN	8	3.70	92	8.2	144	11.7	29.74				4.1	10.2	5.0	7.3	5.5	7.6	47	0.405		9.16	9.84	1.07		
F034	MN	8	5.70	130	11.0	223	13.4	17.91				4.6	12.5	2.8	6.8	7.6	5.0	39	0.367	1.18	10.90	12.68	1.16		
F037	FN	4	4.00	109	9.8	152	11.7	16.08	9.7	7.6	1.27	2.7	17.2	3.7	4.5	11.3	5.9	35	0.333		8.46	9.62	1.14	4.0	4.3
F041	FN	5	4.60	56	6.9	94	8.1	15.72	9.9	8.4	1.18	3.1	12.0	2.5	4.8	7.7	5.3	36	0.290	1.02	9.54	10.48	1.10	3.0	4.0
F042	FN	3	4.30	91	9.2	116	9.7	5.34	9.9	8.7	1.15	4.1	14.5	3.1	7.8	6.7	5.9	31	0.279		10.06	13.36	1.33	3.2	4.7
F043	MN	1	4.50	100	9.1	157	11.2	19.25	10.2	7.8	1.30	2.7	13.6	4.3	5.1	7.7	6.1	43	0.347	0.32	7.90	12.83	1.62	5.1	5.8
F046	MN	10	4.20	115	10.7	155	12.9	17.21	10.8	8.4	1.28	4.1	14.4	3.5	6.6	7.6	6.9	47	0.383	0.73	10.20	12.40	1.22		
F050	FN	1	4.00	150	11.3	236	14.2	20.52	12.8	8.0	1.59	4.6	16.2	5.2	6.7	11.4	7.5	29	0.510	1.68	11.82	13.63	1.15	5.2	7.3
F051	MN	14	6.20	133	10.6	184	13.0	18.03	12.5	8.8	1.42	4.8	17.1	5.0	7.6	9.7	8.6	44	0.335	0.60	10.44	14.72	1.41	3.8	3.5
F053	FN	9	4.00	95	8.9	144	12.5	28.64	10.4	8.5	1.22	4.4	15.4	3.3	5.4	10.2	6.0	34	0.336	1.34	8.30	13.28	1.60		
F054	MN	1	4.50	176	12.4	290	15.8	21.58	13.7	8.4	1.64	4.4	17.4	5.4	6.6	12.1	8.1	30	0.510	1.88	13.10	15.73	1.20	6.1	8.1
F063	MN	4	5.00	108	10.9	189	12.7	14.47	10.6	8.2	1.30	1.9	15.5	4.2	4.7	7.8	7.7	50	0.378	1.32	7.95	13.35	1.68	2.8	4.8
F066	FN	7	3.80	114	9.8	151	10.8	9.12	11.3	6.8	1.66	3.9	14.4	3.8	5.5	8.5	7.0	41	0.374	0.40	8.65	12.90	1.49	4.9	7.2
F080	MN	9	3.90	109	9.4	180	11.9	20.99	11.6	7.1	1.62	3.6	15.9	3.8	6.2	9.9	6.9	38	0.439	1.27	8.55	13.20	1.54	4.3	6.9
F084	MN	9	3.30	100	9.2	162	13.2	30.56	14.1	9.7	1.46	3.7	17.6	4.8	6.6	9.9	8.6	44	0.488	2.94	11.88	17.06	1.44	5.6	8.1
F085	MN	9	4.40	84	8.8	167	13.1	32.88	10.0	7.5	1.33	4.1	15.3	2.5	8.2	5.2	7.7	67	0.298	0.92	7.62	10.32	1.35	2.9	6.1

Appendix B1

Table App.B1- 2D/Doppler echocardiographic variables from normal cats

cat	*Pulmonary artery: Right*				*Aortic valve: Left Apical*								*Mitral valve*										*Tricuspid inflow*				*CFM*		*IVRT (LV)*	
	PA vmax (m/sec)	ET (sec)	PEP (sec)	PEP/ET	R-R (sec)	Ao vmax (m/sec)	Ao VTI (m)	PEP (sec)	ET (sec)	PEP/ET	Acc. t (sec)	R-R (sec)	E (m/sec)	A (m/sec)	E/A	E VTI (m)	A VTI (m)	E dec t (sec)	E acc t (sec)	E dec (sec)	A dur (sec)	R-R (sec)	E vmax (m/sec)	A vmax (m/sec)	E/A	R-R (sec)	PPV (mm/sec)	R-R (sec)	IVRT (sec)	R-R (sec)
F010	0.61				0.330	0.72	0.074	0.050	0.153	0.327	0.050	0.333	0.58	0.60	0.97	0.032	0.026	0.044	0.042	0.095	0.065	0.340	0.42	0.55	0.76	0.325			0.058	0.336
F011	0.74				0.300	0.92	0.075	0.035	0.125	0.280	0.038	0.321	0.80	0.57	1.40	0.040	0.020	0.061	0.025	0.085	0.068	0.329					584	0.308	0.034	0.315
F012	1.10	0.150	0.033	0.221	0.430	0.76	0.075	0.061	0.144	0.424	0.024	0.435	0.82	0.53	1.55	0.050	0.020	0.066	0.034	0.097	0.076	0.444							0.050	0.462
F014	0.71				0.460	0.80	0.082	0.052	0.165	0.315	0.034	0.357	0.59	0.52	1.13	0.030	0.020	0.048	0.051	0.087	0.074	0.397	0.52	0.49	1.06	0.362			0.051	0.374
F015	0.68	0.165	0.042	0.255	0.334	0.68	0.065	0.031	0.159	0.196	0.046	0.307																	0.049	0.314
F025	0.67	0.169	0.028	0.168	0.406	0.83	0.072	0.045	0.134	0.336	0.023	0.370	0.77	0.70	1.10	0.046	0.028	0.068	0.038	0.106	0.079	0.387	0.36	0.55	0.65	0.357	454	0.386	0.054	0.369
F028	0.94	0.116	0.026	0.224	0.282								0.63	0.84	0.75				0.035			0.291	0.26	0.52	0.50	0.283	645	0.295	0.057	0.274
F031	0.63	0.146	0.041	0.279	0.316	0.81	0.080	0.036	0.160	0.225	0.035	0.403	0.61	0.51	1.20							0.315	0.51	0.37	1.38	0.354			0.050	0.461
F033																														
F034	0.78	0.163	0.047	0.290	0.371	0.91	0.090	0.037	0.157	0.236	0.050	0.352														0.341			0.056	0.349
F037						0.84	0.072	0.038	0.145	0.262	0.030	0.322	0.39	0.47	0.83				0.040			0.309	0.37	0.31	1.19	0.400	472	0.312		
F041	0.65		0.029		0.288	0.72	0.056	0.026	0.140	0.186	0.034	0.329	0.70	0.60	1.17				0.032			0.291	0.39	0.68	0.57	0.280	540	0.282	0.053	0.273
F042	0.75	0.146	0.035	0.242	0.331	0.54	0.050	0.040	0.121	0.331	0.031	0.294										0.266					1431	0.267	0.041	0.258
F043	0.71	0.166	0.033	0.198	0.346	0.79	0.064	0.046	0.147	0.313	0.033	0.369	0.88	0.64	1.38	0.042	0.020	0.043	0.042	0.091	0.059	0.354	0.55	0.30	1.83	0.336	618	0.347	0.067	0.366
F046	0.74	0.158	0.035	0.222	0.335	0.67	0.055	0.036	0.157	0.229	0.043	0.353	0.52	0.56	0.93	0.030	0.020	0.042	0.062	0.108	0.068	0.377	0.37	0.49	0.76	0.342	350	0.342		
F050	0.72	0.187	0.051	0.272	0.501	0.85	0.094	0.052	0.181	0.287	0.044	0.480	0.66	0.39	1.69	0.043	0.128	0.048	0.054	0.102	0.071	0.519	0.57	0.35	1.63	0.518	595	0.524	0.055	0.516
F051	0.71	0.158	0.049	0.310	0.339	0.71	0.072	0.049	0.154	0.318	0.037	0.274	0.55	0.64	0.86							0.337	0.33	0.42	0.79	0.335	400	0.328	0.048	0.392
F053	0.73	0.164	0.039	0.235	0.364	0.69	0.048	0.043	0.149	0.289	0.040	0.341	0.46	0.64	0.72				0.039			0.336	0.37	0.50	0.74	0.342	549	0.322		
F054	0.74	0.191	0.049	0.258	0.503	0.86	0.091	0.048	0.195	0.246	0.038	0.506	0.66	0.42	1.57	0.045	0.014	0.062	0.052	0.113	0.073	0.536	0.53	0.44	1.20	0.520	801	0.519	0.055	0.515
F063	0.86	0.141	0.035	0.251	0.386	0.98	0.120	0.038	0.166	0.229	0.049	0.413	0.58	0.52	1.12	0.038	0.018	0.049	0.067	0.117	0.060	0.438	0.74	0.40	1.85	0.341	652	0.405	0.048	0.422
F066	0.85	0.148	0.035	0.234	0.374	0.94	0.093	0.043	0.156	0.276	0.046	0.369	0.68	0.71	0.96	0.045	0.026	0.066	0.037	0.103	0.060	0.370	0.51	0.34	1.50	0.370	581	0.362	0.033	0.368
F080	0.73	0.170	0.035	0.204	0.439	0.88	0.092	0.050	0.170	0.294	0.046	0.396	0.63	0.53	1.19	0.045	0.019	0.061	0.022	0.106	0.075	0.420	0.51	0.37	1.38	0.402	438	0.433	0.039	0.444
F084	0.69	0.223	0.031	0.140	0.488	0.72	0.092	0.047	0.214	0.220	0.056	0.569	0.58	0.57	1.02	0.040	0.030	0.060	0.053	0.114	0.092	0.443	0.33	0.22	1.50	0.576	429	0.567	0.035	0.546
F085	0.71	0.144	0.021	0.149	0.298	0.89	0.076	0.023	0.139	0.165	0.031	0.295	0.78	0.85	0.92							0.290	0.41	0.50	0.82	0.313	483	0.305	0.036	0.294

Appendix B1

Table App.B1- 2D/Doppler echocardiographic variables from normal cats

cat	*Pulmonary venous flow*																					
	Smax (m/sec)	S12 (m/sec)	S1 (m/sec)	S2 (m/sec)	D (m/sec)	Ar (m/sec)	S/D	S VTI (m)	D VTI (m)	Ar VTI (m)	S dur (sec)	D dur (sec)	D dec (sec)	Ar dur (sec)	Adur/Ardur	Q-tS (sec)	Q-Smax (sec)	Q-S12 (sec)	Q-S1 (sec)	Q-S2 (sec)	Q-D (sec)	Q-A (sec)	R-R (sec)
F010																							
F011	0.38	0.38			0.41	0.18	0.94	0.042	0.030	0.010	0.193	0.119	0.050	0.074	0.92	0.023	0.045	0.045			0.268	0.325	0.337
F012	0.30		0.30	0.38	0.57	0.30	0.53	0.055	0.071	0.010	0.197	0.198	0.135			0.061	0.091		0.091	0.181	0.326	0.463	0.479
F014	0.44		0.44	0.18	0.38	0.20	1.16	0.042	0.030	0.010	0.190	0.134	0.058	0.090	0.82	0.024	0.055		0.055	0.171	0.291	0.303	0.326
F015																							
F025	0.44	0.44			0.36	0.19	1.24	0.050	0.046	0.010	0.187	0.198	0.091	0.065	1.22	0.044	0.064	0.064			0.307	0.392	0.404
F028	0.52	0.52			0.48	0.22	1.09	0.042	0.046	0.010	0.137	0.151	0.017	0.091		0.031	0.045	0.045			0.306	0.283	0.292
F031																							
F033																							
F034	0.44	0.44			0.39	0.23	1.14	0.056	0.043	0.010	0.195	0.144	0.048	0.105		0.006	0.038	0.038			0.295	0.305	0.347
F037	0.49	0.49			0.48	0.19	1.03	0.056	0.032	0.010	0.178	0.100	0.035	0.095		0.019	0.040	0.040			0.254	0.252	0.266
F041	0.39	0.39			0.55	0.24	0.70	0.030	0.048	0.010	0.136	0.138	0.030	0.079		0.044	0.071	0.071			0.290	0.254	0.269
F042	0.35		0.35	0.24	0.52	0.39	0.67	0.036	0.032	0.010	0.168	0.101	0.049	0.053		0.021	0.042		0.042	0.162	0.246	0.293	0.258
F043	0.37		0.37	0.29	0.31	0.22	1.19	0.054	0.028	0.010	0.211	0.134	0.075	0.063	0.94	0.027	0.076		0.076	0.190	0.301	0.366	0.370
F046	0.37		0.37	0.28	0.35	0.19	1.07	0.055	0.030	0.010	0.234	0.133	0.092	0.076	0.89		0.065		0.065	0.197	0.276	0.365	0.367
F050	0.20	0.20			0.39	0.15	0.52	0.048	0.043	0.010	0.249	0.203	0.136	0.082	0.87	0.057	0.123	0.123			0.342	0.499	0.568
F051	0.41	0.41			0.43	0.19	0.97	0.068	0.032	0.010	0.237	0.104	0.065	0.059		0.020	0.037	0.037			0.276	0.342	0.345
F053	0.37		0.37	0.28	0.35	0.19	1.07	0.055	0.030	0.010	0.234	0.133	0.092	0.076			0.065		0.065	0.197	0.276	0.365	0.367
F054	0.22	0.22			0.44	0.19	0.51	0.050	0.045	0.010	0.255	0.185	0.102	0.081	0.90	0.019	0.076		0.076	0.197	0.354	0.645	0.610
F063	0.21	0.21			0.32	0.09	0.64	0.018	0.032	0.010	0.162	0.198	0.100	0.071	0.85	0.041	0.098	0.098			0.310	0.412	0.428
F066	0.51		0.51	0.32	0.41	0.41	1.24	0.078	0.032	0.020	0.221	0.113	0.053	0.081	0.74	0.017	0.064		0.064	0.187	0.294	0.368	0.375
F080	0.44		0.44	0.19	0.39	0.31	1.13	0.053	0.034	0.014	0.225	0.172	0.063	0.073	1.02	0.018	0.060		0.060	0.187	0.318	0.437	0.438
F084	0.43		0.43	0.28	0.30	0.36	1.47	0.074	0.036	0.020	0.272	0.211	0.105	0.084	1.10	0.024	0.070		0.070	0.229	0.366	0.570	0.549
F085	0.50		0.50	0.20	0.27	0.19	1.85	0.048	0.012		0.201	0.076	0.039			0.016	0.050	0.050			0.255	0.287	0.300

Table App.B2-2D/Doppler echocardiographic variables from HCM cats

cat	status	sex	age (years)	weight (Kg)	*Two-Dimensional measurements*								*M-mode measurements*											*Mitral annulus m.*	
					LA area d (mm^2)	LA dist d (mm)	LA area s (mm^2)	LA dist s (mm)	LA FS%	LA length d (mm)	Ao diam d (mm)	LAd/Aod	IVSd (mm)	LV diam.d (mm)	LVPW d (mm)	IVSs (mm)	LV diam.s (mm)	LVPWs (mm)	LV FS%	R-R (sec)	MV EPSS (mm)	Aort.v Aod (mm)	Aort.v:LAs (mm)	LAs/Aod	MAM sep (mm)	MAM lat (mm)
F004	asympt.	MN	10	4.50	205	14.8	270	16.8	11	15.2	8.3	1.8	8.3	12.2	5.0	10.0	3.6	10.1	71	0.260	0.20	9.1	16.6	1.83	2.8	4.7
F009	asympt.	MN	7	5.20	117	9.6	204	11.8	18	11.8	8.5	1.4	6.8	15.4	5.7	8.0	6.1	9.1	60	0.394	1.48	10.3	14.0	1.36	5.5	6.4
F013	asympt.	MN	8	6.80						12.6	8.9	1.4	7.3	13.3	5.1	9.9	4.3	9.4	67	0.331		8.3	12.3	1.48		
F018	asympt.	MN	10	4.50	314	14.2	365	16.8	16	14.3	9.0	1.6	7.4	15.2	7.1	10.3	4.9	12.0	67	0.304	1.02	10.3	15.9	1.55	2.6	
F024	asympt.	MN	3	6.45	431	21.1	560	24.2	13	19.8	8.8	2.2	9.2	14.2	7.4	11.1	10.8	10.3	28	0.383		9.3	20.9	2.24	3.3	
F030	asympt.	MN	9	6.30	200	15.2	325	19.2	21	13.6	8.1	1.7	6.9	14.8	6.8	9.9	4.6	9.7	68	0.395	0.75	8.1	15.2	1.88	4.0	7.7
F032	asympt.	MN	12	5.50	154	10.8	219	13.2	18	12.8	8.5	1.5	8.2	9.5	7.8	10.3	3.9	11.0	60	0.271	0.35	9.6	13.6	1.42	4.3	7.5
F038	asympt.	MN	10	5.00	127	11.5	184	14.8	22	14.2	6.9	2.1	6.1	16.9	4.3	11.0	7.8	7.8	54	0.395	1.50	7.8	12.9	1.66		
F044	asympt.	MN	7	4.50	113	9.9	180	11.6	15	12.2	9.3	1.3	5.9	14.4	5.4	8.2	7.4	8.4	50	0.395	2.17	9.4	13.7	1.46		
F052	asympt.	MN	9	4.20	126	10.4	244	14.2	27	11.9	7.9	1.5	3.9	16.4	6.8	7.9	8.3	9.6	50	0.383	1.28	8.7	16.7	1.92	4.7	5.8
F057	asympt.	FN	7	4.40	173	13.6	225	16.2	16	15.4	7.4	2.1	6.7	12.9	7.5	8.1	8.1	9.2	38	0.295	0.68	8.1	16.4	2.02		
F069	asympt.	FN	4	4.15	66	7.1	121	10.6	33	10.0	7.5	1.3	4.6	18.3	4.2	8.8	7.6	7.1	59	0.390	1.08	8.0	12.4	1.54	4.8	4.4
F071	asympt.	MN	7	6.70	112	9.9	217	12.3	20	13.5	9.7	1.4	6.7	15.4	5.8	9.1	6.4	9.3	58	0.398	1.42	10.7	15.3	1.43	4.0	4.9
F073	asympt.	MN	5	6.15	140	11.7	214	15.2	23	12.9	9.3	1.4	4.1	17.2	6.0	8.9	5.9	9.7	67	0.337	1.40	9.8	14.8	1.51	3.4	3.3
F081	asympt.	MN	3	4.75	128	10.5	236	13.6	23	13.9	8.3	1.7	7.4	18.1	5.8	9.8	7.3	9.7	60	0.300	0.53	9.8	14.0	1.43	3.6	4.2
F086	asympt.	MN	7	4.40	82	8.5	142	11.9	29				6.3	15.8	3.9	9.8	4.1	9.3	75	0.359	0.68	7.2	12.8	1.78	3.7	4.9
F091	asympt.	FN	5	4.90	83	8.3	160	11.7	29	10.1	8.2	1.2	6.3	13.7	3.8	8.3	4.3	8.8	69	0.320	0.42	9.8	10.9	1.11	3.4	7.3
F093	asympt.	MN	9	6.70	79	8.8	166	11.2	21				6.9	13.8	4.9	10.7	3.7	9.6	73	0.341	1.42	9.9	11.6	1.17	3.8	4.6
F029	CHF	MN	5	4.90	498	20.8	555	20.3	-2	21.9	8.5	2.6	8.2	14.5	8.0	9.7	8.7	9.0	41	0.315	0.80	9.0	23.2	2.57	2.2	2.2
F060	CHF	MN	2	3.30						19.3	5.7	3.4	4.3	17.6	4.7	8.2	6.6	9.4	63	0.342	0.60	7.4	20.8	2.82		
F067	CHF	MN	9	4.80	221	16.9	267	16.6	-2	15.4	9.0	1.7	6.2	17.6	3.0	5.3	12.8	4.1	27	0.258	1.98	10.0	15.3	1.52	2.1	
F082	CHF	MN	11	5.80	815	30.5	829	31.4	3	28.6	7.8	3.7	5.0	15.9	7.7	5.6	11.7	8.2	27	0.414		7.6	28.1	3.68	1.9	3.0
F092	CHF	MN	4	4.50	514	25.0	593	26.1	4	21.6	8.1	2.7	9.2	14.1	8.7	11.2	7.5	11.6	47	0.350	0.53	11.1	21.5	1.93		

Table App.B2-2D/Doppler echocardiographic variables from HCM cats

cat	*Pulmonary artery: Right*					*Aortic valve: Left Apical*							*Mitral valve*										*Tricuspid inflow*				*CFM*		*IVRT (LV)*	
	PA vmax (m/sec)	ET (sec)	PEP (sec)	PEP/ET	R-R (sec)	Ao vmax (m/sec)	Ao VTI (m)	PEP (sec)	ET (sec)	PEP/ET	Acc. t (sec)	R-R (sec)	E (m/sec)	A (m/sec)	E/A	E VTI (m)	A VTI (m)	E dec t (sec)	E acc t (sec)	E dur (sec)	A dur (sec)	R-R (sec)	E vmax (m/sec)	A vmax (m/sec)	E/A	R-R (sec)	FPV (mm/sec)	R-R (sec)	IVRT (sec)	R-R (sec)
F004						1.16	0.1	0.0366	0.150	0.244	0.05	0.336										0.300					724	0.261	0.030	0.280
F009	1.03	0.157	0.030		0.388	0.93	0.09	0.071	0.174	0.406	0.071	0.401	0.63	0.70	0.90	0.040	0.035	0.072	0.048	0.127	0.096	0.403	0.45	0.41	1.10	0.444	407	0.360	0.056	0.378
F013																														
F018	0.72	0.150	0.047	0.314	0.344	2.49	0.28	0.038	0.167	0.226	0.052	0.353										0.331				0.335			0.068	0.335
F024	1.00	0.136	0.029	0.215	0.383	0.82	0.07	0.028	0.152	0.184	0.050	0.352																		
F030	0.69	0.171	0.041	0.239	0.382	4.92	0.37	0.050	0.129	0.384	0.084	0.389	0.81	0.59	1.37	0.053	0.017	0.061	0.052	0.112	0.051	0.416	0.63	0.46	1.37	0.406			0.052	0.414
F032	1.81	0.153	0.059	0.387	0.271																	0.257								
F038	1.06	0.149	0.047	0.317	0.345																		0.50	0.46	1.09	0.350	303	0.397		
F044	1.00		0.042		0.396	0.96	0.08	0.034	0.166	0.204	0.038	0.439	0.60	0.67	0.89	0.042	0.030	0.069	0.050	0.119	0.085	0.541	0.58	0.34	1.71	0.492	249	0.489	0.072	0.520
F052	0.93	0.135	0.040	0.297	0.388	3.86	0.43	0.049	0.178	0.276	0.116	0.407	0.58	0.75	0.77							0.398	0.68	0.30	2.27	0.414	380	0.379	0.058	0.396
F057	2.13		0.050		0.277																	0.286					397	0.304		
F069	0.78	0.165	0.035	0.214	0.364	3.73	0.35	0.031	0.161	0.193	0.096	0.343	0.58	0.72	0.81							0.313	0.53	0.41	1.29	0.366	448	0.326	0.056	0.331
F071	0.80	0.173	0.036	0.208	0.428	1.20	0.14	0.039	0.162	0.241	0.039	0.385	0.58	0.50	1.16	0.040	0.030	0.086	0.036	0.123	0.091	0.400					397	0.376	0.056	0.359
F073	1.12	0.137	0.041	0.296	0.339	5.01	0.36	0.041	0.140	0.289	0.095	0.339										0.340	0.37	0.35	1.06	0.369	392	0.329	0.084	0.351
F081	1.40	0.110	0.034	0.308	0.314	0.99	0.11	0.033	0.158	0.206	0.065	0.344	0.50	0.55	0.91	0.040		0.089	0.055	0.142		0.364	0.42	0.50	0.84	0.382	263	0.391	0.058	0.375
F086	1.18	0.160	0.042	0.265	0.385	2.86	0.24	0.036	0.150	0.237	0.105	0.374	0.52	0.89	0.58	0.035	0.052	0.078	0.030	0.109	0.101	0.402	0.55	0.48	1.15	0.388			0.040	0.371
F091	1.19	0.141	0.030	0.213	0.311	0.72	0.06		0.129		0.038	0.310										0.286				0.300	514	0.317	0.059	0.321
F093	0.90	0.146	0.044	0.298	0.299	1.36	0.14		0.146		0.062	0.376	0.67	0.75	0.89							0.340	0.48	0.50	0.96	0.340	315	0.354		
F029	0.88	0.137	0.058	0.423	0.307	0.88	0.06	0.055	0.122	0.452	0.045	0.328	0.74	0.36	2.05	0.030		0.035	0.042	0.075		0.327	0.45	0.50	0.89	0.322			0.035	0.325
F060	0.91	0.157	0.051	0.328	0.367																	0.349					199	0.339		
F067	0.61	0.115	0.046	0.397	0.258	0.68	0.06	0.050	0.116	0.429	0.028	0.251										0.260					443	0.254	0.040	0.266
F082	0.29	0.155	0.080	0.518	0.405	0.64	0.06	0.050	0.178	0.278	0.027	0.429	1.12			0.082		0.089	0.041	0.128		0.414				0.378	480	0.455		
F092	1.15	0.144	0.036	0.247	0.369	1.02	0.09	0.051	0.148	0.345	0.030	0.371	0.30	0.25	1.20			0.074	0.049	0.124		0.390								

Table App.B2-2D/Doppler echocardiographic variables from HCM cats

cat	*Pulmonary venous flow*																					
	Smax (m/sec)	S12 (m/sec)	S1 (m/sec)	S2 (m/sec)	D (m/sec)	Ar (m/sec)	S/D	S VTI (m)	D VTI (m)	Ar VTI (m)	S dur (sec)	D dur (sec)	D dec (sec)	Ar dur (sec)	Ader/Ardur	Q-bS (sec)	Q-Smax (sec)	Q-S12 (sec)	Q-S1 (sec)	Q-S2 (sec)	Q-D (sec)	Q-A (sec)	R-R (sec)
F004																							
F009	0.49	0.49			0.37	0.33	1.3	0.080	0.050	0.020	0.232	0.169	0.082	0.103	0.93	0.030	0.073		0.073		0.348	0.442	0.421
F013																							
F018	0.46	0.46			0.36	0.19	1.3	0.048	0.038	0.010	0.176	0.153	0.080	0.099		0.021	0.049		0.049		0.249	0.333	0.379
F024	0.32	0.32			0.21	0.19	1.5	0.037	0.022	0.010	0.189	0.176	0.117	0.133		0.022	0.126		0.126		0.284	0.413	0.399
F030	0.52	0.52			0.34	0.48	1.5	0.068	0.025	0.022	0.197	0.127	0.046	0.086	0.59	0.039	0.091		0.091		0.301	0.373	0.399
F032	0.69	0.69			0.40	0.56	1.7	0.063	0.028	0.018	0.168	0.107	0.045	0.067		0.042	0.088		0.088		0.271	0.325	0.294
F038	0.40		0.40	0.20	0.27	0.21	1.5	0.042	0.023	0.012	0.195	0.135	0.075	0.115		0.023	0.056	0.056		0.189	0.280	0.365	0.369
F044	0.37		0.37	0.19	0.25	0.34	1.5	0.048	0.025	0.015	0.261	0.170	0.111	0.094	0.91	0.022	0.063	0.063		0.227	0.347	0.476	0.457
F052	0.45		0.45	0.32	0.27	0.38	1.6	0.067	0.020	0.010	0.247	0.128	0.068	0.056		0.019	0.085	0.085		0.204	0.328	0.412	0.396
F057																							
F069	0.64	0.64			0.35	0.24	1.8	0.060	0.022	0.010	0.182	0.100	0.063	0.086		0.037	0.122		0.122		0.254	0.268	0.307
F071	0.44		0.44	0.29	0.24	0.43	1.8	0.063	0.018	0.012	0.240	0.123	0.070	0.063	1.44	0.025	0.076	0.076		0.183	0.319	0.399	0.391
F073	0.44		0.44	0.23	0.23	0.27	1.9	0.057	0.012	0.010	0.251	0.102	0.052	0.090		0.021	0.121	0.121		0.227	0.320	0.320	0.352
F081	0.55	0.55			0.27	0.58	2.0	0.050	0.020	0.020	0.203	0.141	0.063	0.064		0.049	0.082		0.082		0.317	0.415	0.406
F086																							
F091	0.47	0.47			0.32	0.21	1.5	0.045	0.041	0.010	0.134	0.172	0.104	0.082									
F093	0.52	0.52			0.29	0.24	1.8	0.065	0.030	0.010	0.204	0.140	0.055	0.081									0.363
F029	0.22	0.22			0.61	0.37	0.4	0.012	0.037	0.010	0.133	0.115	0.059	0.071		0.033	0.084	0.084	0.084		0.261	0.311	0.320
F060																							
F067	0.16	0.16			0.49	0.38	0.3	0.010	0.023	0.018	0.128	0.104	0.048	0.100		0.045	0.071	0.071	0.071		0.222	0.255	0.261
F082					0.57		0.4	0.018	0.080		0.153	0.249	0.148			0.060	0.121	0.121	0.121		0.364		0.492
F092	0.23	0.23			0.24	0.20	1.0	0.022	0.018	0.010	0.154	0.163		0.111		0.059	0.117	0.117	0.117		0.286	0.382	0.363

Appendix B2

Table App.B3 Linear regression and multiple linear regression equations for independent variables significantly influencing 2D/Doppler echocardiographic variables in normal cats

Normal Parameter	Forward stepwise regression analysis	Linear and multiple linear regression equations	R	R^2	Adjusted R^2	p
LA area s	Sex (p=0.020)	LA area s = 239.400 - (49.700 * sex)	0.538	0.290	0.250	<0.05
LA diam.d	R-R (p=0.044)	LA diam.d = 9.040 + (15.671 * R-R)	0.491	0.241	0.205	<0.05
LVPW d	R-R (p=0.002)	LVPW d = 0.823 + (8.086 * R-R)	0.668	0.447	0.420	<0.001
LV diam.s	R-R (p=0.003)	LV diam.s = 0.803 + (20.118 * R-R)	0.627	0.393	0.365	<0.01
Aort.v:LAs	Sex (p=0.014)	Aort.v:LAs= 15.347 - (1.945 * sex)	0.503	0.253	0.219	<0.05
LAs/Aod	Sex (p=0.014)	LAs/Aod = 1.672 - (0.220 * sex)	0.532	0.283	0.251	<0.01
ET RV	RR (p<0.001);sex (p=0.059);weight (p=0.051)	ET RV = 0.127 + (0.243 * RR) - (0.0147 * sex) - (0.00825 * weight)	0.875	0.765	0.715	<0.001
Ao VTI	RR (p=0.020)	Ao VTI = 0.0283 + (0.130 * RR)	0.556	0.309	0.274	<0.01
PEP LV	RR (p=0.004); weight (p=0.015)	PEP LV = -0.0112 + (0.0779 * RR) + (0.00537 * weight)	0.645	0.416	0.354	<0.01
ET LV	RR (p<0.001); sex (p=0.003)	ET LV = 0.0952 + (0.229 * RR) - (0.0167 * sex)	0.906	0.820	0.801	<0.001
PEP/ET LV	Weight (p=0.009); sex (p=0.041)	PEP/ET LV = 0.0136 + (0.0529 * sex) + (0.0400 * weight)	0.576	0.332	0.261	<0.05
Acc. t	Sex (p=0.082)	Acc. t = 0.0510 - (0.00825 * sex)	0.479	0.229	0.191	<0.05
A	RR (p=0.029)	A = 0.991 - (1.066 * RR)	0.641	0.411	0.379	<0.01
E/A	RR (p=0.008); age (p<0.001)	E/A = 0.746 + (1.727 * RR) - (0.0443 * age)	0.866	0.749	0.720	<0.001
E VTI	Sex (p=0.088)	E VTI = 0.0307 + (0.00705 * sex)	0.559	0.313	0.250	0.047
E dec t	Sex (p=0.059)	E dec t = 0.0405 + (0.0107 * sex)	0.558	0.312	0.249	0.047
E dur	RR (p=0.018); age (p=0.082)	E dur = 0.0412 + (0.127 * RR) + (0.00155 * age)	0.763	0.581	0.498	<0.05
FPV	Age (p=0.049)	FPV = 791.433 - (33.003 * age)	0.520	0.270	0.222	<0.05
IVRT	Age (p=0.059); weight (p=0.011)	IVRT = 0.0218 - (0.00114 * age) + (0.00720 * weight)	0.636	0.404	0.334	<0.05
E (tr)	Age (p=0.005)	E vmax = 0.574 - (0.0191 * age)	0.599	0.359	0.319	<0.01
E/A (tr)	Age (p=0.027)	E/A = 1.569 - (0.0684 * age)	0.568	0.323	0.280	<0.05

Table App.B4 Linear regression and multiple linear regression equations for independent variables significantly influencing 2D/Doppler echocardiographic variables in normal cats

Normal						
Parameter	Forward stepwise regression analysis	Linear and multiple linear regression equations	R	R^2	Adjusted R^2	p
Smax	RR (p=0.009); age (p=0.015)	Smax = 0.507 - (0.483 * RR) + (0.0113 * age)	0.744	0.554	0.501	<0.001
D	Sex (p=0.010); weight (p=0.031)	D = 0.0247 + (0.107 * sex) + (0.0487 * weight)	0.714	0.509	0.452	<0.01
S/D	Age (p=0.019); weight (p=0.020)	S/D = 1.418 + (0.0600 * age) - (0.170 * weight)	0.682	0.465	0.402	<0.01
S VTI	Age (p=0.025)	ns	ns			ns
D VTI	RR (p=0.002); sex (p=0.002); weight (p=0.002)	D VTI = -0.056 + (0.014 * sex) + (0.0097 * weight) + (0.071 * RR)	0.824	0.679	0.618	<0.001
Ar VTI	Weight (p<0.017)	Ar VTI = 0.0218 - (0.00232 * weight)	0.525	0.275	0.233	<0.05
S dur	RR (p<0.001); age (p<0.046)	S dur = 0.0693 + (0.291 * RR) + (0.00378 * age)	0.788	0.621	0.576	<0.001
D dur	RR (p<0.001)	D dur = 0.0251 + (0.318 * RR)	0.794	0.630	0.610	<0.001
D dec	RR (p<0.001)	D dec = -0.0342 + (0.275 * RR)	0.827	0.684	0.667	<0.001
Q-Smax	RR (p<0.01)	Q-Smax = 0.00561 + (0.151 * RR)	0.694	0.481	0.452	<0.001
Q-S1	RR (p<0.001)	Q-S1 = -0.0297 + (0.255 * RR)	0.813	0.660	0.618	<0.01
Q-S12	RR (p<0.01)	Q-S12 = 0.0320 + (0.0831 * RR)	0.666	0.444	0.374	<0.05
Q-S2	RR (p<0.002	Q-S2 = 0.143 + (0.113 * RR)	0.668	0.446	0.377	<0.05
Q-D	RR (p<0,001)	Q-D = 0.188 + (0.286 * RR)	0.887	0.787	0.775	<0.001
Q-Ar	RR (p<0.001)	Q-Ar = -0.0103 + (1.005 * RR)	0.975	0.951	0.948	<0.001
MAM lat	Sex (p=0.058); weight (p=0.002)	MAM lat = 14.225 - (1.266 * sex) - (1.523 * weight)	0.739	0.547	0.486	<0.01

Table App.B5 Linear regression and multiple linear regression equations for independent variables significantly influencing 2D/Doppler echocardiographic variables in HCM cats

HCM						
Parameter	Forward stepwise regression analysis	Linear and multiple linear regression equations	R	R^2	Adjusted R^2	p
Ao diam d	Weight (p=0.016)	Ao diam d = 5.395 + (0.563 * weight)	0.586	0.343	0.308	<0.01
IVSd	R-R (p=0.044)	ns	ns			
PA. vmax	RR (p=0.068)	PA. vmax = 2.421 - (3.997 * RR)	0.482	0.232	0.192	<0.05
ET RV	RR (p=0.003)	ET RV = 0.0719 + (0.214 * RR)	0.596	0.355	0.317	<0.01
PEP RV	Age (p=0.032)	ns				
ET LV	RR (p=0.002)	ET LV = 0.0372 + (0.314 * RR)	0.743	0.551	0.521	<0.001
E	Age (p=0.056)	E = 0.245 + (0.0571 * age)	0.704	0.496	0.446	<0.05
A	Age (p=0.065)	A = 0.493 + (0.0158 * age)	0.491	0.242	0.199	<0.05
FPV	RR (p=0.053); age (p=0.043)	FPV = 635.789 - (1123.793 * RR) + (22.525 * age)	0.704	0.495	0.411	<0.05
E (tr)	Age (p=0.034)	ns	ns			ns
Smax	Age (p=0.050); sex (p=0.013)	Smax = 0.302 + (0.0145 * age)	0.555	0.308	0.269	<0.05
S12	Sex (p=0.040)	ns				
S/D	RR (p=0.028); sex (p=0.037)	ns				
D VTI	RR (p=0.043)	D VTI = -0.0208 + (0.133 * RR)	0.479	0.230	0.178	=0.052
D dur	RR (p<0.001)	D dur = -0.0563 + (0.527 * RR)	0.817	0.667	0.645	<0.001
D dec	RR (p=0.002)	D dec = -0.0637 + (0.367 * RR)	0.758	0.575	0.544	<0.001
Q-D	RR (p<0.001)	Q-D = 0.0801 + (0.578 * RR)	0.855	0.731	0.712	<0.001
Q-Ar	RR (p<0.001)	Q-Ar = -0.0440 + (1.115 * RR)	0.929	0.863	0.853	<0.001

Appendix D1

Table App.D1-pulsed TDI indices (sep MA normal group)

cat	sex	age (years)	weight (Kg)	thickness (mm)	R-R (sec)	E'/A'	E' (cm/s)	E' VTI (cm)	E' dur (sec)	E' acc (cm/s^2)	tE' acc (sec)	E' dec (cm/s^2)	tE' dec (sec)	A' (cm/s)	A' VTI (cm)	A' dur (sec)	EA' (cm/s)	EA' VTI (cm)
F010	MN	10	6.3	5.55	0.387	1.10	9.15		0.086	258	0.036	188	0.049	8.33		0.061		
F011	FN	2	4	4.04	0.354	1.15	7.57		0.092	227	0.034	143	0.059	6.59		0.050		
F012	FN	2	5.6	4.22	0.495	1.54	7.50		0.096	307	0.025	112	0.067	4.87		0.076		
F014	MN	6	4.8	4.97	0.381	1.03	8.04		0.090	180	0.045	185	0.047	7.80		0.060	8.59	
F015	MN	6	4.4	3.73	0.337	0.72	7.15			213	0.033			9.97				
F022	MN	3	5.9	4.16	0.437	0.82	11.18	0.72	0.100	235	0.050	236	0.048	13.69	0.53	0.055		
F025	FN	9	4.7	4.87	0.419	0.80	4.52							5.68				
F028	FN	7	4.9	4.26	0.288	0.83	9.67							11.61			12.39	0.78
F031	FN	4	3.5	3.85	0.334	1.14	7.13	0.31	0.080	256	0.028	130	0.056	6.28	0.24	0.057		
F033	FN	8	3.7	5.4	0.400	0.64	3.57	0.18	0.070	137	0.029	77	0.045	5.58	0.22	0.064		
F034	MN	8	5.7	4.93	0.441	0.92	4.73	0.20	0.077	129	0.033	97	0.046	5.14	0.25	0.073		
F037	FN	4	4	3.1	0.352	1.09	5.84	0.28	0.080	182	0.033	113	0.052	5.36	0.25	0.072		
F041	FN	5	4.6	3.64	0.332	1.10	6.28	0.34	0.080	212	0.032	152	0.044	5.72	0.28	0.070		
F042	FN	3	4.3	4.1	0.313	0.90	7.13							7.89				
F043	MN	1	4.5	2.7	0.427	1.10	5.69	0.33	0.083	158	0.040	139	0.045	5.19	0.28	0.090		
F046	MN	10	4.2	3.97	0.393	0.91	5.38	0.34	0.092	113	0.047	112	0.047	5.89	0.28	0.058		
F050	FN	1	4	4.24	0.488	1.43	4.99	0.31	0.086	125	0.041	110	0.050	3.50	0.15	0.062		
F051	MN	14	6.2	5.54	0.361	0.90	4.88	0.23	0.070	197	0.027	114	0.045	5.40	0.25	0.072		
F053	FN	9	4	4.4	0.364	0.76	4.35	0.27	0.090	109	0.039	91	0.046	5.73				
F054	MN	1	4.5	4.4	0.573	1.61	7.73	0.46	0.097	170	0.048	167	0.050	4.79	0.23	0.086		
F063	MN	4	5	4.3	0.387	1.37	6.76	0.31	0.085	202	0.034	144	0.048	4.94	0.17	0.053		
F066	FN	7	3 8	3.41	0.408	0.96	4.98	0.34	0.103	131	0.038	81	0.063	5.21	0.26	0.075		
F080	MN	9	3.9	3.6	0.529	1.16	4.94	0.34	0.107	95	0.053	86	0.058	4.28	0.20	0.073		
F084	MN	9	3.3	4.84	0.587	0.74	5.07	0.29	0.103	117	0.045	86	0.062	6.84	0.32	0.083		
F085	MN	9	4.4	5.22	0.312	0.84	6.84							8.15				

Appendix D1

Table App.D1-pulsed TDI indices (sep MA normal group)

cat	Se' (cm/s)	Sl' (cm/s)	S' VTI (cm)	S' dur (sec)	Se' acc (cm/s^2)	tSe' acc (sec)	bS'-Sl' (sec)	Q-Se' (sec)	Q-Sl' (sec)	Q-bS' (sec)	Q-E' (sec)	Q-A' (sec)	Q-bE' (sec)	IVCt (sec)	IVRt (sec)	IVRb (cm/s)	IVRa (cm/s)	IVCa (cm/s)	IVCb (cm/s)
F010	7.21	6.46		0.150	332	0.022	0.065	0.071	0.088	0.049	0.275	0.380		0.020	0.049	2.94	5.34	4.54	3.44
F011	7.76	5.88		0.142	516	0.017	0.050	0.070	0.101	0.054	0.283	0.365		0.034	0.059	4.39	4.49		
F012	8.25	6.13		0.168	421	0.021	0.071	0.086	0.143		0.317	0.491		0.038	0.058	3.47	3.75	2.78	6.60
F014	7.03	5.54		0.170	242	0.029	0.080	0.090	0.098	0.060	0.312	0.366		0.030	0.044	2.61	3.55	2.69	3.52
F015	9.75	5.63		0.150	310	0.031	0.073	0.076	0.126	0.045	0.276	0.323		0.028	0.046		5.56		
F022	9.91	6.61	0.97	0.168	533	0.022	0.053	0.090	0.145		0.338	0.423	0.296		0.040	4.28	4.10	13.59	6.94
F025	6.68	4.86	0.54	0.144	279	0.025	0.059	0.099	0.134	0.079	0.324	0.426				4.10	3.05		12.16
F028	11.58	7.28	0.81	0.128	526	0.024	0.078	0.070	0.130	0.049				0.016	0.056	5.52	4.56		5.75
F031	10.60	4.91	0.69	0.141	391	0.027	0.071	0.077	0.120	0.053	0.262	0.343	0.235	0.019	0.049		3.28		7.90
F033	5.47	4.30	0.48	0.153	235	0.024	0.056	0.088	0.126	0.070	0.322	0.391	0.293	0.057	0.083	2.93		2.46	3.40
F034	4.40	2.60	0.46	0.187	131	0.032	0.094	0.124	0.192	0.083	0.354	0.435	0.328	0.069	0.073	1.84	2.29	2.72	2.63
F037	7.01	4.01	0.55	0.142	223	0.032	0.079	0.097	0.146	0.068	0.285	0.353	0.253	0.034	0.058	3.46	4.29		
F041	6.32	4.20	0.56	0.143	246	0.027	0.082							0.034	0.051	4.08	4.41	5.00	7.56
F042	5.92	4.18	0.50	0.137	221	0.028	0.079	0.071	0.129	0.042	0.243	0.282	0.225	0.041	0.059	3.17	4.83	3.50	4.91
F043	7.50	3.88	0.62	0.168	291	0.028	0.095	0.068	0.138	0.049	0.308	0.413	0.265	0.030	0.070		4.03		5.01
F046	5.77	3.55	0.50	0.140	242	0.025	0.090			0.069				0.043	0.072	3.08	2.53	4.68	6.99
F050	6.12	3.12	0.47	0.148	324	0.019	0.082	0.096	0.160	0.081	0.351	0.485	0.311	0.055	0.080				5.72
F051	5.37	4.25	0.49	0.138	232	0.025	0.069	0.090	0.128	0.071	0.285	0.377	0.258	0.036	0.054	2.10	3.81		
F053	6.20	3.58	0.47	0.137	306	0.022	0.083	0.087	0.151	0.068	0.300	0.367	0.265	0.041	0.065	4.64	5.21		7.75
F054	5.55	4.92	0.71	0.205	149	0.038	0.093	0.102	0.175	0.065	0.367	0.642	0.323	0.058	0.080				
F063	6.91	3.26	0.54	0.153	239	0.031	0.089	0.096	0.125	0.069	0.327	0.402	0.291	0.031	0.078	4.69	4.10		9.70
F066	5.92	4.38	0.55	0.165	223	0.028	0.077	0.083	0.130	0.059	0.298	0.407	0.264	0.025	0.057		3.30		4.56
F080	4.29	2.95	0.40	0.160	161	0.028	0.081	0.103	0.162	0.086	0.348	0.540	0.305	0.042	0.057			3.69	3.80
F084	5.82	3.69	0.63	0.198	207	0.031	0.100	0.090	0.164	0.065	0.359	0.579	0.347	0.030	0.083	2.62	3.00	3.24	6.93
F085	7.85	6.23	0.69	0.152	292	0.029	0.080	0.082	0.137	0.054	0.271	0.317	0.235	0.017	0.048		4.47	6.70	4.03

Table App.D2-pulsed TDI indices (lat MA normal group)

cat	sex	age (years)	weight (Kg)	thickness (mm)	R-R (sec)	E'/A'	E' (cm/s)	E' VTI (cm)	E' dur (sec)	E' acc (cm/s^2)	tE' acc (sec)	E' dec (cm/s^2)	tE' dec (sec)	A' (cm/s)	A' VTI (cm)	A' dur (sec)	EA' (cm/s)	EA' VTI (cm)
F010	MN	10	6.30	4.28	0.337	1.66	11.01		0.059	307	0.036	482	0.025	6.64		0.043		
F011	FN	2	4.00	4.10	0.338		10.15		0.072	299	0.035	269	0.039					
F012	FN	2	5.60	4.63	0.481	2.49	12.02		0.091	316	0.038	230	0.052	4.82		0.062		
F014	MN	6	4.80	3.60	0.456	1.79	7.09		0.064	207	0.036	190	0.038	3.96		0.059		
F015	MN	6	4.40	3.94	0.364	0.86	8.45		0.076	242	0.034	198	0.045	9.87		0.054		
F022	MN	3	5.90	5.50	0.447	1.74	10.72	0.69	0.114	251	0.043	150	0.072	6.15		0.045		
F025	FN	9	4.70	4.61	0.417	1.00	7.87	0.49	0.100	231	0.039	113	0.069	7.89	0.38	0.068		
F028	FN	7	4.90	3.60	0.313	0.74	10.69				0.030			14.48			14.61	1.13
F031	FN	4	3.50	4.03	0.335	1.77	12.83	0.62	0.074	356	0.036	286	0.046	7.23	0.23	0.050		
F033	FN	8	3.70	4.52	0.399	0.65	4.36	0.18	0.060	184	0.023	127	0.034	6.71	0.30	0.066		
F034	MN	8	5.70	5.54	0.444	0.98	4.84	0.27	0.095	116	0.043	111	0.049	4.92	0.20	0.073		
F037	FN	4	4.00	3.67	0.381	1.30	5.17	0.24	0.076	165	0.034	116	0.048	3.98	0.16	0.065		
F041	FN	5	4.60	3.00	0.342	1.93	10.64	0.50	0.076	394	0.028	220	0.051	5.50	0.21	0.057		
F042	FN	3	4.30	3.10	0.314												8.08	0.56
F043	MN	1	4.50	3.94	0.336	1.60	11.17	0.54	0.092	313	0.030	256	0.043	7.00	0.30	0.068		
F050	FN	1	4.00	4.15	0.599	2.99	8.99	0.37	0.070	240	0.037	227	0.040	3.01	0.12	0.052		
F051	MN	14	6.20	4.42	0.364	1.05	4.85	0.25	0.068	166	0.030	126	0.040	4.62	0.18	0.055		
F053	FN	9	4.00	3.31	0.431	1.34	9.16	0.44	0.080	321	0.030	196	0.050	6.85	0.27	0.065		
F054	MN	1	4.50	3.01	0.523	2.27	10.37	0.63	0.100	232	0.045	200	0.054	4.56	0.22	0.082		
F063	MN	4	5.00	4.01	0.382	1.38	6.07	0.38	0.100	137	0.046	119	0.053	4.41	0.17	0.055		
F066	FN	7	3.80	4.16	0.418	1.19	5.77	0.30	0.094	199	0.030	100	0.059	4.85	0.18	0.055		
F080	MN	9	3.90	4.24	0.466	1.63	7.46	0.37	0.090	179	0.042	158	0.047	4.59	0.16	0.063		
F084	MN	9	3.30	5.33	0.571	1.20	7.88	0.46	0.108	184	0.043	121	0.066	6.56	0.29	0.072		
F085	MN	9	4.40	4.57	0.327	0.91	5.44							6.01				

Table App.D2-pulsed TDI indices (lat MA normal group)

cat	Se' (cm/s)	Sl' (cm/s)	S' VTI (cm)	S' dur (sec)	Se' acc (cm/s^2)	tSe' acc (sec)	bS'-Sl' (sec)	Q-Se' (sec)	Q-Sl' (sec)	Q-bS' (sec)	Q-E' (sec)	Q-A' (sec)	Q-bE' (sec)	IVCt (sec)	IVRt (sec)	IVRb (cm/s)	IVRa (cm/s)	IVCa (cm/s)	IVCb (cm/s)
F010	9.57	4.89		0.140	424	0.023	0.065	0.083	0.119	0.059	0.287	0.338		0.034	0.049	3.66	3.85	4.21	
F011	8.79	5.26		0.139	390	0.020	0.053	0.072	0.112	0.055	0.273				0.050				
F012	7.60	5.42		0.167	401	0.018	0.097	0.086	0.160	0.067	0.328	0.479		0.050	0.044	3.61	3.51	4.79	4.08
F014	6.43	4.57		0.176	232	0.029	0.071	0.089	0.131	0.065	0.317			0.045	0.049	4.53	2.98		2.73
F015	9.06	5.12		0.150	425	0.021	0.051	0.078	0.106	0.059	0.281	0.374		0.032	0.039	2.31	3.20		
F022	6.72	5.10	0.70	0.164	338	0.022	0.075	0.091	0.134	0.073	0.327	0.425	0.274	0.076	0.056	5.09		4.49	7.28
F025	7.49	4.35	0.61	0.160	321	0.024	0.074	0.092	0.143	0.069	0.308	0.441	0.251	0.036	0.040				8.37
F028	13.29	5.77	0.86	0.145	727	0.019	0.077	0.067	0.127	0.052	0.260	0.308	0.231	0.022	0.049	5.08	4.24		
F031	10.38	6.34	0.70	0.134	479	0.023	0.059	0.083	0.121	0.066	0.264	0.341	0.225	0.039	0.047	4.67	4.40		3.51
F033	4.39	3.49	0.45	0.138	182	0.026	0.070	0.107	0.149	0.090	0.320	0.376	0.272	0.075	0.077	2.02	4.16	2.90	4.28
F034	4.55	3.19	0.34	0.165	146	0.026	0.060	0.108	0.148	0.085	0.344	0.404	0.309	0.090	0.054	2.22	2.24	2.94	2.46
F037	5.85	2.74	0.38	0.135	215	0.029	0.064	0.080	0.113	0.055	0.275	0.366	0.244	0.069	0.052			5.07	7.62
F041	6.93	3.84	0.64	0.148	238	0.030	0.094	0.090	0.162	0.069	0.273	0.333	0.237	0.044	0.044	3.93	3.86	4.88	4.71
F042	5.82	2.96	0.52	0.153	199	0.031	0.105	0.092	0.161	0.065				0.043	0.040	3.72		3.28	3.47
F043	12.17	4.20	0.78	0.175	392	0.028	0.096	0.055	0.133	0.046	0.389	0.334	0.238	0.029	0.035	2.80		5.63	5.54
F050	6.95	3.93	0.65	0.164	265	0.028	0.092	0.104	0.172	0.085	0.355	0.560	0.308	0.066	0.070			3.91	3.31
F051	6.32	2.63	0.45	0.143	268	0.024	0.098	0.104	0.187	0.080	0.309	0.381	0.275	0.046	0.070	3.99	3.06	4.82	5.06
F053	5.42	3.72	0.60	0.170	261	0.024	0.095	0.082	0.173	0.063	0.306	0.419	0.276	0.050	0.053	7.27	3.67	4.39	6.83
F054	5.88	2.98	0.72	0.203	201	0.032	0.122	0.089	0.178	0.067	0.343	0.542	0.305	0.060	0.068			3.47	5.54
F063	5.42	4.64	0.47	0.142	297	0.019	0.073	0.093	0.153	0.079	0.324	0.395	0.279	0.041	0.068	5.48	4.41		7.96
F066	4.61	3.10	0.46	0.158	197	0.025	0.090	0.089	0.158	0.069	0.299	0.432	0.273	0.054	0.056	3.40	3.76	7.78	8.28
F080	5.21	4.54	0.56	0.180	173	0.032	0.090	0.109	0.139	0.090	0.346	0.500	0.308	0.051	0.054			3.53	6.02
F084	6.12	4.23	0.76	0.208	324	0.021	0.106	0.098	0.192	0.083	0.378	0.632	0.334	0.040	0.061	3.78	2.70	4.49	5.43
F085	5.59	4.01	0.43	0.137	357	0.018	0.069	0.075	0.119	0.062	0.281	0.331	0.250	0.027	0.067	6.32	3.47	9.46	10.04

Table App.D3-pulsed TDI indices (4ch IVS normal group)

cat	sex	age (years)	weight (Kg)	thickness (mm)	R-R (sec)	E'/A'	E' (cm/s)	E' VTI (cm)	E' dur (sec)	E' acc (cm/s^2)	tE' acc (sec)	E' dec (cm/s^2)	tE' dec (sec)	A' (cm/s)	A' VTI (cm)	A' dur (sec)	EA' (cm/s)	EA' VTI (cm)
F010	MN	10	6.30	5.55	0.344	1.49	11.97		0.081	377	0.032	238	0.051	8.03		0.051		
F011	FN	2	4.00	4.04	0.329	2.08	9.52		0.064	355	0.028	260	0.037	4.58		0.050		
F012	FN	2	5.60	4.22	0.540	1.69	7.10		0.071	249	0.028	178	0.040	4.21		0.061		
F014	MN	6	4.80	4.97	0.420	1.35	8.69		0.090	257	0.040	189	0.050	6.42		0.050		
F015	MN	6	4.40	3.73	0.371	0.96	7.01		0.073	260	0.029	175	0.043	7.34		0.063		
F022	MN	3	5.90	4.16	0.434	1.22	8.64	0.37	0.065	243	0.036	282	0.031	7.08	0.30	0.063		
F025	FN	9	4.70	4.87	0.409	0.88	6.60	0.48	0.110	127	0.052	104	0.063	7.51	0.32	0.058		
F028	FN	7	4.90	4.26	0.294	0.73	7.15	0.26	0.062	279	0.027	188	0.038	9.80	0.35	0.050	11.61	0.62
F031	FN	4	3.50	3.85	0.341	1.03	5.42	0.27	0.068	166	0.035	157	0.037	5.27	0.17	0.050		
F033	FN	8	3.70	5.40	0.406	0.59	2.97	0.11	0.055	122	0.026	98	0.032	5.04	0.19	0.056		
F034	MN	8	5.70	4.93	0.427	1.08	4.73	0.23	0.072	108	0.043	113	0.040	4.39	0.17	0.062		
F037	FN	4	4.00	3.10	0.393	1.60	7.69	0.38	0.082	284	0.030	168	0.055	4.81	0.20	0.068		
F041	FN	5	4.60	3.64	0.342	1.17	6.65	0.30	0.072	180	0.037	161	0.040	5.67	0.21	0.058	7.61	0.36
F042	FN	3	4.30	4.10	0.335	1.18	8.74	0.30	0.053	322	0.028	345	0.027	7.42	0.18	0.043	11.21	0.43
F043	MN	1	4.50	2.70	0.413	1.13	6.45	0.38	0.078	123	0.058	250	0.029	5.71	0.22	0.067		
F046	MN	10	4.20	3.97	0.399	1.01	6.07	0.30	0.072	180	0.034	145	0.042	6.02	0.22	0.054		
F050	FN	1	4.00	4.24	0.547	2.08	6.93	0.40	0.092	195	0.035	117	0.059	3.33	0.14	0.062		
F051	MN	14	6.20	5.54	0.373	0.60	3.98	0.21	0.072	159	0.028	92	0.048	6.63	0.22	0.060		
F053	FN	9	4.00	4.40	0.385	0.91	5.54	0.27	0.090	132	0.041	111	0.047	6.08	0.22	0.060		
F054	MN	1	4.50	4.40	0.536	1.13	5.55							4.90	0.36	0.090		
F063	MN	4	5.00	4.30	0.396	1.08	5.54	0.39	0.102	135	0.044	86	0.063	5.13	0.26	0.065		
F066	FN	7	3.80	3.41	0.412	0.87	5.49	0.32	0.096	141	0.039	90	0.062	6.33	0.25	0.063		
F080	MN	9	3.90	3.60	0.521	1.21	5.82	0.30	0.085	147	0.041	129	0.046	4.79	0.18	0.067		
F084	MN	9	3.30	4.84	0.598	1.00	8.69	0.44	0.085	233	0.037	182	0.047	8.72	0.32	0.068		
F085	MN	9	4.40	5.22	0.334	0.82	7.28	0.35	0.072	181	0.043	208	0.037	8.86	0.32	0.057		

Table App.D3-pulsed TDI indices (4ch IVS normal group)

cat	Se' (cm/s)	SI' (cm/s)	S' VTI (cm)	S' dur (sec)	Se' acc (cm/s^2)	tSe' acc (sec)	bS'-SI' (sec)	Q-Se' (sec)	Q-SI' (sec)	Q-bS' (sec)	Q-E' (sec)	Q-A' (sec)	Q-bE' (sec)	IVCt (sec)	IVRt (sec)	IVRb (cm/s)	IVRa (cm/s)	IVCa (cm/s)	IVCb (cm/s)
F010	5.98	7.35		0.159	235	0.026	0.072	0.077	0.116	0.053	0.282	0.333		0.030	0.038				
F011	7.12	6.91		0.128	392	0.019	0.076	0.067	0.122	0.050	0.265	0.323		0.027	0.064	4.77		5.25	5.28
F012	7.35	5.48		0.166	283	0.026	0.098	0.094	0.173	0.067	0.323	0.529		0.037	0.053	6.26	4.72		4.61
F014	5.95	5.44		0.180	199	0.030	0.070	0.090	0.120	0.060	0.330	0.430		0.030	0.040	2.33	2.87	2.36	3.23
F015	8.02	5.89		0.161	232	0.035	0.082	0.080	0.128	0.047	0.287	0.362		0.018	0.056		5.78		
F022	7.22	5.38	0.66	0.148	237	0.032	0.080	0.089	0.145	0.059	0.338	0.411	0.294	0.044	0.082		5.94	4.39	
F025	7.10	6.85	0.81	0.163	307	0.025	0.083	0.081	0.140	0.071	0.314	0.419	0.279	0.036	0.063				
F028	9.98	8.54	0.80	0.132	446	0.023	0.078	0.068	0.124	0.049	0.245	0.296	0.219	0.021	0.052	5.71	3.73	2.87	6.26
F031	5.73	3.79	0.51	0.143	239	0.025	0.092	0.074	0.143	0.056	0.278	0.355	0.235	0.021	0.056		3.51		
F033	4.99	2.97	0.37	0.130	163	0.031	0.076	0.097	0.140	0.071	0.336	0.397	0.302	0.055	0.101	2.49			2.33
F034	3.05	3.13	0.32	0.148	102	0.027	0.086	0.112	0.175	0.093	0.351	0.423	0.317	0.074	0.045				
F037	4.74	3.91	0.49	0.160	144	0.034	0.098	0.101	0.152	0.069	0.284	0.392	0.258	0.049	0.053				
F041	5.67	4.06	0.48	0.130	187	0.028	0.080	0.091	0.132	0.067	0.276	0.335	0.246	0.036	0.059	2.64	4.16	4.57	4.57
F042	4.76	4.06	0.42	0.135	204	0.024	0.067	0.093	0.131	0.068	0.287	0.323	0.259	0.047	0.068				
F043	7.10	4.26	0.57	0.165	243	0.029	0.087	0.083	0.135	0.054	0.318	0.401	0.267	0.030	0.062				
F046	5.52	3.65	0.51	0.150	246	0.023	0.092	0.081	0.149	0.064	0.325	0.413	0.290	0.028	0.087	3.48	6.73	2.90	4.91
F050	5.49	3.53	0.54	0.176	157	0.036	0.098	0.103	0.167	0.068	0.329	0.548	0.293	0.054	0.056		3.15		
F051	3.93	4.46	0.44	0.138	174	0.023	0.076							0.041	0.063		2.56	4.34	6.05
F053	6.47	4.62	0.59	0.152	235	0.029	0.094	0.083	0.145	0.057	0.285	0.384	0.315	0.032	0.058		8.73		3.57
F054	6.62	4.16	0.67	0.203	170	0.040	0.118	0.077	0.158	0.045	0.328	0.557		0.038					
F063	7.75	3.23	0.59	0.162	216	0.034	0.102	0.094	0.168	0.065	0.301	0.406	0.260	0.030	0.049		4.50	3.20	3.80
F066	6.40	4.81	0.60	0.154	186	0.036	0.097	0.075	0.138	0.049	0.297	0.417	0.256	0.021	0.071				
F080	3.92	3.88	0.45	0.172	128	0.032	0.086	0.116	0.177	0.080	0.361	0.530	0.322	0.042	0.072			3.74	
F084	6.25	4.50	0.77	0.205	193	0.033	0.104	0.104	0.164	0.071	0.377	0.593	0.339	0.033	0.080		8.01		
F085	7.36	4.92	0.63	0.150	309	0.026	0.077	0.064	0.121	0.045	0.281	0.336	0.236	0.022	0.052		5.71		

Table App.D4-pulsed TDI indices (4ch LVPW normal group)

cat	sex	age (years)	weight (Kg)	thickness (mm)	R-R (sec)	E'/A'	E' (cm/s)	E' VTI (cm)	E' dur (sec)	E' acc (cm/s^2)	tE' acc (sec)	E' dec (cm/s^2)	tE' dec (sec)	A' (cm/s)	A' VTI (cm)	A' dur (sec)	EA' (cm/s)	EA' VTI (cm)
F010	MN	10	4.28	6.30	0.361	1.92	9.44		0.062	422	0.025	284	0.037	4.92				
F011	FN	2	4.10	4.00	0.340	2.03	12.66		0.070	392	0.032	336	0.039	6.25		0.051		
F012	FN	2	4.63	5.60	0.516	2.58	13.09		0.079	429	0.031	280	0.047	5.08		0.048		
F014	MN	6	3.60	4.80	0.450	2.59	8.78		0.090	360	0.020	140	0.060	3.39				
F015	MN	6	3.94	4.40	0.356	1.39	8.70		0.060	367	0.024	237	0.038	6.24		0.053	12.72	
F022	MN	3	5.50	5.90	0.452	1.05	7.46	0.42	0.073	239	0.033	183	0.042	7.08	0.32	0.075		
F025	FN	9	4.61	4.70	0.408	1.08	8.60	0.56	0.103	200	0.044	142	0.062	7.98	0.37	0.067		
F028	FN	7	3.60	4.90	0.326	1.22	12.95	0.66	0.080	469	0.027	251	0.051	10.61	0.33	0.060	13.19	1.05
F031	FN	4	4.03	3.50	0.339	2.08	9.99	0.46	0.076	404	0.026	193	0.054	4.80	0.19	0.055		
F033	MN	8	4.52	3.70	0.412	1.85	6.87	0.30	0.063	238	0.030	168	0.044	3.72	0.14	0.050		
F034	FN	8	5.54	5.70	0.456	2.72	8.14	0.40	0.093	265	0.032	123	0.066	2.99	0.10	0.055		
F037	FN	4	3.67	4.00	0.370	2.25	8.49	0.34	0.078	320	0.028	182	0.047	3.78	0.13	0.060		
F041	FN	5	3.00	4.60	0.335	2.34	9.43	0.37	0.082	318	0.029	186	0.049	4.04	0.14	0.058		
F042	FN	3	3.10	4.30	0.332	1.81	9.54	0.40	0.075	389	0.026	202	0.049	5.26	0.18	0.057	10.16	0.56
F043	MN	1	3.94	4.50	0.316	2.48	13.82	0.56	0.078	397	0.041	315	0.044	5.57				
F050	FN	1	4.15	4.00	0.464	2.83	8.82	0.38	0.070	306	0.029	203	0.044	3.12	0.15	0.063		
F051	MN	14	4.42	6.20	0.379	1.14	4.64	0.20	0.067	174	0.028	108	0.044	4.08	0.13	0.046		
F053	FN	9	3.31	4.00	0.404	1.20	7.58	0.49	0.100	214	0.037	138	0.057	6.32	0.23	0.060		
F054	MN	1	3.01	4.50	0.543	2.19	11.28	0.61	0.085	364	0.033	247	0.049	5.15	0.23	0.073		
F063	MN	4	4.01	5.00	0.405	2.24	8.78	0.49	0.098	349	0.027	94	0.071	3.91	0.26	0.082		
F066	FN	7	4.16	3.80	0.413	1.78	7.60	0.44	0.100	267	0.030	106	0.072	4.26	0.14	0.060		
F080	MN	9	4.24	3.90	0.505	2.17	8.84	0.40	0.075	255	0.035	207	0.043	4.08	0.14	0.063		
F084	MN	9	5.33	3.30	0.510	1.01	8.97	0.59	0.107	241	0.039	145	0.064	8.85	0.41	0.080		
F085	MN	9	4.57	4.40	0.345	1.12	8.40	0.40	0.077	245	0.032	150	0.130	7.48	0.25	0.055		

Table App.D4-pulsed TDI indices (4ch LVPW normal group)

cat	Se' (cm/s)	Sl' (cm/s)	S' VTI (cm)	S' dur (sec)	Se' acc (cm/s^2)	tSe' acc (sec)	bS'-Sl' (sec)	Q-Se' (sec)	Q-Sl' (sec)	Q-bS' (sec)	Q-E' (sec)	Q-A' (sec)	Q-bE' (sec)	IVCt (sec)	IVRt (sec)	IVRb (cm/s)	IVRa (cm/s)	IVCa (cm/s)	IVCb (cm/s)
F010	6.24	3.48		0.156	309	0.021	0.095	0.073	0.148	0.051	0.288	0.362		0.035	0.056				
F011	7.09	5.45		0.147	359	0.021	0.058	0.070	0.107	0.050	0.269	0.341		0.029	0.044	3.98			
F012	7.41	4.05		0.161	401	0.019	0.092	0.084	0.158	0.071	0.321	0.507		0.050	0.054	5.45	3.88	4.08	5.01
F014	5.56	3.64		0.180	198	0.030	0.110	0.090	0.180	0.060	0.330	0.460		0.060	0.060	2.94	2.43		2.80
F015	5.99	3.84		0.153	209	0.029	0.065	0.081	0.123	0.058	0.290	0.351		0.034	0.051	4.01	3.97		5.44
F022	4.96	4.83	0.75	0.173	281	0.017	0.110	0.082	0.177	0.075	0.352	0.430	0.314	0.071	0.080	5.33	5.95	3.68	6.56
F025	7.30	3.27	0.74	0.180	191	0.038	0.114	0.087	0.164	0.042	0.320	0.410	0.273	0.010	0.051	3.41	3.75		4.47
F028	12.24	5.35	0.99	0.150	285	0.045	0.122	0.088	0.166	0.056	0.274	0.326	0.238	0.044	0.057	7.84			
F031	9.05	5.43	0.61	0.140	371	0.025	0.064	0.077	0.112	0.055	0.265	0.349	0.233	0.024	0.056	2.94	2.75		8.65
F033	4.22	2.70	0.35	0.015	162	0.024	0.087	0.114	0.176	0.080	0.320	0.383	0.289	0.082	0.059	2.58			5.17
F034	4.29	2.87	0.47	0.184	209	0.020	0.099	0.109	0.197	0.084	0.337	0.428	0.309	0.087	0.061	2.42	2.18		
F037	5.57	2.70	0.44	0.167	195	0.032	0.112	0.080	0.148	0.048	0.275	0.345	0.245	0.040	0.060	3.68			4.53
F041	4.54	4.11	0.45	0.145	233	0.020	0.066							0.036	0.053	3.00	3.70	3.25	5.48
F042	8.25	3.02	0.56	0.158	293	0.027	0.111	0.088	0.173	0.069	0.279	0.339	0.254	0.042	0.050	3.32			3.65
F043	7.91	4.80	0.70	0.165	318	0.028	0.094	0.078	0.130	0.050	0.271	0.328	0.243	0.025	0.044				
F050	5.27	4.32	0.68	0.170	252	0.026	0.087	0.123	0.189	0.101	0.321	0.435	0.305	0.060	0.077	3.97	3.15		2.99
F051	5.26	2.05	0.37	0.143	216	0.025	0.106	0.102	0.168	0.084				0.053	0.074	5.36	2.27		5.90
F053	3.99	4.81	0.57	0.147	306	0.015	0.072	0.083	0.148	0.069	0.293	0.402	0.257	0.050	0.045	4.91	4.45		9.49
F054	6.30	3.17	0.72	0.197	116	0.050	0.101	0.115	0.189	0.068	0.346	0.554	0.315	0.070	0.073	3.90	3.67		3.11
F063	5.74		0.57	0.148	252	0.024		0.100		0.089	0.296	0.402	0.273	0.054	0.047	6.40		4.02	8.02
F066	5.50	2.65	0.48	0.165	217	0.027	0.089	0.086	0.154	0.066	0.303	0.425	0.274	0.042	0.048	3.55			3.83
F080	5.71	2.89	0.54	0.193	256	0.023	0.131	0.108	0.221	0.091	0.353	0.497	0.317	0.055	0.049	2.94	2.22		3.39
F084	5.75	4.64	0.68	0.197	292	0.021	0.200	0.086	0.142	0.067	0.341	0.508	0.302	0.025	0.065	5.69	4.77	4.36	6.50
F085	8.21		0.78	0.155	238	0.038		0.091		0.058	0.274	0.353	0.245	0.027	0.056	2.57	3.82		4.05

Table App.D5-pulsed TDI indices (rpla LVPW normal group)

cat	sex	age (years)	weight (Kg)	thickness (mm)	R-R (sec)	E'/A'	E' (cm/s)	E' VTI (cm)	E' dur (sec)	E' acc (cm/s^2)	tE' acc (sec)	E' dec (cm/s^2)	tE' dec (sec)	A' (cm/s)	A' VTI (cm)	A' dur (sec)	EA' (cm/s)	EA' VTI (cm)
F010	MN	10	6.3	4.28	0.355	1.33	6.39		0.061	219	0.028	175	0.036	4.81		0.051		
F012	FN	2	5.6	4.63	0.507	1.58	5.00		0.046	254	0.020	179	0.028	3.17		0.047		
F014	MN	6	4.8	3.60	0.475	1.11	8.04		0.092	237	0.034	133	0.060	7.26		0.056		
F015	MN	6	4.4	3.94	0.373	0.91	5.28		0.072	145	0.036	150	0.037	5.83		0.058		
F022	MN	3	5.9	5.50	0.408	1.11	10.27	0.54	0.076	304	0.038	262	0.043	9.25	0.43	0.078		
F025	FN	9	4.7	4.61	0.486	1.08	4.99	0.30	0.098	160	0.030	70	0.069	4.60	0.19	0.073		
F028	FN	7	4.9	3.60	0.309	0.75	6.74							9.03				
F031	FN	4	3.5	4.03	0.369	0.78	6.84	0.32	0.085	153	0.045	166	0.040	8.82	0.29	0.058		
F033	FN	8	3.7	4.52	0.404	0.82	3.76	0.11	0.047	216	0.021	181	0.023	4.59	0.15	0.046		
F034	MN	8	5.7	5.54	0.431	0.75	3.81							5.04				
F037	FN	4	4	3.67	0.308	0.81	4.61	0.15	0.063	167	0.027	159	0.028	5.67	0.22	0.058		
F041	FN	5	4.6	3.00	0.325	2.18	6.84	0.31	0.068	280	0.030	171	0.043	3.13	0.14	0.055	10.04	0.38
F042	FN	3	4.3	3.10	0.317	1.37	7.01	0.29	0.067	301	0.023	134	0.051	5.10	0.22	0.063	8.69	0.40
F043	MN	1	4.5	3.94	0.504	1.52	6.78	0.39	0.096	183	0.038	102	0.068	4.46	0.23	0.070		
F046	MN	10	4.2	4.92	0.370	0.85	5.90							6.93	0.36	0.073		
F050	FN	1	4	4.15	0.482	0.92	4.08	0.18	0.072	163	0.032	134	0.036	4.45	0.26	0.087		
F051	MN	14	6.2	4.42	0.371	0.48	3.38	0.16	0.078	124	0.029	68	0.050	7.03	0.29	0.075		
F053	FN	9	4	3.31	0.367	0.92	4.99							5.44				
F054	MN	1	4.5	3.01	0.616	1.56	6.25	0.41	0.102	192	0.039	127	0.060	4.01	0.15	0.057		
F063	MN	4	5	4.01	0.379	0.95	4.99	0.26	0.078	160	0.034	110	0.048	5.23	0.23	0.068		
F066	FN	7	3.8	4.16	0.389	0.79	4.18	0.29	0.100	83	0.056	119	0.040	5.32	0.21	0.062		
F080	MN	9	3.9	4.24	0.564	1.25	4.27	0.31	0.107	85	0.054	80	0.057	3.41	0.17	0.078		
F084	MN	9	3.3	5.33	0.622	0.74	5.49	0.38	0.125	154	0.037	62	0.088	7.41	0.32	0.075		
F085	MN	9	4.4	4.57	0.348	1.18	4.72	0.20	0.068	149	0.033	129	0.037	3.98	0.21	0.077		

Table App.D5-pulsed TDI indices (rpla LVPW normal group)

cat	Se' (cm/s)	Sl' (cm/s)	S' VTI (cm)	S' dur (sec)	Se' acc (cm/s^2)	tSe' acc (sec)	bS'-Sl' (sec)	Q-Se' (sec)	Q-Sl' (sec)	Q-bS' (sec)	Q-E' (sec)	Q-A' (sec)	Q-bE' (sec)	IVCt (sec)	IVRt (sec)	IVRb (cm/s)	IVRa (cm/s)	IVCa (cm/s)	IVCb (cm/s)
F010	6.30	4.26		0.140	195	0.032	0.087	0.094	0.142	0.066	0.293	0.357		0.037	0.052				6.40
F012	6.09	2.96		0.141	120	0.051	0.169	0.137	0.255	0.090	0.348	0.477		0.068	0.039	3.13	4.38		4.92
F014	6.79	6.44		0.159	250	0.027	0.071	0.113	0.158	0.089	0.335	0.436		0.067	0.062		3.00	2.22	3.47
F015	5.68	5.98		0.141	239	0.023	0.049	0.087	0.116	0.066	0.290	0.355		0.047	0.054	3.03		2.50	7.35
F022	6.83	5.36	0.85	0.158	175	0.043	0.109	0.106	0.176	0.070	0.315	0.380	0.275	0.051		5.10		4.63	8.72
F025	4.56	3.47	0.53	0.180	126	0.039	0.101	0.112	0.182	0.083	0.350	0.492	0.320	0.039	0.072	2.69			6.71
F028	9.70	7.14	0.80	0.167	331	0.029	0.087	0.076	0.135	0.051	0.245	0.298		0.025					11.04
F031	7.40		0.58	0.138	168	0.043		0.107		0.068	0.294	0.371	0.254	0.033	0.060				10.71
F033	3.86	3.36	0.34	0.126	204	0.020	0.065	0.098	0.143	0.084	0.328	0.375	0.313	0.080	0.111				4.30
F034	4.58	3.61	0.47	0.150	139	0.035	0.095	0.117	0.182	0.086	0.322	0.406	0.287	0.072	0.071				4.62
F037	6.47		0.39	0.137	241	0.037		0.068		0.043	0.193	0.303	0.170	0.025					9.86
F041	7.08	2.75	0.48	0.128	290	0.025	0.080	0.082	0.140	0.060	0.278	0.370	0.240	0.044	0.053	3.09	3.83	2.90	5.76
F042	5.67	3.21	0.45	0.133	206	0.032	0.090	0.092	0.128	0.073				0.047	0.049	3.59			7.14
F043	5.06	4.28	0.55	0.176	182	0.031	0.079	0.085	0.137	0.068	0.292	0.480	0.262	0.052	0.043				4.18
F046	6.60	3.40	0.58	0.147	217	0.032	0.106	0.108	0.177	0.072	0.312	0.396	0.276	0.041	0.065	4.28		2.96	8.40
F050	5.28	2.52	0.45	0.150	221	0.025	0.084	0.096	0.157	0.075	0.354	0.453	0.314	0.060	0.090	3.24			6.18
F051	5.92	3.52	0.53	0.143	178	0.035	0.090	0.104	0.157	0.074	0.278	0.362	0.259	0.050	0.064	3.25	3.95		5.65
F053	8.57		0.54	0.124	395	0.022		0.077		0.059	0.258	0.349	0.230	0.050	0.059	3.25			10.05
F054	5.19	5.34	0.60	0.170	175	0.027	0.075	0.110	0.155	0.086	0.346	0.593	0.311	0.077	0.066	2.83	2.67		5.63
F063	6.20		0.55	0.143	225	0.029		0.106		0.080	0.304	0.379	0.269	0.050	0.055	4.52			7.62
F066	6.62	3.10	0.57	0.145	168	0.039	0.092	0.105	0.163	0.072	0.326	0.381	0.272	0.041	0.064				7.70
F080	5.57	2.55	0.52	0.180	238	0.025	0.109	0.107	0.201	0.089	0.364	0.550	0.316	0.053	0.062	2.30	2.80		4.42
F084	5.49	3.31	0.72	0.202	165	0.036	0.123	0.095	0.196	0.063	0.340	0.606	0.306	0.046	0.046				6.34
F085	6.58	3.10	0 43	0.122	338	0.020	0.071	0.078	0.124	0.064	0.259	0.338	0.226	0.038	0.045				8.28

Table App.D6-pulsed TDI indices (rpla IVS normal group)

cat	sex	age (years)	weight (Kg)	thickness (mm)	R-R (sec)	E'/A'	E' (cm/s)	E' VTI (cm)	E' dur (sec)	E' acc (cm/s^2)	tE' acc (sec)	E' dec (cm/s^2)	tE' dec (sec)	A' (cm/s)	A' VTI (cm)	A' dur (sec)	EA' (cm/s)	EA' VTI (cm)
F012	FN	2	5.60	4.22	0.456	1.45	5.47		0.095	105	0.052	118	0.046	3.79		0.089		
F031	FN	4	3.50	3.85	0.359	2.62	8.32	0.30	0.058	265	0.031	279	0.028	3.18	0.07	0.040		
F033	FN	8	3.70	5.40	0.383	0.67	3.70							5.53	0.20	0.050		
F034	FN	8	5.70	4.93	0.436	0.54	3.43	0.46	0.160	45	0.099	77	0.059	6.31	0.22	0.053		
F037	FN	4	4.00	3.10	0.329	0.99	3.65							3.71				
F041	FN	5	4.60	3.64	0.430	1.54	6.01	0.31	0.090	139	0.044	138	0.045	3.90	0.22	0.083	7.56	0.32
F042	MN	3	4.30	4.10	0.328	0.43	3.90							9.15			9.89	0.61
F046	MN	10	4.20	3.97	0.416	0.65	4.63	0.19	0.060	148	0.034	156	0.033	7.08	0.34	0.063		
F050	FN	1	4.00	4.24	0.510	2.43	8.03	0.29	0.060	266	0.030	269	0.030	3.30	0.10	0.050		
F051	MN	14	6.20	5.54	0.371	1.15	4.65	0.19	0.063	168	0.027	134	0.034	4.05	0.12	0.045		
F053	FN	9	4.00	4.40	0.382	0.66	4.20	0.21	0.063	148	0.037	156	0.033	6.35	0.24	0.063		
F054	MN	1	4.50	4.40	0.555	1.37	4.96	0.31	0.088	131	0.044	144	0.041	3.64	0.14	0.057		
F063	MN	4	5.00	4.30	0.351	1.69	4.99	0.26	0.077	141	0.036	112	0.046	2.95	0.12	0.055		
F066	FN	7	3.80	3.41	0.409	0.71	4.93	0.29	0.088	156	0.034	101	0.051	6.92	0.22	0.050		
F080	MN	9	3.90	3.60	0.521	1.11	3.91	0.24	0.092	90	0.047	105	0.040	3.52	0.10	0.043		
F084	MN	9	3.30	4.84	0.502	0.64	4.75	0.32	0.110	104	0.048	76	0.066	7.38	0.30	0.065		
F085	MN	9	4.40	5.22	0.353	0.88	8.95	0.56	0.108	160	0.062	204	0.049	10.18	0.39	0.070		

Table App.D6-pulsed TDI indices (rpla IVS normal group)

cat	Se' (cm/s)	Sl' (cm/s)	S' VTI (cm)	S' dur (sec)	Se' acc (cm/s^2)	tSe' acc (sec)	bS'-Sl' (sec)	Q-Se' (sec)	Q-Sl' (sec)	Q-bS' (sec)	Q-E' (sec)	Q-A' (sec)	Q-bE' (sec)	IVCt (sec)	IVRt (sec)	IVRb (cm/s)	IVRa (cm/s)	IVCa (cm/s)	IVCb (cm/s)
F012	5.10			0.129	107	0.047		0.122		0.083	0.304	0.445	0.260	0.058	0.050			7.07	4.96
F031	7.71				309	0.024		0.063		0.040	0.268	0.348	0.238	0.025				4.45	7.10
F033	4.41	2.90	0.37	0.130	166	0.028	0.088	0.079	0.146	0.058	0.315	0.371	0.269	0.045					3.05
F034	5.42	3.43	0.44	0.147	189	0.031	0.076	0.045	0.153	0.020	0.339	0.428	0.238	0.013	0.062				
F037	3.97	3.67	0.28	0.107	130	0.032		0.082		0.065	0.190	0.302	0.170	0.070	0.043				7.28
F041	6.83	4.28	0.46	0.143	247	0.028	0.086	0.066	0.128	0.042	0.294	0.422	0.245	0.030	0.074	2.63	4.20		4.52
F042	6.62	3.93	0.52	0.160	245	0.027	0.092	0.076	0.144	0.053	0.237	0.291	0.222	0.038	0.032		4.92		4.73
F046	5.34	2.75	0.42	0.128	153	0.029	0.064	0.128	0.158	0.107	0.309	0.416	0.275	0.065	0.065	3.02	3.34	5.90	5.42
F050	4.70	2.00	0.40	0.163	202	0.024	0.108	0.065	0.143	0.046	0.357	0.502	0.325	0.027				2.45	5.58
F051	4.23	3.73	0.35	0.133	159	0.024	0.062							0.032	0.045			4.06	3.22
F053	6.09	3.43	0.56	0.163	222	0.030	0.105	0.071	0.148	0.043	0.308	0.372	0.266	0.027	0.078			3.22	6.96
F054	5.59	3.99	0.37	0.133	189	0.029	0.067	0.078	0.119	0.053	0.370	0.621	0.315	0.111	0.136				4.03
F063	7.23	2.67	0.46	0.155	409	0.019	0.093	0.068	0.144	0.050	0.299	0.362	0.268	0.027	0.069		4.82		5.60
F066	4.77	2.70	0.41	0.160	273	0.018	0.094	0.080	0.150	0.062	0.306	0.427	0.285	0.024	0.059		2.90		4.47
F080	3.98	1.92	0.39	0.178	132	0.034	0.103	0.088	0.170	0.059	0.357	0.605	0.316	0.022	0.081			2.50	2.35
F084	6.34	3.11	0.63	0.195	232	0.029	0.114	0.072	0.148	0.047	0.358	0.506	0.321	0.026	0.083	3.15	3.67	3.02	5.27
F085	7.81		0.58	0.117	156	0.050		0.117		0.071	0.289	0.362	0.237	0.029	0.060	4.57	5.87		5.93

Table App.D7-pulsed TDI indices (Tr normal group)

cat	sex	age (years)	weight (Kg)	thickness (mm)	R-R (sec)	E'/A'	E' (cm/s)	E' VTI (cm)	E' dur (sec)	E' acc (cm/s^2)	tE' acc (sec)	E' dec (cm/s^2)	tE' dec (sec)	A' (cm/s)	A' VTI (cm)	A' dur (sec)	EA' (cm/s)	EA' VTI (cm)
F050	FN	1	4.00	0	0.497	1.13	8.67	0.63	0.118	143	0.062	168	0.052	7.64	0.33	0.073		
F051	MN	14	6.20	0	0.355	0.79	7.65	0.62	0.127	178	0.048	111	0.071	9.68	0.37	0.063		
F053	FN	9	4.00	0	0.389	0.71	10.22	0.74	0.117	267	0.038	127	0.080	14.42	0.72	0.088		
F054	MN	1	4.50	0	0.593	1.83	12.65	0.93	0.127	221	0.056	180	0.070	6.90	0.35	0.093		
F066	FN	7	3.80	0	0.416	1.00	11.63	0.82	0.123	227	0.049	164	0.068	11.58	0.51	0.083		
F080	MN	9	3.90	0	0.503	1.25	6.02	0.40	0.112	123	0.050	85	0.072	4.80	0.32	0.097		
F084	MN	9	3.30	0	0.615	0.75	9.58	0.93	0.162	160	0.060	87	0.110	12.83	0.74	0.102		
F085	MN	9	4.40	0	0.341	0.83	11.83	0.63	0.092	307	0.036	202	0.054	14.30	0.58	0.072		

Table App.D7-pulsed TDI indices (Tr normal group)

cat	Se' (cm/s)	Sl' (cm/s)	S' VTI (cm)	S' dur (sec)	Se' acc (cm/s^2)	tSe' acc (sec)	bS'-Sl' (sec)	Q-Se' (sec)	Q-Sl' (sec)	Q-bS' (sec)	Q-E' (sec)	Q-A' (sec)	Q-bE' (sec)	IVCt (sec)	IVRt (sec)	IVRb (cm/s)	IVRa (cm/s)	IVCa (cm/s)	IVCb (cm/s)
F050	10.43	3.78	0.75	0.168	299	0.035	0.091	0.090	0.143	0.058	0.359	0.500	0.296	0.032	0.087				
F051	7.12	6.48	0.67	0.135	241	0.030	0.083	0.087	0.135	0.069	0.258	0.390	0.204	0.036	0.038			8.30	
F053	12.22	7.23	1.10	0.157	326	0.039	0.104	0.072	0.135	0.039	0.263	0.365	0.225	0.025	0.046		6.38	7.23	
F054	25.42	7.20	1.22	0.222	265	0.037	0.103	0.083	0.153	0.053	0.353	0.606	0.304	0.031	0.073		3.87	6.40	
F066	10.92	9.77	1.15	0.167	298	0.034	0.081	0.083	0.138	0.056	0.289	0.412	0.242	0.023	0.033	2.87	4.37	7.33	
F080	5.27	3.91	0.64	0.188	126	0.044	0.107	0.122	0.192	0.086	0.359	0.477	0.315	0.034	0.061			6.88	4.75
F084	14.50	8.13	1.54	0.210	454	0.032	0.098	0.096	0.173	0.065	0.385	0.578	0.318	0.019	0.051		5.92	9.63	
F085	11.60		0.95	0.144	420	0.028		0.077		0.054	0.258	0.345	0.218	0.024	0.038			12.47	

Table App.D8-pulsed TDI indices (sep MA HCM group)

cat	status	sex	age (years)	weight (Kg)	thickness (mm)	R-R (sec)	E'/A'	E' (cm/s)	E' VTI (cm)	E' dur (sec)	E' acc (cm/s^2)	tE' acc (sec)	E' dec (cm/s^2)	tE' dec (sec)	A' (cm/s)	A' VTI (cm)	A' dur (sec)	EA' (cm/s)	EA' VTI (cm)
F004	asympt.	MN	10	4.50	7.36	0.273												15.39	
F009	asympt.	MN	7	5.20	5.84	0.359	0.71	5.06							7.16				
F013	asympt.	MN	3	6.80	7.30	0.384	0.46	4.47							9.72				
F018	asympt.	MN	10	4.50	4.39	0.319												8.94	
F024	asympt.	MN	3	6.45	9.11	0.487	2.41	5.73	0.31	0.088	167	0.037	114	0.052	2.38	0.08	0.048		
F027	asympt.	FN	1	5.20	6.00	0.480	0.48	3.97	0.35	0.138	86	0.050	48	0.085	8.33	0.36	0.070		
F030	asympt.	MN	9	6.30	6.01	0.388	1.45	5.14							3.55				
F032	asympt.	MN	12	5.50	7.00	0.313	0.52	4.12	0.14	0.054	162	0.028	208	0.022	7.86	0.34	0.072		
F038	asympt.	MN	10	5.00	4.87	0.451	0.68	3.10	0.20	0.088	88	0.037	62	0.054	4.58	0.25	0.082		
F044	asympt.	MN	7	4.50	7.20	0.622	0.47	2.69	0.27	0.138	43	0.065	36	0.072	5.67	0.28	0.077		
F052	asympt.	MN	9	4.20	4.70	0.392	0.40	3.10	0.24	0.088	81	0.044	93	0.041	7.65	0.34	0.065		
F057	asympt.	FN	7	4.40	6.70	0.322	0.53	4.27	0.21	0.080	78	0.053	161	0.027	7.99	0.36	0.080		
F069	asympt.	FN	4	4.15	6.42	0.419	0.42	3.55	0.19	0.080	91	0.038	99	0.036	8.46	0.44	0.073		
F071	asympt.	MN	7	6.70	4.93	0.472	0.60	4.93	0.48	0.130	77	0.071	199	0.055	8.27	0.33	0.070		
F073	asympt.	MN	5	6.15	4.10	0.380	0.49	4.03							8.14	0.36	0.070		
F081	asympt.	MN	3	4.75	4.21	0.467	0.63	4.11	0.37	0.117	103	0.046	62	0.074	6.55	0.28	0.073		
F086	asympt.	MN	7	4.40	5.69	0.515	0.59	4.33	0.35	0.128	73	0.062	75	0.059	7.35	0.29	0.065		
F091	asympt.	FN	5	4.90	6.30	0.354	0.69	5.58	0.29	0.090	132	0.036	93	0.051	8.07	0.24	0.050		
F093	asympt.	MN	9	6.70	6.90	0.401	0.47	3.45	0.31	0.110	69	0.060	86	0.051	7.27	0.32	0.068	9.41	0.49
F060	CHF	MN	2	3.30	4.30	0.368	0.91	4.73							5.21				
F067	CHF	MN	9	4.80	7.60	0.281	0.81	2.97	0.13	0.068	79	0.042	109	0.029	3.66	0.16	0.068		
F082	CHF	MN	11	5.80	5.00	0.494		3.40	0.21	0.112	72	0.049	59	0.060					
F092	CHF	MN	4	4.50	7.68	0.459	1.23	3.95	0.33	0.155	113	0.041	38	0.114	3.20	0.16	0.077		

Table App.D8-pulsed TDI indices (sep MA HCM group)

cat	Se' (cm/s)	Sl' (cm/s)	S' VTI (cm)	S' dur (sec)	Se' acc (cm/s^2)	tSe' acc (sec)	bS'-Sl' (sec)	Q-Se' (sec)	Q-Sl' (sec)	Q-bS' (sec)	Q-E' (sec)	Q-A' (sec)	Q-bE' (sec)	IVCt (sec)	IVRt (sec)	IVRb (cm/s)	IVRa (cm/s)	IVCa (cm/s)	IVCb (cm/s)
F004	10.04			0.110	317	0.032		0.075		0.036				0.019	0.070		4.10		
F009	6.35	3.87		0.151	215	0.030	0.089	0.098	0.153	0.070	0.310	0.362	0.281	0.039	0.067		5.16	5.66	4.14
F013	9.04	4.10		0.157	274	0.033	0.097	0.078	0.141	0.047	0.327	0.363	0.269	0.035	0.073		3.74		3.30
F018	8.34	3.33		0.142	269	0.030	0.080	0.079	0.140	0.049				0.020	0.069				6.97
F024	3.83	3.01	0.39	0.150	158	0.026	0.087	0.082	0.146	0.058	0.293	0.476	0.255	0.049	0.071	2.38	3.38	4.17	2.38
F027	8.03	2.51	0.50	0.133	279	0.029	0.083	0.101	0.168	0.074	0.368	0.496	0.314	0.023	0.119	2.16		3.87	7.46
F030	4.63	3.75	0.45	0.157	127	0.034	0.101	0.085	0.155	0.058	0.303	0.375	0.258	0.045	0.075				4.52
F032	8.06	4.20	0.50	0.122	311	0.027	0.069	0.089	0.130	0.069	0.269	0.326	0.249	0.032	0.072				4.92
F038	5.31	2.84	0.41	0.142	220	0.025	0.081	0.095	0.154	0.072	0.329	0.434	0.297	0.050	0.100	3.28	3.18		6.55
F044	5.54	2.77	0.44	0.150	186	0.030	0.096	0.103	0.172	0.076	0.382	0.613	0.317	0.026	0.093				4.15
F052	5.81	3.03	0.53	0.158	260	0.027	0.089	0.080	0.136	0.057	0.335	0.400	0.300	0.026	0.077			5.02	5.75
F057	5.84	2.64	0.39	0.125	174	0.034	0.078	0.086	0.133	0.053	0.242	0.308	0.195	0.026	0.037				
F069	7.42	3.61	0.58	0.153	214	0.037	0.092	0.079	0.134	0.045	0.310	0.391	0.279	0.026	0.110		2.88	3.66	5.14
F071	6.99	3.65	0.66	0.172	212	0.034	0.094	0.088	0.154	0.060	0.290	0.482	0.268	0.028	0.050		3.21	4.31	3.54
F073	4.78	4.07	0.47	0.158	193	0.026	0.078	0.091	0.143	0.067	0.322	0.375	0.277	0.045	0.063			6.96	5.77
F081	6.51	3.51	0.57	0.157	240	0.029	0.100	0.095	0.163	0.067	0.335	0.468	0.287	0.026	0.076				
F086	6.77	4.25	0.58	0.160	199	0.035	0.094	0.072	0.136	0.040	0.304	0.472	0.248	0.049	0.054			3.43	2.90
F091	6.48	3.83	0.51	0.153	267	0.024	0.080	0.076	0.131	0.059	0.308	0.345	0.260	0.037	0.065				4.83
F093	6.27	2.93	0.48	0.153	281	0.023	0.084	0.075	0.145	0.061	0.349	0.414	0.295	0.026	0.092	3.02			6.33
F060	6.39	3.26	0 58	0.158	223	0.033	0.090	0.086	0.138	0.050	0.299	0.347	0.257	0.025	0.069		2.79	3.87	5.72
F067	4.06		0 29	0.115	186	0.024		0.075		0.047	0.205	0.248	0.163	0.047	0.040			2.45	1.94
F082	2.99	2.23	0 28	0.163	84	0.035	0.082	0.081	0.129	0.054	0.358		0.309		0.117				
F092	4.70	2.25	0 38	0.150	156	0.032	0.102	0.106	0.174	0.078	0.322	0.454	0.285	0.044	0.070			4.20	2.63

Table App.D9-pulsed TDI indices (lat MA HCM group)

cat	status	sex	age (years)	weight (Kg)	thickness (mm)	R-R (sec)	E'/A'	E' (cm/s)	E' VTI (cm)	E' dur (sec)	E' acc (cm/s^2)	tE' acc (sec)	E' dec (cm/s^2)	tE' dec (sec)	A' (cm/s)	A' VTI (cm)	A' dur (sec)	EA' (cm/s)	EA' VTI (cm)
F009	asympt.	MN	7	5.20	4.95	0.359	0.95	6.70							7.04				
F013	asympt.	MN	8	6.80	4.95	0.395	0.65	6.25							9.60				
F027	asympt.	FN	1	5.20	8.29	0.462	0.99	3.83							3.85				
F038	asympt.	MN	10	5.00	6.14	0.487	1.03	6.60	0.46	0.115	144	0.049	104	0.069	6.41	0.34	0.077		
F044	asympt.	MN	7	4.50	6.03	0.511	1.19	4.23	0.38	0.136	106	0.050	67	0.076	3.57	0.13	0.053		
F052	asympt.	MN	9	4.20	7.95	0.379	0.76	3.45							4.52	0.12	0.044		
F057	asympt.	FN	7	4.40	6.92	0.301												7.12	0.39
F069	asympt.	FN	4	4.15	4.60	0.356	0.73	4.98	0.27	0.077	160	0.035	145	0.039	6.84	0.31	0.073		
F071	asympt.	MN	7	6.70	6.32	0.467	0.76	6.05	0.40	0.107	120	0.053	107	0.062	7.96	0.29	0.057		
F073	asympt.	MN	5	6.15	7.44	0.368												14.14	0.53
F081	asympt.	MN	3	4.75	5.56	0.437	0.92	6.11	0.55	0.138	97	0.069	90	0.073	6.66	0.21	0.055		
F086	asympt.	MN	7	4.40	4.00	0.511	0.78	5.32	0.48	0.148	144	0.039	51	0.104	6.82	0.19	0.048		
F091	asympt.	FN	5	4.90	4.00	0.350	0.82	5.18	0.32	0.085	132.5	0.044	128.0	0.045	6.28	0.22	0.060		
F093	asympt.	MN	9	6.70	6.34	0.401	0.86	5.20							6.02				
F060	CHF	MN	2	3.30	4.68	0.363	1.06	7.16							6.75				
F067	CHF	MN	9	4.80	3.59	0.284												6.70	0.32
F082	CHF	MN	11	5.80	7.15	0.459		4.30	0.35	0.132	86	0.051	57	0.079					
F092	CHF	MN	4	4.50	8.17	0.448	1.41	3.28	0.17	0.092	98	0.036	48	0.064	2.34	0.15	0.093		

Table App.D9-pulsed TDI indices (lat MA HCM group)

cat	Se' (cm/s)	Sl' (cm/s)	S' VTI (cm)	S' dur (sec)	Se' acc (cm/s^2)	tSe' acc (sec)	bS'-Sl' (sec)	Q-Se' (sec)	Q-Sl' (sec)	Q-bS' (sec)	Q-E' (sec)	Q-A' (sec)	Q-bE' (sec)	IVCt (sec)	IVRt (sec)	IVRb (cm/s)	IVRa (cm/s)	IVCa (cm/s)	IVCb (cm/s)
F009	8.06	3.89		0.136	361	0.022	0.077	0.089	0.145	0.068	0.315	0.356	0.282	0.034	0.076	3.42			4.53
F013	8.20	4.10		0.139	253	0.032	0.092	0.083	0.139	0.053	0.314	0.374	0.231	0.045	0.047				
F027	5.17		0.44	0.138	192	0.031		0.110		0.086	0.356	0.441		0.053		3.90	2.45		7.49
F038	5.56	3.87	0.84	0.237	198	0.031	0.174	0.099	0.244	0.071	0.306	0.424	0.266	0.049	0.051	3.36			4.66
F044	4.63	2.57	0.44	0.166	115	0.044	0.113	0.132	0.202	0.085	0.343	0.501	0.279	0.059	0.054	2.69	2.25		4.77
F052	3.80	3.49	0.37	0.117	278	0.018	0.066	0.080	0.134	0.070	0.324	0.389	0.300	0.049	0.123	3.82		2.73	6.89
F057	4.17	3.00	0.29	0.098	162	0.026	0.059	0.078	0.114	0.057				0.038	0.098	3.68	3.18	4.07	4.57
F069	6.99	4.45	0.55	0.135	213	0.033	0.091	0.071	0.128	0.043	0.289	0.351	0.255	0.030	0.085		4.69	4.27	7.13
F071	11.04	3.35	0.50	0.130	225	0.031	0.091	0.092	0.162	0.066	0.344	0.469	0.281	0.037	0.095	5.36		7.50	5.80
F073	6.42		0.43	0.093	316	0.024		0.091		0.079				0.062	0.146				
F081	7.96		0.61	0.133	158	0.051		0.120		0.074	0.349	0.422	0.278	0.059	0.083	4.01			4.98
F086	6.93	2.80	0.68	0.177	162	0.044	0.120	0.089	0.174	0.053	0.309	0.462	0.275	0.085	0.069				
F091	5.90	3.23	0.53	0.145	209.5	0.032	0.091	0.092	0.147	0.066	0.284	0.341	0.248	0.045	0.069	3.07			4.15
F093	6.16							0.098			0.338	0.392	0.294						
F060	4.87	3.42	0.53	0.187	145	0.035	0.133	0.090	0.191	0.063	0.299	0.338	0.263	0.068	0.042			5.23	5.85
F067	2.97	1.66	0.26	0.130	106	0.030	0.081	0.080	0.125	0.053				0.085	0.039			3.53	3.95
F082	2.72	2.68	0.38	0.200	61	0.045	0.114	0.096	0.193	0.069	0.339		0.290		0.041				
F092	2.48	2.05	0.27	0.170	94	0.027	0.122	0.108	0.204	0.089	0.317	0.419	0.275	0.059	0.033				

Table App.D10-pulsed TDI indices (4ch IVS HCM group)

cat	status	sex	age (years)	weight (Kg)	thickness (mm)	R-R (sec)	E'/A'	E' (cm/s)	E' VTI (cm)	E' dur (sec)	E' acc (cm/s^2)	tE' acc (sec)	E' dec (cm/s^2)	tE' dec (sec)	A' (cm/s)	A' VTI (cm)	A' dur (sec)	EA' (cm/s)	EA' VTI (cm)
F004	asympt.	MN	10	4.50	7.36	0.230												25.07	
F009	asympt.	MN	7	5.20	5.84	0.362	0.86	5.45							6.33				
F013	asympt.	MN	8	6.80	7.30	0.408	0.89	6.10		0.093	105	0.059	150	0.040	6.88		0.049		
F018	asympt.	MN	10	4.50	4.39	0.331												8.17	
F024	asympt.	MN	3	6.45	9.11	0.506	2.56	8.31	0.33	0.078	362	0.025	156	0.053	3.24	0.14	0.070		
F027	asympt.	FN	1	5.20	6.00	0.417	0.84	4.77	0.42	0.138	117	0.043	53	0.090	5.70	0.24	0.066		
F030	asympt.	MN	9	6.30	6.01	0.398	1.11	5.43	0.34	0.097	128	0.045	118	0.050	4.90	0.24	0.085		
F032	asympt.	MN	12	5.50	7.00	0.298	0.48	6.88							14.38			14.85	0.70
F038	asympt.	MN	10	5.00	4.87	0.426	0.79	4.15	0.23	0.078	120	0.034	82	0.050	5.24	0.21	0.072		
F044	asympt.	MN	7	4.50	7.20	0.646	0.53	3.10	0.22	0.098	67	0.043	56	0.061	5.86	0.31	0.075		
F052	asympt.	MN	9	4.20	4.70	0.390	0.62	5.20	0.22	0.068	282	0.019	100	0.054	8.46	0.36	0.065		
F057	asympt.	FN	7	4.40	6.70	0.322	0.60	4.58							7.67	0.35	0.075		
F069	asympt.	FN	4	4.15	6.42	0.394	0.56	3.73	0.17	0.066	118	0.034	93	0.044	6.72	0.24	0.060	10.55	0.46
F071	asympt.	MN	7	6.70	4.93	0.460	0.41	4.82	0.41	0.125	128	0.043	67	0.081	11.72	0.44	0.068		
F073	asympt.	MN	5	6.15	4.10	0.393	0.83	9.94							11.98				
F081	asympt.	MN	3	4.75	4.21	0.412	0.74	7.44	0.46	0.108	163	0.049	118	0.065	10.11	0.37	0.062		
F086	asympt.	MN	7	4.40	5.69	0.395	0.63	6.01	0.38	0.110	132	0.040	92	0.060	9.5	0.37	0.07		
F091	asympt.	FN	5	4.90	6.30	0.344	0.57	5.25	0.26	0.077	220	0.024	131	0.042	9.13	0.29	0.058		
F093	asympt.	MN	9	6.70	6.90	0.388	0.83	5.35	0.29	0.083	140	0.038	121	0.044	6.47	0.21	0.055		
F060	CHF	MN	2	3.30	4.30	0.354	0.80	4.18							5.22			5.34	0.31
F067	CHF	MN	9	4.80	7.60	0.279	0.58	1.91							3.28			3.36	0.13
F082	CHF	MN	11	5.80	5.00	0.494		3.28	0.14	0.067	117	0.031	108	0.034					
F092	CHF	MN	4	4.50	7.68	0.459	0.68	1.73	0.11	0.098	59	0.032	29	0.062	2.54	0.11	0.072		

Table App.D10-pulsed TDI indices (4ch IVS HCM group)

cat	Se' (cm/s)	Sl' (cm/s)	S' VTI (cm)	S' dur (sec)	Se' acc (cm/s^2)	tSe' acc (sec)	bS'-Sl' (sec)	Q-Se' (sec)	Q-Sl' (sec)	Q-bS' (sec)	Q-E' (sec)	Q-A' (sec)	Q-bE' (sec)	IVCt (sec)	IVRt (sec)	IVRb (cm/s)	IVRa (cm/s)	IVCa (cm/s)	IVCb (cm/s)
F004	10.32			0.084	322	0.033		0.068		0.041				0.016	0.076	8.08	5.18		
F009	6.08	3.78		0.148	213	0.029	0.078	0.089	0.152	0.074	0.309	0.362	0.264	0.041	0.051	5.23	3.75		6.71
F013	7.83	5.15		0.162	245	0.032	0.095	0.083	0.142	0.047	0.317	0.391	0.269	0.039	0.062	4.80	3.95		5.04
F018	4.75			0.153	135	0.036		0.086		0.053				0.021	0.073		2.50	3.64	3.28
F024	4.90	2.99	0.45	0.143	204	0.025	0.080	0.113	0.170	0.089	0.321	0.515	0.300	0.041	0.087	3.79	3.49	4.24	4.44
F027	8.62	2.70	0.63	0.166	165	0.050	0.122	0.098	0.176	0.058	0.292	0.440	0.248	0.044	0.044				
F030	4.17	3.03	0.39	0.147	154	0.026	0.073	0.075	0.137	0.060	0.297	0.387	0.257	0.042	0.068	3.05	3.18		3.85
F032	10.78	4.18	0.65	0.127	426	0.026	0.079	0.094	0.143	0.071				0.045	0.050				
F038	5.71	2.92	0.47	0.172	144	0.040	0.098	0.098	0.156	0.060	0.321	0.424	0.290	0.039	0.075	2.75	4.15		4.24
F044	5.75	3.06	0.46	0.155	170	0.033	0.095	0.104	0.166	0.071	0.373	0.677	0.337	0.029	0.094	1.92	3.43	2.72	3.26
F052	7.62		0.38	0.087	262	0.028		0.085		0.058	0.316	0.390	0.298	0.023	0.166	6.59	3.57		
F057	6.07				202	0.029		0.069		0.045	0.239	0.308		0.017					
F069	6.02	3.08	0.37	0.134	132	0.042	0.091	0.076	0.130	0.043	0.305	0.364	0.276	0.048	0.105	3.24			
F071	8.32	4.59	0.74	0.168	220	0.039	0.105	0.077	0.136	0.041	0.292	0.461	0.251	0.052	0.058		3.63		
F073	7.88	6.35	0.73	0.147	194	0.044	0.099	0.071	0.122	0.033	0.322	0.364	0.284	0.017	0.116	3.68			
F081	6.94	4.74	0.72	0.167	195	0.037	0.111	0.095	0.171	0.062	0.320	0.415	0.270	0.024	0.044				
F086	8.23	5.73	0.65	0.140	240	0.030	0.090	0.060	0.120	0.040	0.260	0.340	0.220	0.050	0.050				
F091	7.22	3.55	0.51	0.145	249	0.029	0.085	0.071	0.128	0.050	0.287	0.344	0.261	0.027	0.089	3.43	3.27	3.20	4.57
F093	7.79	4.33	0.59	0.145	288	0.028	0.098	0.080	0.152	0.057	0.328	0.301	0.289	0.034	0.097		3.20		
F060	4.09	2.89	0.28	0.103	152	0.027	0.072	0.094	0.140	0.065	0.325	0.359	0.305	0.034	0.145	4.58	3.21	2.55	5.65
F067	2.78	1.36	0.20	0.150	92	0.028	0.093	0.068	0.128	0.055	0.208	0.273	0.210	0.035	0.053				
F082	2.15										0.337		0.305						
F092	4.78		0.23	0.082	156	0.030		0.101		0.074	0.385	0.385	0.350	0.026	0.101	2.03	1.70		

Table App.D11-pulsed TDI indices (4ch LVPW HCM group)

cat	status	sex	age (years)	weight (Kg)	thickness (mm)	R-R (sec)	E'/A'	E' (cm/s)	E' VTI (cm)	E' dur (sec)	E' acc (cm/s^2)	tE' acc (sec)	E' dec (cm/s^2)	tE' dec (sec)	A' (cm/s)	A' VTI (cm)	A' dur (sec)	EA' (cm/s)	EA' VTI (cm)
F004	asympt.	MN	10	4.50	5.00	0.255												9.88	
F013	asympt.	MN	8	6.80	4.95	0.405	1.38	8.06		0.085	233	0.035	167	0.050	5.86		0.046		
F018	asympt.	MN	10	4.50	5.34	0.352												9.42	
F024	asympt.	MN	3	6.45	5.60	0.500	2.39	6.23	0.24	0.070	167	0.037	219	0.028	2.60	0.09	0.050		
F027	asympt.	FN	1	5.20	8.29	0.383	0.89	6.53							7.35				
F032	asympt.	MN	12	5.50	7.16	0.311	0.45	6.03							13.37				
F038	asympt.	MN	10	5.00	6.14	0.450	1.34	6.92	0.45	0.104	256	0.033	123	0.066	5.17	0.28	0.080		
F044	asympt.	MN	7	4.50	6.03	0.574	0.70	3.56	0.34	0.143	49	0.070	48	0.074	5.12	0.19	0.065		
F052	asympt.	MN	9	4.20	7.95	0.391	0.84	4.55	0.29	0.093	164	0.032	92	0.058	5.44	0.18	0.050		
F057	asympt.	FN	7	4.40	6.92	0.328	0.74	5.12							6.90				
F069	asympt.	FN	4	4.15	4.60	0.384	1.28	6.48	0.36	0.088	193	0.035	143	0.048	5.06	0.18	0.058		
F071	asympt.	MN	7	6.70	6.32	0.465	1.24	6.43	0.33	0.080	227	0.029	134	0.051	5.17	0.24	0.068		
F081	asympt.	MN	3	4.75	5.56	0.444	1.42	5.71	0.45	0.130	98	0.061	85	0.073	4.01				
F086	asympt.	MN	7	4.40	4.00	0.463	0.79	4.18	0.43	0.145	85	0.058	57	0.083	5.30	0.23	0.075		
F091	asympt.	FN	5	4.90	4.00	0.360	1.41	8.40	0.39	0.080	251	0.035	191	0.046	5.97	0.21	0.062		
F060	CHF	MN	2	3.30	4.68	0.381	0.89	5.80							6.51				
F067	CHF	MN	9	4.80	3.59	0.278												5.66	0.26
F082	CHF	MN	1	5.80	7.15	0.495		4.10	0.33	0.135	96	0.045	46	0.090					

Table App.D11-pulsed TDI indices (4ch LVPW HCM group)

cat	Se' (cm/s)	SI' (cm/s)	S' VTI (cm)	S' dur (sec)	Se' acc (cm/s^2)	tSe' acc (sec)	bS'-SI' (sec)	Q-Se' (sec)	Q-SI' (sec)	Q-bS' (sec)	Q-E' (sec)	Q-A' (sec)	Q-bE' (sec)	IVCt (sec)	IVRt (sec)	IVRb (cm/s)	IVRa (cm/s)	IVCa (cm/s)	IVCb (cm/s)
F004	4.72			0.098	150	0.031		0.107		0.078				0.045	0.065	3.44		4.28	3.72
F013	7.96			0.153	259	0.032		0.084		0.059	0.313	0.392	0.278	0.052	0.070	3.54		3.00	3.23
F018	8.00			0.118	237	0.034		0.072		0.060				0.051	0.116	3.30			9.43
F024	4.05	3.30	0.38	0.153	146	0.026	0.082	0.064	0.113	0.048	0.295	0.495	0.252	0.032	0.061				4.10
F027	6.24		0.50	0.138	191	0.034		0.108		0.071	0.367	0.400	0.297		0.098				7.16
F032	6.28	4.71	0.52	0.133	152	0.043	0.089	0.099	0.150	0.069	0.294	0.321	0.258	0.027	0.077				
F038	7.29	4.24	0.60	0.160	244	0.033	0.093	0.096	0.150	0.074	0.314	0.446	0.291	0.059	0.074	6.71			6.01
F044	5.90	2.52	0.58	0.183	144	0.041	0.105	0.119	0.182	0.074	0.394	0.564	0.319	0.046	0.082			3.76	3.91
F052	3.68	4.12	0.41	0.138	211	0.022	0.060	0.084	0.122	0.074	0.328	0.398	0.284	0.031	0.083	4.98			6.36
F057	4.46		0.25	0.096	152	0.031		0.086		0.060	0.265	0.304	0.240	0.061	0.084				3.60
F069	6.36	2.77	0.54	0.168	251	0.025	0.116	0.073	0.168	0.050	0.300	0.356	0.253	0.049	0.060			2.80	4.06
F071	4.00	4.51	0.40	0.122	181	0.027	0.082	0.089	0.143	0.072	0.349	0.472	0.314	0.053	0.115	4.41		5.12	4.67
F081	6.04		0.46	0.117	129	0.053		0.114		0.070	0.345	0.468	0.292	0.035	0.107	2.85			3.62
F086	7.55	2.55	0.54	0.133	265	0.031	0.099	0.075	0.138	0.053	0.331	0.401	0.243	0.065	0.059			3.18	4.75
F091	5.03	4.18	0.37	0.108	250	0.020	0.063	0.070	0.112	0.049	0.291	0.374	0.259	0.033	0.093	5.15			5.53
F060	4.14	4.28	0.61	0.190	150	0.032	0.124	0.098	0.186	0.063	0.305	0.350	0.270	0.075	0.039				4.32
F067	2.46		0.23	0.118	83	0.036		0.098		0.073				0.065	0.030				
F082	2.62	2.05	0.35	0.215	73	0.041	0.124	0.085	0.175	0.054	0.340		0.299		0.041				

Table App.D12-pulsed TDI indices (rpla LVPW HCM group)

cat	status	sex	age (years)	weight (Kg)	thickness (mm)	R-R (sec)	E'/A'	E' (cm/s)	E' VTI (cm)	E' dur (sec)	E' acc (cm/s^2)	tE' acc (sec)	E' dec (cm/s^2)	tE' dec (sec)	A' (cm/s)	A' VTI (cm)	A' dur (sec)	EA' (cm/s)	EA' VTI (cm)
F004	asympt.	MN	10	4.50	5.00	0.282	0.50	6.55							13.15				
F009	asympt.	MN	7	5.20	4.95	0.400	0.66	3.25		0.083	72	0.044	84	0.038	4.95		0.036		
F013	asympt.	MN	8	6.80	4.95	0.408	0.89	7.05		0.109	161	0.045	107	0.067	7.95		0.053		
F018	asympt.	MN	10	4.50	5.34	0.367	0.50	3.25							6.56		0.064		
F024	asympt.	MN	3	6.45	5.60	0.473	0.75	3.81	0.37	0.200	101	0.040	30	0.135	5.08	0.25	0.080		
F027	asympt.	FN	1	5.20	8.29	0.473	0.76	4.01							5.31	0.21	0.067		
F030	asympt.	MN	9	6.30	4.45	0.397	0.80	6.18							7.68	0.32	0.073		
F032	asympt.	MN	12	5.50	7.16	0.299	0.89	10.50							11.85			12.50	0.57
F038	asympt.	MN	10	5.00	6.14	0.479	1.25	9.07	0.57	0.123	245	0.039	114	0.083	7.23	0.39	0.098		
F044	asympt.	MN	7	4.50	6.03	0.548	0.44	3.04	0.19	0.082	95	0.031	58	0.051	6.95	0.26	0.068		
F052	asympt.	MN	9	4.20	7.95	0.343	0.57	2.96	0.13	0.053	156	0.022	104	0.032	5.23	0.17	0.053		
F057	asympt.	FN	7	4.40	6.92	0.316	0.76	5.54							7.28				
F069	asympt.	FN	4	4.15	4.60	0.418	0.67	4.51	0.26	0.085	123	0.038	97	0.051	6.76	0.24	0.067		
F071	asympt.	MN	7	6.70	6.32	0.483	0.64	5.40	0.43	0.120	137	0.042	76	0.074	8.49	0.36	0.068		
F073	asympt.	MN	5	6.15	7.44	0.381	0.80	6.45							8.08				
F081	asympt.	MN	3	4.75	5.56	0.398	0.48	4.25	0.25	0.087	145	0.031	73	0.061	8.81	0.39	0.072		
F086	asympt.	MN	7	4.40	4.00	0.510	0.63	5.08	0.41	0.135	118	0.044	60	0.078	8.03	0.32	0.070		
F091	asympt.	FN	5	4.90	4.00	0.371	0.67	4.77	0.33	0.098	100	0.049	111	0.047	7.12	0.25	0.060		
F093	asympt.	MN	9	6.70	6.34	0.430	0.71	4.79	0.36	0.120	76	0.065	96	0.052	6.72	0.28	0.068		
F060	CHF	MN	2	3.30	4.68	0.308	0.55	3.96	0.13	0.048	173	0.025	171	0.025	7.15	0.25	0.053		
F067	CHF	MN	9	4.80	3.59	0.270												7.53	0.34
F082	CHF	MN	11	5.80	7.15	0.462		2.33	0.23	0.145	49	0.054	31	0.088					
F092	CHF	MN	4	4.50	8.17	0.477	1.73	4.13	0.35	0.133	80	0.054	54	0.079	2.38	0.20	0.108		

Table App.D12-pulsed TDI indices (rpla LVPW HCM group)

cat	Se' (cm/s)	Sl' (cm/s)	S' VTI (cm)	S' dur (sec)	Se' acc (cm/s^2)	tSe' acc (sec)	bS'-Sl' (sec)	Q-Se' (sec)	Q-Sl' (sec)	Q-bS' (sec)	Q-E' (sec)	Q-A' (sec)	Q-bE' (sec)	IVCt (sec)	IVRt (sec)	IVRb (cm/s)	IVRa (cm/s)	IVCa (cm/s)	IVCb (cm/s)
F004	8.58	5.18		0.124	394	0.022	0.076	0.067	0.115	0.047	0.236	0.279	0.212	0.026	0.044			6.36	6.20
F009	5.05	3.58		0.152	279	0.018	0.068	0.102	0.160	0.086	0.340	0.403	0.301	0.052	0.064	3.33		2.86	6.96
F013	8.03	4.43		0.160	197	0.043	0.107	0.096	0.157	0.057	0.295	0.381	0.258	0.049	0.049				3.60
F018	4.85	3.23		0.136	120	0.041	0.097	0.125	0.185	0.088	0.287	0.357	0.268	0.065	0.049				3.75
F024	6.43		0.55	0.145	153	0.043		0.124		0.085	0.284	0.489	0.267	0.032	0.046		2.07	2.07	4.87
F027	5.69	3.93	0.50	0.157	191	0.030	0.077	0.106	0.163	0.079	0.323	0.497	0.281	0.048	0.060	3.25			4.81
F030	7.18		0.78	0.177	155	0.046		0.103		0.060	0.290	0.381	0.254	0.050	0.040				6.97
F032	6.67	4.20	0.55	0.138	212	0.035	0.078	0.107	0.166	0.079	0.311	0.334	0.263	0.030	0.061				6.30
F038	5.69	3.35	0.77	0.183	132	0.047	0.139	0.113	0.208	0.069	0.324	0.433	0.291	0.049	0.055	3.48		3.95	4.60
F044	6.35	3.72	0.55	0.160	230	0.023	0.090	0.098	0.167	0.079	0.387	0.519	0.350	0.051	0.125				5.83
F052	5.42		0.33	0.128	344	0.017		0.086		0.072	0.285	0.339	0.266	0.057	0.077	3.40			8.04
F057	5.15	2.27	0.35	0.132	232	0.024	0.090	0.098	0.168	0.080	0.302	0.335	0.281	0.041	0.094	2.31			5.25
F069	6.65	3.13	0.63	0.178	168	0.041	0.112	0.100	0.171	0.065	0.303	0.398	0.265	0.064	0.054			2.69	5.31
F071	6.32	5.56	0 78	0.165	194	0.036	0.103	0.100	0.152	0.065	0.314	0.473	0.282	0.038	0.065		3.49		4.60
F073	7.25	3.34	0 55	0.143	227	0.033	0.084	0.083	0.134	0.053	0.318	0.353	0.219	0.041	0.092			3.36	4.37
F081	6.82	3.98	0 65	0.148	190	0.036	0.102	0.098	0.165	0.069	0.287	0.394	0.257	0.035	0.056		2.25	2.71	6.48
F086	8.22	5.73	0 72	0.158	298	0.029	0.081	0.077	0.133	0.055	0.329	0.461	0.263	0.071	0.060		2.90	2.62	4.42
F091	7.13		0.61	0.142	171	0.043		0.103		0.070	0.308	0.395	0.257	0.056	0.059			3.30	6.72
F093	5.92	2.80	0.57	0.168	99	0.056	0.105	0.125	0.177	0.075	0.353	0.428	0.294	0.041	0.069	2.00	2.10		5.42
F060	4.77	2.33	0.36	0.137	237	0.020	0.077	0.078	0.136	0.065	0.274	0.314	0.255	0.032	0.069			3.70	7.35
F067	3.53	2.50	0.30	0.123	134	0.029	0.079	0.073	0.120	0.046				0.079	0.021				4.23
F082	2.08	1.88	0.30	0.192	41	0.058	0.153	0.180	0.270	0.119	0.441		0.381		0.065				
F092	5.60	1.83	0.49	0.158	97	0.056	0.111	0.133	0.194	0.081	0.325	0.489	0.276	0.036	0.045			2.53	4.70

Table App.D13-pulsed TDI indices (rpla IVS HCM group)

cat	status	sex	age (years)	weight (Kg)	thickness (mm)	R-R (sec)	E'/A'	E' (cm/s)	E' VTI (cm)	E' dur (sec)	E' acc (cm/s^2)	tE' acc (sec)	E' dec (cm/s^2)	tE' dec (sec)	A' (cm/s)	A' VTI (cm)	A' dur (sec)	EA' (cm/s)	EA' VTI (cm)
F004	asympt.	MN	10	4.50	7.36	0.266												13.20	
F018	asympt.	MN	10	4.50	4.39	0.319	0.52	5.00							9.68				
F027	asympt.	FN	1	5.20	6.00	0.409	0.60	3.63	0.16	0.073	117	0.032	91	0.041	6.05	0.23	0.063		
F038	asympt.	MN	10	5.00	4.87	0.448	0.92	6.35	0.27	0.070	177	0.037	148	0.043	6.88	0.32	0.090		
F044	asympt.	MN	7	4.50	7.20	0.483	0.58	3.41	0.23	0.098	108	0.036	70	0.060	5.87	0.25	0.065		
F052	asympt.	MN	5	4.20	4.70	0.352	0.60	3.50							5.81				
F057	asympt.	FN	7	4.40	6.70	0.311												7.78	0.30
F069	asympt.	FN	4	4.15	6.42	0.399	0.78	4.66	0.35	0.096	165	0.041	112	0.058	5.97	0.23	0.068	8.63	0.50
F071	asympt.	MN	7	6.70	4.93	0.464	0.95	5.76	0.38	0.107	112	0.053	117	0.050	6.07	0.26	0.068		
F073	asympt.	MN	5	6.15	4.10	0.383	0.17	2.29							13.42	0.43	0.058		
F081	asympt.	MN	3	4.75	4.21	0.510	0.71	5.95	0.39	0.102	113	0.056	126	0.050	8.32	0.29	0.067		
F086	asympt.	MN	7	4.40	5.69	0.489	0.84	4.02	0.22	0.093	140	0.031	72	0.058	4.80	0.15	0.053		
F091	asympt.	FN	5	4.90	6.30	0.423	1.06	6.48	0.37	0.092	158	0.037	103	0.057	6.12	0.20	0.052		
F093	asympt.	MN	5	6.70	6.90	0.412	1.13	4.79	0.34	0.110	113	0.044	81	0.060	4.23	0.15	0.057		
F060	CHF	MN	2	3.30	4.30	0.306	0.71	8.29							11.65				
F067	CHF	MN	5	4.80	7.60	0.283												8.49	0.46
F092	CHF	MN	4	4.50	7.68	0.489	1.17	5.02	0.33	0.118	80	0.061	77	0.064	4.28	0.16	0.068		

Table App.D13-pulsed TDI indices (rpla IVS HCM group)

cat	Se' (cm/s)	Sl' (cm/s)	S' VTI (cm)	S' dur (sec)	Se' acc (cm/s^2)	tSe' acc (sec)	bS'-Sl' (sec)	Q-Se' (sec)	Q-Sl' (sec)	Q-bS' (sec)	Q-E' (sec)	Q-A' (sec)	Q-bE' (sec)	IVCt (sec)	IVRt (sec)	IVRb (cm/s)	IVRa (cm/s)	IVCa (cm/s)	IVCb (cm/s)
F004	7.28	4.52		0.124	347	0.021	0.078	0.046	0.104	0.029				0.020	0.083				
F018	8.88			0.099	441	0.021		0.079		0.057	0.281	0.317	0.257	0.026	0.096		3.64		5.08
F027	7.26	3.42	0.63	0.177	215	0.035	0.107	0.072	0.139	0.039	0.354	0.422	0.328	0.090	0.101	3.7	5.14		
F038	4.78		0.52	0.173	89	0.053		0.125		0.081	0.321	0.416	0.293	0.061	0.071		4.53		5.13
F044	4.81	3.98	0.43	0.157	182	0.026	0.068	0.092	0.139	0.072	0.356	0.524	0.332	0.031	0.109		3.05		4.04
F052	6.15		0.50	0.133	171	0.038		0.065		0.040	0.239	0.350	0.217	0.012	0.055				
F057	5.97	2.73	0.38	0.147	205	0.032	0.112	0.076	0.158	0.051				0.034	0.090				
F069	5.06	3.30	0.56	0.190	132	0.041	0.107	0.068	0.153	0.050	0.325	0.475	0.290		0.065				
F071	5.04	3.49	0.50	0.153	190	0.028	0.091	0.233	0.141	0.056	0.343	0.473	0.291	0.029	0.087			3.63	2.90
F073	6.23	3.05	0.44	0.118	183	0.035	0.080	0.064	0.108	0.029	0.233	0.360	0.200	0.033	0.061				4.32
F081	4.79	3.36	0.57	0.172	181	0.037	0.124	0.085	0.171	0.053	0.338	0.489	0.280	0.020	0.059				4.23
F086	6.37	2.91	0.48	0.178	289	0.023	0.112	0.064	0.064	0.044	0.301	0.456	0.277	0.056	0.074			2.14	3.62
F091	5.55	4.23	0.60	0.185	187	0.029	0.106	0.069	0.146	0.047	0.317	0.419	0.278	0.037	0.061			2.78	3.45
F093	5.85	4.60	0.56	0.167	266	0.025	0.096	0.078	0.154	0.057	0.298	0.427	0.257	0.031	0.054			2.27	1.98
F060	6.57	2.96	0.40	0.125	417	0.017	0.088	0.067	0.144	0.054	0.278	0.314	0.254	0.024	0.045			7.15	6.17
F067	7.29	3.06	0.55	0.137	164	0.047	0.095	0.059	0.111	0.019				0.043	0.021				3.45
F092	5.82	2.33	0.54	0.187	103	0.056	0.119	0.082	0.157	0.044	0.345	0.450	0.290	0.037	0.078				

Table App.D14-pulsed TDI indices (Tr HCM group)

cat	status	sex	age (years)	weight (Kg)	thickness (mm)	R-R (sec)	E'/A'	E' (cm/s)	E' VTI (cm)	E' dur (sec)	E' acc (cm/s^2)	tE' acc (sec)	E' dec (cm/s^2)	tE' dec (sec)	A' (cm/s)	A' VTI (cm)	A' dur (sec)	EA' (cm/s)	EA' VTI (cm)
F052	asympt.	MN	9	4.20	0	0.390	0.42	7.75	0.53	0.093	188	0.041	160	0.047	18.62	0.85	0.077		
F057	asympt.	FN	7	4.40	0	0.318												18.45	0.71
F069	asympt.	FN	4	4.15	0	0.368	0.50	8.92	0.72	0.120	200	0.045	141	0.063	17.69	0.73	0.075		
F071	asympt.	MN	7	6.70	0	0.466	0.56	8.08	0.75	0.148	145	0.056	88	0.091	14.50	0.75	0.090		
F073	asympt.	MN	5	6.15	0	0.373												16.37	1.06
F081	asympt.	MN	3	4.75	0	0.430	0.58	5.95	0.52	0.140	106	0.056	77	0.078	10.18	0.51	0.078		
F086	asympt.	MN	7	4.40	0	0.474	0.39	8.20	0.67	0.127	183	0.048	111	0.080	21.20	0.88	0.075		
F091	asympt.	FN	5	4.90	0	0.349	0.47	6.47							13.83				
F093	asympt.	MN	9	6.70	0	0.347	0.31	7.25							23.30	1.00	0.075		
F067	CHF	MN	9	4.80	0	0.351												18.45	0.75
F082	CHF	MN	11	5.80	0	0.416		5.48	0.35	0.113	167	0.035	78	0.073					
F092	CHF	MN	4	4.50	0	0.433	0.51	5.67	0.38	0.100	115	0.050	120	0.048	11.05	0.57	0.088		

Table App.D14-pulsed TDI indices (Tr HCM group)

cat	Se' (cm/s)	Sl' (cm/s)	S' VTI (cm)	S' dur (sec)	Se' acc (cm/s^2)	tSe' acc (sec)	bS'-Sl' (sec)	Q-Se' (sec)	Q-Sl' (sec)	Q-bS' (sec)	Q-E' (sec)	Q-A' (sec)	Q-bE' (sec)	IVCt (sec)	IVRt (sec)	IVRb (cm/s)	IVRa (cm/s)	IVCa (cm/s)	IVCb (cm/s)
F052	15.42	6.65	1.17	0.165	509	0.032	0.092	0.074	0.137	0.053	0.307	0.371	0.248	0.038	0.059	5.93		8.48	
F057	9.50	5.03	0.69	0.127	334	0.029	0.078	0.079	0.131	0.055				0.042	0.097	4.38	4.03		
F069	12.41	8.58	0.99	0.145	399	0.031	0.078							0.046	0.063			10.78	
F071	12.85	8.93	1.27	0.172	396	0.034	0.090	0.085	0.143	0.058	0.319	0.463	0.263	0.019	0.055		4.32	6.92	4.22
F073	8.83	7.13	0.88	0.150	261	0.033	0.087	0.076	0.127	0.058				0.032	0.080			9.43	
F081	7.75	5.70	0.75	0.153	334	0.024	0.090	0.090	0.157	0.068	0.288	0.443	0.239	0.031	0.028			6.03	
F086	10.67	7.50	1.10	0.158	290	0.038	0.102	0.066	0.129	0.034	0.304	0.420	0.258	0.056	0.074	3.53	4.85	7.03	
F091	11.13	6.30	0.83	0.143	424	0.028	0.058	0.074	0.130	0.048	0.275	0.325	0.246	0.035	0.069			5.68	6.67
F093	16.14	8.53	1.09	0.138	440	0.036	0.086	0.074	0.125	0.043	0.266	0.326	0.236	0.029	0.080				
F067	7.35	5.70	0.62	0.133	231	0.034	0.193	0.068	0.115	0.043				0.051	0.039				
F082	5.10	2.97	0.42	0.138	141	0.041	0.086	0.124	0.169	0.088	0.307		0.335		0.095				
F092	8.43	5.95	0.76	0.162	268	0.032	0.091	0.092	0.150	0.066	0.312	0.390	0.264	0.050	0.056		3.90		

Appendix D2

Table App.D15 Linear regression and multiple linear regression equations for independent variables significantly influencing pulsed TDI indices of the septal mitral annulus in the normal group

normal TDI parameter Sep MA	Forward stepwise regression analysis	Linear and multiple linear regression equations	R	R^2	Adjusted R^2	p
E'/A'	Age (p=0.005)	E'/A' = 1.259 - (0.0402 * age)	0.564	0.318	0.288	<0.01
E'	Age (p=0.032); weight (p=0.024)	E' = 2.746 - (0.181 * age) + (1.008 * weight)	0.527	0.277	0.212	<0.05
E' dur	R-R (p<0.001)	E' dur = 0.0514 + (0.0876 * R-R)	0.999	0.997	0.997	<0.001
E' acc	Age (p=0.043); weight (p=0.024)	E' acc = 50.766 - (6.803 * age) + (36.743 * weight)	0.649	0.421	0.356	<0.01
tE' acc	Sex (p=0.028)	tE' acc = 0.0486 - (0.00769 * sex)	0.488	0.238	0.198	<0.05
E' dec	Age (p=0.002); sex (p=0.0170; R-R (p=0.031)	E' dec = 375.250 - (7.242 * age) - (59.815 * sex) - (279.961 * R-R)	0.747	0.558	0.475	<0.01
tE' dec	Sex (p=0.057); R-R (p=0.019)	tE' dec = 0.0190 + (0.00687 * sex) + (0.0531 * R-R)	0.615	0.379	0.305	<0.05
A'	R-R (p=0.055)	ns	ns			ns
A' dur	R-R (p=0.012)	A' dur = 0.0328 + (0.0827 * R-R)	0.558	0.311	0.271	<0.05
Se'	R-R (p=0.051)	Se' = 11.263 - (10.521 * R-R)	0.441	0.195	0.158	<0.05
S' dur	R-R (p=0.004)	S' dur = 0.00770 + (0.320 * R-R)	0.491	0.242	0.207	<0.05
tSe' acc	Sex (p=0.035)	tSe' acc = 0.0325 - (0.00400 * sex)	0.427	0.183	0.145	<0.05
Q-Se'	R-R (p=0.033)	Q-Se' = 0.0511 + (0.0882 * R-R)	0.515	0.266	0.229	<0.05
Q-Sl'	Sex (p=0.022); R-R (p<0.001)	Q-Sl' = -0.300 + (0.0444 * sex) + (0.900 * R-R)	0.999	0.999	0.999	<0.001
Q-E'	R-R (p<0.001)	Q-E' = 0.105 + (0.494 * R-R)	1.000	1.000	1.000	<0.001
Q-A'	R-R (p<0.001)	Q-A' = 0.135 + (0.678 * R-R)	1.000	0.999	0.999	<0.001
Q-bS'	Sex (p=0.004); weight (p=0.009); R-R (p<0.001)	Q-bS' = -6.968 + (0.899 * sex) + (0.454 * weight) + (9.068 * R-R)	0.999	0.999	0.999	<0.001
IVRt	Weight (p=0.015); R-R (p=0.022)	IVRt = 0.0949 - (0.00727 * weight)	0.410	0.168	0.130	<0.05
IVCb	Weight (p=0.048)	ns	ns			ns

Table App.D16 Linear regression and multiple linear regression equations for independent variables significantly influencing pulsed TDI indices of the lateral mitral annulus in the normal group

normal TDI parameter Lat MA	Forward stepwise regression analysis	Linear and multiple linear regression equations	R	R^2	Adjusted R^2	p
E'/A'	Thickness (p=0.071); age (p=0.006); weight (p=0.030) R-R (p=0.002)	E'/A' = 0.320 - (0.268 * thickness) - (0.0831 * age) + (0.227 * weight) + (4.187 * R-R)	0.838	0.702	0.632	<0.001
E'	Age (p=0.028)	E' = 10.690 - (0.383 * age)	0.513	0.264	0.228	<0.05
tE' acc	Sex (p=0.042); R-R (p=0.076)	tE' acc = 0.0295 - (0.00544 * sex) + (0.0347 * R-R)	0.673	0.453	0.396	<0.01
A'	R-R (p=0.052)	A' = 12.284 - (14.851 * R-R)	0.481	0.231	0.193	<0.05
Se'	R-R (p=0.061)	Se' = 12.107 - (12.264 * R-R)	0.416	0.173	0.135	<0.05
S' dur	Sex (p=0.019); R-R (p<0.001)	S' dur = 0.101 - (0.0106 * sex) + (0.180 * R-R)	0.788	0.620	0.584	<0.001
tSe' acc	Thickness (p=0.017)	ns	ns			ns
bS'-SI'	Thickness (p=0.023); R-R (p=0.008)	bS'-SI' = 0.0760 - (0.0118 * thickness) + (0.132 * R-R)	0.605	0.366	0.305	<0.01
Q-Se'	Age (p=0.036); R-R (p=0.005)	Q-Se' = 0.0380 + (0.00163 * age) + (0.0995 * R-R)	0.679	0.461	0.409	<0.01
Q-SI'	R-R (p<0.001)	Q-SI' = 0.0737 + (0.176 * R-R)	0.567	0.322	0.291	<0.01
Q-E'	R-R (p<0.001)	Q-E' = 0.186 + (0.308 * R-R)	0.676	0.458	0.432	<0.001
Q-A'	R-R (p<0.001)	Q-A' = -0.00986 + (1.028 * R-R)	0.962	0.925	0.921	<0.001
Q-bE'	Age (p=0.009); sex (p=0.004); R-R (p<0.001)	Q-bE' = 0.149 + (0.00221 * age) - (0.0191 * sex) + (0.331 * R-R)	0.962	0.926	0.910	<0.001
Q-bS'	Age (p=0.076); R-R (p=0.009)	Q-bS' = 0.0222 + (0.00137 * age) + (0.0946 * R-R)	0.688	0.473	0.423	<0.001

Table App.D17 Linear regression and multiple linear regression equations for independent variables significantly influencing pulsed TDI indices of the IVS along the longitudinal axis in the normal group

normal TDI parameter 4ch IVS	Forward stepwise regression analysis	Linear and multiple linear regression equations	R	R^2	Adjusted R^2	p
E'/A'	Age (p=0.022)	E'/A' = 1.564 - (0.0676 * age)	0.605	0.366	0.339	<0.001
E' dec	Age (p=0.014)	E' dec = 224.119 - (8.752 * age)	0.436	0.190	0.153	<0.05
A' dur	R-R (p=0.004)	A' dur = 0.0291 + (0.0747 * R-R)	0.642	0.412	0.386	<0.001
S' dur	Sex (p=0.014); R-R (p<0.001)	S' dur = 0.0932 - (0.0108 * sex) + (0.192 * R-R)	0.843	0.711	0.685	<0.001
Se' acc	R-R (p=0.047)	Se' acc = 412.025 - (453.795 * R-R)	0.460	0.211	0.177	<0.05
tSe' acc	R-R (p=0.027)	tSe' acc = 0.0135 + (0.0378 * R-R)	0.577	0.333	0.304	<0.01
Sl' acc	R-R (p=0.039)	Sl' acc = 115.857 - (140.929 * R-R)	0.508	0.258	0.226	<0.01
bS'-Sl'	R-R (p=0.003)	bS'-Sl' = 0.0456 + (0.100 * R-R)	0.641	0.411	0.386	<0.001
Q-Se'	R-R (p=0.003)	Q-Se' = 0.0448 + (0.103 * R-R)	0.594	0.352	0.323	<0.01
Q-Sl'	R-R (p<0.001)	Q-Sl' = 0.0715 + (0.176 * R-R)	0.748	0.560	0.540	<0.001
Q-E'	Sex (p=0.061); R-R (p<0.001)	Q-E' = 0.208 - (0.0182 * sex) + (0.309 * R-R)	0.875	0.765	0.743	<0.001
Q-A'	R-R (p<0.001)	Q-A' = -0.00691 + (1.015 * R-R)	0.992	0.984	0.983	<0.001
Q-bE'	R-R (p<0.001)	Q-bE' = 0.136 + (0.345 * R-R)	0.790	0.625	0.601	<0.001
IVCb	Weight (p=0.048)	ns	ns			ns

Table App.D18 Linear regression and multiple linear regression equations for independent variables significantly influencing pulsed TDI indices of the LVPW along the longitudinal axis in the normal group

normal TDI parameter 4ch LVPW	Forward stepwise regression analysis	Linear and multiple linear regression equations	R	R^2	Adjusted R^2	p
E'/A'	Age (p=0.027)	E'/A' = 2.431 - (0.0942 * age)	0.548	0.301	0.269	<0.01
E'	Age (p=0.005)	E' = 11.594 - (0.393 * age)	0.631	0.399	0.371	<0.001
E' acc	Age (p=0.006)	E' acc = 397.983 - (13.671 * age)	0.571	0.326	0.295	<0.01
E' dec	Age (p=0.014)	E' dec = 250.803 - (9.924 * age)	0.511	0.261	0.228	<0.05
SI'	Age (p=0.060)	SI' = 4.535 - (0.123 * age)	0.422	0.178	0.137	0.05
Q-Se'	R-R (p=0.016)	Q-Se' = 0.0445 + (0.114 * R-R)	0.534	0.285	0.251	<0.01
Q-SI'	R-R (p=0.004)	Q-SI' = 0.0588 + (0.247 * R-R)	0.602	0.362	0.328	<0.01
Q-E'	R-R (p<0.001)	Q-E' = 0.146 + (0.390 * R-R)	0.907	0.822	0.813	<0.001
Q-A'	R-R (p<0.001)	Q-A' = 0.0190 + (0.944 * R-R)	0.979	0.959	0.957	<0.001
Q-bE'	RR (p<0.001)	Q-bE' = 0.109 + (0.404 * R-R)	0.924	0.854	0.844	<0.001
IVCt	R-R (p=0.025)	IVCt = -0.0119 + (0.143 * R-R)	0.502	0.252	0.219	<0.05
Q-bS'	R-R (p=0.037)	Q-bS' = 0.0184 + (0.119 * R-R)	0.516	0.266	0.231	<0.05

Table App.D19 Linear regression and multiple linear regression equations for independent variables significantly influencing pulsed TDI indices of the LVPW along the radial axis in the normal group

normal TDI parameter rpla LVPW	Forward stepwise regression analysis	Linear and multiple linear regression equations	R	R^2	Adjusted R^2	p
E'A'	Thickness (p=0.049)	E'/A' = 1.983 - (0.218 * thickness)	0.421	0.177	0.139	<0.05
E'	Age (p=0.036)	E' = 6.739 - (0.182 * age)	0.396	0.156	0.118	0.056
E' dur	R-R (p=0.023)	E' dur = 0.0219 + (0.135 * R-R)	0.638	0.407	0.374	<0.01
E' acc	Age (p=0.060); weight (p=0.054)	E' acc = 83.046 - (8.872 * age) + (33.789 * weight)	0.613	0.375	0.302	<0.05
E' dec	Age (p=0.007); R-R (p=0.029)	E' dec = 272.677 - (6.346 * age) - (233.984 * R-R)	0.618	0.382	0.310	<0.05
tE' dec	R-R (p=0.020)	tE' dec = 0.00139 + (0.106 * R-R)	0.634	0.402	0.368	<0.01
A' VTI	Thickness (p=0.002)	A' VTI = -0.0724 + (0.0745 * thickness)	0.688	0.473	0.438	<0.01
S' dur	R-R (p=0.001)	S' dur = 0.0805 + (0.165 * R-R)	0.749	0.561	0.541	<0.001
Se' acc	Thickness (p=0.024); R-R (p=0.048)	Se' acc = 481.933 - (37.312 * thickness) - (262.552 * R-R)	0.592	0.351	0.289	<0.05
bS'-Sl'	Thickness (p=0.015); sex (p=0.034)	bS'-Sl' = -0.00729 + (0.0180 * thickness) + (0.0158 * sex)	0.536	0.287	0.204	<0.05
Q-Se'	Weight (p=0.036); R-R (p=0.011)	Q-Se' = 0.0231 + (0.00759 * weight) + (0.0963 * R-R)	0.631	0.398	0.341	<0.01
Q-Sl'	Thickness (p=0.026); sex (p=0.014); weight (p=0.051); R-R (p=0.001)	Q-Sl' = -0.132 + (0.0201 * thickness) + (0.0296 * sex) + (0.0131 * weight) + (0.241 * R-R)	0.828	0.686	0.602	<0.001
Q-E'	R-R (p <0.001)	Q-E' = 0.159 + (0.345 * R-R)	0.764	0.583	0.564	<0.001
Q-A'	R-R (p<0.001)	Q-A' = 0.0283 + (0.907 * R-R)	0.979	0.959	0.957	<0.001
Q-bE'	R-R (p<0.001)	Q-bE' = 0.141 + (0.304 * R-R)	0.732	0.535	0.506	<0.001
IVCt	R-R (p=0.020)	IVCt = 0.0129 + (0.0877 * R-R)	0.546	0.298	0.266	<0.01
Q-bS'	R-R (p=0.008)	Q-bS' = 0.0404 + (0.0756 * R-R)	0.566	0.320	0.289	<0.001
IVCb	R-R (p=0.007)	IVCb = 12.473 - (13.285 * R-R)	0.570	0.325	0.295	<0.01

Table App.D20 Linear regression and multiple linear regression equations for independent variables significantly influencing pulsed TDI indices of the IVS along the radial axis in the normal group

normal TDI parameter rpla IVS	Forward stepwise regression analysis	Linear and multiple linear regression equations	R	R^2	Adjusted R^2	p
Q-Sl'	Age (p=0.047)	Q-Sl' = 0.128 + (0.00284 * age)	0.707	0.500	0.450	<0.001
Q-E'	R-R (p<0.001)	Q-E' = 0.0712 + (0.560 * R-R)	0.854	0.729	0.709	<0.001
Q-A'	R-R (p<0.001)	Q-A' = -0.116 + (1.286 * R-R)	0.970	0.940	0.936	<0.001
Q-bE'	R-R (p<0.001)	Q-bE' = 0.0677 + (0.471 * R-R)	0.816	0.665	0.641	<0.001
IVRt	R-R (p=0.010)	IVRt = -0.0451 + (0.269 * R-R)	0.771	0.594	0.560	<0.001

Table App.D21 Linear regression and multiple linear regression equations for independent variables significantly influencing pulsed TDI indices of the tricuspid annulus in the normal group

normal TDI parameter Tr	Forward stepwise regression analysis	Linear and multiple linear regression equations	R	R^2	Adjusted R^2	p
E' dur	R-R (p=0.027)	E' dur = 0.0642 + (0.125 * R-R)	0.669	0.448	0.356	0.069
E' dec	Age (p=0.032); R-R (p=0.061)	E' dec = 365.951 - (9.660 * age) - (332.616 * R-R)	0.854	0.729	0.621	<0.05
tE' dec	Age (p=0.035); R-R (p=0.048)	tE' dec = -0.0306 + (0.00347 * age) + (0.166 * R-R)	0.881	0.776	0.686	<0.001
S' dur	R-R (p=0.057)	S' dur = 0.0442 + (0.280 * R-R)	0.956	0.913	0.899	<0.001
Q-E'	R-R (p=0.014)	Q-E' = 0.0926 + (0.481 * R-R)	0.941	0.886	0.867	<0.001
Q-A'	R-R (p<0.001)	Q-A' = 0.0386 + (0.907 * R-R)	0.975	0.951	0.943	<0.001
Q-bE'	R-R (p<0.001)	Q-bE' = 0.0693 + (0.423 * R-R)	0.932	0.868	0.846	<0.001

Table App.D22 Linear regression and multiple linear regression equations for independent variables significantly influencing pulsed TDI indices of the septal mitral annulus in the HCM group

HCM TDI parameter Sep MA	Forward stepwise regression analysis	Linear and multiple linear regression equations	R	R^2	Adjusted R^2	p
E/A'	Thickness (p=0.014); age (p=0.025); sex (p=0.043)	E'/A' = -0.285 + (0.168 * thickness)	0.475	0.226	0.183	<0.05
E'	Age (p=0.029)	ns	ns			ns
E' VTI	Thickness (p=0.046); age (p=0.009); weight (p=0.032)	E' VTI = 0.314 - (0.0300 * thickness) - (0.0200 * age) + (0.0551 * weight)	0.804	0.646	0.558	<0.01
E' dur	R-R (p=0.033)	E' dur = -0.00300 + (0.247 * R-R)	0.751	0.563	0.532	<0.001
A'	Thickness (p=0.030); sex (p=0.014)	A' = 7.463 - (0.583 * thickness) + (2.228 * sex)	0.551	0.303	0.221	<0.05
A' VTI	Thickness (p=0.012); sex (p=0.018)	A' VTI = 0.413 - (0.0387 * thickness) + (0.0915 * sex)	0.717	0.514	0.439	<0.01
S' dur	Thickness (p=0.005); weight (p=0.043); R-R (p=0.017)	S' dur = 0.115 - (0.00582 * thickness) + (0.00523 * weight) + (0.0987 * R-R)	0.771	0.594	0.530	<0.001
Q-E'	R-R (p=0.001)	Q-E' = 0.163 + (0.355 * R-R)	0.701	0.491	0.464	<0.001
Q-A'	R-R (p<0.001)	Q-A' = -0.00981 + (1.004 * R-R)	0.980	0.961	0.958	<0.001
Q-bE'	R-R (p=0.003)	Q-bE' = 0.144 + (0.299 * R-R)	0.645	0.416	0.385	<0.001
IVRt	R-R (p=0.024)	IVRt = 0.0271 + (0.118 * R-R)	0.456	0.208	0.171	<0.05
IVCb	Thickness (p=0.006)	IVCb = 9.209 - (0.739 * thickness)	0.623	0.389	0.353	<0.01

Table App.D23 Linear regression and multiple linear regression equations for independent variables significantly influencing pulsed TDI indices of the lateral mitral annulus in the HCM group

HCM TDI parameter Lat MA	Forward stepwise regression analysis	Linear and multiple linear regression equations	R	R^2	Adjusted R^2	p
E'	Thickness (p=0.008)	E' = 8.648 - (0.573 * thickness)	0.676	0.457	0.415	<0.01
E' VTI	Thickness (p=0.033)	ns	ns			ns
A'	Thickness (p=0.005); weight (p=0.030)	A' = 7.039 - (0.942 * thickness) + (0.901 * weight)	0.844	0.713	0.661	<0.01
Se'	Thickness (p=0.0320; weight (p=0.008)	Se' = 0.501 + (1.039 * weight)	0.461	0.212	0.163	0.054
S' VTI	R-R (p=0.037)	ns	ns			ns
S' dur	R-R (p=0.011)	S' dur = 0.0254 + (0.303 * R-R)	0.577	0.333	0.289	<0.05
tSe' acc	Thickness (p=0.054); R-R (p=0.014)	tSe' acc = 0.0151 - (0.00275 * thickness) + (0.0830 * R-R)	0.698	0.488	0.415	<0.01
bS'-Sl'	R-R (p=0.045)	bS'-Sl' = -0.00235 + (0.257 * R-R)	0.640	0.410	0.361	<0.05
Q-Se'	R-R (p=0.020)	Q-Se' = 0.0334 + (0.149 * R-R)	0.664	0.441	0.406	<0.01
Q-Sl'	R-R (p=0.020)	Q-Sl' = 0.00872 + (0.384 * R-R)	0.763	0.583	0.548	<0.01
Q-E'	R-R (p=0.020)	Q-E' = 0.234 + (0.206 * R-R)	0.528	0.279	0.224	<0.05
Q-A'	R-R (p<0.001)	Q-A' = 0.0563 + (0.825 * R-R)	0.945	0.893	0.884	<0.001
Q-bS'	Thickness (p=0.006)	Q-bS' = 0.0327 + (0.00585 * thickness)	0.697	0.486	0.451	<0.01

Table App.D24 Linear regression and multiple linear regression equations for independent variables significantly influencing pulsed TDI indices of the IVS along the longitudinal axis in the HCM group

HCM TDI parameter 4ch IVS	Forward stepwise regression analysis	Linear and multiple linear regression equations	R	R^2	Adjusted R^2	p
E'/A'	Thickness (p=0.044); age (p=0.022)	ns	ns			ns
E'	Weight (p=0.015)	E' = 0.639 + (0.859 * weight)	0.432	0.187	0.144	0.05
E' VTI	Thickness (p=0.048); age (p=0.015); weight (p=0.047)	E' VTI = 0.390 - (0.0504 * thickness) - (0.0254 * age) + (0.0688 * weight)	0.773	0.598	0.477	<0.05
E' dur	Age (p=0.027)	ns	ns			ns
tE' dec	Thickness (p=0.045); age (p=0.010)	tE' dec = 0.0736 - (0.00282 * age)	0.552	0.304	0.251	<0.05
A'	Thickness (p=0.021)	A' = 13.930 - (1.085 * thickness)	0.466	0.217	0.174	<0.05
A' VTI	Thickness (p=0.035)	A' VTI = 0.579 - (0.0487 * thickness)	0.674	0.454	0.408	<0.01
S' VTI	Thickness (p=0.027); weight (p=0.017)	S' VTI = 0.344 - (0.0626 * thickness) + (0.104 * weight)	0.694	0.481	0.407	<0.05
S' dur	Weight (p=0.015)	S' dur = 0.0697 + (0.0135 * weight)	0.483	0.233	0.192	<0.05
tSe' acc	Thickness (p=0.020)	tSe' acc = 0.0453 - (0.00204 * thickness)	0.416	0.173	0.131	0.054
Q-Se'	R-R (p=0.053)	Q-Se' = 0.0467 + (0.0960 * R-R)	0.579	0.335	0.302	0.01
Q-E'	R-R (p=0.003)	Q-E' = 0.156 + (0.367 * R-R)	0.707	0.500	0.473	<0.001
Q-A'	R-R (p<0.001)	Q-A' = -0.0511 + (1.093 * R-R)	0.943	0.890	0.883	<0.001
Q-bE'	R-R (p<0.001)	Q-bE' = 0.159 + (0.286 * R-R)	0.625	0.391	0.355	<0.001
Q-bS'	Thickness (p=0.038)	ns	ns			ns

Table App.D25 Linear regression and multiple linear regression equations for independent variables significantly influencing pulsed TDI indices of the LVPW along the longitudinal axis in the HCM group

HCM TDI parameter 4ch LVPW	Forward stepwise regression analysis	Linear and multiple linear regression equations	R	R^2	Adjusted R^2	p
E'/A'	Weight (p=0.044)	ns	ns			ns
E'	Weight (p=0.009); R-R (p=0.028)	E' = 7.078 + (0.686 * weight) - (11.085 * R-R)	0.659	0.435	0.340	<0.05
E' dur	Weight (p=0.039)	ns	ns			ns
tE' acc	Weight (p=0.049)	ns	ns			ns
E' dec	Weight (p=0.048)	ns	ns			ns
A'	R-R (p=0.049)	A' = 15.358 - (22.467 * R-R)	0.652	0.425	0.378	<0.05
A' VTI	Age (p=0.030)	A' VTI = 0.0895 + (0.0170 * age)	0.725	0.525	0.446	<0.05
Sl'	R-R (p=0.044)	Sl' = 6.992 - (7.894 * R-R)	0.632	0.399	0.332	<0.05
S' dur	R-R (p=0.033)	S' dur = 0.0446 + (0.241 * R-R)	0.609	0.370	0.331	<0.01
Q-E'	R-R (p=0.032)	Q-E' = 0.189 + (0.315 * R-R)	0.669	0.447	0.405	<0.01
Q-A'	R-R (p=0.001)	Q-A' = 0.00763 + (0.965 * R-R)	0.947	0.896	0.887	<0.001
Q-bE'	R-R (p=0.017)	Q-bE' = 0.193 + (0.197 * R-R)	0.553	0.305	0.252	<0.05
Q-bS'	Thickness (p=0.050)	ns	ns			ns

Table App.D26 Linear regression and multiple linear regression equations for independent variables significantly influencing pulsed TDI indices of the LVPW along the radial axis in the HCM group

HCM TDI parameter rpla LVPW	Forward stepwise regression analysis	Linear and multiple linear regression equations	R	R^2	Adjusted R^2	p
E' dur	Weight (p=0.035); R-R (p=0.044)	E' dur = -0.0973 + (0.0166 * weight) + (0.276 * R-R)	0.754	0.568	0.496	<0.01
E' dec	R-R (p=0.014)	E' dec = 258.677 - (401.683 * R-R)	0.717	0.514	0.476	<0.01
tE' dec	R-R (p=0.045)	tE' dec = -0.0471 + (0.256 * R-R)	0.606	0.368	0.319	<0.05
S' VTI	R-R (p=0.048)	S' VTI = 0.137 + (0.987 * R-R)	0.490	0.240	0.195	<0.05
S' dur	R-R (p<0.001)	S' dur = 0.0812 + (0.176 * R-R)	0.710	0.504	0.480	<0.001
Q-SI'	Thickness (p=0.067); age (p=0.049); R-R (p=0.058)	Q-SI' = 0.00633 + (0.0105 * thickness) + (0.00428 * age) + (0.164 * R-R)	0.674	0.454	0.345	<0.05
Q-E'	Age (p=0.054); R-R (p=0.002)	Q-E' = 0.128 + (0.00449 * age) + (0.379 * R-R)	0.681	0.464	0.408	<0.05
Q-A'	R-R (p<0.001)	Q-A' = 0.0509 + (0.863 * R-R)	0.952	0.907	0.902	<0.001
Q-bE'	Age (p=0.039); R-R (p=0.002)	Q-E' = 0.128 + (0.00449 * age) + (0.379 * R-R)	0.681	0.464	0.408	<0.01
IVCt	Thickness (p=0.041)	IVCt = 0.0723 - (0.00430 * thickness)	0.432	0.187	0.146	<0.05
Q-bS'	Thickness (p=0.064)	Q-bS' = 0.0409 + (0.00522 * thickness)	0.457	0.209	0.171	<0.05

Table App.D27 Linear regression and multiple linear regression equations for independent variables significantly influencing pulsed TDI indices of the IVS along the radial axis in the HCM group

HCM TDI parameter rpla IVS	Forward stepwise regression analysis	Linear and multiple linear regression equations	R	R^2	Adjusted R^2	p
E' acc	Thickness (p<0.001); age (p<0.001); sex (p=0.012) weight 0.001	E' acc = 152.540 - (14.461 * thickness) + (10.883 * age) + (60.367 * sex) - (15.294 * weight)	0.991	0.982	0.968	<0.001
E' dec	Thickness (p=0.048)	E' dec = 206.431 - (17.729 * thickness)	0.756	0.572	0.518	<0.05
A'	Thickness (p=0.046)	A' = 16.434 - (1.685 * thickness)	0.742	0.551	0.514	<0.01
A' VTI	Thickness (p=0.041)	A' VTI = 0.547 - (0.0520 * thickness)	0.747	0.558	0.509	<0.01
Se'	R-R (p=0.017)	Se' = 9.882 - (9.532 * R-R)	0.672	0.452	0.415	<0.01
S' dur	Thickness (p=0.031) ; sex (p=0.020); R-R (p<0.001)	S' dur = -0.0248 + (0.00681 * thickness) + (0.0263 * sex) + (0.269 * R-R)	0.913	0.833	0.794	<0.001
Q-E'	R-R (p=0.048)	Q-E' = 0.134 + (0.417 * R-R)	0.675	0.456	0.411	<0.01
Q-A'	R-R (p=0.001)	Q-A' = 0.0499 + (0.882 * R-R)	0.883	0.780	0.762	<0.001
Q-bS'	R-R (p=0.024)	Q-bS' = 0.0123 + (0.0909 * R-R)	0.471	0.222	0.170	0.056
IVCb	Thickness (p=0.025); weight (p=0.012)	IVCb = 10.500 - (0.478 * thickness) - (0.758 * weight)	0.910	0.829	0.786	<0.001

Table App.D28 Linear regression and multiple linear regression equations for independent variables significantly influencing pulsed TDI indices of the tricuspid annulus in the HCM group

HCM TDI parameter Tr	Forward stepwise regression analysis	Linear and multiple linear regression equations	R	R^2	Adjusted R^2	p
E' acc	Age (p=0.049)	ns	ns			ns
S' dur	R-R (p=0.054)	S' dur = 0.0648 + (0.213 * R-R)	0.780	0.609	0.570	<0.01
tSe' acc	Age (p=0.017)	tSe' acc = 0.0238 + (0.00133 * age)	0.735	0.540	0.494	<0.01
IVCt	Weight (p=0.022)	IVCt = 0.0825 - (0.00859 * weight)	0.752	0.565	0.517	<0.01

Appendix E

Tissue Mimicking Material

Composition:
All percentages are given in mass % (± 0.02 mass %) and are valid for non-diluted materials:

- 82.97% Demi-water
- 11.21% Glycerol
- 0.46% Rodalon® Benzalkoniumchloride
- 0.53% SiC-powder 400 grain
- 0.94% Al_2O_3-powder 3.0 μm
- 0.88% Al_2O_3-powder 0.3 μm
- 3.00% Agar (Struers)

SiC-powder for scattering: 400 grain (Logitech).

Preparation:

- Weigh all ingredients and mix them in a flask
- Close the flask as well as possible to prevent evaporation
- Place the flask in a water bath
- Heat the bath until 96 ± 3 °C; keep stirring
- Keep at this temperature for one hour; keep stirring
- Cool down to about 42 °C; keep stirring
- Cover the flask-wall with the mixture to allow condensated liquid to slip back into the mixture
- Cast the mixture in the tank
- Allow the mixture to cool down

Appendix F1

Table App.F1 MVG indices from the LVPW of normal cats

cat	sex	age (years)	weight (Kg)	thickness (mm)	R-R (sec)	E1 (sec^{-1})	E2 (sec^{-1})	E1-2 (sec^{-1})	Emax (sec^{-1})	A (sec^{-1})	EA (sec^{-1})	Se (sec^{-1})	SI (sec^{-1})	IVRa (sec^{-1})	IVRb (sec^{-1})	IVCa (sec^{-1})	IVCb (sec^{-1})
F010	MN	10	6.3	4.28	0.374	11.17	3.46		11.17	6.75		-8.69	-5.02	2.31	-0.65	-0.6	5.06
F012	FN	2	5.6	4.63	0.51	9.08	13.45		13.45	6		-12.64	-9.98	0.46	-3.81	-2.05	3.92
F015	MN	6	4.4	3.94	0.385	14.77	5.95		14.77	15.89		-10.78	-3.12	1.65	-3.94	-1.68	3.91
F025	FN	9	4.7	4.61	0.423	12.47	6.93		12.47	13.64		-12.51	-4.76	3.12	-1.66	7.08	10.15
F031	FN	4	3.5	4.03	0.368	9.96	8.1		9.96	6.45		-7.93	-3.7	-0.43	-2.4	-1.62	6.47
F033	FN	8	3.7	4.52	0.407			9.69	9.69	10.14		-9.12	-3.5	0.96	-1.57	-11.7	6.48
F034	MN	8	5.7	5.54	0.428			6.68	6.68	8.31		-5.65	-2.55	1.32	-2	0	2.25
F037	FN	4	4	3.67	0.354	15.54	7.07		15.54	8.44		-11.74	-4.14	0.45	-3.48	0.29	7.86
F041	FN	5	4.6	3	0.323	9.12	5.87		9.12	7.48		-5.24	-2.05	2.41	-2.37	-6.75	1.1
F043	MN	1	4.5	3.94	0.486	9.29	7.14		9.29	5.24		-4.74	-2.51	0.57	-3.75	-4.48	2.56
F046	MN	10	4.2	4.92	0.446	8.24	3.39		8.24	6.57		-5.79	-3.65	0.04	-2.8	-1.34	5.23
F050	FN	1	4	4.15	0.397	10.58	10.28		10.58	7.02		-10.29	-5.46	0.82	-3.15	-1.84	9.34
F051	MN	14	6.2	4.42	0.353			5.79	5.79	10.22		-3.65	-2.81	5.11	-0.79		13.68
F053	FN	9	4	3.31	0.338			8.32	8.32	15.16		-13.06	-8.66	9.76	-1.18	-3.5	
F054	MN	1	4.5	3.01	0.608	18.03	12.42		18.03	6.93		-11.02	-4.46	4.86	-0.87	5.9	5.14
F063	MN	4	5	4.01	0.408	15.22	6.96		15.22	6.4		-10.29	-4.44	1.87	-2.87	-3.41	3.1
F066	FN	7	3.8	4.16	0.398	10.71	5.49		10.71	8.35		-7.83	-3.92	0.99	-1.57	0.61	8.09
F080	MN	9	3.9	4.24	0.53	7.96	6.13		7.96	5.71		-8.33	-2.85	0.88	-2.68	-1	3.7
F084	MN	9	3.3	5.33	0.554	8.68	2.63		8.68	7.38		-6.41	-3.8	1.3	-2.35	-0.89	3.2
F085	MN	9	4.4	4.57	0.347			9.47	9.47	11.6		-7.69	-6	0.39	-4.37	-3.18	5.45

Table App.F2 MVG indices from the LVPW of HCM cats

cat	status	sex	age (years)	weight (Kg)	thickness (mm)	R-R (sec)	E1 (sec^{-1})	E2 (sec^{-1})	E1-2 (sec^{-1})	Emax (sec^{-1})	A (sec^{-1})	EA (sec^{-1})	Se (sec^{-1})	SI (sec^{-1})	IVRa (sec^{-1})	IVRb (sec^{-1})	IVCa (sec^{-1})	IVCb (sec^{-1})
F009	asympt.	MN	7	5.2	4.95	0.35			6.2	6.2	8.42		-5.99	-3.28	0.8	-0.95		2.4
F013	asympt.	MN	8	6.8	4.95	0.443	2.61	3.6		3.6	7.28		-8.09	-3.91	0.71	-1.61	-4.6	3.66
F018	asympt.	MN	10	4.5	5.34	0.363			4.14	4.14	6.21		-4.04	-2.92	0.76	-0.94	-5.19	4.66
F024	asympt.	MN	3	6.45	5.6	0.545	6.73	1.17		6.73	4.89		-6.52		0.08	-2.09		
F027	asympt.	MN	2	5.2	8.29	0.403			2.33	2.33	6.04		-5.93	-1.35			-0.43	3.1
F030	asympt.	MN	9	6.3	4.45	0.383	8.06	5.49		8.06	6.84		-7.71	-4.07	-0.13	-3.5	-1.05	7.51
F032	asympt.	MN	12	5.5	7.16	0.287			6.65	6.65	6.42		-4.45		1.6	-1.95	0.38	2.99
F038	asympt.	MN	10	5	6.14	0.467	6.09	2.29		6.09	6.45		-4.07	-2.81	0.44	0.21	-1.8	0.92
F044	asympt.	MN	7	4.5	6.03	0.63	5.42	1.91		5.42	7.24		-6.58	-3.03	1.08	-1.24	0.07	6.53
F052	asympt.	MN	9	4.2	7.95	0.367			4.41	4.41	5.75		-4.42	-1.76	-0.08	-1.45	0.53	2.97
F057	asympt.	FN	7	4.4	6.92	0.323			7.07	7.07	8.32		-6.26	-2.82	0.06	-1.92	-2.09	6.27
F069	asympt.	FN	4	4.15	4.6	0.405			7.49	7.49	6.84		-6.45	-4.43	-0.44	-2.4		3.97
F071	asympt.	MN	7	6.7	6.32	0.46	4.58	2.64		4.58	4.69		-4.09	-2.44	1.71	-0.47	-0.87	1.16
F073	asympt.	MN	5	6.15	7.44	0.348						5.2	-2.72		0.65	-0.56	-0.83	1.99
F081	asympt.	MN	3	4.75	5.56	0.352			4.57	4.57	8.48		-10.1	-4.57	0.94	-1.2	-1.12	5.13
F086	asympt.	MN	7	4.4	4	0.5	6.5	4.54		6.5	8.75		-6.52	-2.93	1.57	-0.21	-4.14	2.72
F091	asympt.	FN	5	4.9	4	0.354			11.12	11.12	9.75		-10.53	-4.85	0.45	-3.1	-1.59	8.82
F093	asympt.	MN	9	6.7	6.34	0.37			7.44	7.44	10.28		-6.44	-2.96	1.17	-2.18	-1.45	2.2
F029	CHF	MN	5	4.9	7.67	0.333	1.6	4.2		4.2	0.95		-1.21	-0.87	0.48	-0.56	0.22	0.13
F060	CHF	MN	2	3.3	4.68	0.375	9.28	5.42		9.28	12.24		-5.5	-2.35	-0.13	-2.72	4.73	-7.05
F067	CHF	MN	9	4.8	3.59	0.276						12.49	-10.74	-4.48		-2.49	0.24	-1.22
F082	CHF	MN	11	5.8	7.15	0.455			2.46	2.46			-1.72		0.96	-1.37	-0.71	1.48
F092	CHF	MN	4	4.5	8.17	0.445			3.46	3.46	1.24		-3.36	-1.33	0.78	-0.6	-0.12	2.65

Table App.F3 MMV indices from the LVPW of normal cats

cat	sex	age (years)	weight (Kg)	thickness (mm)	R-R (sec)	E1 (mm/s)	E2 (mm/s)	E1-2 (mm/s)	Emax (mm/s)	A (mm/s)	EA (mm/s)	E/A	Se (mm/s)	Sl (mm/s)	IVRa (mm/s)	IVRb (mm/s)	IVCa (mm/s)	IVCb (mm/s)
F010	MN	10	5.30	4.28	0.374	-28.31	-22.56		-28.30	-26.23		1.08	32.76	19.20	2.61	8.86	2.07	-34.98
F012	FN	2	5.60	4.63	0.510	-11.91	-37.51		-37.50	-8.49		4.42	33.06	19.10	-1.84	10.59	-4.42	-34.45
F015	MN	6	4.40	3.94	0.385	-44.10	-27.98		-44.10	-43.11		1.02	42.73	21.88	3.45	16.57	4.46	-39.19
F025	FN	9	4.70	4.61	0.423	-13.05	-19.04		-19.00	-48.01		0.40	46.48	12.09	10.58	11.72	-4.97	-51.79
F031	FN	4	3.50	4.03	0.368	-34.19	-32.66		-34.20	-33.87		1.01	34.74	19.05	2.78	11.46	-1.31	-52.80
F033	FN	8	3.70	4.52	0.407			-40.75	-40.75	-41.55		0.98	32.93	22.64	2.81	5.96	5.25	-34.60
F034	MN	8	5.70	5.54	0.428			-27.63	-27.63	-29.26		0.94	30.27	13.89	6.28	7.72	4.06	-23.47
F037	FN	4	4.00	3.67	0.354	-30.39	-16.96		-30.40	-18.92		1.61	33.08	14.25	7.82	26.27	-3.74	-39.86
F041	FN	5	4.60	3.00	0.323	-35.33	-18.05		-35.30	-24.86		1.42	25.68	12.08	2.77	17.45	3.70	-24.86
F043	MN	1	4.50	3.94	0.486	-46.59	-37.41		-46.60	-17.92		2.60	46.03	22.02	-5.28	9.95	3.87	-33.52
F046	MN	10	4.20	4.92	0.446	-45.08	-14.47		-45.10	-39.16		1.15	26.93	16.13	5.44	18.87	3.09	-25.96
F050	FN	1	4.00	4.15	0.397	-29.41	-35.45		-35.50	-24.63		1.44	49.30	35.58	5.40	17.64	5.11	-59.89
F051	MN	14	6.20	4.42	0.353			-14.52	-14.52	-30.11		0.48	29.32	11.05	-0.82	8.02	-1.17	-46.79
F053	FN	9	4.00	3.31	0.338			-17.60	-17.60	-30.82		0.57	29.84	17.55	-22.76	16.81	5.12	-51.81
F054	MN	1	4.50	3.01	0.608	-40.15	-32.57		-40.20	-23.57		1.71	41.17	27.61	-12.40	11.76	7.38	-39.61
F063	MN	4	5.00	4.01	0.408	-35.72	-16.95		-35.70	-16.66		2.14	37.27	18.96	1.24	19.81	-1.36	-37.71
F066	FN	7	3.80	4.16	0.398	-28.20	-22.31		-28.20	-22.59		1.25	24.38	16.48	-2.40	8.77	3.78	-34.11
F080	MN	9	3.90	4.24	0.530	-22.26	-16.58		-22.30	-13.93		1.60	34.14	15.43	0.10	4.02	-1.34	-27.55
F084	MN	9	3.30	5.33	0.554	-30.80	-16.21		-30.80	-32.78		0.94	31.32	13.05	-2.53	8.75	-0.80	-34.07
F085	MN	9	4.40	4.57	0.347			-29.78	-29.78	-14.73		2.02	32.08	11.03	2.29	13.72	7.89	-46.05

Table App.F3 MMV indices from the LVPW of normal cats

cat	Se acc (mm/s^2)	E1 acc (mm/s^2)	E2 acc (mm/s^2)	E1-2 acc (mm/s^2)	EA acc (mm/s^2)	E1 dec (mm/s^2)	E2 dec (mm/s^2)	E1-2 dec (mm/s^2)	EA dec (mm/s^2)	IVRt (sec)	IVCt (sec)	diast t (sec)	systo t (sec)
F010	2227	718	307			827	676			0.043	0.043	0.155	0.145
F012	2971	398	574			1160	1271			0.040	0.035	0.273	0.200
F015	1775		651			937	1124			0.033	0.048	0.145	0.155
F025	3166	757	437			743	590			0.052	0.068	0.155	0.152
F031	2217		682			573	1088			0.046	0.036	0.150	0.140
F033	1811							714		0.043	0.060	0.137	0.170
F034	1424			758				762		0.050	0.068	0.144	0.170
F037	1613	849	217			1029	495			0.044	0.060	0.112	0.130
F041	2216		367			1345	1216			0.042	0.044	0.115	0.117
F043	2841	766	326			994	1383			0.040	0.047	0.235	0.163
F046	1612		97			1266	382			0.042	0.048	0.200	0.135
F050	2381		578			1073	1037			0.043	0.035	0.275	0.193
F051	2856			639				364		0.035	0.050	0.132	0.133
F053	1729							276		0.044	0.060	0.108	0.130
F054	1564		483			628	1003			0.060	0.073	0.300	0.177
F063	2354		187			572	368			0.050	0.060	0.160	0.140
F066	1992	833	282			1176	718			0.030	0.040	0.180	0.150
F080	1876	700	149			722	535			0.048	0.055	0.273	0.188
F084	601	786	169			841	445			0.045	0.045	0.265	0.175
F085	2644			725				1148		0.058	0.055	0.125	0.110

Table App.F4 MMV indices from the LVPW of HCM cats

cat		sex	age (years)	weight (Kg)	thickness (mm)	R-R (sec)	E1 (mm/s)	E2 (mm/s)	E1-2 (mm/s)	Emax (mm/s)	A (mm/s)	EA (mm/s)	E/A	Se (mm/s)	SI (mm/s)	IVRa (mm/s)	IVRb (mm/s)	IVCa (mm/s)	IVCb (mm/s)
F009	asympt.	MN	7	5.20	4.95	0.350			-24.76	-24.76	-22.28		1.11	35.68	9.30	1.19	9.88	-6.95	-37.78
F013	asympt.	MN	8	6.80	4.95	0.443	-39.99	-19.82		-39.99	-28.22		1.42	52.46	14.76	-12.33	-5.06	7.14	-23.51
F018	asympt.	MN	10	4.50	5.34	0.363			-13.27	-13.27	-24.88		0.53	29.54	14.17	-5.53	3.10	6.48	-29.22
F024	asympt.	MN	3	6.45	5.60	0.545	-20.81	-8.53		-20.81	-23.58		0.88	42.12	12.18	-11.20	-3.29	12.14	-16.44
F027	asympt.	MN	2	5.20	8.29	0.403			-12.00	-12.00	-30.91		0.39	44.14	7.34		5.73	-4.05	-25.95
F030	asympt.	MN	9	6.30	4.45	0.383	-44.37	-30.55		-44.37	-39.24		1.13	38.62	23.28	2.00	7.44	7.49	-15.03
F032	asympt.	MN	12	5.50	7.16	0.285			-39.99	-39.99	-37.21		1.07	31.43	13.55	-5.86	12.89	7.69	-12.50
F038	asympt.	MN	10	5.00	6.14	0.467	-49.61	-13.64		-49.61	-47.69		1.04	26.13	17.87	4.18	17.11	12.33	-17.33
F044	asympt.	MN	7	4.50	6.03	0.630	-19.84	-13.56		-19.84	-34.44		0.58	40.49	26.89	0.52	6.02	0.16	-34.68
F052	asympt.	MN	9	4.20	7.95	0.367			-11.19	-11.19	-41.92		0.27	37.27	14.92	-2.36	7.82	-7.10	-54.47
F057	asympt.	FN	7	4.40	6.92	0.323			-29.63	-29.63	-47.32		0.63	31.67	12.43	5.89	7.20	10.14	-14.88
F069	asympt.	FN	4	4.15	4.60	0.405			-12.43	-12.43	-12.37		1.00	28.42	5.42	-1.79	2.39	0.30	-22.45
F071	asympt.	MN	7	6.70	6.32	0.460	-31.03	-9.27		-31.03	-30.36		1.02	32.40	20.48	-22.36	-5.46	-1.20	-11.19
F073	asympt.	MN	5	6.15	7.44	0.348						-37.60		16.69	7.64	-2.79	-1.36	7.23	-7.83
F081	asympt.	MN	3	4.75	5.56	0.352			-22.14	-22.14	-27.57		0.80	40.62	7.82	-14.00	-1.06	0.67	-14.75
F086	asympt.	MN	7	4.40	4.00	0.500	-25.79	-29.58		-29.58	-39.05		0.76	43.92	14.20	-15.23	-5.85	7.20	-21.88
F091	asympt.	FN	5	4.90	4.00	0.354			-29.89	-29.89	-39.13		0.76	33.23	10.69	0.33	4.31	2.85	-30.87
F093	asympt.	MN	9	6.70	6.34	0.370			-25.64	-25.64	-49.72		0.52	34.60	9.97	-6.71	-3.43	1.24	-42.50
F029	CHF	MN	5	4.90	7.67	0.333	-3.47	-44.17		-44.17	-12.02		3.67	21.30	16.79	5.60	13.52	2.15	-29.48
F060	CHF	MN	2	3.30	4.68	0.375	-31.58	-47.86		-47.86	-47.20		1.01	30.14	16.52	4.46	14.26	19.05	-7.30
F067	CHF	MN	9	4.80	3.59	0.276						-41.72		22.56	14.92			10.63	-14.94
F082	CHF	MN	11	5.80	7.15	0.455			-16.30	-16.30				11.18		1.86	11.29	-0.54	-12.18
F092	CHF	MN	4	4.50	8.17	0.445			-33.04	-33.04	-10.32		3.20	54.21	8.50	-8.32	-0.75	10.13	-20.32

Table App.F4 MMV indices from the LVPW of HCM cats

cat	Se acc (mm/s^2)	E1 acc (mm/s^2)	E2 acc (mm/s^2)	E1-2 acc (mm/s^2)	EA acc (mm/s^2)	E1 dec (mm/s^2)	E2 dec (mm/s^2)	E1-2 dec (mm/s^2)	EA dec (mm/s^2)	IVRt (sec)	IVCt (sec)	diast t (sec)	systo t (sec)
F009	2456			841				559		0.058	0.055	0.150	0.125
F013	2784	903	13			653	517			0.040	0.063	0.180	0.167
F018	1541			544				458		0.055	0.060	0.135	0.108
F024	1390	367	27			545	247			0.068	0.048	0.303	0.138
F027	2467			87				221		0.057	0.050	0.160	0.153
F030	1585	799	299			908	1032			0.037	0.040	0.193	0.153
F032	1987			1369				1274		0.110	0.030	0.073	0.078
F038	1514		169			1371	480			0.055	0.065	0.195	0.150
F044	2089	618	76			279	297			0.065	0.043	0.367	0.165
F052	2824			372				324		0.080	0.050	0.120	0.115
F057	1218			918				788		0.100	0.043	0.085	0.098
F069	1888			428				556		0.060	0.050	0.153	0.133
F071	1406	909	64			475				0.063	0.050	0.193	0.153
F073	495				791				1939		0.040		0.170
F081	2003			643				378		0.075	0.053	0.115	0.108
F086	1464	593	199			816	605			0.055	0.060	0.230	0.150
F091	2400							1034		0.035	0.048	0.135	0.150
F093	2697			760				540		0.065	0.050	0.123	0.130
F029	627	565	947			163	3264			0.040	0.068	0.153	0.093
F060	1846		855			962	1076			0.060	0.047	0.113	0.200
F067	768				730				1991		0.075	0.098	
F082	213			460				158		0.063	0.073	0.200	0.140
F092	1171			516				380		0.074	0.051	0.204	0.105

Appendix F2

Table App.F5 Linear regression and multiple linear regression equations for independent variables significantly influencing MVG indices in normal and HCM cats

Normal MVG parameters	Forward stepwise regression analysis	Linear and multiple linear regression equations	R	R^2	Adjusted R^2	p
E2	Age (p=0.006); sex (p=0.009); weight (p=0.043); R-R (p=0.007)	E2 = -7.114 - (0.576 * age) + (2.855 * sex) + (1.131 * weight) + (18.498 * R-R)	0.934	0.873	0.822	<0.001
IVRa	Thickness (p=0.003); age (p=0.010)	IVRa = 9.572 - (2.375 * thickness) + (0.366 * age)	0.661	0.437	0.371	<0.01
IVRb	Thickness (p=0.040); age (p=0.004); R-R (p=0.036)	ns	ns			ns
HCM MVG parameters						
E2	Thickness (p=0.049); R-R (p=0.011)	E2 = 13.438 - (0.699 * thickness) - (13.260 * R-R)	0.896	0.804	0.738	<0.01
E1-2	Sex (p=0.028)	E1-2 = 0.698 + (3.931 * sex)	0.701	0.491	0.440	<0.05
E max	Thickness (p=0.005)	E max = 12.111 - (1.050 * thickness)	0.645	0.416	0.386	<0.01
A	Thickness (p=0.009)	A = 13.967 - (1.194 * thickness)	0.611	0.373	0.338	<0.01
Se	Thickness (p<0.001)	Se = 13.198 - (1.239 * thickness)	0.697	0.486	0.462	<0.001
SI	Thickness (p<0.001)	SI = 6.749 - (0.646 * thickness)	0.820	0.672	0.653	<0.001
IVCb	Sex (p=0.012)	IVCb = -1.729 + (4.041 * sex)	0.434	0.188	0.148	<0.05

Table App.F6 Linear regression and multiple linear regression equations for independent variables significantly influencing MMV indices in normal and HCM cats

normal MMV parameter	Forward stepwise regression analysis	Linear and multiple linear regression equations	R	R^2	Adjusted R^2	p
E1	Sex (p<0.001); weight (p=0.023); R-R (p=0.017)	E1 = -47.184 + (10.558 * sex)	0.523	0.273	0.218	<0.05
E2	Age (p=0.008)	E2 = 34.950 - (1.921 * age)	0.758	0.575	0.542	0.001
E max	Age (p=0.004)	E max = 42.250 - (1.550 * age)	0.616	0.379	0.345	<0.01
E/A	Age (p=0.012)	E/A = 2.413 - (0.150 * age)	0.605	0.366	0.331	<0.01
Se	Age (p=0.056)	Se = 41.245 - (1.011 * age)	0.519	0.269	0.229	<0.05
SI	Age (p=0.032)	SI = 25.051 - (1.092 * age)	0.654	0.428	0.396	<0.05
IVRa	Thickness (p=0.017)	IVRa = -20.800 + (5.002 * thickness)	0.450	0.202	0.158	<0.05
IVRb	R-R (p=0.034)	ns	ns			ns
Se acc	Weight (p=0.029)	Se acc = 611.744 + (328.185 * weight)	0.451	0.203	0.159	<0.05
E1 acc	Weight (p=0.042)	ns	ns			ns
diast t	R-R (p<0.001)	diast t = -0.118 + (0.712 * R-R)	0.871	0.759	0.746	<0.001
systo t	R-R (p=0.001)	systo t = 0.0547 + (0.235 * R-R)	0.727	0.529	0.502	<0.001
HCM MMV parameter						
E2	Weight (p=0.042); R-R (p=0.012)	E2 = -112.959 + (6.790 * weight) + (113.964 * R-R)	0.929	0.863	0.817	<0.01
SI	Age (p=0.027); R-R (p=0.028)	SI = -5.379 + (0.957 * age) + (31.917 * R-R)	0.638	0.408	0.345	<0.01
IVRb	Weight (p=0.023)	IVRb = 19.987 - (3.001 * weight)	0.418	0.175	0.134	0.054
E1-2 dec	R-R (p=0.029)	E1-2 dec = 2497.670 - (5210.653 * R-R)	0.762	0.581	0.539	<0.01
IVRt	Thickness (p=0.044)	IVRt = 0.0239 + (0.00645 * thickness)	0.473	0.223	0.183	<0.05

Appendix G

Table App.G1 Repeatability results for 2D/Doppler echocardiographic variables

		Two-Dimensional measurements								M mode measurements											Mitral ann. mot	
		LA area d RPS	LA dist d RPS	LA area s RPS	LA dist s RPS	LA FS%	LA length d	Ao diam d	LAd/Aod	IVSd	LV diam.d	LVPW d	IVSs	LV diam.s	LVPWs	FS%	MV EPSS	Aort v Aod	Aort v LAs	LAs/Aod	MAM sep.	MAM lat.
cat 1	scan 1	133	11	184	13	18	12	9	1	4.80	17.10	5.00	7.55	9.70	8.60	44	0.60	10	15	1.41	3.82	3.46
	scan 2	133	11	151	12	7	13	10	1	4.50	14.95	4.60	6.95	8.10	7.75	46	0.56	8	15	1.73	3.62	3.38
difference		0	-1	32	1	11	0	-1	0	0.30	2.15	0.40	0.60	1.60	0.85	-3	0.04	2	0	-0.32	0.20	0.08
mean		133	11	167	13	12	13	9	1	4.65	16.03	4.80	7.25	8.90	8.18	45	0.58	9	15	1.57	3.72	3.42
sd mean		0	1	23	0	8	0	1	0	0.21	1.52	0.28	0.42	1.13	0.60	2	0.03	1	0	0.22	0.14	0.06
CV%		0	5	14	4	65	1	6	5	5	9	6	6	13	7	4	5	15	1	14	4	2
cat 2	scan 1	93	9	157	10	11	11	7	2	3.90	14.50	3.70	5.50	8.45	7.00	42	0.40	9	13	1.45	5.95	7.50
	scan 2	114	10	151	11	9	11	7	2	3.93	14.37	3.77	5.47	8.48	6.97	41	0.40	9	13	1.49	4.85	7.20
difference		-22	-1	5	0	2	0	0	0	-0.03	0.13	-0.07	0.03	-0.03	0.03	1	0.00	0	0	-0.04	1.10	0.30
mean		103	10	154	11	10	11	7	2	3.92	14.43	3.73	5.48	8.47	6.98	41	0.40	9	13	1.47	5.40	7.35
sd mean		15	0	4	0	1	0	0	0	0.02	0.09	0.05	0.02	0.02	0.02	0	0.00	0	0	0.03	0.78	0.21
CV%		15	4	3	3	14	3	2	1	1	1	1	0	0	0	1	0	1	1	2	14	3
cat 3	scan 1	176	12	283	15	20	13	8	2	4.45	17.35	5.20	7.05	11.75	7.85	32	1.93	9	14	1.66	4.43	7.70
	scan 2	176	12	290	16	22	14	8	2	4.35	17.42	5.43	6.55	12.12	8.08	30	1.88	13	16	1.20	6.08	8.10
difference		1	0	-8	-1	-2	-1	0	0	0.10	-0.07	-0.23	0.50	-0.37	-0.23	2	0.05	-5	-1	0.46	-1.65	-0.40
mean		176	12	287	15	21	13	8	2	4.40	17.38	5.32	6.80	11.93	7.97	31	1.91	11	15	1.43	5.26	7.90
sd mean		0	0	5	1	1	1	0	0	0.07	0.05	0.16	0.35	0.26	0.16	1	0.04	3	1	0.33	1.17	0.28
CV%		0	2	2	3	6	5	0	4	2	0	3	5	2	2	4	2	29	7	23	22	4
cat 4	scan 1	116	10	187	13	22	11	8	1	4.30	16.32	4.26	7.10	10.35	7.05	37	1.27	9	13	1.52	3.78	7.02
	scan 2	150	11	236	14	21	13	8	2	4.58	16.17	5.21	6.65	11.41	7.53	29	1.68	12	14	1.15	5.20	7.25
difference		-34	-1	-50	-1	2	-2	0	0	-0.28	0.15	-0.95	0.45	-1.05	-0.48	8	-0.40	-3	-1	0.37	-1.42	-0.24
mean		133	11	212	14	22	12	8	1	4.44	16.25	4.74	6.87	10.88	7.29	33	1.48	10	13	1.34	4.49	7.13
sd mean		24	1	35	1	1	1	0	0	0.20	0.10	0.67	0.32	0.74	0.34	5	0.29	2	0	0.26	1.00	0.17
CV%		18	7	17	6	6	11	2	9	4	1	14	5	7	5	16	19	23	3	19	22	2
cat 5	scan 1	163	11	246	14	22	15	8	2	5.40	17.60	5.40	9.10	9.65	8.50	45	0.56	10	17	1.68	4.80	
	scan 2	163	12	254	17	29	15	8	2	6.25	17.30	5.95	10.00	8.80	9.50	49	0.66	8	17	2.17	4.60	
difference		0	-1	-9	-3	-7	1	0	0	-0.85	0.30	-0.55	-0.90	0.85	-1.00	-4	-0.10	2	-1	-0.49		
mean		163	11	250	15	26	15	8	2	5.83	17.45	5.68	9.55	9.23	9.00	47	0.61	9	17	1.92	4.70	
sd mean		0	1	6	2	5	0	0	0	0.60	0.21	0.39	0.64	0.60	0.71	3	0.07	1	1	0.34	0.14	
CV%		0	6	2	12	19	2	0	2	10	1	7	7	7	8	6	12	15	3	18	3	
cats 1,2,3,4,5																						
mean of differ.		-11	-1	-6	-1	1	-1	0	0	-0.15	0.53	-0.28	0.14	0.20	-0.17	1	-0.08	-1	-1	0.00	-0.44	-0.06
sd of differ.		16	0	30	1	7	1	0	0	0.44	0.91	0.51	0.62	1.04	0.68	4	0.19	3	1	0.41	1.32	0.31
upper lim. agr.		21	0	53	2	15	1	0	0	0.73	2.36	0.73	1.37	2.28	1.20	10	0.29	5	1	0.83	2.19	0.56
lower lim. agr.		-43	-1	-65	-3	-12	-2	-1	0	-1.04	-1.29	-1.29	-1.10	-1.88	-1.53	-8	-0.46	-7	-2	-0.83	-3.08	-0.69
coef.of repeat.		32	1	59	2	13	2	1	0	0.89	1.83	1.01	1.24	2.08	1.37	9	0.38	6	1	0.83	2.63	0.63
cats 1,2,3,4																						
mean of differ.		-14	-1	-5	0	3	-1	0	0	0.02	0.59	-0.21	0.39	0.04	0.04	2	-0.08	-1	-1	0.12	-0.44	-0.06
sd of differ.		17	0	34	1	6	1	0	0	0.24	1.04	0.56	0.25	1.12	0.58	4	0.22	3	1	0.36	1.32	0.31
upper lim. agr.		20	0	63	1	14	1	0	0	0.51	2.68	0.91	0.89	2.29	1.20	10	0.36	5	1	0.84	2.19	0.56
lower lim. agr.		-48	-1	-73	-2	-8	-2	-1	0	-0.46	-1.50	-1.33	-0.10	-2.21	-1.11	-7	-0.51	-7	-2	-0.61	-3.08	-0.69
coef.of repeat.		34	1	68	2	11	1	1	0	0.49	2.09	1.12	0.50	2.25	1.15	8	0.44	6	1	0.72	2.63	0.63
mean (cats 1,2,3,4)		136.19	10.88	204.868	13	16.188	12	8.042	1.53	4.35	16.022	4.65	6.60	10.04	7.60	37.491	1.09	9.796	13.946	1.452	4.716	6.451
real upper value		156.19	10.83	268.13	14	30.677	13	8.406	1.71	4.86	18.701	5.55	7.50	12.33	8.80	47.716	1.45	14.366	14.796	2.294	6.908	7.014
real lower value		88.61	9.49	131.67	11	8.531	10	7.064	1.23	3.89	14.524	3.32	6.50	7.83	6.49	30.951	0.58	2.401	12.058	0.847	1.640	5.759

Appendix G

Table App.G1 Repeatability results for 2D/Doppler echocardiographic variables

		Pulmonary artery: Right				Aortic valve: Left Apical						Mitral valve									CFM: pro IVRT (LV) Tricuspid valve				
		PA vmax	ET	PEP	PEP/ET	Ao vmax	Ao VTI	PEP	ET	PEP/ET	Acc. t	E	A	E/A	E VTI	A VTI	E dec t	E acc t	E dur.	A dur.	FPV	IVRT	E vmax	A vmax	E/A
cat 1	scan 1	0.71	0.158	0.049	0.310	0.71	0.72	0.049	0.154	0.318	0.037	0.55	0.64	0.86							400	0.048	0.33	0.42	0.79
	scan 2	0.86	0.152	0.046	0.304	0.84	0.76	0.039	0.148	0.264	0.039	0.46	0.54	0.85				0.040			383	0.055	0.42	0.46	0.91
difference		-0.15	0.006	0.003	0.006	-0.13	-0.04	0.010	0.006	0.055	-0.002	0.09	0.10	0.01							17	-0.007	-0.09	-0.04	-0.13
mean		0.79	0.155	0.048	0.307	0.78	0.74	0.044	0.151	0.291	0.038	0.51	0.59	0.86							391	0.051	0.38	0.44	0.85
sd mean		0.11	0.004	0.002	0.004	0.09	0.03	0.007	0.004	0.039	0.001	0.06	0.07	0.01							12	0.005	0.06	0.03	0.09
CV%		14	3	4	1	12	4	16	3	13	4	13	12	1							3	10	17	6	11
cat 2	scan 1	0.77	0.154	0.036	0.234	0.95	0.90	0.043	0.142	0.303	0.040	0.67	0.78	0.86	0.05	0.03	0.06	0.04	0.10	0.06	497	0.040	0.61	0.30	2.03
	scan 2	0.85	0.148	0.035	0.234	0.94	0.93	0.043	0.156	0.276	0.046	0.68	0.71	0.96	0.05	0.03	0.07	0.04	0.10	0.06	581	0.033	0.51	0.34	1.50
difference		-0.08	0.006	0.001	0.000	0.01	-0.03	0.000	-0.014	0.027	-0.006	-0.01	0.07	-0.10	0.00	0.00	0.00	0.00	0.00	0.00	-84	0.007	0.10	-0.04	0.53
mean		0.81	0.151	0.035	0.234	0.95	0.92	0.043	0.149	0.289	0.043	0.68	0.75	0.91	0.05	0.03	0.06	0.04	0.10	0.06	539	0.037	0.56	0.32	1.77
sd mean		0.06	0.004	0.001	0.000	0.01	0.02	0.000	0.010	0.019	0.004	0.01	0.05	0.07	0.00	0.00	0.00	0.00	0.00	0.00	60	0.005	0.07	0.03	0.38
CV%		7	3	3	0	1	3	0	7	7	10	1	7	8	0	10	3	3	3	1	11	13	13	9	21
cat 3	scan 1	0.72	0.191	0.038	0.199	0.79	0.87	0.051	0.197	0.259	0.039	0.69	0.40	1.73	0.04	0.02	0.07	0.05	0.12	0.08	677	0.056	0.56	0.42	1.33
	scan 2	0.74	0.191	0.049	0.258	0.86	0.92	0.048	0.195	0.246	0.038	0.66	0.42	1.57	0.05	0.01	0.06	0.05	0.11	0.07	801	0.055	0.53	0.44	1.20
difference		-0.02	0.000	-0.011	-0.059	-0.07	-0.05	0.003	0.002	0.013	0.001	0.03	-0.02	0.15	-0.01	0.00	0.01	0.00	0.01	0.01	-124	0.001	0.03	-0.02	0.13
mean		0.73	0.191	0.044	0.229	0.83	0.89	0.050	0.196	0.253	0.039	0.68	0.41	1.65	0.04	0.02	0.07	0.05	0.12	0.08	739	0.055	0.55	0.43	1.27
sd mean		0.01	0.000	0.008	0.042	0.05	0.04	0.002	0.001	0.009	0.001	0.02	0.01	0.11	0.00	0.00	0.01	0.00	0.01	0.01	88	0.001	0.02	0.01	0.09
CV%		2	0	18	18	6	4	4	1	4	2	3	3	7	8	7	12	5	5	10	12	1	4	3	7
cat 4	scan 1	0.71	0.188	0.039	0.206	0.83	0.95	0.053	0.171	0.310	0.043	0.64	0.45	1.42	0.04	0.02	0.06	0.04	0.11	0.08	485	0.054	0.51	0.30	1.70
	scan 2	0.72	0.187	0.051	0.272	0.85	0.94	0.052	0.181	0.287	0.044	0.66	0.39	1.69	0.04	0.02	0.05	0.05	0.10	0.07	595	0.055	0.57	0.35	1.63
difference		-0.01	0.001	-0.012	-0.066	-0.02	0.00	0.001	-0.010	0.023	-0.001	-0.02	0.06	-0.27	0.00	-0.01	0.01	-0.01	0.01	0.00	-110	-0.001	-0.06	-0.05	0.07
mean		0.72	0.188	0.045	0.239	0.84	0.94	0.053	0.176	0.299	0.044	0.65	0.42	1.56	0.04	0.02	0.05	0.05	0.11	0.07	540	0.055	0.54	0.33	1.66
sd mean		0.01	0.001	0.009	0.046	0.01	0.00	0.001	0.007	0.016	0.001	0.01	0.04	0.19	0.00	0.00	0.01	0.01	0.01	0.00	78	0.000	0.04	0.04	0.05
CV%		1	0	19	19	2	0	1	4	5	2	2	10	12	0	20	17	14	7	4	14	1	8	11	3
cat 5	scan 1					0.82	0.07	0.046	0.161	0.286	0.050	0.41	0.38	1.08	0.03	0.02	0.10	0.05	0.15	0.09	287	0.056	0.43	0.38	1.13
	scan 2	0.78	0.186			0.82	0.11		0.182		0.051	0.52	0.39	1.33	0.04	0.02	0.11	0.06	0.16	0.09	278	0.062	0.29	0.37	0.78
difference						0.00	-0.04		-0.021		-0.001	-0.11	-0.01	-0.25	-0.01	0.00	0.00	-0.01	-0.01	0.00	9	-0.007	0.14	0.01	0.35
mean		0.78	0.186			0.82	0.09	0.046	0.172	0.286	0.051	0.46	0.39	1.20	0.04	0.02	0.10	0.05	0.16	0.09	282	0.059	0.36	0.38	0.96
sd mean						0.00	0.03		0.015		0.001	0.08	0.01	0.18	0.01	0.00	0.00	0.00	0.01	0.00	6	0.005	0.10	0.01	0.25
CV%						0	31		9		2	16	2	15	20	8	3	9	5	1	2	8	27	2	26
cats 1,2,3,4,5																									
mean of differ.		-0.07	0.003	-0.005	-0.030	-0.04	-0.03	0.004	-0.007	0.029	-0.002	0.00	0.04	-0.09	0.00	0.00	0.00	-0.01	0.00	0.00	-58	-0.001	0.02	-0.03	0.19
sd of differ.		0.06	0.003	0.008	0.038	0.06	0.02	0.005	0.011	0.018	0.003	0.07	0.05	0.18	0.01	0.00	0.01	0.00	0.01	0.01	67	0.006	0.10	0.02	0.26
upper lim. agr.		0.06	0.010	0.011	0.046	0.07	0.01	0.013	0.015	0.065	0.003	0.14	0.14	0.26	0.01	0.01	0.02	0.00	0.02	0.01	75	0.010	0.22	0.02	0.70
lower lim. agr.		-0.19	-0.003	-0.021	-0.106	-0.16	-0.07	-0.006	-0.030	-0.007	-0.007	-0.15	-0.06	-0.45	-0.01	-0.01	-0.01	-0.01	-0.02	-0.01	-192	-0.013	-0.17	-0.08	-0.32
coef.of repeat.		**0.13**	**0.006**	**0.016**	**0.076**	**0.12**	**0.04**	**0.009**	**0.023**	**0.036**	**0.005**	**0.15**	**0.10**	**0.36**	**0.01**	**0.01**	**0.02**	**0.01**	**0.02**	**0.01**	**134**	**0.011**	**0.20**	**0.05**	**0.51**
cats 1,2,3,4																									
mean of differ.		-0.07	0.003	-0.005	-0.030	-0.05	-0.03	0.004	-0.004	0.029	-0.002	0.02	0.05	-0.05	0.00	0.00	0.01	0.00	0.00	0.00	-75	0.000	0.00	-0.04	0.15
sd of differ.		0.06	0.003	0.008	0.038	0.06	0.02	0.005	0.010	0.018	0.003	0.05	0.05	0.18	0.00	0.00	0.01	0.00	0.01	0.01	64	0.006	0.09	0.01	0.28
upper lim. agr.		0.06	0.010	0.011	0.046	0.07	0.01	0.013	0.015	0.065	0.004	0.12	0.15	0.30	0.00	0.01	0.02	0.00	0.02	0.02	53	0.011	0.17	-0.01	0.71
lower lim. agr.		-0.19	-0.003	-0.021	-0.106	-0.18	-0.08	-0.006	-0.023	-0.007	-0.008	-0.08	-0.05	-0.41	-0.01	-0.01	-0.01	-0.01	-0.01	-0.01	-203	-0.011	-0.18	-0.06	-0.40
coef.of repeat.		**0.13**	**0.006**	**0.016**	**0.076**	**0.12**	**0.05**	**0.009**	**0.019**	**0.036**	**0.006**	**0.10**	**0.10**	**0.36**	**0.01**	**0.01**	**0.02**	**0.01**	**0.02**	**0.01**	**128**	**0.011**	**0.17**	**0.03**	**0.55**
mean (cats 1,2,3,4)		0.760	0.171	0.043	0.252	0.846	0.873	0.047	0.168	0.283	0.041	0.626	0.541	1.242	0.044	0.020	0.062	0.045	0.108	0.070	552.329	0.049	0.505	0.379	1.387
real upper value		0.824	0.181	0.054	0.298	0.916	0.888	0.060	0.183	0.348	0.045	0.749	0.696	1.547	0.047	0.030	0.087	0.049	0.128	0.087	604.849	0.061	0.673	0.366	2.093
real lower value		0.566	0.168	0.022	0.146	0.671	0.798	0.042	0.145	0.276	0.033	0.549	0.491	0.833	0.036	0.011	0.052	0.032	0.098	0.063	349.648	0.038	0.327	0.316	0.985

Appendix G

Table App.G1 Repeatability results for 2D/Doppler echocardiographic variables

		Pulmonary venous flow																				
		Sinus	S12	S1	S2	D	Ar	S/D	S VTI	D VTI	Ar VTI	S dur.	D dur.	D dec	Ar dur.	Adur/Ardur	Q-tS	Q-S12	Q-S1	Q-S2	Q-D	Q-A
cat 1	scan 1	0.41	0.41			0.43	0.19	0.97	0.07	0.03	0.01	0.237	0.104	0.065	0.059	0.000	0.020	0.037			0.276	0.342
	scan 2	0.40	0.40			0.40	0.21	1.00	0.06	0.04	0.01	0.214	0.126	0.065	0.065	0.000						
difference		0.01	0.01			0.03	-0.02	-0.03	0.01	-0.01	0.00	0.023	-0.022	0.000	-0.006	0.000						
mean		0.41	0.41			0.41	0.20	0.99	0.06	0.04	0.01	0.226	0.115	0.065	0.062	0.000	0.020	0.037			0.276	0.342
sd mean		0.01	0.01			0.02	0.02	0.02	0.01	0.01	0.00	0.016	0.016	0.000	0.004	0.000						
CV%		2	2			4	8	2	9	16	0	7	14	0	7							
cat 2	scan 1	0.57		0.57	0.41	0.48	0.41	1.19	0.09	0.04	0.02	0.221	0.112	0.067	0.076	0.776	0.021		0.070	0.183	0.291	0.373
	scan 2	0.51		0.51	0.32	0.41	0.41	1.24	0.08	0.03	0.02	0.221	0.113	0.053	0.081	0.741	0.017		0.064	0.187	0.294	0.368
difference		0.06		0.06	0.09	0.07	0.00	-0.05	0.01	0.00	0.00	0.000	-0.001	0.014	-0.005	0.036	0.004		0.006	-0.004	-0.004	0.005
mean		0.54		0.54	0.37	0.45	0.41	1.21	0.08	0.03	0.02	0.221	0.113	0.060	0.079	0.759	0.019		0.067	0.185	0.292	0.370
sd mean		0.04		0.04	0.06	0.05	0.00	0.04	0.00	0.00	0.00	0.000	0.001	0.010	0.004	0.025	0.003		0.004	0.003	0.003	0.004
CV%		7		7	17	11	0	3	6	6	0	0	1	16	5	3	15		7	2	1	1
cat 3	scan 1	0.19	0.19			0.36	0.23	0.54	0.03	0.04	0.01	0.226	0.218	0.110	0.077	1.091						
	scan 2	0.22	0.22			0.44	0.19	0.51	0.05	0.05	0.01	0.255	0.185	0.102	0.081	0.901	0.019		0.076	0.197	0.354	0.645
difference		-0.03	-0.03			-0.09	0.03	0.04	-0.02	-0.01	0.00	-0.029	0.033	0.008	-0.004	0.190						
mean		0.21	0.21			0.40	0.21	0.52	0.04	0.04	0.01	0.241	0.202	0.106	0.079	0.996	0.019		0.076	0.197	0.354	0.645
sd mean		0.02	0.02			0.06	0.02	0.02	0.01	0.01	0.00	0.021	0.023	0.006	0.003	0.134						
CV%		11	11			15	12	5	35	15	0	9	12	5	4	13						
cat 4	scan 1	0.29		0.29	0.19	0.40	0.20	0.72	0.03	0.04	0.01	0.205	0.211	0.086	0.067	1.119	0.040		0.094	0.178	0.327	0.440
	scan 2	0.20				0.39	0.15	0.52	0.05	0.04	0.01	0.249	0.203	0.136	0.082	0.866	0.057		0.123		0.342	0.499
difference		0.09	0.09			0.01	0.05	0.20	-0.01	-0.01	0.00	-0.044	0.008	-0.050	-0.015	0.254	-0.017		-0.029		-0.015	-0.059
mean		0.25	0.25			0.40	0.18	0.62	0.04	0.04	0.01	0.227	0.207	0.111	0.075	0.993	0.048		0.109	0.178	0.335	0.469
sd mean		0.06	0.06			0.01	0.04	0.14	0.01	0.00	0.00	0.031	0.006	0.035	0.011	0.179	0.012		0.020		0.011	0.041
CV%		24	24			2	21	22	23	11	7	14	3	32	14	18	25		19		3	9
cat 5	scan 1	0.59	0.59			0.36	0.40	1.64	0.07	0.04	0.02	0.191	0.149	0.081	0.092	0.946	0.056	0.127			0.313	0.421
	scan 2	0.42	0.42			0.23	0.39	1.79	0.05	0.02	0.02	0.214	0.173	0.107	0.120	0.708						
difference		0.17	0.17			0.13	0.01	-0.16	0.02	0.01	-0.01	-0.023	-0.024	-0.026	-0.028	0.238						
mean		0.51	0.51			0.30	0.39	1.72	0.06	0.03	0.02	0.203	0.161	0.094	0.106	0.827	0.056	0.127			0.313	0.421
sd mean		0.12	0.12			0.09	0.01	0.11	0.02	0.01	0.00	0.016	0.017	0.019	0.020	0.168						
CV%		24	24			30	1	6	26	28	20	8	11	20	19	20						
cats 1,2,3,4,5																						
mean of differ.		0.06	0.06			0.03	0.01	0.00	0.00	0.00	0.00	-0.015	-0.001	-0.011	-0.012	0.143	-0.007		-0.011		-0.009	-0.027
sd of differ.		0.08	0.09			0.08	0.03	0.13	0.02	0.01	0.00	0.026	0.024	0.027	0.010	0.118	0.015		0.025		0.008	0.045
upper lim. agr.		0.21	0.24			0.19	0.07	0.26	0.04	0.02	0.00	0.038	0.046	0.043	0.009	0.379	0.023		0.038		0.007	0.064
lower lim. agr.		-0.09	-0.12			-0.13	-0.04	-0.26	-0.03	-0.02	-0.01	-0.067	-0.048	-0.064	-0.032	-0.092	-0.037		-0.061		-0.026	-0.117
coef.of repeat.		0.15	0.18			0.16	0.06	0.26	0.03	0.02	0.01	0.053	0.047	0.054	0.021	0.235	0.030		0.049		0.016	0.090
cats 1,2,3,4																						
mean of differ.		0.03	0.02			0.00	0.02	0.04	0.00	-0.01	0.00	-0.013	0.004	-0.007	-0.008	0.120	-0.007		-0.011		-0.009	-0.027
sd of differ.		0.05	0.06			0.06	0.03	0.11	0.01	0.01	0.00	0.030	0.023	0.029	0.005	0.121	0.015		0.025		0.008	0.045
upper lim. agr.		0.13	0.14			0.13	0.08	0.26	0.02	0.01	0.00	0.047	0.050	0.051	0.003	0.363	0.023		0.038		0.007	0.064
lower lim. agr.		-0.07	-0.09			-0.13	-0.05	-0.19	-0.03	-0.02	0.00	-0.072	-0.041	-0.065	-0.018	-0.123	-0.037		-0.061		-0.026	-0.117
coef.of repeat.		0.10	0.12			0.13	0.07	0.23	0.03	0.01	0.00	0.060	0.046	0.058	0.010	0.243	0.030		0.049		0.016	0.090
mean (cats 1,2,3,4)		0.351	0.287			0.414	0.249	0.837	0.057	0.038	0.013	0.229	0.159	0.086	0.074	0.687	0.026		0.084		0.314	0.457
real upper value		0.484	0.427			0.548	0.331	1.101	0.081	0.044	0.014	0.276	0.209	0.137	0.076	1.049	0.050		0.122		0.321	0.521
real lower value		0.281	0.193			0.288	0.198	0.648	0.024	0.022	0.012	0.156	0.118	0.020	0.056	0.564	-0.010		0.023		0.288	0.340

Table App.G2 Repeatability results for pulsed TDI indices from the septal mitral annulus

		E'	E' VTI	E' dur	E' acc	tE' acc	E' dec	tE' dec	A'	A' VTI	A' dur	E/A	Se'	SI'	S' VTI	S' dur	Se' acc	tSe' acc	bS'-SI'	Q-Se'	Q-SI'	Q-E'	Q-A'	Q-bE'	IVCt	Q-bS'	IVRt	IVCb	RR
cat 1	scan 1	4.88	0.23	0.070	197	0.027	114	0.045	5.40	0.25	0.072	0.90	5.37	4.25	0.49	0.138	232	0.025	0.069	0.090	0.128	0.285	0.377	0.258	0.036	0.071	0.054		0.379
	scan 2	3.89							6.89	0.33	0.077	0.56	5.87				261	0.023		0.083	0.123	0.282	0.375		0.037	0.060			0.356
difference		0.99							-1.50	-0.08	-0.005	0.34	-0.50				-29	0.002		0.007	0.005	0.003	0.002		-0.002	0.011			0.024
mean		4.38							6.14	0.29	0.074	0.73	5.62				246	0.024		0.087	0.125	0.284	0.376		0.036	0.065			0.367
sd mean		0.70							1.06	0.05	0.004	0.24	0.35				20	0.001		0.005	0.003	0.002	0.001		0.001	0.007			0.017
CV%		16							17	19	5	33	6				8	5		5	3	1	0		3	11			5
cat 2	scan 1	4.98	0.34	0.103	131	0.038	81	0.063	5.21	0.26	0.075	0.96	5.92	4.38	0.55	0.165	223	0.028	0.077	0.083	0.130	0.298	0.407	0.264	0.025	0.059	0.057	4.6	0.413
	scan 2	7.73	0.43	0.103	284	0.027	103	0.072	6.95	0.31	0.072	1.11	6.57	5.00	0.65	0.170	232	0.030	0.086	0.087	0.146	0.291	0.398	0.264	0.032	0.061	0.055	4.2	0.376
difference		-2.75	-0.10	0.000	-153	0.011	-23	-0.009	-1.74	-0.04	0.003	-0.16	-0.65	-0.62	-0.10	-0.005	-9	-0.002	-0.009	-0.003	-0.016	0.007	0.009	0.000	-0.007	-0.002	0.003	0.3	0.037
mean		6.35	0.38	0.103	208	0.033	92	0.067	6.08	0.28	0.073	1.03	6.25	4.69	0.60	0.168	228	0.029	0.081	0.085	0.138	0.294	0.402	0.264	0.028	0.060	0.056	4.4	0.394
sd mean		1.94	0.07	0.000	108	0.008	16	0.007	1.23	0.03	0.002	0.11	0.46	0.44	0.07	0.004	6	0.001	0.007	0.002	0.011	0.005	0.007	0.000	0.005	0.001	0.002	0.2	0.026
CV%		31	18	0	52	24	17	10	20	10	3	11	7	9	12	2	3	4	8	3	8	2	2	0	17	2	3	5	7
cat 3	scan 1	5.99	0.35	0.083	183	0.034	115	0.053	4.35	0.21	0.070	1.38	5.01	3.59	0.52	0.170	141	0.036	0.088	0.099	0.161	0.353	0.521	0.322	0.056	0.069	0.082	3.2	0.573
	scan 2	7.73	0.46	0.097	170	0.048	167	0.050	4.79	0.23	0.086	1.61	5.55	4.92	0.71	0.205	149	0.038	0.093	0.102	0.175	0.367	0.642	0.323	0.058	0.065	0.080		0.543
difference		-1.74	-0.12	-0.014	13	-0.015	-52	0.003	-0.44	-0.02	-0.016	-0.24	-0.54	-1.33	-0.19	-0.035	-8	-0.002	-0.005	-0.003	-0.014	-0.013	-0.120	-0.002	-0.001	0.004			0.031
mean		6.86	0.41	0.090	176	0.041	141	0.052	4.57	0.22	0.078	1.50	5.28	4.25	0.62	0.188	145	0.037	0.090	0.100	0.168	0.360	0.581	0.323	0.057	0.067	0.081		0.558
sd mean		1.23	0.08	0.010	9	0.010	37	0.002	0.31	0.01	0.011	0.17	0.38	0.94	0.13	0.025	6	0.001	0.003	0.002	0.010	0.009	0.085	0.001	0.001	0.003	0.001		0.022
CV%		18	20	11	5	25	26	4	7	5	15	11	7	22	22	13	4	3	4	2	6	3	15	0	2	4	2		4
cat 4	scan 1	4.99	0.31	0.086	125	0.041	110	0.050	3.50	0.15	0.062	1.43	6.12	3.12	0.47	0.148	324	0.019	0.082	0.096	0.160	0.351	0.485	0.311	0.055	0.081	0.080	5.7	0.464
	scan 2	8.93	0.53	0.090	207	0.040	173	0.050	4.32	0.17	0.058	2.07	5.29	4.13	0.56	0.155	265	0.021	0.079	0.103	0.165	0.323	0.489	0.285	0.063	0.085	0.050	3.7	0.399
difference		-3.94	-0.22	-0.004	-82	0.001	-63	0.000	-0.82	-0.02	0.004	-0.64	0.83	-1.00	-0.09	-0.007	59	-0.002	0.003	-0.007	-0.005	0.029	-0.004	0.026	-0.008	-0.004	0.030	2.1	0.065
mean		6.96	0.42	0.088	166	0.041	141	0.050	3.91	0.16	0.060	1.75	5.71	3.62	0.52	0.152	295	0.020	0.080	0.099	0.163	0.337	0.487	0.298	0.059	0.083	0.065	4.7	0.431
sd mean		2.78	0.16	0.003	58	0.001	45	0.000	0.58	0.01	0.003	0.45	0.59	0.71	0.06	0.005	42	0.001	0.002	0.005	0.004	0.020	0.003	0.018	0.006	0.003	0.021	1.5	0.046
CV%		40	37	3	35	2	32	1	15	9	5	26	10	20	12	3	14	6	3	5	2	6	1	6	10	3	32	31	11
cat 5	scan 1	4.03	0.36	0.166	79	0.050	37	0.107	6.60	0.38	0.108	0.61	7.32	4.29	0.67	0.192	185	0.038	0.086	0.100	0.145	0.334	0.538	0.290	0.018	0.061	0.073		0.428
	scan 2	3.28	0.19	0.090	118	0.030	57	0.069	6.71	0.31	0.085	0.49	7.01	4.99	0.57	0.155	226	0.032	0.075	0.090	0.132	0.311	0.417	0.279	0.021	0.065	0.081		0.540
difference		0.76	0.17	0.076	-38	0.020	-19	0.038	-0.10	0.08	0.023	0.12	0.32	-0.71	0.10	0.037	-40	0.007	0.011	0.010	0.013	0.023	0.121	0.011	-0.004	-0.003	-0.009		-0.112
mean		3.65	0.28	0.128	98	0.040	47	0.088	6.65	0.34	0.097	0.55	7.16	4.64	0.62	0.173	205	0.035	0.081	0.095	0.139	0.322	0.477	0.285	0.019	0.063	0.077		0.484
sd mean		0.53	0.12	0.054	27	0.014	14	0.027	0.07	0.05	0.016	0.09	0.23	0.50	0.07	0.026	28	0.005	0.008	0.007	0.009	0.016	0.085	0.008	0.002	0.002	0.006		0.079
CV%		15	44	42	28	35	29	31	1	16	17	16	3	11	11	15	14	14	10	7	7	5	18	3	13	4	8		16
cats 1,2,3,4,5																													
mean of differ.		-1.34	-0.06	0.014	-65	0.004	-39	0.008	-0.92	-0.02	0.002	-0.11	-0.11	-0.91	-0.07	-0.003	-5	0.001	0.000	0.001	-0.003	0.010	0.001	0.009	-0.004	0.001	0.008	1.2	0.009
sd of differ.		2.16	0.17	0.041	70	0.015	22	0.021	0.69	0.06	0.014	0.37	0.65	0.32	0.12	0.030	39	0.004	0.009	0.007	0.012	0.017	0.085	0.013	0.003	0.006	0.020	1.2	0.069
upper lim. agr.		2.99	0.27	0.097	76	0.034	4	0.049	0.46	0.10	0.031	0.63	1.19	-0.27	0.17	0.056	72	0.008	0.018	0.015	0.021	0.043	0.172	0.034	0.002	0.013	0.047	3.6	0.147
lower lim. agr.		-5.66	-0.40	-0.068	-206	-0.025	-82	-0.034	-2.31	-0.13	-0.027	-0.86	-1.41	-1.55	-0.31	-0.062	-82	-0.007	-0.018	-0.014	-0.028	-0.024	-0.169	-0.017	-0.011	-0.011	-0.031	-1.2	-0.130
coef.of repeat.		4.32	0.34	0.083	141	0.030	43	0.042	1.38	0.11	0.029	0.74	1.30	0.64	0.24	0.059	77	0.007	0.018	0.014	0.024	0.034	0.171	0.025	0.006	0.012	0.039	2.4	0.138
cats 1,2,3,4																													
mean of differ.		-1.86	-0.14	-0.006	-74	-0.001	-46	-0.002	-1.13	-0.04	-0.003	-0.17	-0.21	-0.98	-0.13	-0.016	3	-0.001	-0.004	-0.002	-0.008	0.006	-0.028	0.008	-0.004	0.002	0.016		0.039
sd of differ.		2.10	0.07	0.007	83	0.013	21	0.007	0.60	0.03	0.009	0.40	0.70	0.35	0.05	0.017	38	0.002	0.006	0.006	0.009	0.017	0.062	0.015	0.004	0.006	0.019		0.018
upper lim. agr.		2.34	-0.01	0.009	93	0.025	-4	0.011	0.08	0.02	0.015	0.63	1.19	-0.27	-0.02	0.018	80	0.003	0.009	0.010	0.011	0.041	0.095	0.039	0.003	0.015	0.055		0.075
lower lim. agr.		-6.06	-0.28	-0.021	-241	-0.027	-88	-0.015	-2.33	-0.09	-0.022	-0.98	-1.61	-1.69	-0.23	-0.049	-74	-0.004	-0.016	-0.013	-0.026	-0.028	-0.152	-0.023	-0.012	-0.011	-0.022		0.003
coef.of repeat.		4.20	0.14	0.015	167	0.026	42	0.013	1.20	0.06	0.019	0.80	1.40	0.71	0.11	0.034	77	0.003	0.012	0.012	0.019	0.034	0.123	0.031	0.007	0.013	0.039		0.036
mean (cats 1,2,3,4)		6.14	0.40	0.094	183	0.038	125	0.056	5.18	0.24	0.071	1.25	5.71	4.19	0.58	0.169	228	0.027	0.084	0.093	0.148	0.319	0.462	0.295	0.045	0.069	0.067		0.438
real upper value		8.48	0.39		276	0.063	121	0.067	5.25	0.26	0.087	1.88	6.90	3.92	0.56	0.187	309	0.030	0.093	0.103	0.159	0.359	0.556	0.334	0.048	0.084	0.122		0.512
real lower value		0.08	0.12		-58	0.012	37	0.041	2.85	0.15	0.049	0.28	4.10	2.50	0.34	0.120	155	0.023	0.068	0.080	0.122	0.290	0.310	0.272	0.033	0.058	0.045		0.441

Table App.G3 Repeatability results for pulsed TDI indices from the lateral mitral annulus

		E'	E' VTI	E' dur	E' acc	tE' acc	E' dec	tE' dec	A'	A' VTI	A' dur	E/A	Se'	Sl'	S' VTI	S' dur	Se' acc	tSe' acc	bS'-Sl'	Q-Se'	Q-Sl'	Q-E'	Q-A'	Q-bE'	IVCt	Q-bS'	IVRt	IVCb	RR
cat 1	scan 1	4.85	0.25	0.068	166	0.030	126	0.040	4.62	0.18	0.055	1.05	6.32	2.63	0.45	0.143	268	0.024	0.098	0.104	0.187	0.309	0.381	0.275	0.046	0.080	0.070	5.06	0.364
	scan 2	5.78	0.25	0.068	228	0.026	134	0.044	7.01	0.23	0.055	0.82	4.66	3.89	0.42	0.133	207	0.024	0.072	0.075	0.128	0.283	0.356	0.257	0.030	0.055	0.082	6.89	0.350
difference		-0.93	0.00	0.000	-62	0.004	-8	-0.005	-2.39	-0.05	0.000	0.23	1.66	-1.26	0.03	0.010	60	0.000	0.026	0.029	0.059	0.026	0.025	0.018	0.016	0.025	-0.012	-1.83	0.014
mean		5.32	0.25	0.068	197	0.028	130	0.042	5.82	0.21	0.055	0.94	5.49	3.26	0.44	0.138	237	0.024	0.085	0.090	0.157	0.296	0.368	0.266	0.038	0.068	0.076	5.97	0.357
sd mean		0.66	0.00	0.000	44	0.003	6	0.003	1.69	0.04	0.000	0.16	1.17	0.89	0.02	0.007	43	0.000	0.018	0.021	0.041	0.018	0.017	0.013	0.011	0.018	0.009	1.29	0.010
CV%		**12**	**0**	**0**	**22**	**9**	**4**	**8**	**29**	**17**	**0**	**17**	**21**	**27**	**5**	**5**	**18**	**1**	**21**	**23**	**26**	**6**	**5**	**5**	**29**	**26**	**12**	**22**	**3**
cat 2	scan 1	6.34	0.35	0.088	222	0.031	103	0.063	8.04	0.31	0.068	0.79	5.90	3.40	0.57	0.162	203	0.032	0.082	0.084	0.159	0.303	0.394	0.272	0.026	0.061	0.063	9.71	0.381
	scan 2	5.77	0.30	0.094	199	0.030	100	0.059	4.85	0.18	0.055	1.19	4.61	3.10	0.46	0.158	197	0.025	0.090	0.089	0.158	0.299	0.432	0.273	0.054	0.069	0.056	8.28	0.418
difference		0.57	0.05	-0.006	23	0.001	3	0.003	3.19	0.13	0.013	-0.40	1.29	0.30	0.10	0.004	6	0.007	-0.008	-0.005	0.001	0.005	-0.038	-0.002	-0.028	-0.008	0.007	1.43	-0.037
mean		6.06	0.33	0.091	211	0.031	102	0.061	6.45	0.24	0.062	0.99	5.26	3.25	0.51	0.160	200	0.028	0.086	0.087	0.159	0.301	0.413	0.272	0.040	0.065	0.060	8.99	0.400
sd mean		0.40	0.03	0.004	16	0.001	2	0.002	2.26	0.09	0.009	0.28	0.91	0.21	0.07	0.003	4	0.005	0.006	0.004	0.001	0.003	0.027	0.001	0.020	0.006	0.005	1.01	0.026
CV%		**7**	**11**	**4**	**8**	**2**	**2**	**4**	**35**	**36**	**15**	**29**	**17**	**7**	**14**	**2**	**2**	**17**	**7**	**4**	**0**	**1**	**7**	**0**	**49**	**9**	**8**	**11**	**7**
cat 3	scan 1	10.37	0.63	0.100	232	0.045	200	0.054	4.56	0.22	0.082	2.27	5.88	2.98	0.72	0.203	201	0.032	0.122	0.089	0.178	0.343	0.542	0.305	0.060	0.067	0.068	5.54	0.523
	scan 2	8.74	0.50	0.103	330	0.028	114	0.082	3.36	0.14	0.063	2.60	5.42	3.02	0.66	0.193	114	0.046	0.118	0.113	0.200	0.348	0.580	0.320	0.069	0.074	0.071	3.40	0.566
difference		1.63	0.13	-0.003	-97	0.017	86	-0.027	1.20	0.07	0.019	-0.32	0.46	-0.04	0.06	0.010	88	-0.014	0.004	-0.025	-0.022	-0.005	-0.038	-0.015	-0.009	-0.007	-0.003	2.14	-0.043
mean		9.56	0.56	0.102	281	0.037	157	0.068	3.96	0.18	0.073	2.44	5.65	3.00	0.69	0.198	158	0.039	0.120	0.101	0.189	0.346	0.561	0.313	0.065	0.070	0.069	4.47	0.544
sd mean		1.15	0.09	-0.002	69	0.012	61	0.019	0.85	0.05	0.013	0.23	0.33	0.03	0.04	0.007	62	0.010	0.003	0.017	0.015	0.003	0.027	0.011	0.006	0.005	0.002	1.52	0.030
CV%		**12**	**16**	**2**	**24**	**33**	**39**	**28**	**21**	**29**	**18**	**9**	**6**	**1**	**6**	**4**	**39**	**26**	**2**	**17**	**8**	**1**	**5**	**3**	**10**	**7**	**3**	**34**	**6**
cat 4	scan 1	8.99	0.37	0.070	240	0.037	227	0.040	3.01	0.12	0.052	2.99	6.95	3.93	0.65	0.164	265	0.028	0.092	0.104	0.172	0.355	0.560	0.308	0.066	0.085	0.070	3.31	0.599
	scan 2	11.91	0.63	0.080	444	0.033	245	0.047	6.01	0.30	0.080	1.98	7.56	6.03	0.68	0.160	358	0.023	0.075	0.084	0.138	0.320	0.413	0.282	0.059	0.068	0.078	4.36	0.473
difference		-2.92	-0.26	-0.010	-204	0.004	-18	-0.008	-3.00	-0.19	-0.028	1.00	-0.61	-2.10	-0.03	0.004	-93	0.005	0.017	0.020	0.034	0.036	0.147	0.026	0.008	0.018	-0.008	-1.05	0.127
mean		10.45	0.50	0.075	342	0.035	236	0.044	4.51	0.21	0.066	2.48	7.26	4.98	0.67	0.162	311	0.025	0.084	0.094	0.155	0.337	0.486	0.295	0.062	0.076	0.074	3.83	0.536
sd mean		2.06	0.18	0.007	144	0.003	13	0.006	2.12	0.13	0.020	0.71	0.43	1.48	0.02	0.003	66	0.004	0.012	0.014	0.024	0.025	0.104	0.018	0.005	0.012	0.006	0.74	0.090
CV%		**20**	**37**	**9**	**42**	**8**	**6**	**13**	**47**	**62**	**30**	**29**	**6**	**30**	**3**	**2**	**21**	**14**	**15**	**15**	**16**	**7**	**21**	**6**	**9**	**16**	**8**	**19**	**17**
cat 5	scan 1	3.45							5.61			0.61	4.28	3.64	0.55	0.187	95	0.052	0.129	0.121	0.189	0.305	0.362	0.269	0.056	0.081	0.035		0.370
	scan 2	4.63	0.48	0.170	67	0.073	54	0.088	4.56			1.02	5.77	2.40	0.66	0.217	90	0.067	0.151	0.138	0.212	0.350	0.468	0.286	0.052	0.066	0.057		0.552
difference		-1.18							1.05			-0.40	-1.50	1.24	-0.12	-0.030	4	-0.015	-0.022	-0.017	-0.023	-0.045	-0.106	-0.017	0.004	0.015	-0.022		-0.182
mean		4.04							5.08			0.82	5.02	3.02	0.60	0.202	93	0.059	0.140	0.129	0.200	0.328	0.415	0.278	0.054	0.074	0.046		0.461
sd mean		0.84							0.74			0.28	1.06	0.88	0.08	0.021	3	0.010	0.015	0.012	0.016	0.032	0.075	0.012	0.003	0.010	0.015		0.128
CV%		**21**							**15**			**35**	**21**	**29**	**14**	**11**	**3**	**17**	**11**	**9**	**8**	**10**	**18**	**4**	**6**	**14**	**33**		**28**
cats 1,2,3,4,5																													
mean of differ.		-0.57	-0.02	-0.005	-85	0.006	16	-0.009	0.01	-0.01	0.001	0.02	0.26	-0.37	0.01	0.000	13	-0.003	0.003	0.001	0.010	0.003	-0.002	0.002	-0.002	0.008	-0.008	0.18	-0.024
sd of differ.		1.74	0.17	0.004	94	0.007	48	0.013	2.62	0.14	0.021	0.61	1.31	1.32	0.09	0.017	69	0.010	0.019	0.023	0.036	0.031	0.095	0.019	0.017	0.015	0.011	1.91	0.111
upper lim. agr.		2.92	0.31	0.004	103	0.021	111	0.017	5.25	0.27	0.043	1.24	2.89	2.26	0.18	0.033	151	0.018	0.041	0.047	0.081	0.066	0.188	0.040	0.032	0.039	0.014	4.00	0.199
lower lim. agr.		-4.05	-0.36	-0.013	-273	-0.008	-80	-0.035	-5.23	-0.29	-0.041	-1.20	-2.36	-3.00	-0.16	-0.034	-125	-0.024	-0.035	-0.046	-0.062	-0.060	-0.193	-0.037	-0.036	-0.022	-0.029	-3.65	-0.247
coef.of repeat.		**3.49**	**0.34**	**0.008**	**188**	**0.014**	**95**	**0.026**	**5.24**	**0.28**	**0.042**	**1.22**	**2.63**	**2.63**	**0.17**	**0.034**	**138**	**0.021**	**0.038**	**0.046**	**0.071**	**0.063**	**0.190**	**0.038**	**0.034**	**0.030**	**0.021**	**3.82**	**0.223**
cats 1,2,3,4																													
mean of differ.		-0.41	-0.02	-0.005	-85	0.006	16	-0.009	-0.25	-0.01	0.001	0.13	0.70	-0.77	0.04	0.007	15	0.000	0.010	0.005	0.018	0.015	0.024	0.007	-0.003	0.007	-0.004		0.015
sd of differ.		1.97	0.17	0.004	94	0.007	48	0.013	2.95	0.14	0.021	0.65	1.01	1.11	0.06	0.004	80	0.010	0.015	0.024	0.035	0.019	0.087	0.018	0.019	0.017	0.008		0.079
upper lim. agr.		3.53	0.31	0.004	103	0.021	111	0.017	5.65	0.27	0.043	1.42	2.71	1.44	0.15	0.014	175	0.019	0.039	0.053	0.089	0.053	0.198	0.044	0.035	0.041	0.012		0.173
lower lim. agr.		-4.36	-0.36	-0.013	-273	-0.008	-80	-0.035	-6.14	-0.29	-0.041	-1.17	-1.31	-2.99	-0.07	0.000	-144	-0.020	-0.020	-0.044	-0.053	-0.022	-0.151	-0.030	-0.042	-0.027	-0.021		-0.142
coef.of repeat.		**3.95**	**0.34**	**0.008**	**188**	**0.014**	**95**	**0.026**	**5.89**	**0.28**	**0.042**	**1.30**	**2.01**	**2.22**	**0.11**	**0.007**	**159**	**0.019**	**0.030**	**0.049**	**0.071**	**0.037**	**0.175**	**0.037**	**0.038**	**0.034**	**0.017**		**0.158**
mean (cats 1,2,3,4)		7.84	0.41	0.084	258	0.033	156	0.054	5.18	0.21	0.064	1.71	5.91	3.62	0.58	0.165	227	0.029	0.094	0.093	0.165	0.320	0.457	0.286	0.051	0.070	0.070		0.459
real upper value		11.38	0.72		350	0.053	267	0.070	10.83	0.48	0.107	3.14	8.63	5.07	0.73	0.179	401	0.048	0.133	0.146	0.254	0.372	0.655	0.330	0.086	0.110	0.082		0.632
real lower value		3.49	0.05		-15	0.025	77	0.018	-0.96	-0.08	0.023	0.54	4.60	0.63	0.51	0.164	83	0.009	0.074	0.049	0.112	0.298	0.306	0.256	0.009	0.043	0.049		0.317

Table App.G4 Repeatability results for pulsed TDI indices from the IVS along the longitudinal axis

		E'	E' VTI	E' dur	E' acc	tE' acc	E' dec	tE' dec	A'	A' VTI	A' dur	E/A	Se'	Sl'	S' VTI	S' dur	Se' acc	tSe' acc	bS'-Sl'	Q-Se'	Q-Sl'	Q-E'	Q-A'	Q-bE'	IVCt	Q-bS'	IVRt	IVCb	RR
cat 1	scan 1	3.98	0.21	0.072	159	0.028	92	0.048	6.63	0.22	0.060	0.60	3.93	4.46	0.44	0.138	174	0.023	0.076						0.041		0.063	6.05	0.373
	scan 2	6.32	0.24	0.060	231	0.028	192	0.035	6.42			0.98	5.36	2.44	0.41	0.148	207	0.027	0.101	0.092	0.165	0.294	0.332	0.265		0.069	0.059		0.363
difference		-2.34	-0.03	0.012	-72	0.000	-100	0.013	0.21			-0.38	-1.42	2.02	0.03	-0.009	-34	-0.004	-0.024								0.004		0.010
mean		5.15	0.22	0.066	195	0.028	142	0.042	6.53			0.79	4.64	3.45	0.42	0.143	190	0.025	0.088								0.061		0.368
sd mean		1.65	0.02	0.008	51	0.000	71	0.009	0.15			0.27	1.01	1.43	0.02	0.007	24	0.003	0.017								0.003		0.007
CV%		32	10	13	26	0	50	22	2			34	22	41	5	5	12	10	19								5		2
cat 2	scan 1	6.01	0.41	0.120	138	0.046	84	0.072	7.56	0.31	0.068	0.79	8.84	5.10	0.75	0.163	336	0.027	0.088	0.080	0.139	0.288	0.393	0.250	0.020	0.053	0.046	6.29	0.390
	scan 2	5.49	0.32	0.096	141	0.039	90	0.062	6.33	0.25	0.063	0.87	6.40	4.81	0.60	0.154	186	0.036	0.097	0.075	0.138	0.297	0.417	0.256	0.021	0.049	0.071		0.412
difference		0.51	0.09	0.024	-3	0.007	-5	0.010	1.23	0.06	0.006	-0.07	2.44	0.29	0.15	0.009	150	-0.010	-0.009	0.005	0.001	-0.008	-0.024	-0.006	-0.001	0.005	-0.025		-0.022
mean		5.75	0.37	0.108	139	0.042	87	0.067	6.95	0.28	0.065	0.83	7.62	4.96	0.67	0.159	261	0.031	0.092	0.077	0.138	0.292	0.405	0.253	0.021	0.051	0.058		0.401
sd mean		0.36	0.06	0.017	2	0.005	4	0.007	0.87	0.04	0.004	0.05	1.72	0.20	0.11	0.007	106	0.007	0.006	0.003	0.001	0.006	0.017	0.004	0.001	0.003	0.018		0.016
CV%		6	17	16	1	11	4	11	12	14	6	6	23	4	16	4	41	21	7	4	0	2	4	2	3	6	31		4
cat 3	scan 1	5.55							4.90	0.36	0.090	1.13	6.62	4.16	0.67	0.203	170	0.040	0.118	0.077	0.158	0.328	0.557		0.038	0.045			0.536
	scan 2	6.68	0.41	0.088	238	0.029	117	0.058	4.44	0.20	0.065	1.51	5.48	3.40	0.59	0.188	163	0.035	0.102	0.099	0.162	0.345	0.569	0.321	0.056	0.074	0.063		0.531
difference		-1.13							0.46	0.15	0.025	-0.37	1.14	0.75	0.08	0.015	8	0.006	0.016	-0.022	-0.004	-0.017	-0.012		-0.018	-0.029			0.005
mean		6.11							4.67	0.28	0.078	1.32	6.05	3.78	0.63	0.195	166	0.037	0.110	0.088	0.160	0.337	0.563		0.047	0.059			0.533
sd mean		0.80							0.33	0.11	0.018	0.26	0.80	0.53	0.05	0.011	5	0.004	0.011	0.016	0.003	0.012	0.008		0.013	0.020			0.003
CV%		13							7	39	23	20	13	14	9	5	3	10	10	18	2	4	1		27	34			1
cat 4	scan 1	6.93	0.40	0.092	195	0.035	117	0.059	3.33	0.14	0.062	2.08	5.49	3.53	0.54	0.176	157	0.036	0.098	0.103	0.167	0.329	0.548	0.293	0.054	0.068	0.056		0.547
	scan 2	6.58	0.36	0.072	234	0.035	192	0.041	4.24	0.17	0.060	1.55	6.24	3.23	0.44	0.162	250	0.025	0.105	0.090	0.179	0.317	0.407	0.291	0.053	0.068	0.068	3.36	0.405
difference		0.34	0.04	0.020	-39	0.000	-75	0.018	-0.91	-0.02	0.002	0.53	-0.75	0.30	0.10	0.014	-93	0.011	-0.007	0.013	-0.012	0.012	0.141	0.002	0.001	0.000	-0.012		0.142
mean		6.76	0.38	0.082	214	0.035	155	0.050	3.78	0.16	0.061	1.82	5.87	3.38	0.49	0.169	204	0.030	0.102	0.096	0.173	0.323	0.477	0.292	0.054	0.068	0.062		0.476
sd mean		0.24	0.03	0.014	27	0.000	53	0.013	0.64	0.02	0.001	0.37	0.53	0.21	0.07	0.010	65	0.008	0.005	0.009	0.008	0.008	0.100	0.001	0.001	0.000	0.008		0.101
CV%		4	8	17	13	0	34	26	17	11	2	21	9	6	14	6	32	27	5	9	5	3	21	0	1	0	13		21
cat 5	scan 1	6.31	0.30	0.085	145	0.046	181	0.037	8.03	0.35	0.080	0.79	8.25	5.45	0.70	0.152	220	0.039	0.084	0.089	0.132	0.296	0.413	0.253	0.029	0.062	0.059		0.380
	scan 2	7.14	0.41	0.113	145	0.051	112	0.063	6.23	0.30	0.085	1.15	7.06	4.58	0.73	0.185	166	0.043	0.103	0.093	0.160	0.323	0.461	0.279	0.030	0.061	0.073		0.569
difference		-0.83	-0.10	-0.028	1	-0.005	70	-0.025	1.80	0.05	-0.005	-0.36	1.19	0.87	-0.03	-0.033	54	-0.004	-0.020	-0.004	-0.028	-0.027	-0.048	-0.026	-0.002	0.000	-0.013		-0.189
mean		6.73	0.35	0.099	145	0.049	146	0.050	7.13	0.33	0.083	0.97	7.65	5.01	0.72	0.168	193	0.041	0.093	0.091	0.146	0.309	0.437	0.266	0.029	0.061	0.066		0.475
sd mean		0.59	0.07	0.020	0	0.003	49	0.018	1.27	0.04	0.004	0.25	0.84	0.61	0.02	0.024	38	0.003	0.014	0.003	0.020	0.019	0.034	0.018	0.001	0.000	0.009		0.134
CV%		9	21	20	0	7	34	36	18	11	4	26	11	12	3	14	20	7	15	3	14	6	8	7	4	0	14		28
cats 1,2,3,4,5																													
mean of differ.		-0.69	-0.08	0.007	-28	0.000	-28	0.004	0.56	0.06	0.007	-0.13	0.52	0.85	0.07	-0.001	17	0.000	-0.009	-0.002	-0.011	-0.010	0.014	-0.010	-0.005	-0.006	-0.012		-0.011
sd of differ.		1.17	0.20	0.024	34	0.005	76	0.020	1.03	0.07	0.013	0.39	1.57	0.71	0.07	0.021	92	0.008	0.015	0.015	0.013	0.016	0.086	0.014	0.009	0.015	0.012		0.118
upper lim. agr.		1.65	0.31	0.055	40	0.010	125	0.044	2.62	0.20	0.033	0.65	3.66	2.26	0.20	0.040	201	0.017	0.022	0.028	0.015	0.023	0.186	0.019	0.013	0.024	0.012		0.226
lower lim. agr.		-3.02	-0.48	-0.041	-96	-0.009	-180	-0.036	-1.51	-0.09	-0.019	-0.92	-2.63	-0.57	-0.07	-0.042	-167	-0.017	-0.040	-0.032	-0.036	-0.043	-0.157	-0.039	-0.022	-0.036	-0.036		-0.248
coef.of repeat.		2.33	0.40	0.048	68	0.009	152	0.040	2.07	0.14	0.026	0.78	3.15	1.42	0.13	0.041	184	0.017	0.031	0.030	0.025	0.033	0.172	0.029	0.018	0.030	0.024		0.237
cats 1,2,3,4																													
mean of differ.		-0.65	-0.08	0.019	-38	0.002	-60	0.014	0.25	0.06	0.011	-0.08	0.35	0.84	0.09	0.007	8	0.001	-0.006	-0.002	-0.005	-0.004	0.035	-0.002	-0.006	-0.008	-0.011		0.034
sd of differ.		1.34	0.23	0.006	35	0.004	49	0.004	0.88	0.09	0.012	0.43	1.76	0.82	0.05	0.011	103	0.009	0.016	0.018	0.006	0.015	0.092	0.006	0.010	0.018	0.015		0.074
upper lim. agr.		2.04	0.38	0.031	31	0.010	38	0.022	2.01	0.24	0.036	0.78	3.88	2.48	0.19	0.030	215	0.020	0.027	0.035	0.008	0.025	0.219	0.010	0.015	0.028	0.018		0.181
lower lim. agr.		-3.34	-0.53	0.006	-107	-0.005	-158	0.005	-1.52	-0.12	-0.014	-0.93	-3.18	-0.79	-0.01	-0.016	-199	-0.018	-0.039	-0.038	-0.018	-0.034	-0.149	-0.014	-0.027	-0.044	-0.040		-0.114
coef.of repeat.		2.69	0.46	0.01	69.04	0.01	97.93	0.01	1.77	0.18	0.02	0.86	3.53	1.64	0.10	0.02	206.74	0.02	0.03	0.04	0.01	0.03	0.18	0.01	0.02	0.04	0.03		0.147
mean (cats 1,2,3,4)		5.94	0.32	0.085	183	0.035	128	0.053	5.48	0.24	0.068	1.19	6.04	3.89	0.55	0.166	205	0.031	0.098	0.087	0.157	0.317	0.482	0.272	0.041	0.059	0.060		0.445
real upper value		7.98	0.70		214	0.045	166	0.075	7.50	0.48	0.104	1.97	9.92	6.37	0.74	0.196	420	0.051	0.125	0.122	0.165	0.342	0.700	0.282	0.055	0.087	0.079		0.626
real lower value		2.60	-0.21		76	0.030	-30	0.058	3.96	0.12	0.054	0.26	2.87	3.10	0.54	0.151	7	0.013	0.059	0.049	0.139	0.284	0.333	0.259	0.014	0.015	0.020		0.331

Table App.G5 Repeatability results for pulsed TDI indices from the LVPW along the longitudinal axis

		E'	E' VTI	E' dur	E' acc	tE' acc	E' dec	tE' dec	A'	A' VTI	A' dur	E/A	Se'	Sl'	S' VTI	S' dur	Se' acc	tSe' acc	bS'-Sl'	Q-Se'	Q-Sl'	Q-E'	Q-A'	Q-bE'	IVCt	Q-bS'	IVRt	IVCb	RR
cat 1	scan 1	4.64	0.20	0.067	174	0.028	108	0.044	4.08	0.13	0.046	1.14	5.26	2.05	0.37	0.143	216	0.025	0.106	0.102	0.168				0.053	0.084	0.074	5.90	0.379
	scan 2	6.02							4.35			1.38	5.84	2.52															0.356
difference		-1.38							-0.26			-0.25	-0.58	-0.47															0.024
mean		5.33							4.21			1.26	5.55	2.29															0.367
sd mean		0.97							0.18			0.18	0.41	0.33															0.017
CV%		18							4			14	7	15															5
cat 2	scan 1	7.60	0.44	0.100	267	0.030	106	0.072	4.26	0.14	0.060	1.78	5.50	2.65	0.48	0.165	217	0.027	0.089	0.086	0.154	0.303	0.425	0.274	0.042	0.066	0.048	3.83	0.413
	scan 2	8.99	0.46	0.088	254	0.039	194	0.050	5.55	0.16	0.052	1.62	8.08	3.72	0.60	0.158	305	0.028	0.084	0.088	0.149	0.307	0.377	0.261	0.034	0.062	0.054	5.21	0.376
difference		-1.39	-0.03	0.012	12	-0.010	-88	0.022	-1.29	-0.02	0.008	0.16	-2.59	-1.07	-0.13	0.007	-88	-0.002	0.005	-0.002	0.004	-0.004	0.049	0.013	0.008	0.004	-0.006	-1.38	0.037
mean		8.29	0.45	0.094	261	0.034	150	0.061	4.91	0.15	0.056	1.70	6.79	3.18	0.54	0.162	261	0.027	0.086	0.087	0.152	0.305	0.401	0.267	0.038	0.064	0.051	4.52	0.394
sd mean		0.99	0.02	0.008	9	0.007	62	0.016	0.91	0.01	0.006	0.11	1.83	0.76	0.09	0.005	62	0.001	0.004	0.002	0.003	0.003	0.034	0.009	0.006	0.003	0.004	0.97	0.026
CV%		12	4	9	3	20	41	26	19	9	11	7	27	24	16	3	24	4	4	2	2	1	9	3	15	4	8	22	7
cat 3	scan 1	9.01	0.35	0.073	364	0.025	171	0.052	4.33	0.17	0.060	2.08	4.95	2.90	0.54	0.178	120	0.040	0.139	0.132	0.216	0.344	0.543	0.326	0.076	0.081	0.070	4.58	0.573
	scan 2	11.28	0.61	0.085	364	0.033	247	0.049	5.15	0.23	0.073	2.19	6.30	3.17	0.72	0.197	116	0.050	0.101	0.115	0.189	0.346	0.554	0.315	0.070	0.068	0.073	3.11	0.543
difference		-2.27	-0.26	-0.013	0	-0.009	-76	0.003	-0.82	-0.07	-0.013	-0.11	-1.35	-0.27	-0.18	-0.019	3	-0.010	0.038	0.017	0.027	-0.003	-0.011	0.011	0.006	0.014	-0.003	1.47	0.031
mean		10.14	0.48	0.079	364	0.029	209	0.050	4.74	0.20	0.066	2.14	5.62	3.03	0.63	0.187	118	0.045	0.120	0.124	0.202	0.345	0.548	0.320	0.073	0.074	0.071	3.84	0.558
sd mean		1.61	0.18	0.009	0	0.006	53	0.002	0.58	0.05	0.009	0.08	0.96	0.19	0.13	0.014	2	0.007	0.027	0.012	0.019	0.002	0.008	0.007	0.004	0.010	0.002	1.04	0.022
CV%		16	38	11	0	21	26	4	12	23	13	4	17	6	21	7	2	16	23	10	10	1	1	2	6	13	3	27	4
cat 4	scan 1	5.07	0.41	0.132	98	0.056	76	0.071	6.33	0.22	0.063	0.80	6.14		0.54	0.148	102	0.061		0.131		0.317	0.425	0.263	0.054	0.077	0.053	3.57	0.464
	scan 2	4.46	0.38	0.138	87	0.056	62	0.074	6.40	0.24	0.070	0.70	4.22	3.45	0.57	0.212	91	0.048	0.138	0.157	0.238	0.345	0.448	0.297	0.105	0.108	0.028		0.399
difference		0.62	0.03	-0.006	11	0.000	14	-0.003	-0.07	-0.03	-0.008	0.10	1.92		-0.03	-0.064	11	0.012		-0.026		-0.029	-0.022	-0.033	-0.051	-0.031	0.026		0.065
mean		4.77	0.40	0.135	92	0.056	69	0.073	6.37	0.23	0.066	0.75	5.18		0.55	0.180	96	0.055		0.144		0.331	0.436	0.280	0.080	0.093	0.040		0.431
sd mean		0.44	0.02	0.004	8	0.000	10	0.002	0.05	0.02	0.005	0.07	1.36		0.02	0.045	8	0.009		0.019		0.020	0.016	0.024	0.036	0.022	0.018		0.046
CV%		9	5	3	9	0	14	3	1	8	8	10	26		3	25	8	16		13		6	4	8	45	24	45		11
cat 5	scan 1	8.82	0.38	0.070	306	0.029	203	0.044	3.12	0.15	0.063	2.83	5.27	4.32	0.68	0.170	252	0.026	0.087	0.123	0.189	0.321	0.435	0.305	0.060	0.101	0.077	2.99	0.428
	scan 2	13.85	0.64	0.072	454	0.031	311	0.046	5.72	0.24	0.058	2.42	6.54	5.37	0.70	0.173	263	0.026	0.085	0.087	0.149	0.316	0.401	0.290	0.050	0.068	0.055		0.540
difference		-5.03	-0.26	-0.002	-148	-0.003	-109	-0.002	-2.60	-0.09	0.005	0.41	-1.27	-1.05	-0.02	-0.003	-11	0.000	0.002	0.036	0.040	0.005	0.035	0.014	0.010	0.033	0.022		-0.112
mean		11.34	0.51	0.071	380	0.030	257	0.045	4.42	0.20	0.060	2.63	5.91	4.84	0.69	0.172	258	0.026	0.086	0.105	0.169	0.319	0.418	0.297	0.055	0.084	0.066		0.484
sd mean		3.56	0.19	0.001	105	0.002	77	0.001	1.84	0.06	0.004	0.29	0.90	0.74	0.01	0.002	8	0.000	0.001	0.025	0.028	0.004	0.024	0.010	0.007	0.023	0.015		0.079
CV%		31	37	2	28	6	30	3	42	32	6	11	15	15	2	1	3	0	2	24	17	1	6	3	13	28	23		16
cats 1,2,3,4,5																													
mean of differ.		-1.89	-0.13	-0.002	-31	-0.005	-64	0.005	-1.01	-0.05	-0.002	0.06	-0.77	-0.71	-0.09	-0.020	-21	0.000	0.015	0.006	0.024	-0.007	0.013	0.001	-0.007	0.005	0.010	0.05	0.009
sd of differ.		2.05	0.15	0.010	78	0.005	54	0.012	1.01	0.03	0.010	0.25	1.67	0.41	0.08	0.031	45	0.009	0.020	0.027	0.018	0.015	0.034	0.023	0.030	0.027	0.016	2.01	0.069
upper lim. agr.		2.21	0.18	0.018	125	0.004	44	0.028	1.01	0.02	0.018	0.57	2.57	0.10	0.07	0.043	70	0.019	0.055	0.059	0.060	0.022	0.081	0.047	0.052	0.058	0.042	4.07	0.147
lower lim. agr.		-5.99	-0.44	-0.023	-188	-0.014	-173	-0.018	-3.03	-0.12	-0.022	-0.44	-4.12	-1.53	-0.25	-0.083	-112	-0.019	-0.025	-0.047	-0.012	-0.037	-0.056	-0.045	-0.066	-0.049	-0.023	-3.98	-0.130
coef.of repeat.		4.10	0.31	0.021	157	0.009	108	0.023	2.02	0.07	0.020	0.51	3.34	0.81	0.16	0.063	91	0.019	0.040	0.053	0.036	0.029	0.069	0.046	0.059	0.054	0.033	4.03	0.138
cats 1,2,3,4																													
mean of differ.		-1.11	-0.08	-0.002	8	-0.006	-50	0.007	-0.61	-0.04	-0.004	-0.02	-0.65	-0.60	-0.11	-0.026	-24	0.000	0.022	-0.004	0.016	-0.012	0.005	-0.003	-0.012	-0.005	0.006		0.039
sd of differ.		1.22	0.15	0.013	7	0.005	56	0.013	0.55	0.03	0.011	0.19	1.90	0.42	0.08	0.036	55	0.011	0.024	0.022	0.016	0.015	0.038	0.026	0.034	0.023	0.017		0.018
upper lim. agr.		1.34	0.22	0.023	21	0.004	62	0.033	0.49	0.01	0.018	0.36	3.16	0.23	0.05	0.046	86	0.023	0.069	0.039	0.048	0.018	0.081	0.048	0.055	0.042	0.041		0.075
lower lim. agr.		-3.55	-0.39	-0.028	-5	-0.016	-161	-0.019	-1.71	-0.09	-0.026	-0.40	-4.45	-1.43	-0.27	-0.097	-134	-0.023	-0.025	-0.047	-0.016	-0.041	-0.071	-0.055	-0.079	-0.051	-0.029		0.003
coef.of repeat.		2.44	0.31	0.025	13	0.010	111	0.026	1.10	0.05	0.022	0.38	3.81	0.83	0.16	0.072	110	0.023	0.047	0.043	0.032	0.029	0.076	0.052	0.067	0.047	0.035		0.036
mean (cats 1,2,3,4)		7.13	0.44	0.103	239	0.040	143	0.061	5.06	0.19	0.063	1.46	5.79	2.83	0.57	0.176	158	0.042	0.103	0.118	0.177	0.327	0.462	0.289	0.063	0.077	0.054		0.438
real upper value		8.47	0.66		260	0.044	204	0.095	5.55	0.21	0.081	1.82	8.94	3.06	0.62	0.222	244	0.065	0.171	0.157	0.225	0.344	0.543	0.338	0.118	0.119	0.095		0.512
real lower value		3.58	0.05		234	0.023	-19	0.042	3.34	0.11	0.037	1.06	1.33	1.40	0.30	0.079	24	0.020	0.077	0.071	0.161	0.286	0.391	0.234	-0.016	0.026	0.025		0.441

Table App.G6 Repeatability results for pulsed TDI indices from the LVPW along the radial axis

		E'	E' VTI	E' dur	E' acc	tE' acc	E' dec	tE' dec	A'	A' VTI	A' dur	E/A	Se'	SI'	S' VTI	S' dur	Se' acc	tSe' acc	bS'-SI'	Q-Se'	Q-SI'	Q-E'	Q-A'	Q-bE'	IVCt	Q-bS'	IVRt	IVCb	RR
cut 1	scan 1	2.80							5.15			0.54	5.25															6.84	0.350
	scan 2	3.38	0.16	0.078	124	0.029	68	0.050	7.03	0.29	0.075	0.48	5.92	3.52	0.53	0.143	178	0.035	0.090	0.104	0.157	0.278	0.362	0.259	0.050	0.074	0.064	5.65	0.370
difference		-0.58							-1.89			0.06	-0.67															1.19	-0.020
mean		3.09							6.09			0.51	5.58															6.24	0.360
sd mean		0.41							1.34			0.04	0.47															0.84	0.014
CV%		13							22			9	8															13	4
cut 2	scan 1	4.18	0.29	0.100	83	0.056	119	0.040	5.32	0.21	0.062	0.79	6.62	3.10	0.57	0.145	168	0.039	0.092	0.105	0.163	0.326	0.381	0.272	0.041	0.072	0.064	7.70	0.406
	scan 2	4.22							5.77	0.21	0.065	0.73	6.26	3.00	0.57	0.148	155	0.041	0.096	0.108	0.163	0.305	0.391	0.260	0.045	0.071	0.053	8.63	0.409
difference		-0.05							-0.45	0.00	-0.003	0.05	0.36	0.10	0.00	-0.003	13	-0.002	-0.005	-0.003	0.000	0.022	-0.010	0.012	-0.004	0.001	0.011	-0.93	-0.003
mean		4.20							5.54	0.21	0.063	0.76	6.44	3.05	0.57	0.147	162	0.040	0.094	0.107	0.163	0.315	0.386	0.266	0.043	0.071	0.058	8.17	0.408
sd mean		0.03							0.32	0.00	0.002	0.04	0.25	0.07	0.00	0.002	9	0.002	0.003	0.002	0.000	0.015	0.007	0.008	0.003	0.001	0.008	0.66	0.002
CV%		1							6	2	4	5	4	2	0	2	6	4	3	2	0	5	2	3	6	1	14	8	1
cut 3	scan 1	5.30	0.33	0.102	144	0.040	101	0.056					5.15	3.00	0.60	0.185	207	0.026	0.108	0.095	0.183	0.330	0.498	0.288	0.065	0.072	0.047	5.42	0.501
	scan 2	6.25	0.41	0.102	192	0.039	127	0.060	4.01	0.15	0.057	1.56	5.19	5.34	0.60	0.170	175	0.027	0.075	0.110	0.155	0.346	0.593	0.311	0.077	0.086	0.066	5.63	0.555
difference		-0.95	-0.08	0.000	-48	0.001	-26	-0.004					-0.04	-2.34	0.01	0.015	32	-0.002	0.033	-0.016	0.028	-0.016	-0.095	-0.023	-0.013	-0.014	-0.020	-0.21	-0.054
mean		5.77	0.37	0.102	168	0.040	114	0.058					5.17	4.17	0.60	0.178	191	0.026	0.092	0.102	0.169	0.338	0.546	0.300	0.071	0.079	0.056	5.53	0.528
sd mean		0.67	0.06	0.000	34	0.001	19	0.003					0.03	1.65	0.00	0.011	23	0.001	0.023	0.011	0.020	0.011	0.067	0.016	0.009	0.010	0.014	0.15	0.038
CV%		12	15	0	20	2	16	5					1	40	1	6.0	12	4	26	11	12	3	12	5	12	12	25	3	7
cut 4	scan 1	4.08	0.18	0.072	163	0.032	134	0.036	4.45	0.26	0.087	0.92	5.28	2.52	0.45	0.150	221	0.025	0.084	0.096	0.157	0.354	0.453	0.314	0.060	0.075	0.090	6.18	0.458
	scan 2	4.76							4.17	0.17	0.064	1.14	5.09	3.28	0.54	0.158	215	0.024	0.099	0.104	0.180	0.331	0.475	0.303	0.073	0.086	0.071	7.36	0.510
difference		-0.68							0.28	0.08	0.023	-0.22	0.19	-0.75	-0.09	-0.008	5	0.001	-0.015	-0.008	-0.023	0.023	-0.022	0.011	-0.013	-0.011	0.019	-1.18	-0.052
mean		4.42							4.31	0.21	0.075	1.03	5.19	2.90	0.49	0.154	218	0.024	0.092	0.100	0.169	0.343	0.464	0.309	0.067	0.080	0.081	6.77	0.484
sd mean		0.48							0.20	0.06	0.016	0.16	0.13	0.53	0.06	0.005	4	0.001	0.011	0.006	0.016	0.016	0.016	0.008	0.009	0.008	0.013	0.83	0.037
CV%		11							5	27	21	15	3	18	13	3	2	2	12	6	10	5	3	3	14	9	17	12	8
cut 5	scan 1	2.52	0.15	0.087	75	0.036	49	0.054	6.10	0.26	0.077	0.41	5.23	3.63	0.43	0.140	206	0.027	0.068	0.110	0.155	0.316	0.414	0.292	0.046	0.088	0.075	5.53	0.449
	scan 2	2.23	0.33	0.187	29	0.076	18	0.148	5.20	0.25	0.090	0.43	4.91		0.53	0.178	141	0.038		0.130		0.389	0.618	0.326	0.050	0.095	0.086	4.30	0.606
difference		0.30	-0.18	-0.100	46	-0.040	31	-0.094	0.90	0.02	-0.013	-0.01	0.31		-0.10	-0.038	66	-0.011		-0.020		-0.073	-0.204	-0.035	-0.004	-0.007	-0.011	1.23	-0.157
mean		2.37	0.24	0.137	52	0.056	33	0.101	5.65	0.25	0.083	0.42	5.07		0.48	0.159	173	0.032		0.120		0.352	0.516	0.309	0.048	0.091	0.081	4.91	0.527
sd mean		0.21	0.13	0.071	33	0.029	22	0.067	0.63	0.01	0.009	0.01	0.22		0.07	0.027	46	0.007		0.014		0.052	0.144	0.024	0.003	0.005	0.008	0.87	0.111
CV%		9	53	52	62	51	66	66	11	4	11	2	4		15	17	27	23		12		15	28	8	6	6	10	18	21
cuts 1,2,3,4,5																													
mean of differ.		-0.39	-0.13	-0.050	-1	-0.020	2	-0.049	-0.29	0.03	0.002	-0.03	0.03	-1.00	-0.05	-0.009	29	-0.003	0.004	-0.012	0.002	-0.011	-0.083	-0.009	-0.008	-0.008	0.000	0.02	-0.057
sd of differ.		0.50	0.07	0.071	67	0.029	41	0.064	1.20	0.05	0.019	0.13	0.42	1.24	0.06	0.022	27	0.005	0.025	0.008	0.025	0.045	0.089	0.024	0.005	0.007	0.018	1.14	0.060
upper lim. agr.		0.62	0.01	0.091	132	0.039	84	0.078	2.11	0.12	0.039	0.24	0.87	1.48	0.07	0.036	83	0.006	0.055	0.003	0.052	0.079	0.096	0.039	0.002	0.006	0.036	2.30	0.063
lower lim. agr.		-1.40	-0.27	-0.191	-134	-0.078	-79	-0.177	-2.69	-0.06	-0.035	-0.30	-0.81	-3.47	-0.16	-0.053	-25	-0.013	-0.046	-0.027	-0.049	-0.101	-0.261	-0.056	-0.018	-0.021	-0.037	-2.27	-0.177
coef.of repeat.		1.01	0.14	0.141	133	0.059	81	0.127	2.40	0.09	0.037	0.27	0.84	2.48	0.12	0.044	54	0.010	0.050	0.015	0.051	0.090	0.178	0.048	0.010	0.013	0.036	2.28	0.120
cuts 1,2,3,4																													
mean of differ.		-0.56	-0.08	0.000	-48	0.001	-26	-0.004	-0.69	0.04	0.010	-0.04	-0.04	-1.00	-0.03	0.001	17	-0.001	0.004	-0.009	0.002	0.010	-0.042	0.000	-0.010	-0.008	0.004		-0.032
sd of differ.		0.38							1.10	0.06	0.018	0.16	0.45	1.24	0.05	0.012	14	0.002	0.025	0.006	0.025	0.022	0.046	0.020	0.005	0.008	0.020		0.025
upper lim. agr.		0.19							1.52	0.16	0.046	0.29	0.86	1.48	0.08	0.025	44	0.002	0.055	0.004	0.052	0.054	0.050	0.040	0.001	0.008	0.044		0.017
lower lim. agr.		-1.32							-2.89	-0.08	-0.027	-0.36	-0.94	-3.47	-0.14	-0.023	-11	-0.004	-0.046	-0.022	-0.049	-0.034	-0.135	-0.040	-0.020	-0.024	-0.037		-0.081
coef.of repeat.		0.75							2.21	0.12	0.037	0.33	0.90	2.48	0.11	0.024	28	0.003	0.050	0.013	0.051	0.044	0.093	0.040	0.010	0.016	0.041		0.049
mean (cuts 1,2,3,4)		4.37	0.37	0.102	168	0.040	114	0.058	5.31	0.21	0.069	0.77	5.59	3.37	0.55	0.159	190	0.030	0.092	0.103	0.167	0.332	0.465	0.291	0.060	0.077	0.065		0.445
real upper value		4.56	0.37		168	0.040	114	0.058	6.83	0.37	0.116	1.06	6.45	4.85	0.63	0.185	234	0.032	0.147	0.107	0.219	0.386	0.516	0.331	0.061	0.085	0.109		0.462
real lower value		3.05	0.37		168	0.040	114	0.058	2.42	0.13	0.042	0.40	4.66	-0.10	0.42	0.137	179	0.026	0.046	0.081	0.118	0.298	0.330	0.251	0.040	0.053	0.028		0.363

Table App.G7 Repeatability results for pulsed TDI indices from the IVS along the radial axis

		E'	E' VTI	E' dur	E' acc	tE' acc	E' dec	tE' dec	A'	A' VTI	A' dur	E/A	Se'	Sl'	S' VTI	S' dur	Se' acc	tSe' acc	bS'-Sl'	Q-Se'	Q-Sl'	Q-E'	Q-A'	Q-bE'	IVCt	Q-bS'	IVRt	IVCb	RR
cut 1	scan 1	3.24							4.02			0.81	6.26	2.92	0.41	0.130	227	0.030	0.081									4.28	0.350
	scan 2	4.65	0.19	0.063	168	0.027	134	0.034	4.05	0.12	0.045	1.15	4.23	3.73	0.35	0.133	159	0.024										3.22	0.370
difference		-1.41							-0.03			-0.34	2.02	-0.82	0.06	-0.003	69	0.006										1.06	-0.020
mean		3.95							4.03			0.98	5.24	3.32	0.38	0.132	193	0.027										3.75	0.360
sd mean		1.00							0.02			0.24	1.43	0.58	0.04	0.002	49	0.004										0.75	0.014
CV%		25							1			25	27	17	11	2	25	16										20	4
cut 2	scan 1	5.31	0.32	0.092	170	0.033	87	0.060	6.06	0.21	0.055	0.88	6.43	2.85	0.48	0.160	281	0.024	0.093	0.072	0.140	0.299	0.418	0.274	0.034	0.046	0.074	5.54	0.406
	scan 2	4.93	0.29	0.088	156	0.034	101	0.051	6.92	0.22	0.050	0.71	4.77	2.70	0.41	0.160	273	0.018	0.094	0.080	0.150	0.306	0.427	0.285	0.024	0.062	0.059	4.47	0.409
difference		0.38	0.03	0.004	14	-0.001	-13	0.009	-0.86	-0.01	0.005	0.16	1.67	0.15	0.07	0.000	8	0.006	-0.001	-0.008	-0.010	-0.007	-0.009	-0.011	0.010	-0.016	0.015	1.07	-0.003
mean		5.12	0.31	0.090	163	0.033	94	0.056	6.49	0.22	0.053	0.79	5.60	2.78	0.44	0.160	277	0.021	0.094	0.076	0.145	0.303	0.422	0.279	0.029	0.054	0.066	5.00	0.408
sd mean		0.27	0.02	0.003	10	0.001	9	0.006	0.61	0.01	0.004	0.12	1.18	0.11	0.05	0.000	5	0.004	0.001	0.006	0.007	0.005	0.007	0.008	0.007	0.011	0.011	0.76	0.002
CV%		5	7	3	6	2	10	11	9	4	7	15	21	4	11	0	2	20	1	7	5	2	2	3	24	21	16	15	1
cut 3	scan 1	6.15	0.35	0.096	130	0.049	133	0.048	2.50			2.46	3.97							0.071		0.363		0.314		0.053		5.30	0.501
	scan 2	4.96	0.31	0.088	131	0.044	144	0.041	3.64	0.14	0.057	1.37	5.59	3.99	0.37	0.133	189	0.029	0.067	0.078	0.119	0.370	0.621	0.315	0.111	0.053	0.136	4.03	0.555
difference		1.18	0.04	0.008	-1	0.005	-11	0.007	-1.14			1.09	-1.62							-0.007		-0.007		-0.001		0.000		1.27	-0.054
mean		5.56	0.33	0.092	131	0.047	138	0.044	3.07			1.91	4.78							0.074		0.367		0.315		0.053		4.67	0.528
sd mean		0.84	0.03	0.006	0	0.003	8	0.005	0.80			0.77	1.15							0.005		0.005		0.001		0.000		0.90	0.038
CV%		15	9	6	0	7	6	11	26			40	24							7		1		0		1		19	7
cut 4	scan 1	5.69	0.35	0.106	121	0.054	127	0.051	3.40	0.10	0.050	1.67	4.63	3.40	0.56	0.195	139	0.035	0.118	0.063	0.155	0.330	0.495	0.283	0.038	0.043	0.085	4.41	0.458
	scan 2	8.03	0.29	0.060	266	0.030	269	0.030	3.30	0.10	0.050	2.43	4.70	2.00	0.40	0.163	202	0.024	0.108	0.065	0.143	0.357	0.502	0.325	0.027	0.046		5.58	0.510
difference		-2.34	0.07	0.046	-145	0.024	-142	0.021	0.10	0.00	0.000	-0.76	-0.07	1.40	0.16	0.032	-63	0.011	0.010	-0.003	0.012	-0.027	-0.007	-0.043	0.011	-0.004		-1.17	-0.052
mean		6.86	0.32	0.083	194	0.042	198	0.041	3.35	0.10	0.050	2.05	4.67	2.70	0.48	0.179	171	0.030	0.113	0.064	0.149	0.344	0.499	0.304	0.032	0.044		5.00	0.484
sd mean		1.65	0.05	0.033	102	0.017	100	0.015	0.07	0.00	0.000	0.54	0.05	0.99	0.11	0.022	45	0.008	0.007	0.002	0.008	0.019	0.005	0.030	0.007	0.002		0.83	0.037
CV%		24	15	39	53	40	51	37	2	2	0	26	1	37	24	12	26	26	6	3	6	6	1	10	23	6		17	8
cut 5	scan 1	5.26	0.37	0.117	109	0.050	77	0.068	5.98	0.20	0.065	0.88	5.61	4.33	0.50	0.163	187	0.032	0.090	0.086	0.148	0.333	0.470	0.284	0.026	0.060	0.076	4.42	0.449
	scan 2	6.60	0.47	0.135	109	0.063	89	0.077	4.39	0.21	0.082	1.50	5.08	2.70	0.46	0.178	106	0.050	0.131	0.088	0.175	0.353	0.570	0.302	0.031	0.055	0.084		0.606
difference		-1.34	-0.10	-0.018	-1	-0.012	-12	-0.009	1.60	0.00	-0.017	-0.62	0.53	1.63	0.04	-0.015	81	-0.018	-0.042	-0.003	-0.027	-0.020	-0.100	-0.018	-0.006	0.005	-0.008		-0.157
mean		5.93	0.42	0.126	109	0.056	83	0.072	5.18	0.21	0.073	1.19	5.34	3.51	0.48	0.171	146	0.041	0.110	0.087	0.161	0.343	0.520	0.293	0.028	0.058	0.080		0.527
sd mean		0.94	0.07	0.013	1	0.009	8	0.006	1.13	0.00	0.012	0.44	0.37	1.15	0.03	0.011	57	0.013	0.030	0.002	0.019	0.014	0.071	0.013	0.004	0.004	0.006		0.111
CV%		16	17	10	1	15	10	8	22	1	16	37	7	33	6	6	39	31	27	2	12	4	14	4	14	6	7		21
cuts 1,2,3,4,5																													
mean of differ.		-0.70	0.01	0.010	-33	0.004	-45	0.007	-0.07	0.00	-0.004	-0.09	0.51	0.59	0.08	0.003	23	0.001	-0.011	-0.005	-0.008	-0.015	-0.039	-0.018	0.005	-0.004	0.004	0.56	-0.057
sd of differ.		1.44	0.07	0.027	75	0.015	65	0.012	1.07	0.01	0.011	0.75	1.46	1.14	0.05	0.020	66	0.013	0.027	0.003	0.020	0.010	0.053	0.018	0.009	0.009	0.016	1.16	0.060
upper lim. agr.		2.18	0.16	0.063	117	0.034	85	0.032	2.07	0.01	0.019	1.41	3.42	2.88	0.19	0.043	155	0.027	0.043	0.001	0.031	0.005	0.067	0.017	0.023	0.014	0.036	2.87	0.063
lower lim. agr.		-3.59	-0.14	-0.043	-183	-0.026	-174	-0.017	-2.20	-0.02	-0.027	-1.60	-2.41	-1.69	-0.02	-0.037	-108	-0.025	-0.065	-0.011	-0.048	-0.035	-0.144	-0.054	-0.014	-0.022	-0.029	-1.75	-0.177
coef.of repeat.		2.89	0.15	0.053	150	0.030	130	0.025	2.14	0.02	0.023	1.50	2.91	2.29	0.10	0.040	132	0.026	0.054	0.006	0.039	0.020	0.106	0.035	0.018	0.018	0.033	2.31	0.120
cuts 1,2,3,4																													
mean of differ.		-0.55	0.05	0.019	-44	0.009	-56	0.012	-0.48	0.00	0.003	0.04	0.50	0.24	0.10	0.009	4	0.008	0.004	-0.006	0.001	-0.014	-0.008	-0.018	0.010	-0.007	0.015		-0.032
sd of differ.		1.62	0.02	0.023	88	0.013	75	0.008	0.61	0.01	0.004	0.80	1.68	1.11	0.05	0.019	66	0.003	0.007	0.003	0.015	0.012	0.002	0.022	0.001	0.008			0.025
upper lim. agr.		2.68	0.08	0.066	132	0.035	94	0.028	0.73	0.02	0.010	1.64	3.87	2.47	0.20	0.048	136	0.013	0.019	0.000	0.032	0.010	-0.005	0.025	0.011	0.010			0.017
lower lim. agr.		-3.78	0.01	-0.027	-220	-0.016	-205	-0.003	-1.70	-0.03	-0.005	-1.56	-2.87	-1.98	-0.01	-0.029	-127	0.002	-0.011	-0.012	-0.030	-0.037	-0.011	-0.062	0.009	-0.023			-0.081
coef.of repeat.		3.23	0.04	0.046	176	0.026	150	0.015	1.22	0.02	0.007	1.60	3.37	2.22	0.11	0.039	132	0.006	0.015	0.006	0.031	0.023	0.003	0.043	0.001	0.017			0.049
mean (cuts 1,2,3,4)		5.37	0.32	0.088	162	0.041	144	0.047	4.23	0.16	0.051	1.43	5.07	2.93	0.43	0.157	214	0.026	0.103	0.071	0.147	0.338	0.460	0.299	0.031	0.050	0.066		0.445
real upper value		8.05	0.40		295	0.076	238	0.075	4.97	0.17	0.061	3.07	8.94	5.40	0.64	0.205	350	0.039	0.122	0.071	0.179	0.347	0.455	0.325	0.042	0.060	0.066		0.462
real lower value		1.59	0.33		-57	0.024	-62	0.044	2.54	0.13	0.047	-0.12	2.21	0.95	0.42	0.128	86	0.028	0.093	0.059	0.117	0.301	0.449	0.238	0.040	0.027	0.066		0.363

Table App.G8 Repeatability results for pulsed TDI indices from the tricuspid annulus

		E'	E' VTI	E' dur	E' acc	tE' acc	E' dec	tE' dec	A'	A' VTI	A' dur	E/A	Se'	Sl'	S' VTI	S' dur	Se' acc	tSe' acc	bS'-Sl'	Q-Se'	Q-Sl'	Q-E'	Q-A'	Q-bE'	IVCt	Q-bS'	IVRt	IVCb	RR
cat 1	scan 1	4.97	0.37	0.110	95	0.048	96	0.050	7.29			0.68	8.82	4.85	0.74	0.170	268	0.027	0.102	0.063	0.143	0.275	0.393	0.219		0.045			0.374
	scan 2	7.65	0.62	0.127	178	0.048	111	0.071	9.68	0.37	0.063	0.79	7.12	6.48	0.67	0.135	241	0.030	0.083	0.087	0.135	0.258	0.390	0.204	0.036	0.069	0.038		0.355
difference		-2.68	-0.26	-0.017	-84	0.000	-15	-0.022	-2.39			-0.11	1.70	-1.63	0.06	0.035	26	-0.003	0.020	-0.024	0.007	0.017	0.003	0.015		-0.024			0.019
mean		6.31	0.49	0.118	136	0.048	104	0.060	8.48			0.74	7.97	5.66	0.70	0.153	254	0.029	0.092	0.075	0.139	0.267	0.392	0.212		0.057			0.364
sd mean		1.90	0.18	0.012	59	0.000	11	0.015	1.69			0.08	1.20	1.15	0.05	0.025	19	0.002	0.014	0.017	0.005	0.012	0.002	0.011		0.017			0.013
CV%		30	37	10	43	0	10	25	20			10	15	20	7	16	7	7	15	23	4	5	1	5		30			4
cat 2	scan 1	11.45	0.69	0.103	248	0.047	197	0.059	11.68	0.65	0.095	0.98	13.07	9.48	1.23	0.167	418	0.031	0.084	0.083	0.137	0.290	0.393	0.246	0.020	0.052	0.042		0.399
	scan 2	11.63	0.82	0.123	227	0.049	164	0.068	11.58	0.51	0.083	1.00	10.92	9.77	1.15	0.167	298	0.034	0.081	0.083	0.138	0.289	0.412	0.242	0.023	0.056	0.033		0.416
difference		-0.18	-0.13	-0.020	21	-0.002	33	-0.009	0.10	0.14	0.012	-0.02	2.15	-0.29	0.08	0.000	120	-0.003	0.003	-0.001	-0.001	0.002	-0.019	0.005	-0.004	-0.004	0.009		-0.016
mean		11.54	0.76	0.113	237	0.048	181	0.063	11.63	0.58	0.089	0.99	11.99	9.62	1.19	0.167	358	0.032	0.083	0.083	0.138	0.290	0.402	0.244	0.021	0.054	0.038		0.407
sd mean		0.13	0.09	0.014	15	0.002	23	0.006	0.07	0.10	0.008	0.02	1.52	0.21	0.06	0.000	85	0.002	0.002	0.001	0.001	0.001	0.013	0.003	0.003	0.003	0.006		0.012
CV%		1	12	12	6	3	13	10	1	17	9	2	13	2	5	0	24	7	3	1	0	0	3	1	12	5	17		3
cat 3	scan 1	10.41	0.71	0.117	194	0.054	175	0.060	6.86	0.30	0.073	1.52	8.09	6.46	0.92	0.190	219	0.036	0.099	0.089	0.155	0.339	0.563	0.291	0.053	0.059	0.055		0.563
	scan 2	12.65	0.93	0.127	221	0.056	180	0.070	6.90	0.35	0.093	1.83	9.67	7.20	1.22	0.222	265	0.037	0.103	0.083	0.153	0.353	0.606	0.304	0.031	0.053	0.073		0.593
difference		-2.24	-0.22	-0.010	-28	-0.002	-5	-0.011	-0.04	-0.05	-0.020	-0.32	-1.58	-0.74	-0.30	-0.032	-46	-0.001	-0.004	0.006	0.002	-0.014	-0.044	-0.013	0.022	0.006	-0.018		-0.029
mean		11.53	0.82	0.122	207	0.055	177	0.065	6.88	0.33	0.083	1.68	8.88	6.83	1.07	0.206	242	0.036	0.101	0.086	0.154	0.346	0.584	0.297	0.042	0.056	0.064		0.578
sd mean		1.58	0.15	0.007	20	0.002	3	0.007	0.03	0.03	0.014	0.22	1.12	0.52	0.21	0.022	33	0.000	0.002	0.004	0.001	0.010	0.031	0.009	0.016	0.004	0.013		0.021
CV%		14	19	6	9	3	2	11	0	10	17	13	13	8	20	11	13	1	2	5	1	3	5	3	37	8	20		4
cat 4	scan 1	8.67	0.63	0.118	143	0.062	168	0.052	7.64	0.33	0.073	1.13	10.43	3.78	0.75	0.168	299	0.035	0.091	0.090	0.143	0.359	0.500	0.296	0.032	0.058	0.087		0.497
	scan 2	7.79	0.44	0.097	135	0.060	217	0.036	5.72	0.24	0.065	1.36	6.61	3.09	0.59	0.165	247	0.028	0.097	0.100	0.169	0.344	0.411	0.290	0.056	0.072	0.065		0.417
difference		0.87	0.19	0.021	9	0.002	-50	0.016	1.92	0.09	0.008	-0.23	3.83	0.68	0.15	0.003	51	0.008	-0.006	-0.010	-0.026	0.015	0.089	0.006	-0.024	-0.014	0.022		0.080
mean		8.23	0.53	0.107	139	0.061	192	0.044	6.68	0.28	0.069	1.25	8.52	3.43	0.67	0.166	273	0.031	0.094	0.095	0.156	0.352	0.456	0.293	0.044	0.065	0.076		0.457
sd mean		0.62	0.14	0.015	6	0.001	35	0.011	1.36	0.06	0.006	0.16	2.70	0.48	0.11	0.002	36	0.005	0.005	0.007	0.018	0.010	0.063	0.004	0.017	0.010	0.015		0.057
CV%		8	26	14	4	2	18	26	20	22	9	13	32	14	16	1	13	17	5	7	12	3	14	1	39	15	20		12
cats 1,2,3,4																													
mean of differ.		-1.06	-0.10	-0.006	-20	-0.001	-9	-0.006	-0.10	0.06	0.000	-0.17	1.52	-0.49	0.00	0.001	38	0.000	0.003	-0.007	-0.004	0.005	0.007	0.003	-0.002	-0.009	0.004		0.013
sd of differ.		1.69	0.20	0.019	47	0.002	34	0.016	1.77	0.09	0.017	0.13	2.26	0.96	0.20	0.027	68	0.005	0.012	0.013	0.015	0.014	0.058	0.012	0.023	0.013	0.020		0.049
upper lim. agr.		2.31	0.31	0.031	74	0.003	59	0.026	3.43	0.25	0.035	0.09	6.05	1.43	0.41	0.056	175	0.010	0.026	0.019	0.025	0.033	0.123	0.026	0.044	0.017	0.045		0.111
lower lim. agr.		-4.43	-0.51	-0.044	-114	-0.004	-77	-0.038	-3.63	-0.13	-0.035	-0.43	-3.00	-2.41	-0.41	-0.053	-99	-0.010	-0.020	-0.033	-0.034	-0.023	-0.108	-0.020	-0.048	-0.035	-0.036		-0.085
coef.of repeat.		3.37	0.41	0.037	94	0.004	68	0.032	3.53	0.19	0.035	0.26	4.52	1.92	0.41	0.054	137	0.010	0.023	0.026	0.029	0.028	0.115	0.023	0.046	0.026	0.040		0.098
mean (cats 1,2,3,4)		9.40	0.65	0.115	180	0.053	163	0.058	8.42	0.40	0.081	1.16	9.34	6.39	0.91	0.173	282	0.032	0.092	0.085	0.146	0.313	0.458	0.261	0.036	0.058	0.059		0.452
real upper value		11.72	0.96	0.146	254	0.056	222	0.084	11.85	0.65	0.115	1.25	15.39	7.81	1.31	0.229	456	0.043	0.119	0.103	0.172	0.346	0.581	0.288	0.080	0.075	0.104		0.563
real lower value		4.98	0.14	0.071	66	0.048	86	0.020	4.79	0.27	0.046	0.74	6.34	3.98	0.50	0.120	183	0.022	0.072	0.052	0.113	0.290	0.350	0.241	-0.012	0.023	0.023		0.367

Table App.G9 Repeatabiltiy results for MVG indices

		E1	E2	E12	Emax	A	Se	Sl	IVRa	IVRb	IVCa	IVCb	R-R
cat 1	scan 1			5.79	5.79	10.22	3.65	2.81	5.11	0.79		13.68	0.370
	scan 2			7.15	7.15	8.35	6.05	3.65	2.90	0.61		4.75	0.353
differnce				-1.36	-1.36	1.87	-2.40	-0.84	2.21	0.18		8.93	0.02
mean				6.47	6.47	9.29	4.85	3.23	4.01	0.70		9.22	0.36
sd mean				0.96	0.96	1.32	1.70	0.59	1.56	0.13		6.32	0.01
CV%				**15**	**15**	**14**	**35**	**18**	**39**	**18**		**69**	**3**
cat 2	scan 1	10.71	5.49		10.71	8.35	7.83	3.92	0.99	1.57	0.61	8.09	0.398
	scan 2	9.61	4.38		9.61	7.61	7.03	5.93	0.84	2.18	-1.53	6.35	0.403
differnce		1.11	1.10		1.11	0.74	0.80	-2.01	0.15	-0.61	2.13	1.74	-0.006
mean		10.16	4.93		10.16	7.98	7.43	4.93	0.91	1.88	-0.46	7.22	0.400
sd mean		0.78	0.78		0.78	0.52	0.57	1.42	0.11	0.43	1.51	1.23	0.004
CV%		**8**	**16**		**8**	**7**	**8**	**29**	**12**	**23**	**-328**	**17**	**1**
cat 3	scan 1	18.03	12.42		18.03	6.93	11.02	4.46	4.86	0.87	5.90	5.14	0.604
	scan 2	14.31	5.47		14.31	5.23	6.93	3.65	2.56	1.48		3.36	0.545
differnce		3.73	6.95		3.73	1.71	4.09	0.81	2.30	-0.61		1.77	0.059
mean		16.17	8.94		16.17	6.08	8.98	4.06	3.71	1.18		4.25	0.575
sd mean		2.63	4.91		2.63	1.21	2.89	0.57	1.63	0.43		1.25	0.042
CV%		**16**	**55**		**16**	**20**	**32**	**14**	**44**	**37**		**29**	**7**
cat 4	scan 1	10.58	10.28		10.58	7.02	10.29	5.46	0.82	3.15	1.84	9.34	0.520
	scan 2	10.89	8.31		10.89	7.89	13.93	5.99	3.06	3.87	1.52	11.09	0.417
differnce		-0.31	1.97		-0.31	-0.87	-3.64	-0.53	-2.24	-0.72	0.32	-1.75	0.103
mean		10.73	9.30		10.73	7.45	12.11	5.73	1.94	3.51	1.68	10.22	0.468
sd mean		0.22	1.39		0.22	0.62	2.57	0.37	1.58	0.51	0.23	1.23	0.073
CV%		**2**	**15**		**2**	**8**	**21**	**7**	**82**	**15**	**13**	**12**	**16**
cat 5	scan 1			4.33	4.33	6.17	6.38		0.81	0.71	0.19	2.11	0.612
	scan 2			4.17	4.17	8.05	8.38		0.93	0.93	0.50	4.14	0.405
differnce				0.15	0.15	-1.88	-2.00		-0.12	-0.22	-0.31	-2.04	0.207
mean				4.25	4.25	7.11	7.38		0.87	0.82	0.35	3.12	0.508
sd mean				0.11	0.11	1.33	1.41		0.08	0.16	0.22	1.44	0.146
CV%				**3**	**3**	**19**	**19**		**10**	**19**	**64**	**46**	**29**
cats 1,2,3,4,5													
mean of differ.		1.51	3.34	-0.60	0.66	0.31	-0.63	-0.64	0.46	-0.40	0.71	1.73	0.076
sd of differ.		2.05	3.15	1.07	1.93	1.64	3.10	1.16	1.88	0.37	1.27	4.42	0.084
upper lim. agr.		5.60	9.65	1.54	4.52	3.59	5.57	1.68	4.22	0.35	3.25	10.57	0.244
lower lim. agr.		-2.59	-2.97	-2.75	-3.20	-2.97	-6.83	-2.96	-3.30	-1.14	-1.82	-7.11	-0.092
coef.of repeat.		**4.10**	**6.31**	**2.14**	**3.86**	**3.28**	**6.20**	**2.32**	**3.76**	**0.75**	**2.54**	**8.84**	**0.168**
cats 1,2,3,4													
mean of differ.		1.51	3.34		0.79	0.86	-0.29	-0.64	0.61	-0.44	1.23	2.67	0.043
sd of differ.		2.05	3.15		2.20	1.26	3.47	1.16	2.14	0.42	1.28	4.49	0.048
upper lim. agr.		5.60	9.65		5.20	3.38	6.65	1.68	4.88	0.39	3.79	11.65	0.140
lower lim. agr.		-2.59	-2.97		-3.62	-1.66	-7.22	-2.96	-3.67	-1.27	-1.34	-6.30	-0.053
coef.of repeat.		**4.10**	**6.31**		**4.41**	**2.52**	**6.93**	**2.32**	**4.28**	**0.83**	**2.57**	**8.98**	**0.096**
mean (cats 1,2,3,4)		12.35	7.72	6.47	10.88	7.70	8.34	4.48	2.64	1.82	0.61	7.73	0.451
real upper value		17.96	17.37		16.08	11.08	14.99	6.16	7.52	2.21	4.40	19.37	0.591
real lower value		9.76	4.76		7.27	6.04	1.12	1.52	-1.03	0.54	-0.73	1.42	0.398

Table App.G10 Repeatability results for MMV indices

		E1	E2	E12	Emax	E/A	A	Se	Sl	IVRa	IVRb	IVCa	IVCb	Se acc	E1 acc	E1 dec	E2 dec	E12 acc	E12 dec	IVRt	IVCt	Diast. t	Systo. T	R-R
cat 1	scan 1			18.57	18.57	0.59	31.73	19.25		2.77	9.39	5.00	47.50	2658				758	97	0.047	0.053	0.133	0.133	0.370
	scan 2			14.52	14.52	0.48	30.11	11.05		0.82	8.02	1.20	46.80	2856				639	364	0.035	0.050	0.132	0.133	0.353
differnce				4.05	4.05	0.11	1.62	8.21		1.95	1.37	3.80	0.70	-198				119	-267	0.012	0.003	0.002	0.000	
mean				16.55	16.55	0.54	30.92	15.15		1.80	8.70	3.10	47.15	2757				698	230	0.041	0.052	0.132	0.133	0.362
sd mean				2.86	2.86	0.08	1.15	5.80		1.38	0.97	2.69	0.49	140				84	189	0.008	0.002	0.001	0.000	0.012
CV%				**17**	**17**	**15**	**4**	**38**		**77**	**11**	**87**	**1**	**5**				**12**	**82**	**20**	**5**	**1**	**0**	**3**
cat 2	scan 1	29.70	23.92		29.77	1.20	24.74	35.77	11.93	6.77	6.71	6.50	58.00	3584		1311	593			0.037	0.040	0.190	0.147	0.407
	scan 2	28.20	22.31		28.20	1.25	22.59	27.93	16.48	2.40	8.77	3.80	34.10	1992	833	1176	718			0.030	0.040	0.180	0.150	0.398
differnce		1.50	1.61		1.57	-0.05	2.15	7.84	-4.55	4.37	-2.06	2.70	23.90	1592		135	-125			0.007	0.000	0.010	-0.003	
mean		28.95	23.12		28.99	1.23	23.67	31.85	14.21	4.59	7.74	5.15	46.05	2788		1244	655			0.033	0.040	0.185	0.148	0.402
sd mean		1.06	1.14		1.11	0.04	1.52	5.54	3.22	3.09	1.46	1.91	16.90	1126		96	88			0.005	0.000	0.007	0.002	0.006
CV%		**4**	**5**		**4**	**3**	**6**	**17**	**23**	**67**	**19**	**37**	**37**	**40**		**8**	**14**			**14**	**0**	**4**	**2**	**2**
cat 3	scan 1	47.62	24.56		47.62	2.20	21.63	35.54	26.83	3.92	8.50	2.95	31.90	1121			955			0.050	0.070	0.267	0.170	0.545
	scan 2	40.15	32.57		40.15	1.70	23.57	41.17	27.61	12.40	11.76	7.38	39.60	1564		628	1003			0.060	0.073	0.300	0.177	0.608
differnce		7.47	-8.01		7.47	0.50	-1.94	-5.63	-0.78	-8.48	-3.26	-4.43	-7.70	-443			-48			-0.010	-0.002	-0.033	-0.007	
mean		43.89	28.57		43.89	1.95	22.60	38.35	27.22	8.16	10.13	5.16	35.75	1342			979			0.055	0.071	0.283	0.173	0.577
sd mean		5.28	5.66		5.28	0.35	1.37	3.98	0.55	6.00	2.30	3.14	5.44	313			34			0.007	0.002	0.024	0.005	0.045
CV%		**12**	**20**		**12**	**18**	**6**	**10**	**2**	**73**	**23**	**61**	**15**	**23**			**3**			**13**	**2**	**8**	**3**	**8**
cat 4	scan 1	29.41	35.45		35.45	1.44	24.63	51.28	35.58	5.40	17.64	5.11	60.00	2381		1073	1037			0.043	0.035	0.275	0.193	0.523
	scan 2	16.54	15.18		16.54	0.68	24.17	28.19	14.70	-2.18	20.62	-1.24	60.00	2071	1672	631	463			0.058	0.053	0.170	0.148	0.417
differnce		12.87	20.27		18.91	0.76	0.46	23.09	20.88	7.58	-2.98	6.36	0.00	310		441	574			-0.015	-0.018	0.105	0.045	
mean		22.98	25.32		26.00	1.06	24.40	39.73	25.14	1.61	19.13	1.93	60.00	2226		852	750			0.050	0.044	0.223	0.170	0.470
sd mean		9.10	14.33		13.37	0.54	0.33	16.33	14.76	5.36	2.11	4.49	0.00	219		312	406			0.011	0.012	0.074	0.032	0.075
CV%		**40**	**57**		**51**	**51**	**1**	**41**	**59**	**334**	**11**	**232**	**0**	**10**		**37**	**54**			**21**	**28**	**33**	**19**	**16**
cat 5	scan 1			17.60	17.60	0.56	31.70	38.86		10.90	3.47	6.80	27.30	2054				435	279	0.063	0.053	0.147	0.127	0.405
	scan 2			12.16	12.16	0.91	13.43	24.28		5.85	0.47	8.51	18.10	1102				295	141	0.070	0.068	0.320	0.140	0.612
differnce				5.44	5.44	-0.35	18.27	14.57		5.05	3.01	-1.71	9.20	952				140	137	-0.007	-0.014	-0.173	-0.013	
mean				14.88	14.88	0.74	22.57	31.57		8.38	1.97	7.66	22.70	1578				365	210	0.067	0.060	0.233	0.133	0.508
sd mean				3.85	3.85	0.25	12.92	10.30		3.57	2.13	1.21	6.51	673				99	97	0.005	0.010	0.123	0.009	0.146
CV%				**26**	**26**	**34**	**57**	**33**		**43**	**108**	**16**	**29**	**43**				**27**	**46**	**7**	**17**	**53**	**7**	**29**
cats 1,2,3,4,5																								
mean of differ.		7.28	4.62	4.75	7.49	0.19	4.11	9.62	5.19	2.09	-0.78	1.34	5.22	443		288	134	129	-65	-0.003	-0.006	-0.018	0.004	0.076
sd of differ.		5.69	14.38	0.98	6.74	0.44	8.07	10.53	13.72	6.24	2.81	4.35	12.04	836		216	383	15	286	0.011	0.009	0.101	0.023	0.084
upper lim. agr.		18.65	33.38	6.71	20.96	1.08	20.25	30.68	32.63	14.58	4.83	10.04	29.29	2114		721	901	159	508	0.020	0.012	0.184	0.051	0.244
lower lim. agr.		-4.09	-24.13	2.78	-5.98	-0.69	-12.03	-11.45	-22.26	-10.39	-6.40	-7.36	-18.85	-1229		-145	-633	99	-637	-0.025	-0.024	-0.220	-0.042	-0.092
coef.of repeat.		**11.37**	**28.76**	**1.97**	**13.47**	**0.88**	**16.14**	**21.07**	**27.44**	**12.48**	**5.62**	**8.70**	**24.07**	**1671.34**		**432.95**	**766.99**	**30.13**	**572.42**	**0.02**	**0.02**	**0.20**	**0.05**	**0.168**
cats 1,2,3,4																								
mean of differ.		7.28	4.62		8.00	0.33	0.57	8.38	5.19	1.36	-1.73	2.11	4.23	315		288	134			-0.002	-0.004	0.021	0.009	0.043
sd of differ.		5.69	14.38		7.66	0.37	1.82	11.73	13.72	6.95	2.13	4.62	13.66	907		216	383			0.013	0.009	0.059	0.024	0.048
upper lim. agr.		18.65	33.38		23.33	1.07	4.21	31.85	32.63	15.26	2.53	11.35	31.54	2130		721	901			0.024	0.014	0.139	0.057	0.140
lower lim. agr.		-4.09	-24.13		-7.33	-0.41	-3.06	-15.09	-22.26	-12.55	-5.99	-7.14	-23.09	-1499		-145	-633			-0.027	-0.023	-0.097	-0.040	-0.053
coef.of repeat.		**11.37**	**28.76**		**15.33**	**0.74**	**3.64**	**23.47**	**27.44**	**13.90**	**4.26**	**9.24**	**27.32**	**1814.31**		**432.95**	**766.99**			**0.03**	**0.02**	**0.12**	**0.05**	**0.096**
mean (cats 1,2,3,4)		31.94	25.67	16.55	28.85	1.19	25.40	31.27	22.19	4.04	11.43	3.84	47.24	2278.21		1047.70	794.67	698.26	230.19	0.04	0.05	0.21	0.16	0.451
real upper value		50.59	59.05		52.18	2.26	29.60	63.12	54.82	19.29	13.95	15.19	78.78	4407.75		1768.83	1695.33	698.26	230.19	0.07	0.07	0.34	0.21	0.591
real lower value		27.84	1.53		21.52	0.79	22.33	16.18	-0.07	-8.51	5.44	-3.30	24.15	779.14		902.92	161.35	698.26	230.19	0.02	0.03	0.11	0.12	0.398

Table G11- Results of intraobserver (intra) and interobserver (inter) variability in analysing MVG and MMV indices

	E1	E2	A	Se	Sl	IVRa	IVRb	IVCa	IVCb
MVG[a] Intra[b]	12.74 0.2 (0.6 to -0.2)	8.28 0.3 (0 to -1.1)	6.99 0.4 (0.6 to -1.1)	-9.52 0.7 (1.4 to -1.2)	-3.76 0.5 (1 to -1.2)	1.33 0.3 (0.8 to -0.4)	-2.15 0.5 (0.8 to -1)	-2.7 0.3 (1 to -0.3)	-6.67 0.8 (1.3 to -1.9)
MVG[a] Inter[b]	12.3 0.5 (0.2 to -2)	7.97 0.4 (0.4 to -1.3)	6.64 0.7 (0.9 to -1.9)	-9.69 1 (2 to -2.2)	-3.84 0.7 (1.2 to -1.5)	1.37 0.2 (0.3 to -0.6)	-2.08 0.3 (0.5 to -0.5)	-1.9 0.4 (1 to -0.4)	6.23 0.8 (1 to -2.1)
MMV[a] Intra[b]	-33.6 0.7 (1.2 to -1.7)	-27.4 0.7 (1.5 to -1.4)	-24.5 0.2 (0.3 to -0.3)	38.7 0.6 (0.8 to -1.7)	20.1 0.6 (0.8 to -1.7)	-2.3 0.2 (0.5 to -0.3)	13.5 0.2 (0.3 to -0.5)	2.7 0.2 (0.3 to -0.3)	-44.6 0.5 (1.3 to -0.7)
MMV[a] Inter[b]	-32.9 2 (3.7 to -4.4)	-27.4 0.7 (2.1 to -0.8)	-23.7 1.2 (2.5 to -2.1)	38.6 1.1 (2.1 to -2.4)	20.9 1.4 (2.4 to -3.3)	-1.6 1.5 (2.4 to -3.6)	13.6 1.5 (3.2 to -2.7)	1.9 2.7 (7.6 to -3.3)	-44.4 1.2 (2.3 to -2.5)

[a] Mean of two observations

[b] Standard deviation of difference (limits of agreement)

J Vet Intern Med 2003;17:510–524

Peak Mean Myocardial Velocities and Velocity Gradients Measured by Color M-Mode Tissue Doppler Imaging in Healthy Cats

H. Koffas, J. Dukes-McEwan, B.M. Corcoran, C.M. Moran, A. French, V. Sboros, T. Anderson, P. Smith, K. Simpson, and W.N. McDicken

We sought to assess the feasibility of recording the myocardial velocity gradients (MVGs) and mean myocardial velocities (MMVs) measured by color M-mode tissue Doppler imaging (TDI) in the free wall of unsedated normal cats (n = 18) with a 7.4-MHz probe equipped to record TDI images. The peak MVG and MMV values during the different phases of the cardiac cycle corresponded to certain color velocity patterns occurring in the left ventricular free wall (LVFW). Biphasic shifts were recorded in the tracings of both the MVG and MMV during early diastole (E1 and E2) as well as during the isovolumic relaxation (IVR) and isovolumic contraction (IVC) phases. Stepwise regression analysis showed that age was the only significant predictor for the peak MVG values during the 2nd phase of early diastole (E2) ($r = -0.79$, $r^2 = 0.63$, and $P < .001$). The peak late diastolic MVG values were associated positively with age ($r = 0.50$, $r^2 = 0.25$, and $P < .05$). The peak MMV values showed a negative association with age during E2 ($r = -0.71$, $r^2 = 0.50$, and $P < .001$) as well as during early systole (Se) ($r = -0.55$, $r^2 = 0.30$, and $P < .05$) and late systole (Sl) ($r = -0.62$, $r^2 = 0.39$, and $P < .01$). A positive association was found between age and the peak MMV values during late diastole ($r = 0.54$, $r^2 = 0.29$, and $P < .05$). The MVG values showed cyclic variations consistent with wall thickness changes. The accuracy of velocity determination and the spatial resolution of the system used were validated with a phantom. To our knowledge, this study is the 1st report of the application of this technique to the myocardium of cats, providing insights into the physiology of myocardial motion. It provides reference ranges of the peak MVG and MMV values for future studies of feline myocardial diseases.

Key words: Age effects on myocardium; Cardiac; Doppler tissue imaging; Echocardiography; Heart; Myocardial velocity gradients.

Myocardial disease is a major cause of morbidity and mortality of cats, particularly hypertrophic cardiomyopathy (HCM).[1–3] HCM in this species is characterized by a concentrically hypertrophied, nondilated left ventricle, with diastolic dysfunction being the main abnormality of the disease.[3] However, diastolic dysfunction is also thought to be involved in other cardiac diseases of cats, which have been labeled "restrictive cardiomyopathy,"[4] "unclassified cardiomyopathy,"[5] and "intermediate cardiomyopathy."[6] These entities are poorly classified, and often, their assessment is subjective and based on morphologic features. Consequently, much effort has been spent in the investigation and improvement of the classification of feline myocardial disease in recent years. Moreover, studies of feline myocardial disease have shown the potential of using cats as an animal model for human cardiac disease.[3,7,8] This possibility further emphasizes the importance of investigating the myocardial function of cats in a more detailed way.

Tissue Doppler imaging (TDI) recently has emerged as a new ultrasonic technique, which is able to quantify myocardial motion.[9,10] On the basis of the Doppler principle, which is applied to the myocardium instead of to the blood pool, the technique selects only the high-amplitude, low-frequency ultrasonic shifts returning from the interrogated myocardium and therefore allows the estimation of myocardial velocities.[9,11] A series of studies have proven the usefulness of TDI in investigating the different cardiac diseases of humans and animals.[5,12–14] More particularly, color M-mode TDI allows the estimation of the myocardial velocity gradient (MVG) and the mean myocardial velocity (MMV). The MVG describes the spatial distribution of transmyocardial velocities throughout the myocardium from the endocardium to the epicardium and reflects wall thickness changes during diastole and systole.[11] It is one of the few ultrasonic variables that is independent of preload and also of the overall heart motion and correlates strongly with invasive hemodynamic variables such as the positive rate of pressure development (dP/dt) and the time constant of pressure decay in isovolumetric relaxation (τ). Thus, the MVG is a very sensitive tool for noninvasively assessing regional and global myocardial systolic and diastolic function.[11,15–17] The MVG can differentiate between myocardial hypertrophy of different etiologies and is also a useful tool in the investigation of different myocardial diseases of humans.[14,16,18–21] Moreover, it has shown a correlation with age-related changes in the normal human myocardium.[22,23] The MMV describes the mean value of myocardial velocity estimates from the endocardium to the epicardium and has been widely used in the investigation of human myocardial physiology and myocardial diseases.[22–24] In addition, color M-mode TDI has offered a unique opportunity to assess the different phases of the cardiac cycle accurately and noninvasively.[24]

From the Department of Veterinary Clinical Studies (Koffas, Dukes-McEwan, Corcoran, French, Smith, Simpson), and the Department of Medical Physics and Engineering (Moran, Sboros, Anderson, McDicken), University of Edinburgh, Scotland, UK. Dr Dukes-McEwan is presently affiliated with Cardiology Service, Division of Small Animal Clinical Studies, Institute of Comparative Medicine, University of Glasgow Veterinary School, Bearsden, Glasgow, Scotland, UK.

Part of the results of this paper were presented at the 33rd British Medical Ultrasound Society and the 13th Euroson congress, December 11–14, 2001, Edinburgh, UK.

Reprint requests: Haralambos Koffas, DVM, Hospital for Small Animals, Easter Bush Veterinary Centre, Department of Veterinary Clinical Studies, Royal (Dick) School of Veterinary Studies, University of Edinburgh, Easter Bush, Nr. Roslin, Midlothian, EH25 9RG, Scotland, UK; e-mail: h.koffas@sms.ed.ac.uk.

Submitted August 13, 2002; Revised February 7, 2003; Accepted March 26, 2003.

0891-6640/03/1704-0006/$3.00/0

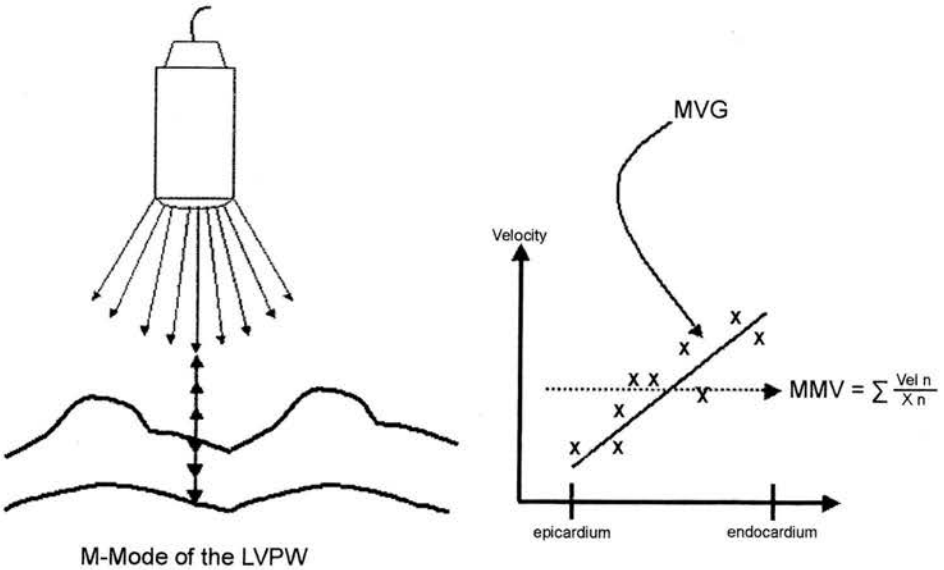

Fig 1. Graphic representation of the calculation of the myocardial velocity gradient and the mean myocardial velocity. The myocardial velocity gradient is defined as the slope of the linear regression of the velocity estimates across every single M-mode scan line throughout the myocardium from the endocardium and epicardium. The mean myocardial velocity was defined as the mean value of the velocity estimates along each M-mode scan line from the endocardium to the epicardium.

We sought to assess the feasibility of measuring the MVG and MMV in the free wall of normal cats with a purpose-designed 7.4-MHz transducer equipped to record color M-mode TDI. The velocity estimation accuracy and the spatial resolution of the system used to record color M-mode TDI images were assessed by rotating phantoms made with tissue-mimicking material (TMM). The cyclic variation of the MVG and its consistency with wall thickness changes as determined by the normalized rate of change of wall thickness (nRCWT) were assessed. We also attempted to provide reference data for the MVG and MMV from healthy cats to aid in ongoing studies of feline myocardial disease. Such data may offer an additional tool in the classification of myocardial disease in this species.

Materials and Methods

Study Group

The study population comprised 18 unsedated normal cats, which were pets owned by students and staff at the University of Edinburgh. None of the animals had clinical evidence of cardiovascular disease or other clinically relevant abnormalities. Each cat underwent a complete 2-dimensional, M-mode, color flow, and spectral Doppler echocardiographic examination and had results within normal limits.[3,25] All cats older than 7 years underwent a CBC and biochemical testing and had values within reference ranges. Cats with azotemia and high total thyroxine hormone (T4) concentration were excluded. All cats had normal systolic blood pressure (<180 mm Hg) as measured by the Doppler technique.

Ultrasound Equipment

Conventional 2-dimensional, M-mode, color flow, and spectral Doppler echocardiographic examinations were obtained with an Esaote SIM 7000 Challenge ultrasound system[a] with a 7.5-MHz transducer. Images were recorded onto S-VHS videotapes, and measurements were obtained and analyzed off-line.

All color M-mode TDI recordings were made with an ATL HDI 5000 ultrasound system[b] with a 7.4-MHz phased-array transducer, which used prototype TDI software. Off-line analysis of the images was performed by special analysis software (HDIlab)[c] on a personal computer.

TDI Echocardiography

Color M-mode TDI provides the potential for assessing the spatial distribution of transmyocardial velocities throughout the myocardium by detecting the consecutive Doppler shifts returning from the interrogated myocardium.[9,10] On the basis of this information, the MVG and MMV can be calculated.[9,11] In this study, the MVG was defined as the slope of the linear regression of the velocity estimates across each M-mode scan line throughout the myocardium, from the endocardium to the epicardium (Fig 1). The peak MVG was defined as the maximal value of the MVG during a particular cardiac phase. The MMV was defined as the mean value of the myocardial velocity estimates along each M-mode scan line from the endocardium to the epicardium (Fig 1). The peak MMV was the maximal MMV value over the duration of each cardiac phase.

Color M-mode TDI images of the left ventricular posterior wall (LVPW) were obtained from the right parasternal long-axis view at the mitral valve. The mitral valve was chosen to permit the timing of cardiac events and to optimize alignment. Throughout the study, care was taken to ensure that the ultrasonic beam was always parallel to the movement of the free wall. The Doppler velocity range was set at the minimal point at which no aliasing occurred. Doppler velocity gain was adjusted to achieve proper color filling of the free wall. Gray-scale gain was optimized so that the endocardial and epicardial borders could be clearly seen. The maximal available M-mode sweep rate was used (values were obtained every 3 milliseconds). The focus of the ultrasonic beam was set at the free wall to optimize the quality of the gray and color scales.

Both the gray and color scales were captured simultaneously with the color scale being superimposed on the gray scale. The assessment of the quality of the gray scale was possible by turning the color scale off before downloading the images. To assess the region of interest, the endocardial and epicardial borders were traced manually on the gray scale (Fig 2). This method was chosen because the wall boundaries were seen more clearly on the digitized gray-scale image. These

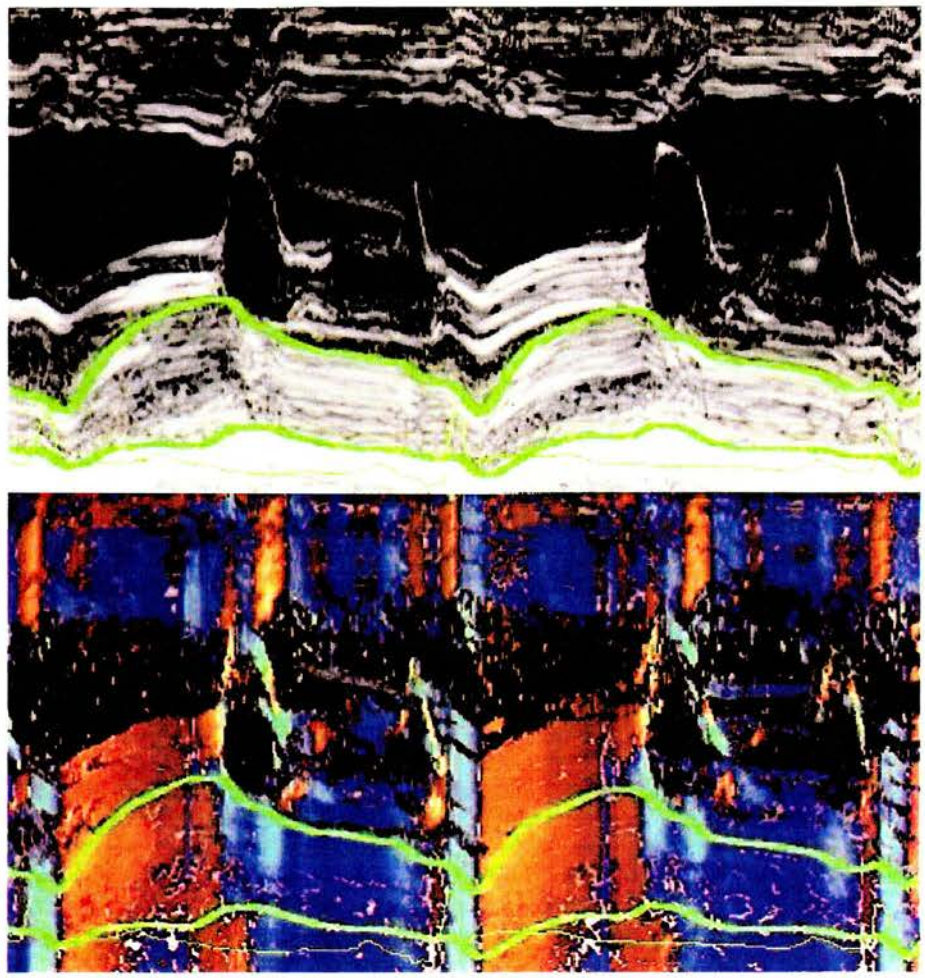

Fig 2. M-mode imaging at the mitral valve (right parasternal long-axis view). Tracing of the cardiac boundaries took place on the gray-scale image. Color M mode images were automatically superimposed onto the corresponding gray-scale image.

traces were automatically superimposed onto the corresponding color image (Fig 2). In previous studies of humans in which color M-mode TDI was used, myocardial velocities were calculated by converting color-coded velocities into velocity estimates with the color bar data as a reference table.[14,18,22,23] In contrast to these studies, an advantage of the system used in the current study was that a determination of the velocity estimates was possible from the direct quantification of the image data, so a conversion from the color bar velocities was not required (the number of data points collected for each column of M-mode data was 512). However, the use of color played an important role in selecting the optimal velocity range for every frame.

Phantom Study

To test the velocity estimation accuracy of the system used to record TDI images, a rotating circular-shaped phantom (4.2 cm in diameter; chosen to mimic a cat heart) made from TMM was used. The mean Doppler velocities measured by the system along different scan lines were compared with the actual velocities of the rotating phantom at the same points. The calculation of the actual velocities was based on the concept that a straight line through a rotating phantom has a constant velocity component in the direction of the line at all points along it.[26] This velocity can be calculated by the following equation:

$$v = 2\pi rf \cos \theta \qquad (1)$$

where v is the velocity; r is the distance between the scan line and the center of rotation; f is the rotational frequency (revolutions per second); and θ is the angle of incidence of the scan line. The rotational speed of the phantom was set at 17, 26, and 47 rpm. Actual velocities were measured at 7 different points from either side of the center of the phantom. The mean Doppler velocities were calculated from color M-mode TDI images acquired from the same points by the special analysis software (HDIlab). All actual velocities were then compared with the Doppler velocities.

To assess the spatial resolution of the current system, a rotating circular-shaped TMM phantom (diameter = 4.2 cm) with a wedge was used (Fig 3A,B). The spatial resolution was assessed as the minimal distance in which the 2 edges of the wedge could be resolved while in the 2-dimensional TDI mode, and it was calculated as the mean value of several measurements obtained at 8 different levels and 2 different rotating velocities (26 and 40 rpm). All phantom measurements were obtained with echocardiographic settings similar to those used during the acquisition of images from animals.

MVG and Wall Thickness Changes

Fleming et al[11] proposed that velocity gradients are linear in the myocardium and can be estimated from Doppler velocity estimates throughout the muscle. According to their initial study, if the ultrasound beam is parallel to the movement of the interrogated muscle, then the following relationship between the MVG and the wall thickness holds:

$$\text{MVG} = -d\text{PW}/\text{PW} \times dt \quad (\text{cm/cm} \times \text{seconds}) \qquad (2)$$

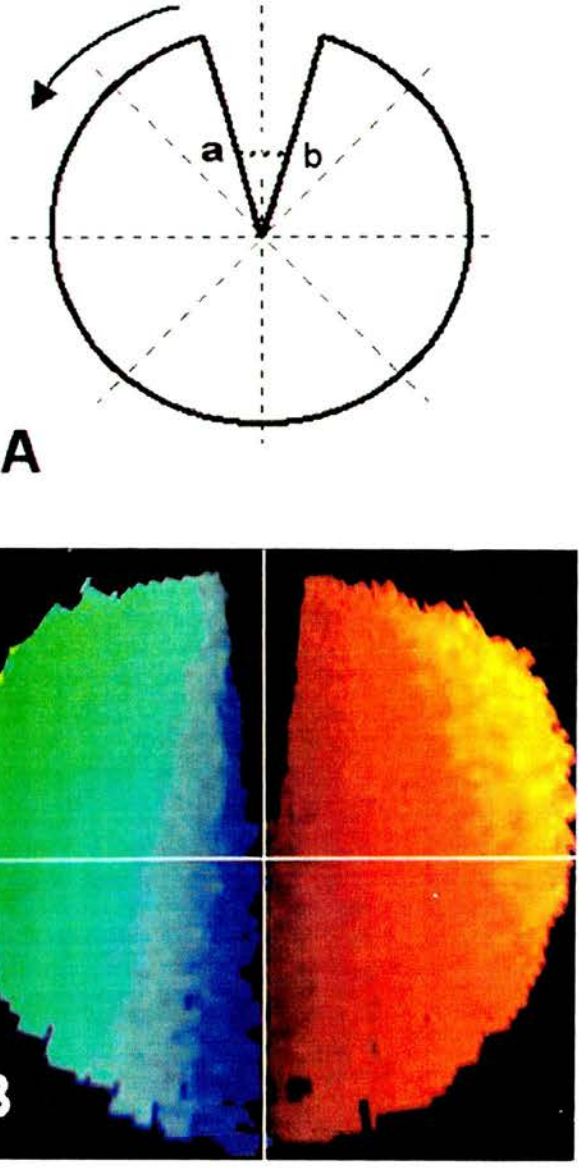

Fig 3. **(A)** Diagram of rotating wedged phantom. Spatial resolution was assessed as the minimal distance (thick vertical dashed line) in which the 2 edges of the wedge (a and b) could be clearly resolved. Thin dashed lines indicate levels at which spatial resolution was assessed. **(B)** Actual image of rotating wedged phantom.

where *d*PW is the change in wall thickness that occurs during time *dt*, and PW is the average wall thickness during *dt*. The 2nd part of the above equation represents the nRCWT.

To assess whether the MVG follows wall thickness changes measured by the nRCWT in the free wall of cats, 2 methods were used. (1) The correlation coefficient between the overall amplitude of the MVG and nRCWT was calculated for each M-mode sequence. (2) The correspondence between peaks of the MVG and nRCWT during systole and diastole was assessed. These determinations were made by noting the presence or absence of an MVG peak when an nRCWT peak was used as a reference and vice versa. Only peaks of the MVG and nRCWT that reached 1/s were considered. Peaks less than 1/s were ignored. The calculation of the nRCWT was achieved by means of the data acquired by tracing the cardiac boundaries on the digitized gray scale (Fig 2). Figure 4b shows a characteristic tracing of the nRCWT. The peak nRCWT was the maximal nRCWT value during a particular cardiac phase.

The assessment of every cardiac phase was performed by means of the combined information obtained from the M-mode images of both the color and gray scales at the mitral valve and the simultaneously recorded ECG (Fig 5). Each cardiac cycle was divided into 6 standardized phases: (1) early ventricular filling (opening of the mitral valve to the P wave of the ECG), (2) atrial contraction (P wave of the ECG to the mitral valve closure), (3) early ventricular ejection (systolic inward movement indicated by a red color velocity pattern occurring in the LVPW after the S wave of the ECG to the end of the T wave of the ECG), (4) late ventricular ejection (from the end of the T wave of the ECG to the end of the inward systolic movement indicated by the end of the red color velocity pattern), (5) isovolumic contraction (IVC), and (6) isovolumic relaxation (IVR) (the last 2 are intervals occurring between diastole and systole).

All peak values for the MVG, MMV, and nRCWT are expressed as the mean value of at least 6 cardiac cycles.

Repeatability

The same experienced echocardiographer (JDMcE) acquired all of the scans for the study. A single observer (HK) measured all of the scans in this study, including the repeatability study (observer 1). Interobserver and intraobserver variability for every peak myocardial index were assessed in 5 randomly selected images by calculating the mean difference and limits of agreement (mean difference $\pm$ 2 $\times$ SD of difference) of the image readings between 2 observers (1 experienced and 1 inexperienced observer [observer 2, PS]) to assess interobserver variability and between the 2 separate readings of the experienced observer (observer 1) to assess intraobserver variability.[27]

Statistical Analysis

Statistical analysis was carried out by SigmaStat software.[9] Values are expressed as the mean plus or minus the standard deviation. The Kolmogorov-Smirnov test was used to assess the distribution of the variables. To achieve normality of nonnormally distributed variables, logarithmic transformation was used. Pearson's correlation coefficients were calculated to assess the linear relationship between 2 variables (eg, the MVG and nRCWT). Linear regression analysis was used to assess the association between the following variables of interest: peak TDI myocardial indices with age and heart rate and Doppler-derived and actual velocities in the phantom study. Stepwise regression was used to assess the influence of age and heart rate as independent predictors of the peak MVG and MMV values. A P value $<.05$ was considered statistically significant.

Results

Study Population

Cats of the following breeds were included in the study: 14 domestic shorthaired, 1 domestic semilonghaired, 1 Maine coon, 1 Abyssinian, and 1 Siamese. There were 11 female and 7 male neutered cats. The mean plus or minus standard deviation body weight was 4.3 $\pm$ 0.5 kg. All cats were in good body condition (none were obese or excessively thin). The mean plus or minus standard deviation age was 6.2 $\pm$ 3.7 years, with ages ranging from 10 months to 14 years. The results of 2-dimensional, M-mode, and conventional Doppler echocardiographic analysis were all within previously published reference ranges.[3,25] The M-mode results are presented in Table 1. The mean plus or minus standard deviation heart rate measured by the R to R interval recorded during the acquisition of images from at least 6 cardiac cycles was 151 $\pm$ 28 beats/min.

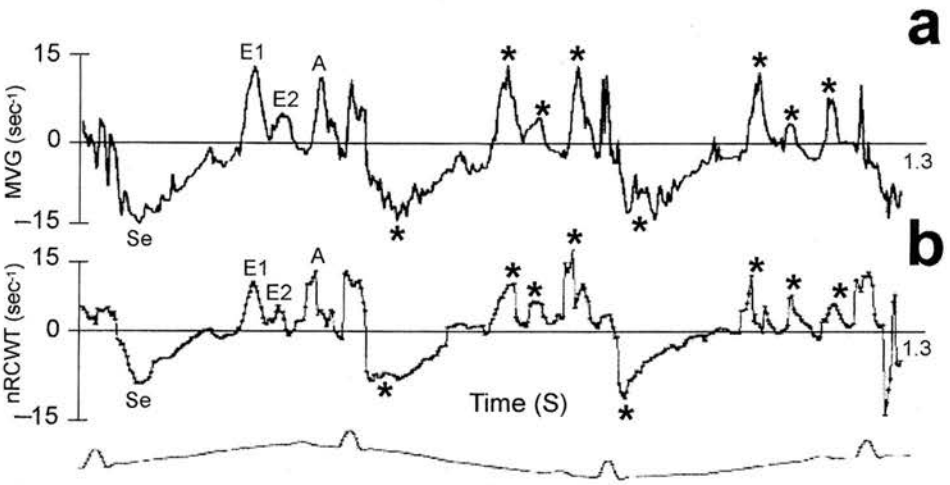

Fig 4. Examples of tracings of the myocardial velocity gradient (MVG) **(a)** and the normalized rate of change of wall thickness (nRCWT) **(b)** from the free wall (at the mitral valve, long-axis view) of a 7-year-old domestic shorthaired cat. Note that there is a very good correspondence in terms of timing in all 3 cardiac cycles between peaks in both curves. However, the peak values for the nRCWT are lower than the corresponding peak values for the MVG. Asterisks indicate peak values during the different phases of the cardiac cycle.

Description of Color M-mode TDI

By an analysis of the combined information obtained from the simultaneously recorded ECG and the digitized gray scale, we were able to determine that several distinct color phases were present in the color TDI images (Fig 6). Systole was represented by a red-colored strip, which began immediately after the S wave of the ECG and was, in most cases, composed of 2 distinct phases: an early phase that corresponded to a bright red band (early systole, Se) and then a dark red band (late systole, Sl), which commenced during the terminal portion of the T wave of the ECG. The beginning of the IVR phase was marked by the occurrence of a very brief-duration blue strip (IVRa) at the end of systole and coincided with a slight descending motion of the endocardium, which was clearly seen in the digitized gray scale. A red and relatively wider strip followed immediately after and represented the inward movement of the free wall during the IVR (IVRb). Diastole was represented by a blue band, which commenced at the mitral valve opening and ended with the appearance of a red, brief-duration strip during the QR wave of the ECG and mitral valve closure (inward movement of the free wall during the IVC phase, IVCa). Early diastole showed 2 brighter blue columns, which reflected the biphasic motion of the free wall of cats during this particular phase of the cardiac cycle. In some animals, a short-duration red strip was noticed between the 2 bright columns of early diastole, probably reflecting a rebounding movement of the free wall during the middle part of this phase (Fig 5). Late diastole was represented by another bright blue column appearing after the P wave of the ECG (Fig 6). In only a few animals (n = 4), a 2nd bright blue column was noticed during this phase, reflecting the biphasic motion of the free wall of cats that occasionally may occur during late diastole. A bright blue band occurred throughout the myocardium between the R and the end of the S wave of the ECG (outward movement of the free wall during the IVC phase, IVCb). This band actually consisted of successive narrow strips with an interchangeable pattern (Fig 7): 2 narrow bright blue strips separated by a deep blue strip appearing at the beginning and end of the sequence. The movement of the free wall of cats during the IVCb was very prominent and involved the endocardial and epicardial regions equally.

MVG and MMV Traces

Both tracings of the MVG and MMV showed consistent characteristic peaks during the different phases of the cardiac cycle (Fig 6) that corresponded to the color velocity patterns described above. The early (Se) and late (Sl) ventricular systolic peaks of the MMV were positive, indicating the inward movement of the free wall during the corresponding phases of the cardiac cycle. The Se peak of the MMV was biphasic and consisted of 2 smaller subpeaks. Early diastole in the MMV tracing was represented by 2 distinct negative shifts, E1 and E2, which, in some cases, were separated by a positive shift corresponding to the inward movement of the myocardium during mid-early diastole. A 3rd negative peak occurred during late diastole. The IVC and IVR in the MMV tracing showed 2 oppositely directed biphasic peaks. In many cases, the outward movement of the free wall during the IVCb provided the most prominent negative peak in the MMV tracing and showed the same biphasic pattern, composed of 2 smaller subpeaks, as the one seen during Se. The same pattern of peaks occurred in the MVG tracing, although the peaks in it showed the opposite direction from those in the corresponding MMV tracing (Fig 6).

Peak MVG and MMV Values and Influence of Heart Rate and Age

The peak mean values for the MVG and MMV during the defined cardiac phases and the influence of age and heart rate are given in Table 2. A significant and relatively strong inverse association was found between E2 of the MMV and age ($r = -0.71$, $r^2 = 0.50$, and $P < .01$) (Fig 8). The relationship between E1 of the MMV and age was similarly inverse but did not achieve statistical significance.

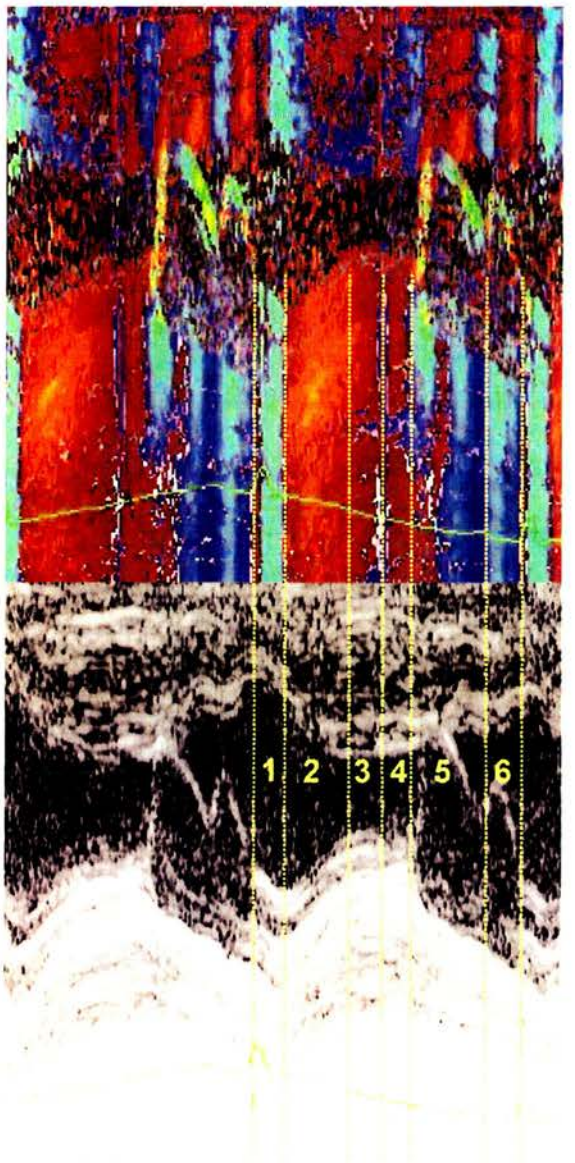

Fig 5. Color M-mode tissue Doppler imaging (TDI) and the corresponding gray scale. 1 = isovolumic contraction phase. The beginning of the isovolumic contraction (IVC) was marked by a narrow red strip, which coincided with the closure of the mitral valve (after left atrial contraction) and the QR wave of the ECG. A bright blue strip (RS wave of the ECG) followed immediately (2nd part of the IVC). 2 = early systole. This phase was represented by a yellow-red color transition coming after the S wave of the ECG. 3 = late systole; corresponds to a dark red strip, which coincided with the last part of the T wave of the ECG. 4 = the isovolumic relaxation (IVR) phase. The beginning of the IVR is marked with a blue strip, which corresponded to a descending movement of the myocardium more easily seen in the endocardial area at the gray scale. The 2nd part of the IVR is represented by a red strip before the opening of the mitral valve. 5 = early diastole. This phase started immediately after the opening of the mitral valve (1st bright blue transition) and lasted until the opening of the mitral valve during left atrial contraction (P wave of the ECG). 6 = late diastole. Note that early diastole shows 2 bright blue columns separated by a red column.

Table 1. M-mode measurement (mean ± SD) of clinically normal cats (n = 18).

IVSd (mm)	3.8 ± 0.9
LVd (mm)	14.4 ± 2.1
LVPWd (mm)	3.8 ± 0.9
IVSs (mm)	6.3 ± 1.2
LVs (mm)	8.1 ± 1.9
LVPWs (mm)	6.7 ± 1.1
FS (%)	42.5 ± 8.4
LA:Aod	1.4 ± 0.35

IVSd, interventricular septal wall thickness (diastolic); LVd, left ventricular end-diastolic diameter; LVPWd, left ventricular posterior wall thickness (diastolic); IVSs, interventricular septal wall thickness (systolic); LVs, left ventricular end-systolic diameter; LVPWs, left ventricular posterior wall thickness (systolic); FS, fractional shortening; LA:Aod, left atrium (systole) to aorta ratio (diastole).

The peak MMV during late diastole showed a positive association with age ($r = 0.54$, $r^2 = 0.29$, and $P < .05$) (Fig 8). With advancing age, both Se and Sl peaks of the MMV decreased significantly ($r = -0.55$, $r^2 = 0.30$, and $P < .05$ and $r = -0.62$, $r^2 = 0.39$, and $P < .01$, respectively) (Fig 8).

A relatively strong inverse association was found between E2 and age for the MVG ($r = -0.79$, $r^2 = 0.63$, and $P < .001$) (Fig 8) but not between E1 of the MVG and age. The late diastolic peak MVG was associated positively with age ($r = 0.50$, $r^2 = 0.25$, and $P < .05$). We did not find any age association for the peak MVG during Se or Sl. Neither of the peak values for the IVR or IVC showed a marked association with age. A comparison between a 2-year-old cat and a 10-year-old cat for the MMV and MVG is illustrated in Figure 9.

The peak values for the MVG and MMV were influenced by heart rate but to a variable extent during the different phases of the cardiac cycle (Table 2). In the group of normal cats of our study, only E2 of the MVG showed a statistically significant inverse association with heart rate ($r = -0.64$, $r^2 = 0.41$, and $P < .01$). E2 was absent in 3 cats with heart rates >170 beats/min. In these 3 cats, the myocardial motion during early diastole became monophasic. However, E2 also was absent in 2 animals (both of them 8 years of age) with relatively low heart rates (146 and 140 beats/min). No other peak values for the MVG and MMV showed a marked association with heart rate. Stepwise regression analysis in which age and heart rate were used as independent predictors of the peak MVG and MMV showed that age was the only significant independent predictor of these indices.

Phantom Study

A very strong association ($r^2 = 0.99$ and $P < .001$) was found between measured and calculated velocities in all speeds used (17, 26, and 47 rpm) (Fig 10). Spatial resolution assessed by the method used was 1.3 ± 0.4 mm.

Comparison between the MVG and Wall Thickness Changes (nRCWT)

The overall amplitude correlation (r) between the MVG and nRCWT ranged between 0.34 and 0.8 (mean ± SD,

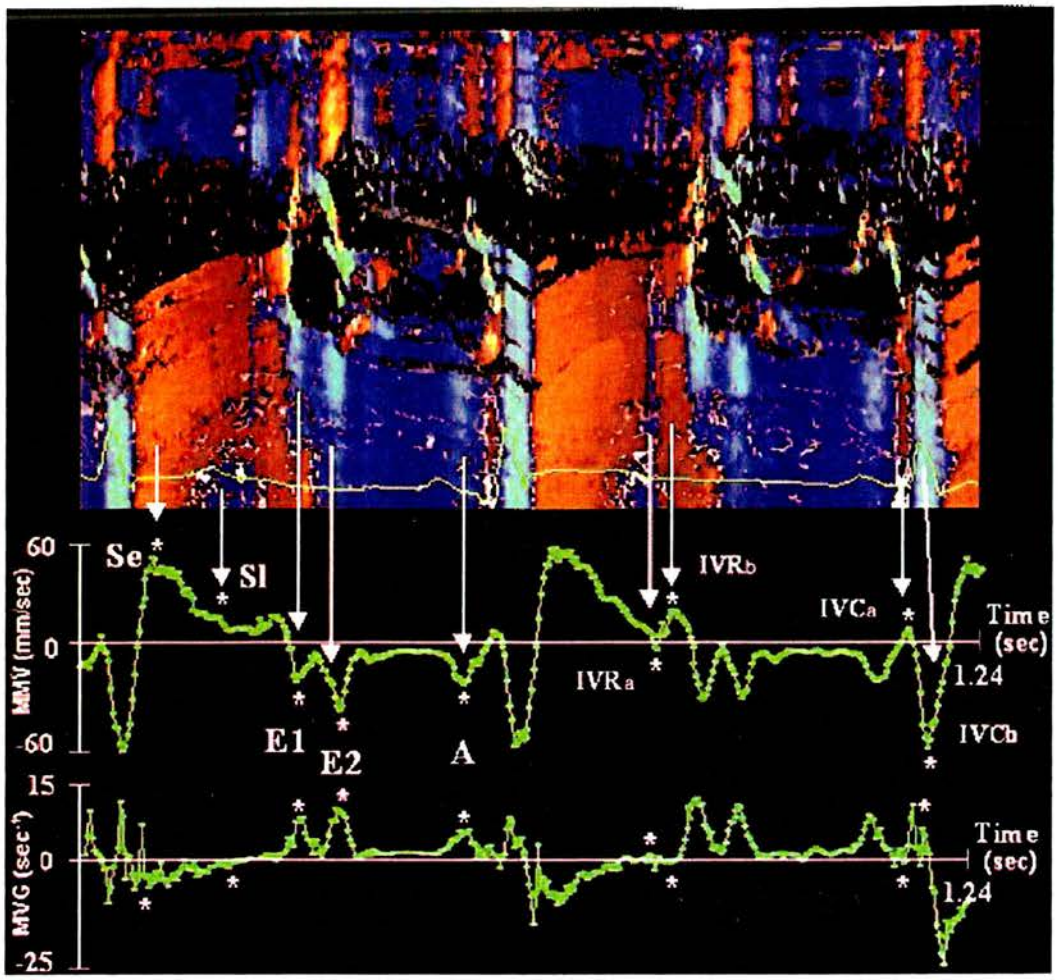

Fig 6. Color M-mode tissue Doppler imaging (TDI) from a 10-month-old domestic shorthaired cat (right parasternal long-axis view, at the mitral valve). Early systole is represented by a prominent peak (Se) in both tracings of the mean myocardial velocity (MMV) and the myocardial velocity gradient (MVG) occurring after the S wave of the QRS complex of the ECG (yellow-red phase in the TDI image). During late systole (T wave), a less prominent peak (late systole, Sl) appears (dark red strip). Early diastole shows a biphasic shift (E1 and E2 peaks), each corresponding to one of the 2 bright blue strips occurring in the color TDI image during this phase. Late diastole is represented by peak A, which corresponds to the 3rd bright blue strip of diastole coming after the P wave of the ECG. During the isovolumic relaxation (IVR) and isovolumic contraction (IVC) phases, oppositely directed shifts were recorded in both tracings. Note that at the beginning of the IVR, the free wall undergoes an outward movement (narrow blue strip in the color TDI image; IVRa peak), which is followed by an inward movement (red strip before the opening of the mitral valve; IVRb peak). In contrast, during the IVC, the movement of the free wall follows the opposite pattern. An inward movement of the free wall (narrow red strip during the QR wave of the ECG; IVCa peak) is followed by a very prominent outward movement (blue strip during the RS wave of the ECG; IVC phase, IVCb). The asterisk indicates where peak values were measured during the different phases of the cardiac cycle.

0.6 ± 0.13). The correspondence between the peak values for the 2 variables during diastole and systole is shown in Table 3. An example is shown in Figure 4. All peaks of the MVG during early diastole and systole had a corresponding peak of the nRCWT. The peak values for the MVG occurred more consistently than the peak values for the nRCWT mainly during E2.

Reproducibility

Results of the interobserver and intraobserver variability are presented in Table 4.

Discussion

This study documents the successful application of color M-mode TDI in the myocardium of cats. Because of the very high temporal and spatial resolution of the system used, a recording of the MVG and MMV was feasible in the myocardium of cats despite the very small size of their hearts and the very fast heart rates that may develop.

The cat population of this study was similar to the population of diseased cats referred to the cardiopulmonary service of the Small Animal Hospital of the University of Edinburgh with respect to breed and age. To produce reliable reference data, we excluded cats with obesity, hypertension, chronic renal failure, hyperthyroidism, and acromegaly because of the influence these conditions might have on myocardial properties.[28–31] However, this exclusion made it more difficult to recruit older healthy cats, particularly those older than 10 years.

Several different studies of humans have shown the abil-

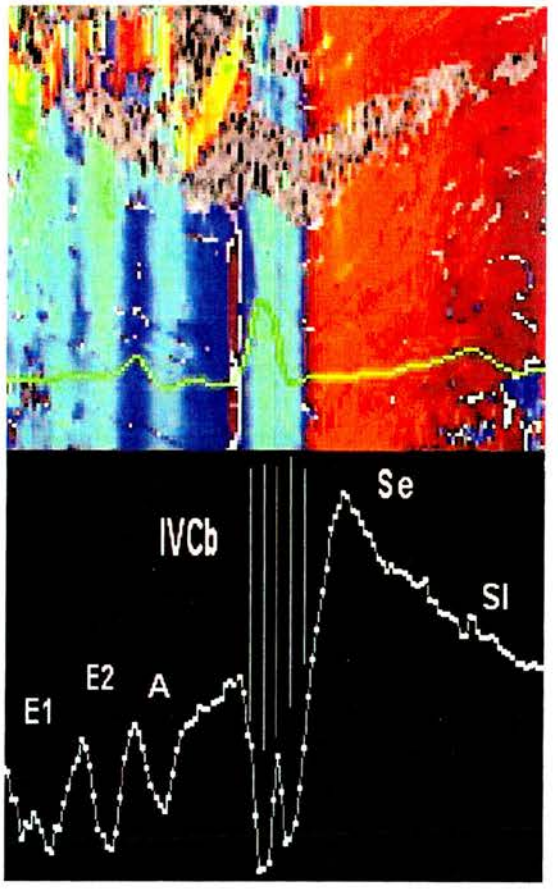

Fig 7. Color M-mode image (free wall, at the mitral valve). Note that during the second part of the isovolumic contraction phase (IVCb), the free wall shows a sequence of very short-duration blue strips, with the interchangeable pattern representing the oscillating movements of the myocardium during this phase. The tracing of the mean myocardial velocity (MMV) depicts the corresponding pattern of motion.

ity of color M-mode TDI to describe changes in wall motion during individual phases of the cardiac cycle by certain color velocity patterns.[22,24,32] Color M-mode TDI measurements in the free wall of humans have shown that this part of the myocardium is shown alternatively in red and blue as it moves toward and away from the transducer, respectively. Our study shows that similar velocity patterns occur in the LV free wall (LVFW) of cats.[22,24]

Zamorano et al[24] have proven that color M-mode TDI has the potential to accurately assess the different phases of the cardiac cycle noninvasively. Their study showed that color velocity patterns recorded by color M-mode TDI echocardiography in the IVS of humans correlated very well with the different phases of the cardiac cycle as assessed by invasive hemodynamic measurements. In our noninvasive study, the assessment of the cardiac phases in the free wall of cats was performed by means of the combined information obtained from the color and gray scales, including mitral valve motion and the simultaneously recorded ECG. However, the consistency of the color velocity patterns, along with their good correlation with the events seen on the gray scale and with ECG timing, ensures that the assessment of the cardiac phases was performed accurately.

Differences in the color intensity between early and late ventricular ejection reflected differences in the type of motion (fast acceleration during Se and deceleration during Sl). Studies of humans in which color M-mode TDI has been used have shown that anteroseptal endocardial motion shows biphasic shifts during early diastole.[33,34] Ventricular interdependence and right ventricular filling were proposed as 2 possible factors contributing to this phenomenon. Our study documented the biphasic character of the early diastolic movement in the free wall of cats. This movement actually involved the entire myocardium and was not confined to the endocardial area. This observation was confirmed by the quantification of myocardial motion for different layers of the LV wall. The 1st shift (E1) coincided with the opening of the anterior mitral valve leaflet, as shown in the gray scale of the M-mode, whereas the 2nd shift (E2) was associated with the descending movement of

Table 2. Color M-mode tissue Doppler imaging measurements (mean ± SD) from the free wall of normal cats and their association with age and heart rate.[a]

		Age		HR			Age		HR	
	MVG	r	r^2	r	r^2	MMV	r	r^2	r	r^2
EI	11.4 ± 3.7	NS	NS	NS	NS	−31.8 ± 11.5	NS	NS	NS	NS
E2	7.4 ± 3	−0.79	0.63, $P < .001$	−0.64	0.41, $P < .01$	−22.3 ± 15.9	−0.71	0.50, $P < .01$	NS	NS
A	8.8 ± 3.2	0.50	0.25, $P < .05$	NS	NS	−28.2 ± 10.5	0.54	0.29, $P < .05$	NS	NS
Se	−8.9 ± 2.9	NS	NS	NS	NS	36 ± 7.2	−0.55	0.30, $P < .05$	NS	NS
Sl	−4.4 ± 2.1	NS	NS	NS	NS	18.8 ± 6.3	−0.62	0.39, $P < .01$	NS	NS
IVRa	2.3 ± 2.4	NS	NS	NS	NS	1.9 ± 10.2	NS	NS	NS	NS
IVRb	−1.7 ± 1.9	NS	NS	NS	NS	12.7 ± 4.1	NS	NS	NS	NS
IVCa	−1.1 ± 3.6	NS	NS	NS	NS	2 ± 3.9	NS	NS	NS	NS
IVCb	5.6 ± 3.3	NS	NS	NS	NS	−39.1 ± 10.4	NS	NS	NS	NS

NS, not significant; HR, heart rate; MVG, myocardial velocity gradient (per second); MMV, mean myocardial velocity (mm/s); E1, 1st early diastolic peak; E2, 2nd early diastolic peak; A, late diastolic peak; Se, early systolic peak; Sl, late systolic peak; IVRa and IVRb, 1st and 2nd phases of isovolumic relaxation; IVCa and IVCb, 1st and 2nd phases of isovolumic contraction.

[a] The r values were calculated by means of absolute values of myocardial indices.

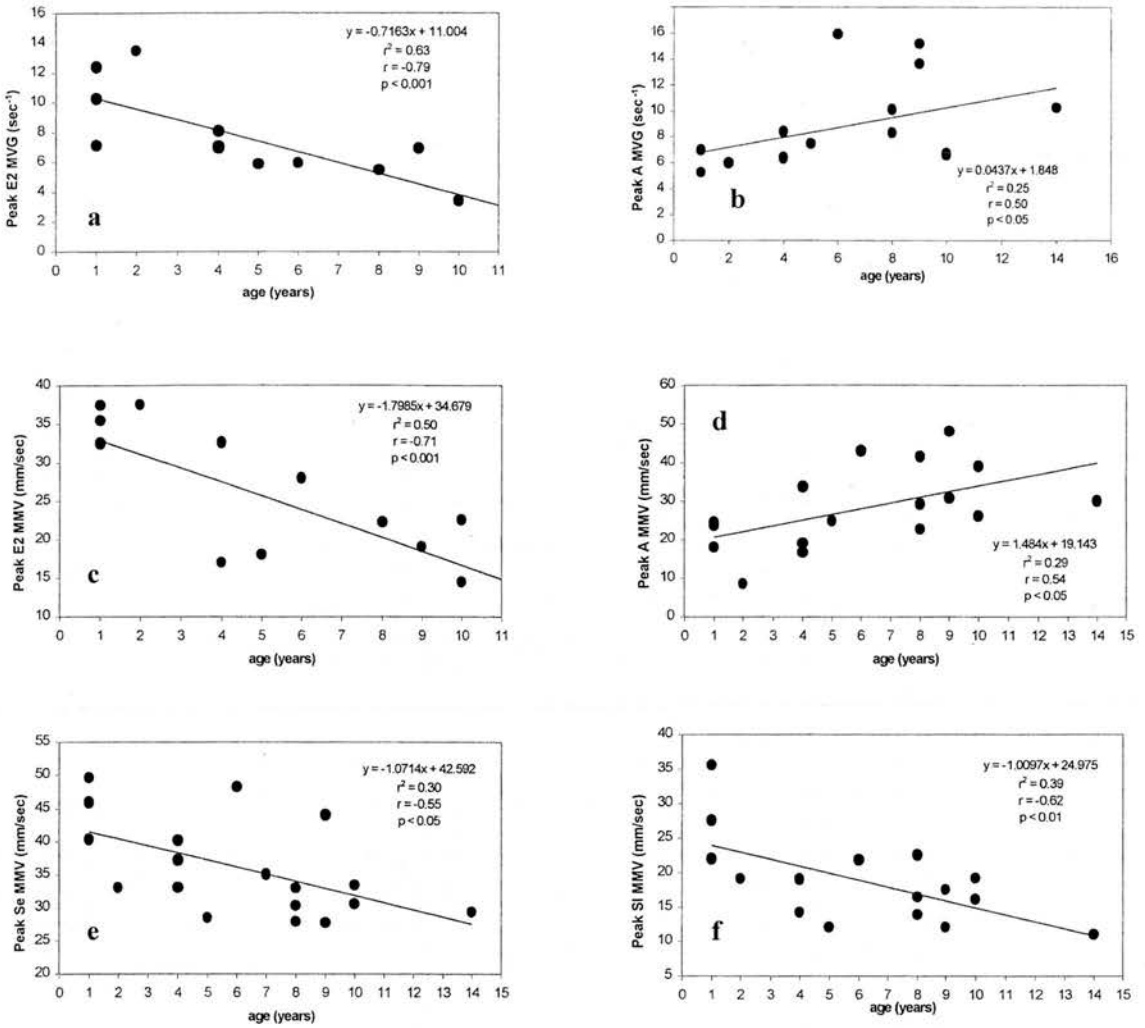

Fig 8. Linear regression plots showing **(a)** the association between age and the peak myocardial velocity gradient (MVG) during the 2nd phase of early diastole, **(b)** the association between age and the peak MVG during late diastole, **(c)** the association between age and the peak mean myocardial velocity (MMV) during the 2nd phase of early diastole, **(d)** the association between age and the peak MMV during late diastole, **(e)** the association between age and the peak MMV during early systole, and **(f)** late systole.

the mitral valve during E2. Although the energy dependence of myocardial relaxation during early diastole is well known, it is still unclear whether E2 is part of this energy-dependent process or whether it merely reflects a passive movement of the myocardium caused by the influx of blood into the left ventricle. Additional studies are needed to investigate the physiologic significance of this biphasic movement during early diastole in the myocardium of cats. According to the pattern of color strips seen in the IVS during early diastole (2 red strips separated by a narrower blue strip) (data not shown), this part of the myocardium is thought to undergo a similar biphasic motion during early diastole, as shown in the free wall of this species and reported in the anteroseptal endocardium of humans.[33,34] The passive dependence of myocardial motion due to the influx of blood into the LV cavity after atrial contraction has been described by other researchers.[35]

Quantification of the motion of the human myocardium with TDI has identified the oppositely directed shifts that occur during the IVR and IVC.[32,36–38] Our study recorded a similar pattern of motion in the free wall of cats during these phases. During both parts of the IVR and IVC, a uniform motion was recorded along the entire myocardium and resulted in relatively low MVG values, especially during their initial phases. However, myocardial motion was more prominent during the IVRb and IVCb. This finding was reflected in the higher MMV recorded during these phases and especially during the IVCb. Pellerin et al,[39] by means of the color M-mode TDI technique, described a "bayadere" color pattern of successive vertical strips with reverse velocity signals in the IVS and free wall of humans during the preejection period (from the beginning of the Q wave of the ECG to the onset of the ejection). However, in the free wall of cats, reverse velocity signs existed only between the IVCa and IVCb, with the latter presenting a pattern of very narrow successive strips, which were depicted more clearly in the MMV tracing (Fig 7). The presence of these successive strips reflects the very brief duration of the oscillating movements occurring in the myocardium of cats during the IVCb.

Several different studies of humans and experimental animals have attempted to analyze LV volume and shape

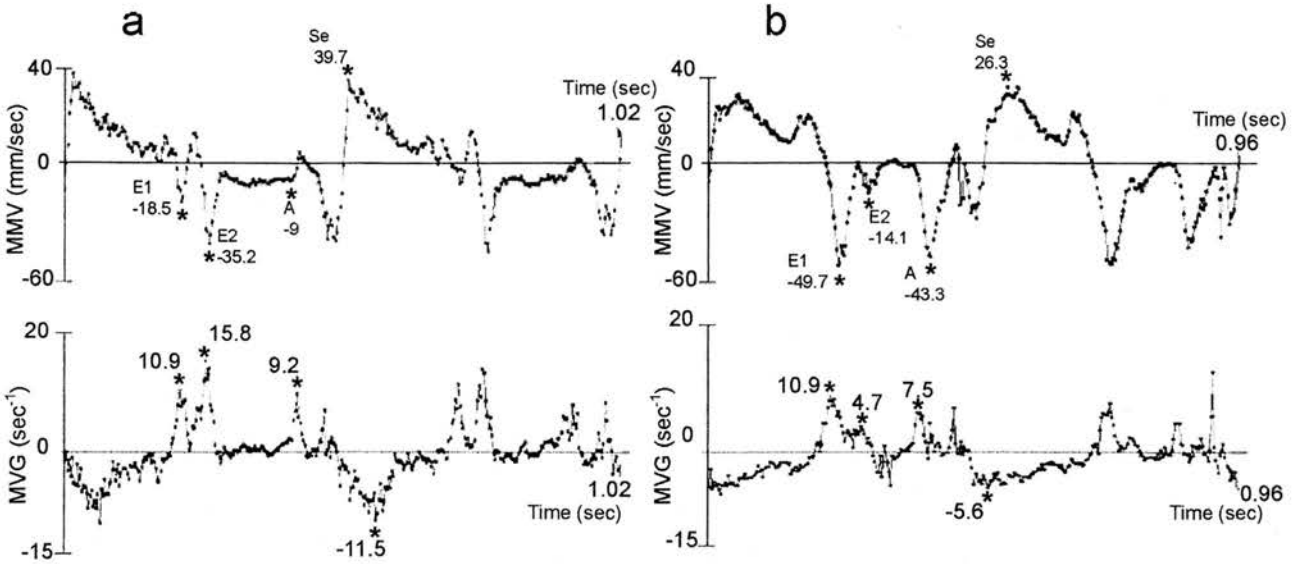

Fig 9. Tracings of the myocardial velocity gradients (MVGs) and mean myocardial velocities (MMVs) from **(a)** a 2-year-old Maine coon cat and **(b)** a 10-year-old domestic shorthaired cat. Note that during early diastole (E1), the MMV in the older animal was higher than in the younger animal. However, there was no difference in the peak MVG during this phase between the 2 animals. During the 2nd phase of early diastole (E2), the peak MMV and MVG values were substantially higher in the younger animal. Similarly, the peak MMV and MVG values were higher during early systole (Se) in the younger animal than in the older one. A = late diastolic peak. Asterisk indicates peak values during the different cardiac phases.

changes during the 2 isovolumic periods and to correlate them with myocardial motion. Some researchers have proposed that the IVC phase is characterized by asynchronous contraction during which the early activation and contraction of papillary muscles and trabeculae carnae result in the sudden downward movement of the atrioventricular valves and the passive outward stretch of the circumferentially oriented fibers, particularly those in the basilar two thirds of the ventricle.[40,41] This sequence of events results in a more spheric configuration of the LV during the IVC.[40–42] During the IVR period, an outward movement of the anterior wall and the apex, accompanied by an inward movement of the inferior and posterior wall of the basal area of the LV, has been described by others.[43,44] The outward movement during the 2nd part of the IVC phase as well as the inward movement during the 2nd part of the IVR period seen in the free wall of the cats of our study may be explained by the aforementioned findings of older, invasive, physiologic studies. However, none of these studies provides a substantial clue for the 1st part of the 2 isovolumic periods. Rankin et al[45] documented occasional biphasic changes in the thickness of the anterior wall consisting of alternative thickening and thinning during the IVC. We believe that the oppositely directed shifts recorded during the 2 isovolumic periods represent adjustment movements of the myocardial fibers determined by the Frank-Starling law.[46] The outward movement of the myocardium during the IVCb precedes the initiation of the main inward movement during systole, and the IVRa follows the cessation of it. The same relationship holds between the observed inward movements (IVRb and

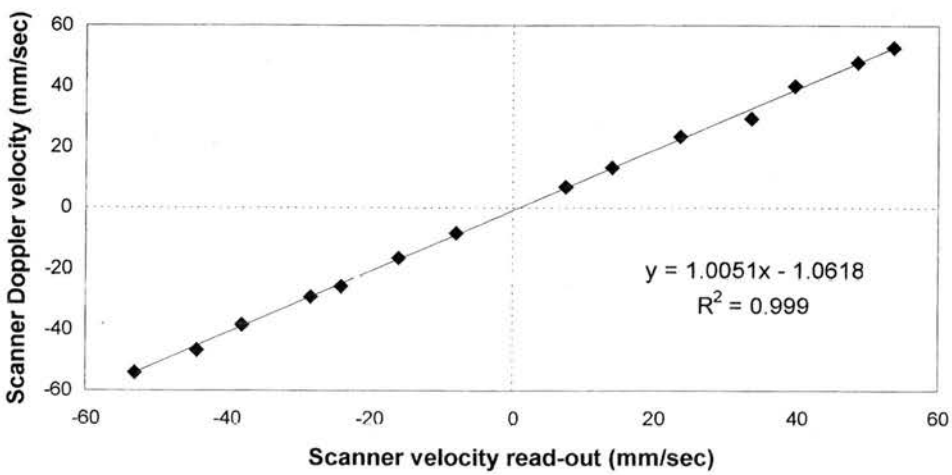

Fig 10. Phantom study. Comparison of calculated actual velocities from a rotating tissue-mimicking phantom with the Doppler velocities measured by the ultrasound machine (26 rpm).

Table 3. Percentage of cardiac cycles with MVG peaks having a concurrent peak of the nRCWT and vice versa. Also, percentage of cardiac cycles with the peak MVG and nRCWT values during 4 different cardiac phases. Only the peaks of the MVG and nRCWT that reached 1/s were considered.

	% E1	% E2	% A	% Se
MVG peaks with a concurrent nRCWT peak	100	82	98	100
nRCWT peaks with a concurrent MVG peak	100	93	100	100
Cycles with an MVG peak	100	94	100	100
Cycles with an nRCWT peak	100	70	97	100

MVG, myocardial velocity gradient; nRCWT, normalized rate of change of wall thickness; E1, 1st phase of early diastole; E2, 2nd phase of early diastole; A, late diastole; Se, early systole.

IVCa) during the 2 isovolumic periods and the diastolic movement. An investigation of the timing of occurrence of these biphasic shifts in different myocardial segments when sampled from different projections would offer valuable clues for the role and interrelation between longitudinal and circumferential fibers during these periods. Moreover, myocardial motion during the 2 isovolumic phases has been shown to affect overall myocardial performance, and its quantification may be of value in assessing LV properties.[32,47,48]

The peak MVG in the group of normal cats of our study was higher than that reported in sedentary humans during all cardiac phases.[14,22,23] However, values for the peak MVG of cats during E1 (11.4 ± 3.7/s) were close to those reported during early diastole from the free wall of athletes (10.2 ± 1.5/s).[23] On the other hand, the peak MMV during E1 was substantially lower in the free wall of cats (31.8 ± 11.5 mm/s) than in the free wall of humans (66 ± 22 mm/s).[14,22,23] Only the peak MMV during the IVCb (39.1 ± 10.4 mm/s) exceeded the corresponding value recorded from the human myocardium (13 ± 12 mm/s).[14,22,23] The above differences in the peak MVG and MMV values reflect physiologic differences in myocardial function between the 2 species. We speculate that the high-velocity gradient between endocardium and epicardium in the free wall of cats is a compensatory mechanism that allows the normal myocardium of cats to perform efficiently despite the very short R to R intervals that occur normally in this species.

Many studies of humans and experimental animals have shown the influence of aging on LV properties. Prolongation of both contraction and relaxation times is believed to be due to an altered active state and to changes in viscoelasticity.[49,50] Increased myocardial stiffness due to an increased quantity of interstitial connective tissue, along with an increase of the connective tissue of the fibrous skeleton of the heart, may play a dramatic role in the age-related decrease in LV diastolic function. Furthermore, with increasing age, a decline in the ability of β-adrenergic receptor stimulation to increase contractility has been reported in isolated myocytes of rats.[51] Age-related changes in the myocardium of humans have been reflected in color M-mode TDI measurements. The peak velocity gradient and peak mean velocity during late diastole were positively associated with age, whereas the peak MVG during rapid ventricular filling decreased with increasing age in the free wall of normal humans.[22] No association between age and systolic indices has been reported for humans.[22] However, our study showed that the systolic performance of the myocardium of cats also is reduced in association with aging. This association was shown mainly in the decrease of the peak systolic MMV values during both the early and late ventricular ejection periods. Another study has shown that the negative correlation between the peak early diastolic MVG and age was more prominent in the free wall of sedentary humans than in the free wall of athletes.[23] In the group of normal cats of our study, the influence of aging in diastolic performance proved to be more prominent in the E2 of early diastole with a marked decrease in the amplitude of the peak MVG and MMV (Fig 9). All animals without a defined separate E2 wave, regardless of their heart rate, were older than 7 years. This finding suggests that the absence of this wave may reflect, at least in part, the failure of the older myocardium to relax adequately during early diastole. On the other hand, our results show that the E1 wave remains uninfluenced by age-related changes in the myocardium of nondiseased animals. The peak MVG during late diastole showed a relatively weak positive association with age in contrast to the strong relationship reported with age in the free wall of normal humans. However, the above findings complement the results of the study by Santilli and Bussadori[52] in which a positive correlation was found between the A wave of mitral inflow and age of healthy cats. A negative association was also found between age and the velocity time integral of the E mitral inflow wave but not with the peak E mitral inflow wave velocity.[52] That the E1 wave remains unaltered by advancing age may partially explain why the peak E wave of mitral inflow did not correlate with age in the study by Santilli and Bussadori.[52] The augmentation of the passive myocardial motion of cats during late diastole (peak A wave of the MVG and MMV) is due to the increasingly dominant role of left atrial contraction in LV filling (increased A wave of mitral inflow) with increasing age.[35]

Although heart rate appeared to markedly influence only E2 of the MVG, stepwise regression analysis showed that this factor was not a significant independent predictor of myocardial indices for any stage of the cardiac cycle. This heart rate independence offers advantages over other methods for assessing systolic or diastolic function. However, we believe that only an invasive study in which heart rate is controlled by pacing will reliably assess the influence of this factor on the MMV or MVG indices.[53]

Fleming et al[26] previously showed that the measurement of the MVG is feasible only within a distance double the spatial resolution available. Therefore, we thought that an in vitro assessment of the spatial resolution of our system

Table 4. Results of intraobserver (intra) and interobserver (inter) variability of myocardial indices.

	E1	E2	A	Se	Sl	IVRa	IVRb	IVCa	IVCb
MVG[a]	12.74	8.28	6.99	−9.52	−3.76	1.33	−2.15	−2.7	−6.67
Intra[b]	0.2 (0.6 to −0.2)	0.3 (0 to −1.1)	0.4 (0.6 to −1.1)	0.7 (1.4 to −1.2)	0.5 (1 to −1.2)	0.3 (0.8 to −0.4)	0.5 (0.8 to −1)	0.3 (1 to −0.3)	0.8 (1.3 to −1.9)
MVG[a]	12.3	7.97	6.64	−9.69	−3.84	1.37	−2.08	−1.9	6.23
Inter[b]	0.5 (0.2 to −2)	0.4 (0.4 to −1.3)	0.7 (0.9 to −1.9)	1 (2 to −2.2)	0.7 (1.2 to −1.5)	0.2 (0.3 to −0.6)	0.3 (0.5 to −0.5)	0.4 (1 to −0.4)	0.8 (1 to −2.1)
MMV[a]	−33.6	−27.4	−24.5	38.7	20.1	−2.3	13.5	2.7	−44.6
Intra[b]	0.7 (1.2 to −1.7)	0.7 (1.5 to −1.4)	0.2 (0.3 to −0.3)	0.6 (0.8 to −1.7)	0.6 (0.8 to −1.7)	0.2 (0.5 to −0.3)	0.2 (0.3 to −0.5)	0.2 (0.3 to −0.3)	0.5 (1.3 to −0.7)
MMV[a]	−32.9	−27.4	−23.7	38.6	20.9	−1.6	13.6	1.9	−44.4
Inter[b]	2 (3.7 to −4.4)	0.7 (2.1 to −0.8)	1.2 (2.5 to −2.1)	1.1 (2.1 to −2.4)	1.4 (2.4 to −3.3)	1.5 (2.4 to −3.6)	1.5 (3.2 to −2.7)	2.7 (7.6 to −3.3)	1.2 (2.3 to −2.5)

MVG, mycardial velocity gradient (1/s); MMV, mean myocardial velocity (mm/s); E1, 1st early diastolic peak; E2, 2nd early diastolic peak; A, late diastolic peak; Se, early systolic peak; Sl, late systolic peak; IVRa and IVRb, 1st and 2nd phases of isovolumic relaxation; IVCa and IVCb, 1st and 2nd phases of isovolumic contraction.

[a] Mean of 2 observations.

[b] Standard deviation of difference (limits of agreement).

would be essential, considering the normal, thin LV wall of cats (3–4 mm). The TMM phantoms used in this study were designed to be similar in size to those of the heart of a cat. Rotational velocities and echocardiographic settings resembled those used during the acquisition of images from cats. Our results show that with the current system, the successful determination of the MVG is possible only over a distance exceeding twice the spatial resolution assessed in this study ($2 \times 1.3 \pm 0.4$ mm). This finding provides further evidence for the potentially accurate measurement of the MVG of cats under most circumstances. The lower spatial resolution documented in our study when compared with that reported by Fleming et al[26] (3 mm) is due to the higher frequency probe used in the current study. The very good correlation found between actual and estimated velocities shows the ability of the system used to accurately assess myocardial velocities and further validates the use of this technique for cats.

Several studies have proven the usefulness of assessing wall thickness changes in investigating LV properties in the different cardiac diseases of humans.[54–58] However, the calculation of the rate of thinning and thickening from the digitized M-mode images has some inherent disadvantages.[11] First, it is based only on the displacement of endocardial and epicardial borders and therefore does not accurately reflect changes within the myocardium. Furthermore, it is highly dependent on the clear identification of the cardiac boundaries, which sometimes are blurred or ambiguous. It also is affected by the overall heart motion.

On the other hand, the calculation of the MVG and MMV from color M-mode TDI images is based on the estimation of myocardial estimates along the entire thickness of the myocardium. Therefore, it more accurately depicts the inherent properties of the myocardium, assuming that myocardial velocity estimates reflect the structural and functional characteristics of different points along the myocardium.[11] Moreover, the estimation of the MVG is independent of the accurate identification of endocardial and epicardial borders; also, it is not affected by translational effects.

The results of our study are in agreement with those reported from studies of humans, in which it has been shown that the MVG follows wall thickness changes[11] (Fig 4). Differences in the overall amplitude between the 2 variables reflect the difficulty in obtaining optimal images rather than the failure to prove that Equation 2 is valid. Blurred cardiac boundaries, especially in animals with increased subcutaneous or intrathoracic fat, resulted in a less accurate calculation of the nRCWT from the digitized gray scale and, consequently, in a poor correlation between the 2 variables. Another factor that explains the discrepancy observed in the amplitude of the MVG and nRCWT is the fact that even subtle errors in accurately tracing the cardiac boundaries resulted in marked changes in the amplitude of the nRCWT. Overall heart motion also may have contributed to the difference seen in the overall amplitude between the 2 variables because it affects the nRCWT and not the MVG.

That peak values for the MVG occurred more consistently during E2 shows that the color M-mode TDI was more sensitive than the nRCWT in accurately depicting changes in wall movement during this particular phase of

the cardiac cycle. The correspondence between the peak values for the MVG and nRCWT was very strong during all phases of the cardiac cycle. This finding further supports our argument that the MVG is consistent with wall thickness changes and therefore can be used as a more accurate and sensitive means of quantifying the myocardial motion of cats.

Intraobserver and interobserver limits of agreement are satisfactory for most indices of both variables (the MMV and MVG) (Table 4). Very wide interobserver limits of agreement for some indices (the IVCa and IVRa of the MMV) may reflect differences in analyzing experience between observers rather than true difficulties in reproducing peak values successfully during these phases. In general, intraobserver variability was lower than interobserver variability. This observation emphasizes that the analysis of color M-mode TDI images requires a minimal amount of analyzing experience. Narrower limits of agreement of the MMV indices than those of the MVG occurred because the MMV tracings showed a more consistent and recognizable sequence of peaks than the MVG tracings. The peak indices with very low mean values (especially the MVG during the IVC and IVR phases) were difficult to identify consistently and thus more prone to measurement error.

Ours was a noninvasive study carried out on pet animals. Consequently, we were unable to generate any invasively determined hemodynamic data to provide gold standards with which to compare our results. Because of the angle dependence of Doppler measurements, the estimation of the MVG and MMV was confined to the free wall by means of the right parasternal long-axis view in which the ultrasonic beam was visually determined to be parallel to myocardial movement. Although this study showed a marked influence of age on the MMV, this parameter is influenced by the translational movement of the heart within the thorax. Analysis of very short-duration events, such as those occurring during the 2 isovolumic periods and especially their 1st part, requires a very high temporal resolution. Higher rates of data acquisition than those used in the current study will allow a more accurate quantification of myocardial motion during these periods. The lack of a simultaneous recording of the phonocardiogram may have caused a less accurate estimation of the duration of the different cardiac phases than that reported in other studies. However, we believe that the color and gray-scale events and the simultaneously recorded ECG offered a consistent definition of the phases of the cardiac cycle used to define our analyses. Although previous studies have reported the influence of respiration on the amplitude of the MMV and MVG,[32] we were unable to simultaneously record phases of respiration during the acquisition of images, and it was impossible for us to investigate the relationship between the timing of each phase of respiration and the occurrence of the peak MVG or MMV.

Myocardial disease is a major cause of morbidity and mortality of cats, with patients presenting with dyspnea or thromboembolism.[1,4,59] Dilated cardiomyopathy, related or unrelated to taurine deficiency, is now rare.[4] At present, HCM is the most common cardiac disease of cats, and it is well described and diagnosed by echocardiography.[1–3] Restrictive cardiomyopathy is another known cardiac disease of cats, but its diagnosis by echocardiography is difficult or controversial. Pathologic confirmation usually is required.[59] On the other hand, some poorly defined myocardial disease presentations have been identified in a subset of feline patients and are believed to be associated with clinically relevant diastolic dysfunction. These cats present with a marked left atrial enlargement with a high risk of thromboembolism without meeting the criteria for the diagnosis of HCM or restrictive cardiomyopathy. These atypical cases are poorly characterized on the basis of ultrasonography, and their etiopathogenesis is not understood. Various terms such as "restrictive," "intermediate," "intergrade," and "unclassified" have been used to describe such cardiomyopathy cases, and so far, their classification is based mainly on morphologic features and subjective assessment.[6,59] Major limitations occur in assessing myocardial diastolic function, even with traditional echocardiographic approaches, including mitral inflow and pulmonary venous flow studies. Mitral inflow is subject to loading conditions, and pulmonary venous flow is technically difficult to measure.[16,60]

Recently, in the 1st application of pulsed TDI in cats, Gavaghan et al[5] reported that some cats with unclassified cardiomyopathy showed a "restrictive" myocardial pattern of motion, whereas others had an entirely "unclassified" myocardial pattern. Studies of humans have shown that the MVG is preload independent and correlates well with invasive hemodynamic indices, which reflect global systolic and diastolic myocardial properties, such as dP/dt and τ.[15–17] Furthermore, in contrast to the myocardial velocities measured by pulsed TDI, the MVG is not affected by overall heart motion.[16] Palka et al[18] have shown that the MVG recorded in the LVFW of humans can be used to differentiate between myocardial hypertrophy of different etiologies, reflecting the great sensitivity of this novel echocardiographic variable in assessing and differentiating LV properties of various cardiac entities with similar morphologic characteristics. These advantages of the MVG render it a more sensitive tool in assessing LV properties, and it will therefore be of value in better classifying cardiac diseases of cats and elucidating the mechanisms of their pathophysiology. These findings may help further establish better therapeutic regimens for the treatment of cardiac diseases of cats.

To our knowledge, this is the 1st study to record the myocardial velocities and velocity gradients of cats by means of color M-mode TDI. On the basis of the very high temporal resolution of this particular application of TDI, we identified valuable physiologic aspects of the myocardial movement of cats. Our results describe these features, including the influence of aging and biphasic motion during early diastole and the isovolumic periods. The MVG showed cyclic variation consistent with wall thickness changes, suggesting that it has the potential to be a very useful tool in the assessment of the myocardial function of cardiac diseases of cats. Furthermore, the study proved that the measurement of the MVG and MMV was feasible in the myocardium of this species despite the small size of the heart of the cat and the very fast heart rates that may develop. This study provides evidence for the utility of color

TDI in human neonatal hearts or in experimental models of small animals.

Footnotes

[a] SIM 7000 Challenge ultrasound system, Esaote Biomedica, Firenze, Italy

[b] ATL HDI 5000 ultrasound system, Advanced Technology Laboratories (ATL), Bothell, WA

[c] Special analysis software (HDIlab), Advanced Technology Laboratories (ATL), Bothell, WA

[d] SigmaStat, version 2.03, SPSS Inc, Chicago, IL

Acknowledgments

This work was performed at the Department of Veterinary Clinical Studies, Cardiopulmonary Service, and the Department of Medical Physics and Engineering, University of Edinburgh, Edinburgh, Scotland, UK. This study and HK were supported by the Greek State Scholarships Foundation. JDMcE was supported by the British Heart Foundation (PG/98060). The transducer and KS were funded by Pet Plan Charitable Trust. We are grateful to Dr Graham Mackenzie for his assistance with the analysis software and, also, to Amanda Lee for her statistical advice for the reproducibility study. The work would not have been possible without the support and cooperation of the cat owners and handlers, especially Dr Irini Christodoulou.

References

1. Atkins CE, Gallo AM, Kurzman ID, et al. Risk factors, clinical signs, and survival in cats with a clinical diagnosis of idiopathic hypertrophic cardiomyopathy: 74 cases (1985–1989). J Am Vet Med Assoc 1992;201:613–618.

2. Bright JM, Golden AL, Daniel GB. Feline hypertrophic cardiomyopathy: Variations on a theme. J Small Anim Pract 1992;33:266–274.

3. Fox PR, Liu SK, Maron BJ. Echocardiographic assessment of spontaneously occurring feline hypertrophic cardiomyopathy. An animal model of human disease. Circulation 1995;92:2645–2651.

4. Fox PR. Feline cardiomyopathies. In: Fox PR, Sisson D, Moise NS, ed. Textbook of Canine and Feline Cardiology. Principles and Clinical Practice, 2nd ed. Philadelphia, PA: WB Saunders; 1998:621–678.

5. Gavaghan BJ, Kittleson MD, Fisher KJ, et al. Quantification of left ventricular diastolic wall motion by Doppler tissue imaging in healthy cats and cats with cardiomyopathy. Am J Vet Res 1999;60: 1478–1486.

6. Harpster NK. Feline myocardial diseases. In: Kirk RW, ed. Current Veterinary Therapy. Philadelphia, PA: WB Saunders; 1986:380–398.

7. Kittleson MD, Meurs KM, Munro MJ, et al. Familial hypertrophic cardiomyopathy in Maine coon cats: An animal model of human disease. Circulation 1999;99:3172–3180.

8. Fox PR, Maron BJ, Basso C, et al. Spontaneously occurring arrhythmogenic right ventricular cardiomyopathy in the domestic cat: A new animal model similar to the human disease. Circulation 2000;102: 1863–1870.

9. Miyatake K, Yamagishi M, Tanaka N, et al. New method for evaluating left ventricular wall motion by color-coded tissue Doppler imaging: In vitro and in vivo studies. J Am Coll Cardiol 1995;25:717–724.

10. McDicken WN, Sutherland GR, Moran CM, et al. Colour Doppler velocity imaging of the myocardium. Ultrasound Med Biol 1992;18:651–654.

11. Fleming AD, Xia X, McDicken WN, et al. Myocardial velocity gradients detected by Doppler imaging. Br J Radiol 1994;67:679–688.

12. Edvardsen T, Aakhus S, Endresen K, et al. Acute regional myocardial ischemia identified by 2-dimensional multiregion Doppler imaging tissue technique. J Am Soc Echocardiogr 2000;13:986–994.

13. Oki T, Tabata T, Yamada H, et al. Left ventricular diastolic properties of hypertensive patients measured by pulsed tissue Doppler imaging. J Am Soc Echocardiogr 1998;11:1106–1112.

14. Palka P, Lange A, Wright RA, et al. Myocardial velocity gradient measured throughout the cardiac cycle in dilated cardiomyopathy hearts—A potential new parameter of systolic and diastolic myocardial function by Doppler myocardial imaging. Eur J Ultrasound 1997;5: 141–154.

15. Oki T, Mishiro Y, Yamada H, et al. Detection of left ventricular regional relaxation abnormalities and asynchrony in patients with hypertrophic cardiomyopathy with the use of tissue Doppler imaging. Am Heart J 2000;139:497–502.

16. Shimizu Y, Uematsu M, Shimizu H, et al. Peak negative myocardial velocity gradient in early diastole as a noninvasive indicator of left ventricular diastolic function: Comparison with transmitral flow velocity indices. J Am Coll Cardiol 1998;32:1418–1425.

17. Ueno Y, Nakamura Y, Ohbayashi Y, et al. Evaluation of left ventricular systolic and diastolic global function: Peak positive and negative myocardial velocity gradients in M-mode Doppler tissue imaging. Echocardiography 2002;19:15–25.

18. Palka P, Lange A, Fleming AD, et al. Differences in myocardial velocity gradient measured throughout the cardiac cycle in patients with hypertrophic cardiomyopathy, athletes and patients with left ventricular hypertrophy due to hypertension. J Am Coll Cardiol 1997;30: 760–768.

19. Palka P, Lange A, Donnelly JE, et al. Differentiation between restrictive cardiomyopathy and constrictive pericarditis by early diastolic Doppler myocardial velocity gradient at the posterior wall. Circulation 2000;102:655–662.

20. Dutka DP, Donnelly JE, Nihoyannopoulos P, et al. Marked variation in the cardiomyopathy associated with Friedreich's ataxia. Heart 1999;81:141–147.

21. Marcos-Alberca P, Garcia-Fernandez MA, Ledesma MJ, et al. Intramyocardial analysis of regional systolic and diastolic function in ischemic heart disease with Doppler tissue imaging: Role of the different myocardial layers. J Am Soc Echocardiogr 2002;15:99–108.

22. Palka P, Lange A, Fleming AD, et al. Age-related transmural peak mean velocities and peak velocity gradients by Doppler myocardial imaging in normal subjects. Eur Heart J 1996;17:940–950.

23. Palka P, Lange A, Nihoyannopoulos P. The effect of long-term training on age-related left ventricular changes by Doppler myocardial velocity gradient. Am J Cardiol 1999;84:1061–1067.

24. Zamorano J, Wallbridge DR, Ge J, et al. Non-invasive assessment of cardiac physiology by tissue Doppler echocardiography. A comparison with invasive haemodynamics. Eur Heart J 1997;18:330–339.

25. Sisson DD, Knight DH, Helinski C, et al. Plasma taurine concentrations and M-mode echocardiographic measures in healthy cats and in cats with dilated cardiomyopathy. J Vet Intern Med 1991;5: 232–238.

26. Fleming AD, McDicken WN, Sutherland GR, et al. Assessment of colour Doppler tissue imaging using test-phantom. Ultrasound Med Biol 1994;20:937–951.

27. Bland JM, Altman DG. Statistical methods for assessing agreement between two methods of clinical measurement. Lancet 1986;1: 307–310.

28. Taugner F, Baatz G, Nobiling R. The renin-angiotensin system in cats with chronic renal failure. J Comp Pathol 1996;115:239–252.

29. Snyder PS, Sadek D, Jones GL. Effect of amlodipine on echo-

cardiographic variables in cats with systemic hypertension. J Vet Intern Med 2001;15:52–56.

30. Peterson ME, Taylor RS, Greco DS, et al. Acromegaly in 14 cats. J Vet Intern Med 1990;4:192–201.

31. Bond BR, Fox PR, Peterson ME, et al. Echocardiographic findings in 103 cats with hyperthyroidism. J Am Vet Med Assoc 1988; 192:1546–1549.

32. Palka P, Lange A, Fleming AD, et al. Doppler tissue imaging: Myocardial wall motion velocities in normal subjects. J Am Soc Echocardiogr 1995;8:659–668.

33. Gorcsan J, Gulati VK, Mandarino WA, et al. Color-coded measures of myocardial velocity throughout the cardiac cycle by tissue Doppler imaging to quantify regional left ventricular function. Am Heart J 1996;131:1203–1213.

34. Gorcsan J, Deswal A, Mankad S, et al. Quantification of the myocardial response to low-dose dobutamine using tissue Doppler echocardiographic measures of velocity and velocity gradient. Am J Cardiol 1998;81:615–623.

35. Yamada H, Oki T, Mishiro Y, et al. Effect of aging on diastolic left ventricular myocardial velocities measured by pulsed tissue Doppler imaging in healthy subjects. J Am Soc Echocardiogr 1999;12:574–581.

36. Garcia MJ, Rodriguez L, Ares M, et al. Myocardial wall velocity assessment by pulsed Doppler tissue imaging: Characteristic findings in normal subjects. Am Heart J 1996;132:648–656.

37. Galiuto L, Ignone G, DeMaria AN. Contraction and relaxation velocities of the normal left ventricle using pulsed-wave tissue Doppler echocardiography. Am J Cardiol 1998;81:609–614.

38. Naqvi TZ, Neyman G, Broyde A, et al. Comparison of myocardial tissue Doppler with transmitral flow Doppler in left ventricular hypertrophy. J Am Soc Echocardiogr 2001;14:1153–1160.

39. Pellerin M, Cohen P, Larrazet F, et al. Preejectional left ventricular wall motion in normal subjects using Doppler tissue imaging and correlation with ejection fraction. Am J Cardiol 1997;80:601–607.

40. Rushmer RF. Initial phase of ventricular systole: Asynchronous contraction. Am J Physiol 1956;184:188–194.

41. Hawthorne EW. Symposium on measurements of left ventricular volume. Part III. Dynamic geometry of the left ventricle. Am J Cardiol 1966;18:566–573.

42. Jones CJH, Raposo L, Gibson DG. Functional importance of the long axis dynamics of the human left ventricle. Br Heart J 1990; 63:215–220.

43. Altieri PI, Wilt SM, Leighton RF. Left ventricular wall motion during the isovolumic relaxation period. Circulation 1973;48:499–505.

44. Hammermeister KE, Gibson DG, Hughes D. Regional variation in the timing and extent of left ventricular wall motion in normal subjects. Br Heart J 1986;56:226–235.

45. Rankin JS, McHale PA, Arentzen CE, et al. The three-dimensional dynamic geometry of the left ventricle in the conscious dog. Circ Res 1976;39:304–313.

46. Hawthorne EW. Instantaneous dimensional changes of the left ventricle in dogs. Circ Res 1961;9:110–119.

47. Gibson DG, Doran JH, Traill TA, et al. Abnormal left ventricular wall movement during early systole in patients with angina pectoris. Br Heart J 1978;40:758–766.

48. Gibson DG, Prewitt TA, Brown DJ. Analysis of left ventricular wall movement during isovolumic relaxation and its relation to coronary artery disease. Br Heart J 1976;38:1010–1019.

49. Weisfeldt ML, Loeven WA, Shock NW. Resting and active mechanical properties of trabeculae carnae from aged male rats. Am J Physiol 1971;220:1921–1927.

50. Lakatta EG, Gerstenblith G, Angell CS, et al. Prolonged contraction duration in aged myocardium. J Clin Invest 1975;55:61–68.

51. Xiao RP, Spurgeon HA, O'Connor F, et al. Age-associated changes in beta-adrenergic modulation on rat cardiac excitation-contraction coupling. J Clin Invest 1994;94:2051–2059.

52. Santilli RA, Bussadori C. Doppler echocardiographic study of left ventricular diastole in non-anaesthetized healthy cats. Vet J 1998; 156:203–215.

53. Vogel M, Schmidt MR, Kristiansen SB, et al. Validation of myocardial acceleration during isovolumic contraction as a novel noninvasive index of right ventricular contractility: Comparison with ventricular pressure-volume relations in an animal model. Circulation 2002;105:1693–1699.

54. Sutton MG, Tajik AJ, Gibson DG, et al. Echocardiographic assessment of left ventricular filling and septal and posterior wall dynamics in idiopathic hypertrophic subaortic stenosis. Circulation 1978; 57:512–520.

55. Carvalho JS, Silva CM, Shinebourne EA, et al. Prognostic value of posterior wall thickness in childhood dilated cardiomyopathy and myocarditis. Eur Heart J 1996;17:1233–1238.

56. Lee CH, Hogan JC, Gibson DG. Diastolic disease in left ventricular hypertrophy: Comparison of M mode and Doppler echocardiography for the assessment of rapid ventricular filling. Br Heart J 1991;65:194–200.

57. Papademetriou V, Gottdiener JS, Fletcher RD, et al. Echocardiographic assessment by computer-assisted analysis of diastolic left ventricular function and hypertrophy in borderline or mild systemic hypertension. Am J Cardiol 1985;56:546–550.

58. Traill TA, Gibson DG, Brown DJ. Study of left ventricular wall thickness and dimension changes using echocardiography. Br Heart J 1978;40:162–169.

59. Kittleson MD. Small Animal Cardiovascular Medicine. St Louis, MO: Mosby; 1999:347–369.

60. Ommen SR, Nishimura RA, Appleton CP, et al. Clinical utility of Doppler echocardiography and tissue Doppler imaging in the estimation of left ventricular filling pressures: A comparative simultaneous Doppler-catheterization study. Circulation 2000;102:1788–1794.